United Nations
Educational, Scientific and
Cultural Organization

Intergovernmental
Oceanographic
Commission

Technical Series 129

What are Marine Ecological Time Series telling us about the ocean?

A STATUS REPORT



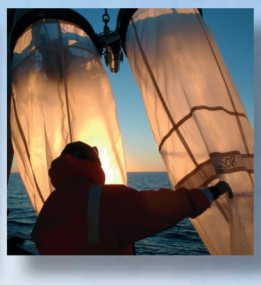
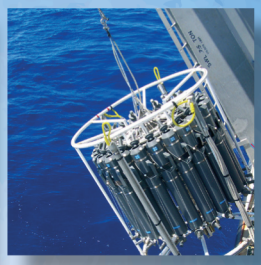

IGMETS

UNESCO 2017

Intergovernmental Oceanographic Commission of UNESCO (IOC-UNESCO)

UNESCO's Intergovernmental Oceanographic Commission (IOC), established in 1960, promotes international cooperation and coordinates programmes in marine research, services, observation systems, hazard mitigation, and capacity development in order to understand and effectively manage the resources of the ocean and coastal areas. By applying this knowledge, the Commission aims to improve the governance, management, institutional capacity, and decision-making processes of its 148 Member States with respect to marine resources and climate variability and to foster sustainable development of the marine environment, in particular in developing countries.

Disclaimer

For bibliographic purposes, this document should be cited as:

O'Brien, T. D.[1], Lorenzoni, L.[2], Isensee, K.[3], and Valdés, L.[4] (Eds). 2017. What are Marine Ecological Time Series telling us about the ocean? A status report. IOC-UNESCO, IOC Technical Series, No. 129: 297 pp.

[1] National Oceanic and Atmospheric Administration (NOAA), Silver Spring, Maryland, United States
[2] University of South Florida (USF), St. Petersburg, Florida, United States
[3] Intergovernmental Oceanographic Commission of UNESCO (IOC-UNESCO), Paris, France
[4] Instituto Español de Oceanografía (IEO), Santander, Spain

What are Marine Ecological Time Series telling us about the ocean? A status report
is available online in electronic format at:

http://ioc.unesco.org

IOC/2017/TS/129

Technical Series 129

Intergovernmental Oceanographic Commission

What are Marine Ecological Time Series telling us about the ocean?

A status report

Editors:

Todd D. O'Brien

Laura Lorenzoni

Kirsten Isensee

Luis Valdés

United Nations
Educational, Scientific and
Cultural Organization

Intergovernmental
Oceanographic
Commission

With the support of the Korea Institute
for Ocean Science and Technology (KIOST)

KIOST
KOREA INSTITUTE OF
OCEAN SCIENCE & TECHNOLOGY

UNESCO 2017

Table of Contents

Foreword

The systematic collection of data on essential variables is fundamental to taking the pulse of our world ocean. Contemporary oceanography is an increasingly integrated endeavor relying on synergies between manned and unmanned, *in situ* and remote observations. Yet, ship based time series – the focus of this report – continue constituting a critical contribution to the knowledge basis for understanding patterns and identifying trends in biogeochemical processes.

The world ocean is vast. Different ocean basins react differently to direct human pressures and to climate change. Understanding the diversity of the effects of global change on the various ocean basins helps us understand better how they interact and how the ocean is responding to change at a global scale. Conversely, there is a need to assess and predict the effects of global change at sub-regional to local scales.

The adoption of the 2030 Agenda for Sustainable Development by the global community in 2015 calls upon ocean science to play a significant role for the achievement of this new agenda. The recently held United Nations Ocean Conference (New York, June 2017) issued a call for action in which ocean science is called upon responding to Member States' needs for coordinated ocean observations; assessing the state of the ocean; assisting informed decision-making; and supporting marine and ocean spatial planning and integrated management – *inter alia*.

The Intergovernmental Oceanographic Commission of UNESCO (IOC) fully realizes the importance of such clear and reinforced enabling policy framework for ocean science. IOC is fully committed to delivering an effective contribution of ocean science to the realization of the 2030 Agenda and its Sustainable Development Goal 14 on conserving and sustainably using the oceans, seas and marine resources for sustainable development. In this context, the Commission provides a platform for promoting international scientific cooperation in ocean science, from research to observations, modelling and related predictions, the set-up of early warning systems, and open access to data and information for management purposes.

The wealth of ecological ship-based time series contributing to this report is to be acknowledged and praised, especially in light of the voluntary nature of the contribution of ship time and efforts to the gathering of data on essential ocean biogeochemical variables. I wish to thank sincerely all time-series programmes having contributed to this report; this has allowed us to present for the first time the status of time series around the world – an essential step towards coordinating such efforts, and to fill existing gaps in ocean research and observations.

In an era of global change we should be ambitious and scale up ocean science activities. IOC Member States at the Twenty-ninth session of the IOC Assembly adopted a resolution on an International Decade of Ocean Science for Sustainable Development (2021-2030) under the auspices of the United Nations. It is in the framework of the Decade, and with the crucial assistance of the IOC International Group for Marine Ecological Time Series (IGMETS), that I see ecological time series be expanded and sustained and become a source of data flowing on a systematic basis into future projections, delivery of ocean services important for human well being such as food security, climate regulation, health, and recreation.

Vladimir Ryabinin
Executive Secretary of IOC

Preface

Some of most valuable scientific discoveries and some of the most beautiful and iconic illustrations in environmental sciences (e.g. the Keeling Curve[1]) were only possible thanks to the data obtained by long-term systematic observations – the so called Time Series- of natural events and conditions. Such time series have been carried out to discover facts about them and to formulate laws and principles based on these facts.

Data provided by ship-based biogeochemical and ecological ocean time-series provide the information to quantify the rate and range of variability of many oceanographic parameters, environmental variables and biological communities. These time series enable estimates of the rate of ocean warming and the effects of global change on the ecosystem processes, e.g. production and sedimentation. They provide reference baselines that are essential to define the extent of environmental disturbances and estimate recovery times. In short, the time series are instrumental in providing the data required to describe, characterize, and quantify the cycles, patterns, variability, and trends of the marine environment and its biota.

Almost since its foundation, the Intergovernmental Oceanographic Commission of UNESCO (IOC-UNESCO) has promoted and advocated for the establishment of ocean observatories. However, it was only in 2013 that the IOC- UNESCO decided to support the International Group for Marine Ecological Time Series (IGMETS) as a result of synergistic activities of the Ocean Carbon and Biogeochemistry Program (OCB), the International Ocean Carbon Coordination Project (IOCCP), and the International Council for the Exploration of the Sea (ICES), with generous funding provided by the Republic of Korea. This initiative aims to aggregate and analyse the existing biogeochemical and ecological time series distributed around the world in an effort to augment the observing power to look at changes within different ocean regions, to explore plausible reasons for their similarities and differences, and to seek connections in the driving forces at ocean basin and global scale. The global perspective will highlight locations of especially large changes that may be of particular ecological importance.

In a first step, IGMETS identified and compiled the metadata from a large number of ship-based biogeochemical and ecological ocean time-series that are currently conducting regular measurements. This exercise -as if we were following a treasure map - resulted in the identification of many existing time series which now comprise part of IGMETS and their locations are displayed in a graphical world map[2] with the metadata accessible in the IOC website. The experts engaged with IGMETS, including the IOC Secretariat, were strongly motivated and convinced that the collective value of these data is greater than that provided by each time series individually. Because the individual time series are distributed across different oceans and managed by different countries, collaboration with countries' institutions conducting the time-series was essential. Their aggregation and synthesis would provide a quantum jump in regional and global ocean ecosystem science. This was how this publication came about.

The statistical analysis and writing process was a rewarding process. We realized very soon that if we wanted to use the existing time series to predict future changes or drifts in the ecosystem dynamics we had to overcome obstacles like the limited number, the non-uniform dispersion, and variable length of the time series themselves. The message was clear: more sampling sites and much longer series are needed in order to gain statistical accuracy if the data are to be used for a plausible prognosis.

[1] https://scripps.ucsd.edu/programs/keelingcurve/
[2] http://unesdoc.unesco.org/images/0023/002346/234627e.pdf

Another realization that occurred over and over again in the IGMETS discussions was that, in spite of their scientific value and relevance, long-term monitoring programmes are often heavily dependent on the personal effort and dedication of individual scientists whose tenure is finite. Thus, many sampling programmes are abandoned after a few years. It is hard to understand why it has proved to be so difficult to establish sustained long-term environmental monitoring programmes. In some cases, it is due to the reluctance from funding agencies to commit long-term support for projects that are constantly seen as "work in progress" and/or treated as "repetitive monitoring". Hopefully this situation will reverse in the near future, as the environmental pressures the ocean is facing and the associated information needs (e.g. Climate change and the UN Sustainable Development Goals) are largely dependent on dedicated and widely distributed observation networks and therefore more long-term monitoring projects should be established worldwide.

With this report, the Intergovernmental Oceanographic Commission of UNESCO is showcasing the importance of the ship-based biogeochemical and ecological time series as one of the most valuable tools to characterize and quantify ocean ecosystems. These results are intended to encourage other colleagues and their institutions to establish new time series and/or continue the sustained systematic sampling of the existing ones and promote data sharing.

The preparation of the report was only possible thanks to the colleagues that run the time-series programmes across different oceans, month after month and year after year, and who generously gave us access to their data. We gratefully acknowledge all of them. I would like to thank my fellow IGMETS members for their commitment, talent, and hard work to summarize the existing, fragmented science, and assemble and make sense of the time series used in this analysis. I also want to thank everyone who contributed to the reviewing and editing of this volume for their dedication and time. Working together, a comprehensive assessment has been produced of ocean biogeochemical and ecological knowledge that demonstrates the scientific potential of ship-based and ecological ocean time-series around the world.

Luis Valdés

Instituto Español de Oceanografía, Santander, Spain

Former head of the Ocean Science Section,
IOC Secretariat - UNESCO

Co-founder of IGMETS

Plankton sampling using a Bongo Net.
© María Luz Fernández de Puelles

Guide to the Report

This section describes the format of the ***IOC-UNESCO Technical Series 129 Report*** and its chapter's structure. The report was peer reviewed by experts specializing in the different regions of the ocean addressed within the report. The report was written for an audience with a certain level of scientific knowledge, with exception of the Executive Summary, which is designed to be accessible to a broader audience.

Executive Summary

The Executive Summary describes the major findings of this report, the ***IOC-UNESCO Technical Series 129 Report*** "What are Marine Ecological Time Series telling us about the ocean? A status report", and highlights some of the significant points of each chapter.

Introduction, Methodology and Ocean Basin Chapters

A general introduction, highlighting the purpose of and scientific questions behind this report, is followed by a section describing the methodology applied in the ocean basin chapters. These chapters include key findings, which are based on the authors' analysis of the available time-series data and scientific, peer-reviewed literature from that region. The time-series analysis in this report only considers data through the end of 2012. This time gap was necessary to ensure that the participating institutions/time-series sites had sufficient time to process their samples (especially plankton counts) and to complete verification of their data. In brief, the results presented herein provide an overview of information from time-series sites and describe general hydrographic, climatic, and biological characteristics and trends, as well as changes over different time scales. Additional analyses integrate relationships to major climatic indices for the different ocean basins.

The order of the chapters follows the ocean conveyor belt (thermohaline circulation), starting up north with the Arctic Ocean, followed by the North and South Atlantic Ocean, subsequently analyzing time-series information in the Southern, Indian, South Pacific and finally North Pacific Ocean. The Global Chapter aims at understanding connections between ocean basins and assessing changes at a larger, global scale.

Annex

The Annex includes detailed information about the time-series sites and surveys that participated in this analysis. For each chapter, a table lists the different time-series sites/surveys located in the ocean basin, the duration, the country conducting the sampling and analysis, and the parameter groups measured. Each site is described with a short paragraph accompanied with a geographic location map. More detailed information on all of the programmes and time series can be accessed online at http://igmets.net/metabase/.

List of Acronyms

A short list of regularly used acronyms is located on the last page of this report.

Executive Summary

Sustained ocean observations, including ships, autonomous platforms, and satellites, are critical for monitoring the health of our marine ecosystems and developing effective management strategies to ensure long-term provision of the marine ecosystem services upon which human societies depend. Ocean observations are also essential in the development and validation of ocean and climate models used to predict future conditions. Ship-based biogeochemical time series provide the high-quality biological, physical and chemical measurements that are needed to detect climate change-driven trends in the ocean, assess associated impacts on marine food webs, and to ultimately improve our understanding of changes in marine biodiversity and ecosystems. While the spatial 'footprint' of a single time series may be limited, coupling observations from multiple time series with synoptic satellite data can improve our understanding of critical processes such as ocean productivity, ecosystem variability, and carbon fluxes on a larger spatial scale. The International Group for Marine Ecological Time Series (IGMETS) analyzed over 340 open ocean and coastal datasets, ranging in duration from five years to greater than 50 years. Their locations are displayed in a world map (Discover Ocean Time Series, http://igmets.net/discover) and in the IGMETS information database (http://igmets.net/metabase). These cross-time-series analyses yielded important insights on climate trends occurring both on a global and regional scale.

At a global level, a generalized warming trend is observed over the past thirty years, consistent with what has been published by the IPCC (2013) report as well as other research. There are regional differences in temperature trends, depending on the time window considered, which are driven by regional and temporal expressions of large-scale climatic forcing and atmospheric teleconnections. This warming is accompanied by shifts in the biology and biogeochemical cycling (i.e. oxygen, nutrient, carbon), which impact marine food webs and ecosystem services.

The surface waters of the **Arctic Ocean** have been **steadily warming** over the past 30 years, from 1983-2012. **Chlorophyll biomass**, as determined by satellite observations, has **increased slightly** over the past fifteen years, from 1998-2012. The complexity of the Arctic marginal seas and central basin settings, and the scarcity of in situ data, limit the analysis of biogeochemical and biological community changes across the pan-Arctic.

The first comprehensive analysis of in situ time series provided for the **North Atlantic Ocean** revealed that, despite being the most studied region of the global ocean, there are large areas in this region still lacking multidisciplinary in situ observations. However, over the 25- and 30-year analysis periods, > 95% of the North Atlantic Ocean **significantly warmed and the chlorophyll concentrations decreased ($p < 0.05$)**. At the same time, **negative trends in salinity, oxygen and nutrients**, as exemplified by nitrate, were noted. The analysis of existing time series showed that even in adjacent areas that appear to be relatively homogenous, there is large variability in ecosystem behaviour over time, as observed in the continental shelves at both sides of the North Atlantic Ocean.

In general, over the **5-year period** prior to 2012, **~70% of the area of the South Atlantic showed cooling** and **66% decreasing chlorophyll concentrations**. However, over the **past 30 years, > 85% of the South Atlantic increased in temperature**. The paucity of in situ time series in this region, and the striking changes that have been reported in South Atlantic ecosystems over the past two decades, highlight the need to have a better observing system in place.

Both **long-term trends and sub-decadal cycles** are evident in the **Southern Ocean** on multiple trophic levels, and they are strongly related in complex ways to climate forcings and their effects on the physical oceanographic system. **Antarctic marine ecosystems have changed over the past 30 years** in response to changing ocean conditions and changes in the extent and seasonality of **sea ice**. These changes have been spatially heterogeneous which suggests that ecological responses depend on the magnitude and direction of the changes, and their interactions with other factors.

Of all the ocean basins, the **Indian Ocean** showed the greatest extent of warming, with **92% of its area showing a significant ($p < 0.05$) positive trend** over 30 years, compared with the Atlantic (89%), the Pacific (66%), the Arctic (79%) and the Southern (32%) oceans. In addition to having a high degree of warming, the Indian Ocean also had the greatest proportion of its area **(55%) showing a significant** ($p < 0.05$) **decline of chlorophyll** between 1998 and 2012. Given the spatial scale of warming in the Indian Ocean, it does seem likely that climate impacts on marine ecosystems will be most pronounced in this basin. The Indian Ocean has very few in situ biogeochemical time series that can be used to assess impacts of climate change on biota or biodiversity.

Over the past **30 years, significant ($p < 0.05$) surface warming** has been recorded for 67% of the area of the **South Pacific Ocean**. A strong physical coupling with planktonic ecology and biology is evident in the South Pacific, with a dominant warming pattern and significantly **declining phytoplankton populations**.

The **North Pacific Ocean** has undergone significant changes in ocean climate during the past three decades. Based on both satellite and ship-based SST measurements, over **65% of its surface area has undergone significant warming since 1983 ($p < 0.05$)**. The patterns of change suggest that the **PDO** has been the dominant mode of climate variability in the North Pacific Ocean **between 1983 and 2012**. However, marked variability in SST has been observed, with episodes of warming in 2002, 2004 and 2010 interspersed with periods of cooling, particularly since 2008 due to the combined effects of La Niña and a negative, cooling PDO phase.

Long-term time series in the **central, subarctic northeast and western North Pacific Ocean show an increase in phytoplankton biomass** during the past 30 years. However, **satellite observations suggest that over 65% of the surface of the North Pacific has experienced a decline in chlorophyll** concentration since 1998. Available time series show an increase in zooplankton biomass in the waters off Hawaii, southern Vancouver Island and the western United States during the last 15 years but an overall decrease at most other locations, with no significant correlation between zooplankton biomass and chlorophyll. **Nutrients, salinity and dissolved oxygen at the ocean surface appear to be negatively correlated with SST across the North Pacific**.

The IGMETS effort highlights the value of biogeochemical time series as essential tools for assessing, and predicting, global and regional climate change and its impacts on ecosystem services. The capacity to identify and differentiate anthropogenic and natural climate variations and trends depends largely on the length of the time-series, as well as on the location. Most of the ship based ecological time series are concentrated in the coastal ocean. While coastal zones in North America and Europe are being monitored, there is a conspicuous lack of biogeochemical time-series in other coastal regions around the world, and an almost complete absence of such observational platforms in the open ocean, which limits the capacity of analyses such as this. A more globally distributed network of time-series observations over multiple decades will be needed to differentiate between natural and anthropogenic variability.

1 New light for ship-based time series (Introduction)

Luis Valdés and Michael W. Lomas

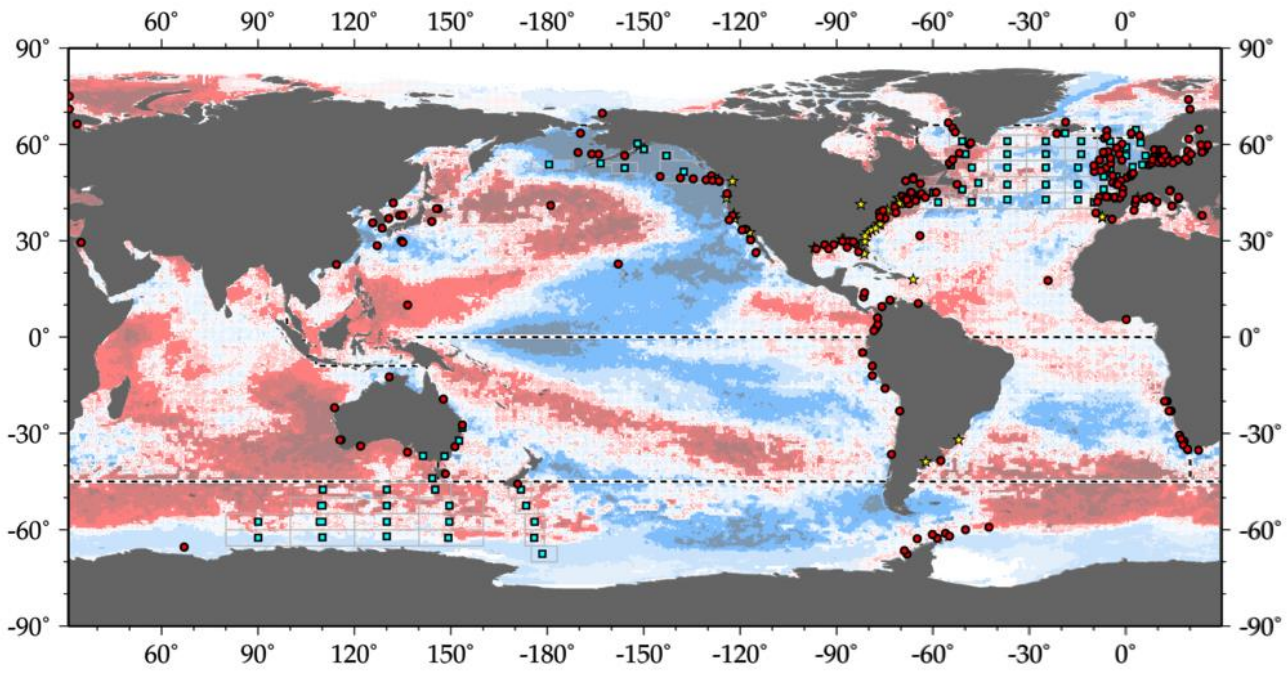

Figure 1.1. Map of IGMETS-participating time series on a background of 10-year (2003–2012) sea surface temperature trends. This map shows 344 time series (coloured symbols of any type), of which 71 were from Continuous Plankton Recorder subareas (blue boxes) and 46 were from estuarine areas (yellow stars). The dashed lines indicate boundaries between IGMETS regions, which are further examined in the chapters of this report. Additional information on the sites in this study is also presented in the Annex.

This chapter should be cited as: Valdés, L., and Lomas, M.W. 2017. New light for ship-based time series. *In* What are Marine Ecological Time Series telling us about the ocean? A status report, pp. 11–17. Ed. by T. D. O'Brien, L. Lorenzoni, K. Isensee, and L. Valdés. IOC-UNESCO, IOC Technical Series, No. 129. 297 pp.

1.1 Global importance of time series

The observation of nature and the understanding that there are underlying regularities (cause-and-effect relationships) dates back to the very origin of human culture. In fact, this knowledge allowed for the management of natural resources and for the establishment of the earliest human settlements, e.g. the very first agricultural societies. The prediction of Nile flooding was critical not only for food security, but it was also a matter of political power.

There are many examples of records of long-term systematic observations of natural events and conditions from crop yields, planet movements, sun spots, river discharges, and freezing records dating from ancient times (Bell and Walker, 2013). Many of the most beautiful scientific discoveries were possible thanks to data obtained by regular observations – time series – carried out with the purpose of discovering facts about certain phenomena and to formulate laws and principles based on these facts. [1]

The biogeochemistry of the ocean (Figure 1.1) varies naturally across a range of temporal and spatial scales (Figure 1.2), which is often further conflated with anthropogenic forcing (warming, acidification, pollution, etc.). In a growing effort to distinguish between natural and human-induced earth system variability, sustained ocean time-series measurements have taken on a renewed importance as they represent one of the most valuable tools that scientists have to characterize and quantify ocean ecosystem cycles and fluxes and their associated links to changing climate.

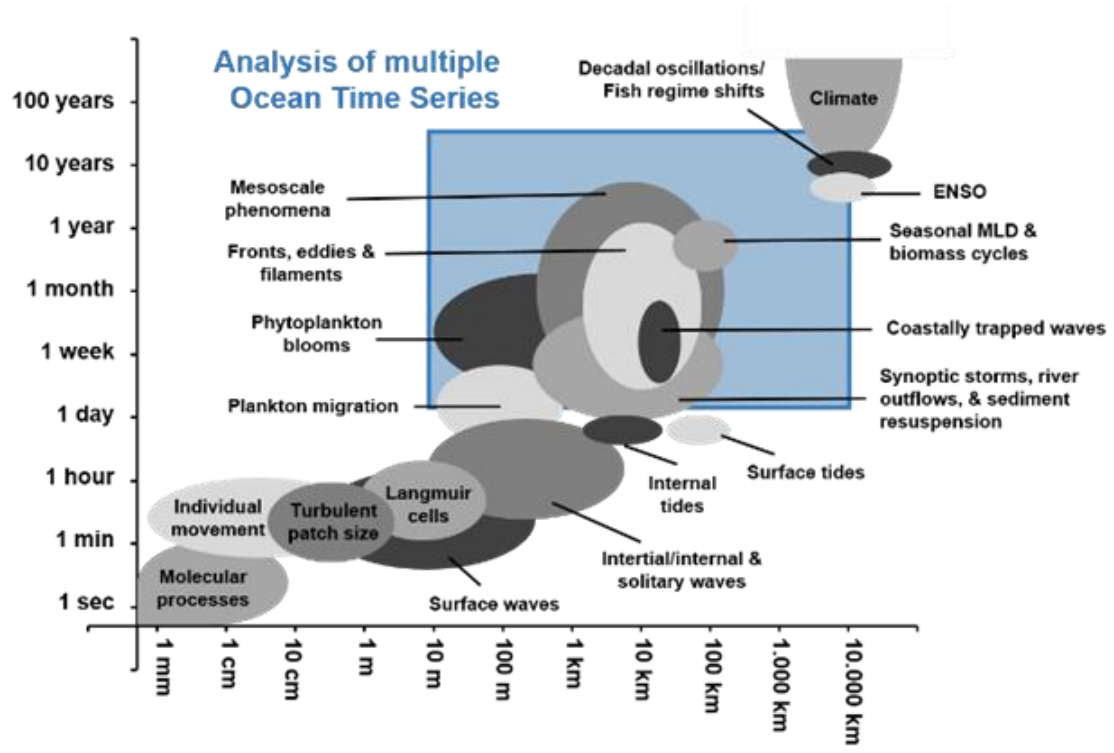

Figure 1.2. Temporal and spatial scales of a range of ocean processes. The blue square highlights the range of space- and time-scales that can be addressed by ship-based, time-series measurements (Adapted from Dickey, 2002).

[1] To state that a particular phenomenon always occurs if certain conditions are present is a principle of conservation laws of physics, which reflects the homogeneity of a process in space and time. The search for patterns and symmetries is one of the main goals of science, and reducing uncertainties in a given phenomenon makes us feel comfortable as if we were able to reduce the entropy and minimize the occurrence, or the impacts, of unexpected events.

Ocean time series, particularly ship-based repeated measurements, consist of one type of observation programmes which are crucial to answering scientific questions and improving decision-making in ocean and coastal management (Edwards *et al.*, 2010). They provide the oceanographic community with the long, temporally resolved datasets and high-quality data needed to characterize ocean physics, climate, biogeochemistry, and ecosystem variability and to change what can be used to examine, test, and refine many paradigms and hypotheses about the functioning of the ocean (Henson, 2014). They also help to disentangle natural and human-induced changes in marine ecosystems (Reid and Valdés, 2011).

1.2 Levels of understanding and need for continued sampling

Time-series data help resolve both short- and long-term scales of variability, depending on sampling frequency, and provide context for traditional process-oriented studies.

Depending on motivation, sampling frequency, and length, time series can be used for different purposes (Figure 1.3) and are of critical importance to enable or facilitate: (i) the acquisition of ecosystem baselines and rate and scale of environmental change, including climate change and biodiversity loss, (ii) the understanding of ocean, earth, and climate system processes, (iii) to monitor ecosystem dynamics and its variability, (iv) the detection of hazards and environmental disturbances and the estimation of recovery times, (v) to forecast and anticipate ecosystem changes, and (vi) effective policy-making and sustainable management of the seas and oceans.

Significant advances in our understanding of ocean processes in some well-studied systems have shown that not all ocean regions are changing at the same rate or following the same pattern. This is, in part, because the ocean is characterized by interacting processes, which operate over nearly 10 orders of magnitude in time and space (Dickey, 2001, 2002). Indeed, some regions are more sensitive to environmental change than others. Exploring this temporal and spatial variability of ocean change, at a basin-scale or greater, is largely the realm of earth ecosystem models at present. Indeed, it is only through models that we can learn about the spatial representativeness of existing time series (i.e. the footprint of a time series) and, therefore, inform decisions about where to site new time series (Henson *et al.*, 2016).

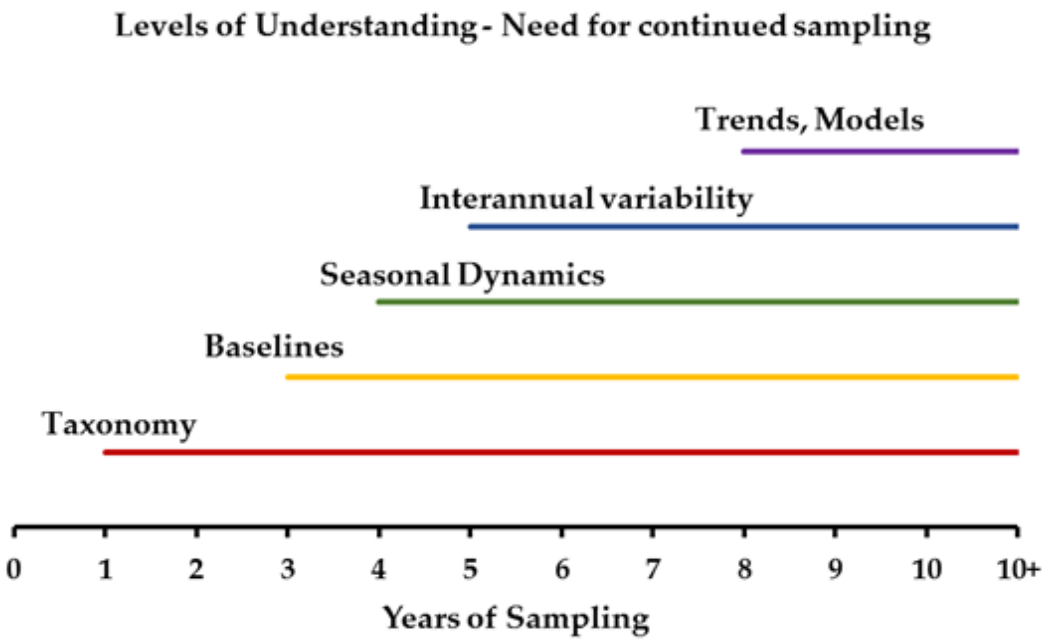

Figure 1.3. Representative sampling time-scales needed to establish a minimum level of understanding across levels of complexity within an ecosystem.

While our understanding of first-order ocean biogeochemical concepts in these models and their coupling to atmospheric forcing is reasonably well developed (Keller *et al*., 2014), these models are still limited by lack of mechanistic and observational knowledge in time and space of how the ocean is changing physically, chemically, and biologically and, worse yet, the interactions between these levels of variability (Heinze *et al*., 2015). This is further exacerbated by the fact that observational time series generally have to be several-fold longer than the time-scale they are trying to resolve, while models can produce multidecadal output with relative ease. For example, published model output suggests that at least three decades would be needed to resolve climate-change response in the North Atlantic in certain variables (e.g. primary production), but less in others (e.g. sea surface temperature) (Henson *et al*., 2010, 2016).

Obviously, the "pay check" you receive from consistent long-term, ship-based marine time series is not regular, but many times it is surprising, as demonstrated by recent discoveries, e.g. proof of ocean acidification, ecosystem regime shifts, and exploration of the deep sea, which illustrate that sustained multidecadal observations are ecological and economical important research investments for future generations.

In a time of increasing pressures on the marine environment, time series are central to understanding past, current, and future alterations in ocean biology and to monitoring future responses to climate change (Valdés *et al*., 2010; Karl, 2014). With many time series now having accumulated sufficient data to quantify variability and trends (see Figures 2.2 and 2.3 in the "Methods and visualization" chapter), it would be foolish to allow reductions or long gaps in sampling to occur, and replacing the ship-based, long-term series with autonomous platforms should not be the ultimate path to follow.

While these tools provide high-quality and high-frequency data for certain, generally physical and geochemical, parameters, ship-based time series are unique in their multidisciplinarity: physical, chemical, and biological parameters can be measured simultaneously. Many ecosystem processes and functions (e.g. primary production, phytoplankton composition, utilization of specific nutrients) cannot be directly obtained from these autonomous sensors, and only some can be derived through proxy measurements. Furthermore, regular and consistent calibration of independent sensors, moorings, and remote-sensing techniques can only be assured with standardized *in-situ* measurements.

1.3 New light for time series: international collaboration in ship-based ecosystem monitoring

The history of long-term ocean time series started more than 100 years ago. In the Western English Channel and around the British Isles, records go back to the late 19th century. A broad suite of marine time-series sites was established in the middle of the 20th century in the Northern Hemisphere, e.g. Station M in the Norwegian Sea (1948), NOAA Ocean Station P Sea in the North Pacific (1947), Henry Stommel's 'Hydrostation S' in the Sargasso Sea (1954), and Boknis Eck Time Series Station where monthly sampling began in April 1957 (Owens, 2014).

Many other coastal and oceanic time series were established across different oceans and managed by different countries since the 1980s and 1990s following recommendations from international programmes such as JGOFS (1990) and GLOBEC (1997).

The value of these measurements has not been fully appreciated, and several sampling sites face severe funding difficulties. Some could not sustain measurements with the same sampling frequency in time, resulting in temporal gaps of observations, and financial resources even ceased, and no alternatives could be obtained (Frost *et al*., 2006). However, many others survived and gained international prestige (e.g. HOT, BATS, CARIACO, ESTOC, Plymouth L4, Helgoland Roads, RADIALES) particularly for providing the reference baselines for different variables at local–regional scales and in different ocean biogeographical provinces.

Difficulties in harmonizing the data, digitalizing results to enhance broad accessibility, and evaluating methods hampered the utilization of these historical datasets. As a contribution to GLOBEC, ICES encouraged the international comparison and analysis of time series, which was adopted by the ICES Working Group on Zooplankton Ecology (Valdés *et al*., 2005; O'Brien *et al*., 2012; Wiebe *et al*., 2016) and then continued by SCOR WG125 and WG137 (WG125: *Global Comparisons of Zooplankton Time Series* and WG137: *Patterns of Phytoplankton Dynamics in Coastal Ecosystems: Comparative Analysis of Time Series Observation*). Now, the International Group for Marine Ecological Time Series (IGMETS; Figure 1.4), under the auspices of the IOC-UNESCO, is taking on the mantle of improving access to time series. All of these groups stressed the need to broaden the scientific utilization of existing time-series datasets and to link current and past studies.

Figure 1.4. Previous and ongoing activities within the scientific community leading up to the IGMETS effort.

The goals of IGMETS are to look at holistic changes in different ocean regions, explore plausible reasons and explanations at regional and global scales, and highlight locations of especially large change that might be of particular importance for model projections or ongoing management policies. In the process, IGMETS intends to aggregate existing time-series sampling sites, establish global baselines, assess spatial variability and response to climate at the basin-scale and greater, and provide the basis for projection and forecasting.

1.4 The ocean time series heritage

A time-series workshop in November 2012 was organized by OCB, IOCCP, and IOC-UNESCO. One of the key outcomes of this workshop was the development of a global time-series network compiling more than 140 ship-based time series and to improve evaluation and coordination of methods and communication among marine biogeochemical time series. The compilation of metadata of time series continued under the IGMETS umbrella; more than 340 open ocean and coastal datasets (Figure 1.1), ranging in length from 5 to >50 years and having a similar set of minimal observations, have so far been identified. Their locations are now displayed in a world map (inner cover of this volume) and in the metadata search on the http://IGMETS.net website. These time-series sampling sites represent a phenomenal heritage legacy, and intergovernmental bodies such as ICES, European Marine Board, or IOC-UNESCO strongly recommend continuing the systematic sampling of the existing sites and establishing new time series based on the knowledge gained.

Given that individual time series are distributed across different oceans and managed by different countries, open collaboration with national institutions managing the time series is essential. Sustaining a ship-based time series requires careful planning, periodic evaluation of approach and methods (including implementation of new methods and measurements as appropriate), and a good data-dissemination policy (Karl, 2010).

IGMETS advocates:

1) **Observations which are not made today are lost forever!**
2) **Existing observations are lost if they are not made accessible.**
3) **The collective value of datasets is far greater than their dispersed value.**
4) **No substitute exists for adequate observations.**
5) **The value of time-series observations is positively correlated with the duration of continuous measurements. Measurements encompassing a time-span of several decades allows identification of seasonal, interannual, and decadal patterns.**
6) **The analysis of multiple datasets from different time-series stations allows the separation of stressors and the evaluation of connected ecosystem responses.**
7) **During previous decades, science and technology evolved along with time-series observations. Anticipated development of new techniques will allow streamlining the measurements and improving their geographical coverage.**
8) **Advanced analysis, including global assessments and improved computation, using existing data, creates new science.**
9) **Models will evolve and improve, but, without data, will be untestable – projections and forecasting require considerable diversification of *in situ* data.**
10) **Today's climate models will likely prove of little interest in 100 years. But, adequately sampled, carefully quality controlled, and archived data for key elements of the climate system will be useful indefinitely.**

1.5 Overview of this report

There are an extraordinary number of unexploited datasets obtained by long-term ocean time series. Large spatial-scale analyses using many different time series allow us to augment our capacity to detect and interpret links between climate variability and ocean biogeochemistry, ultimately improving our understanding of marine ecosystem change. However, in order to bring together datasets from different time series, it is important that the sampling and analytical protocols used at each site are homogenous, consistent, and intercomparable.

For the purposes of analyses presented in this report, we define a time series as a location that is sampled at least once per season (such that strong seasonal patterns can be removed to study lower-frequency variability). We also only examined near-surface observations. This is, in part, due to taking a global view for this analysis and thus avail ourselves of satellite observations to fill in spatial gaps between *in situ* observations, but also because there are far fewer ecological time series that sample in the vertical domain. Within the time-series compilation records, 214 contain information on zooplankton, 142 on phytoplankton, and 145 on nutrients. Data obtained after 2012 were not included in the analysis, which allows the data owner to be the first to publish new findings in the peer-reviewed literature.

The result presented herein provide a brief overview of the information provided from the long-term time-series sites and describe general hydrographic, climatic, and biological characteristics and trends, explaining the change over time. This analysis allows for comparisons of changes occurring in distant locations and helps to detect changes occurring at broad scales and to distinguish them from local imbalances or fluctuations. Additional analyses integrate relationships to major climatic indices for the different ocean basins.

Analyzing the datasets obtained at multiple ocean time-series sites has high scientific value, but sharing data has also important economic and social benefits. The demand from different stakeholders and decision-makers for answers to the challenges posed by changes in the marine environment is growing rapidly. Sharing and accessing time-series data would reduce uncertainties in the management of marine resources and ecosystem services.

This document reviews the dynamics and climate trends that have been reported from different ocean basins and discusses potential future changes to the ecological processes of marine systems. Forecasting the dynamics of ocean processes requires the use of mathematical models, which are often limited by data availability. Challenges are highlighted in this publication in the hope that continuing research efforts will fill knowledge gaps and thus improve our ability to predict future trends and facilitate the successful management and conservation of marine species, habitats, living marine resources, and ecosystem services.

In summary, this IGMETS report aims to deliver new insights into existing biogeochemical and ecological ship-based times-series and to reduce scientific uncertainty regarding environmental change. The report also features an overview of the gaps and needs for better sampling coverage in the different ocean basins and seas.

1.6 References

Bell, M., and Walker, M. J. C. 2013. Late Quaternary Environmental Change: Physical and Human Perspectives. Routledge, New York. 355 pp.

Dickey, T. 2001. The role of new technology in advancing ocean biogeochemical research. Oceanography, 14(4): 108–120.

Dickey, T. 2002. A vision of oceanographic instrumentation and technology in the early 21st century. *In* Oceans 2020: Science, Trends, and the Challenge of Sustainability, pp. 209–254. Ed. by J. G. Field, G. Hempel, and C. P. Summerhayes. Island Press, Washington, DC. 296 pp.

Edwards, M., Beaugrand, G., Hays, G. C., Koslow, J. A., and Richardson, A. J. 2010. Multidecadal oceanic ecological datasets and their application in marine policy and management. Trends in Ecology & Evolution, 25: 602–610, doi:10.1016/j.tree.2010.07.007.

Frost, M. T., Jefferson, R., and Hawkins, S. J. (Eds). 2006. The evaluation of time series: their scientific value and contribution to policy needs. Report prepared by the Marine Environmental Change Network (MECN) for the Department for Environment, Food and Rural Affairs (DEFRA), Marine Biological Association, Plymouth. Marine Biological Association Occasional Publications No. 22. 94 pp.

GLOBEC. 1997. Global Ocean Ecosystem Dynamics (GLOBEC) Science Plan. Final editing by R. Harris and the members of the GLOBEC Scientific Steering Committee (SSC). IGBP Report 40. 83 pp.

Heinze, C., Meyer, S., Goris, N., Anderson, L., Steinfeldt, R., Chang, N., Le Quéré, C., *et al*. 2015. The ocean carbon sink – impacts, vulnerabilities, and challenges. Earth System Dynamics, 6: 327–358.

Henson, S. A. 2014. Slow science: the value of long ocean biogeochemistry records. Philosophical Transactions of the Royal Society A, 372: doi: 10.1098/rsta.2013.0334.

Henson, S. A., Beaulieu, C., and Lampitt, R. 2016. Observing climate change trends in ocean biogeochemistry: when and where. Global Change Biology, 22(4): 1561–1571, doi:10.1111/gcb.13152.

Henson, S. A., Sarmiento, J., Dunne, J., Bopp, L., Lima, I., Doney, S., John, J., *et al.* 2010. Detection of anthropogenic climate change in the satellite records of ocean chlorophyll and productivity. Biogeosciences, 7: 621–640.

JGOFS. 1990. Joint Global Ocean Flux Study (JGOFS) Science Plan. JGOFS Report No 5. 67 pp.

Karl, D. M. 2010. Oceanic ecosystem time-series programs: Ten lessons learned. Oceanography, 23(3): 104–125.

Karl, D. M. 2014. The contemporary challenge of the sea: Science, society, and sustainability. Oceanography, 27(2): 208–225, http://dx.doi.org/10.5670/oceanog.2014.57.

Keller, K. M., Joos, F., and Raible, C. C. 2014. Time of emergence of trends in ocean biogeochemistry. Biogeosciences, 11: 3647–3659.

O'Brien, T. D., Li, W. K. W., and Morán, X. A. G. (Eds). 2012. ICES Phytoplankton and Microbial Plankton Status Report 2009/2010. ICES Cooperative Research Report No. 313. 196 pp.

Owens, N. J. P. 2014. Sustained UK marine observations. Where have we been? Where are we now? Where are we going? Philosophical Transactions of the Royal Society A, 372: http://dx.doi.org/10.1098/rsta.2013.0332.

Reid, P. C., and Valdés, L. 2011. ICES status report on climate change in the North Atlantic. ICES Cooperative Research Report No. 310. 262 pp.

Valdés, L., Fonseca, L., and Tedesco, K. 2010. Looking into the future of ocean sciences: an IOC perspective. Oceanography, 23(3): 160–175.

Valdés, L., O'Brien, T. D., and López-Urrutia, A. (Eds). 2005. Zooplankton monitoring results in the ICES area, Summary Status Report 2003/2004. ICES Cooperative Research Report No. 276. 34 pp.

Wiebe, P., Harris, R., Gislason, A., Margonski, P., Skjoldal, H. R., Benfield, M., Hay, S., *et al*. 2016. The ICES Working Group on Zooplankton Ecology: Accomplishments of the first 25 years. Progress in Oceanography, 141: 179–201, doi:10.1016/j.pocean.2015.12.009.

2 Methods and Visualizations

Todd D. O'Brien

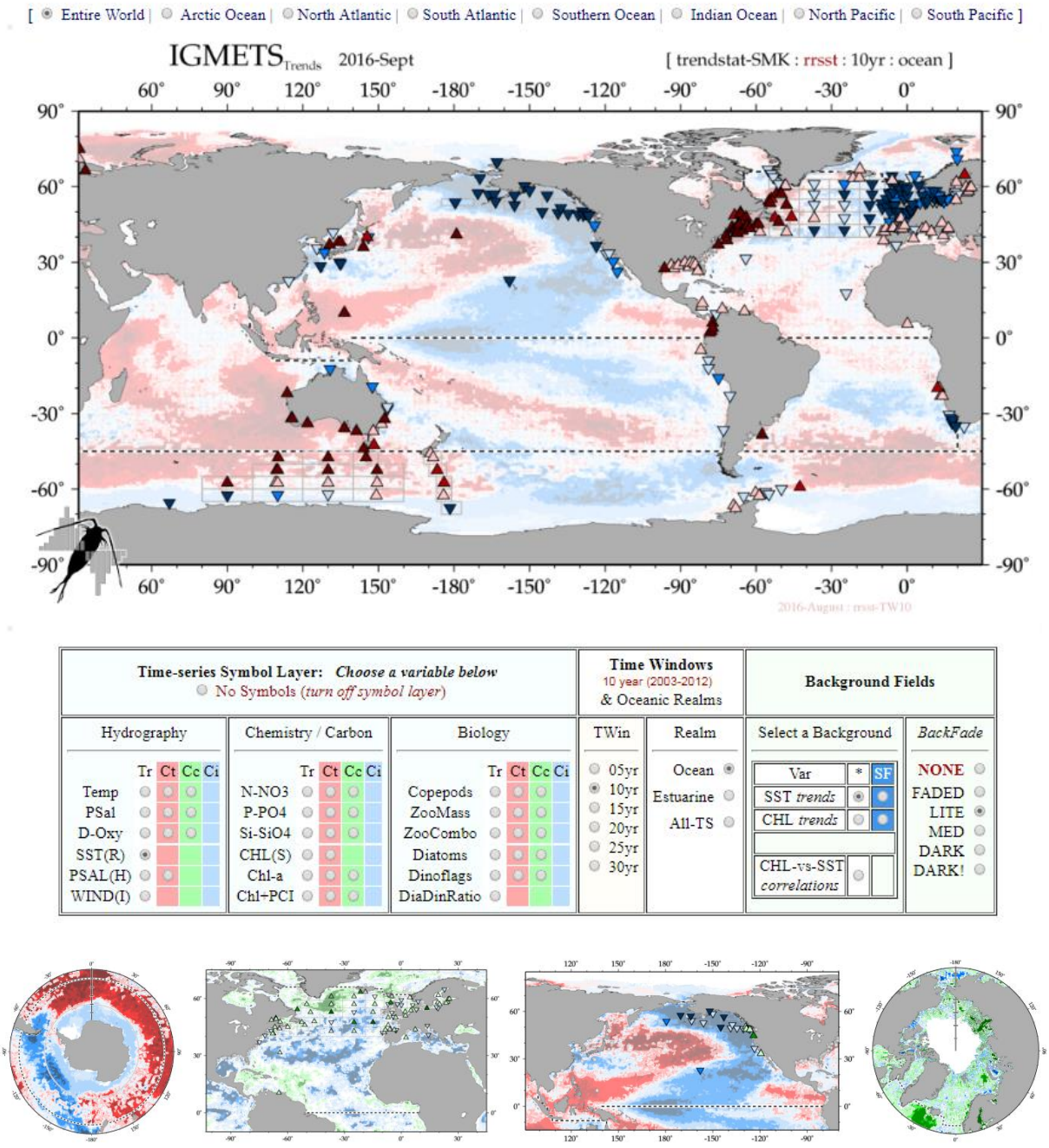

Figure 2.1. An example screenshot from the IGMETS time series Explorer available online at http://igmets.net/explorer and a selection of additional spatio-temporal visualizations available via the Explorer and used throughout this report.

This chapter should be cited as: O'Brien, T. D. 2017. Methods and Visualizations. *In* What are Marine Ecological Time Series telling us about the ocean? A status report, pp. 19–35. Ed. by T. D. O'Brien, L. Lorenzoni, K. Isensee, and L. Valdés. IOC-UNESCO, IOC Technical Series, No. 129. 297 pp.

2.1 Introduction

With a collection of over 340 marine ecological time series, the data-assembling effort behind IGMETS was considerable (Figure 2.1). As these time series also varied in their available variables, methodologies, months of coverage, and years in length (Figures 2.2 and 2.3), a flexible yet robust analytical method was required to synthesize and compare the information. For over 12 years, the Coastal & Oceanic Plankton Ecology, Production, & Observation Database (COPEPOD) been working with marine ecological time-series data assembly, analysis, and visualization when it provided the data backbone for the SCOR Global Comparisons of Zooplankton Time Series working group (WG125). COPEPOD continued its support with other time-series groups, such as the ICES Working Group on Zooplankton Ecology (WGZE), the ICES Working Group on Phytoplankton and Microbial Ecology (WGPME), and the SCOR Global Patterns of Phytoplankton Dynamics in Coastal Ecosystems working group (WG137).

During these years of collaboration, a suite of analytical and visualization tools has been created, modified, and expanded to support the specific needs of each of these groups (Mackas *et al*., 2012; O'Brien *et al*., 2012, 2013; Paerl *et al*., 2015). These tools were again adapted and expanded to fit the requirements of IGMETS, creating the first-of-its-kind interactive time series visual explorer (http://igmets.net/explorer) as well as the spatio-temporal trend fields seen throughout the following chapters of the report.

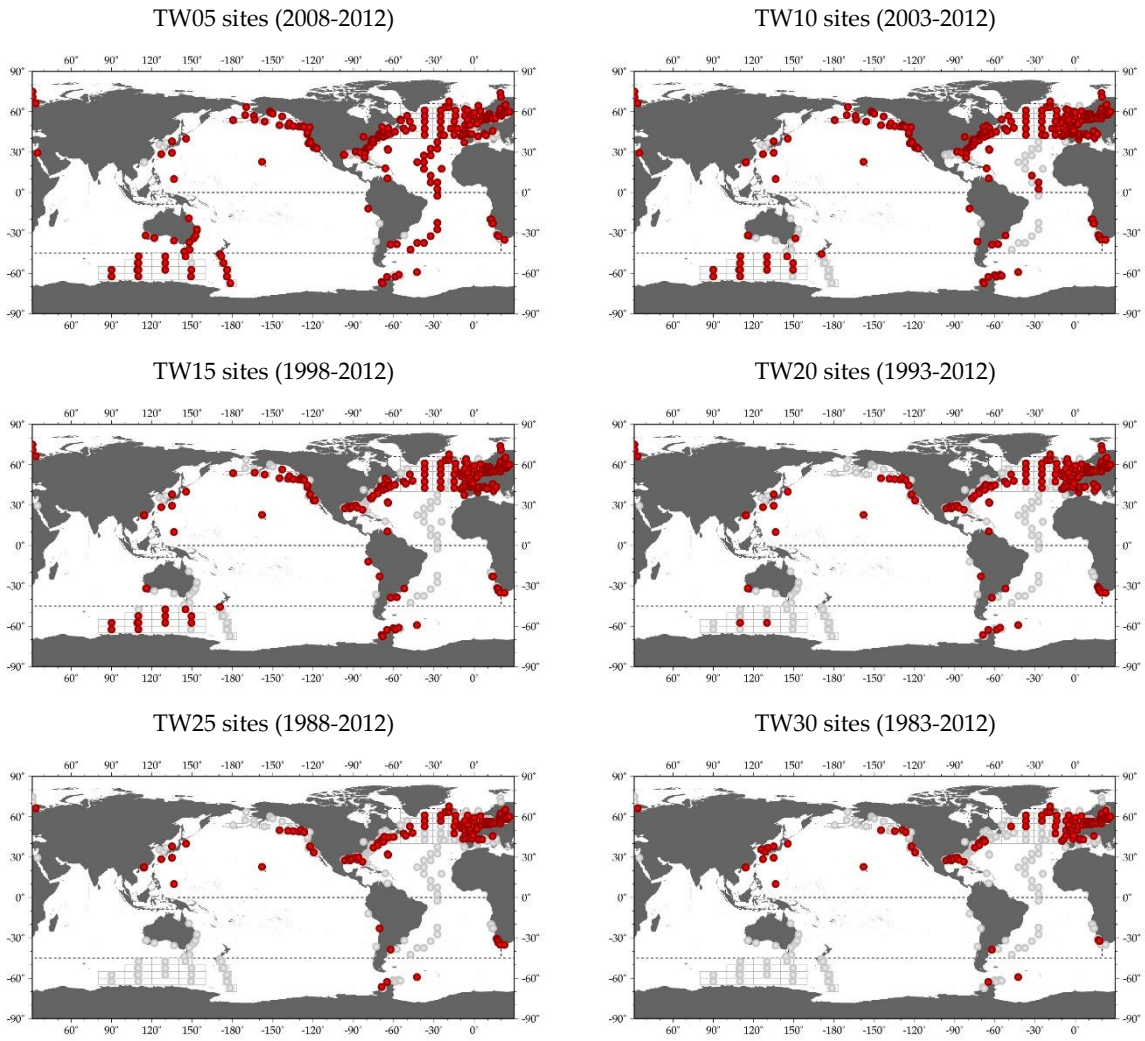

Figure 2.2. Panel of maps showing locations of IGMETS-participating time series based on time-window qualification. Red symbols indicate time-series sites with at least one biological or biogeochemical variable (i.e. excluding temperature- and salinity-only time series) that qualified for that time-window (e.g. TW05, TW20). The time-window concept and method are described in Section 2.3.2. Light gray symbols indicate sites that did not have enough data from the given time-window to be included in that analysis.

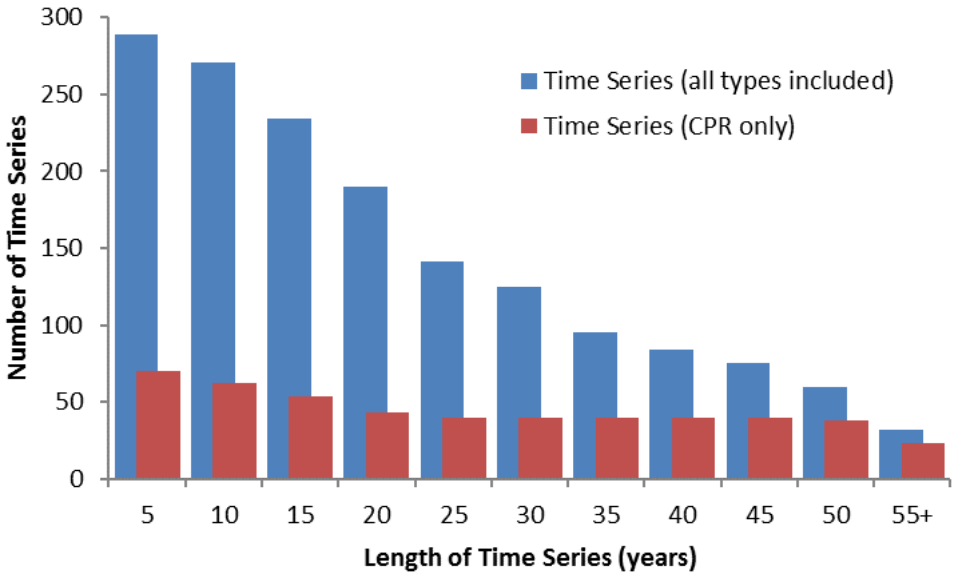

Figure 2.3. Histogram of all IGMETS-participating time series sorted by their length in years. The Continuous Plankton Recorder (CPR) time series is also plotted separately, highlighting its significant contributions to the longer time-spans.

2.2 *In situ* data sources

The International Group for Marine Ecological Time Series effort focused on ship-based, *in situ* time series with chemical and/or biological data elements. IGMETS did not pursue data from buoys, floats, pier-mounted sensors, or automated underwater vehicles (AUV). With an interest in ecological time series, IGMETS most heavily pursued datasets that had chemical or biological variables (e.g. nutrients, pigments, or plankton data).

At the time of preparation of this report, more than 340 time series were participating in IGMETS. These sites are listed at the end of each chapter in the "Regional listing of participating time series" tables and are presented in more detail in the Annex of this report. The IGMETS online metabase (http://igmets.net/metabase) also includes this information and offers additional content and search tools (e.g. search by variable, length in years, programme, investigator, or country). Finally, the metabase also contains any additional time series identified and added after this initial report was published.

The term "participating time series" was used to identify time series that provided data for the IGMETS numerical analysis. Time series acknowledged in the report, but not classified as "participating", implies that their data were not available for the analysis. Reasons for this unavailability included receiving no response after repeated attempts to contact the data holders or, in some rare cases, non-public proprietary data.

The chapters of the IGMETS report are divided into larger ocean-based regions (e.g. North Atlantic, South Pacific, Arctic Ocean), separated by land masses, or, in the case of an in-water division, indicated with black dashed lines (Figure 2.4). Each regional chapter only discusses time series and trends found within that specific region. For the purpose of this report, most of the analyses and visualizations also only focused on trends within oceanic, non-estuarine sites.

2.3 Analytical methods

The IGMETS time series vary greatly in their available variables, methodologies, months of coverage, and years in length (Figures 2.2 and 2.3). A flexible yet robust analytical method was required to conduct the analyses and compare them in a meaningful way. The following sections describe the methods used and the challenges addressed by the IGMETS analysis. Many of these methods are refinements and expansions of earlier work developed by COPEPOD to support other time-series working groups.

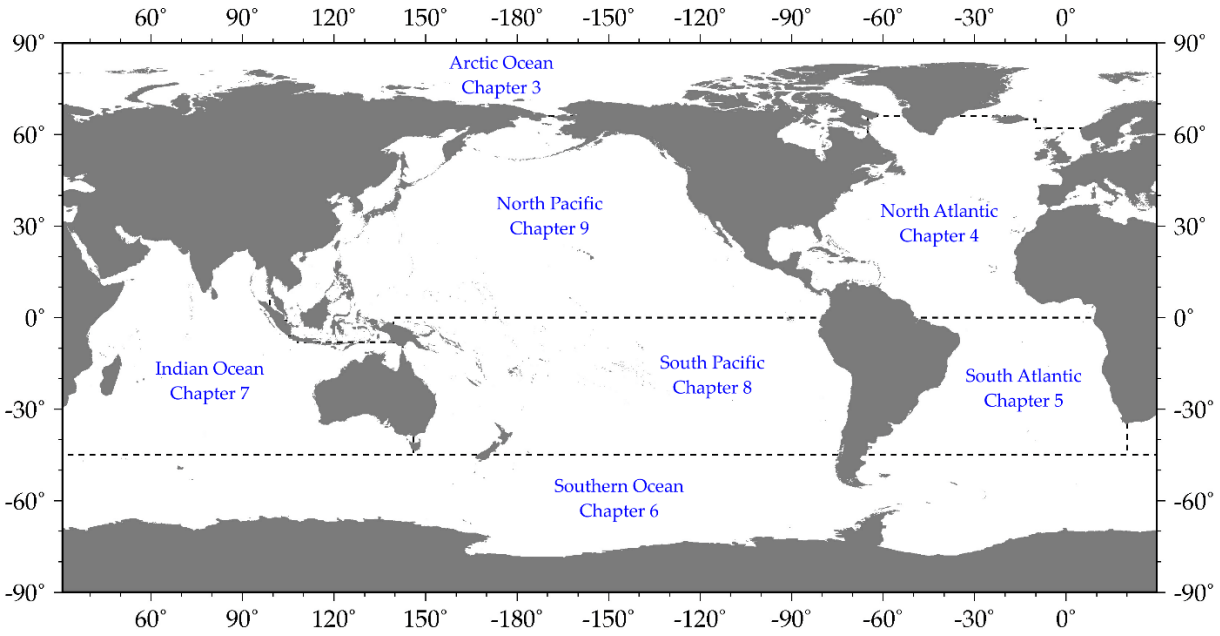

Figure 2.4. Global map illustrating the geographical boundaries of each chapter. The geographical separation of the ocean-basin chapters is set by land masses or, in the case of an in-water division, indicated with black dashed lines.

The IGMETS analysis addressed the following questions:

- How to compare time series with different methods or measuring units (Section 2.3.1),
- How to address time series with different seasonal influences (Section 2.3.1),
- How to compare time series with different time spans (Section 2.3.2),
- How to get a spatially-coherent overview from sparse data (Section 2.3.3).

2.3.1 The IGMETS statistical methodology

The comparison of variables sampled using different methods requires a careful yet flexible analysis. These differences not only include the measurement technique itself (e.g. instrumentation used, chemical method, counting method), but also sampling protocols and depth at which such measurements were collected (e.g. "surface" vs. a bottle triggered at 10 m vs. an average of the top 10 m vs. an integration of values over the top 10 m). Quantitatively, these values are not easily intercomparable, if at all. In terms of a time-series study, however, the focus is on how these variables are changing over time relative to themselves and to each other. Using data from different methods, one cannot necessarily intercompare how much they are changing, but it is possible to detect if these variables are similarly increasing or decreasing over time. As long as the method used within each individual time series is consistent over the duration of that individual time series, a comparison of relative trends among multiple time series, even with different methodologies, is possible.

2.3.1.1 Calculation of trends over time

A monotonic upward (or downward) trend means that the variable consistently increases (or decreases) over time, even though that trend may or may not be linear. Previous time-series studies by SCOR WG125 (Mackas *et al.*, 2012) and ICES WGZE/WGPME (O'Brien *et al.*, 2012, 2013) looked at trends by calculating the linear regression (slope) of annual anomalies within a time series. These annual anomalies were, in turn, calculated using "the Mackas method" (Mackas *et al.*, 2001; O'Brien *et al.*, 2013), which removed the seasonal cycle during the calculations. The Mackas method is also very tolerant of sparse data or time series with missing years or months (Mackas *et al.*, 2001).

While the Mackas method itself was robust, ICES WGPME/WGZE found that the (parametric) linear regressions used to estimate trends were limited (e.g. yielded weak *p* values) when accounting for the statistical complexity in some shorter ecological time series, especially those less than ten years in length. Following the suggestion of these working groups, the IGMETS time-series analysis used the non-parametric seasonal Mann-Kendall (SMK) test to test for monotonic trend in time series with seasonal variation (Hirsch *et al*., 1982). The SMK works by calculating the Mann-Kendall score (Mann, 1945; Kendall, 1975; Gilbert, 1987) separately for each month; the sum of these values gives the final test statistic. The variance of the test statistic is likewise obtained by summing the variances of each month, and a normal approximation is then used to evaluate the significance level. IGMETS found results from the SMK to be equivalent to the Mackas method for time series longer than ten years and that it also frequently helped near-but-not-quite-significant shorter time series cross the "$p < 0.05$" borderline.

2.3.1.2 Statistical significance

The IGMETS analyses provide tables and visualization figures that differentiate between statistically significant ($p < 0.05$) and non-significant trends within the *in situ* variables and satellite-based background fields. In terms of estimating the statistical significance of a monotonic trend, the calculations behind the *p* value depend on the:

a) number of observations (e.g. the number of years in the time series),
b) strength of the trend (e.g. the magnitude of change over time), and
c) error/variance/noise of the variable.

In terms of time series, this means:

a) A shorter time series may require a stronger trend to be considered statistically significant, while a less pronounced trend may require more years in length before being considered statistically significant.
b) A variable with a large, but natural, variance (e.g. biological or biologically influenced variables) may require more years in length and/or a stronger trend (to be considered statistically significant) than a variable with a relatively lower variance (e.g. temperature).

These patterns are easily seen in the "Spatial frequency" tables (Section 2.4.4), where the ratio of significant to non-significant trends greatly increases with length of time. Statistically significant or not, spatially coherent patterns of "increasing" and "decreasing" were evident in both temperature and chlorophyll spatio-temporal fields (Section 2.4.4 and Figures 2.8, 2.9, and 2.10).

2.3.1.3 Combined variables

Within the IGMETS variables set, a handful of related, but slightly different, variables were present. For example, some time series had chlorophyll *a* measurements, others had total chlorophyll, or fluorescence, and the Continuous Plankton Recorder (CPR) time series had data from its Phytoplankton Colour Index (PCI). As stated in the beginning of this section (Section 2.3.1), as long as the method used in each individual time series was consistent over the duration of that individual time series, one can compare general trends among time series, even if they used different methodologies to measure the same variable. By grouping the trends from these three methods into a loose "combined chlorophyll" category, it is possible to obtain a larger and more coherent spatial picture than if only considering one method-specific variable at a time. For example, in the North Atlantic, the combined chlorophyll included the CPR PCI trends that fill the entire central transbasin North Atlantic region, an area where no chlorophyll *a* time series were otherwise available.

Similar combinations were done for the "combined zooplankton" grouping, which included trends from the "total copepods" abundance time series and trends from various total zooplankton biomass methods (e.g. total wet weights, total dry weights, or total sample volumes). This approach has been used by SCOR WG125 as well as the ICES WGZE and WGPME plankton time-series groups (Mackas *et al*., 2012; O'Brien *et al*., 2012, 2013).

For those who wish to not combine similar variables, the IGMETS Explorer (http://igmets.net/explorer) can display the distributions and trends of time-series variables both individually and in their combined grouping forms.

Table 2.1. Year-span and minimum year requirements for the IGMETS time-windows.

IGMETS time-window	Year-span	Minimum year requirement
"TW05" (5 years)	2008–2012	4 of 5
"TW10" (10 years)	2003–2012	8 of 10
"TW15" (15 years)	1998–2012	12 of 15
"TW20" (20 years)	1993–2012	16 of 20
"TW25" (25 years)	1988–2012	20 of 25
"TW30" (30 years)	1983–2012	24 of 30

2.3.2 IGMETS time-windows

While it is not really meaningful to compare long-term trends from a 31-year time series with a 12-year time series, it is possible to compare the 10-year trends created from the overlapping 10-year periods shared by these two time series. By splitting each time series into multiple "time-windows" with common starting and ending dates, the IGMETS analysis looked at patterns of change over time (trends) at a variety of shared time-intervals (e.g. 5 years, 10 years, 30 years).

O'Brien *et al.* (2012) used a similar approach to look at 10-year and 30-year trends in major North Atlantic phytoplankton taxonomic groups. IGMETS expanded upon this approach to include 5-, 10-, 15-, 20-, 25-, and 30-year time-windows. For this study, an analysis ending date of December 2012 was selected to allow the time-series researchers sufficient time to process complex biological samples (e.g. complete microscope identification and enumeration of plankton samples) and to conduct any necessary quality control on their data. The IGMETS time-windows were then calculated by counting backwards from 2012 (Table 2.1).

Table 2.1 summarizes the year span and minimum number-of-years-present requirements for the six IGMETS time-windows used in this report. Using this criteria, a time series with data for 2007–2012 would be eligible for the 5-year (TW05) time-window, but none of the longer windows. A time series encompassing 1981–2012, with no missing years, would be eligible for all six time-windows.

To ensure that a minimum number of years of data were available for statistical-trend calculations within each time-window, it was required that 80% of the years within the time-window must have data present to qualify for that window. For example, a time series with ten years of data from 2001 to 2010 could qualify for the 10-year (TW10) time-window, but would not qualify for the 5-year time-window as it only had data for three of the required four TW05 years (e.g. 2008, 2009, and 2010 are present, but 2011 and 2012 are both missing). In this example, if data for 2011 or 2012 could also be added, the time series would then qualify for the 5-year (TW05) window. Adding values for both 2011 and 2012 together would also allow this time series to participate in the 15-year time-window, as it would now have the 12 years minimum required by TW15. Under this criterium, a "60-year" time series from 1950 to 2010, but missing data every other year, would fail to qualify for any of the IGMETS time-windows.

2.3.3 Calculation of spatio-temporal trend fields

Within some oceanic regions, participating time series were sparse or simply did not exist (e.g. upper Indian Ocean and South Atlantic, central South Pacific). Even within data-rich regions like the North Atlantic, the available sites still often had vast areas with no information (Figure 2.2). While IGMETS is focused on *in situ*, ship-based measurements, satellite data were used to create globally covered, spatially complete fields that could shed light on the general physical (e.g. sea surface temperature) and biological (e.g. surface chlorophyll) changes that occurred during the different IGMETS time-windows.

The IGMETS spatio-temporal analysis used temperature data from the NOAA Optimum Interpolation Sea Surface Temperature dataset (OISST version 2.0, https://www.ncdc.noaa.gov/oisst) and chlorophyll data from the ESA Ocean Colour CCI dataset (OC-CCI version 2.0, http://www.esa-oceancolour-cci.org/). Both datasets were acquired in a prepared-product form, downloaded as a regular global grid of monthly mean values by year. By using these preprepared products, the typical concerns and issues with satellite data (e.g. instrument intercalibration, handling of clouds, aerosols, and ice) were already expertly accounted for and documented by the OISST and OC-CCI product teams.

For both datasets, the global datafields were calculated into 0.5° × 0.5° latitude–longitude grids of mean monthly values by year. This process created a global coverage set of nearly 160 000 individual time series, which were then run through the standard IGMETS analysis to calculate trends for each 0.5° box and IGMETS time-window. The OISST, with temperature data from 1982 to present, qualified for all six IGMETS time-windows (TW05–TW30), while the OC-CCI, with chlorophyll data for 1998–2013, only qualified for the 15-year and shorter time-windows (TW05–TW15). The spatio-temporal trends obtained from these datasets were used to create the visual background fields (Section 2.4.4) and to calculate the spatial frequency tables (Section 2.4.5) used in the report.

Table 2.2. Summary of correlation strengths based on Pearson correlation coefficient (*r*) values, modified from Hinkle *et al.* (2003).

Pearson correlation coefficient (*r*)	Interpretation
–1.00 to –0.70 (< –0.70)	High/strong negative correlation
–0.70 to –0.50 (< –0.50)	Moderate negative correlation
–0.50 to –0.30 (< –0.30)	Low/weak negative correlation
–0.30 to –0.15 (< –0.15)	Negligible negative correlation
–0.15 to 0.15	not plotted
0.15 to 0.30 (> 0.15)	Negligible positive correlation
0.30 to 0.50 (> 0.30)	Low/weak positive correlation
0.50 to 0.70 (> 0.50)	Moderate positive correlation
0.70 to 1.00 (> 0 .70)	High/strong positive correlation

2.3.4 Correlations with SST and chlorophyll

To detect relationships between *in situ* variables and surface seawater temperatures or chlorophyll concentrations, the Pearson product-moment correlation coefficient was calculated for each *in situ* variable against its geographically-corresponding, 0.5° × 0.5° satellite-based SST and chlorophyll time series (as discussed in Section 2.3.3). Satellite data were used, instead of at-site *in situ* data, in an attempt to create a globally uniform correlation base variable (e.g. not all of the sites had *in situ* chlorophyll data, and some did not have even *in situ* temperature data).

The Pearson product-moment correlation is a measure of the strength of a linear association between two variables calculated by trying to draw a best-fit line through these two variables (Hinkle *et al*., 2002). The Pearson correlation coefficient *r* indicates how far away these data points are from that best-fit line. This *r* value indicates the strength of the correlation. Unlike a linear regression, the Pearson product-moment correlation does not declare either variable as dependent or independent and treats all variables equally. Similar to the spatio-temporal trend fields (Section 2.3.4), spatio-temporal correlation fields were run for each of the 0.5° × 0.5° time-series boxes. Table 2.2 provides interpretations for nine, range-based *r* value groupings of the Pearson correlation coefficient.

2.4 Visualization of trends

With results from over 340 time series and thousands of variables spanning multiple time-windows, one major challenge IGMETS faced was presenting the results in a way that quickly discerned spatio-temporal trends and patterns within and among variables and regions. This was done by mapping colour-coded symbols that represented *in situ* trends (Section 2.4.1) and correlations (Section 2.4.2), creating graphical summary tables (Section 2.4.3), adding colour-coded backgrounds of spatially complete satellite trends (Section 2.4.4), and summarizing basin-wide statistics of the background field data in a table format (Section 4.5). With thousands of possible variables and time-window configurations, this printed report still only illustrates a small subset of the many different ways to explore the available datasets. For those results not found in this report, the IGMETS Explorer (Section 2.5) provides an online interface that allows the user to view the full set and variety of all combinations and analyses generated by this first IGMETS analysis.

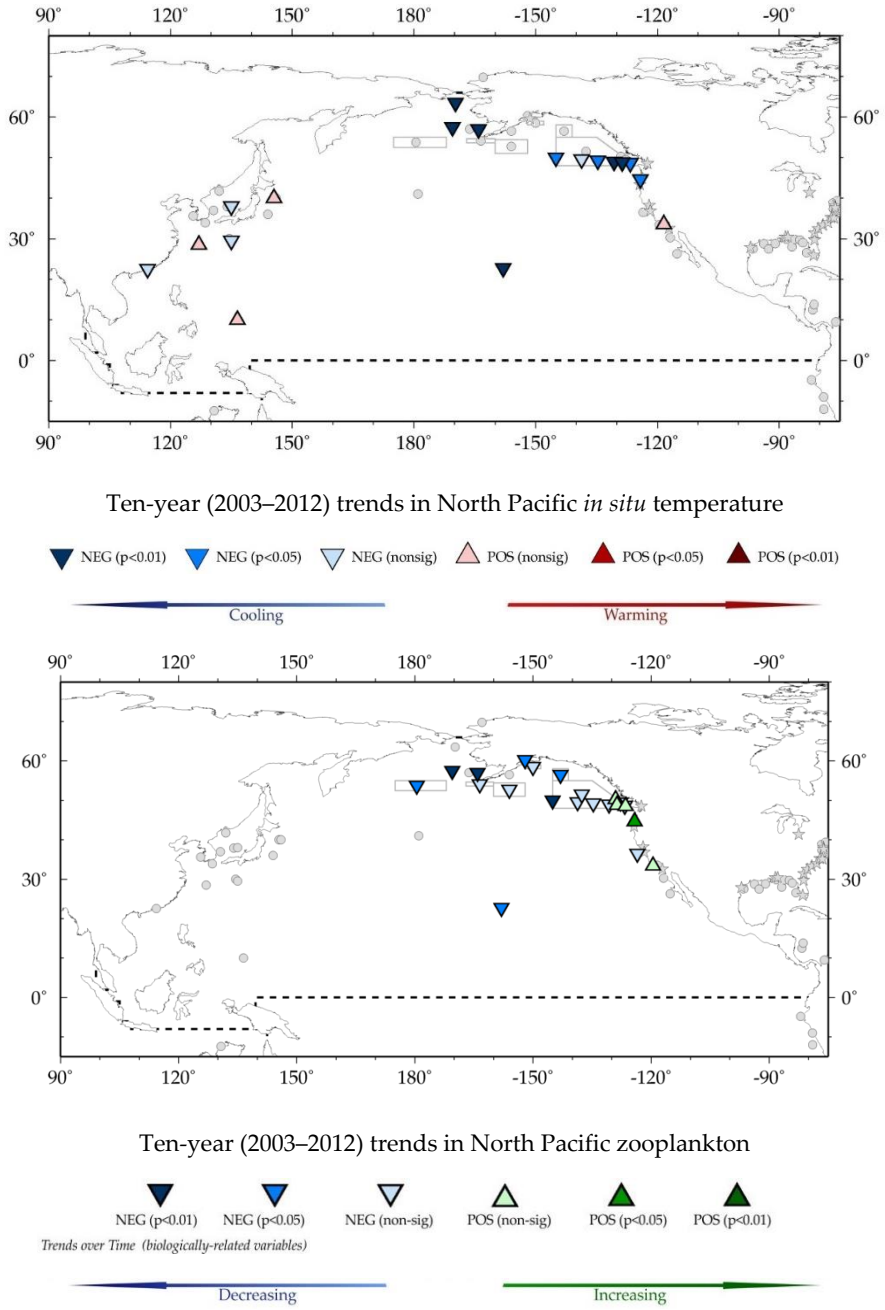

Figure 2.5. Examples of *in situ* trend maps displaying 10-year (TW10) trends in temperature (upper panel) and zooplankton (lower panel) in the IGMETS North Pacific region. Gray circles indicate time series locations in which data were not available or of insufficient years (Section 2.3.2).

2.4.1 *In situ* trend maps

For each *in situ* variable, time-window, and geographic region, IGMETS used colour-coded symbols (triangles) to map both variable trend state and the location of time-series sites (e.g. Figure 2.5). The upward- or downward-pointing orientation of the triangle, along with its base colour (i.e. red, green, or blue) indicates its trend direction. Non-biological variables (e.g. temperature, salinity, nutrients) are illustrated in red for positive/increasing trends and blue for negative/decreasing trends (Figure 2.5, upper panel). Symbols showing the trends in biological variables (e.g. chlorophyll, phytoplankton, zooplankton) are green (if positive) and blue (if negative) (Figure 2.5, lower panel). The shading of the triangle colour indicates the statistical significance of that trend, with the darkest colours representing the strongest trend ($p < 0.01$) and the lightest colour indicating a non-significant trend.

Within a given IGMETS trend map, if a time series did not have the variable being plotted or if its data did not qualify for the current time-window, a gray circle (or star, in the case of an "estuarine" site) was used to indicate the location of the time series. For example, in Figure 2.5, the gray circles mark time-series sites without the displayed variable and/or sites that did not qualify for the TW10 time-window. These gray symbols were also used to indicate time series that were discussed in a different IGMETS regional chapter (e.g. South Pacific, Arctic Ocean, or North Atlantic).

2.4.2 *In situ* correlation maps

Similar to the approach used with the *in situ* trend maps, correlation maps between *in situ* variables and satellite SST or chlorophyll fields were also created (Figure 2.6). Slightly different from the *in situ* trend maps, the up or down orientation of the triangle, along with its base colour (i.e. red, green, or blue) indicate its correlation direction and strength. Correlations against satellite SST use the red/blue symbol colour set (Figure 2.6, upper panel)

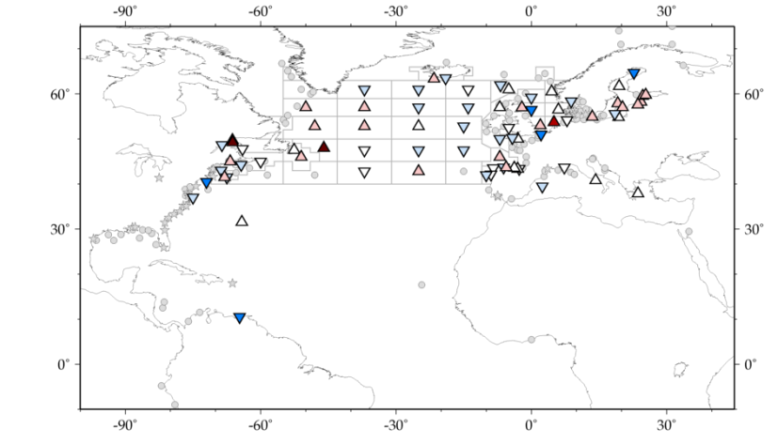

Ten-year (2003–2012) trends in North Atlantic *in situ* temperature

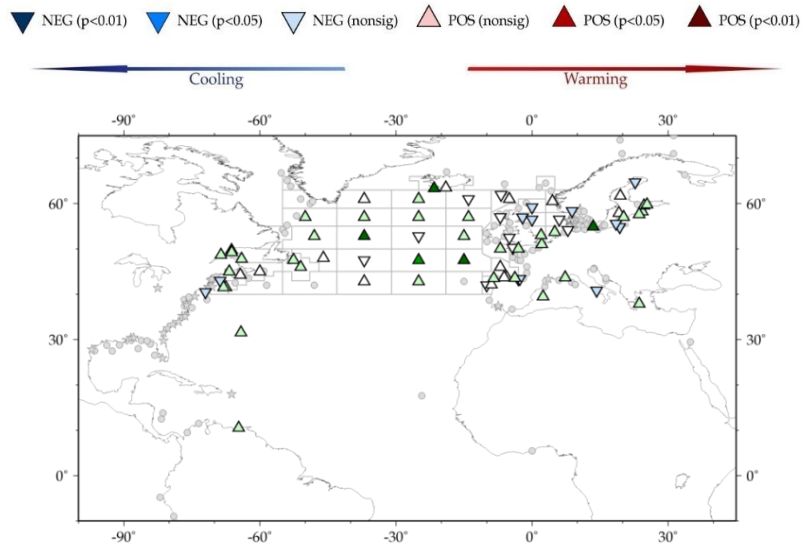

Ten-year (2003–2012) trends in North Atlantic zooplankton

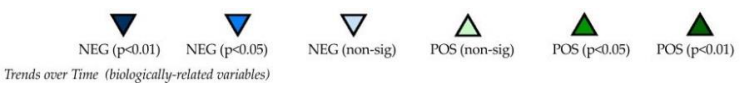

Figure 2.6. Examples of *in situ* correlation maps displaying 10-year (TW10) correlations between zooplankton and satellite SST (upper panel) and satellite chlorophyll (lower panel). Gray circles indicate time series locations in which data were not available or of insufficient years (Section 2.3.2).

and correlations against satellite chlorophyll use the symbol green/blue colour set (Figure 2.6, lower panel). As with the *in situ* trend maps, gray circles and stars indicated non-time-window-qualifying and/or out-of-region time series.

2.4.3 BODE plots

The brief overviews of dynamic ecosystems (BODE) plot is a visualization showing the relative amounts of positive and negative trends (or correlations) within a given time-window and across a set of select *in situ* variables. The upper map in Figure 2.5 has 18 symbols indicating 10-year trends in *in situ* temperature, of which 4 were positive (red) and 14 were negative (blue). The lower map in Figure 2.5 has 22 symbols indicating 10-year trends in zooplankton, of which 5 were positive (green) and 17 were negative (blue). This numerical information, along with that from seven other additional *in situ* variables, is represented in the single BODE plot shown in Figure 2.7a. The left side of the BODE plot shows the number of time-series sites having each respective trend (e.g. 4 positive and 14 negative temperature trends). The right side of the BODE plot shows the same information calculated as a percentage of all sites present with that variable [e.g. 78% (14 of 18) of the sites with temperature data had a negative trend]. A dashed gray line marks the 50% proportion level on both the positive and negative *y*-axis. A coloured star above the figure's upper gray line indicates that the proportion of positive vs. negative trends was statistically different ($p < 0.05$, two-tailed Z test for difference between proportions). In Figure 2.7a, the proportions of positive to negative trends in temperature (Temp), zooplankton (Zoop), and the ratio of diatoms to dinoflagellates (Ratio) were significantly different. The BODE plot can also be used with correlation data. Correlations of *in situ* variables with sea surface temperature, as seen in Figure 2.6 (upper panel), are represented in Figure 2.7b. Correlations of *in situ* variables with satellite chlorophyll, as seen in Figure 2.6c, are represented in Figure 2.7c. The three BODE plot types can be quickly distinguish by their colour sets: trend (red/blue), correlations with SST (red-only), correlations with satellite chlorophyll (green-only).

a) BODE plot of 10-year *in situ* variable trends in the **North Pacific**

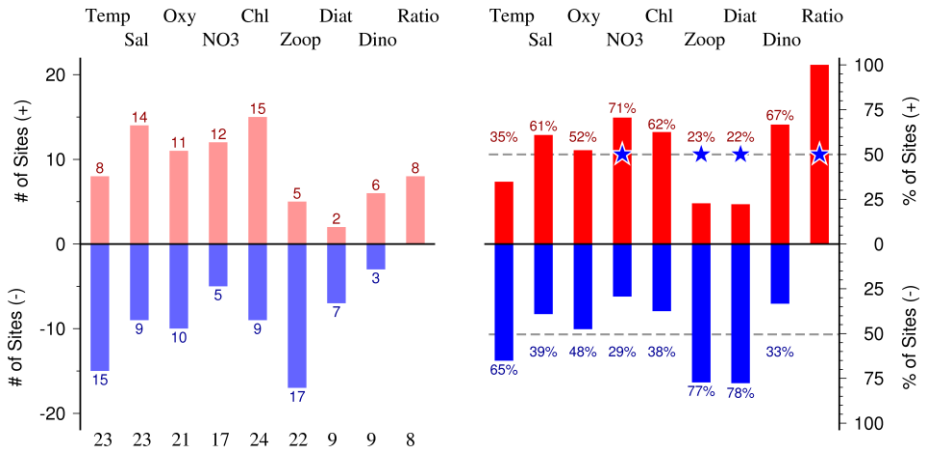

b) BODE plot of 10-year correlations with SST in the North Atlantic

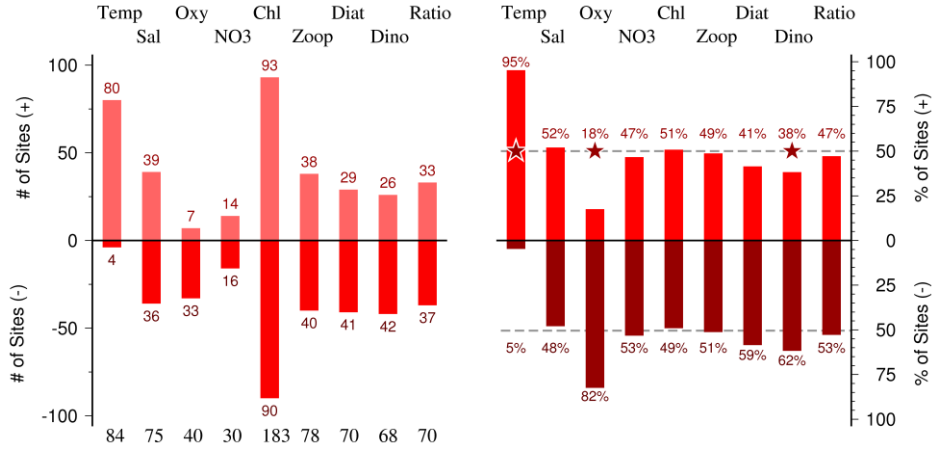

c) BODE plot of 10-year correlations with chlorophyll in the North Atlantic

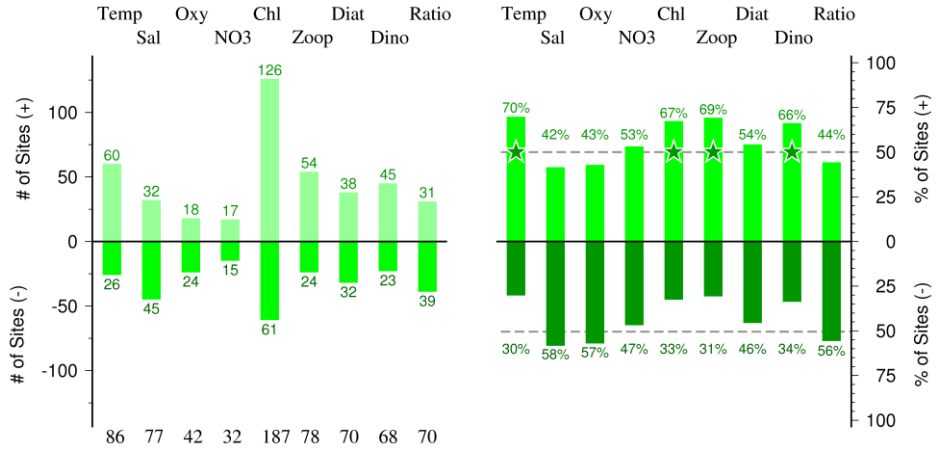

Figure 2.7. Brief overviews of dynamic ecosystems (BODE) plots illustrating *in situ* data (10-year window) (a) trends over time in the North Pacific (*see also* Figure 2.5), (b) correlations with satellite SST in the North Atlantic (*see also* Figure 2.6), and (c) correlations with satellite chlorophyll in the North Atlantic (*see also* Figure 2.6). See Section 2.4.3 for an explanation of the methodology and visualization. Column headings (*In situ* variables): Temp-temperature, Sal-salinity, Oxy-dissolved oxygen, NO3-nitrate, Chl-chlorophyll, Zoop-total zooplankton or copepods, Diat-total diatoms, Dino-total dinoflagellates, Ratio-ratio of diatoms to dinoflagellates.

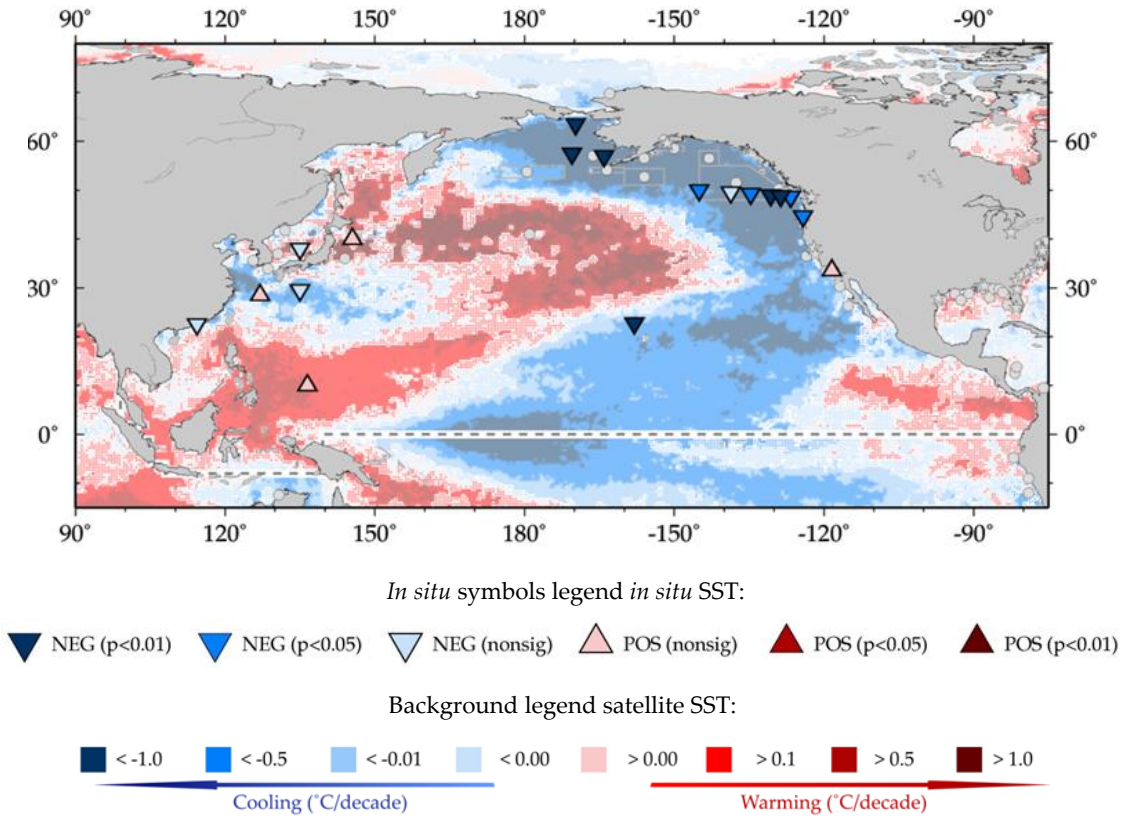

Figure 2.8. Enhanced version of Figure 2.4 (symbols indicating 10-year trends of *in situ* temperature, see also Section 2.4.1) with a background of 10-year trends in sea surface temperature trends calculated from the OISST global SST product (Sections 2.3.3 and 2.4.4). Note that the colours of the *in situ* symbols indicate trend direction and statistical strength, while the colours of the background OISST field represent the direction and rate of change (e.g. °C decade^{-1}).

2.4.4 Spatio-temporal trend backgrounds

While *in situ* time-series data were not available for all the world's ocean, satellite-based data were used to create a global grid of time series to describe the general physical (e.g. satellite sea surface temperature) and biological (e.g. satellite ocean colour chlorophyll) environments that surround and influence the *in situ* time series in the IGMETS study.

As mentioned in Section 2.3.3., the satellite variables were divided in 0.5° latitude–longitude grid boxes and run through the same time-series analysis used for the *in situ* data. Unlike the *in situ* data, these satellite data also share a common method and units, which allows these data to be compared both qualitatively (e.g. is the variable increasing or decreasing) and quantitatively (e.g. at what rate is the variable increasing or decreasing over time). The slope of the SMK trend (Section 2.3.1.1) captures this numerical rate of change, initially °C year^{-1} for temperature and mg m^{-3} year^{-1} for chlorophyll. IGMETS recalculated these rates into units of change per decade and then plotted them as a background trend field using a similar colour scheme to that used for the *in situ* time series (Figure 2.8).

By plotting and comparing different *in situ* variables together with these background trend fields, it is possible to spatially examine how the *in situ* variables generally correspond to changes in the larger spatial area environments surrounding them. For example, were zooplankton in warming ocean areas (e.g. Figure 2.9, upper panel – red background areas) responding differently than those in cooling areas (e.g. Figure 2.9, upper panel –blue background areas)? If a temperature relationship was not clear, were the zooplankton responding instead to increasing or decreasing phytoplankton biomass, as estimated using OC-CCI satellite chlorophyll and plotting it as the background field (e.g. Figure 2.9, lower panel)?

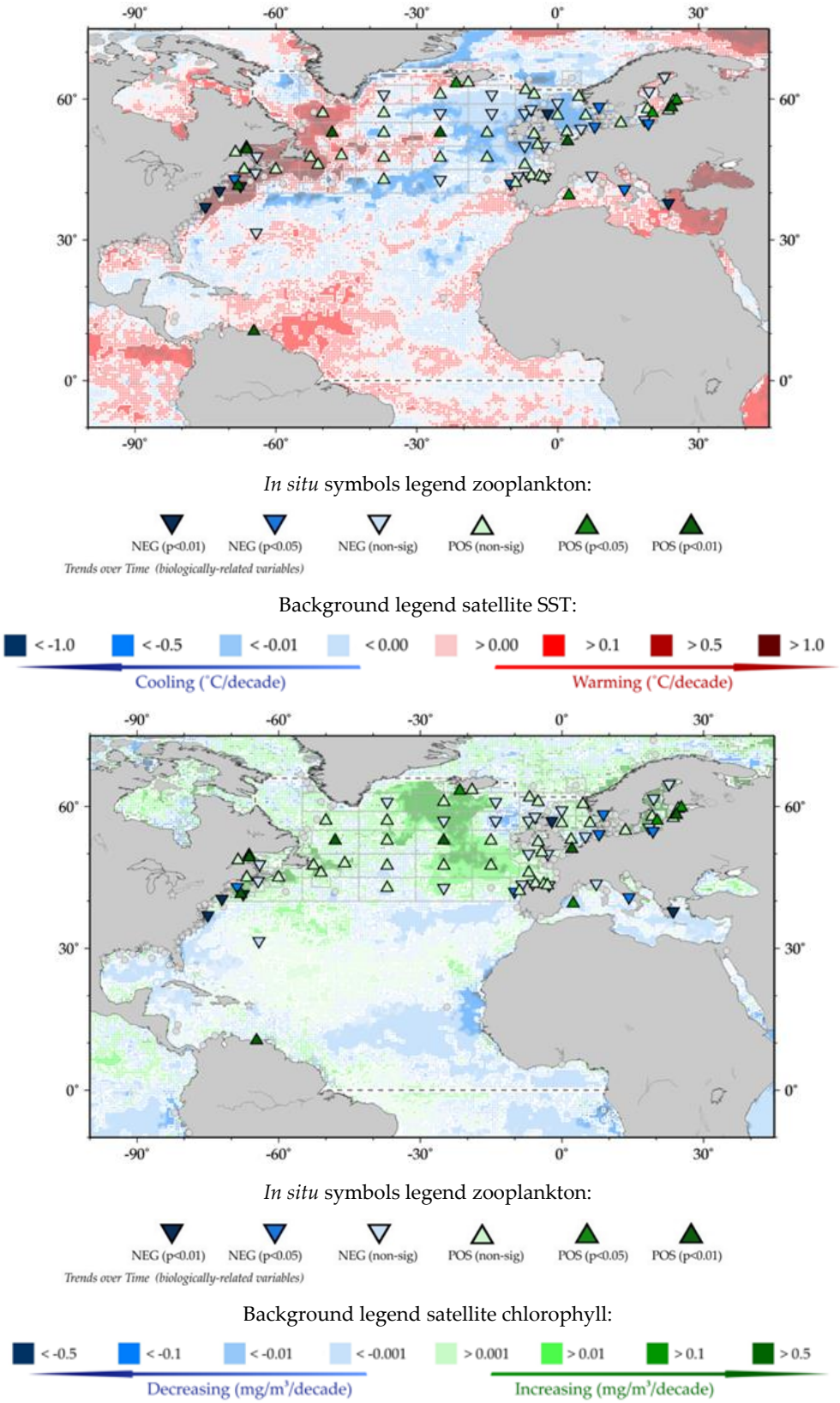

Figure 2.9. Illustrative examples of how spatio-temporal trend fields can be used to look at *in situ* data (zooplankton) in relation to their physical (SST, top) and biological (chlorophyll, bottom) environment.

2.4.5 Spatial frequency tables

Visually, the spatial areas of red- and blue-coloured SST trends (or of green- and blue-coloured chlorophyll trends) within the plotted spatio-temporal trend backgrounds (Section 2.4.4) differ across time-windows both within regions and between regions. For example, in the North Atlantic, the 10-year SST trends visually seem to have roughly equal areas of increasing (red) and decreasing (blue) trend areas (Figure 2.10, left), but this changes to almost entirely increasing (red) trends in the 30-year plot (Figure 2.10, right). To quantify the actual oceanic surface area of these trends, the areas of the various trend categories were calculated by summing the latitude-adjusted surface areas of each 0.5° latitude–longitude satellite data grid falling within that region (e.g. the IGMETS North Atlantic region). These spatial totals were then divided by the total area of that region to give the relative amount (percentage) of area having each trend direction or trend rate category. These subtotals were then recorded in table form, representing each region and the time-windows available for that background variable (Table 2.3).

Within the spatial-frequency table (Table 2.3), the upper table section summarizes the relative spatial areas of the total increasing or decreasing trends, without dividing these trends into any rate-based subcategories. For example, in the North Atlantic (Table 2.3, column 3), 50.3% of the 10-year SST trends were increasing, while 49.7% were decreasing. In contrast, 95.7% of the 20-year SST trends were increasing (Table 2.3, column 5). The lower number in parenthesis in the spatial-frequency table indicates the spatial area of statistically significant ($p < 0.05$) trends. Only 14.6% of the increasing 10-year SST trends were $p < 0.05$, while 95.0% of the increasing 30-years were $p < 0.05$. This noticeable difference in statistical significance is an artefact caused by the smaller number of measurements (n) available in the shorter time-windows. (See Section 2.3.1.2 for a discussion on how time-window length, strength of trend, and variable type affect statistical significance calculations.)

The lower section of the spatial-frequency table divides the trends into the same rate and colour categories as used in the spatial-trends background figures (Figure 2.10). For example, 9.2% of the 20-year SST trends fell in the 0.5–1.0°C decade^{-1} warming category. Of these, all of the trends were statistically significant ($p < 0.05$).

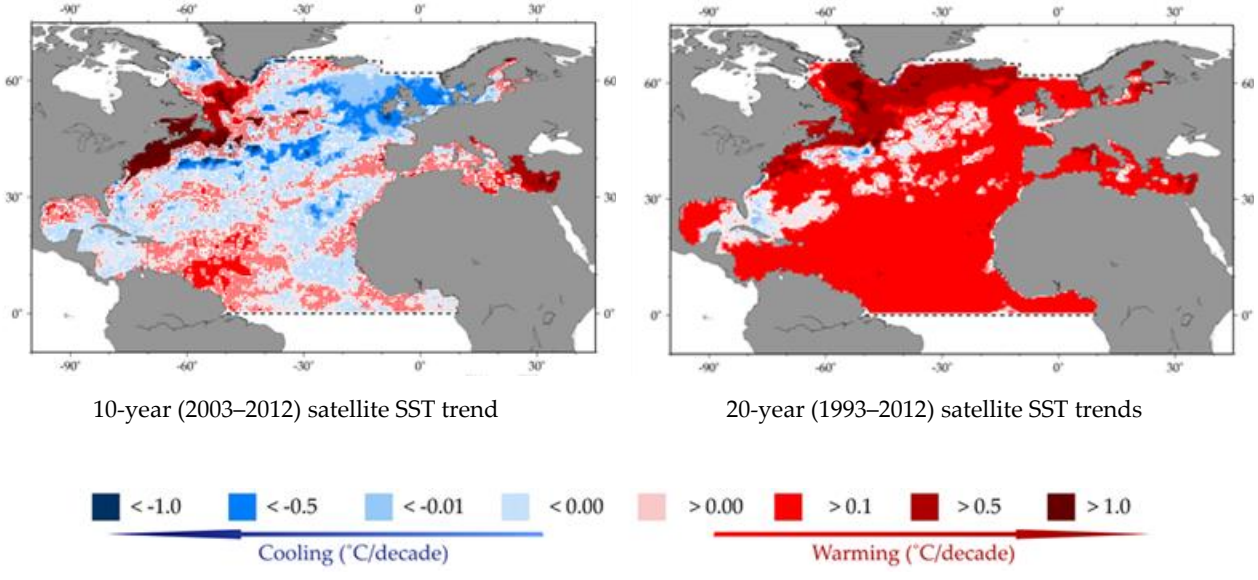

Figure 2.10. Sea surface temperature (SST) trends within the IGMETS-defined North Atlantic region for the 10-year time-window (left panel) and 20-year time-window (right panel) (Table 2.3).

Table 2.3. Spatial-frequency table showing sea surface temperature (SST) trends within the IGMETS-defined North Atlantic region. Percentage values represent the fraction of trends within the entire North Atlantic that fall within that category. Percentages in parenthesis indicate the fraction of trends (within the entire North Atlantic) with a $p < 0.05$ significance level. (See Section 2.3.1.2 for discussion on significance levels, trends, and time-windows).

Latitude-adjusted SST data field surface area = 46.1 million km²	**5-year** (2008–2012)	**10-year** (2003–2012)	**15-year** (1998–2012)	**20-year** (1993–2012)	**25-year** (1988–2012)	**30-year** (1983–2012)
Area (%) w/ increasing SST trends ($p < 0.05$)	**52.5%** (*13.3%*)	**50.3%** (*14.6%*)	**76.8%** (*54.8%*)	**95.7%** (*87.4%*)	**98.1%** (*95.0%*)	**99.1%** (*97.3%*)
Area (%) w/ decreasing SST trends ($p < 0.05$)	47.5% (*18.6%*)	49.7% (*15.5%*)	23.2% (*7.1%*)	4.3% (*1.1%*)	1.9% (*0.6%*)	0.9% (*0.3%*)
> 1.0°C decade^{-1} warming ($p < 0.05$)	13.5% (*8.1%*)	3.4% (*3.3%*)	0.9% (*0.9%*)	0.7% (*0.7%*)	0.1% (*0.1%*)	0.0% (*0.0%*)
0.5 to 1.0°C decade^{-1} warming ($p < 0.05$)	18.0% (*4.6%*)	5.0% (*4.1%*)	5.4% (*5.4%*)	10.0% (*10.0%*)	9.2% (*9.2%*)	6.7% (*6.7%*)
0.1 to 0.5°C decade^{-1} warming ($p < 0.05$)	17.0% (*0.6%*)	27.3% (*7.1%*)	**56.3%** (*47.4%*)	**77.1%** (*74.3%*)	**83.3%** (*82.5%*)	**86.7%** (*86.4%*)
0.0 to 0.1°C decade^{-1} warming ($p < 0.05$)	4.1% (*0.0%*)	14.6% (*0.2%*)	14.2% (*1.2%*)	8.0% (*2.4%*)	5.4% (*3.2%*)	5.6% (*4.2%*)
0.0 to –0.1°C decade^{-1} cooling ($p < 0.05$)	3.9% (*0.0%*)	13.1% (*0.1%*)	10.0% (*0.2%*)	2.6% (*0.1%*)	1.3% (*0.1%*)	0.7% (*0.1%*)
–0.1 to –0.5°C decade^{-1} cooling ($p < 0.05$)	13.3% (*0.7%*)	29.2% (*8.7%*)	12.4% (*6.1%*)	1.4% (*0.8%*)	0.6% (*0.4%*)	0.2% (*0.1%*)
–0.5 to –1.0°C decade^{-1} cooling ($p < 0.05$)	15.7% (*6.6%*)	6.7% (*6.1%*)	0.7% (*0.6%*)	0.2% (*0.2%*)	0.1% (*0.1%*)	0.0% (*0.0%*)
> –1.0°C decade^{-1} cooling ($p < 0.05$)	14.6% (*11.3%*)	0.6% (*0.6%*)	0.2% (*0.2%*)	0.0% (*0.0%*)	0.0% (*0.0%*)	0.0% (*0.0%*)

2.5 The IGMETS time series Explorer

This initial IGMETS analysis and summary report featured seven geographic regions and one global overview, six time-windows, 18 *in situ* variables, and three background fields, generating a set of over 2500 possible image combinations (i.e. 8 × 6 × 18 × 3 = 2592). This number easily reaches 100 000 after including possibilities to select correlations vs. trends, to plot data subsets based on statistical significance level, or to focus on estuarine vs. open-ocean sites. While only a small number of these figures could be included in this report, the full figure set and interactive options are available in the IGMETS Explorer (http://igmets.net/explorer) (Figure 2.11).

The Explorer is an online companion to the IGMETS report, providing interactive (point and click) access and expansion to the figures and tables shown throughout the report. It further provides information on the participating time series found in each of the report chapters and the Annex. As IGMETS work continues, new data and sites will be added to the Explorer and to the IGMETS Metabase (http://igmets.net/metabase).

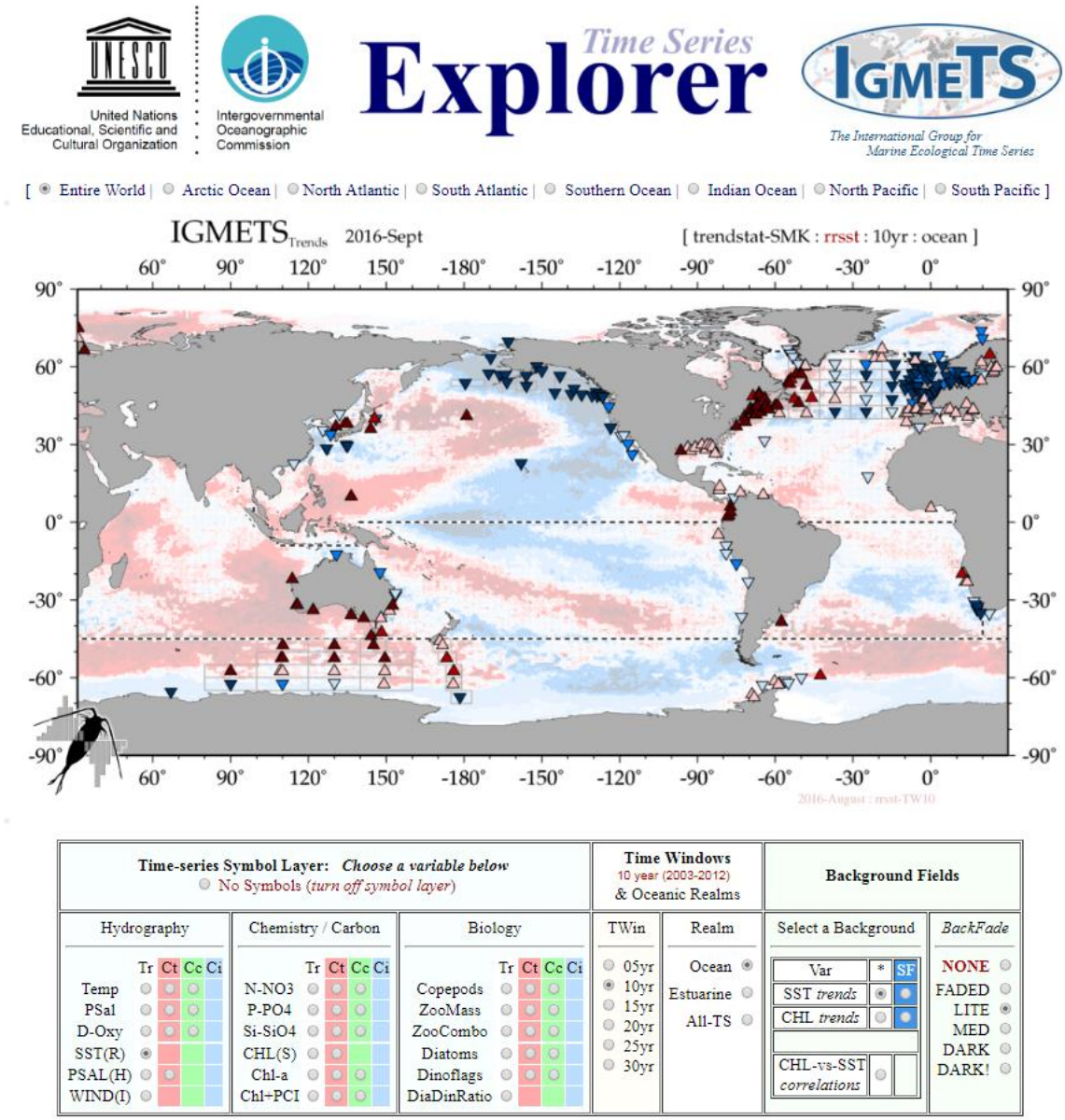

Figure 2.11. An example screenshot from the IGMETS time series Explorer available online at http://Igmets.net/explorer.

2.6 References

Gilbert, R. O. 1987. Statistical Methods for Environmental Pollution Monitoring. John Wiley & Sons, NY. 320 pp.

Hinkle, D. E., Wiersma, W., and Jurs, S. G. 2002. Applied Statistics for the Behavioral Sciences, 5th edn. Houghton Mifflin, Boston. 756 pp.

Hirsch, R. M., Slack, J. R., and Smith, R. A. 1982. Techniques of trend analysis for monthly water quality data, Water Resources Research, 18(1): 107–121.

Kendall, M. G. 1975. Rank Correlation Methods, 4th edn. Charles Griffin, London. 272 pp.

Mackas, D. L., Pepin, P., and Verheye, H. 2012. Interannual variability of marine zooplankton and their environments: Within- and between-region comparisons. Progress in Oceanography, 97–100: 1–14.

Mackas, D. L., Thomson, R. E., and Galbraith, M. 2001. Changes in the zooplankton community of the British Columbia continental margin, 1985–1999, and their covariation with oceanographic conditions. Canadian Journal of Fisheries and Aquatic Sciences, 58: 685–702.

Mann, H. B. 1945. Non-parametric tests against trend, Econometrica, 13: 163–171.

O'Brien, T. D., Li, W. K. W., and Morán, X. A. G. (Eds). 2012. ICES Phytoplankton and Microbial Plankton Status Report 2009/2010. ICES Cooperative Research Report No. 313. 196 pp.

O'Brien, T. D., Wiebe, P. H., and Falkenhaug, T. (Eds). 2013. ICES Zooplankton Status Report 2010/2011. ICES Cooperative Research Report No. 318. 208 pp.

Paerl, H. W., Yin, K., and O'Brien, T. D. 2015. SCOR Working Group 137: Global Patterns of Phytoplankton Dynamics in Coastal Ecosystems'': An introduction to the special issue of Estuarine, Coastal and Shelf Science. Estuarine, Coastal and Shelf Science, 162: 1–3.

3 Arctic Ocean

Nicholas R. Bates, Todd D. O'Brien, and Laura Lorenzoni

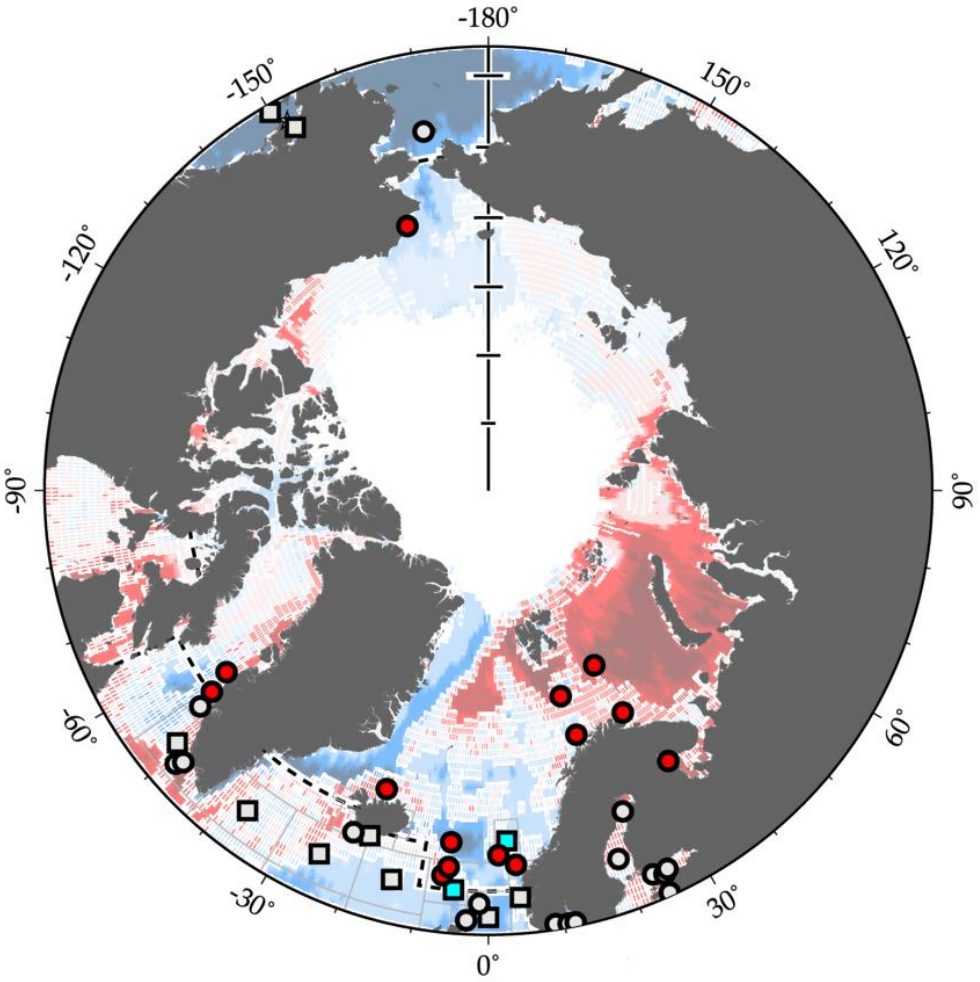

Figure 3.1. Map of IGMETS-participating Arctic Ocean time series on a background of 10-year time-window (2003–2012) sea surface temperature trends (see also Figure 3.3). At the time of this report, the Arctic Ocean collection consisted of 16 time series (coloured symbols of any type), of which two were from Continuous Plankton Recorder subareas (blue boxes). Un-coloured (gray) symbols indicate time series being addressed in a different regional chapter (e.g. North Atlantic, North Pacific). Dashed lines indicate boundaries between IGMETS regions. See Table 3.3 for a listing of this region's participating sites. Additional information on the sites in this study is presented in the Annex.

Participating time-series investigators

Alexey Babkov, Cecilie Broms, Claudia Castellani, Padmini Dalpadado, Martin Edwards, Lisa Eisner, Ed Farley, Eilif Gaard, Astthor Gislason, Hafsteinn Gudfinnsson, Kristinn Gudmundsson, Solva Jacobsen, Inna Kutcheva, Priscilla Licandro, Daria Martynova, Webjørn Melle, Jeffrey Napp, S.A. Pedersen, Igor Primakov, Regina Prygunkova, Rowena Stern, and Nikolay Usov

This chapter should be cited as: Bates, N. R., O'Brien, T. D., and Lorenzoni, L. 2017. Arctic Ocean. *In* What are Marine Ecological Time Series telling us about the ocean? A status report, pp. 37–53. Ed. by T. D. O'Brien, L. Lorenzoni, K. Isensee, and L. Valdés. IOC-UNESCO, IOC Technical Series, No. 129. 297 pp.

3.1 Introduction

The Arctic Ocean has experienced rapid and complex environmental changes over the last few decades in response to changes in climate and physical forcing that influence Arctic atmospheric properties, air–cryosphere–ocean interaction and exchanges, and terrestrial inputs. Atmospheric warming (Overland *et al*., 2014) and changes in the terrestrial hydrological cycle of the region, combined with physical circulation and gateway exchange of the Arctic have contributed to well-documented summertime sea ice loss (Serreze *et al*., 2000; Polyakov *et al*., 2002, 2012; Maslanik *et al*., 2007; Markus *et al*., 2009; Perovich *et al*., 2007, 2014; Stroeve *et al*., 2007, 2014; Perovich and Richter-Menge, 2009; Wang and Overland, 2009; Screen *et al*., 2013; Overland and Wang, 2013; Simmonds and Goverkar, 2014; Frey *et al*., 2014a,b, 2015). The rapid loss of sea ice is the most recognizable phenomena associated with the emerging "new Arctic" climate (Carmack *et al*., 2015).

These physical changes have resulted in changes in the biology and biogeochemistry of the shallow and deep areas of the Arctic Ocean (Grebmeier *et al*., 2010; Wassmann *et al*., 2011). Increased ice-free waters and warmer temperatures appear to have caused changes in rates of primary production in the deep Arctic (Pabi *et al*., 2008; Arrigo et al., 2008, 2012, 2014; Arrigo and van Dijken, 2011) and associated shelves (Ardyna *et al*., 2014). They have affected the seasonal timing of the annual phytoplankton bloom (Kahru *et al*., 2010), the

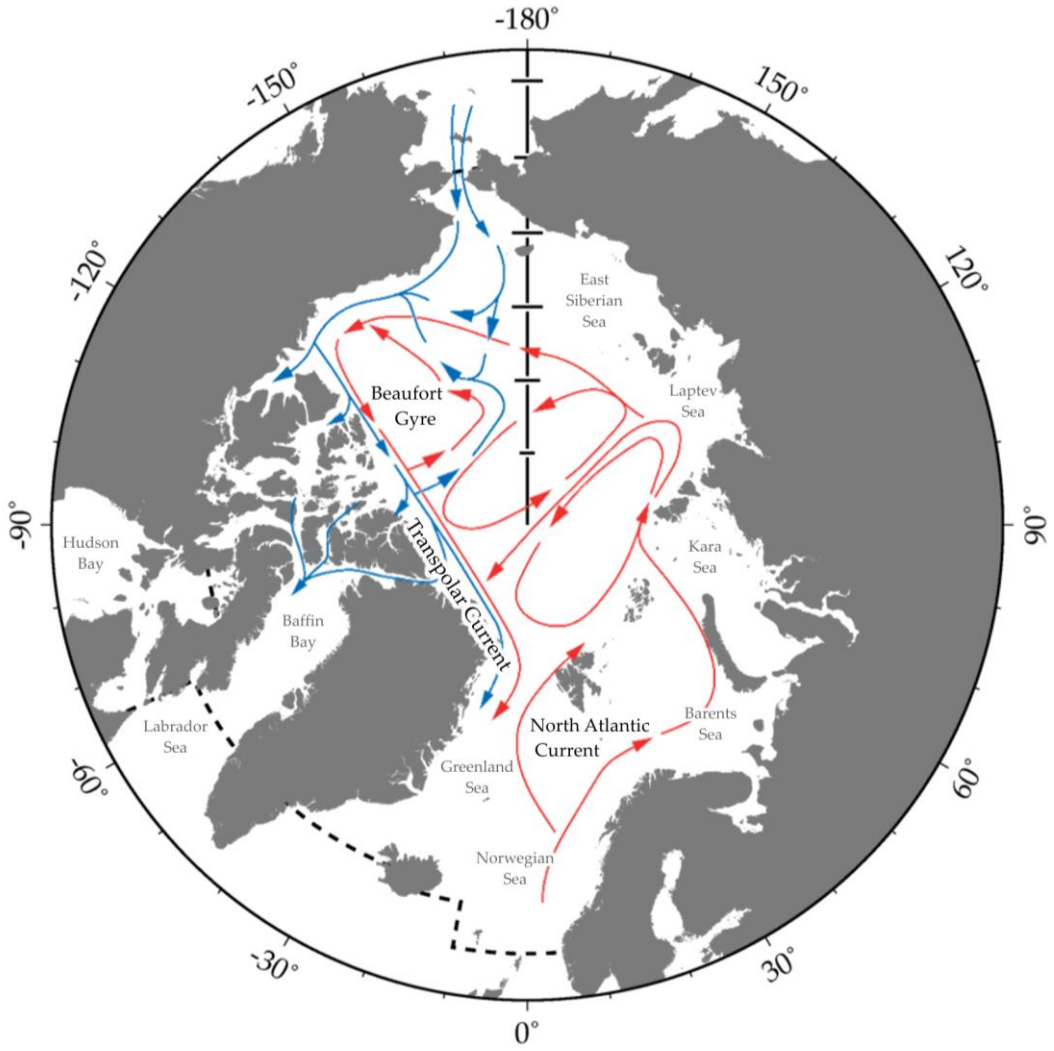

Figure 3.2. Schematic of major current systems, bays, and seas in the IGMETS-defined Arctic Ocean region. Red arrows indicate generally warmer water currents; blue arrows indicate generally cooler water currents. In this and subsequent figures, the Arctic Ocean region includes the Barents Sea, Siberian Shelf seas, Chukchi Sea, Beaufort Sea, Canadian Archipelago, and the central Arctic basins, but does not include the marginal seas (i.e. Greenland–Iceland–Norwegian Sea, Labrador Sea, Hudson Bay, Bering Sea). See "Methods" chapter for a complete description and methodology used.

composition of the phytoplankton (Li *et al*., 2009), and have shifted higher trophic-level pelagic and benthic communities (Grebmeier *et al*., 2015). The biogeochemical dynamics of carbon and nutrients have also been altered (McGuire *et al*., 2006; Macdonald *et al*., 2008), with an acceleration in the biological pump of carbon leading to enhanced export of carbon to the deep ocean (Lalande *et al*., 2009, 2014a; Nishino *et al*., 2011), and ultimately ocean carbon dioxide (CO_2) uptake and ocean acidification (OA) impacts in the region (Orr *et al*., 2005; Bates *et al*., 2006; Bates and Mathis, 2009; Steinacher *et al*., 2009; Takahashi *et al*., 2009; Manizza *et al*., 2013; Schuster *et al*., 2013; Bates, 2015). Loss of sea ice appears to be increasing momentum transfer to the ocean, increasing gateway inflows and outflows (Woodgate *et al*., 2015), and increasing circulation and mixing (Rippeth *et al*., 2014). This may have additional unknown implications for the biological communities and biogeochemical cycling of carbon and nutrients in the region.

The harsh polar climate and difficulties in sampling the Arctic Ocean have resulted in few sustained observations of ocean physics, biology, and biogeochemistry. As such, there remains much uncertainty about the present ocean function and understanding about the future response of the Arctic Ocean to rapid environmental change. However, the few existing time series that occupy Arctic waters have provided invaluable information that has enabled the understanding we now have of the dramatic changes the region has undergone (Figure 3.1).

3.2 Physical setting of the Arctic Ocean

The relatively small Arctic Ocean (ca. 10.7×10^6 km^2) is almost completely landlocked except for the gateways at the Bering Strait and Canadian Archipelago and the Fram Strait and Barents Sea that allow exchanges with the Pacific and Atlantic oceans, respectively (Figure 3.2). The Arctic Ocean is dominated by interocean exchanges between the Pacific and Atlantic oceans (Macdonald *et al*., 2008) and subsequent physical and biogeochemical modifications and transformations of water. This includes river inputs of freshwater and materials (McGuire *et al*., 2006; Cooper *et al*., 2008), sea ice production and melting (Peterson *et al*., 2002; Carmack and Chapman, 2003), and atmosphere–ocean interaction (Rigor *et al*., 2002; Overland and Wang, 2005; Wang *et al*., 2005) and exchanges, which combined, act to dictate water column stratification (Aagaard *et al*., 1981; Rudels *et al*., 1996) and circulation and residence time in the Arctic. The inputs to the Arctic in descending order include: Atlantic inflow through Fram Strait and via the Barents Sea of ca. 5–6 Sv (Sv = sverdrup = 10^6 m^3 s^{-1}); Pacific inflow (through Bering Strait) of ca. 1 Sv (Woodgate *et al*., 2005; 2015); and freshwater inputs of ca. 0.10–0.14 (Aagaard and Carmack, 1989; Wijffels *et al*., 1992; Fahrbach *et al*., 2001; Macdonald *et al*., 2008), with outflow through the Canadian Archipelago, across the Barents Sea, and through Fram Strait.

The relatively broad, generally shallow (< 200 m deep) continental shelves surrounding the central basin comprise about 53% of the area of the Arctic Ocean (Macdonald *et al*., 2008). Each of the Arctic continental shelves is unique and thus difficult to characterize generically. As a simplification, the Chukchi and Barents seas can be characterized as "inflow" shelves (Carmack and Wassmann, 2006), with inflow of warm, nutrient-rich waters from the Pacific and Atlantic, respectively (Müller-Karger *et al*., 1987; Nihoul *et al*., 1993; Hopcroft and Day, 2013; Cai *et al*., 2014; Grebmeier *et al*., 2015). The Siberian shelves (i.e. Kara, Laptev, and East Siberian Sea) and the Beaufort Sea (Mackenzie Shelf) constitute "interior shelves" and are highly influenced by exchanges with other shelves and freshwater inputs. The Canadian Archipelago represents an "outflow shelf" where Arctic water is exported via Hudson Bay and Baffin Bay to the Atlantic Ocean. In the deep central basin of the Arctic Ocean, waters of the Canada Basin or Beaufort Gyre are separated from the Eurasian Basin by the surface transpolar drift. Strong seasonal atmosphere–ocean interaction (e.g. changes in Arctic Dipole Anomaly; Ogi and Wallace, 2012; Overland *et al*., 2012), sea ice production and melting (e.g. associated with Arctic Sea Ice Oscillation; Frey *et al*., 2014a, 2015), lateral transports of water (Coachman, 1993; Danielson *et al*., 2014), and freshwater inputs dictate the physical setting of the Arctic and its biological and biogeochemical characteristics.

The geographic scope of this review encompasses the Arctic Ocean shelves (i.e. Barents, Kara, Laptev, East Siberian, Chukchi, Beaufort, and Canadian Archipelago seas) and central basin (i.e. Canada and Eurasian Basin), but does not extend past the gateways of the Arctic Ocean to the Greenland, Iceland, Norwegian, and Bering seas, and Hudson and Baffin bays.

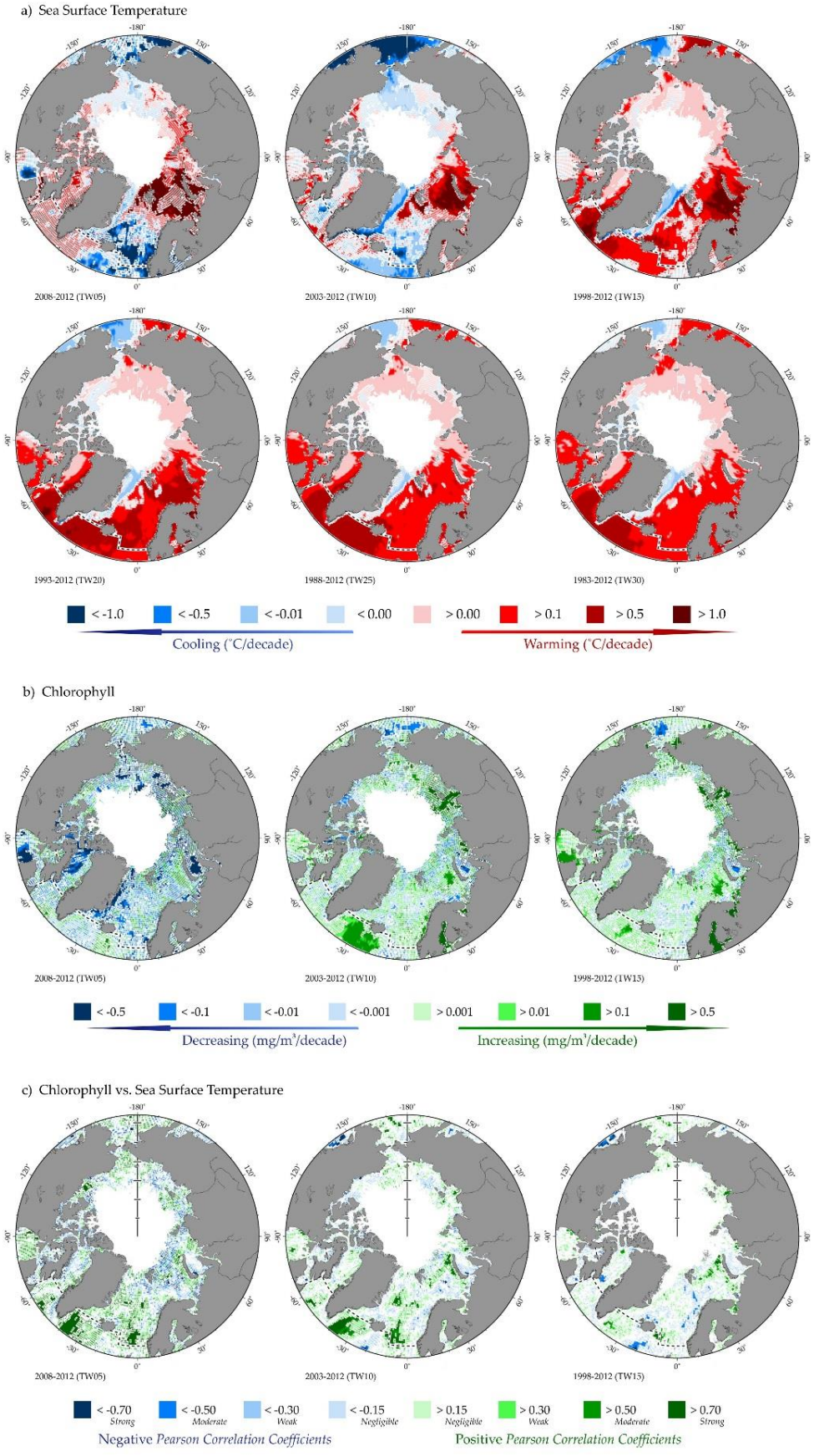

Figure 3.3. Annual trends in the Arctic Ocean region sea surface temperature and chlorophyll for each of the standard IGMETS time-windows. See "Methods" chapter for a complete description and methodology used.

3.3 Trends in the Arctic Ocean

3.3.1 Pan-Arctic Ocean sea ice and hydrological changes

The synergistic interactions among atmospheric warming, pressure changes associated with the Arctic Dipole Anomaly, air–sea interaction, and Arctic amplification (e.g. the drivers of pan-Arctic change; Holland and Bitz, 2003; IPCC, 2007, 2014; Serreze *et al*., 2007; Serreze and Stroeve, 2009; Stroeve *et al*., 2014) have brought about an Arctic-wide reduction in sea ice extent and thickness, especially during the last decade (Polyakov *et al*., 2012; Lindsay and Schweiger, 2015). The loss of multiyear ice and summer sea ice has been accompanied by earlier melt onset in spring and later freeze-up in autumn (Stroeve *et al*., 2012; Parkinson, 2014; Frey *et al*., 2015; Wood *et al*., 2015). Summer sea ice concentrations have declined in most Arctic marginal seas (Stroeve *et al*., 2014), particularly in areas where multiyear sea ice used to prevail. In the central Arctic, annual mean sea ice thickness has decreased by 65% from 3.59 to 1.25 m since 1975 (Lindsay and Schweiger, 2015). As noted by Wood *et al*. (2015), the primary regulation of the upper ocean environment has shifted from a once stable sea ice-dominated system (Kwok and Unstersteiner, 2011) toward a system more sensitive to variable meteorological forces, especially wind and waves, and to cloud-cover-mediated radiation (Kay *et al*., 2008; Perovich and Polashenski, 2012; Jeffries *et al*., 2013; Timmermans, 2015; Wang *et al*., 2015).

Analysis of sea surface temperature from available gridded satellite data indicates that over 85% (79% at $p < 0.05$) of the Arctic Ocean has warmed over the past 30 years (Table 3.1, Figure 3.2). This warming trend has been sustained in the Chukchi, Barents, and Kara seas, and in Baffin Bay and Davis Strait (Figure 3.3a). Of the limited number of sustained field observations in the Arctic, several time-series sites in the Barents Sea (i.e. Fugløya-Bjørnøya North, Fugløya-Bjørnøya South, Vardø-Nord North, and Vardø-Nord South) exhibit similar trends over the past 15–30 years. Across much of the central basins and several of the marginal seas of the Arctic, there are insufficient data to establish trends due primarily to cloud cover and sea ice extent. At the periphery of the Arctic Ocean, warming has been observed in the Greenland–Iceland–Norwegian (GIN) seas, whilst modest regional cooling has been observed in the Bering Strait and in the Fram Strait in the region of the outflow from the central Arctic Basin.

Over shorter time-scales, regional variability of the coupled atmosphere–ocean system does not show ubiquitous warming trends within the Arctic Ocean. In the Chukchi Sea, modest cooling is observed over the past ten years or so (Wood *et al*., 2015) (Figure 3.3a). However, this appears to relate to a shift in the Arctic Dipole (and its related wind field) in 2012 that allowed sea ice to persist in the Chukchi Sea longer during summer despite a record-low sea ice extent for the pan-Arctic. Fluctuations in regional wind fields also contribute to gateway flows through the Bering Strait (Coachman, 1993; Danielson *et al*., 2014) that, in turn, impact the upwelling and transport of nutrient-rich Pacific water into the Arctic (Coachman and Shigaev, 1992; Nihoul *et al*., 1993; Hopcroft and Day, 2013). In the Barents Sea, two out of the four longer-term time series show modest cooling. These examples illustrate the complex short-term and longer-term feedbacks operating in the Arctic Ocean.

The warming is also likely to have been accompanied by salinity changes, with a freshening of the polar mixed layer associated with increased sea ice melt and freshwater inputs. While significant freshening has been observed over the past 30 years in the periphery of the Arctic (e.g. Baltic Sea and near Iceland), lack of sustained observations precludes any summary of salinity changes in the Arctic Ocean itself. In the Barents Sea, four time-series sites (i.e. Fugløya-Bjørnøya North, Fugløya-Bjørnøya South, Vardø-Nord North, and Vardø-Nord South) show increased salinity over the past 15–30 years, presumably reflecting the influence of increased Atlantic water in the surface ocean (Table 3.1, Figure 3.4). This mixture of trends underscores the regional complexities in surface stratification, dictated by a balance of buoyancy input, freshwater inflow, and mixing processes (Tremblay and Gagnon, 2009; Carmack and McLaughlin, 2011; Popova *et al*., 2012).

3.3.2 Sea surface chlorophyll and primary production in the Arctic Ocean

Observations of chlorophyll biomass derived from MODIS and Sea-viewing Wide Field-of-view Sensor (SeaWiFS) in the Arctic Ocean during 1998–2012 are limited by the presence of clouds and sea ice cover in the region. During 1998–2010, cloudiness has increased,

Table 3.1. Relative spatial areas (% of the total region) and rates of change within the Arctic Ocean region that are showing increasing or decreasing trends in sea surface temperature (SST) for each of the standard IGMETS time-windows. Numbers in brackets indicate the % area with significant ($p < 0.05$) trends. See "Methods" chapter for a complete description and methodology used.

Latitude-adjusted SST data field surface area = 10.6 million km²	**5-year** (2008–2012)	**10-year** (2003–2012)	**15-year** (1998–2012)	**20-year** (1993–2012)	**25-year** (1988–2012)	**30-year** (1983–2012)
Area (%) w/ increasing SST trends ($p < 0.05$)	**59.9%** (*22.1%*)	46.0% (*26.6%*)	**83.0%** (*66.2%*)	**83.8%** (*74.3%*)	**86.5%** (*75.0%*)	**85.3%** (*79.2%*)
Area (%) w/ decreasing SST trends ($p < 0.05$)	40.1% (*13.6%*)	**54.0%** (*27.2%*)	17.0% (*7.7%*)	16.2% (*6.8%*)	13.5% (*5.5%*)	14.7% (*7.4%*)
> 1.0°C decade^{-1} warming ($p < 0.05$)	17.6% (*12.9%*)	5.4% (*5.4%*)	4.9% (*4.9%*)	0.8% (*0.8%*)	0.2% (*0.2%*)	0.1% (*0.1%*)
0.5 to 1.0°C decade^{-1} warming ($p < 0.05$)	9.3% (*3.9%*)	8.3% (*8.0%*)	9.8% (*9.8%*)	17.2% (*17.2%*)	4.4% (*4.4%*)	1.8% (*1.8%*)
0.1 to 0.5°C decade^{-1} warming ($p < 0.05$)	20.5% (*4.7%*)	15.7% (*8.9%*)	29.4% (*25.4%*)	24.9% (*24.3%*)	37.0% (*36.7%*)	38.6% (*38.5%*)
0.0 to 0.1°C decade^{-1} warming ($p < 0.05$)	12.7% (*0.5%*)	16.6% (*4.3%*)	39.0% (*26.2%*)	40.9% (*32.1%*)	44.9% (*33.6%*)	44.8% (*38.8%*)
0.0 to –0.1°C decade^{-1} cooling ($p < 0.05$)	15.6% (*1.8%*)	28.4% (*8.8%*)	11.0% (*2.6%*)	12.9% (*4.0%*)	11.8% (*4.0%*)	12.9% (*5.9%*)
–0.1 to –0.5°C decade^{-1} cooling ($p < 0.05$)	11.4% (*3.0%*)	19.7% (*12.8%*)	4.9% (*3.9%*)	3.3% (*2.7%*)	1.7% (*1.4%*)	1.7% (*1.4%*)
–0.5 to –1.0°C decade^{-1} cooling ($p < 0.05$)	6.7% (*3.4%*)	4.8% (*4.5%*)	1.1% (*1.1%*)	0.0% (*0.0%*)	0.0% (*0.0%*)	0.0% (*0.0%*)
> –1.0°C decade^{-1} cooling ($p < 0.05$)	6.3% (*5.4%*)	1.1% (*1.1%*)	0.1% (*0.1%*)	0.0% (*0.0%*)	0.0% (*0.0%*)	0.0% (*0.0%*)

Table 3.2. Relative spatial areas (% of the total region) and rates of change within the Arctic Ocean that are showing increasing or decreasing trends in phytoplankton biomass (CHL) for each of the standard IGMETS time-windows. Numbers in brackets indicate the % area with significant ($p < 0.05$) trends. See "Methods" chapter for a complete description and methodology used.

Latitude-adjusted CHL data field surface area = 10.7 million km²	**5-year** (2008–2012)	**10-year** (2003–2012)	**15-year** (1998–2012)
Area (%) w/ increasing CHL trends ($p < 0.05$)	25.7% (*1.8%*)	**56.5%** (*14.3%*)	**60.8%** (*21.7%*)
Area (%) w/ decreasing CHL trends ($p < 0.05$)	**74.3%** (*30.2%*)	43.5% (*9.0%*)	39.2% (*8.3%*)
> 0.50 mg m^{-3} decade^{-1} increasing ($p < 0.05$)	7.1% (*1.0%*)	10.1% (*5.8%*)	9.7% (*7.2%*)
0.10 to 0.50 mg m^{-3} decade^{-1} increasing ($p < 0.05$)	11.0% (*0.7%*)	20.9% (*6.8%*)	20.3% (*9.8%*)
0.01 to 0.10 mg m^{-3} decade^{-1} increasing ($p < 0.05$)	6.7% (*0.1%*)	22.6% (*1.6%*)	26.0% (*4.5%*)
0.00 to 0.01mg m^{-3} decade^{-1} increasing ($p < 0.05$)	0.9% (*0.1%*)	3.0% (*0.0%*)	4.8% (*0.2%*)
0.00 to –0.01mg m^{-3} decade^{-1} decreasing ($p < 0.05$)	0.9% (*0.0%*)	2.9% (*0.1%*)	4.2% (*0.1%*)
–0.01 to –0.10 mg m^{-3} decade^{-1} decreasing ($p < 0.05$)	9.6% (*0.5%*)	20.7% (*1.9%*)	23.1% (*3.8%*)
–0.10 to –0.50 mg m^{-3} decade^{-1} decreasing ($p < 0.05$)	31.0% (*10.7%*)	15.4% (*4.9%*)	9.9% (*3.4%*)
> –0.50 mg m^{-3} decade^{-1} decreasing ($p < 0.05$)	32.8% (*19.0%*)	4.4% (*2.1%*)	2.0% (*1.0%*)

leading to reduced incoming solar radiation across the pan-Arctic region (Belanger *et al*., 2013). In addition, satellite retrieval algorithms of chlorophyll are confounded by the signals of river turbidity in coastal regions (Demidov *et al*., 2014), chlorophyll maxima deeper than the optical depth of satellite sensor capabilities (Ardyna *et al*., 2013), and the contribution of coloured dissolved organic material (CDOM) to assessment of chlorophyll *a* biomass (Siegel *et al*., 2005). This latter confounding signal is of particular importance to Arctic marginal seas where substantial riverine CDOM or coloured detrital materials are supplied from the Arctic watersheds.

Given the above caveats, chlorophyll biomass has increased during 1998–2012 in over 60% (22% at $p < 0.05$) of the Arctic Ocean, and especially over continental margins (Table 3.2, Figure 3.3b). This finding is consistent with other studies showing increases in Arctic Ocean chlorophyll biomass (Arrigo *et al*., 2008, 2012, 2014; Pabi *et al*., 2008; Arrigo and van Dijken, 2011; Ardyna *et al*., 2014). More recently, Frey *et al*. (2014b) report higher chlorophyll biomass in 2014 relative to mean values in 2003–2013. As we show in Figures 3.3b, 3.4b, and 4.4c, the largest increases in chlorophyll biomass occurred in the Laptev, Kara, and Barents seas, with this finding similar to studies of Petrenko *et al.* (2013) and Frey *et al*. (2014). These longer-term trends in chlorophyll biomass appear consistent with global ocean increases over the past 20–50 years shown by McQuatters-Gollop *et al.* (2011) (in contrast to declines in marine phytoplankton reported by Boyce *et al*., 2010 using Secchi disk and other data). The seasonal timing of the annual phytoplankton bloom has become earlier (Kahru *et al*., 2010), and there is evidence for an autumn bloom now occurring in the Arctic marginal seas (Ardyna *et al*., 2014). Early satellite studies of the Bering Sea also showed evidence of an autumn bloom (Müller-Karger *et al*., 1990), with either the Arctic now experiencing similar phenomena to the Bering Sea or increased observations in the Arctic have simply revealed the occurrence of a pre-existing seasonal phenomenon.

Over the past five years (2008–2012), chlorophyll biomass in the marginal seas decreased over 74% (30% at $p < 0.05$) of the Arctic Ocean (Figures 3.3b, 3.4b, and 3.4c; Table 3.2). The causes for this decline in marine phytoplankton are uncertain. It may be related to reduced solar radiation due to increased cloudiness (Belanger *et al*., 2013), or deepening of the chlorophyll maximum (Monier *et al*., 2014). For example, Bergaron and Tremblay (2014) have shown a deepening of the nitracline and subsurface chlorophyll maximum, with diatoms consuming nutrients over a greater water depth. Light and nutrient availability in the Arctic Ocean appears to be one of the primary drivers of marine phytoplankton biomass and primary production (Popova *et al*., 2010).

Challenges remain in establishing trends in marine phytoplankton abundance, depth-integrated chlorophyll concentration, and rates such as primary production in the Arctic Ocean. For example, Petrenko *et al*. (2013) suggest that the Barents and Greenland seas are the most productive in the Arctic, with the East Siberian and Chukchi seas the least productive. This satellite-derived finding contrasts markedly with evidence that the highest rates of *in situ* primary production (Müller-Karger *et al*., 1987; Walsh *et al*., 1989; Cota *et al*., 2004; Arrigo *et al*., 2012) and net community production (from inorganic nutrient and dissolved inorganic carbon changes; Bates and Mathis, 2009; Codispoti *et al*., 2013) in the Arctic are found in the Chukchi Sea, with the Barents Sea a close second (Dalpadado *et al*., 2014). What remains consistent is that the Arctic marginal seas are productive (Müller-Karger and Alexander, 1987; Müller-Karger *et al*., 1987, 1990; Walsh *et al*., 1989; Hill and Cota, 2005; Arrigo *et al*., 2014; Ulfsbo *et al*., 2014) compared to the highly oligotrophic central basins (English, 1961; Moran *et al*., 1997; Wheeler *et al*., 1996; Lalande *et al*., 2014b).

The loss of sea ice will also affect the standing stocks of sea ice algae, their rates of primary production, and their importance to the marine biochemical cycles of the Arctic (Legendre *et al*., 1992). Dupont (2012) estimates that sea ice biology contributes about 7.5% of the total primary production for the entire Arctic Ocean, with declining sea ice extent presumably reducing the contribution to carbon and nutrient cycling in the Arctic (Boetius *et al*., 2014).

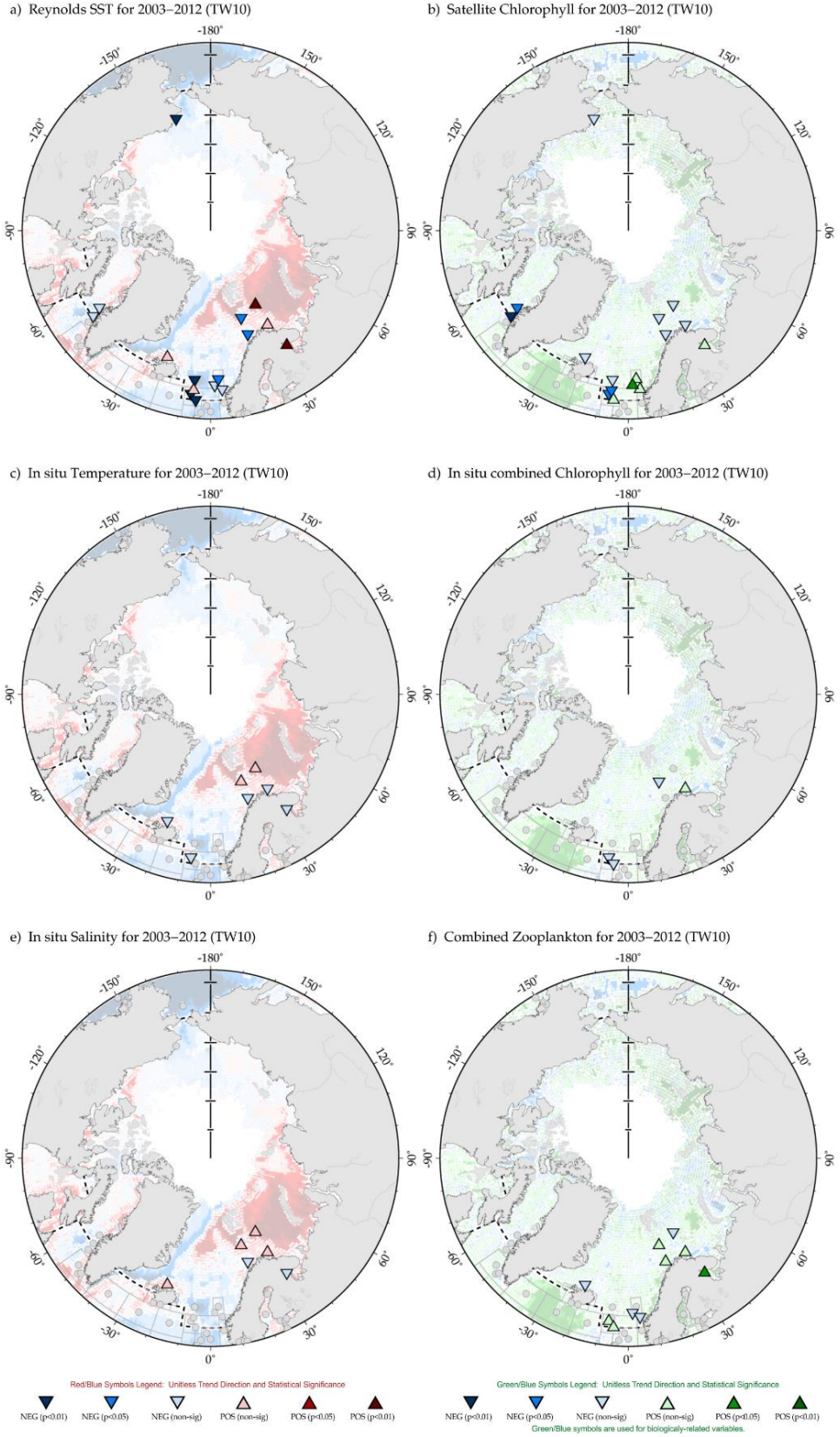

Figure 3.4. Map of Arctic Ocean region time-series locations and trends for select variables and IGMETS time-windows. The Arctic Ocean region is defined in the Figure 3.2 caption. Upward-pointing triangles indicate positive trends; downward triangles indicate negative trends. Gray circles indicate time-series site that fell outside of the current study region or time-window. Additional variables and time-windows are available through the IGMETS Explorer (http://IGMETS.net/explorer). See "Methods" chapter for a complete description and methodology used.

3.4 Zooplankton changes

The response of zooplankton to the physical and biological changes occurring in the Arctic is mixed and difficult to assess due to limited time-series observations. Over the past ten years, zooplankton appear to have increased in the White Sea (Usov *et al.*, 2013) and in the Barents Sea, the latter often concomitant with surface warming, increased chlorophyll biomass, and primary production (Dalpadado *et al*., 2014). Such increases in primary production are also observed in the Fram Strait adjacent to the Barents Sea (Cherkasheva *et al*., 2014). Over longer time-scales (15+ years), zooplankton appear to have declined at three of the four Barents Sea time-series sites and at the White Sea site. Unfortunately, other concomitant ecological data (e.g. diatom, dinoflagellate, and nutrient concentrations) were lacking from these sites.

Elsewhere on the Siberian shelves and central basins of the Arctic, ecological data are scarce, making it difficult to assess trends. However, in the Chukchi Sea, Ershova *et al*. (2015) report a significant increase in large copepod biomass (primarily *Calanus glacialis* and other calanid taxa) between 1946 and 2012, concomitant with longer-term warming. Of note is a more recent decline in copepod biomass (2004–2012) that accompanies the modest cooling of the region and a decline in primary production (Lee *et al*., 2013).

3.5 Conclusions

In general, the surface Arctic Ocean has been steadily warming over the past 30 years. Chlorophyll biomass, as determined by satellite observations, has increased slightly over the past 15 years. The complexity of the Arctic marginal seas and the central basin settings coupled with a scarcity of *in situ* data only allows us to superficially assess biogeochemical and biological community changes across the pan-Arctic.

Table 3.3. Time-series sites located in the IGMETS Arctic Ocean subarea. Participating countries: Denmark (dk), Faroe Islands (fo), Iceland (is), Norway (no), Russia (ru), United Kingdom (uk), and United States (us). Year-spans in red text indicate time series of unknown or discontinued status. IGMETS-IDs in red text indicate time series without a description entry in the Annex A1.

No.	IGMETS-ID	Site or programme name	Year-span	T	S	Oxy	Ntr	Chl	Mic	Phy	Zoo
1	dk-10101	Hellefiske Bank – S1 *(West Greenland)*	1950–1984 (?)	X	-	-	-	-	-	-	X
2	dk-10102	Sukkertop Bank – S2 *(West Greenland)*	1950–1984 (?)	X	-	-	-	-	-	-	X
3	fo-30101	Faroe Islands Shelf *(Faroe Islands)* *see North Atlantic Annex (A2)*	1991–present	X	-	-	X	X	-	-	X
4	fo-30102	Norwegian Sea Transect – North *(North Faroe Islands)*	1990–present	X	-	-	-	X	-	-	X
5	fo-30103	Norwegian Sea Transect – South *(North Faroe Islands)*	1990–present	X	-	-	-	X	-	-	X
6	is-30101	Siglunes Transect *(North Iceland)*	1952–present	X	X	-	-	X	-	-	X
7	no-50101	Svinøy Transect – East *(Norwegian Sea)*	1994–present	-	-	-	-	X	-	-	X
8	no-50102	Svinøy Transect – West *(Norwegian Sea)*	1994–present	-	-	-	-	X	-	-	X
9	no-50201	Fugløya-Bjørnøya Transect – North *(Western Barents Sea)*	1990–present	X	X	-	-	X	-	-	X
10	no-50202	Fugløya-Bjørnøya Transect – South *(Western Barents Sea)*	1990–present	X	X	-	-	X	-	-	X
11	no-50301	Vardø-Nord Transect – North *(Central Barents Sea)*	1990–present	X	X	-	-	X	-	-	X
12	no-50302	Vardø-Nord Transect – South *(Central Barents Sea)*	1990–present	X	X	-	-	X	-	-	X
13	ru-10101	Kartesh D1 *(White Sea)*	1961–present	X	X	-	-	-	-	-	X
14	uk-40101	SAHFOS-CPR A01 *(Norwegian Sea)*	1958–present	-	-	-	-	X	-	X	X
15	uk-40114	SAHFOS-CPR B04 *(Southern Norwegian Sea)*	1958–present	-	-	-	-	X	-	X	X
16	us-50604	EMA-4: Chukchi Sea *(Chukchi Sea)*	2003–present	X	X	-	X	X	-	-	-

3.6 References

Aagaard, K., and Carmack, E. C. 1989. The role of sea ice and other fresh water in the Arctic circulation. Journal of Geophysical Research, 94(C10): 14485–14498.

Aagaard, K., Coachman, L. K., and Carmack, E. C. 1981. On the halocline of the Arctic Ocean. Deep-Sea Research, 28: 529–545.

Ardyna, M., Babin, M., Gosselin, M., Devred, E., Bélanger, S., Matsuoka, A., and Tremblay, J-É. 2013. Parameterization of vertical chlorophyll *a* in the Arctic Ocean: impact of the subsurface chlorophyll maximum on regional, seasonal, and annual primary production estimates. Biogeosciences, 10: 4383–4404, doi:10.5194/bg-10-4383-2013.

Ardyna, M., Babin, M., Gosselin, M., Devrad, E., Rainville, L., and Tremblay, J-E. 2014. Recent Arctic Ocean sea-ice loss triggers novel fall phytoplankton blooms. Geophysical Research Letters, 41: 6207–6212, doi:10.1002/2014GL061047.

Arrigo, K. R., and van Dijken, G. 2011. Secular trends in Arctic Ocean net primary production. Journal of Geophysical Research, 116(C9): C09011, doi:10.1029/2011JC007151.

Arrigo, K. R., van Dijken, G., and Pabi, S. 2008. Impact of a shrinking Arctic ice cover on marine primary production. Geophysical Research Letters, 35: L19603, doi:10.1029/2008GL035028.

Arrigo, K. J., Perovich, D. K., Pickart, R. S., Brown, Z. W., van Dijken, G. L., Lowry, K. E., Mills, M. M., *et al*. 2012. Massive phytoplankton blooms under Arctic sea-ice. Science, 336(6087): 1408–1409, doi:10.1126/science.1215065.

Arrigo, K. R., Perovich, D. K., Pickart, R. S., Brown, Z. W., van Dijken, G. L., Lowry, K. E., Mills, M. M., *et al*. 2014. Phytoplankton blooms beneath the sea ice in the Chukchi Sea. Deep-Sea Research, 105: 1–16.

Bates, N. R. 2015. Assessing ocean acidification variability in the Pacific-Arctic Region (PAR) as part of the Russian-American Long-term Census of the Arctic (RUSALCA). Oceanography, 28(3): 36–45, http://dx.doi.org/10.5670/oceanog.2015.56.

Bates, N. R., and Mathis, J. T. 2009. The Arctic Ocean marine carbon cycle: Evaluation of air-sea CO_2 exchanges, ocean acidification impacts and potential feedbacks. Biogeosciences, 6(11): 2433–2459.

Bates, N. R., Moran, S. B., Hansell, D. A., and Mathis, J. T. 2006. An increasing CO_2 sink in the Arctic Ocean due to sea-ice loss? Geophysical Research Letters, 33: L23609, doi:10.1029/2006GL027028.

Bélanger, S., Babin, M., and Tremblay, J-É. 2013. Increasing cloudiness in Arctic damps the increase in phytoplankton primary production due to sea ice receding. Biogeosciences, 10(6): 4087–4101, doi:10.5194/bg-10-4087-2013.

Bergeron, M., and Tremblay, J-É. 2014. Shifts in biological productivity inferred from nutrient drawdown in the southern Beaufort Sea (2003-2011) and northern Baffin Bay (1997-2011), Canadian Arctic. Geophysical Research Letters, 41: 3979–3987, doi:10.1002/2014GL059649.

Boetius, A., Albrecht, S., Bakker, K., Bienhold, C., Felden, J., Fernández-Méndez, M., Hendricks, A., *et al*. 2014. Export of algal biomass from the melting Arctic sea ice. Science, 339(6126): 1430–1432, doi:10.1126/science.1231346.

Boyce, D. G., Lewis, M. R., and Worm, B. 2010. Global phytoplankton decline over the past century. Nature, 466: 591–596.

Cai, W. J., Bates, N. R., Guo, L., Anderson, L. G., Mathis, J. T., Wanninkhof, R., Hansell, D. A., *et al*. 2014. Carbon fluxes across boundaries in the Pacific Arctic region in a changing environment. *In* The Pacific Arctic Region: Ecosystem Status and Trends in a Rapidly Changing Environment, pp. 199–222. Ed. by J. M. Grebmeier**, W.** Maslowski, and J. Zhao. Springer, Dordrecht. 450 pp.

Carmack, E. C., and Chapman, D. 2003. Wind-driven shelf/basin exchange on an Arctic shelf: The joint roles of ice cover extent and shelf-break bathymetry. Geophysical Research Letters, 30: 1778, doi:10.1029/2003GL017526.

Carmack, E., and McLaughlin, F. 2011. Towards recognition of physical and geochemical change on Subarctic and Arctic Seas. Progress in Oceanography, 90: 90–104, doi:10.1016/j.pocean.2011.02.007.

Carmack, E., Polyakov, I., Padman, L., Fer, I., Hunke, E., Hutchings, J., Jackson, J., *et al*. 2015. Towards quantifying the increasing role of oceanic heat in sea ice loss in the new Arctic. Bulletin of the American Meteorological Society, 96: 2079–2105, doi:10.1175/BAMS-D-13-00177.1.

Carmack, E., and Wassman, P. 2006. Food webs and physical-biological coupling on pan-Arctic shelves: Unifying concepts and comprehensive perspectives. Progress in Oceanography, 71: 446–477.

Coachman, L. K. 1993. On the flow field in the Chirikov Basin. Continental Shelf Research, 13(5–6): 481–508, doi:10.1016/0278-4343(93)90092-C.

Coachman, L. K., and Shigaev, V. V. 1992. Northern Bering-Chukchi Sea ecosystem: The physical basis. *In* Results of the Third Joint US-USSR Bering & Chukchi Seas Expedition (BERPAC): Summer 1988, p. 448. Ed. by J. F. Turner, and P. A. Nagel. US Fish and Wildlife Service, Washington, DC.

Cherkasheva, A., Bracher, A., Melsheimer, C., Koeberle, C., Gerdes, R., Noethig, E-M., Bauerfeind, E., *et al*. 2014. Influence of the physical environment on polar phytoplankton blooms: A case study in the Fram Strait. Journal of Marine Systems, 132: 196–207, doi: 10.1016/j.jmarsys.2013.11.008.

Codispoti, L. A., Kelly, V., Thessen, A., Matrai, P., Suttles, S., Hill, V., Steele, M., *et al*. 2013. Synthesis of primary production in the Arctic Ocean: III. Nitrate and phosphate based estimates of net community production. Progress in Oceanography, 110: 126–150, doi:10.1016/j.pocean.2012.11.006.

Cooper, L. W., McClelland, J. W., Holmes, R. M., Raymond, P. A., Gibson, J. J., Guay, C. K., and Peterson, B. J. 2008. Flow-weighted tracer content ($\delta^{18}O$, DOC, Ba, alkalinity) of the six largest Arctic rivers. Geophysical Research Letters, 35: L18606, doi:10.1029/2008GL035007.

Cota, G., Wang, G., and Comiso, J. C. 2004. Transformation of global satellite chlorophyll retrievals with a regionally tuned algorithm. Remote Sensing of the Environment, 90: 373–377.

Dalpadado, P., Arrigo, K. R., Hjollo, S. S., Rey, F., Ingvaldsen, R. B., Sperfeld, E., van Dijken, G. L., *et al*. 2014. Productivity in the Barents Sea - response to recent climate variability. Plos ONE, 9(5): doi:10.1371/journal.pone.0095273.

Danielson, S. L., Weingartner, T. J., Hedstrom, K. S., Aagaard, K., Woodgate, R., Curchitser, E., and Stabeno, P. J. 2014. Coupled wind-forced controls of the Bering–Chukchi shelf circulation and the Bering Strait throughflow: Ekman transport, continental shelf waves, and variations of the Pacific–Arctic sea surface height gradient. Progress in Oceanography, 125: 40–61, doi:10.1016/j.pocean.2014.04.006.

Demidov, A. B., Mosharov, S. A., and Makkaveev, P. N. 2014. Patterns of the Kara Sea primary production in autumn: Biotic and abiotic forcing of subsurface layer. Journal of Marine Systems, 132: 130–149, doi:10.1016/j.jmarsys.2014.01.014.

Dupont, F. 2012. Impact of sea-ice biology on overall primary production in a biophysical model of the pan-Arctic Ocean. Journal of Geophysical Research, 117: C00D17, doi:10.1029/2011JC006983.

English, T. S. 1961. Some biological oceanographic observations in the central north Polar Sea, Drift Station Alpha, 1957–1958. Science Arctic Institute of North America - University of Calgary, Report 15.

Ershova, E. A., Hopcroft, R. R., Kosobokova, K. N., Matsuno, K., Nelson, R. J., Yamaguchi, A., and. Eisner, L. B. 2015. Long-term changes in summer zooplankton communities of the western Chukchi Sea, 1945–2012. Oceanography, 28(3): 100–115, doi:10.5670/oceanog.2015.60.

Fahrbach, E., Meincke, J., Østerhus, S., Rohardt, G., Schauer, U., Tverberg, V., and Verduin, J. 2001. Direct measurements of volume transports through Fram Strait. Polar Research, 20(2): 217–224.

Frey, K. E., Comiso, J. C., Cooper, L. W., Gradinger, R. R., Grebmeier, J. M., Saitoh, S-I., and Tremblay, J-E. 2014. Arctic Ocean primary productivity. *In* Arctic Report Card 2014, pp. 44–54. Ed. by M. Jeffries, J. Richter-Menge, and J. Overland. 75 pp. ftp://ftp.oar.noaa.gov/arctic/documents/ArcticReportCard_full_report2014.pdf.

Frey, K. E., Maslanik, J. A., Kinney, J. C., and Maslowski, W. 2014a. Recent variability in sea-ice cover, age, and thickness in the Pacific Arctic Region. *In* The Pacific Arctic Region: Ecosystem Status and Trends in a Rapidly Changing Environment, pp. 31–63. Ed. by J. M. Grebmeier, W. Maslowski, and J. Zhao. Springer, Dordrecht. 450 pp.

Frey, K. E., Moore, G. W. K., Cooper, L. W., and Grebmeier, J. M. 2015. Divergent patterns of recent sea ice cover across the Bering, Chukchi, and Beaufort seas of the Pacific Arctic Region. Progress in Oceanography, 136: 32–49, http://dx.doi.org/10.1016/j.pocean.2015.05.009.

Grebmeier, J. M., Bluhm, B. A., Cooper, L. W., Denisenko, S. G., Iken, K., Kędra, M., and Serratos, C. 2015. Time series benthic community composition and biomass and associated environmental characteristics in the Chukchi Sea during the RUSALCA 2004–2012 Program. Oceanography, 28(3): 116–133, doi:10.5670/oceanog.2015.61.

Grebmeier, J. M., Moore, S. E., Overland, J. E., Frey, K. E., and Gradinger, R. 2010. Biological response to recent Pacific Arctic sea-ice retreats. EOS Transactions, 91(18): 161–162.

Hill, V. J., and Cota, G. F. 2005. Spatial patterns of primary production in the Chukchi Sea in the spring and summer of 2002. Deep-Sea Research II, 52: 3344–3354.

Holland, M. M., and Bitz, C. M. 2003. Polar amplification of climate change in coupled models. Climate Dynamics, 21: 221–232.

Hopcroft, R. R., and Day, R. H. 2013. Introduction to the special issue on the ecology of the northeastern Chukchi Sea. Continental Shelf Research, 67: 1–4, doi:10.1016/j.csr.2013.06.017.

IPCC. 2007. Climate Change 2007: Synthesis Report. Contribution of Working Groups I, II and III to the Fourth Assessment Report of the Intergovernmental Panel on Climate Change [Core Writing Team, R. K. Pachauri, and A. Reisinger]. IPCC, Geneva, Switzerland. 104 pp.

IPCC. 2014. Climate Change 2014: Synthesis Report. Contribution of Working Groups I, II and III to the Fifth Assessment Report of the Intergovernmental Panel on Climate Change [Core Writing Team, R.K. Pachauri, and L.A. Meyer]. IPCC, Geneva, Switzerland. 151 pp.

Jeffries, M. O., Overland, J. E., and Perovich, D. K. 2013. The Arctic shifts to a new normal. Physics Today, 66(10): 35–40, http://dx.doi.org/10.1063/PT.3.2147.

Kahru, M., Kudela, R. M., Murtugudde, R., Strutton, P. G., Manzano-Sarabia, M., Wang, H., and Mitchell, B. G. 2010. Global correlations between winds and ocean chlorophyll. Journal of Geophysical Research, 115: C12, doi:10.1029/2010JC006500.

Kay, J. E., L'Ecuyer, T., Gettelman, A., Stephens, G., and O'Dell, C. 2008. The contribution of cloud and radiation anomalies to the 2007 Arctic sea ice extent minimum. Geophysical Research Letters, 35: L08503, doi:10.1029/2008GL033451.

Kwok, R., and Untersteiner, N. 2011. The thinning of Arctic sea ice. Physics Today, 64(4): 36–41, http://dx.doi.org/10.1063/1.3580491.

Lalande, C., Belanger, S., and Fortier, L. 2009. Impact of a decreasing sea ice cover on the vertical export of particulate organic carbon in the northern Laptev Sea, Siberian Arctic Ocean. Geophysical Research Letters, 36: L21604, doi:10.1029/2009GL040570.

Lalande, C., Nöthig, E-M., Somavilla, R., Bauerfeind, E., Shevchenko, V., and Okolodkov, Y. 2014a. Variability in under-ice export fluxes of biogenic matter in the Arctic Ocean. Global Biogeochemical Cycles, 28(5): 571–583, doi:10.1002/2013gb004735.

Lalande, C., Nöthig, E-M., Bauerfeind, E., and Fortier, L. 2014b. Export fluxes of biogenic matter in the Siberian Arctic Ocean. Ocean Sciences Meeting, Honolulu, Hawaii.

Lee, S. H., Yun, M. S., Kim, B. K., Saitoh, S., Kang, C. K., Kang, S. H., and Whitledge, T. E. 2013. Latitudinal carbon productivity in the Bering and Chukchi Seas during the summer in 2007. Continental Shelf Research, 59: 28–36, doi:10.1016/j.csr.2013.04.004.

Legendre, L., Ackley, S. F., Dieckmann, G. S., Gullicksen, B., Horner, R., Hoshiai, T., Melnikov, I. A., *et al.* 1992. Ecology of sea ice biota: 2. Global significance. Polar Biology, 12: 429–444.

Li, W. K. W., McLaughlin, F. A., Lovejoy, C., and Carmack, E. C. 2009. Smallest algae thrive as the Arctic Ocean freshens. Science, 326(5952): 539, doi:10.1126/science.1179798.

Lindsay, R., and Schweiger, A. 2015. Arctic sea ice thickness loss determined using subsurface, aircraft, and satellite observations. The Cryosphere, 9(1): 269–283, doi:10.5194/tc-9-269-2015.

Macdonald, R. W. Anderson, L. G., Christensen, J. P., Miller, L. A., Semiletov, I. P., and Stein, R. 2008. The Arctic Ocean. *In* Carbon and Nutrient Fluxes in Continental Margins: A Global Synthesis, pp. 291–303. Ed. by K. K. Liu, L. Atkinson, R. Quinones, and L. Talue-McManus Springer, New York. 741 pp.

Manizza, M., Follows, M. J., Dutkiewicz, S., Menemenlis, D., Hill, C. N., and Key, R. M. 2013. Changes in the Arctic ocean CO_2 sink (1996-2007): A regional model analysis. Global Biogeochemical Cycles, 27: 1108–1118, doi:10.1002/2012GB004491.

Markus, T., Stroeve, J., and Miller, J. 2009. Recent changes in Arctic sea ice melt onselt, freezeup and melt season length. Journal of Geophyiscal Research, 114(C12): C12024.

Maslanik, J., Drobot, S., Fowler, C., Emery, W., and Barry, R. 2007. On the Arctic climate paradox and the continuing role of atmospheric circulation in affecting sea ice conditions. Geophysical Research Letters, 34: L03711.

McGuire, A. D., Chapin III, F. S., Walsh, J. E., and Wirth, C. 2006. Integrated regional changes in arctic climate feedbacks: implications for the global climate system. Annual Review of Environment and Resources, 31: 61–91.

McQuatters-Gollop, A., Reid, P. C., Edwards, M., Burkill, P. H., Castellani, C., Batten, S., Gieskes, W., *et al*. 2011. Is there a decline in marine phytoplankton. Nature, 472: E6–E7, doi:10.1038/nature09950.

Monier, A., Comte, J., Babin, M., Forest, A., Matsuoka, A., and Lovejoy, C. 2014. Oceanographic structure drives the assembly processes of microbial eukaryotic communities. The International Society for Microbial Ecology Journal, 9(4): 990–1002, doi:10.1038/ismej.2014.197.

Moran, S. B., Ellis, K. M., and Smith, J. N. 1997. $^{234}Th/^{238}U$ disequilibrium in the central Arctic Ocean: Implications for particulate organic carbon export. Deep-Sea Research II, 44: 1593–1606.

Müller-Karger, F. E., and Alexander, V. 1987. Nitrogen dynamics in a marginal sea-ice zone. Continental Shelf Research, 7: 805–823.

Müller-Karger, F. E., McClain, C. R., and Ray, G. C. 1987. Primary Productivity. Chapter in the Strategic Atlas of Economic Resources of the Bering Sea. NOAA Strategic Assessment Branch, Rockville, MD.

Müller-Karger, F. E., McClain, C. R., Sambrotto, R. N., and Ray, C. G. 1990. Measurements of phytoplankton distribution in the southeastern Bering Sea using the CZCS: A note of caution. Journal of Geophysical Research, 95(C7): 11483–11499.

Nihoul, J. C. J., Adam, P., Brasseur, P., Deleersnijder, E., Djenidi, S., and Haus, J. 1993. Three-dimensional general circulation model of the northern Bering Sea's summer ecohydrodynamics. Continental Shelf Research, 13: 509–542, http://dx.doi.org/10.1016/0278-4343(93)90093-D.

Nishino, S., Kikichi, T., Yamamoto-Kawai, M., Kawaguchi, Y., Hirawake, T., and Itoh, M. 2011. Enhancement/reduction of biological pump depends on ocean circulation in the sea-ice reduction regions of the Arctic Ocean. Journal of Oceanography, 67(3): 305–311.

Ogi, M., and Wallace, J. M. 2012. The role of summer surface wind anomalies in the summer Arctic sea ice extent in 2010 and 2011. Geophysical Research Letters, 39: L09704, doi.org/10.1029/2012GL051330.

Orr, J. C., Fabry, V. J., Aumont, O., Bopp, L., Doney, S. C., Feely, R. A., Gnanadesikan, A., *et al.* 2005. Anthropogenic ocean acidification over the twenty-first century and its impacts on calcifying organisms. Nature, 437(7059): 681–686.

Overland, J. E., Francis, J. A., Hanna, E., and Wang, M. 2012. The recent shift in early summer Arctic atmospheric circulation. Geophysical Research Letters, 39: L19804, doi:10.1029/2012GL053268.

Overland, J. E., Hanna, E., Hanssen-Bauer, I., Kim, S-J., Walsh, J., Wang, M., and Bhatt, U. S. 2014. Air temperature. *In* Arctic Report Card 2014, pp. 9–15. Ed. by M.. Jeffries, J. Richter-Menge, and J. Overland. 75 pp. ftp://ftp.oar.noaa.gov/arctic/documents/ArcticReportCard_full_report2014.pdf.

Overland, J. E., and Wang, M. 2005. The Arctic climate paradox: The recent decrease of the Arctic Oscillation. Geophysical Research Letters, 32(6): L06701, doi:10.1029/2004GL021752, 2005.

Overland, J. E, and Wang, M. 2013. When will the summer Arctic be nearly sea-ice free? Geophysical Research Letters, 40(10): 2097–2101, doi:10.1002/grl.50316.

Pabi, S., van Dijken, G. L., and Arrigo, K. R. 2008. Primary production in the Arctic Ocean, 1998-2006, Journal of Geophysical Research, 113: C08005, doi:10.1029/2007JC004578.

Parkinson, C. L. 2014. Spatially mapped reductions in the length of the Arctic sea ice season. Geophysical Research Letters, 41: 4316–4322, doi.org/10.1002/2014GL060434.

Perovich, D. K., Gerland, S., Hendricks, S., Meier, W., Nicolaus, M., and Tschudi, M. 2014. Sea Ice. *In* Arctic Report Card 2014, pp. 32–38. Ed. by M. Jeffries, J. Richter-Menge, and J. Overland. 75 pp. ftp://ftp.oar.noaa.gov/arctic/documents/ArcticReportCard_full_report2014.pdf.

Perovich, D. K., Light, B., Eicken, H., Jones, K. F., Runciman, K., and Nghiem, S. V. 2007. Increasing solar heating of the Arctic Ocean and adjacent seas, 1979-2005: Attribution and role in the ice-albedo feedback. Geophysical Research Letters, 34(19): L19505.

Perovich, D. K., and Polashenski, C. 2012. Albedo evolution of seasonal Arctic sea ice. Geophysical Research Letter, 39: L08501, doi:org/10.1029/2012GL051432.

Perovich, D. K., and Richter-Menge, J. A. 2009. Loss of sea ice in the Arctic. Annual Revue Marine Science, 1(1): 417–441.

Peterson, B. J., Holmes, R. M., McClelland, J. W., Vorosmarty, C. S. J., Lammers, R. B., Shiklomanov, A. I., Shiklomanov, I. A., *et al.* 2002, Increasing river discharge to the Arctic Ocean. Science, 298: 2171–2173, doi:10.1126/science.1077445.

Petrenko, D., Pozdnyakov, D., Johannessen, J, Counillon, F., and Sychov, V. 2013. Satellite-derived multiyear trend in primary production in the Arctic Ocean. International Journal of Remote Sensing, 34: 3903–3937, doi:10.1080/01431161.2012.762698.

Polyakov, I. V., Alekseev, G. V., Bekryaev, R. V., Bhatt, U., Colony, R. L., Johnson, M. A., Karklin, V. P., *et al.* 2002. Observationally based assessment of polar amplification of global warming. Geophysical Research Letters, 29: 1878, doi:10.1029.2001GL011111.

Polyakov, I. V., Walsh, J. E., and Kwok, R. 2012. Recent changes of Arctic multiyear sea ice coverage and the likely causes. Bulletin of the American Meteorological Society, 93(2): 145–151, doi:10.1175/BAMS-D-11-00070.1.

Popova, E. E., Yool, A., Coward, A. C., Aksenov, Y. K., Alderson, S. G., de Cuevas, B. A., and Anderson, T. R. 2010. Control of primary production in the Arctic by nutrients and light: insights from a high resolution ocean general circulation model. Biogeosciences, 7: 3569–3591, doi:10.5194/bg-7-3569-2010.

Popova, E. E., Yool, A., Coward, A. C., Dupont, F., Deal, C., Ellot, S., Hunke, E., *et al.* 2012. What controls primary production in the Arctic Ocean? Results from an intercomparison of five general circulation models with biogeochemistry. Journal of Geophysical Research, 117: C00D12, doi:10.1029/2011JC007112.

Rigor, I. G., Wallace, J. M., and Colony, R. L. 2002. Response of sea ice to the Arctic Oscillation. Journal of Climate, 15(18): 2648.

Rippeth, T. P., Lincoln, B. J., Kennedy, H. J., Palmer, M. R., Sharples, J., and Williams, C. A. J. 2014. Impact of vertical mixing on sea surface pCO_2 in temperate seasonally stratified shelf seas. Journal of Geophysical Research, 119: 3868–3882, doi:10.1002/2014JC010089.

Rudels, B., Anderson, L. G., and Jones, E. P. 1996. Formation and evolution of the surface mixed layer and halocline of the Arctic Ocean. Journal of Geophysical Research-Oceans, 101(C4): 8807–8821, doi:10.1029/96JC00143..

Schuster, U., McKinley, G., Bates, N. R., Chevallier, F., Doney, S., Fay, A., Gonzaléz-Dávila, M., *et al*. 2013. Atlantic and Arctic air-Sea CO_2 fluxes, 1990-2009. Biogeosciences, 10(1): 607–627, doi:10.5194/bg-10-607-2013.

Screen, J. A., Deser, C., Simmonds, I., and Tomas, R. 2013. Atmospheric impacts of Arctic sea-ice loss, 1979-2009: separating forced changed from atmospheric internal variability. Climate Dynamics, 43: 333–344.

Seigel, D. A., Maritorena, S., Nelson, N. B., and Behrenfield, M. J. 2005. Independence and interdependence among global ocean color properties: Reassessing the bio-optical assumption. Journal of Geophysical Research, 111: C07011, doi:10.1029/2004JC002527.

Serreze, J. C., and Stroeve, J. 2009. Atmospheric circulation feedbacks. *In* Arctic Climate Feedbacks: Global Implications, pp. 18–27. Ed. by M. Sommerkorn, and S. J. Hassol. WWF International Arctic Program, Oslo. 97 pp.

Serreze, M. C., Holland, M. M., and Stroeve, J. 2007. Perspectives on the Arctic's shrinking sea-ice cover, Science, 315(5818): 1533–1536.

Serreze, M. C., Walsh, J. E., Chapnill, F. S., Osterkamp, T., Dyurgerov, M., Romanovsky, V., Oechel, W. C., *et al*. 2000. Observational evidence of recent change in the northern high-latitude environment. Climatic Change, 46: 159–207.

Simmonds, I., and Govekar, P. D. 2014. What are the physical links between Arctic sea-ice loss and Eurasian winter climate? Environmental Research Letters, 9: 101003, doi:10.1088/1748-9326/9/10/101003.

Steinacher, M., Joos, F., Frölicher, T. L., Plattner, G-K., and Doney, S. C. 2009. Imminent ocean acidification in the Arctic projected with the NCAR global coupled carbon cycle-climate model. Biogeosciences, 6: 515–533.

Stroeve, J. C, Holland, M. M., Meier, W., Scambos, T., and Serreze, M. 2007. Arctic sea ice decline: Faster than forecast. Geophysical Research Letters, 41(4): 1216–1225, doi:10.1002/2013GL058951.

Stroeve, J. C, Markus, T., Boisvert, L., Miller, J., and Barrett, A. 2014. Changes in Arctic melt season and implications for sea-ice loss. Geophysical Research Letters, 41: 1216–1225, doi:10.1002/2013GL058951.

Stroeve, J. C., Serreze, M. C., Holland, M. M., Kay, J. E., Maslanik, J., and Barrett, A. P. 2012. The Arctic's rapidly shrinking sea ice cover: A research synthesis. Climatic Change, 110: 1005–1027, doi:10.1007/s10584-011-0101-1.

Takahashi, T., Sutherland, S. C., Wanninkhof, R., Sweeney, C., Feely, R. A., Chipman, D. W., Hales, B., *et al*. 2009. Climatological mean and decadal change in surface ocean pCO_2, and net sea-air CO_2 flux over the global oceans. Deep-Sea Research II, 56(8–10): 554–577, doi:10.1016.

Timmermans, M. L. 2015. The impact of stored solar heat on Arctic sea ice growth. Geophysical Research Letters, 42(6): 399–406, doi:10.1002/2015GL064541.

Tremblay, J. E., and Gagnon, J. 2009. The effects of irrandiance and nutrient supply on the productivity of Arctic waters: a perspective on climate change. *In* Influence of Climate Change on the Changing Arctic and Sub-Arctic Conditions, pp. 73–93. Ed. by J. C. J. Nihoul, and A. G. Kostianov.Springer, New York. 232 pp.

Ulfsbo, A., Cassar, N., Korhonen, M., van Heuven, S., Hoppema, M., Kattner, G., and Anderson, L. G. 2014. Late summer net community production in the central Arctic Ocean using multiple approaches. Global Biogeochemical Cycles, 28(10): 1129–1148, doi:10.1002/2014GB004833.

Usov, N., Kutcheva, I., Primakov, I., and Martynova, D. 2013. Every species is good in its season: Do the shifts in the annual temperature dynamics affect the phenology of the zooplankton species in the White Sea? Hydrobiologia, 706(1): 11–33.

Walsh, J. J., McRoy, C. P., Coachman, L. K., Goering, J. J., Nihoul, J. J., Whitledge, T. E., Blackburn, T. H., *et al*. 1989. Carbon and nitrogen cycling within the Bering/Chukchi Seas: source regions of organic matter effecting AOU demands of the Arctic Ocean. Progress in Oceanography, 22: 279–361.

Wang, J., Ikeda, M., Zhang, S., and Gerdes, R. 2005. Linking the northern hemisphere sea-ice reduction trend and the quasi-decadal arctic sea-ice oscillation. Climate Dynamics, 24(2–3): 115–130.

Wang, M., and Overland, J. E. 2009. A sea ice free summer Arctic within 30 years? Geophyical. Research Letters, 39: L18501, doi:10.1029/2012GL052868.

Wang, X., Feng, Y., Swail, V., and Cox, A. 2015. Historical changes in the Beaufort-Chukchi-Bering Seas surface winds and waves, 1971–2013. Journal of Climate, http://dx.doi.org/10.1175/JCLI-D-15-0190.1.

Wassman, P., Duarte, C. M., Agusti, S., and Sejr, M. K. 2011. Footprints of climate change in the Arctic marine ecosystem. Global Change Biology, 17: 1235–1249; doi:10.1111/j.1365-2486.2010.02311.x.

Wheeler, P. A., Gosselin, M., Sherr, E., Thibault, D., Kirchman, D. L., Benner, R., and Whitledge, T. E. 1996. Active cycling of organic carbon in the central Arctic Ocean. Nature, 380(6576): 697–699.

Wijffels, S. E., Schmitt, R. W., Bryden, H. L., and Stigebrandt, A. 1992. Transport of freshwater by the oceans, Journal of Geophysical Research, 22: 155–162.

Wood, K. R., Wang, J., Salo, S. A., and Stabeno, P. J. 2015. The climate of the Pacific Arctic during the first RUSALCA decade 2004–2013. Oceanography, 28(3): 24–35, doi.org/10.5670/oceanog.2015.55.

Woodgate, R. A., Aagaard, K., and Weingartner, T. J. 2005. Monthly temperature, salinity and transport variability of the Bering Strait Throughflow. Geophysical Research Letters, 32(4): L04601, doi:10.1029/2004GL021880.

Woodgate, R. A., Stafford, K. M., and Prahl, F. G. 2015. A synthesis of year-round interdisciplinary mooring measurements in the Bering Strait (1990–2014) and the RUSALCA years (2004–2011). Oceanography, 28(3): 46–67, doi:10.5670/oceanog.2015.57.

4 North Atlantic Ocean

Antonio Bode, Hermann W. Bange, Maarten Boersma, Eileen Bresnan, Kathryn Cook, Anne Goffart, Kirsten Isensee, Michael W. Lomas, Patricija Mozetic, Frank E. Muller-Karger, Laura Lorenzoni, Todd D. O'Brien, Stéphane Plourde, and Luis Valdés

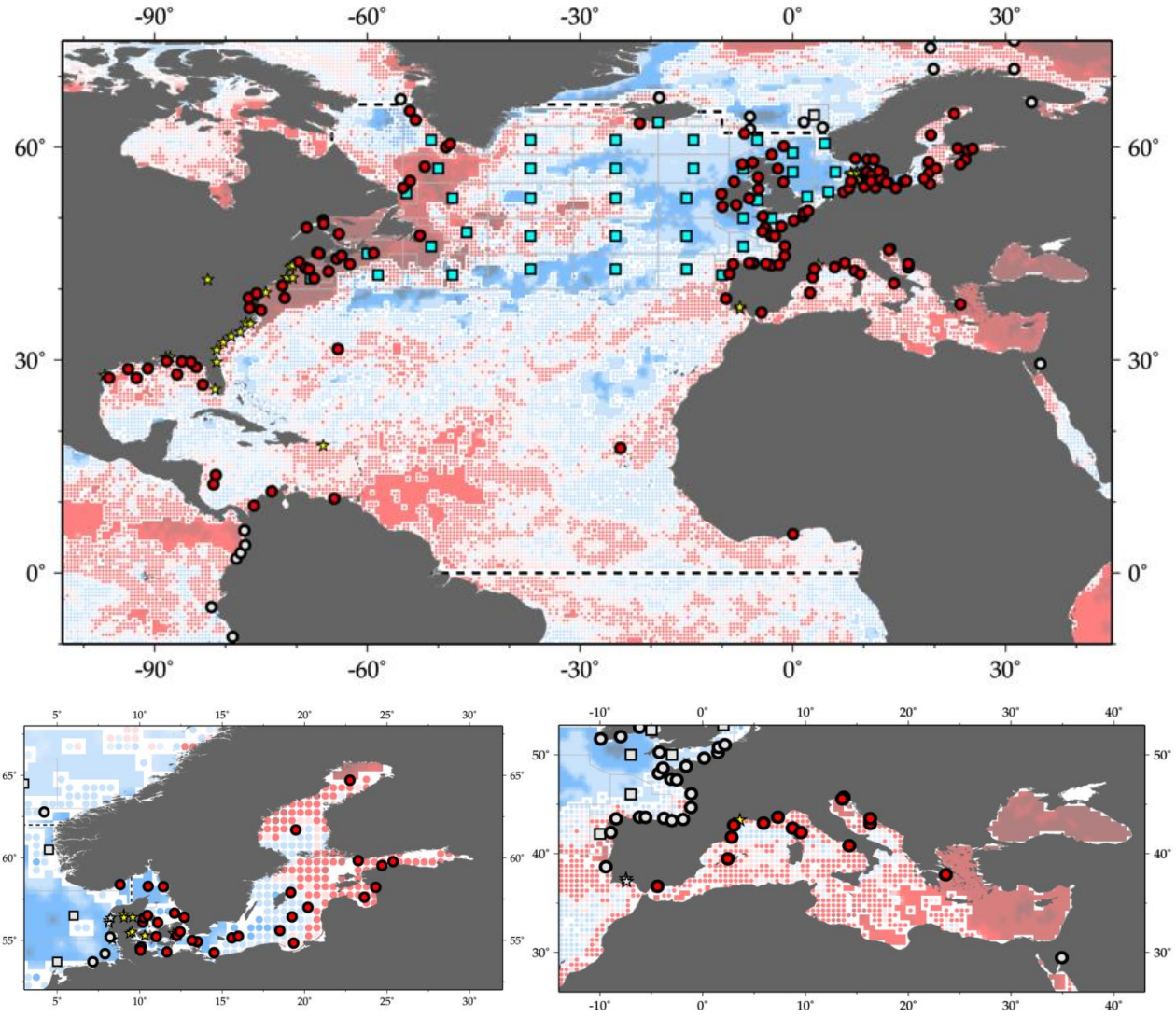

Figure 4.1. Map of IGMETS-participating North Atlantic time series, with zoomed insets for the Baltic Sea and Mediterranean Sea, on a background of a 10-year time-window (2003–2012) sea surface temperature trends (see also Figures 4.3, 4.8, and 4.9). At the time of this report, the North Atlantic collection consisted of 211 time series (coloured symbols of any type), of which 39 were from Continuous Plankton Recorder subareas (blue boxes), and 37 were from estuarine areas (yellow stars). Dashed lines indicate boundaries between IGMETS regions. Uncoloured (gray) symbols indicate time series being addressed in a different regional chapter (e.g. Arctic Ocean, South Pacific). See Tables 4.3–4.5 for a listing of this region's participating sites. Additional information on the sites in this study is presented in the Annex.

Participating time-series investigators

Eric Abadie, Jose L. Acuna, M. Teresa Alvarez-Ossorio, Anetta Ameryk, Jeff Anning, Elvire Antajan, Georgia Asimakopoulou, Yrene Astor, Angus Atkinson, Hermann Bange, Ana Barbosa, Nick Bates, Beatrice Bec, Radhouan Ben-Hamadou, Claudia Benitez-Nelson, Antonio Bode, Maarten Boersma, Angel Borja, Eileen Bresnan, Juan Bueno, Craig Carlson, Jacob Carstensen, Gerardo Casas, Claudia Castellani, Jacky Chauvin, Luis Chicharo, Epaminondas Christou, Nathalie Cochennec-Laureau, Amandine Collignon, Yves Collos, Kathryn Cook, Dolores Cortes, Joana Cruz, Maurizio Ribera D'Alcalà, Alejandro de la Sota, Alessandra de Olazabal, Laure Devine, Emmanuel Devred, Iole Di Capua, Rita Domingues, Anne Doner, Antonina dos Santos, Joerg Dutz, Martin Edwards, Joao Pedro Encarnacao, Luisa Espinosa, Tone Falkenhaug, Ana Faria, Maria Luz Fernandez de Puelles, Susana Ferreira, Bjorn Fiedler, James Fishwick, Serena Fonda-Umani, Almudena Fontan, Janja France, Javier Franco, Eilif Gaard, Peter Galbraith, Helena Galvao, Pep Gasol, Astthor Gislason, Anne Goffart, Renata Goncalves, Rafael Gonzalez-Quiros, Gabriel Gorsky, Annika Grage, Hafsteinn Gudfinnsson, Kristinn Gudmundsson, David Hanisko, Jon Hare, Roger Harris, Erica Head, Jean-Henri Hecq, Anda Ikauniece, Arantza Iriarte, Solva Jacobsen, Marie Johansen, Catherine Johnson, Jacqueline Johnson, Kevin Kennington, Georgs Kornilovs, Arne Kortzinger, Alexandra Kraberg, Nada Krstulovic, Aitor Laza-Martinez, Alain Lefebvre, Sirpa Lehtinen, Maiju Lehtiniemi, William Li, Priscilla Licandro, Michael Lomas, Christophe Loots, Angel Lopez-Urrutia, Laura Lorenzoni, Francesca Margiotta, Piotr Margonski, Jennifer Martin, Daniele Maurer, Maria Grazia Mazzocchi, Jesus M. Mercado, Claire Méteigner, Ana Miranda, Pedro Morais, Patricija Mozetic, Teja Muha, Frank Muller-Karger, Florence Nedelec, Vanessa Neves, Lena Omli, Emma Orive, Hans Paerl, Kevin Pauley, S.A. Pedersen, Ben Peierls, Pierre Pepin, Myriam Perriere Rumebe, Tim Perry, David Pilo, Sophie Pitois, Stephane Plourde, Arno Pollumae, Dwayne Porter, Lutz Postel, Nicole Poulton, A. Miguel P. Santos, Andy Rees, Michael Reetz, Beatriz Reguera, Jasmin Renz, Mickael Retho, Marta Revilla, M. Carmen Rodriguez, Gunta Rubene, Tatiana Rynearson, Rafael Salas, Danijela Santic, Diana Sarno, Michael Scarratt, Renate Scharek, Mary Scranton, Sergio Seoane, Stefanija Sestanovic, Mike Sieracki, Joe Silke, Ioanna Siokou-Frangou, Milijan Sisko, Tim Smyth, Mladen Solic, Dominique Soudant, Jeff Spry, Michel Starr, Deborah Steinberg, Lars Stemmann, Rowena Stern, Solvita Strake, Patrik Stromberg, Glen Tarran, Gordon Taylor, Maria Alexandra Teodosio, Robert Thunell, Valentina Tirelli, Ibon Uriarte, Luis Valdés, Victoriano Valencia, Marta M. Varela, Olja Vidjak, Fernando Villate, Norbert Wasmund, George Wiafe, Claire Widdicombe, Karen H. Wiltshire, Malcolm Woodward, Lidia Yebra, Cordula Zenk, Soultana Zervoudaki, and Adriana Zingone

This chapter should be cited as: Bode, A., Bange, H. W., Boersma, M., Bresnan, E., Cook, K., Goffart, A., Isensee, K., *et al.* 2017. North Atlantic Ocean. *In* What are Marine Ecological Time Series telling us about the ocean? A status report, pp. 55–82. Ed. by T. D. O'Brien, L. Lorenzoni, K. Isensee, and L. Valdés. IOC-UNESCO, IOC Technical Series, No. 129. 297 pp.

4.1 Introduction

The North Atlantic Ocean represents 46 million km² of the global ocean. This region (Figure 4.1) is characterized by unique geomorphological features that greatly affect water circulation and oceanographic processes, showing an asymmetry in surface temperature fields and currents that have no homologues in other ocean basins (Worthington, 1986; Marshall *et al*., 2001). In the North Atlantic, surface circulation at mid-latitudes is dominated by the Gulf Stream (Figure 4.2). This current veers off the American continent around Cape Hatteras (34°N). A divergence of this current around 40°N creates the southeasterly flow of the Azores Current and the northeasterly flow of the North Atlantic Current, both contributing to the gyre circulation in the central basin. The whole current system greatly influences heat flow and transport of water in the entire North Atlantic basin. The protuberance of Brazil and the Guianas in South America produces an asymmetry in the westward flow of the trade winds, allowing the flow of equatorial surface waters into the North Atlantic and eventually into the Gulf Stream and northern waters. The influence of the tropical heat carried by these waters extends northward of 60°N off Iceland. Restrictions to the bottom circulation imposed by the Mid-Atlantic Ridge topography also induce an asymmetry in the circulation between the eastern and western subbasins, thus causing measurable differences in the corresponding marine ecosystems (Longhurst, 2007).

The North Atlantic is one of the main regions of origin of deep ocean water. The North Atlantic Deep Water (NADW) is composed of several water masses formed by the winter cooling of surface waters at high latitudes. It is subsequently modified by deep convection and also by overflow of dense water across the Greenland–Iceland–Scotland Ridge (Dickson and Brown, 1994). In the North Atlantic, there are also several semi-enclosed seas (marginal seas) with specific oceanographic conditions, including the Caribbean Sea and Gulf of Mexico, Mediterranean, Black Sea, North Sea, and Baltic Sea.

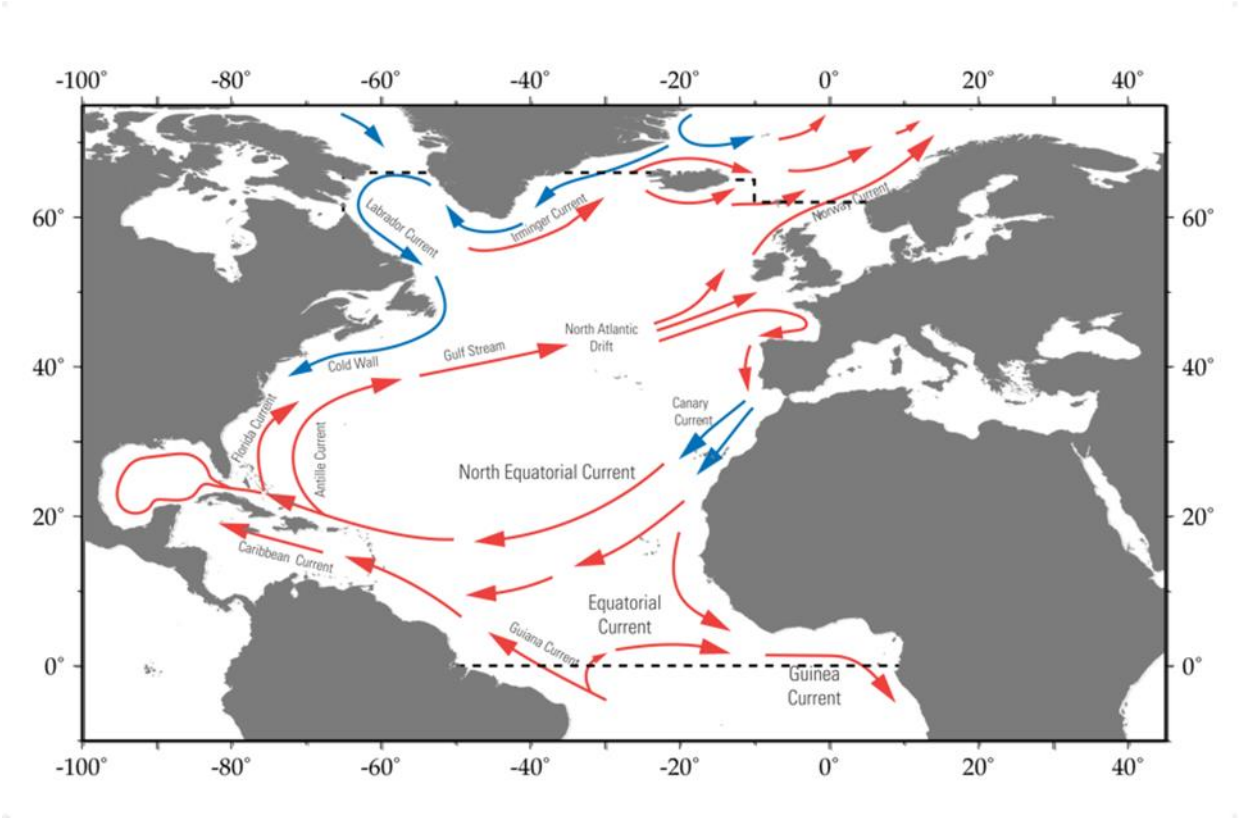

Figure 4.2. Schematic of major current systems in the IGMETS-defined North Atlantic region. Red arrows indicate generally warmer water currents; blue arrows indicate generally cooler water currents.

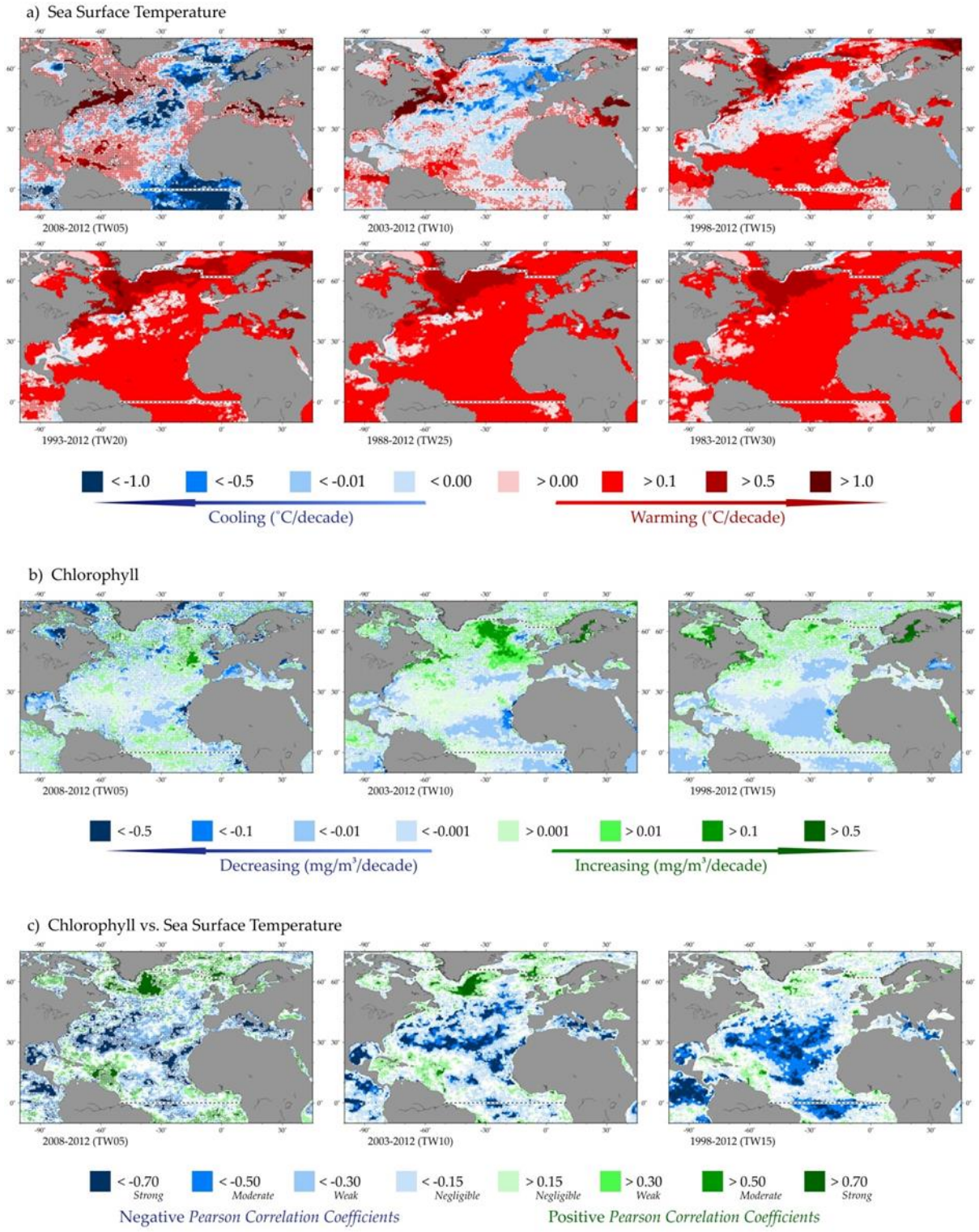

Figure 4.3. Annual trends in North Atlantic region (a) sea surface temperature (SST), (b) sea surface chlorophyll (CHL), and (c) correlations between CHL and SST for each of the standard IGMETS time-windows. See "Methods" chapter for a complete description and methodology behind this figure.

The general oceanography of the North Atlantic can be affected, but also affects the climatic index known as North Atlantic Oscillation (NAO), which is measured as variations in atmospheric pressure fields over the basin. The NAO influences the fluxes of heat and water, including precipitation, with important consequences for most ecosystem components (Hurrell and Dickson, 2004). However, there are additional climatic drivers modulating or even compensating the effects of the NAO at regional or local scale (Hemery *et al*., 2008). The North Atlantic shows periodic changes in surface temperature fields that are tracked as the Atlantic Multidecadal Oscillation (AMO, Knudsen *et al*., 2011), with measurable effects on ecosystems (Hernández-Fariñas *et al*., 2014).

In this chapter, we describe the main patterns derived from analysis of ecological time series compiled by IGMETS during 1983–2012 to illustrate some of the variability of marine ecosystems at multiannual and regional scales. More detailed tables and maps can be accessed in the interactive IGMETS Explorer:

http://igmets.net/explorer/

4.2 General patterns of temperature and phytoplankton biomass

Time series of gridded, large-scale observations derived from reanalysed *in situ* and satellite data (Reynolds OIv2-SST and OCCCI-Chl, see "Methods" chapter) indicated a general warming paralleled by a decrease in phytoplankton biomass. These trends were consistent across various time-windows (Table 4.1, Figure 4.3). Warming at a rate of 0.1–0.5°C decade^{-1} was significant for 86% of the region for the 30-year time-period (1983–2012), while during short time-periods, regional variability became increasingly important (Figure 4.3a). Indeed, some regions, such as the Mediterranean Sea, were almost completely affected by warming. Notwithstanding this general trend, local cooling was observed in the eastern and central Atlantic when considering recent years (10- and 5-year time-windows).

In contrast to the SST trends, changes in chlorophyll were more heterogeneous and, considering the 15-year time-window, the general decrease of up to 0.01 mg Chl *a* m^{-3} decade^{-1} observed was only significant for 38% of the region (Table 4.2). However, changes in enclosed seas affected over a larger area, as in the Mediterranean, or were completely divergent from the general trend, as occurred in the Baltic where surface chlorophyll increased >0.5 mg Chl *a* m^{-3} decade^{-1} in the 10- and 15-year time-windows (Figure 4.3b). In all cases, the spatial patchiness in the trends increased in the analysis of shorter time-windows, likely as a result of local drivers. For example, when comparing the 10- and 5-year time-windows for SST (Figure 4.3a), some regions showed reversed trends, such as the Caribbean (which cooled over the 10-year time-window, but warmed over the 5-year window). The same occurred with satellite-derived chlorophyll, particularly in the Northwest Atlantic where it decreased over the 5-year time-window, but showed an increasing trend for the 10-year period (Figure 4.3b). Nevertheless, over the past 15 years, there has been a consistent increase in surface chlorophyll over most of the continental margins and the open North Atlantic (north of 50°N), while there was a decrease in the central regions of the North Atlantic (Figure 4.3b).

Warming was negatively correlated with chlorophyll in most of the region (Figure 4.3c), including the subtropical gyre and marginal seas (Caribbean and Mediterranean), but there was a positive correlation between SST and chlorophyll in some regions, such as at East Greenland and the subpolar North Atlantic. At the longest time-window considered (15-year time-window), there was a distinct latitudinal difference in the correlations, with most of the area located south of 50°N showing negative correlations both variables. Not excluding direct effects of temperature on the physiological processes of phytoplankton, these relationships also support a key role of stratification as the driver of changes in phytoplankton production either by limiting the input of nutrients from deep layers in already stratified regions (Behrenfeld *et al*., 2015) or by enhancing the access of phytoplankton to light in already mixed waters (Tremblay and Gagnon, 2009).

Table 4.1. Relative spatial areas (% of the total region) and rates of change within the North Atlantic region (including the Baltic Sea and Mediterranean Sea) region that are showing increasing or decreasing trends in sea surface temperature (SST) for each of the standard IGMETS time-windows. Numbers in brackets indicate the % area with significant ($p < 0.05$) trends. See "Methods" chapter for a complete description and methodology used.

Latitude-adjusted SST data field surface area = 46.1 million km²	**5-year** (2008–2012)	**10-year** (2003–2012)	**15-year** (1998–2012)	**20-year** (1993–2012)	**25-year** (1988–2012)	**30-year** (1983–2012)
Area (%) w/ increasing SST trends ($p < 0.05$)	**52.5%** (*13.3%*)	**50.3%** (*14.6%*)	**76.8%** (*54.8%*)	**95.7%** (*87.4%*)	**98.1%** (*95.0%*)	**99.1%** (*97.3%*)
Area (%) w/ decreasing SST trends ($p < 0.05$)	47.5% (*18.6%*)	49.7% (*15.5%*)	23.2% (*7.1%*)	4.3% (*1.1%*)	1.9% (*0.6%*)	0.9% (*0.3%*)
> 1.0°C decade^{-1} warming ($p < 0.05$)	13.5% (*8.1%*)	3.4% (*3.3%*)	0.9% (*0.9%*)	0.7% (*0.7%*)	0.1% (*0.1%*)	0.0% (*0.0%*)
0.5 to 1.0°C decade^{-1} warming ($p < 0.05$)	18.0% (*4.6%*)	5.0% (*4.1%*)	5.4% (*5.4%*)	10.0% (*10.0%*)	9.2% (*9.2%*)	6.7% (*6.7%*)
0.1 to 0.5°C decade^{-1} warming ($p < 0.05$)	17.0% (*0.6%*)	27.3% (*7.1%*)	**56.3%** (*47.4%*)	**77.1%** (*74.3%*)	**83.3%** (*82.5%*)	**86.7%** (*86.4%*)
0.0 to 0.1°C decade^{-1} warming ($p < 0.05$)	4.1% (*0.0%*)	14.6% (*0.2%*)	14.2% (*1.2%*)	8.0% (*2.4%*)	5.4% (*3.2%*)	5.6% (*4.2%*)
0.0 to –0.1°C decade^{-1} cooling ($p < 0.05$)	3.9% (*0.0%*)	13.1% (*0.1%*)	10.0% (*0.2%*)	2.6% (*0.1%*)	1.3% (*0.1%*)	0.7% (*0.1%*)
–0.1 to –0.5°C decade^{-1} cooling ($p < 0.05$)	13.3% (*0.7%*)	29.2% (*8.7%*)	12.4% (*6.1%*)	1.4% (*0.8%*)	0.6% (*0.4%*)	0.2% (*0.1%*)
–0.5 to –1.0°C decade^{-1} cooling ($p < 0.05$)	15.7% (*6.6%*)	6.7% (*6.1%*)	0.7% (*0.6%*)	0.2% (*0.2%*)	0.1% (*0.1%*)	0.0% (*0.0%*)
> –1.0°C decade^{-1} cooling ($p < 0.05$)	14.6% (*11.3%*)	0.6% (*0.6%*)	0.2% (*0.2%*)	0.0% (*0.0%*)	0.0% (*0.0%*)	0.0% (*0.0%*)

4.3 Trends from *in situ* time series

The North Atlantic is home to the largest fraction of *in situ* marine ecological time series globally, though most of them are clustered around continental margins, many in coastal waters (Table 4.3). The distribution of sites is also skewed to the temperate regions of the basin, with very few stations located in subtropical and tropical waters (Figure 4.4). Nevertheless, the data obtained still serve as an invaluable tool to examine the consistency between local and regional changes in environmental and plankton variables. Trends in *in situ* SST match well those derived by satellite. For the 10-year time-window, both *in situ* observations and gridded values showed almost an equivalent number of cases of increasing and decreasing trends (Table 4.2, Figure 4.5). This equivalence indicates that it is not possible to determine a regional coherent trend for this time-window, highlighting the importance of local heterogeneity in the responses of individual variables to climate.

The increasing SST trends tended to dominate in the 20- and 30-year analysis periods (Figure 4.5). Conversely, negative trends in oxygen and nutrients, as exemplified by nitrate, were more frequent over these time-windows. However, given the uneven distribution of *in situ* time series, no clear trend in chemical variables was evident at a basin-scale. For example, during 2003–2012, nitrate increased in most coastal locations across the Northeast Atlantic and in some locations in the northwest subbasin, such as the southern Bay of Biscay and Helgoland, while it decreased at some locations in the Baltic Sea and at the two sites available for the Mediterranean (Figure 4.4). Considering all the compiled time series, even those with shorter dataperiods, the number of series showing increasing trends in phytoplankton slightly exceeded those with decreasing trends, but particularly over long time windows (> 20 years; Figure 4.5). Sites with decreasing phytoplankton were

found in waters north of 50°N, in the southern Bay of Biscay and in the northern Mediterranean (Figure 4.4). Similarly, most sites recorded increases in diatoms (but not in dinoflagellates) in time-windows exceeding 20 years, but, conversely, dinoflagellates increased in periods < 10 years (Figure 4.5).

Consequently, the trends in the ratio diatom/dinoflagellate changed from negative to positive when extending the time-window from 5 to 30 years. Increasing trends in zooplankton also exceeded 50% of available time series over short time-windows (< 10 years), but their frequency decreased for time-windows > 10 years and even switched to a negative-trend dominance for some periods, suggesting an uncoupling with the trends in phytoplankton (Figure 4.5). During 2003–2012, sites with increasing zooplankton were sometimes associated with decreasing phytoplankton, as observed in ocean waters east of Greenland and in some locations on the continental shelf area south of Newfoundland, but there were also examples of zooplankton decreases and a concomitant increase in phytoplankton, e.g. along the coast of North America (Figure 4.4).

The asymmetry in the trends observed can be illustrated by comparing the differences among time series in the marginal seas, such as the Baltic and Mediterranean (Figures 2.6b,c). We will only consider the 5-year time-window (2008–2012) for this example because it contains the largest number of time series. Over this time-window, there was a clear dominance of positive trends in zooplankton and dinoflagellates for the North Atlantic basin as a whole (Figure 4.5a). For time series not included in marginal seas (Figure 4.6a), this pattern was not observed for oxygen, but still holds for zooplankton and dinoflagellates. In the Baltic, trends were mostly characterized by a cooling and decrease in phytoplankton, most notably diatoms (Figure 4.6b). Interestingly, the change in the phytoplankton community indicated by a decrease in the value of the diatom/dinoflagellate ratio was apparently similar in the North Atlantic proper and in the Baltic, but in the former case, the change

Table 4.2. Relative spatial areas (% of the total region) and rates of change within the North Atlantic region (including the Baltic Sea and Mediterranean Sea) that are showing increasing or decreasing trends in phytoplankton biomass (CHL) for each of the standard IGMETS time-windows. Numbers in brackets indicate the % area with significant ($p < 0.05$) trends. See "Methods" chapter for a complete description and methodology used.

Latitude-adjusted CHL data field surface area = 46.1 million km^2	**5-year** (2008–2012)	**10-year** (2003–2012)	**15-year** (1998–2012)
Area (%) w/ increasing CHL trends ($p < 0.05$)	30.2% (*3.6%*)	43.9% (*14.4%*)	38.0% (*12.7%*)
Area (%) w/ decreasing CHL trends ($p < 0.05$)	**69.8%** (*25.0%*)	**56.1%** (*28.2%*)	**62.0%** (*38.3%*)
> 0.50 mg m^{-3} decade^{-1} increasing ($p < 0.05$)	0.8% (*0.2%*)	1.2% (*1.0%*)	2.3% (*2.2%*)
0.10 to 0.50 mg m^{-3} decade^{-1} increasing ($p < 0.05$)	5.7% (*1.7%*)	6.3% (*4.5%*)	4.1% (*3.4%*)
0.01 to 0.10 mg m^{-3} decade^{-1} increasing ($p < 0.05$)	14.9% (*1.6%*)	17.8% (*6.8%*)	16.6% (*5.9%*)
0.00 to 0.01 mg m^{-3} decade^{-1} increasing ($p < 0.05$)	8.7% (*0.0%*)	18.5% (*2.2%*)	15.1% (*1.2%*)
0.00 to –0.01 mg m^{-3} decade^{-1} decreasing ($p < 0.05$)	11.0% (*0.4%*)	18.4% (*3.9%*)	30.4% (*15.3%*)
–0.01 to –0.10 mg m^{-3} decade^{-1} decreasing ($p < 0.05$)	40.8% (*15.0%*)	33.1% (*21.2%*)	30.5% (*22.3%*)
–0.10 to –0.50 mg m^{-3} decade^{-1} (decreasing) ($p < 0.05$)	13.5% (*6.6%*)	3.8% (*2.4%*)	1.0% (*0.7%*)
> –0.50 mg m^{-3} decade^{-1} (decreasing) ($p < 0.05$)	4.4% (*3.0%*)	0.9% (*0.7%*)	0.0% (*0.0%*)

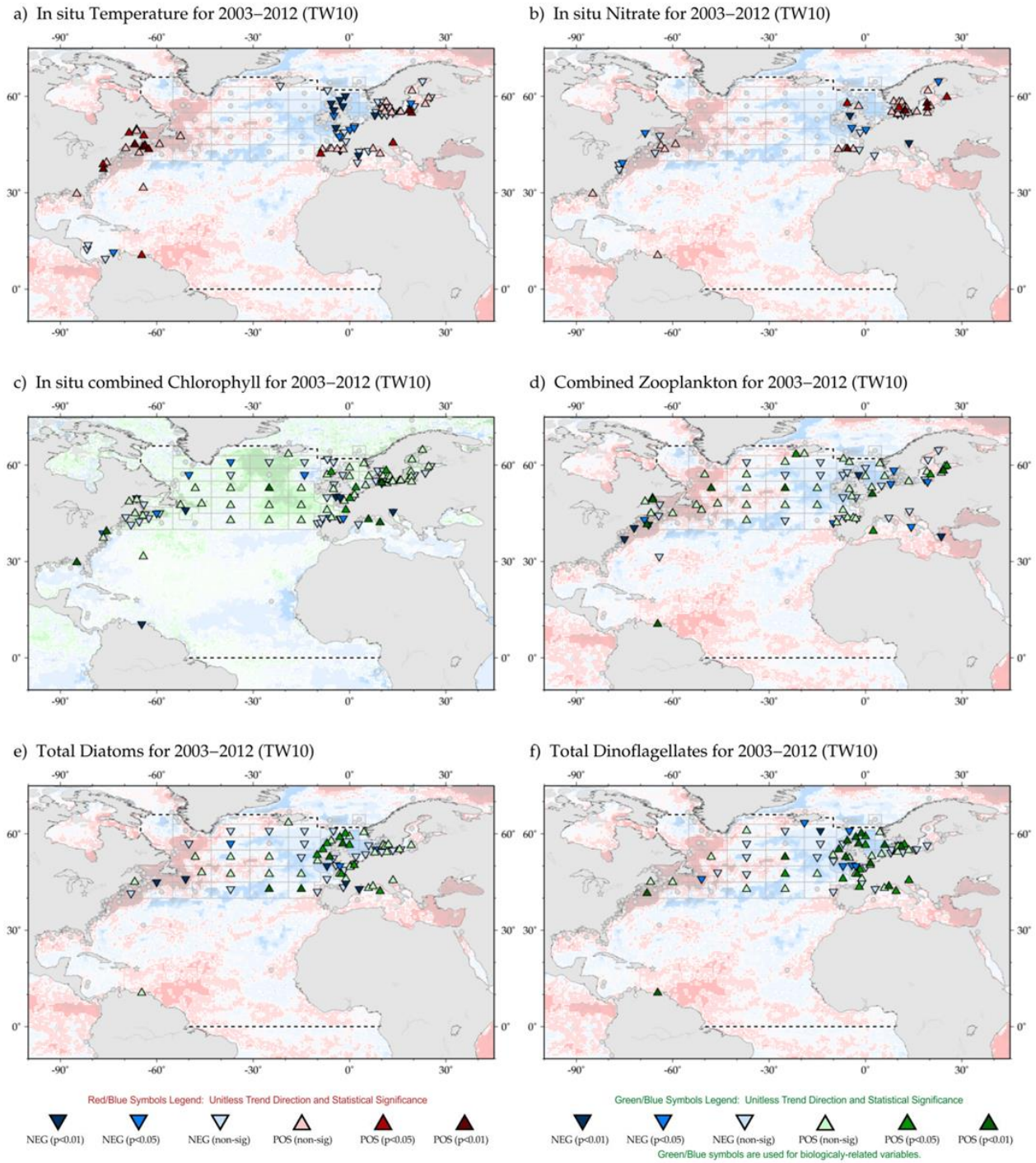

Figure 4.4. Map of North Atlantic region time-series locations and trends for select variables and IGMETS time-windows. Upward-pointing triangles indicate positive trends; downward triangles indicate negative trends. Gray circles indicate time-series site that fell outside of the current study region or time-window. Additional variables and time-windows are available through the IGMETS Explorer (http://IGMETS.net/explorer). See "Methods" chapter for a complete description and methodology used.

was due to an increase in dinoflagellates, while in the latter, it was caused by a decrease in diatoms. In contrast with the changes in the North Atlantic proper, the Mediterranean showed no change in SST, a decrease in nitrate, and an increase in all phytoplankton groups (Figure 4.6c). It is important to note that stations in the Mediterranean are located in coastal waters (see Figure 4.4), and these observations cannot be extrapolated to open Mediterranean waters.

A first examination of potential causal factors of these trends can be provided by the pairwise correlation of time-series, as exemplified for the 10-year time-window (Figure 4.7). Changes in Reynolds SST trends were well represented in nearly all *in situ* series, with a few exceptions (Figure 4.4). Over this 10-year time-window, only oxygen and dinoflagellates varied inversely with SST (Figure 4.7a).

In contrast, satellite-derived chlorophyll appeared more clearly associated with changes in *in situ* plankton variables, as shown by the positive correlations with phytoplankton and zooplankton series (Figure 4.7c). However, it is difficult to generalize about these relationships as there is large heterogeneity throughout the North Atlantic. For example, during 2003–2012, there was an equivalent number of marine ecological time series showing positive and negative correlations between some *in situ* phytoplankton variables (e.g. the abundance of diatoms or the diatom/dinoflagellate ratio) and satellite chlorophyll (Figure 4.7c), suggesting divergent changes in pigment content or cell size.

It must also be noted that only a small fraction of the correlations were significant (for more details, see the IGMETS Explorer), and that there are still large regions of the North Atlantic, particularly in subtropical and tropical regions, that were not covered by *in situ* time-series observations, as they do not exist or were not appropriate for the purpose of IGMETS. In addition, these correlations also vary at different time-scales, as indicated by the increase in the proportion of positive trends in most variables with increasing time-window (Figure 4.5).

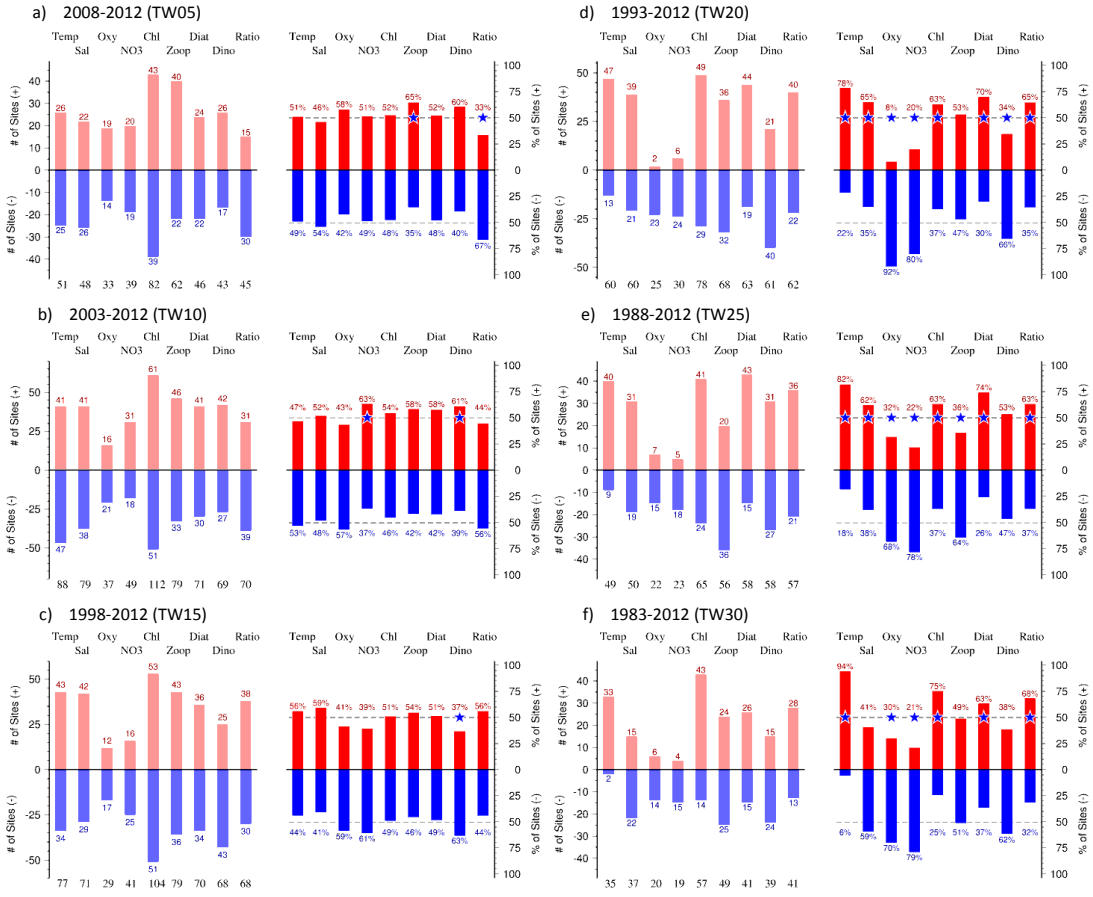

Figure 4.5. Absolute (left) and relative (%, right) frequency of positive and negative trends in selected variables from *in situ* time series in the North Atlantic region computed for different IGMETS time-windows. The 50% relative frequency is indicated by dashed lines in the right panels. A star symbol on this dashed line indicates that the trend was statistically different ($p < 0.05$) from 50%. See "Methods" chapter for a complete description and methodology used.

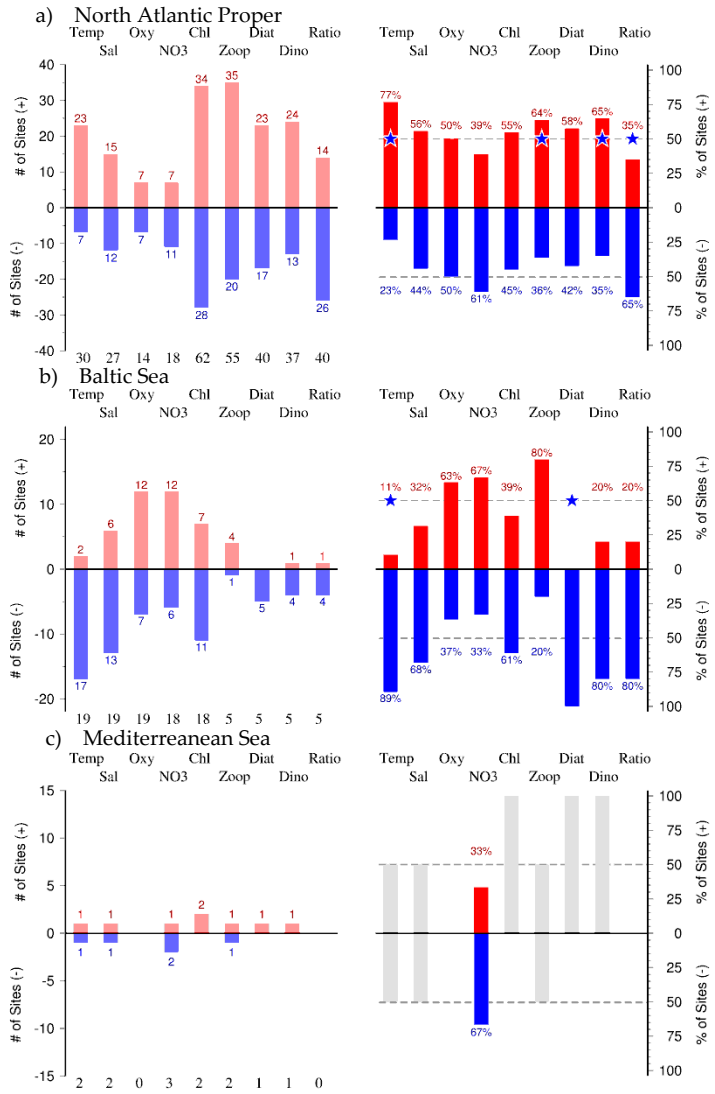

Figure 4.6. Absolute (left) and relative (%, right) frequency of positive and negative trends in variables from *in situ* time-series in the North Atlantic proper, a) excluding semi-enclosed seas, b) Baltic, and c) Mediterranean seas computed for a 5-year time-window. The 50% relative frequency is indicated by dashed lines in the right panels. See "Methods" chapter for a complete description and methodology used.

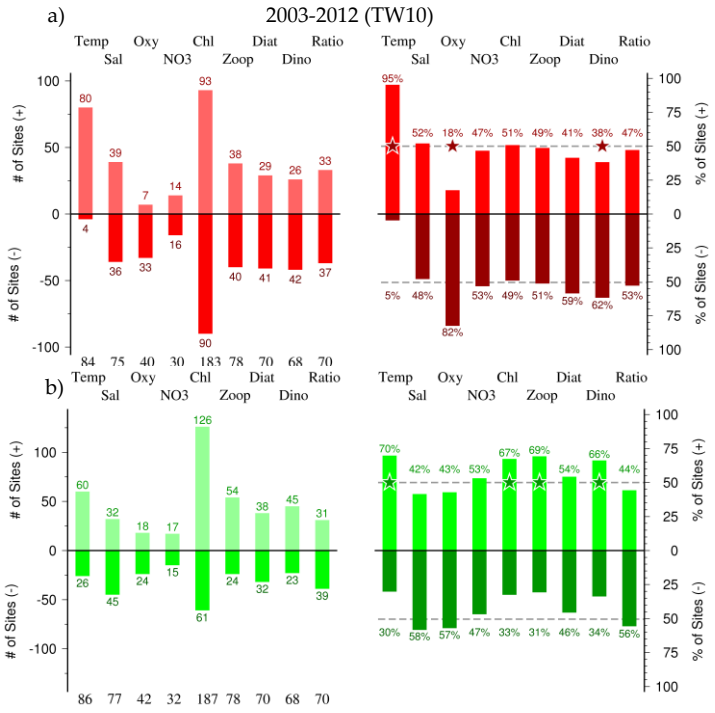

Figure 4.7. Absolute (left) and relative (%, right) frequency of positive and negative correlations between selected *in situ* North Atlantic time-series variables and corresponding gridded SST (red bars – a) and chlorophyll (green bars – b) for the 10-year time-window (2002–2012). The 50% relative frequency is indicated by dashed lines in the right panels. A star symbol on this dashed line indicates that the trend was statistically different ($p < 0.05$) from 50%. See "Methods" chapter for a complete description and methodology used.

4.4 Consistency with previous analysis

Previous analyses of trends in oceanographic variables over the North Atlantic, some using time-series data collected by IGMETS, already showed some of the changes illustrated here. The increasing warming trends in the North Atlantic are some of the most repeated examples of global change in the ocean (Levitus *et al*., 2000; Hoegh-Guldberg *et al*., 2014). These changes were related to various climate forcings over the North Atlantic basin, highlighting the role of multidecadal oscillations and other natural phenomena (Hurrell *et al*., 2009; Knudsen *et al*., 2011). There is evidence that spring blooms initiated later than average in the mid-1980s, but earlier in the 1990s due to fluctuations in the NAO over the central North Atlantic (Zhai *et al*., 2013). Different trends in SST are expected, driven by changes in upwelling intensity along the eastern margin of the North Atlantic (the Canary–Iberian upwelling system). Some authors indicate that upwelling in this region is either decreasing (Pardo *et al*., 2011, Santos *et al*., 2012) or increasing (McGregor *et al*., 2007). Benazzouz *et al*. (2015) suggest that, in contrast to other upwelling regions, recent increases in wind intensity in the Canary–Iberian upwelling system may lead to upwelling of warm waters at the regional level, and at the same time, this may allow for an increase in local primary production (Demarcq and Benazzouz, 2015). The divergent trends in SST and other variables observed in local time series in the southern Bay of Biscay (Figure 4.4) may be an indication of small-scale interaction between regional and local factors. More long-term ecological observations along the subtropical eastern North Atlantic are needed in order to improve the analysis of changes in upwelling and their consequences for ecosystems.

Large changes in North Atlantic ecosystems resulted in regime shifts over long time-periods. The regime shifts that occurred in the North Sea and adjacent regions were well studied, as the consequences affected many ecosystem components (McQuatters-Gollop *et al*., 2007; Reid *et al*., 2010; Beaugrand *et al*., 2015). There were also regime shifts identified in other regions both in the eastern (Hatun *et al*., 2009) and western basins (Plourde *et al*., 2014; Meyer-Gutbrod *et al*., 2015) that affected plankton and also upper trophic-level consumers. While the time-window approach selected in this first IGMETS analysisi is not well suited to identify regime shifts, the large intraregional variability in these regime shifts calls for more comparative analysis to understand the scale-dependent dynamics of climate effects (Fisher *et al*., 2015). Changes in nutrient inputs were addressed mainly as consequence of oceanographic variability in water masses and anthropogenic inputs (Llope *et al*., 2007; Heath and Beare, 2008; Pérez *et al*., 2010), often with divergent trends that were difficult to untangle without a good geographic distribution of *in situ* observations.

The general decrease observed in satellite chlorophyll in the North Atlantic (Table 4.1) has already been noted in previous studies (Boyce *et al*., 2014). Behrenfeld *et al*. (2015) suggested that this may result from physiological adaptations related to thermal stratification rather than a true decrease in primary production. There are areas that exhibit an increase in satellite chlorophyll (e.g. most of the non-subtropical North Atlantic and subarctic waters). Local series of coastal phytoplankton biomass often reflect the interaction of several factors, as exemplified in the study of the effects of wind and water temperature on nutrient replenishment and phytoplankton dynamics during the winter– spring period between 1979 and 2011 in the northern Mediterranean (Goffart *et al*., 2015). Analysis of primary production observations has pointed out the large heterogeneity in local responses (Bode *et al*., 2011), and several studies have also shown a shift in the relative dominance of diatoms, dinoflagellates, and other phyotplankton groups (Leterme *et al*., 2006; O'Brien *et al*., 2012; Suikkanen *et al*., 2013). Recently, underlying changes at the species-specific level have been highlighted, which ultimately affect the composition of phytoplankton communities (Hinder *et al*., 2012; Bode *et al*., 2015). These observations stress the value and need of *in situ* marine ecological time series; most of the changes observed have been identified by using detailed species composition, data than can only be provided by *in situ* time series.

While the long-term (30-year time-window) trends presented in this study are in general agreement with results from previous studies using remote sensing data, time-series measurements from individual stations as well as climatological fields, the interpretation of patterns observed with the selected time-windows must be made with caution. For example, the Baltic Sea shows long-term trends in increasing water temperatures (i.e. warming), decreasing oxygen (i.e. deoxygenation), and decreasing nitrate (i.e. reduced eutrophication). However, the results for the 5-year time-window (Figure 4.6) reveal a statistically significant majority of trends with opposite signs for water temperature and oxygen concentrations, which, in turn, imply cooling and increasing

oxygen concentrations during 2008–2012. These apparent differences between short- and long-term trends can be attributed to the choice of time-window and, of course, do not imply regime shifts and reversals of the observed long-term trends.

Similarly, direct comparison of trends in concurrently measured variables may lead to misinterpretations. Time-series measurements of nitrate in the surface layer of the Baltic Sea show maximum concentrations during the late 1980s, but the input of nitrate to the Baltic Sea has subsequently been reduced drastically and has resulted in a significant decrease in nitrate surface concentrations in some basins (Feistel *et al*., 2008; HELCOM, 2009, 2014). However, chlorophyll *a* trends still show no signs of decrease or have even increased in recent years in some Baltic Sea basins. The long residence time of water as well as phosphorus release from anoxic sediments in combination with blooms of nitrogen fixing cyanobacteria have been identified as slowing the decrease in eutrophication in the Baltic Proper. The obvious paradox of ongoing oxygen loss despite decreasing eutrophication in the coastal regions of the Baltic Sea has been attributed to warming-induced enhanced organic matter respiration in combination with an extended period of water-column stratification (Lennartz *et al*., 2014). In contrast, Carstensen *et al*. (2014) showed that ongoing eutrophication is still the main reason for the observed long-term trend in enhanced oxygen loss in the deep basins of the Baltic Proper.

The effects of climate and oceanographic changes in temperature and circulation affecting nutrient inputs and displacement of plankton are more difficult to trace through the foodweb, as there is a mixture of direct and indirect effects affecting the different trophic levels. This can cause mismatches between observed trends, such as those of phytoplankton and zooplankton at different time-windows (Figure 4.4) and shown by previous studies (Richardson and Schoeman, 2004; McGinty *et al*., 2012).

4.5 Conclusions

The first comprehensive analysis of *in situ* time series provided by IGMETS in the North Atlantic revealed that, despite being the most studied region of the global ocean, there are large areas in this region still not covered by multidisciplinary *in situ* observations. Most of the time series are located in areas very close to the coasts; even in regions well covered by regular observations, such as north of the subtropical gyre, there is no physical (e.g. temperature, salinity) or chemical (e.g. oxygen, nutrients) information to match the biological data. The analysis of existing time series revealed that, even in adjacent areas that appear to be relatively homogenous, there is large variability in ecosystem behaviour over time as observed in the continental shelves at both sides of the North Atlantic.

Table 4.3 Time-series sites located in the IGMETS North Atlantic (not including Baltic Sea and Mediterranean Sea) region. Participating countries: Canada (ca), Colombia (co), Germany (de), Denmark (dk), Spain (es), Faroe Islands (fo), France (fr), Ireland (ie), Isle of Man (im), Iceland (is), Norway (no), Portugal (pt), United Kingdom (uk), United States (us), and Venezuela (ve). Year-spans in red text indicate time series of unknown or discontinued status. IGMETS-IDs in red text indicate time series without a description entry in Annex 2.

No.	IGMETS-ID	Site or programme name	Year-span	T	S	Oxy	Ntr	Chl	Mic	Phy	Zoo
1	ca-50101	AZMP Halifax Line 2 *(Scotian Shelf)*	1997–present	X	-	-	-	X	-	-	X
2	ca-50102	AZMP Prince 5 *(Bay of Fundy)*	1999–present	X	-	-	-	X	-	-	X
3	ca-50201	AR7W Zone 1 *(Labrador Shelf)*	1996–present	X	X	-	-	X	-	-	X
4	ca-50202	AR7W Zone 2 *(Labrador Slope)*	1996–present	X	X	-	-	X	-	-	X
5	ca-50203	AR7W Zone 3 *(Central Labrador Sea)*	1996–present	X	X	-	-	X	-	-	X
6	ca-50204	AR7W Zone 4 *(Eastern Labrador Sea)*	1996–present	X	X	-	-	X	-	-	X
7	ca-50205	AR7W Zone 5 *(Greenland Shelf)*	1996–present	X	X	-	-	X	-	-	X
8	ca-50401	Bedford Basin *(Northwestern North Atlantic)*	1967–present	X	X	-	X	X	X	-	-
9	ca-50501	Bay of Fundy *(Northwestern Atlantic shelf)*	1988–2012 discontinued	X	X	-	-	X	-	X	-
10	ca-50601	AZMP Station 27 *(Newfoundland Shelf)*	1960–present	X	-	-	-	X	-	-	X
11	ca-50701	AZMP Anticosti Gyre *(Gulf of St Lawrence)*	1999–present	X	-	-	-	X	-	-	X
12	ca-50702	AZMP Gaspe Current *(Gulf of St Lawrence)*	1999–present	X	-	-	-	X	-	-	X
13	ca-50703	AZMP Rimouski *(Gulf of St Lawrence)*	2005–present	X	X	-	X	X	-	-	X
14	ca-50704	AZMP Shediac *(Gulf of St Lawrence)*	1999–present	X	X	-	X	X	-	-	X
15	ca-50801	Central Scotian Shelf *(Northwestern Atlantic shelf)*	1996–present	X	X	-	X	X	X	-	-
16	ca-50802	Eastern Scotian Shelf *(Northwestern Atlantic)*	1997–present	X	X	-	X	X	X	-	-
17	ca-50803	Western Scotian Shelf *(Northwestern Atlantic)*	1997–present	X	X	-	X	X	X	-	-
18	co-30101	REDCAM Isla de San Andres *(Southwestern Caribbean)*	2002–present	X	X	X	-	-	-	-	-
19	co-30102	REDCAM Isla de Provencia *(Southwestern Caribbean)*	2002–present	X	X	X	-	-	-	-	-

No.	IGMETS-ID	Site or programme name	Year-span	T	S	Oxy	Ntr	Chl	Mic	Phy	Zoo
20	co-30103	REDCAM Western Colombia–Caribbean Shelf *(Southwestern Caribbean)*	2002–present	X	X	X	-	-	-	-	-
21	co-30104	REDCAM Eastern Colombia–Caribbean Shelf *(Southwestern Caribbean)*	2002–present	X	X	X	-	-	-	-	-
22	de-10101	Nordeney WQ-W2 *(Southern North Sea)*	1999–2008 (?)	X	X	-	X	-	-	X	-
23	de-30201	Helgoland Roads *(Southeastern North Sea)*	1962–present	X	X	-	X	-	X	X	X
24	de-30301	Cape Verde Ocean Observatory *(Tropical Eastern North Atlantic)*	2006–present	X	X	X	X	-	-	-	-
27	dk-30101	North Sea: DNAMAP-1510007 *(Baltic Sea)* *see Baltic Sea Annex (A2)*	1989–present	X	X	X	X	X	-	X	-
28	dk-30105	Ringkobing Fjord: DNAMAP-1 *(Baltic Sea)* *see Baltic Sea Annex (A2)*	1980–present	X	X	X	X	X	-	X	-
29	dk-30106	Nissum Fjord: DNAMAP-22 *(Baltic Sea)* *see Baltic Sea Annex (A2)*	1983–present	X	X	X	X	X	-	X	-
30	dk-30107	Nissum Bredning: DNAMAP-3702-1 *(Baltic Sea)* *see Baltic Sea Annex (A2)*	1982–present	X	X	X	X	X	-	X	-
31	dk-30110	Lister Dyb: DNAMAP-3 *(Baltic Sea)* *see Baltic Sea Annex (A2)*	1993–present	X	X	X	X	X	-	X	-
32	es-30101	BILBAO 35 Time Series *(Inner Bay of Biscay)*	1998–present	X	X	X	-	X	-	-	X
33	es-30102	URDAIBAI 35 Time Series *(Inner Bay of Biscay)*	1997–present	X	Xs	X	-	X	-	-	X
34	es-30201	AZTI Station D2 *(Southeastern Bay of Biscay)*	1986–present	X	X	X	X	X	-	X	-
35	es-30401	Nervion River Estuary E1 *(Southern Bay of Biscay)*	2000–present	X	X	-	-	-	-	X	-
36	es-50101	RADIALES Santander Station 4 *(Southern Bay of Biscay)*	1991–present	X	X	*	X	*	*	-	X
37	es-50102	RADIALES A Coruna Station 2 *(Northwestern Iberian coast)*	1988–present	X	X	X	X	X	X	X	X
38	es-50103	RADIALES Gijon/Xixon Station 2 *(Southern Bay of Biscay)*	2001–present	X	X	*	X	X	X	X	X
39	es-50104	RADIALES Vigo Station 3 *(Northwest Iberian coast)*	1994–present	X	X	-	X	X	-	-	X
40	es-50105	RADIALES Cudillero Station 2 *(Southern Bay of Biscay)*	1992–present	X	X	X	X	X	*	-	X

No.	IGMETS-ID	Site or programme name	Year-span	T	S	Oxy	Ntr	Chl	Mic	Phy	Zoo
41	fo-30101	Faroe Islands Shelf *(Faroe Islands)*	1991–present	X	-	-	X	X	-	-	X
42	fr-50101	REPHY Antifer Ponton Petrolier *(English Channel)*	1989–present	X	X	X	X	X	-	X	-
43	fr-50102	REPHY At So *(English Channel)*	1987–present	X	X	-	X	X	-	X	-
44	fr-50103	REPHY Donville *(English Channel)*	2002–present	X	X	X	X	X	-	X	-
45	fr-50104	REPHY Pen al Lann *(English Channel)*	1987–present	X	X	X	-	X	-	X	-
46	fr-50105	REPHY Point 1 SRN Boulogne *(English Channel)*	1992–present	X	X	-	X	X	-	X	-
47	fr-50106	REPHY Kervel *(Bay of Biscay)*	1987–present	X	X	-	-	X	-	X	-
48	fr-50107	REPHY Le Cornard *(Bay of Biscay)*	1987–present	X	X	X	-	X	-	X	-
49	fr-50108	REPHY Men er Roue *(Bay of Biscay)*	1987–present	X	X	-	X	X	-	X	-
50	fr-50109	REPHY Ouest Loscolo *(Bay of Biscay)*	1987–present	X	X	-	X	X	-	X	-
51	fr-50110	REPHY Teychan Bis *(Bay of Biscay)*	1999–present	X	X	-	X	X	-	X	-
52	fr-50201	Gravelines Station *(English Channel)*	1993–present	-	-	-	-	-	-	-	X
53	ie-30101	East Coast Ireland *(Ireland)*	1990–present	-	-	-	-	-	-	X	-
54	ie-30102	Northwest Coast Ireland *(Ireland)*	1990–present	-	-	-	-	-	-	X	-
55	ie-30103	South Coast Ireland *(Ireland)*	1990–present	-	-	-	-	-	-	X	-
56	ie-30104	Southwest Coast Ireland *(Ireland)*	1990–present	-	-	-	-	-	-	X	-
57	ie-30105	West Coast Ireland (*Ireland*)	1990–present	-	-	-	-	-	-	X	-
58	im-10101	Cypris Station – Isle of Man *(Irish Sea)*	1954–2009 (?)	X	X	X	X	X	-	X	-
59	is-30102	Selvogsbanki Transect *(South Iceland)*	1971–present	X	X	-	-	X	-	-	X
60	no-50401	Arendal Station 2 *(North Sea)*	1994 – present	X	X	X	X	X	-	-	X
61	pt-30101	Cascais Bay *(Portuguese Coast)*	2005–present	X	X	-	-	-	-	-	X

No.	IGMETS-ID	Site or programme name	Year-span	T	S	Oxy	Ntr	Chl	Mic	Phy	Zoo
62	pt-30201	Guadiana Lower Estuary *(Southwest Iberian Peninsula)*	1996–present	X	X	-	-	X	-	-	X
63	pt-30301	Guadiana Upper Estuary *(Southwest Iberian Peninsula)*	1996–present	X	X	-	X	X	X	X	-
64	uk-30101	Stonehaven *(Northwest North Sea)*	1997–present	X	X	-	X	X	-	X	X
65	uk-30102	Loch Ewe *(West coast Scotland)*	2002–present	X	X	-	X	X	-	X	X
66	uk-30103	Loch Maddy *(West coast Scotland)*	2003–2011 (?)	X	X	-	X	-	-	X	-
67	uk-30104	Mill Port *(West coast Scotland)*	2005–2013 (?)	X	-	-	-	-	-	X	-
68	uk-30105	Scalloway – Shetland Isles *(Northwest North Sea)*	2001–present	X	X	-	X	-	-	X	-
69	uk-30106	Scapa Bay – Orkney *(Northwest North Sea)*	2001–present	X	X	-	X	-	-	X	-
70	uk-30201	Plymouth L4 *(Western English Channel)*	1988–present	X	X	X	X	X	X	X	X
71	uk-30301	Dove *(North Sea)*	1971–2002 discontinued	-	-	-	-	-	-	-	X
72	uk-30601	Atlantic Meridional Transect (AMT)	1995-present	X	X	X	X	X		X	X
73	uk-40106	SAHFOS–CPR A06 *(South Iceland)*	1958–present	-	-	-	-	X	-	X	X
74	uk-40111	SAHFOS–CPR B01 *(Northeastern North Sea)*	1958–present	-	-	-	-	X	-	X	X
75	uk-40112	SAHFOS–CPR B02 *(Northwestern North Sea)*	1958–present	-	-	-	-	X	-	X	X
76	uk-40114	SAHFOS–CPR B04 *(Southern Norwegian Sea)*	1958–present	-	-	-	-	X	-	X	X
77	uk-40115	SAHFOS–CPR B05 *(Southeast Iceland)*	1958–present	-	-	-	-	X	-	X	X
78	uk-40116	SAHFOS–CPR B06 *(Southwest Iceland)*	1958–present	-	-	-	-	X	-	X	X
79	uk-40117	SAHFOS–CPR B07 *(Southeast Greenland)*	1958–present	-	-	-	-	X	-	X	X
80	uk-40118	SAHFOS–CPR B08 *(Southwest Greenland)*	1962–present	-	-	-	-	X	-	X	X
81	uk-40121	SAHFOS–CPR C01 *(Eastern Central North Sea)*	1958–present	-	-	-	-	X	-	X	X
82	uk-40122	SAHFOS–CPR C02 *(Western Central North Sea)*	1958–present	-	-	-	-	X	-	X	X

No.	IGMETS-ID	Site or programme name	Year-span	T	S	Oxy	Ntr	Chl	Mic	Phy	Zoo
83	uk-40123	SAHFOS–CPR C03 *(Irish Sea)*	1958–present	-	-	-	-	X	-	X	X
84	uk-40124	SAHFOS–CPR C04 *(Northwest Scotland and Ireland)*	1958–present	-	-	-	-	X	-	X	X
85	uk-40125	SAHFOS–CPR C05 *(Northeast Central North Atlantic)*	1958–present	-	-	-	-	X	-	X	X
86	uk-40126	SAHFOS–CPR C06 *(Central North Atlantic)*	1958–present	-	-	-	-	X	-	X	X
87	uk-40127	SAHFOS–CPR C07 *(Northwest Central North Atlantic)*	1959–present	-	-	-	-	X	-	X	X
88	uk-40128	SAHFOS–CPR C08 *(Labrador)*	1959–present	-	-	-	-	X	-	X	X
89	uk-40131	SAHFOS–CPR D01 *(Southeast North Sea)*	1958–present	-	-	-	-	X	-	X	X
90	uk-40132	SAHFOS–CPR D02 *(Southwest North Sea)*	1958–present	-	-	-	-	X	-	X	X
91	uk-40133	SAHFOS–CPR D03 *(English Channel)*	1958–present	-	-	-	-	X	-	X	X
92	uk-40134	SAHFOS–CPR D04 *(South Ireland)*	1958–present	-	-	-	-	X	-	X	X
93	uk-40135	SAHFOS–CPR D05 *(Eastern Central North Atlantic)*	1958–present	-	-	-	-	X	-	X	X
94	uk-40136	SAHFOS–CPR D06 *(Central North Atlantic)*	1958–present	-	-	-	-	X	-	X	X
95	uk-40137	SAHFOS–CPR D07 *(Western Central North Atlantic)*	1959–present	-	-	-	-	X	-	X	X
96	uk-40138	SAHFOS–CPR D08 *(Western Central North Atlantic)*	1959–present	-	-	-	-	X	-	X	X
97	uk-40139	SAHFOS–CPR D09 *(Labrador Shelf)*	1959–present	-	-	-	-	X	-	X	X
98	uk-40144	SAHFOS–CPR E04 *(Bay of Biscay)*	1958–present	-	-	-	-	X	-	X	X
99	uk-40145	SAHFOS–CPR E05 (*Eastern Southern North Atlantic*)	1958–present	-	-	-	-	X	-	X	X
100	uk-40146	SAHFOS–CPR E06 (*Southern North Atlantic*)	1961–present	-	-	-	-	X	-	X	X
101	uk-40147	SAHFOS–CPR E07 (*Southern North Atlantic*)	1961–present	-	-	-	-	X	-	X	X
102	uk-40148	SAHFOS–CPR E08 (*Western Southern North Atlantic*)	1960–present	-	-	-	-	X	-	X	X
103	uk-40149	SAHFOS–CPR E09 (*Off Newfoundland Shelf*)	1960–present	-	-	-	-	X	-	X	X

No.	IGMETS-ID	Site or programme name	Year-span	T	S	Oxy	Ntr	Chl	Mic	Phy	Zoo
104	uk-40150	SAHFOS–CPR E10 (*Off Scotian Shelf*)	1961–present	-	-	-	-	X	-	X	X
105	uk-40154	SAHFOS–CPR F04 (*Off Iberian Shelf*)	1958–present	-	-	-	-	X	-	X	X
106	uk-40155	SAHFOS–CPR F05 (*Eastern Southern North Atlantic*)	1963–present	-	-	-	-	X	-	X	X
107	uk-40156	SAHFOS–CPR F06 (*Central Southern North Atlantic*)	1967–present	-	-	-	-	X	-	X	X
108	uk-40157	SAHFOS–CPR F07 (*Central Southern North Atlantic*)	1963–present	-	-	-	-	X	-	X	X
109	uk-40158	SAHFOS–CPR F08 (*Central Southern North Atlantic*)	1963–present	-	-	-	-	X	-	X	X
110	uk-40159	SAHFOS–CPR F09 (*Western Southern North Atlantic*)	1962–present	-	-	-	-	X	-	X	X
111	uk-40160	SAHFOS–CPR F10 (*Off Gulf of Maine*)	1961–present	-	-	-	-	X	-	X	X
112	us-10101	Bermuda Atlantic Time Series (*BATS*)	1982–present	X	X	X	X	X	X	-	X
113	us-10401	Boothbay (*Northwestern Atlantic shelf*)	2000–present	X	X	-	-	X	X	-	-
114	us-30101	Upper Chesapeake – Maryland (*Chesapeake Bay*)	1984–2002 (?)	-	-	-	-	-	-	-	X
115	us-30102	Lower Chesapeake – Virginia (*Chesapeake Bay*)	1985–2002 (?)	-	-	-	-	-	-	-	X
116	us-30201	Narragansett Bay (*Northwestern Atlantic*)	1959–present	X	X	-	X	X	-	-	-
117	us-30301	Neuse River Estuary NR000 (*Outer Banks – North Carolina*)	1994–present	X	X	X	X	X	-	-	-
118	us-30302	Pamlico Sound PS1 (*Outer Banks – North Carolina*)	2000–present	X	X	X	X	X	-	-	-
119	us-50101	EcoMon Gulf of Maine – GOM (*Gulf of Maine*)	1977–present	-	-	-	-	-	-	-	X
120	us-50102	EcoMon Georges Bank – GBK (*Georges Bank*)	1977–present	-	-	-	-	-	-	-	X
121	us-50103	EcoMon Southern New England – SNE (*Southern New England*)	1977–present	-	-	-	-	-	-	-	X
122	us-50104	EcoMon Mid-Atlantic Bight – MAB (*Mid-Atlantic Bight*)	1977–present	-	-	-	-	-	-	-	X
123	us-50105	EcoMon Gulf of Maine CPR line (*Gulf of Maine*)	1961–2012 discontinued	-	-	-	-	-	-	-	-
124	us-50106	EcoMon Mid-Atlantic Bight CPR line (*Mid-Atlantic Bight*)	1975–2012 discontinued	-	-	-	-	-	-	-	-

No.	IGMETS-ID	Site or programme name	Year-span	T	S	Oxy	Ntr	Chl	Mic	Phy	Zoo
125	us-50201	SEAMAP: Texas/Lousiana Shelf WEST (*Gulf of Mexico*)	1982–present	-	-	-	-	-	-	-	X
126	us-50202	SEAMAP: Texas/Louisiana Shelf CENTRAL (*Gulf of Mexico*)	1982–present	-	-	-	-	-	-	-	X
127	us-50203	SEAMAP: Texas/Lousiana Shelf EAST (*Gulf of Mexico*)	1982–present	-	-	-	-	-	-	-	X
128	us-50204	SEAMAP: Mississippi/Alabama Shelf (*Gulf of Mexico*)	1982–present	-	-	-	-	-	-	-	X
129	us-50205	SEAMAP: Florida Shelf NORTH-WEST (*Gulf of Mexico*)	1986–present	-	-	-	-	-	-	-	X
130	us-50206	SEAMAP: Florida Shelf NORTH-EAST (*Gulf of Mexico*)	1986–present	-	-	-	-	-	-	-	X
131	us-50207	SEAMAP: Florida Shelf SOUTH (*Gulf of Mexico*)	1982–present	-	-	-	-	-	-	-	X
132	us-50208	Northeast Off-shelf Region – SEAMAP (*Gulf of Mexico*)	1982–present	-	-	-	-	-	-	-	X
133	us-50209	Northwest Off-Shelf Region – SEAMAP (*Gulf of Mexico*)	1982–present	-	-	-	-	-	-	-	X
134	us-60101	NERRS ACE Basin	2001–present	X	X	X	X	X	-	-	-
135	us-60102	NERRS Apalachicola	2002–present	X	X	X	X	X	-	-	-
136	us-60103	NERRS Chesapeake Bay MD	2003–present	X	X	X	X	X	-	-	-
137	us-60104	NERRS Chesapeake Bay VA	2002–present	X	X	X	X	X	-	-	-
138	us-60105	NERRS Delaware	2001–present	X	X	X	X	X	-	-	-
139	us-60107	NERRS Grand Bay	2004–present	X	X	X	X	X	-	-	-
140	us-60108	NERRS Great Bay	2001–present	X	X	X	X	X	-	-	-
141	us-60109	NERRS Guana Tolomato Matanzas	2002–present	X	X	X	X	X	-	-	-
142	us-60111	NERRS Jacques Cousteau	2002–present	X	X	X	X	X	-	-	-
143	us-60112	NERRS Jobos Bay – Puerto Rico	2001–present	X	X	X	X	X	-	-	-
144	us-60115	NERRS Mission-Aransas	2007–present	X	X	X	X	X	-	-	-

No.	IGMETS-ID	Site or programme name	Year-span	T	S	Oxy	Ntr	Chl	Mic	Phy	Zoo
145	us-60116	NERRS Narragansett Bay	2002–present	X	X	X	X	X	-	-	-
146	us-60117	NERRS North Inlet – Winyah Bay	2001–present	X	X	X	X	X	-	-	-
147	us-60118	NERRS North Carolina	2001–present	X	X	X	X	X	-	-	-
148	us-60119	NERRS Old Woman Creek	2002–present	X	X	X	X	X	-	-	-
149	us-60121	NERRS Rookery Bay	2002–present	X	X	X	X	X	-	-	-
150	us-60122	NERRS Sapelo Island	2004–present	X	X	X	X	X	-	-	-
151	us-60126	NERRS Wells	2004–present	X	X	X	X	X	-	-	-
152	us-60127	NERRS Weeks Bay	2001–present	X	X	X	X	X	-	-	-
153	us-60128	NERRS Waquoit Bay	2002–present	X	X	X	X	X	-	-	-
154	ve-10101	CARIACO Ocean Time Series (*Cariaco Basin off Venezuela*)	1995–present	X	X	X	X	X	X	X	X

Baltic Sea

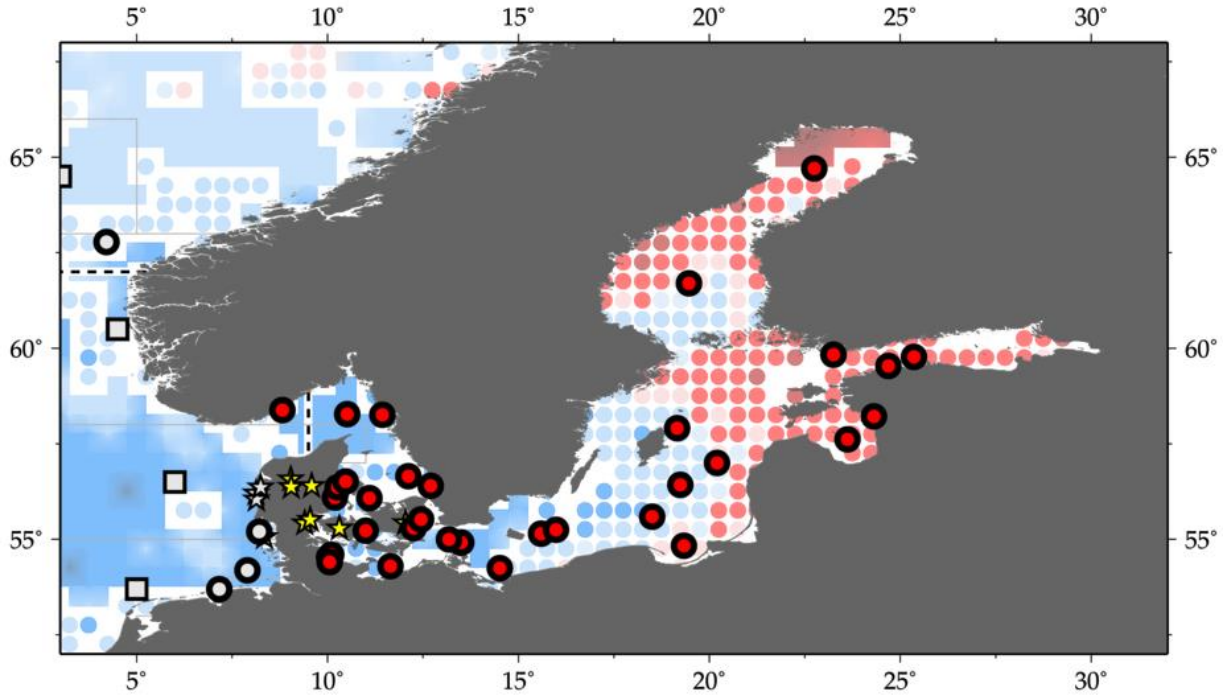

Figure 4.8. Map of IGMETS-participating Baltic Sea time series on a background of a 10-year time-window (2003–2012) sea surface temperature trends. At the time of this report, the Baltic Sea consisted of 41 time series (coloured symbols of any type, see also Table 4.4), of which 7 were from estuarine areas (yellow stars). Uncoloured (gray) symbols indicate time series being addressed in a different regional chapter (e.g. Arctic Ocean) or in separate subregions (e.g. North Atlantic Proper, Figure 4.1/Table 4.3; Mediterranean Sea, Figure 4.9/Table 4.5).

Table 4.4. Regional listing of participating time series for the IGMETS Baltic Sea. Participating countries: Germany (de), Denmark (dk), Estonia (ee), Finland (fi), Latvia (lv), Poland (pl), and Sweden (se).

No.	IGMETS-ID	Site or programme name	Year-span	T	S	Oxy	Ntr	Chl	Mic	Phy	Zoo
1	de-10201	Boknis Eck Time Series Station *(Eckernfoerde Bay – SW Baltic Sea)*	1957–present	X	X	X	X	X	X	-	-
2	de-30101	Arkona Basin (*Southern Baltic Sea*)	1979–present	X	X	X	X	X	X	X	X
3	de-30102	Bornholm Basin (*Southern Baltic Sea*)	1979–present	X	X	X	X	X	X	X	-
4	de-30103	Mecklenburg Bight (*Southern Baltic Sea*)	1980–present	X	X	X	X	X	X	X	-
5	de-30104	Eastern Gotland Basin (*Southern Baltic Sea*)	1979–present	X	X	X	X	X	X	X	-
6	dk-30102	Arhus Bugt: DNAMAP-170006 (*Baltic Sea*)	1979–present	X	X	X	X	X	-	X	-
7	dk-30103	Koge Bugt: DNAMAP-1727 (*Baltic Sea*)	1985–present	X	X	X	X	X	-	X	-
8	dk-30104	Hevring Bugt: DNAMAP-190004 (*Baltic Sea*)	1985–present	X	X	X	X	X	-	X	-

No.	IGMETS-ID	Site or programme name	Year-span	T	S	Oxy	Ntr	Chl	Mic	Phy	Zoo
9	dk-30108	Logstor Bredning: DNAMAP-3708-1 (*Baltic Sea*)	1980–present	X	X	X	X	X	-	X	-
10	dk-30109	Skive Fjord: DNAMAP-3727-1 (*Baltic Sea*)	1980–present	X	X	X	X	X	-	X	-
11	dk-30111	Alborg Bugt: DNAMAP-409 (*Baltic Sea*)	1981–present	X	X	X	X	X	-	X	-
12	dk-30112	Anholt East: DNAMAP-413 (*Baltic Sea*)	1981–present	X	X	X	X	X	-	X	-
13	dk-30113	Vejle Fjord: DNAMAP-4273 (*Baltic Sea*)	1982–present	X	X	X	X	X	-	X	-
14	dk-30114	Ven: DNAMAP-431 (*Baltic Sea*)	1979–present	X	X	X	X	X	-	X	-
15	dk-30115	Arkona: DNAMAP-444 (*Baltic Sea*)	1979–present	X	X	X	X	X	-	X	-
16	dk-30116	Mariager Fjord: DNAMAP-5503 (*Baltic Sea*)	1979–present	X	X	X	X	X	-	X	-
17	dk-30117	Horsens Fjord: DNAMAP-5790 (*Baltic Sea*)	1981–present	X	X	X	X	X	-	X	-
18	dk-30118	Roskilde Fjord: DNAMAP-60 (*Baltic Sea*)	1979–present	X	X	X	X	X	-	X	-
19	dk-30119	Lillebaelt-South: DNAMAP-6300043 (*Baltic Sea*)	1979–present	X	X	X	X	X	-	X	-
20	dk-30120	Lillebaelt-North: DNAMAP-6870 (*Baltic Sea*)	1979–present	X	X	X	X	X	-	X	-
21	dk-30121	Odense Fjord: DNAMAP-6900017 (*Baltic Sea*)	1979–present	X	X	X	X	X	-	X	-
22	dk-30122	Gniben: DNAMAP-925 (*Baltic Sea*)	1979–present	X	X	X	X	X	-	X	-
23	dk-30123	Storebaelt: DNAMAP-939 (*Baltic Sea*)	1982–present	X	X	X	X	X	-	X	-
24	dk-30124	Bornholm Deep: DNAMAP-bmpk2 (*Baltic Sea*)	1980–present	X	X	X	X	X	-	X	-
27	ee-10101	Pärnu Bay (*Gulf of Riga*)	1957–present	X	X	-	-	X	-	-	X
28	ee-10201	Tallinn Bay (*Gulf of Finland*)	1959–present	X	X	-	-	X	-	-	X
29	fi-30101	Bothnian Bay Region: Bo3+F2 (*Northern Baltic Sea*)	1959–present	X	X	X	X	X	X	X	X
30	fi-30102	Bothnian Sea Region: SR5+US5b+F64 (*Northern Baltic Sea*)	1959–present	X	X	X	X	X	X	X	X

No.	IGMETS-ID	Site or programme name	Year-span	T	S	Oxy	Ntr	Chl	Mic	Phy	Zoo
31	fi-30103	Gulf of Finland Region: LL3A+LL7+LL12 (*Northern Baltic Sea*)	1959–present	X	X	X	X	X	X	X	X
32	fi-30104	Northern Baltic Proper Region: BY15+BY38+LL17+LL23 (*Northern Baltic Sea*)	1959–present	X	X	X	X	X	X	X	X
33	lv-10101	Station 121 (*Gulf of Riga*)	1959–present	X	X	-	-	X	-	-	X
34	lv-10201	Eastern Gotland Basin (*Central Baltic Sea*)	1959–present	X	X	X	X	X	-	-	X
35	pl-30101	Gdansk Basin (*Baltic Sea*)	1959–present	X	X	-	X	X	X	X	X
36	pl-30102	Bornholm Basin (*Baltic Sea*)	1959–present	X	X	-	X	X	X	X	X
37	pl-30103	Pomeranian Bay (*Baltic Sea*)	1979–present	X	X	-	X	X	X	X	-
38	pl-30104	Southern Gotland Basin (*Baltic Sea*)	1959–present	X	X	X	-	X	-	-	X
39	se-50101	SMHI A17 (*Sweden*)	1982–present	X	X	X	X	X	X	X	X
40	se-50102	SMHI Anholt East (*Kattegat*)	1959–present	X	X	X	X	X	X	X	X
41	se-50103	SMHI Slaggo (*Sweden*)	1959–present	X	X	X	X	X	X	X	X

Mediterranean Sea

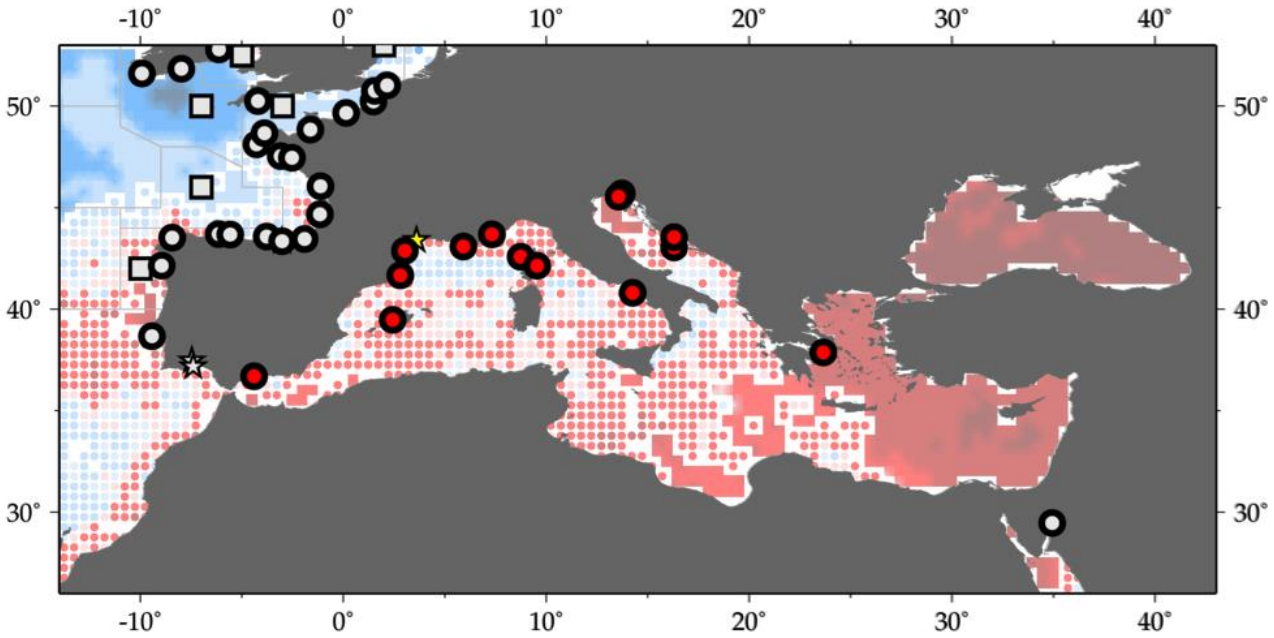

Figure 4.9. Map of IGMETS-participating Mediterranean Sea time series on a background of a 10-year time-window (2003–2012) sea surface temperature trends. At the time of this report, the Mediterranean Sea consisted of 16 time series (coloured symbols of any type; see also Table 4.5), of which one was from estuarine areas (yellow stars). Uncoloured (gray) symbols indicate time series being addressed in a different subregion (e.g. North Atlantic Proper, Figure 4.1/Table 4.3).

Table 4.5. Regional listing of participating time series for the IGMETS Mediterranean Sea. Participating countries: Belgium (be), Spain (es), France (fr), Greece (gr), Croatia (hr), Italy (it), Slovenia (si).

No.	IGMETS-ID	Site or programme name	Year-span	T	S	Oxy	Ntr	Chl	Mic	Phy	Zoo
1	be-10101	PHYTOCLY Time Series *(Bay of Calvi)*	1988–present	-	-	-	X	X	-	-	-
2	es-30301	Blanes Bay *(Northwest Mediterranean)*	1992–present	X	X	-	X	X	X	-	-
3	es-50201	IEO Mallorca Baleares Station *(Mallorca Channel)*	1994–present	X	X	-	-	X	-	-	X
4	es-50301	IEO ECOMÁLAGA *(Alboran Sea)*	1992–present	X	X	-	X	X	-	-	X
5	fr-10101	Villefranche Point B *(Cote d'Azur)*	1995–present	-	-	-	-	-	-	-	X
6	fr-10201	Thau Lagoon *(Mediterranean Sea)*	1965–present	X	X	-	X	X	X	X	-
7	fr-50111	REPHY Diana Centre *(Mediterranean Sea)*	1987–present	X	X	X	X	X	-	X	-
8	fr-50112	REPHY Lazaret A *(Western Mediterranean)*	1987–present	X	X	X	-	X	-	X	-

No.	IGMETS-ID	Site or programme name	Year-span	T	S	Oxy	Ntr	Chl	Mic	Phy	Zoo
9	fr-50113	REPHY Parc Leucate 2 *(Mediterranean Sea)*	1987–present	X	X	-	-	X	-	X	-
10	fr-50114	REPHY Villefranche *(Mediterranean Sea)*	1995–present	X	X	-	-	-	-	X	-
11	gr-10101	Saronikos Gulf S11 *(Aegean Sea)*	1987–present	-	-	-	-	X	-	-	X
12	hr-10101	Stoncica *(Central Adriatic Sea)*	1959–present	-	-	-	-	-	X	-	X
13	hr-10102	Kastela Bay *(Central Adriatic Sea)*	1994–present	-	-	-	-	-	X	-	-
14	it-30101	Gulf of Naples LTER-MC *(Tyrrhenian Sea)*	1984–present	X	X	-	X	X	-	X	X
15	it-30201	C1-LTER Gulf of Trieste *(Northern Adriatic Sea)*	1970–present	-	-	-	-	-	-	-	X
16	si-10101	Gulf of Trieste – MBS Buoy *(Northern Adriatic Sea)*	1990–present	X	X	X	X	X	-	X	-

4.6 References

Beaugrand, G., Conversi, A., Chiba, S., Edwards, M., Fonda-Umani, S., Greene, C., Mantua, N., *et al*. 2015. Synchronous marine pelagic regime shifts in the Northern Hemisphere. Philosophical Transactions of the Royal Society B, 370: (20130272), doi:10.1098/rstb.2013.0272.

Behrenfeld, M. J., O'Malley, R. T., Boss, E. S., Westberry, T. K., Graff, J. R., Halsey, K. H., Milligan, A. J., *et al*. 2015. Revaluating ocean warming impacts on global phytoplankton. Nature Climate Change, 5: doi:10.1038/NCLIMATE2838.

Benazzouz, A., Demarcq, H., and González-Nuevo, G. 2015. Recent changes and trends of the upwelling intensity in the Canary Current Large Marine Ecosystem. *In* Oceanographic and biological features in the Canary Current Large Marine Ecosystem, pp. 321–330. Ed. by L. Valdés, and I. Déniz-González. IOC-UNESCO, IOC Technical Series, No. 115. 383 pp.

Bode, A., Estévez, M. G., Varela, M., and Vilar, J. A. 2015. Annual trend patterns of phytoplankton species abundance belie homogeneous taxonomical group responses to climate in the NE Atlantic upwelling. Marine Environmental Research, 110: 81–91.

Bode, A., Hare, J., Li, W. K. W., Morán, X. A. G., and Valdés, L. 2011. Chlorophyll and primary production in the North Atlantic. *In* ICES status report on climate change in the North Atlantic, pp. 77–102. Ed. by P. C. Reid, and L. Valdés. ICES Cooperative Research Report No. 310. 262 pp.

Boyce, D. G., Dowd, M., Lewis, M. R., and Worm, B. 2014. Estimating global chlorophyll changes over the past century. Progress in Oceanography, 122: 163–173.

Carstensen, J., Andersen, J. H., Gustafsson, B. G., and Conley, D. J. 2014. Deoxygenation of the Baltic Sea during the last century. Proceedings of the National Academy of Sciences of the United States of America, 111(15): 5628–5633.

Demarcq, H., and Bénazzouz, A. 2015. Trends in phytoplankton and primary productivity off Northwest Africa. *In* Oceanographic and biological features in the Canary Current Large Marine Ecosystem, pp. 331–342. Ed. by L. Valdés, and I. Déniz-González. IOC-UNESCO, IOC Technical Series, No. 115. 383 pp.

Dickson, R. R., and Brown, J. 1994. The production of North Atlantic Deep Water: Sources, rates, and pathways. Journal of Geophysical Research, C. Oceans, 99(C6): 12319–12341.

Feistel, R., Nausch, G., and Wasmund, N. E. 2008. State and evolution of the Baltic Sea, 1952-2005. Wiley Interscience, Hoboken, NJ, USA. 703 pp.

Fisher, J. A. D., Casini, M., Frank, K. T., Möllmann, C., Leggett, W. C., and Daskalov, G. 2015. The importance of within-system spatial variation in drivers of marine ecosystem regime shifts. Philosophical Transactions of the Royal Society B, 370: (20130271), doi:10.1098/rstb.2013.0271.

Goffart, A., Hecq, J-H., and Legendre, L. 2015. Drivers of the winter-spring phytoplankton bloom in a pristine NW Mediterranean site, the Bay of Calvi (Corsica): A long-term study (1979-2011). Progress in Oceanography, 137: 121–139.

Hátún, H., Payne, M. R., Beaugrand, G., Reid, P. C., Sando, A. B., Drange, H., Hansen, B., *et al*. 2009. Large bio-geographical shifts in the north-eastern Atlantic Ocean: From the subpolar gyre, via plankton, to blue whiting and pilot whales. Progress in Oceanography, 80: 149–162.

Heath, M. R., and Beare, D. J. 2008. New primary production in northwest European shelf seas, 1960-2003. Marine Ecology Progress Series, 363: 183–203.

HELCOM. 2009. Eutrophication in the Baltic Sea - An integrated thematic assessment of the effects of nutrient enrichment and eutrophication in the Baltic Sea region. Baltic Sea Environment Proceedings, 115B. 148 pp.

HELCOM. 2014. Eutrophication status of the Baltic Sea 2007-2011. Baltic Sea Environment Proceedings, 143. 40 pp.

Hemery, G., D'Amico, F., Castege, I., Dupont, B., D'Elbee, J., Lalanne, Y., and Mouches, C. 2008. Detecting the impact of oceano-climatic changes on marine ecosystems using a multivariate index: The case of the Bay of Biscay (North Atlantic-European Ocean). Global Change Biology, 14: 27–38.

Hernández-Fariñas, T., Soudant, D., Barillé, L., Belin, C., Lefebvre, A., and Bacher, C. 2014. Temporal changes in the phytoplankton community along the French coast of the eastern English Channel and the southern Bight of the North Sea. ICES Journal of Marine Science, 71: 821–833.

Hinder, S. L., Hays, G. C., Edwards, M., Roberts, E., Walne, A. W., and Gravenor, M. B. 2012. Changes in marine dinoflagellate and diatom abundance under climate change. Nature Climate Change, 2: 271–275.

Hoegh-Guldberg, O., Cai, R., Poloczanska, E. S., Brewer, P. G., Sundby, S., Hilmi, K., Fabry, V. J., *et al.* 2014. The Ocean. *In* Climate Change 2014: Impacts, Adaptation, and Vulnerability. Part B: Regional Aspects, pp. 1655–1731. Ed. by V. R. Barros, C. B. Field, D. J. Dokken, M. D. Mastrandrea, K. J. Mach, T. E. Bilir, M. Chatterjee, *et al.* Contribution of Working Group II to the Fifth Assessment Report of the Intergovernmental Panel on Climate Change, Cambridge University Press, Cambridge and New York. 688 pp.

Hurrell, J. W., and Dickson, R. R. 2004. Climate variability over the North Atlantic. *In* Marine Ecosystems and Climate Variation - The North Atlantic, pp. 15–31. Ed. by N. C. Stenseth, G. Ottersen, J. W. Hurrell, and A. Belgrano. Oxford University Press, Oxford. 252 pp.

Hurrell, J., Meehl, G. A., Bader, D., Delworth, T. L., Kirtman, B., and Wielicki, B. 2009. A unified modeling approach to climate system prediction. Bulletin of the American Meteorological Society, 90(12): 1819–1832.

Knudsen, M. F., Seidenkrantz, M-S., Jacobsen, B. H., and Kuijpers, A. 2011. Tracking the Atlantic Multidecadal Oscillation through the last 8,000 years. Nature Communications, 2(178): doi:10.1038/ncomms1186.

Lennartz, S. T., Lehmann, A., Herrford, J., Malien, F., Hansen, H-P., Biester, H., and Bange, H. W. 2014. Long-term trends at the Time Series Station Boknis Eck (Baltic Sea), 1957-2013: does climate change counteract the decline in eutrophication? Biogeosciences, 11: 6323–6339.

Leterme, S. C., Seuront, L., and Edwards, M. 2006. Differential contribution of diatoms and dinoflagellates to phytoplankton biomass in the NE Atlantic Ocean and the North Sea. Marine Ecology Progress Series, 312: 57–65.

Levitus, S., Antonov, J. I., Boyer, T. P., and Stephens, C. 2000. Warming of the world ocean. Science, 287: 2225–2229.

Longhurst, A. 2007. Ecological Geography of the Sea, 2nd edn. Academic Press. 560 pp.

Llope, M., Anadón, R., Sostres, J. A., and Viesca, L. 2007. Nutrients dynamics in the southern Bay of Biscay (1993-2003): Winter supply, stoichiometry, long-term trends, and their effects on the phytoplankton community. Journal of Geophysical Research, 112: doi:10.1029/2006JC003573.

Marshall, J., Kushnir, Y., Battisti, D., Chang, P., Czaja, A., Dickson, R., Hurrell, J., *et al.* 2001. North Atlantic climate variability: phenomena, impacts and mechanisms. International Journal of Climatology, 21: 1863–1898.

McGinty, N., Power, A. M., and Johnson, M. P. 2012. Trophodynamics and stability of regional scale ecosystems in the Northeast Atlantic. ICES Journal of Marine Science, 69: 764–775.

McGregor, H. V., Dima, M., Fischer, H. W., and Mulitza, S. 2007. Rapid 20th-century increase in coastal upwelling off Northwest Africa. Science, 315: 637–639.

McQuatters-Gollop, A., Raitsos, D. E., Edwards, M., Pradhan, Y., Mee, L. D., Lavender, S. J., and Attrill, M. J. 2007. A long-term chlorophyll dataset reveals regime shift in North Sea phytoplankton biomass unconnected to increasing nutrient levels. Limnology and Oceanography, 52: 635–648.

Meyer-Gutbrod, E. L., Greene, C. H., Sullivan, P. J., and Pershing, A. J. 2015. Climate-associated changes in prey availability drive reproductive dynamics of the North Atlantic right whale population. Marine Ecology Progress Series, 535: 243–258.

O'Brien, T. D., Li, W. K. W., and Morán, X. A. G. (Eds). 2012. ICES Phytoplankton and Microbial Plankton Status Report 2009/2010. ICES Cooperative Research Report No. 313. 196 pp.

Pardo, P. C., Padín, X. A., Gilcoto, M., Farina-Busto, L., and Pérez, F. F. 2011. Evolution of upwelling systems coupled to the long-term variability in sea surface temperature and Ekman transport. Climate Research, 48: 231–246.

Pérez, F. F., Padin, X. A., Pazos, Y., Gilcoto, M., Cabanas, M., Pardo, P. C., Doval, M. D., *et al*. 2010. Plankton response to weakening of the Iberian coastal upwelling. Global Change Biology, 16: 1258–1267.

Plourde, S., Grégoire, F., Lehoux, C., Galbraith, P. S., and Castonguay, M. 2014. Effect of environmental variability on the Atlantic Mackerel (*Scomber scombrus* L.) stock dynamics in the Gulf of St. Lawrence. DFO Canadian Science Advisory Secretariat Research Document, 2014/092. 30 pp.

Reid, P. C., Edwards, M., McQuatters-Gollop, A., Beaugrand, G., Bresnan, E., Brierley, A., Davidson, K., *et al.* 2010. Charting Progress 2 Healthy and Biological Diverse Seas Feeder Report: Section 3.3: Plankton. *In* Charting Progress 2 Healthy and Biological Diverse Seas Feeder Report, pp. 286–377. Ed. by M. Frost, and J. Hawkridge. Department for Environment Food and Rural Affairs on behalf of UKMMAS, London.

Richardson, A. J., and Schoeman, D. S. 2004. Climate impact on plankton ecosystems in the Northeast Atlantic. Science, 305: 1609–1612.

Santos, F., Gómez-Gesteira, M., deCastro, M., and Álvarez, I. 2012. Variability of coastal and ocean water temperature in the upper 700 m along the Western Iberian Peninsula from 1975 to 2006. PLoS ONE, 7(12): e50666), doi:10.1371/journal.pone.0050666.

Suikkanen, S., Pulina, S., Engström-Öst, J., Lehtiniemi, M., Lehtinen, S., and Brutemark, A. 2013. Climate change and eutrophication induced shifts in northern summer plankton communities. PLoS ONE, 8(6): e66475, doi:10.1371/journal.pone.0066475.

Tremblay, J. E., and Gagnon, J. 2009. The effects of irrandiance and nutrient supply on the productivity of Arctic waters: a perspective on climate change. *In* Influence of Climate Change on the Changing Arctic and Sub-Arctic Conditions, pp. 73–93. Ed. by J. C. J. Nihoul, and A. G. Kostianov. Springer, Netherlands. 232 pp.

Worthington, L. V. 1986. On the North Atlantic circulation. Johns Hopkins Oceanographic Studies, 6: 1–110.

Zhai, L., Platt, T., Tang, C., Sathyendranath, S., and Walne, A. 2013. The response of phytoplankton to climate variability associated with the North Atlantic Oscillation. Deep-Sea Research II, 93: 159–168.

5 South Atlantic Ocean

Frank E. Muller-Karger, Alberto Piola, Hans M. Verheye, Todd D. O'Brien, and Laura Lorenzoni

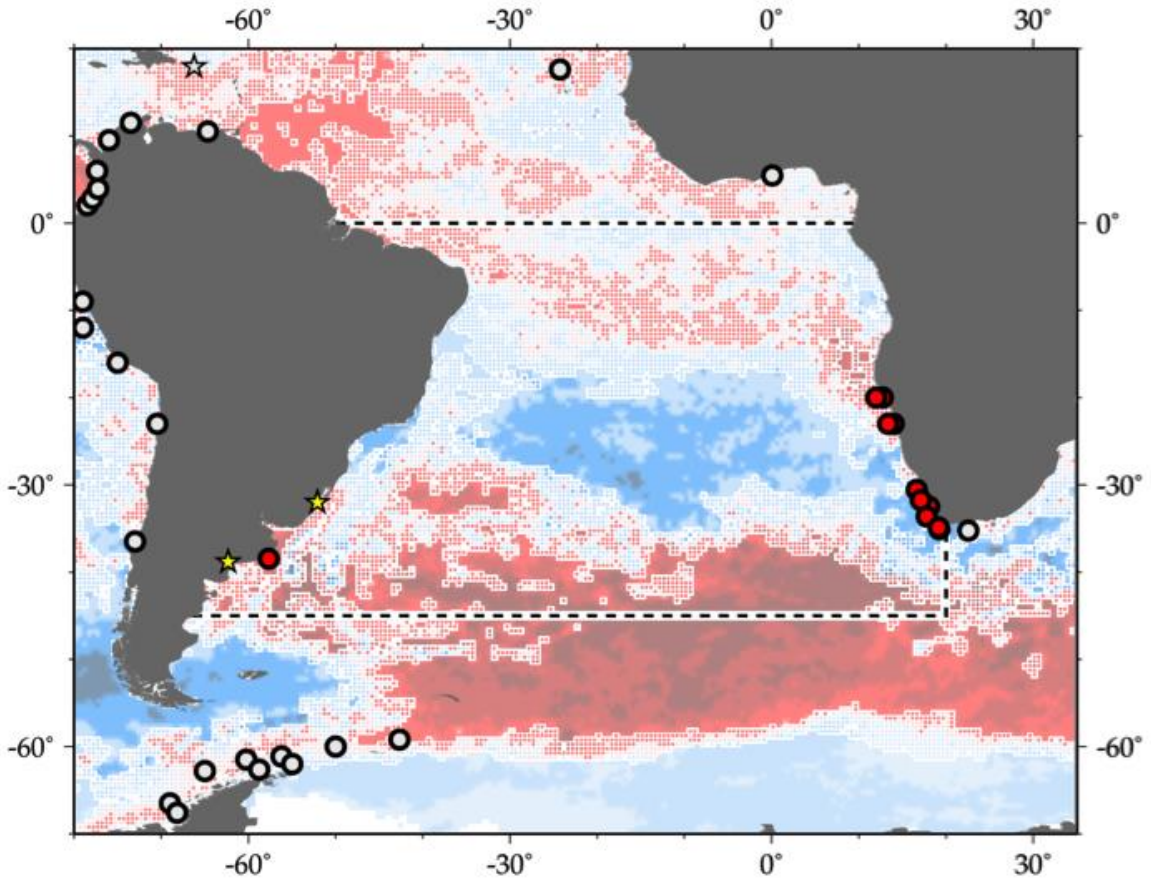

Figure 5.1. Map of IGMETS-participating South Atlantic time series on a background of a 10-year time-window (2003–2012) sea surface temperature trends (see also Figure 5.3). At the time of this report, the South Atlantic collection consisted of 13 time series (coloured symbols of any type), of which two were from estuarine areas (yellow stars). Dashed lines indicate boundaries between IGMETS regions. Uncoloured (gray) symbols indicate time series being addressed in a different regional chapter (e.g. Southern Ocean, South Pacific, North Atlantic). See Table 5.3 for a listing of this region's participating sites. Additional information on the sites in this study is presented in the Annex.

Participating time-series investigators

Carla F. Berghoff, Mario O. Carignan, Fabienne Cazassus, Georgina Cepeda, Paulo Cesar Abreu, Rudi Cloete, Maria Constanza Hozbor, Daniel Cucchi Colleoni, Valeria Guinder, Richard Horaeb, Jenny Huggett, Anja Kreiner, Ezequiel Leonarduzzi, Vivian Lutz, Jorge Marcovecchio, Graciela N. Molinari, Nora Montoya, Ruben Negri, Clarisse Odebrecht, Luciano Padovani, Marcelo Pajaro, Andy Rees, M. Guillermina Ruiz, Valeria Segura, Ricardo I. Silva, Carla Spetter, Sakhile Tsotsobe, Marina Vera Diaz, Hans Verheye, and Maria Delia Viñas

This chapter should be cited as: Muller-Karger, F. E., Piola, A., Verheye, H.M., O'Brien, T. D., and Lorenzoni, L. 2017. South Atlantic Ocean. I*n* What are Marine Ecological Time Series telling us about the ocean? A status report, pp. 83–96. Ed. by T. D. O'Brien, L. Lorenzoni, K. Isensee, and L. Valdés. IOC-UNESCO, IOC Technical Series, No. 129. 297 pp.

5.1 Introduction

5.1.1 Geographic setting

The southern delimitation of the South Atlantic has been historically debated; oceanographically, the Subantarctic Front has been considered the southern limit of this ocean basin. The position of this front fluctuates between about 38°S and 58°S in the Atlantic. Here, we defined the South Atlantic as the area between the equator and 45°S and between the continental land masses of Africa and South America. Depending on this southern boundary delimitation, the South Atlantic covers an area of 30–40 million km^2 (ca. 10% of the total area of the world's oceans), with a volume of ca. 160 million km^3 (ca. 12% of the world's oceans volume) (Figure 5.1, Eakins and Sharman, 2010). It has an average depth of 3973 m and a maximum depth of 8240 m.

The South Atlantic started forming about 160 million years ago (late Jurassic and early Cretaceous) and is still spreading today. The western continental margins of the South Atlantic are broad between the equator, where the Amazon River discharges, and about 5°S (the bulge of Brazil). They become relatively narrow between this region and about 15°S. The margins become broader again to the south, with the Argentine (Patagonia) Shelf extending well over 400 km into the ocean, reaching around 850 km in width at about 50°S (Violante *et al.*, 2014). In the eastern South Atlantic, the broadest shelf is located off western South Africa around 29°S, becoming narrower in Namibia and to the north. Off the Congo River Delta, the shelf is only about 150 km wide and cut by a deep canyon (Savoye *et al.*, 2009).

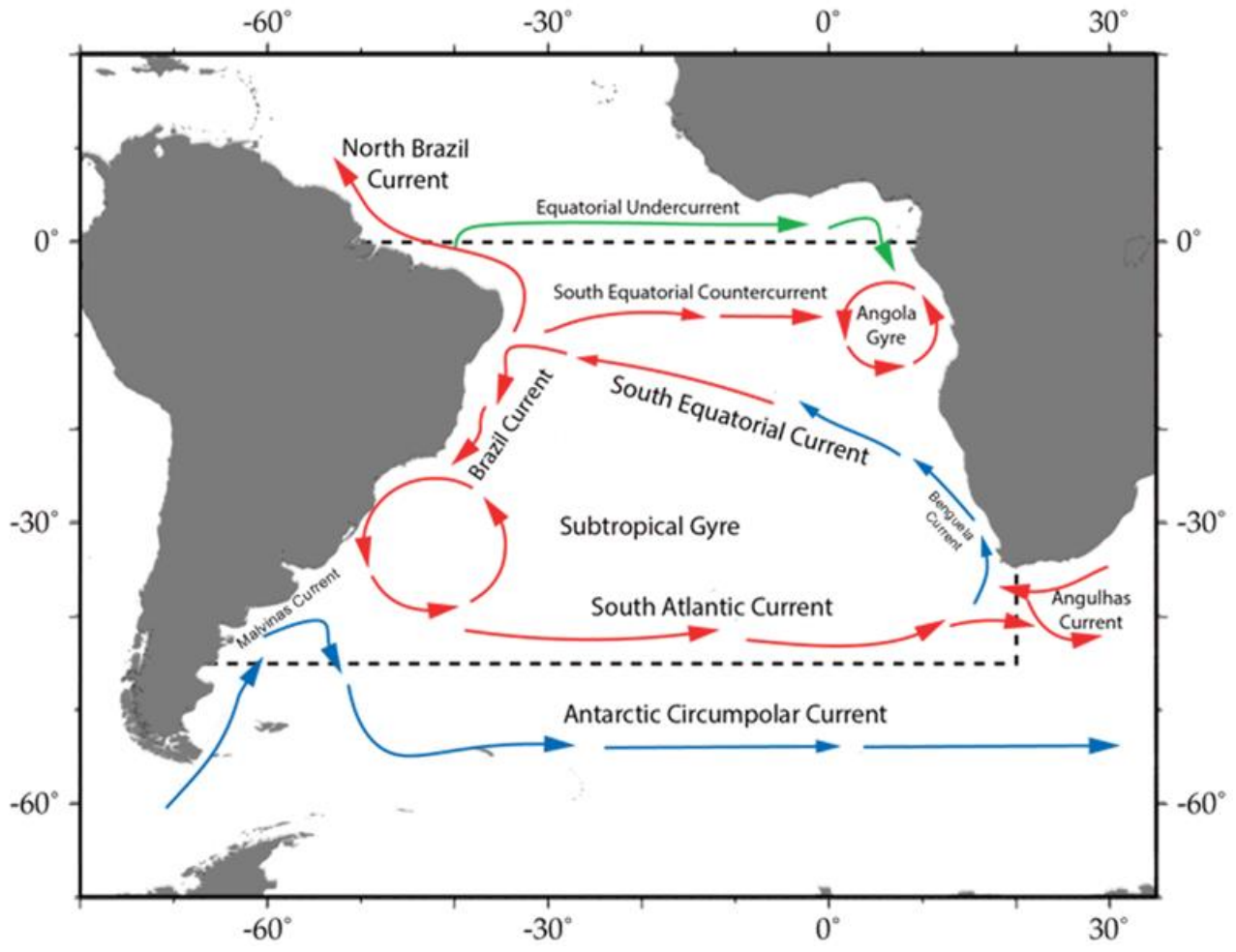

Figure 5.2. Schematic major current systems in the IGMETS-defined South Atlantic region. Red arrows indicate generally warmer water currents; blue arrows indicate generally cooler water currents.

5.1.2 Circulation patterns

The major physical oceanographic features of the South Atlantic have been described in numerous publications (Krummel, 1882; Deacon, 1933; Wefer *et al*., 1996; Garzoli and Matano, 2011; and many others). Only a brief overview of the circulation that results from these forces is provided below for background.

The circulation of this basin is driven partly by winds and partly by the large-scale circulation that overturns the ocean over the scale of the entire Atlantic because of thermohaline imbalances. The atmosphere over the South Atlantic shows a high pressure system between Africa and South America, typically centred around 30°S. Toward the equator, the South Atlantic winds are dominated by the southeast trade winds. South of about 40°S there is a belt of prevailing westerlies that extends south over the Southern Ocean. Trade winds and the westerly wind belts define northern and southern regions, respectively, of the South Atlantic atmospheric high-pressure system. The region around 40°S, where the strong westerlies begin, represents a maximum in wind convergence (i.e. a maximum in Ekman forcing) in the South Atlantic. These patterns are strongly seasonal.

There is a net northward transport of heat from the South Atlantic to the North Atlantic across the equator. This significant cross-equatorial oceanic heat flux is characteristic in the Atlantic Ocean. Heat is carried north in surface layers of the South Atlantic via the southern branch of the South Equatorial Current, which originates with the Benguela Current in the southeastern Atlantic around 15–25°S off Africa (Figure 5.2). The current generally flows toward the northwest across the Atlantic and bifurcates in the central western portion of the Atlantic, with one branch going to the south/southwest (Brazil Current) and another going to the east/northeast merging into the North Brazil Current. This overall pattern is part of what is called the global Meridional Overturning Circulation (MOC; Lumpkin and Speer, 2007; Lopez *et al*., 2016).

The South Atlantic is a mixing basin for many water masses that form in different parts of the world's oceans (Garzoli and Matano, 2011). The South Atlantic gyre, centered approximately at 50°W and 30°S, is bound by a number of major surface ocean currents, including the Antarctic Circumpolar Current, the Benguela Current, the South Equatorial Current, the South Equatorial Counter Current, the Brazil Current, and the Malvinas (or Falkland) Current (Whitworth and Nowlin, 1987; Guhin *et al*., 2003). There are strong variations in the Brazil and Malvinas (Falkland) currents and in the location and intensity of the Brazil/Malvinas Confluence in the western South Atlantic. These variations are important in defining the circulation, including the upwelling regime, and the biological productivity of the Patagonian Shelf (Matano *et al*., 2010). Off South Africa, variation in the Agulhas Current and the Agulhas Retroflection lead to variation in the Benguela Current. This is another important upwelling region in the South Atlantic (Andrews and Hutchings, 1980; Nelson and Hutchings, 1983; Shillington *et al*., 2006). These changes, in turn, affect the northward flow of water across the South Atlantic that eventually crosses the equator into the North Atlantic.

The South Atlantic basin receives the discharge of many small rivers and some of the largest rivers of the world. These include the Congo-Chambeshi River and the Niger River off Africa and the Paraná-Rio de La Plata, Rio Negro, and São Francisco rivers off South America. The Amazon–Tocantins rivers discharge their water close to the equator off South America, but the majority of this water is advected northward toward the Caribbean Sea and toward the western North Atlantic (Müller-Karger *et al*., 1988, 1995; Hu *et al*., 2004; Johns *et al*., 2014). Thus, it is not discussed in this chapter.

In the following sections, we summarize trends observed in ocean biogeochemistry time series for the South Atlantic region (Figure 5.1). The time series are discussed in the context of sea surface temperature (SST), sea surface chlorophyll concentration derived from satellites, and long-term gridded shipboard and model results for the South Atlantic for 1983–2012.

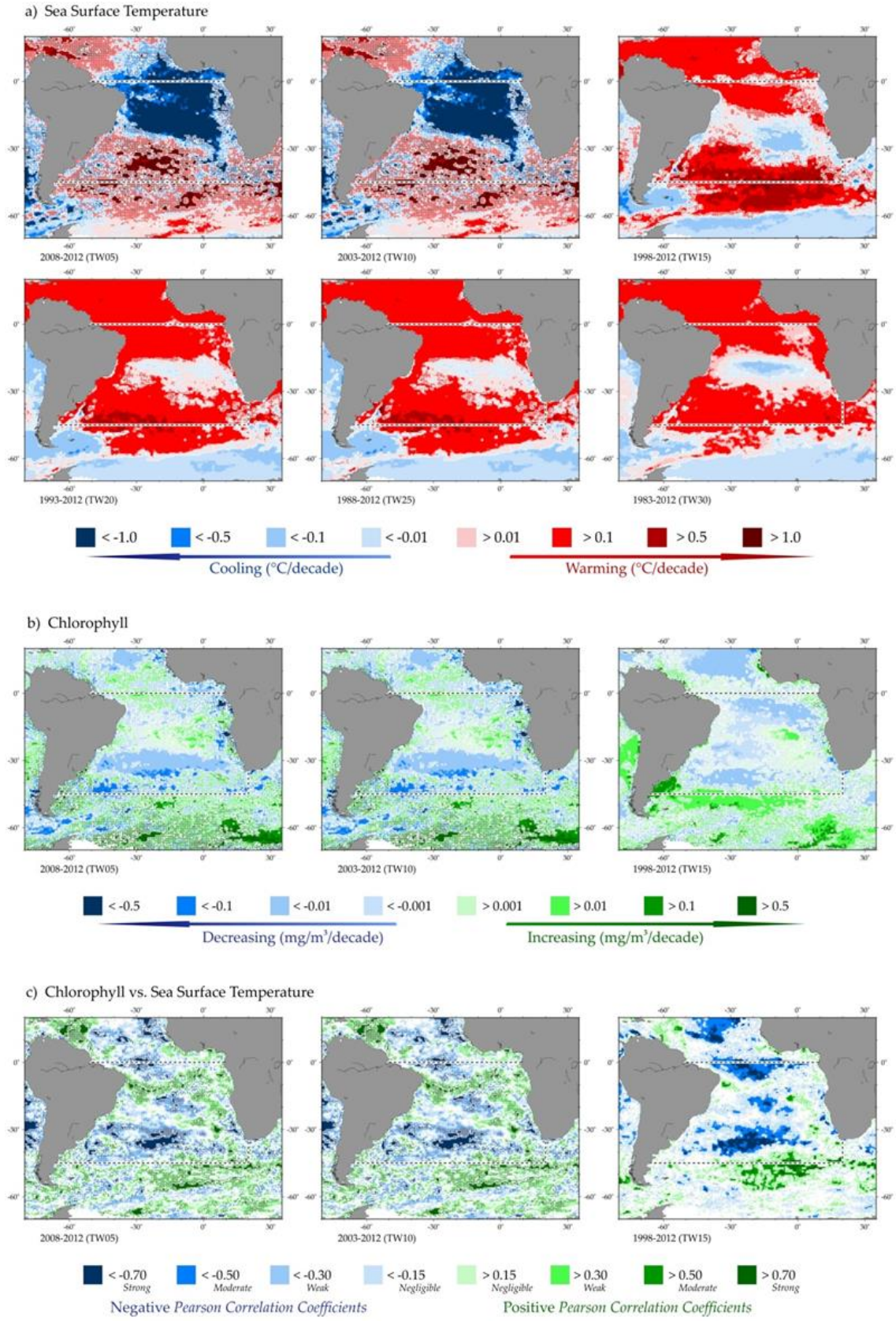

Figure 5.3. Annual trends in the South Atlantic sea surface temperature (a) and sea surface chlorophyll concentration (b), and correlations between chlorophyll and sea surface temperature (c) for each of the standard IGMETS time-windows. See "Methods" chapter for a complete description and methodology used.

5.2 General patterns of temperature and phytoplankton biomass

Different trends are described for particular variables over different time-frames. The reader is cautioned that changing the length of the time series examined will yield different trends. Some of the differences in the long-term trends examined may be due to shifts in the position of fronts and boundaries between water masses rather than changes within a single water mass. Such displacement in water masses can lead to an apparent increase or decrease in a property relative to conditions that may have prevailed in a particular region prior to such change.

The IGMETS time series of regional SST and satellite-derived chlorophyll *a* provide a means to assess change in the marine environment. Over the 30 years before 2012, nearly 86% of the South Atlantic warmed (75% at $p < 0.05$; Figure 5.3; Table 5.1). However, the South Atlantic gyre featured a cooling trend. In contrast, over the more recent 10-year time-window (2003–2012), only about 45% of the South Atlantic showed warming and 55% showed cooling (Table 5.1). Even more recently, between 2008 and 2012, there was a large area between about 30°S and 10°N that showed cooling at 0.1°C year^{-1}. Overall, 68% of the South Atlantic showed cooling during this period (Figure 5.3; Table 5.1). These results suggest that over the more recent 5-and-10-year time-periods, strong warming occurred primarily in temperate latitudes (i.e. south of ca. 30°S), with large areas showing >0.1°C year^{-1} (or warming by ca. 1°C if extrapolated over a decade). The areas showing fastest warming south of the mid-ocean gyre are waters of the South Atlantic Current and of the Antarctic Circumpolar Current (Figures 5.3 and 5.2).

Trends of satellite-derived chlorophyll concentration showed significant increases in some areas over the different time-windows, but overall, chlorophyll decreased consistently over most of the South Atlantic between 1998 and 2012 (Table 5.2). A decrease in chlorophyll concentration of 0.001–0.01 mg m^{-3} year^{-1} was observed in the central gyre between the South Atlantic Current and the Benguela Current trends around 40°S over each of the time-periods examined (i.e. 2008–2012, 2003–2012, and 1998–2012). Much of this area experienced warming of > 0.1°C year^{-1} during these periods.

To the south near the boundary defined for the South Atlantic region, there was some increase in chlorophyll concentration between 1998 and 2012 in areas where moderate warming was also observed. Concentrations increased considerably, particularly in the core of the Antarctic Circumpolar Current (Figures 5.3 and 5.2; Table 5.2; see also the "Southern Ocean" chapter, as these regions overlap). Indeed, over the 10-year time-window (2003–2012), most of the significant chlorophyll increase occurred south of 40°S (over 10% of the area of the basin; Table 5.2; Figure 5.3).

The fastest increase in chlorophyll in the South Atlantic occurred over the Patagonian Shelf, with rates > 0.05 mg m^{-3} year^{-1} observed between 1998 and the early part of the 2000s. A large positive anomaly in chlorophyll concentration was observed in the composite between 1998 and 2003 and is driven by an intrusion of the Malvinas Current onto the shelf near 41°S in 2003 (Signorini *et al*., 2009; Piola *et al*., 2010). The analysis of the satellite-derived time series of chlorophyll concentration over the central area of the Patagonian Middle Shelf (around 40°S) by Delgado *et al.* (2015) shows that concentrations after 2003 and through 2010 were lower, with a decrease in the amplitude of the seasonal cycle.

Several large areas of high chlorophyll concentration and positive biomass trends corresponded to areas of high temperature and warming trends (Figure 5.3, lower panels). Such changes can be due to either increased stability in the water column (Signorini *et al*., 2015), physiological changes in the phytoplankton and phytoplankton community composition changes over time (c.f. Behrenfeld *et al*., 2015), a shift in the position of water masses, or a combination of these.

5.2.1 Potential correlations with climate indices

The North Atlantic Oscillation (NAO) tracks the difference between atmospheric pressures near Iceland and over the Azores. Fluctuations in the strength of these features change the jet stream, temperature, and precipitation in the North Atlantic. We examined whether there were correlations between chlorophyll concentration and the NAO in the South Atlantic over 5-, 10-, or 15-year periods. Overall, the spatial pattern of correlation between chlorphyll concentration and the NAO was patchy, and correlations were low. The only area where a spatially-coherent pattern emerged was in the central area of the South Atlantic along the Subantarctic Front. Here, significant inverse correlations were observed between chlorophyll concentration and the NAO.

Table 5.1. Relative spatial areas (% of the total region) and rates of change within within the South Atlantic region that are showing increasing or decreasing trends in sea surface temperature (SST) for each of the standard IGMETS time-windows. Numbers in brackets indicate the % area with significant ($p < 0.05$) trends. See "Methods" chapter for a complete description and methodology used.

Latitude-adjusted SST data field surface area = 30.6 million km²	**5-year** (2008–2012)	**10-year** (2003–2012)	**15-year** (1998–2012)	**20-year** (1993–2012)	**25-year** (1988–2012)	**30-year** (1983–2012)
Area (%) w/ increasing SST trends ($p < 0.05$)	32.0% (*10.7%*)	44.9% (*17.4%*)	**71.8%** (*45.9%*)	**90.5%** (*70.2%*)	**91.0%** (*74.2%*)	**85.7%** (*75.3%*)
Area (%) w/ decreasing SST trends ($p < 0.05$)	**68.0%** (*45.5%*)	**55.1%** (*26.2%*)	28.2% (*9.2%*)	9.5% (*0.5%*)	9.0% (*0.4%*)	14.3% (*6.6%*)
> 1.0°C decade^{-1} warming ($p < 0.05$)	12.5% (*8.3%*)	5.4% (*5.4%*)	0.7% (*0.7%*)	0.1% (*0.1%*)	0.0% (*0.0%*)	0.0% (*0.0%*)
0.5 to 1.0°C decade^{-1} warming ($p < 0.05$)	9.6% (*2.1%*)	8.3% (*6.8%*)	12.2% (*12.0%*)	4.8% (*4.8%*)	0.7% (*0.7%*)	0.5% (*0.5%*)
0.1 to 0.5°C decade^{-1} warming ($p < 0.05$)	7.8% (*0.3%*)	20.7% (*5.2%*)	43.9% (*32.5%*)	**67.4%** (*61.7%*)	**66.9%** (*65.4%*)	**59.1%** (*58.9%*)
0.0 to 0.1°C decade^{-1} warming ($p < 0.05$)	2.1% (*0.0%*)	10.4% (*0.1%*)	15.0% (*0.7%*)	18.3% (*3.6%*)	23.3% (*8.1%*)	26.1% (*15.9%*)
0.0 to –0.1°C decade^{-1} cooling ($p < 0.05$)	2.0% (*0.0%*)	10.3% (*0.0%*)	13.6% (*0.5%*)	8.5% (*0.1%*)	8.7% (*0.2%*)	11.9% (*4.2%*)
–0.1 to –0.5°C decade^{-1} cooling ($p < 0.05$)	9.5% (*0.6%*)	30.7% (*12.9%*)	14.3% (*8.5%*)	0.9% (*0.4%*)	0.3% (*0.2%*)	2.4% (*2.4%*)
–0.5 to –1.0°C decade^{-1} cooling ($p < 0.05$)	16.3% (*8.7%*)	13.6% (*12.9%*)	0.3% (*0.2%*)	0.1% (*0.1%*)	0.0% (*0.0%*)	0.0% (*0.0%*)
> –1.0°C decade^{-1} cooling ($p < 0.05$)	40.2% (*36.2%*)	0.5% (*0.4%*)	0.0% (*0.0%*)	0.0% (*0.0%*)	0.0% (*0.0%*)	0.0% (*0.0%*)

Most of the South Atlantic SST showed low correlations with the NAO except for tropical and subtropical waters of the western Atlantic around the bulge of Brazil and southeastern South America to ca. 30°S in the area of the southern branch of the Brazil Current, with an inverse correlation with the NAO ($p < –0.40$). This pattern is part of the spatial patterns of correlation observed over much of the tropical and subtropical North Atlantic.

During a positive NAO, there is a strengthening of the Icelandic low and Azores high. This strengthening results in an increased pressure gradient over the North Atlantic, which causes westerlies to increase in strength and cold air to move off the North American continent onto the ocean. Thus, when the NAO is positive, the North Atlantic and the tropical and subtropical South Atlantic tend to cool down, and when the NAO is negative, these areas warm up.

Another climate index is the Southern Oscillation Index (SOI). The SOI is based on the sea level atmospheric pressure differences between Tahiti and Darwin, Australia. It is a measure of the differences in the atmosphere between the western and eastern tropical Pacific and tracks El Niño and La Niña episodes. Negative SOI values typically coincide with abnormally warm ocean waters across the eastern tropical Pacific, which is a characteristic of El Niño episodes. When the SOI is positive, colder waters typically occur across the eastern tropical Pacific (a characteristic of La Niña).

SST in tropical areas of the South Atlantic outside of, but adjacent to, the equatorial upwelling areas were strongly positively correlated with the SOI. Another area of positive correlation between SST and the SOI was the southern South Atlantic, south of the Subantarctic Front, i.e. in the Antarctic Circumpolar Current. SST of the central gyre of the South Atlantic showed a significant strong negative correlation with the SOI. In the central gyre, there were also areas of coherent positive correlations between chlorophyll and the SOI ($p = 0.3$–0.7). These occurred mostly in an approximately 10° × 10° area centred around 30°S and 15°W and in a

20° wide band that occupied most of the Patagonia Shelf and extended east toward Africa along about 50°S. Everywhere else, correlations between chlorophyll and the SOI were poor, including in the tropical and central South Atlantic.

5.3 Trends from *in situ* time series

There are very few *in situ* oceanographic time series of biological, ecological, and biogeochemical observations in this part of the world's oceans (Figures 5.1 and 5.4). Most *in situ* observations in the South Atlantic have been collected either once at particular locations or over short periods. Most sampling programmes are not designed to examine changes in time. One station that provides longer-term (15 years), comprehensive *in situ* measurements in the coastal marine environment is located on the Argentinian coast near Mar de Plata (Station EPEA). Another time series is located in Bahia Blanca, Argentina (1974–2016; Popovich *et al.*, 2008; Arias *et al.*, 2012; Spetter *et al.*, 2015).

The Patos Lagoon and estuary have time series from inland sites with temperature, salinity, and chlorophyll observations since 1993 (Abreu *et al.*, 2010; Odebrecht *et al.*, 2010; Haraguchi *et al.*, 2015). Since this summary chapter focuses on coastal and marine environments of the South Atlantic, the estuarine data are not discussed here.

Table 5.2 Relative spatial areas (% of the total region) and rates of change within the South Atlantic region that are showing increasing or decreasing trends in phytoplankton biomass (CHL) for each of the standard IGMETS time-windows. Numbers in brackets indicate the % area with significant ($p < 0.05$) trends. See "Methods" chapter for a complete description and methodology used.

Latitude-adjusted CHL data field surface area = 30.6 million km^2	**5-year** (2008–2012)	**10-year** (2003–2012)	**15-year** (1998–2012)
Area (%) w/ increasing CHL trends ($p < 0.05$)	33.5% (*5.5%*)	38.9% (*10.1%*)	31.1% (*10.9%*)
Area (%) w/ decreasing CHL trends ($p < 0.05$)	**66.5%** (*31.4%*)	**61.1%** (*28.5%*)	**68.9%** (*42.4%*)
> 0.50 mg m^{-3} decade^{-1} increasing ($p < 0.05$)	1.3% (*0.6%*)	0.4% (*0.2%*)	0.6% (*0.5%*)
0.10 to 0.50 mg m^{-3} decade^{-1} increasing ($p < 0.05$)	3.0% (*0.8%*)	2.8% (*1.7%*)	3.4% (*2.7%*)
0.01 to 0.10 mg m^{-3} decade^{-1} increasing ($p < 0.05$)	17.4% (*3.5%*)	15.0% (*6.0%*)	9.9% (*4.9%*)
0.00 to 0.01 mg m^{-3} decade^{-1} increasing ($p < 0.05$)	12.0% (*0.7%*)	20.8% (*2.1%*)	17.2% (*2.8%*)
0.00 to –0.01 mg m^{-3} decade^{-1} decreasing ($p < 0.05$)	10.9% (*1.1%*)	26.6% (*8.0%*)	37.8% (*20.1%*)
–0.01 to –0.10 mg m^{-3} decade^{-1} decreasing ($p < 0.05$)	41.2% (*21.3%*)	30.3% (*17.7%*)	30.3% (*21.8%*)
–0.10 to –0.5 mg m^{-3} decade^{-1} (decreasing) ($p < 0.05$)	12.0% (*7.4%*)	3.4% (*2.3%*)	0.8% (*0.5%*)
> –0.50 mg m^{-3} decade^{-1} (decreasing) ($p < 0.05$)	2.4% (*1.5%*)	0.8% (*0.5%*)	0.0% (*0.0%*)

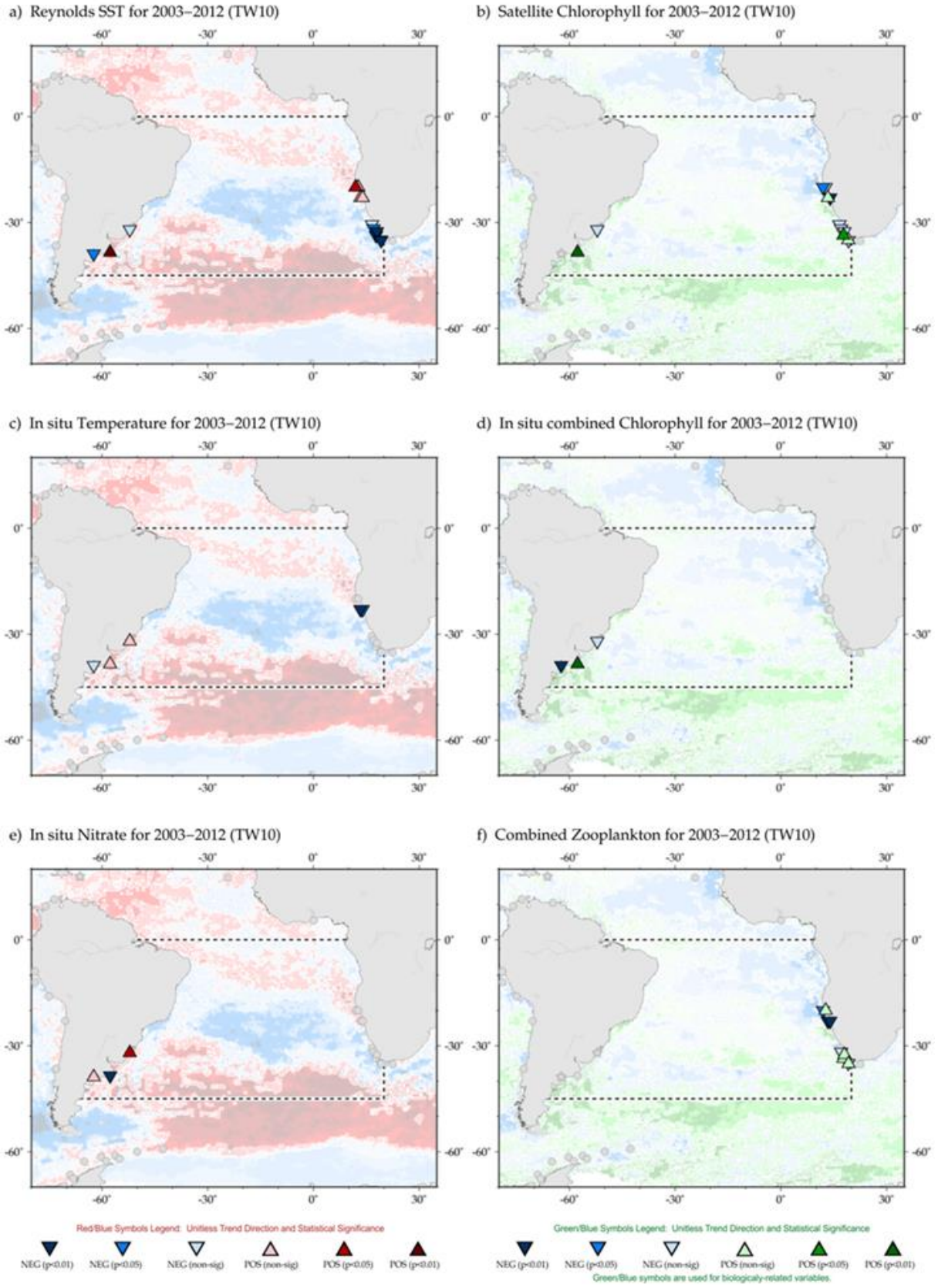

Figure 5.4. Map of South Atlantic region time-series locations and trends for select variables and IGMETS time-windows. Upward-pointing triangles indicate positive trends; downward triangles indicate negative trends. Gray circles indicate time-series site that fell outside of the current study region or time-window. Additional variables and time-windows are available through the IGMETS Explorer (http://IGMETS.net/explorer). See "Methods" chapter for a complete description and methodology used.

Along the southwestern coast of Africa, zooplankton measurements are intermittently available for the past 30 years (zooplankton and chlorophyll *a* time-series data are available from Walvis Bay off Namibia at 23°S; zooplankton data are available from Palgrave Point at 20°S off Namibia and various stations off South Africa). We present a summary of the trends observed with some of these time-series stations, but it is unfortunately impossible to extrapolate these trends to other regions of the central South Atlantic or to coastal areas removed from these locations.

The EPEA *in situ* chlorophyll time series shows a significant ($p < 0.01$) increase in chlorophyll concentration during 2003–2012. The trend is not significant for the 15-year period 1998–2012 nor for the 5-year period spanning 2008–2012; the increase was, however, still visible. These observations are inconsistent with the satellite data over the middle shelf (Signorini *et al*., 2009; Piola *et al*., 2010), but they are consistent with satellite observations over the inner shelf (Delgado *et al*., 2015). EPEA also reported increasing salinity and decreasing nitrate concentrations during this period. The trends remained consistent regardless of the time-window examined (5, 10, or 15 years; Figure 5.4).

In the northern Benguela, the *in situ* integrated (0–30 m) chlorophyll *a* concentration time series (2001–2012) off Walvis Bay showed a decline during 2001–2006, followed by an increase with peak values during 2009–2011. This is in contrast to the satellite-derived time series (1998–2012), which suggests an increase in surface chlorophyll *a* concentration since 2003. This is contrary to what would be expected from increasing SST associated with decreasing upwelling (Jarre *et al*., 2015). There is no comparable uninterrupted, long-term, *in situ* chlorophyll *a* concentration time series for the southern Benguela. However, the phytoplankton data from ship (1980–2007) and satellite observations (1998–2012) indicate multiannual variability and a seasonal cycle, with very high concentrations due to dinoflagellate blooms in late local summer/autumn.

Again, there is also no obvious overall decade-scale trend in chlorophyll concentration (Hutchings *et al*., 2009; Jarre *et al*., 2015; Verheye *et al*., 2016).

There have been long-term shifts in the abundance, biomass, production, and community structure (species and size composition) of zooplankton, and specifically copepods, in both the northern and southern Benguela over the past six decades (Verheye *et al*., 2016). Copepods had been increasing in abundance since the 1950s. However, there was a turning point in the mid-1990s in the south and also in the mid-2000s in the north, after which zooplankton seemed to decline or stabilize. Indeed, a declining trend in copepod abundance was observed off the coast of Namibia and South Africa from the 1990s until the early-mid 2000's (15- and 20-year time windows). Conversely, over shorter 10- and 5-year time-windows, copepod abundance shows an increase again in those locations. A shift from large to smaller species dominating the copepod communities was observed in both Benguela subsystems. In the southern Benguela, copepod biomass and daily production were higher in the north (North and Central West Coast) than in the south (Southwest Coast and Western Agulhas Bank). They were higher in late local spring/early summer than in late autumn/early winter (Huggett *et al*., 2009). Species and size composition of the copepod community also varied both spatially and seasonally.

Copepod biomass on the Western Agulhas Bank has declined by about 22% since 1988. In particular, the abundance of the large calanoid copepod *Calanus agulhensis* decreased by 44% (Jenny Huggett, pers. comm). This could be due to predation from an increase in pelagic fish biomass as well as an increase in SST. Marked declines in copepod biomass have also been observed on the Agulhas Bank off Mossel Bay, which falls within the Indian Ocean region (see Chapter 7).

5.4 Consistency with previous analyses

Several studies have described the general biogeography of the surface South Atlantic in terms of basic oceanographic characteristics (bathymetry, hydrography, productivity, and trophic structure). The most notable are the descriptions provided by Longhurst (1998, 2007) and those under the Large Marine Ecosystems (LME) classification (see summary in Sherman, 1991). Here, we provide a brief summary of major characteristics of marine ecosystems in the context of hydrology and chlorophyll concentration in the South Atlantic and how they compare with results from the observations presented here.

Sherman *et al*. (2009) point out that all of the LMEs of the world except for two (the California Current and Humboldt Current, both in the Eastern Pacific Ocean) showed warming between 1982 and 2006. In the South Atlantic, the temperature in tropical and subtropical LMEs rose 0.3–0.6°C during this period, while more temperate LMEs farther south warmed by < 0.1°C. Fisheries yields in the Patagonian Shelf LME increased

over this period, while declining over the East and South Brazil Shelf LME (Müller-Karger *et al*., 2017). Trends in these areas are likely due to high levels of fisheries exploitation rather than oceanographic or climate-related bottom–up controls (Sherman *et al*., 2009). The Benguela Current LME off southwest Africa showed a declining trend in fisheries yields due to both heavy exploitation and environmental controls (van der Lingen *et al*., 2006; Travers-Trolet *et al*., 2014). Gherardi *et al*. (2010) attempted to examine large-scale drivers, including El-Niño Southern Oscillation (ENSO) and the Pacific Decadal Oscillation (PDO), and concluded that the features that defined the original LME will evolve with climate change, leading to possible changes in the core ecological criteria used to define these areas.

Similar to what was observed in this analysis, Signorini *et al*. (2015) found that the South Atlantic gyre, centred around 50°W and 30°S, showed a slight, but not significant, negative trend in chlorophyll concentration. This result covered a 16-year (1998–2013) record of combined SeaWiFS and MODIS chlorophyll *a* data, SST, and other complementary data. Vantrepotte and Mélin (2011) also found a decreasing trend in chlorophyll *a* concentration of ca. –1 to –3% year^{-1} in the core of the South Atlantic gyre using a 10-year time series of SeaWiFS data (1997–2007). Polovina *et al.* (2008) had earlier suggested that there was both a negative trend in chlorophyll concentration as well as an expansion in the surface area occupied by low concentrations in the South Atlantic gyre area. However, the analysis by Gregg and Rousseux (2014) did not find a significant negative trend or an expansion of the area of low concentration in the South Atlantic gyre region using satellite chlorophyll time series spanning 1998–2012.

Consistent with the observations presented here, these prior studies also showed an increasing trend (>3% year^{-1}) in chlorophyll concentration in a broad band that traces the Benguela–South Equatorial Current, i.e. extending from southwest Africa to the bulge of Brazil in the eastern tropical South Atlantic. This increase is to the east and northeast of the South Atlantic gyre. The positive trend in chlorophyll *a* concentration along the edge of the Patagonian Shelf and extending across the southern South Atlantic basin just south of 45°S, i.e. in the area of the Subantarctic Front, was also reported in all these previous studies. As discussed earlier, changes in chlorophyll concentration on and along the mid- and outer Patagonian Shelf were related to changes in the physical structure of waters over the shelf and adjacent areas (Saraceno *et al*., 2005; Romero *et al*., 2006; Machado *et al*., 2013; Valla and Piola, 2015).

Signorini *et al.* (2015) showed that the seasonal dynamics of chlorophyll concentration in the major ocean gyres, including the South Atlantic gyre, are closely tied to the depth of the mixed layer. In all basins, the seasonal chlorophyll peak coincided with the deepest mixed-layer depth. The analysis of satellite-derived chlorophyll *a* concentration and numerical model results of the South Atlantic basin by da Silveira Pereira *et al*. (2014) showed that chlorophyll and physical parameters, including surface temperature and salinity, exhibited correlations at zero lag, but also at frequencies that coincide with ENSO signals throughout the interior of the South Atlantic.

The eastern South Atlantic showed very dynamic oceanographic features. Rings (large eddies), shed periodically from the Agulhas Current, move to the northwest into the interior of the South Atlantic (see summary by Villar *et al*., 2015). Agulhas rings, as well as Agulhas filaments and cyclonic eddies, interact with the shelf ecosystem. This exports large volumes of water and biological material (phytoplankton, zooplankton, and fish, fish eggs, and larvae) from the Agulhas Bank to the open ocean in the Indian Ocean, and far into the Atlantic Ocean (Duncombe Rae, 1991; Duncombe Rae *et al*., 1992; Hutchings *et al*., 1998).

5.5 Conclusions

In general, in the 5-year period prior to 2012, over 30% of the area of the South Atlantic showed warming, with nearly 70% of the area showing cooling (Table 5.1). However, when considering the two to three decades prior to 2012, nearly 90% of the area of the South Atlantic showed warming, with only about 10% showing no change or slightly decreasing SST trends (Table 5.1). About 30% of the area of the South Atlantic showed increasing chlorophyll *a* concentrations in the 5-year period prior to 2012, with over 66% of the area showing decreasing concentrations. The trends over the decade and a half spanning 1998–2012 were similar (Table 5.2).

The paucity of *in situ* time series in this region and the striking changes that have been reported in South Atlantic ecosystems over the past two decades highlight the need to have a better observing system in place. Such an observing system is needed to collect concurrent time series of physical, ecological, and biogeochemical observations.

Table 5.3. Time-series sites located in the IGMETS South Atlantic region. Participating countries: Argentina (ar), Brazil (br), Namibia (na), United Kingdom, (uk), and South Africa (za). Year-spans in red text indicate time series of unknown or discontinued status. IGMETS-IDs in red text indicate time series without a description entry in this Annex.

No.	IGMETS-ID	Site or programme name	Year-span	T	S	Oxy	Ntr	Chl	Mic	Phy	Zoo
1	ar-10101	Puerto Cuatreros *(Bahia Blanca Estuary)*	1975–present	X	X	X	X	X	-	-	-
2	ar-10201	EPEA – Estacion Permanente de Estudios Ambientales *(Argentine Coastal Waters)*	2000–present	X	X	-	X	X	X	-	-
3	br-10101	Patos Lagoon Estuary – Phytoplankton Time Series *(Southeastern Brazil)*	1993–present	X	X	-	X	X	X	X	-
4	na-10101	Walvis Bay 23S shelf *(Northern Benguela Current)*	1978–present	X	X	X	-	-	-	-	X
5	na-10102	Namibia 20S shelf *(Northern Benguela Current)*	2002–present	-	-	-	-	-	-	-	X
6	na-10103	Walvis Bay 23S offshore *(Northern Benguela Current)*	1978–present	X	X	X	-	-	-	-	X
7	na-10104	Namibia 20S offshore *(Northern Benguela Current)*	2002–present	-	-	-	-	-	-	-	X
8	uk-30601	Atlantic Meridional Transect (AMT)	1995–present	X	X	X	X	X		X	X
9	za-10101	St Helena Bay *(Southern Benguela Current)*	1951–present	X	X	-	-	-	-	-	X
10	za-30101	SBCTS-A: North West Coast *(Southern Benguela Current)*	1988–present	-	-	-	-	-	-	-	X
11	za-30102	SBCTS-B: Central West Coast *(Southern Benguela Current)*	1988–present	-	-	-	-	-	-	-	X
11	za-30103	SBCTS-C: South West Coast *(Southern Benguela Current)*	1988–present	-	-	-	-	-	-	-	X
12	za-30104	SBCTS-D: Western Agulhas Bank *(Southern Benguela Current)*	1988–present	-	-	-	-	-	-	-	X
13	za-30201	ABCTS Danger Point Monitoring Line *(Agulhas Bank)*	1988–present	-	-	-	-	-	-	-	X

5.6 References

Abreu, P. C, Bergesch, M., Proença, L. A., Garcia, C. A. E., and Odebrecht, C. 2010. Short- and long-term chlorophyll a variability in the shallow microtidal Patos Lagoon Estuary, Southern Brazil. Estuaries and Coasts, 33: 554–569, doi:10.1007/s12237-009-9181-9.

Andrews, W. R. H., and Hutchings, L. 1980. Upwelling in the Southern Benguela Current. Progress in Oceanography, 9(1): 1–81, doi:10.1016/0079-6611(80)90015-4.

Arias, A. H., Piccolo, M. C., Spetter, C. V., Freije, R. H., and Marcovecchio, J. E. 2012. Lessons from multi-decadal oceanographic monitoring at an estuarine ecosystem in Argentina. International Journal of Environmental Research, 6(1): 219–234.

Behrenfeld, M. J., O'Malley, R. T., Boss, E. S., Westberry, T. K., Graff, J. R., Halsey, K. H., Milligan, A. J., *et al*. 2015. Revaluating ocean warming impacts on global phytoplankton. Nature Climate Change, 5: doi:10.1038/NCLIMATE2838.

Deacon, G. E. R. 1933. A general account of the hydrology of the South Atlantic Ocean. Discovery Reports, 7: 171–238.

da Silveira Pereira, N. E., Harari, J., and de Camargo, R. 2014. Correlations of remote sensing chlorophyll-a data and results of a numerical model of the tropical and South Atlantic Ocean circulation. Journal of Geology and Geosciences, 3: 171, doi:10.4172/2329-6755.1000171.

Delgado, A. L., Loisel, H., Jamet, C., Vantrepotte, V., Perillo, G. M. E., and Piccolo, M. C. 2015. Seasonal and inter-annual analysis of chlorophyll-a and inherent optical properties from satellite observations in the inner and mid-shelves of the south of Buenos Aires Province (Argentina). Remote Sensing, 7: 11821–11847, doi:10.3390/rs70911821.

Duncombe Rae, C. M. 1991. Agulhas retroflection rings in the South Atlantic: an overview. South African Journal of Marine Science, 11: 327–344.

Duncombe Rae, C. M, Shillington, F., Agenbag, J., Taunton-Clark, J., and Grundlingh, M. 1992. An Agulhas ring in the South Atlantic ocean and its interaction with the Benguela upwelling frontal system. Deep-Sea Research, 39: 2009–2027.

Eakins, B. W., and Sharman, F. 2010. Volumes of the World's Oceans from ETOPO1. NOAA National Geophysical Data Center, Boulder, CO.

Garzoli, S. L., and Matano, R. 2011. The South Atlantic and the Atlantic meridional overturning circulation. Deep-Sea Research II, 58(17–18): 1837–1847, doi:10.1016/j.dsr2.2010.10.063.

Gherardi, D. F. M, Tavares Paes, E., Cahanhuk Soares, H., Ponzi Pezzi, L., and Kayano, M. T. 2010. Differences between spatial patterns of climate variability and large marine ecosystems in the western South Atlantic. Pan-American Journal of Aquatic Sciences, 5(2): 310–319.

Gregg, W. W., and Rousseaux, C. S. 2014. Decadal trends in global pelagic ocean chlorophyll: A new assessment integrating multiple satellites, in situ data, and models, Journal of Geophysical Research Oceans, 119: 5921–5933, doi:10.1002/2014JC010158.

Guhin, S., Ray, P, Mariano, A. J., and Ryan, E. H. 2003. The South Atlantic Current. Ocean Surface Currents. http://oceancurrents.rsmas.miami.edu/southern/south-atlantic.html.

Haraguchi, L., Carstensen, J., Abreu, P. C., and Odebrecht, C. 2015. Long-term changes of the phytoplankton community and biomass in the subtropical shallow Patos Lagoon Estuary, Brazil. Estuarine, Coastal and Shelf Science, 162: 76–87.

Huggett, J., Verheye, H., Escribano, R., and Fairweather, T. 2009. Copepod biomass, size composition and production in the Southern Benguela: Spatio–temporal patterns of variation, and comparison with other eastern boundary upwelling systems. Progress in Oceanography, 83(1): 197–207.

Hutchings, L., Barange, M., Bloomer, S. F., Boyd, A. J., Crawford, R. J. M., Huggett, J. A., Kerstan, M., *et al.* 1998. Multiple factors affecting South African anchovy recruitment in the spawning, transport, and nursery areas. *In* Benguela Dynamics: Impacts of Variability on Shelf-Sea Environments and their Living Resources, pp. 211–225. Ed. by S. C. Pillar, C. L. Moloney, A. I. L. Payne, and F.A. Shillington. South African Journal of Marine Science, 19.

Hutchings, L., van der Lingen, C. D., Shannon, L. J., Crawford, R. J. M., Verheye, H. M. S., Bartholomae, C. H., van der Plas, A. K., *et al*. 2009. The Benguela Current: An ecosystem of four components, Progress in Oceanography, 83: 15–32.

Hu, C., Montgomery, E. T., Schmitt, R. W., and Muller-Karger, F. E. 2004. The Amazon and Orinoco River plumes in the tropical Atlantic and Caribbean Sea: Observation from space and S-PALACE floats. Deep-Sea Research Part II. Topical Studies in Oceanography, 51(10–11): 1151–1171.

Jarre, A., Hutchings, L., Kirkman, S. P., Kreiner, A., Tchipalanga, P., Kainge, P., Uanivi, U., *et al*. 2015. Synthesis: climate effects on biodiversity, abundance and distribution of marine organisms in the Benguela. Fisheries Oceanography, 24 (Suppl. 1): S122–S149.

Johns, E. M., Muhling, B. A., Perez, R. C., Müller-Karger, F. E., Melo, N., Smith, R. H., Lamkin, J. T., *et al*. 2014. Amazon River water in the northeastern Caribbean Sea and its effect on larval reef fish assemblages during April 2009. Fisheries Oceanography, 23: 472–494, doi:10.1111/fog.12082.

Krummel, O. 1882: Bemerkungen uber die Meeresstromungen und Temperaturen in der Falklandsee. Aus dem Archiv der Deutschen Seewarte, V(2). 25 pp.

Longhurst, A. R. A. 1998. Ecological Geography of the Sea. Academic Press, San Diego. 398 pp.

Longhurst, A. R. A. 2007. Ecological Geography of the Sea, 2nd edn. Academic Press, San Diego. 542 pp.

Lopez, H., Dong, S., Lee, S-K., and Goni, G. 2016. Decadal modulations of interhemispheric global atmospheric circulations and monsoons by the South Atlantic Meridional Overturning Circulation. Journal of Climate, 29: 1831–1851, doi:http://dx.doi.org/10.1175/JCLI-D-15-0491.1.

Lumpkin, R., and Speer, K. 2007. Global ocean meridional overturning. Journal of Physical Oceanography, 37: 2550–2562.

Machado, I., Barreiro, M., and Calliari, D. 2013. Variability of chlorophyll-*a* in the Southwestern Atlantic from satellite images: Seasonal cycle and ENSO influences. Continental Shelf Research, 53: 102–109.

Matano, R. P., Palma, E. D., and Piola, A. R. 2010. The influence of the Brazil and Malvinas Currents on the southwestern Atlantic shelf circulation. Ocean Science, 6: 983–995.

Muller-Karger, F. E., McClain, C. R., and Richardson, P. L. 1988. The dispersal of the Amazon's water. Nature, 333: 56–59.

Muller-Karger, F. E., Richardson, P. L., and McGillicuddy, D. 1995. On the offshore dispersal of the Amazon's Plume in the North Atlantic. Deep-Sea Research I, 42(11–12): 2127–2137.

Muller-Karger, F., Rueda-Roa, D., Chavez, F., Kavanaugh, M., and Roffer, M A. 2017. Megaregions among the Large Marine Ecosystems of the Americas. Environmental Development, http://dx.doi.org/10.1016/j.envdev.2017.01.005.

Nelson, G., and Hutchings, L. 1983. The Benguela upwelling area. Progress in Oceanography, 12(3): 333–356.

Odebrecht, C., Abreu, P. C., Bemvenuti, C. E., Copertino, M., Muelbert, J. H., Vieira, J. P., and Seeliger, U. 2010. The Patos Lagoon Estuary: Biotic responses to natural and anthropogenic impacts in the last decades (1979-2008). *In* Coastal Lagoons: Critical Habitats of Environmental Change, pp. 433–455. Ed. by M. J. Kennish, and H. W. Paerl. CRC Press, Boca Raton, FL. 568 pp.

Piola, A. R., Martinez Avellaneda, N., Guerrero, R. A., Jardon, F. P., Palma, E. D., and Romero, S. I. 2010. Malvinas-slope water intrusions on the northern Patagonia continental shelf. Ocean Science, 6: 345–359.

Polovina, J. J., Howell, E. A., and Abecassis, M. 2008. Ocean's least productive waters are expanding. Geophysical Research Letters, 35: L03618, doi:10.1029/2007GL031745.

Popovich, C. A., Spetter, C. V., Marcovecchio, J. E., and Freije, R. H. 2008. Dissolved nutrient availability during winter diatom bloom in a turbid and shallow estuary (Bahia Blanca, Argentina). Journal of Coastal Research, 24(1): 95–102.

Romero, S. I., Piola, A. R., Charo, M., and Garcia, C. A. E. 2006. Chlorophyll-a variability off Patagonia based on SeaWiFS data, Journal of Geophysical Research, 111: C05021, doi:10.1029/2005JC003244.

Saraceno, M., Provost, C., and Piola, A. R. 2005. On the relationship between satellite-retrieved surface temperature fronts and chlorophyll a in the western South Atlantic. Journal of Geophysycal Research, Oceans, 110(C11): doi:10.1029/2004JC002736.

Savoye, B., Babonneau, N., Dennielou, B., and Bez, M. 2009. Geological overview of the Angola–Congo margin, the Congo deep-sea fan and its submarine valleys. Deep-Sea Research Part II: Topical Studies in Oceanography, 56(23): 2169–2182.

Sherman, K. 1991. The Large Marine Ecosystem concept: research and management strategy for living marine resources. Ecological Applications, 1: 349–360, http://dx.doi.org/10.2307/1941896.

Sherman, K., Belkin, I. M., Friedland, K. D., O'Reilly, J., and Hyde, K. 2009. Accelerated warming and emergent trends in fisheries biomass yields of the world's large marine ecosystems. Ambio, 4: 215–224.

Shillington, F. A., Reason, C. J. C., Duncombe, C. M., Florenchie, R. P., and Penven, P. 2006. Large scale physical variability of the Benguela Current Large Marine Ecosystem (BCLME). *In* Large Marine Ecosystems, Vol. 14, pp. 47–68. Ed. by V. Shannon, G. Hempel, P. Malanotte-Rizzoli, C. Moloney, and J. Woods. Elsevier. 410 pp.

Signorini, S. R., Franz, B. A., and McClain, C. R. 2015. Chlorophyll variability in the oligotrophic gyres: mechanisms, seasonality and trends. Frontiers in Marine Science, 02: http://dx.doi.org/10.3389/fmars.2015.00001.

Signorini, S. R., Garcia, V. M. T., Piola, A. R., Evangelista, H., McClain, C. R., Garcia, C. A. E., and Mata, M. M. 2009. Further studies on the physical and biogeochemical causes for large interannual changes in the Patagonian Shelf spring-summer phytoplankton bloom biomass. NASA/TM-2009-214176, NASA Goddard Space Flight Center, Greenbelt, MD, USA.

Spetter, C. A., Popovich, C. A., Arias, A., Asteasuain, R. O., Freije, R. H., and Marcovecchio, J. E. 2015. Role of nutrients in the phytoplankton development during a winter diatom bloom in a eutrophic South American estuary (Bahia Blanca, Argentina). Journal of Coastal Research, 31(1): 76–87.

Travers-Trolet, M., Shin, Y-J., Shannon, L. J., Moloney, C. L., and Field, J. G. 2014. Combined fishing and climate forcing in the Southern Benguela upwelling ecosystem: an end-to-end modelling approach reveals dampened effects. PLOS ONE, 9(4): e94286, doi:10.1371/journal.pone.0094286.

Valla, D., and Piola, A. R. 2015. Evidence of upwelling events at the northern Patagonian shelf break. Journal of Geophysical Research Oceans, 120(11): 7635–7656, doi:10.1002/2015JC011002.

van der Lingen, C., Freon, P., Hutchings, L., Roy, C., Bailey, G., Bartholomae, C., Cockcroft, A., *et al*. 2006. Resource and ecosystem variability, including regime shifts, in the Benguela Current system. *In* Benguela: Predicting a Large Marine Ecosystem, pp. 147–184. Ed. by V. Shannon, G. Hempel, P. Malanotte-Rizzoli, C. Moloney, and J. Woods. Elsevier. 438 pp.

Vantrepotte, V., and Melin, F. 2011. Inter-annual variations in the SeaWiFS global chlorophyll *a* concentration (1997–2007). Deep-Sea Research Part I, 58: 429–441.

Verheye, H., Lamont, T., Huggett, J. A., Kreiner, A., and Hampton, I. 2016. Plankton productivity of the Benguela Current Large Marine Ecosystem (BCLME). Environmental Development, 17: http://dx.doi.org/10.1016/j.envdev.2015.07.011i

Villar, E, Farrant, G. K., Follows, M., Garczarek, L., Speich, S., Audic, S., Bittner, L., *et al*. 2015. Ocean plankton. Environmental characteristics of Agulhas rings affect inter-ocean plankton transport. Science, 348(6237): 1261447, doi:10.1126/science.1261447.

Violante, R. A., Paterlini, C. M., Marcolini, S. I., Costa, I. P., Cavallotto, J. L., Laprida, C., Dragani, W., *et al*. 2014. The Argentine continental shelf: morphology, sediments, processes and evolution since the Last Glacial Maximum. *In* Continental Shelves of the World: Their Evolution During the Last Glacio-Eustatic Cycle, pp. 55–68. Ed. by F. L. Chiocci, and A. R. Chiva. Geological Society Memoir No. 41, The Geological Society, London. 343 pp.

Wefer, G., Berger, W. H., Siedler, G., and Webb, D. J. 1996. The South Atlantic: Present and Past Circulation. Springer, Berlin Heidelberg. 644 pp.

Whitworth, T., and Nowlin Jr., W. D. 1987: Water masses and currents of the southern ocean at the Greenwich meridian, Journal of Geophysical Research, 92: 6462–6476.

6 Southern Ocean

Peter H. Wiebe, Angus Atkinson, Todd D. O'Brien, Peter A. Thompson, Graham Hosie, Laura Lorenzoni, Michael Meredith, and Hugh Venables

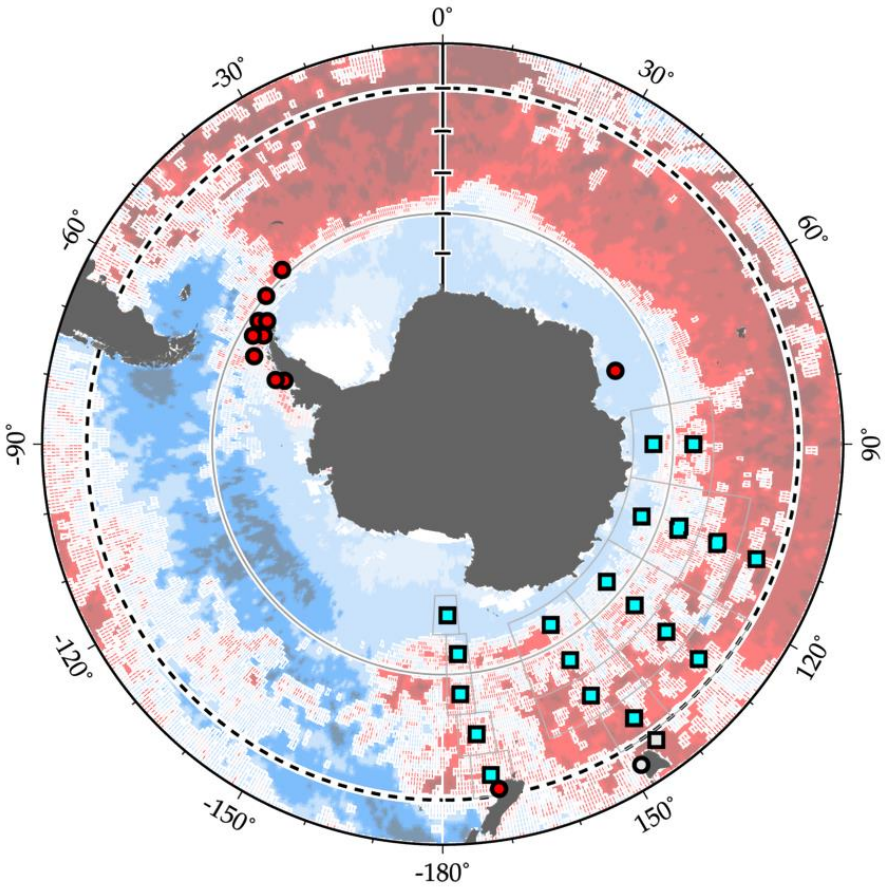

Figure 6.1. Map of IGMETS-participating Southern Ocean time series on a background of a 10-year time-window (2003–2012) sea surface temperature trends (see also Figure 6.3). At the time of this report, the Southern Ocean collection consisted of 32 time series (coloured symbols of any type), of which 21 were from Continuous Plankton Recorder subareas (blue boxes). The dashed line at 45°S indicates the boundary between the IGMETS Southern Ocean region and other IGMETS regions in this report (e.g. South Pacific, South Atlantic, Indian Ocean), while the gray line at 60°S indicates the Antarctic Treaty boundary. Uncoloured (gray) symbols indicate time series being addressed in a different regional chapter. See Table 6.3 for a listing of this region's participating sites. Additional information on the sites in this study is presented in the Annex.

Participating time-series investigators

Angus Atkinson, Uli Bathmann, Alexander Brearley, Andrew Clarke, Kim Currie, Hugh Ducklow, Mitsuo Fukuchi, Simeon Hill, Graham Hosie, Keith Hunter, So Kawaguchi, Takahashi Kunio, Douglas Martinson, Michael Meredith, Evgeny Pakhomov, Malcolm Reid, Christian Reiss, Don Robertson, Karen Robinson, Oscar Schofield, Volker Siegel, Debbie Steinberg, and Hugh Venables

This chapter should be cited as: Wiebe, P. H., Atkinson, A., O'Brien, T. D., Thompson, P. A., Hosie, G., Lorenzoni, L., Meredith, M., *et al.* 2017. Southern Ocean. I*n* What are Marine Ecological Time Series telling us about the ocean? A status report, pp. 97–112. Ed. by T. D. O'Brien, L. Lorenzoni, K. Isensee, and L. Valdés. IOC-UNESCO, IOC Technical Series, No. 129. 297 pp.

6.1 Introduction

The Southern Ocean is a vast ocean region that surrounds the Antarctic continent. It forms the southern connections to the Atlantic, Pacific, and Indian oceans and, while its northern boundary is not clearly defined ecologically, the northern limit, by treaty, is defined as 60°S (Figure 6.1, gray line). Based on hydrographic regimes, the Southern Ocean extends to the Subtropical Front (Figure 6.2), which can be found north of 40°S in some regions (Orsi *et al*., 1995; Belkin and Gordon, 1996; Moore and Abbott, 2000; Sokolov and Rintoul, 2009a, b; Talley *et al*., 2011).

The cold (< ~5°C) waters associated with the Southern Ocean occupy this ~60 million km² region south of the Antarctic Polar Front. This is a mainly deep ocean habitat, especially in the eastern Atlantic, Indian, and Pacific sectors; only 12% of the area south of the Antarctic Polar Front comprises shelf and slope waters shallower than 2000 m (Atkinson *et al*., 2009). Using ETOPO2-v2 bottom topography data (National Geophysical Data Center, 2006), 12.4% of the IGMETS-defined Southern Ocean area was shallower than 2000 m, 9.8% shallower than 1000 m, 6.3% shallower than 500 m, and 4.6% shallower than 250 m. Despite the depth of these shelves (most > 200 m) and their limited spatial extent, they are still important biogeochemically and ecologically due to their effect on hydrography, nutrient supply, carbon drawdown, and the Southern Ocean foodweb. For example, the elevated productivity of the Southwest Atlantic sector relates to its relatively shallow and rugged, complex bathymetry and concomitantly high inputs of iron into the generally low iron environment of the Antarctic Circumpolar Current (Atkinson *et al*., 2008).

The circulation in the Southern Ocean is unique in the world's oceans with the Antarctic Circumpolar Current (ACC), which circulates clockwise around the continent continuously, driven by wind stress and buoyancy forcing, and transports about 100 Sv (1 Sv = 106 $m^3 s^{-1}$) eastward (Orsi *et al*., 1995) (Figure 6.2a). The ACC has a structured frontal system composed of three major surface fronts: the Subantarctic Front (SAF), the Polar Front (PF) in the middle, and the Southern ACC Front (SF) (Figure 6.2b). The SAF defines the northern boundary of the ACC, marked by a major change in temperature, salinity, sea surface height, and speed and direction of current flow, all which act as a major biogeographic boundary for plankton (McLeod *et al*., 2010; Hosie *et al*., 2014). Farther south of the SF is the southern limit of the ACC (Southern Boundary; Orsi *et al*., 1995). Average sea surface temperature (SST) is > 4°C north of the SAF and < 2°C south of the PF. Closer to the Antarctic continent and on the continental shelf, a westward flowing counter-current flows during some portions of the year (e.g. Moffat *et al*., 2008). Between the SF and the Antarctic continent, SST is about –1.0°C.

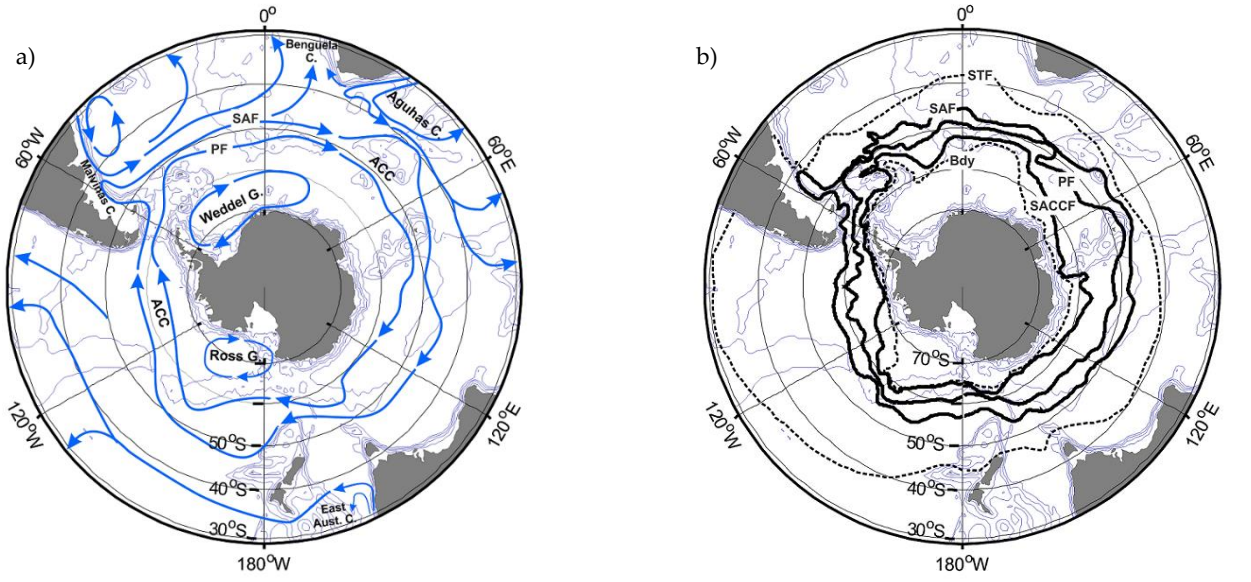

Figure 6.2. a) Major Southern Ocean currents (redrawn from/retrieved from the Encyclopedia of Earth, http://www.eoearth.org). b) Southern Ocean frontal features: ACC - Antarctic Circumpolar Current, STF - Subtropical Front; SAF – Subantarctic Front; PF – Polar Front; SACCF – Southern ACC Front; Bdy – Southern boundary of the ACC (Fronts data from Orsi and Harris, 2001).

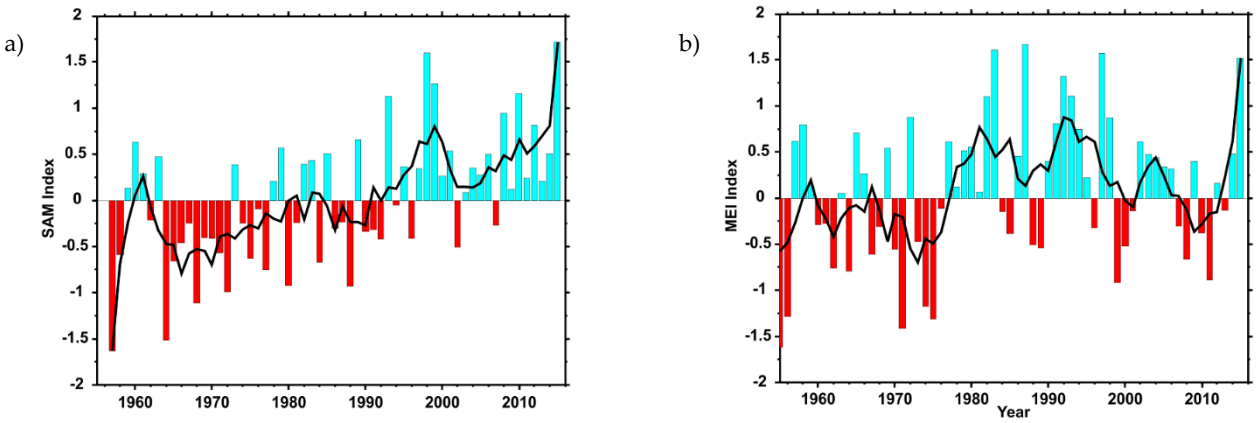

Figure 6.3. a) The Southern Annular Mode (SAM) index changes since 1957 (data: https://legacy.bas.ac.uk/met/gjma/sam.html); b) The Multivariate ENSO Index (MEI) changes since 1957 (data: http://www.esrl.noaa.gov/psd/enso/mei/).

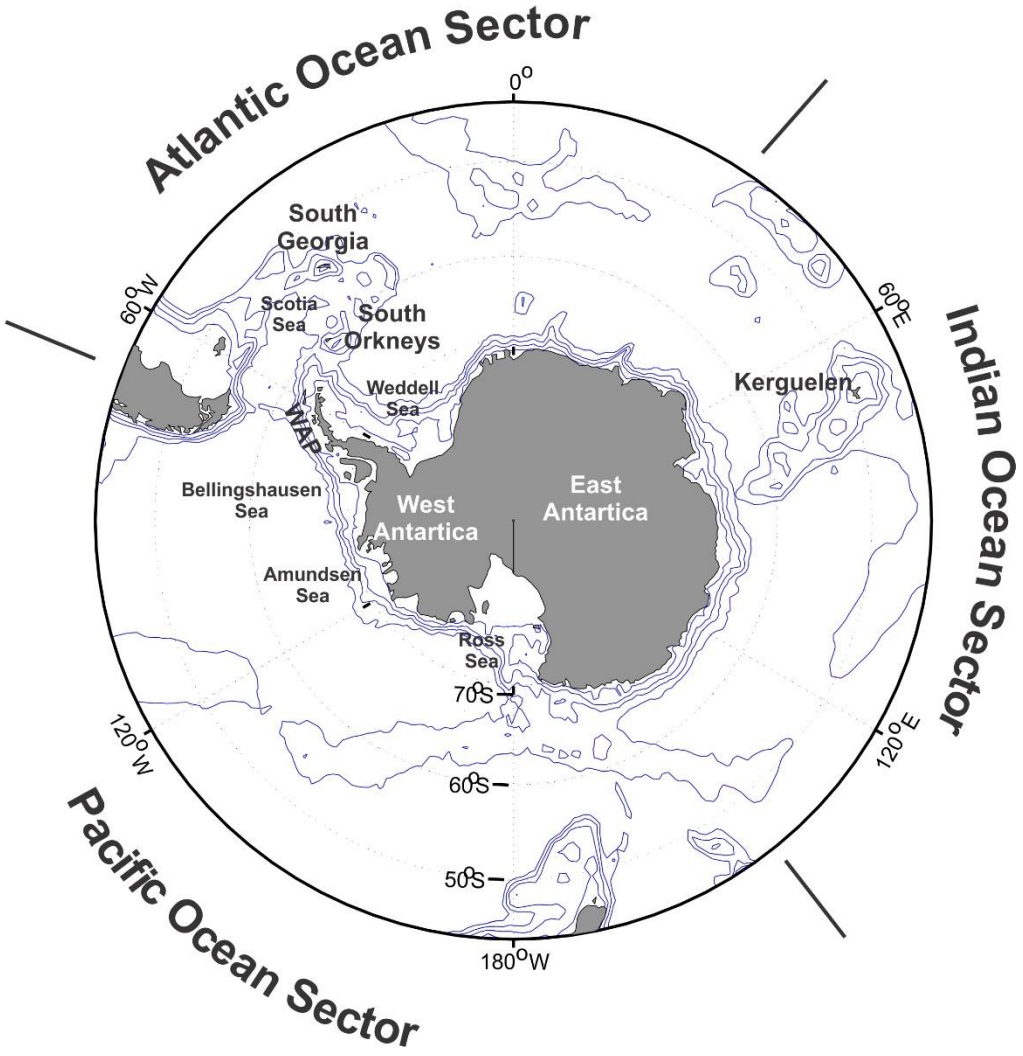

Figure 6.4. Map indicating regions of importance with the Southern Ocean and Antarctica landmass.

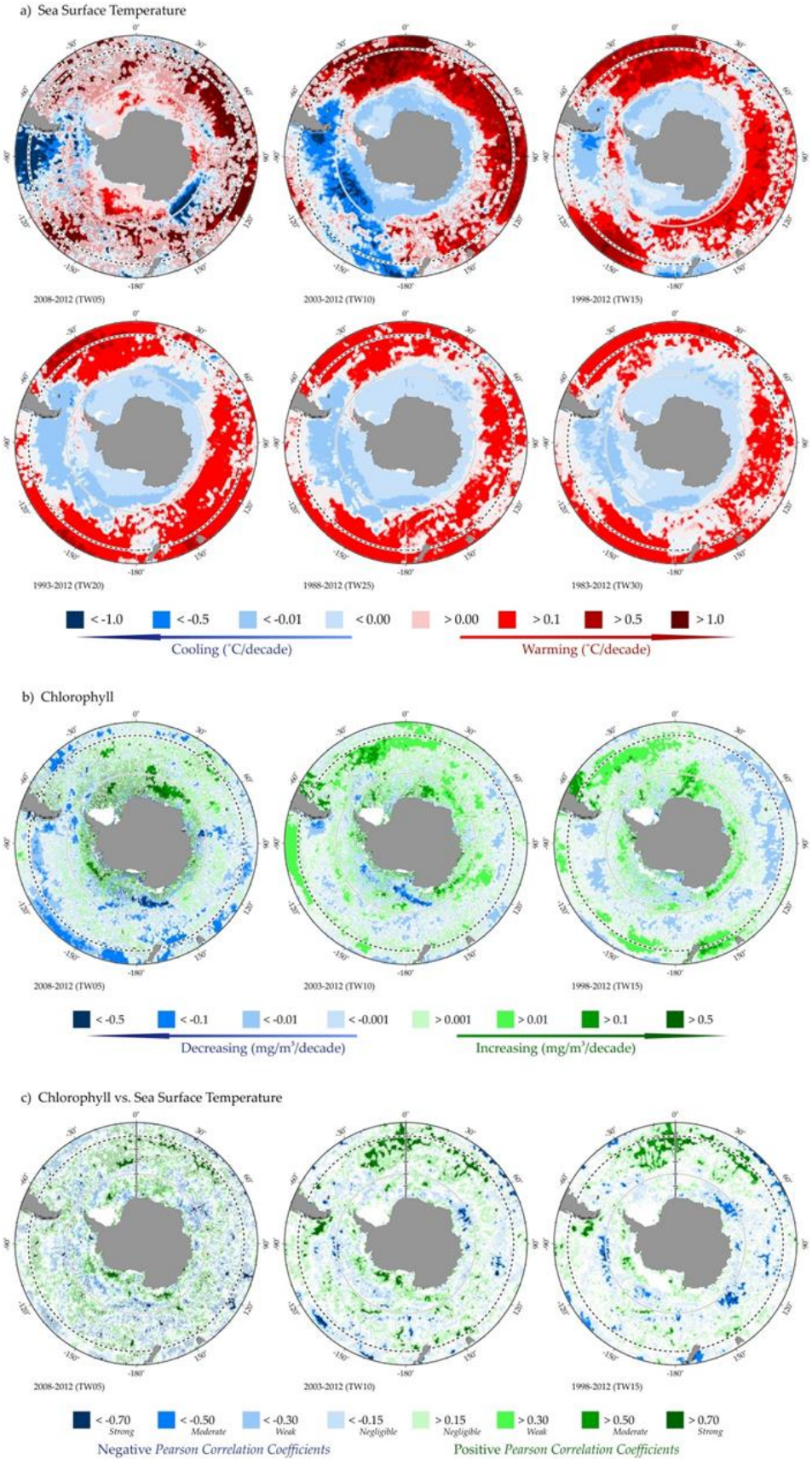

Figure 6.5. Annual trends in Southern Ocean sea surface temperature (SST) (a) and sea surface chlorophyll (CHL) (b), and correlations between chlorophyll and sea surface temperature for each of the standard IGMETS time-windows (c). See "Methods" chapter for a complete description and methodology used.

Over the past 50+ years, environmental conditions in portions of the Southern Ocean have been changing rapidly, while in other portions, the change has been moderate, but still substantial (Turner *et al*., 2005; Gille, 2008; Whitehouse *et al*., 2008; Constable *et al*., 2014; Gutt *et al*., 2014). The changes may be related to the Southern Hemisphere Annular Mode (SAM), also known as the Antarctic Oscillation (AAO), which describes the north–south movement of the westerly winds that circle Antarctica between the mid-high latitudes (poleward of 40°S; Ho *et al*., 2012). A high positive SAM has dominated for nearly two decades (Abram *et al*., 2014; Figure 6.3). A positive SAM is associated with significant decreases in mean sea level pressure (MSLP) and a contraction of the westerly wind belt towards Antarctica. The increased wind speeds may drive the Polar Front of the ACC poleward.

6.2 General patterns of temperature and phytoplankton biomass

IGMETS' time series of satellite-derived surface temperatures show that, over the past 30 years (1983–2012), around half (55.9%, 44% at $p < 0.05$) of the Antarctic Ocean has cooled (Figure 6.5; Table 6.1). Most of this cooling was observed in the areas closer to the Antarctic continent. This cooling trend was sustained over shorter time-windows (e.g. 15 and 10 years) until the 5-year time-window; in the latter, there was warming throughout much of the entire Antarctic Ocean (66.8% warmed, 26.1% at $p < 0.05$; Figure 6.5; Table 6.1). These results may seem contradictory to numerous studies which have reported warming in the Antarctic Ocean (Aoki *et al*., 2003; Fyfe, 2006; Ducklow *et al*., 2007, Böning *et al*., 2008; Gille, 2008; Dinniman *et al*., 2012; Constable *et al*., 2014). The differences lay in the time-windows selected and the spatial areas used for the calculations. Overall, an average of temperature changes across the entire Antarctic Ocean region over the past 30 years yields an overall warning trend.

It is important to remember that satellite-derived temperature only captures surface waters. Since the 1930s, the Southern Ocean has warmed progressively from the subsurface to > 700 m depth (Gille, 2008). The strength of this long-term warming trend appears to be highly variable, and depends on the time-window and location of the study. Around South Georgia in the Southwest Atlantic sector, where records were compared over an 81-year period, the warming extended to > 700 m and occurred at a faster rate than the overall average noted by Gille (2008), with a 2.3°C increase in near-surface waters in austral winter and a 0.9°C increase in summer. On the Antarctic continent, the central West Antarctic is one of the fastest warming regions globally (Bromwich *et al*., 2012). The nearby West Antarctic Peninsula (WAP) is also a region with rapid change, and average air temperatures have risen about 2.9°C from 1951 to 2005 (Vaughan *et al*., 2003; Meredith and King, 2005; Stammerjohn *et al*., 2008). In this region, substantial increases in water heat content and SST have also been reported (Martinson *et al*., 2008; Steinberg *et al*., 2015). The north/south orientation of the WAP results in a latitudinal climate gradient, with warmer temperatures and much less sea ice in the north and colder and higher ice conditions in the south (Ducklow *et al*., 2013; Steinberg *et al*., 2015).

Changes in ocean temperature are also concomitant with trends in sea ice. Sea ice is a major ecological habitat for many marine species, and the timing of sea ice advance and retreat, as well as its seasonal duration, affects the ecology of the region. While observational data suggest that sea ice has decreased since the 1950s (Clarke and Harris, 2003; Curran *et al*., 2003; de la Mare, 1997, 2009), the most recent 30 years of satellite data suggest an increase in maximum sea ice extent for the Southern Ocean as a whole (Gagné *et al*., 2015). However, there is vast heterogeneity in sea ice extent (Stammerjohn *et al*., 2012). For example, in the area west of the WAP, including the Bellingshausen Sea, sea ice duration has been significantly shortened due to earlier spring retreat and later autumn advance. The summer ice-free season is now three months longer than it was in 1979/80. An opposite pattern has been observed in the western Ross Sea region, where the summer ice-free water period has been shortened by 2.5 months (Stammerjohn *et al*., 2012). For much of the rest of the Southern Ocean, the pattern of sea ice seasonal change has been modest.

Trends in satellite-derived chlorophyll have been variable, with different regions showing significant positive or negative trends over the past 15 years (Figure 6.5; Table 6.2). Over the entire Southern Ocean, the spatial distribution of trends has been quite evenly balanced. For example, during 1998–2012, 53.3% (20.4% at $p < 0.05$) of the Antarctic Ocean exhibited an increase in chlorophyll, while 46.7% (17.7% at $p < 0.05$) showed a decrease. One area of increased concentration was close to the

Antarctic continent, consistent with regions of cooling temperature (Figure 6.5). Near the Antarctic continent, the spring bloom is occurring earlier and persisting longer due to a shallowing of the surface mixed layer and increasing solar radiation (Sokolov, 2008; Johnston and Gabric, 2011). The Southern Ocean is largely a high-nutrient, low-chlorophyll (HNLC) region (Banse, 1996; Moore and Abbott, 2000). In northern portions of the Southern Ocean that are in the "Permanently Open Ocean Zone" (POOZ; Moore and Abbott, 2000) and away from land areas and fronts, chlorophyll levels remain low year-round, largely because of iron limitation (Meskhidze *et al*., 2007), light limitation (van Oijen *et al*., 2004), and a result of grazing by zooplankton (Banse, 1996). Increasing chlorophyll and strong phytoplankton blooms occur in areas in the vicinity of land masses, such as the southern tips of South America, Africa, Australia, New Zealand, and downstream of islands such as Kerguelen, where iron inputs are greater (von der Heyden *et al*., 2012). There were 10- and 15-year trends of strongly increasing chlorophyll along the STF, particularly through the South Atlantic sectors (Figure 6.5). When a positive SAM aligns with a positive ENSO (MEI, see Figure 6.3) event, eddy kinetic energy increases significantly along the STF (Langlais *et al*., 2015), potentially stimulating blooms of coccolithophores (Balch *et al*., 2011) during austral summer (December–January).

Areas of positive covariation between temperature and chlorophyll were strongest along the STF in the Atlantic sector, reflecting the close connection between phytoplankton and physics in this environment (Carranza and Gille, 2015).

Table 6.1. Relative spatial areas (% of the total region) and rates of change within within the Southern Ocean region that are showing increasing or decreasing trends in sea surface temperature (SST) for each of the standard IGMETS time-windows. Numbers in brackets indicate the % area with significant ($p < 0.05$) trends. See "Methods" Chapter for a complete description and methodology used.

Latitude-adjusted SST data field surface area = 59.4 million km^2	**5-year** (2008–2012)	**10-year** (2003–2012)	**15-year** (1998–2012)	**20-year** (1993–2012)	**25-year** (1988–2012)	**30-year** (1983–2012)
Area (%) w/ increasing SST trends ($p < 0.05$)	**66.8%** (*26.1%*)	45.8% (*31.5%*)	**57.5%** (*40.0%*)	45.7% (*33.4%*)	46.7% (*34.4%*)	44.1% (*31.8%*)
Area (%) w/ decreasing SST trends ($p < 0.05$)	33.2% (*11.9%*)	**54.2%** (*41.6%*)	42.5% (*29.8%*)	**54.3%** (*42.9%*)	**53.3%** (*45.2%*)	**55.9%** (*44.0%*)
> 1.0°C decade^{-1} warming ($p < 0.05$)	15.7% (*12.8%*)	4.6% (*4.6%*)	0.1% (*0.1%*)	0.0% (*0.0%*)	0.0% (*0.0%*)	0.0% (*0.0%*)
0.5 to 1.0°C decade^{-1} warming ($p < 0.05$)	15.3% (*6.9%*)	16.2% (*16.0%*)	9.8% (*9.8%*)	0.8% (*0.8%*)	0.0% (*0.0%*)	0.0% (*0.0%*)
0.1 to 0.5°C decade^{-1} warming ($p < 0.05$)	20.9% (*4.6%*)	18.9% (*10.7%*)	35.6% (*29.1%*)	31.9% (*30.2%*)	27.8% (*27.2%*)	20.0% (*19.9%*)
0.0 to 0.1°C decade^{-1} warming ($p < 0.05$)	14.9% (*1.7%*)	6.1% (*0.2%*)	12.1% (*1.1%*)	13.0% (*2.4%*)	18.9% (*7.2%*)	24.1% (*11.9%*)
0.0 to –0.1°C decade^{-1} cooling ($p < 0.05$)	6.7% (*0.4%*)	12.2% (*6.2%*)	24.5% (*15.4%*)	31.1% (*21.2%*)	36.6% (*28.7%*)	43.6% (*31.7%*)
–0.1 to –0.5°C decade^{-1} cooling ($p < 0.05$)	12.4% (*2.2%*)	29.0% (*22.5%*)	17.2% (*13.7%*)	23.1% (*21.7%*)	16.7% (*16.5%*)	12.4% (*12.3%*)
–0.5 to –1.0°C decade^{-1} cooling ($p < 0.05$)	8.4% (*4.4%*)	10.9% (*10.8%*)	0.7% (*0.7%*)	0.1% (*0.1%*)	0.0% (*0.0%*)	0.0% (*0.0%*)
> –1.0°C decade^{-1} cooling ($p < 0.05$)	5.7% (*4.9%*)	2.1% (*2.1%*)	0.0% (*0.0%*)	0.0% (*0.0%*)	0.0% (*0.0%*)	0.0% (*0.0%*)

Table 6.2 Relative spatial areas (% of the total region) and rates of change within the South Ocean region that are showing increasing or decreasing trends in phytoplankton biomass (CHL) for each of the standard IGMETS time-windows. Numbers in brackets indicate the % area with significant ($p < 0.05$) trends. See "Methods" chapter for a complete description and methodology used.

Latitude.-adjusted CHL data field surface area = 59.6 million km^2	**5-year** (2008–2012)	**10-year** (2003–2012)	**15-year** (1998–2012)
Area (%) w/ increasing CHL trends ($p < 0.05$)	45.8% (*9.9%*)	**60.8%** (*21.8%*)	**53.3%** (*20.4%*)
Area (%) w/ decreasing CHL trends ($p < 0.05$)	**54.2%** (*19.5%*)	39.2% (*10.8%*)	46.7% (*17.7%*)
> 0.50 mg m^{-3} decade^{-1} increasing ($p < 0.05$)	5.3% (*2.5%*)	0.7% (*0.4%*)	0.3% (*0.2%*)
0.10 to 0.50 mg m^{-3} decade^{-1} increasing ($p < 0.05$)	15.4% (*5.1%*)	7.6% (*4.8%*)	3.8% (*2.7%*)
0.01 to 0.10 mg m^{-3} decade^{-1} increasing ($p < 0.05$)	20.6% (*2.2%*)	41.2% (*16.3%*)	34.4% (*16.9%*)
0.00 to 0.01 mg m^{-3} decade^{-1} increasing ($p < 0.05$)	4.4% (*0.1%*)	11.3% (*0.3%*)	14.9% (*0.6%*)
0.00 to –0.01 mg m^{-3} decade^{-1} decreasing ($p < 0.05$)	4.2% (*0.0%*)	10.3% (*0.5%*)	16.5% (*2.1%*)
–0.01 to –0.10 mg m^{-3} decade^{-1} decreasing ($p < 0.05$)	35.3% (*11.8%*)	24.7% (*8.2%*)	28.7% (*15.0%*)
–0.10 to –0.50 mg m^{-3} decade^{-1} (decreasing) ($p < 0.05$)	11.8% (*6.2%*)	3.9% (*1.9%*)	1.4% (*0.5%*)
> –0.50 mg m^{-3} decade^{-1} (decreasing) ($p < 0.05$)	2.8% (*1.5%*)	0.3% (*0.2%*)	0.1% (*0.1%*)

6.3 Trends from *in situ* time series

At the time of this report, the IGMETS Southern Ocean region had 32 participating *in situ* time series (Figure 6.1; Table 6.3). The largest collection of time series came from the SCAR Southern Ocean Continuous Plankton Recorder (SO-CPR) survey (Hosie *et al.*, 2003; McLeod *et al.*, 2010), followed by time series from KRILLBASE, the US-AMLR programme, and the Palmer-LTER. While few in number, many of these time series were 10+ years in length. Examples of trends for selected variables over the 10-year (2003–2012) time-window are shown in Figure 6.6. The full suite of time-windows and available variables can be viewed in the IGMETS Explorer (http://igmets.net/explorer).

Based on the limited data available, *in situ* temperature trends were mixed (Figure 6.6, top left panel). There was some agreement between satellite and *in situ* SST, but the level of agreement varied over different time-windows and over different subregions. This was likely due to spatial and temporal variability of the *in situ* and satellite data. For example, there was general agreement between *in situ* and satellite data in the area of the WAP. However, in the ACC, the level of correspondence between the CPR time series and satellite data varied, depending on the time-window. The CPR boxes each represent a large spatial area, compared to a transect line or single station, which could have contained subareas both warming and cooling. The overall trend shown is an average of all those trends. In addition, the CPR transect was a single cruise within that month, while the satellite data is a monthly average. It has also been suggested that there is distinct seasonality to the temperature trends observed in Antarctica (Schneider *et al.*, 2012); it is possible that this also played a role in the difference observed between the satellite-derived and *in situ* temperature trends. Munida, off the southeast of New Zealand (see Table 6.3), was one of the stations that showed consistent cooling in all time-windows (15, 10, and 5 years). Munida is poleward of the STF and in Subantarctic surface waters (SASW) in the Subantarctic zone (SAZ), in a region strongly influenced by these mixing

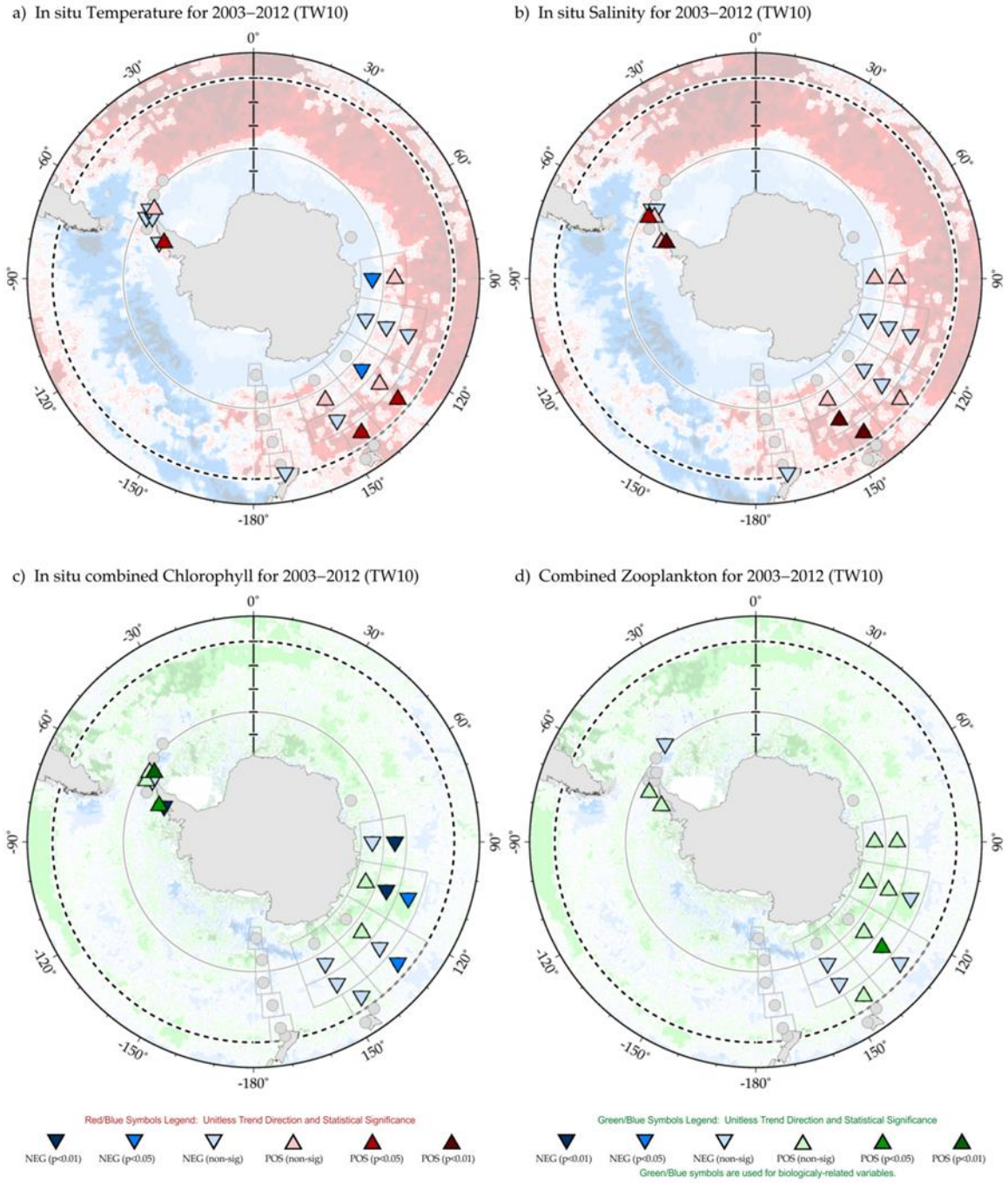

Figure 6.6. Map of Southern Ocean region time-series locations and trends for select variables and IGMETS time-windows. Upward-pointing triangles indicate positive trends; downward triangles indicate negative trends. Gray circles indicate time-series site that fell outside of the current study region or time-window. Additional variables and time-windows are available through the IGMETS Explorer (http://IGMETS.net/explorer). See "Methods" chapter for a complete description and methodology used.

and current regimes (Currie and Wowk, 2009). Although there is considerable small-scale spatial and temporal variability in SST trends in this region off southeast New Zealand, the SASW has been cooling for the last 30 years (Figure 6.3), possibly induced by the positive SAM. During a positive SAM, the southern hemisphere westerly winds tend to move farther southwards and increase in intensity (Thompson *et al*., 2000), resulting in stronger cold water upwelling in the SAZ and declining SST (Hall and Visbeck, 2002; Oke and England, 2004). Munida also showed decreasing salinity trends over the 10- and 15-year time-windows (1998–2012 and 2003–2012, respec-

tively), possibly indicating more SASW. Salinity trends from the SO-CPR time series showed a mixture of trends, possibly reflecting variations in the circulation patterns.

Over the 15- and 10-year time-windows, most of the chlorophyll trends around the Antarctic Peninsula (the left-most arm of Antarctic pointing towards South America) were positive (increasing) (Figure 6.6, bottom left panel), while most of the chlorophyll trends from the SO-CPR areas were decreasing (many at $p < 0.05$). Over this time-period, the Antarctic Peninsula area was a region of general SST cooling and increasing chlorophyll. A notable exception was the WAP. In spite of changes at the surface, the ocean heat content over the WAP shelf showed an increasing trend due predominantly to enhanced upwelling of warm upper circumpolar deep water (UCDW) onto the shelf (Martinson *et al*., 2008; Steinburg *et al*., 2012; Ducklow *et al*., 2013). The SO-CPR areas were mostly located over the warming ACC and thus yielded decreasing chlorphyll trends. However, in two locations over the 10-year time-window, the trends were positive. These positive chlorophyll trends are potentially associated with variability in wind stress throughout summer (Carranza and Gille, 2015). The negative chlorophyll trend at Munida is possibly related to dynamics of the SAZ (Matear *et al*., 2013). In the SAZ, phytoplankton might be seasonally limited by iron (Boyd *et al*., 2001) or grazing (Banse, 1996), but they are undoubtedly limited by irradiance for most of the year (van Oijen *et al*., 2004). Thus, they are unlikely to respond positively to the greater vertical mixing implied by declining SST.

Between 2003 and 2012 (and also over the 15-year time-window), nitrate and phosphate concentrations increased significantly at Munida; an increase in surface phosphate concentrations was also reported by Currie and Wowk (2009). These observations support the model prediction of a more vigorous upwelling in the SAZ resulting from the positive phase of the SAM (Matear and Lenton, 2008). In contrast, surface macronutrient concentrations (silicate, phosphate, and nitrate) showed a consistent decrease over the 10- and 5-year time-windows at the PALMER station. It has been suggested that UCDW represents one of the major sources of nutrients to the WAP region (Prézelin *et al*., 2000) and that nutrient concentrations track temperature in the UCDW; thus, nutrient concentrations are expected to increase with increasing temperature (Ducklow *et al*., 2012). It is possible that the declining trends observed in macronutrients are a reflection of increased phytoplankton populations measured in the area. It has been noted that seasonal nutrient depletions reflect abundance and type of phytoplankton (Ducklow *et al*., 2012).

Time-window-qualifying diatom and dinoflagellate data were not available from any of the time-series sites at the time of this report. Montes-Hugo *et al*. (2009) found that, in the northern WAP during 1998–2012, there was a shift from diatoms to dinoflagellates due to increased winds and deeper mixed layers. Near the Antarctic continent, the seasonal cycle of phytoplankton production in the Southern Ocean is strongly tied to solar radiation, cloud cover, the ebb and flow of sea ice, and mixed-layer dynamics. In the ice-covered regions of the Southern Ocean during winter, under-ice algae and other microorganisms provide a source of food for larger zooplankton, including krill (Arrigo and Thomas, 2004). During spring, nutrients are released by the melting sea ice and stimulate the bloom of algae in the vicinity of the retreating ice edge. Although there is evidence of data collection by researchers (Cassar *et al*., 2015), the lack of available information on phytoplankton species in most areas of the Southern Ocean precludes any conclusions regarding regional community changes over time.

Extensive datasets on meso- and macrozooplankton from various nations span the last 100 years; combining these is still a work in progress. In the Atlantic sector, the greatest abundance of macrozooplankton generally occurred in the vicinity of the STF, while abundance was lower in the more southern regions (Mackey *et al*., 2012, a trend also seen in the mesozooplankton (Ward *et al*., 2014). A warming of the Antarctic Circumpolar Current and the shift of the currents poleward has been predicted to cause decreases in the cold-water species, especially those living closest to the Antarctic continent, and increases in the warm-water species (Mackey *et al*., 2012).

Krill (principally *Euphausia superba*) and salps (especially *Salpa thompsoni*) play key roles in the Antarctic ecosystem, and their distribution and abundance has been studied by a number of investigators (Foxton, 1966; Loeb *et al*., 1997; Atkinson *et al*., 2004, 2008, 2009; Pakhomov *et al*., 2006; Lee *et al*., 2010; Loeb and Santora, 2012). *E. superba* is a cold-water species that predominately lives in ACC waters south of the PF to the ice shelves to the south. As adolescents and adults, *E. superba* aggregates in swarms and schools and is known for avoidance of capture by traditional net sampling. It occurs in highest abundance in the southwestern Atlantic sector of the Southern Ocean (Atkinson *et al*., 2008). In contrast, *S.*

thompsoni is found in warmer, less-productive waters than krill, and while its abundance fluctuates greatly between years in a similar manner to krill, its overall circumpolar distribution is more even (Pakhomov *et al*., 2002; Lee *et al*., 2010).

The distributions and abundance of these two species of krill and salps are related to a range of factors including sea surface temperature, water depth, productivity, and the extent of seasonal sea ice cover (Stammerjohn *et al*., 2008; Lee *et al*., 2010). Over the past several decades, an inverse relationship between these two species has been observed (Lee *et al*., 2010; Loeb and Santora, 2012). In spite of strong 3–5-year oscillations, the longer-term (ca. 30-year) data compilations provided by KRILLBASE suggest that krill populations have been decreasing and salps increasing over parts of their ranges (Atkinson *et al*., 2004). The population trends and oscillations of both species have now been linked to a variety of factors including winter sea ice (Loeb *et al*., 1997; Atkinson *et al*., 2004), the Southern Annular Mode (Saba *et al*., 2014; Steinberg *et al*., 2015), ENSO (Loeb and Santora, 2012), and the Antarctic Circumpolar Wave (Lee *et al*., 2010), as well as to changing top–down controls (Ainley *et al*., 2007). Researchers agree that the duration and the location of the time series are critical factors that will determine which forcing function is found to dominate species dynamics (Loeb and Santora, 2012). In addition, a better mechanistic understanding is still needed to make informed projections on how these key species will respond with future climatic variations (Alcaraz *et al*., 2014).

The IGMETS zooplankton trends (e.g. Figure 6.6, bottom right panel) only looked at the state of the entire zooplankton community, while the literature studies mentioned in the above paragraphs discussed changes in dominant species or groups. It is possible that the trends seen in the IGMETS zooplankton reflect this shift in species dominance. However, without looking deeper into species assemblages, coupled with additional physical and chemical variables, it is difficult to draw any conclusions at this point. It is also important to note that, superimposed on the long-term trends, 4–6-year abundance oscillations have been identified for certain zooplankton species and have been linked to both the SAM and the ENSO climate indices (Steinberg *et al*., 2015), adding further complexity to the picture.

6.4 Conclusions

Both long-term trends and subdecadal cycles are evident in the Southern Ocean on multiple trophic levels and are strongly related in complex ways to climate forcings and their effects on the physical oceanographic system. Antarctic marine ecosystems have changed over the past 30 years in response to changing ocean conditions and the extent and seasonality of sea ice. These changes have been spatially heterogeneous, which suggests ecological responses depend on the magnitude and direction of the changes and their interactions with other factors. In the Southern Ocean, there are few *in situ* time series that measure a comprehensive suite of biological, ecological, and hydrographic measurements; this handicap precludes a deeper understanding of changing conditions in the region. With predictions of an overall strengthening of westerly winds in response to the positive SAM index, it is expected that higher phytoplankton concentrations will be found southward (Constable *et al*., 2014). The response of zooplankton may be more regionally specific, depending on sea ice, primary production, and seasonal dynamics of the physical forcings.

6.5 Acknowledgements

The SCAR SO-CPR data were sourced from the Scientific Committee on Antarctic Research (SCAR) sponsored Southern Ocean CPR (SO-CPR) Survey Database, hosted by the Australian Antarctic Data Centre (AADC). The AADC is part of the Australian Antarctic Division (AAD, a division of the Department of the Environment). The SO-CPR Survey and database are also funded, supported, and populated by the Australian Government through the Department of the Environment-AAD approved AAS projects 472 and 4107, Australian Integrated Marine Observing System (IMOS), the Japanese National Institute of Polar Research (NIPR), the New Zealand National Institute of Water and Atmospheric Research (NIWA), the German Alfred Wegener Institute (AWI), the United States of America – Antarctic Marine Living Resources programme (NOAA US-AMLR), the Russian Arctic and Antarctic Research Institute (AARI), the Brazilian Programa Antartico Brasileiro (PROANTAR), the Chilean Instituto Antartico Chileno (INACH), the South African Departmental of Environmental Affairs (DEA), and the French Institut polaire francais – Paul-Emile Victor (IPEV) and Universite Pierre-et-Marie-Curie (UPMC).

Table 6.3. Time-series sites located in the IGMETS Southern Ocean region. Participating countries: New Zealand (nz), United Kingdom, (uk), United States (us), and multiple-country efforts (zz). Year-spans in red text indicate time series of unknown or discontinued status.

No.	IGMETS-ID	Site or programme name	Year-span	T	S	Oxy	Ntr	Chl	Mic	Phy	Zoo
1	nz-10101	Munida Time Series (*Western South Pacific*)	1998–present	X	X	-	X	X	-	-	-
2	uk-30401	KRILLBASE: Atkinson Krill Study (*Southern Ocean*)	1976–2003 (?)	-	-	-	-	-	-	-	X
3	uk-30402	KRILLBASE: Antarctic Peninsula and western Scotia Sea (*Southern Ocean*)	1975–present	-	-	-	-	-	-	-	X
4	uk-30403	KRILLBASE: Eastern Scotia Sea and South Georgia (*Southern Ocean*)	1975–present	-	-	-	-	-	-	-	X
5	uk-30404	KRILLBASE: Indian Ocean Sector (*Southern Ocean*)	1981–2006 (?)	-	-	-	-	-	-	-	X
6	uk-30501	Rothera Time Series (RaTS) (*Southern Ocean*)	1998–present	X	X	-	-	X	-	-	-
7	us-30501	Palmer Station Antarctica LTER (*Antarctic*)	1989–present	X	X	X	X	X	-	-	X
8	us-50701	AMLR Elephant Island – EI (*Southern Ocean*)	1995–present	X	X	-	-	X	-	-	-
9	us-50702	AMLR South – SA (*Southern Ocean*)	1995–present	X	X	-	-	X	-	-	-
10	us-50703	AMLR West – WA (*Southern Ocean*)	1995–present	X	X	-	-	X	-	-	-
11	us-50704	AMLR Joinville Island – JI (*Southern Ocean*)	1997–present	X	X	-	-	X	-	-	-
12	zz-40101	SCAR SO-CPR Aurora 080-100-B5560 (*Southern Ocean*)	1991–present	X	X	-	-	X	-	-	X
13	zz-40102	SCAR SO-CPR Aurora 080-100-B6065 (*Southern Ocean*)	1991–present	X	X	-	-	X	-	-	X
14	zz-40103	SCAR SO-CPR Aurora 100-120-B5055 (*Southern Ocean*)	1998–present	X	X	-	-	X	-	-	X
15	zz-40104	SCAR SO-CPR Aurora 100-120-B5560 (*Southern Ocean*)	1991–present	X	X	-	-	X	-	-	X
16	zz-40105	SCAR SO-CPR Aurora 100-120-B6065 (*Southern Ocean*)	1997–present	X	X	-	-	X	-	-	X
17	zz-40106	SCAR SO-CPR Aurora 120-140-B4550 (*Southern Ocean*)	1998–present	X	X	-	-	X	-	-	X
18	zz-40107	SCAR SO-CPR Aurora 120-140-B5055 (*Southern Ocean*)	1997–present	X	X	-	-	X	-	-	X
19	zz-40108	SCAR SO-CPR Aurora 120-140-B5560 (*Southern Ocean*)	1995–present	X	X	-	-	X	-	-	X

No.	IGMETS-ID	Site or programme name	Year-span	T	S	Oxy	Ntr	Chl	Mic	Phy	Zoo
20	zz-40109	SCAR SO-CPR Aurora 120-140-B6065 (*Southern Ocean*)	1995–present	X	X	-	-	X	-	-	X
21	zz-40110	SCAR SO-CPR Aurora 140-160-B4550 (*Southern Ocean*)	1999–present	X	X	-	-	X	-	-	X
22	zz-40111	SCAR SO-CPR Aurora 140-160-B5055 (*Southern Ocean*)	1995–present	X	X	-	-	X	-	-	X
23	zz-40112	SCAR SO-CPR Aurora 140-160-B5560 (*Southern Ocean*)	1995–present	X	X	-	-	X	-	-	X
24	zz-40113	SCAR SO-CPR Aurora 140-160-B6065 (*Southern Ocean*)	1997–present	X	X	-	-	X	-	-	X
25	zz-40131	SCAR SO-CPR Shirase E108111-S4550 (*Southern Ocean*)	2000–present	X	X	-	-	X	-	-	X
26	zz-40132	SCAR SO-CPR Shirase E108111-S5055 (*Southern Ocean*)	1999–present	X	X	-	-	X	-	-	X
27	zz-40133	SCAR SO-CPR Shirase E108111-S5560 (*Southern Ocean*)	1999–present	X	X	-	-	X	-	-	X
28	zz-40151	SCAR SO-CPR Aotea B4550 (*Southern Ocean*)	2008–present	-	-	-	-	-	-	-	X
29	zz-40152	SCAR SO-CPR Aotea B5055 (*Southern Ocean*)	2008–present	-	-	-	-	-	-	-	X
30	zz-40153	SCAR SO-CPR Aotea B5560 (*Southern Ocean*)	2008–present	-	-	-	-	-	-	-	X
31	zz-40154	SCAR SO-CPR Aotea B6065 (*Southern Ocean*)	2008–present	-	-	-	-	-	-	-	X
32	zz-40155	SCAR SO-CPR Aotea B6570 (*Southern Ocean*)	2008–present	-	-	-	-	-	-	-	X

6.6 References

Abram, N. J., Mulvaney, R., Vimeux, F., Phipps, S. J., Turner, J., and England, M. H. 2014. Evolution of the Southern Annular Mode during the past millennium. Nature Climate Change, 4(7): 564–569, doi:10.1038/nclimate2235.

Ainley, D. G., Ballard, G., Ackley, S., Blight, L. K., Eastman, J. T., Emslie, S. D., Lescroël, A., *et al*. 2007. Paradigm lost, or is top-down forcing no longer significant in the Antarctic marine ecosystem? Antarctic Science, 19: 283–290.

Alcaraz, M., Almeda, R., Duarte, C. M., Horstkotte, B., Lasternas, S., and Agustí, S. 2014. Changes in the C, N, and P cycles by the predicted salps-krill shift in the Southern Ocean. Frontiers in Marine Science, 1: 45, doi:10.3389/fmars.2014.00045.

Aoki, S., Yoritaka, M., and Masuyama, A. 2003. Multidecadal warming of subsurface temperature in the Indian sector of the Southern Ocean, Journal of Geophysical Research, 108: 8081, doi:10.1029/2000JC000307.

Arrigo, K. R., and Thomas, D. N. 2004. Large scale importance of sea ice biology in the Southern Ocean. Antarctic Science, 16(04): 471–486.

Atkinson, A., Siegel, V., Pakhomov, E. A., Jessopp, M. J., and Loeb, V. 2009. A re-appraisal of the total biomass and annual production of Antarctic krill. Deep-Sea Research I, 56: 727–740.

Atkinson, A., Siegel, V., Pakhomov, E., and Rothery, P. 2004. Long-term decline in krill stock and increase in salps within the Southern Ocean. Nature, 432: 100–103.

Atkinson, A., Siegel, V., Pakhomov, E. A., Rothery, P., Loeb, V., Ross, R. M., Quetin, L. B., *et al.* 2008. Oceanic circumpolar habitats of Antarctic krill. Marine Ecology Progress Series, 362: 1–23.

Balch, W. M., Drapeau, D. T., Bowler, B. C., Lyczskowski, E., Booth, E. S., and Alley, D. 2011. The contribution of coccolithophores to the optical and inorganic carbon budgets during the Southern Ocean Gas Exchange Experiment: New evidence in support of the "Great Calcite Belt" hypothesis. Journal of Geophysical Research: Oceans, 116(C4): doi:10.1029/2011JC006941.

Banse, K. 1996. Low seasonality of low concentrations of surface chlorophyll in the Subantarctic water ring: underwater irradiance, iron, or grazing? Progress in Oceanography, 37(3): 241–291.

Belkin, I. M., and Gordon, A. L. 1996. Southern Ocean fronts from the Greenwich meridian to Tasmania, Journal of Geophysical Research, 101: 3675–3696.

Böning, C. W., Dispert, A., Visbeck, M., Rintoul, S. R., and Schwarzkopf, F. U. 2008. The response of the Antarctic Circumpolar Current to recent climate change. Nature Geoscience, 1: 864–869.

Boyd, P. W., Crossley, A. C., DiTullio, G. R., Griffiths, F. B., Hutchins, D. A., Queguiner, B., Sedwick, P. N., *et al*. 2001. Control of phytoplankton growth by iron supply and irradiance in the subantarctic Southern Ocean: Experimental results from the SAZ Project. Journal of Geophysical Research: Oceans, 106(C12): 31573–31583.

Bromwich, D. H., Nicolas, J. P., Hines, K. M., Kay, J. E., Key, E. L., Lazzara, M. L., Lubin, D., *et al*. 2012. Tropospheric clouds in Antarctica. Reviews of Geophysics, 50: RG1004, doi:10.1029/2011RG000363.

Carranza, M. M., and Gille, S. T. 2015. Southern Ocean wind-driven entrainment enhances satellite chlorophyll-*a* through the summer. Journal of Geophysical Research: Oceans, 120: 304–323, doi:10.1002/2014JC010203.

Cassar, N., Wright, S. W., Thomson, P. G., Trull, T. W., Westwood, K. J., de Salas, M., Davidson, A., *et al*. 2015. The relation of mixed-layer net community production to phytoplankton community composition in the Southern Ocean, Global Biogeochemical Cycles, 29: 446–462, doi:10.1002/2014GB004936.

Clarke, A., and Harris, C. M. 2003. Polar marine ecosystems: major threats and future change. Environmental Conservation, 30: 1–25.

Constable, A. J., Melbourne-Thomas, J., Corney, S. P., Arrigo, K. R., Barbraud, C., Barnes, D. K. A., Bindoff, N. L., *et al*. 2014. Climate change and Southern Ocean ecosystems I: How changes in physical habitats directly affect marine biota. Global Change Biology, 20: 3004–3025, doi:10.1111/gcb.12623.

Curran, M. A. J., van Ommen, T. D., Morgan, V. I., Phillips K. L., and Palmer, A. S. 2003. Ice core evidence for Antarctic sea ice decline since the 1950s. Science, 302: 1203–1206.

Currie, D. E., and Wowk, K. 2009. Climate change and CO_2 in the oceans and global oceans governance. Carbon & Climate Law Review, 3(4): 18.

de la Mare, W. K. 1997. Abrupt mid-twentieth-century decline in Antarctic sea ice from whaling records. Nature, 389: 57–60.

de la Mare, W. K. 2009. Changes in Antarctic sea-ice extent from direct historical observations and whaling records. Climatic Change, 92(3–4): 461–493, doi:10.1007/s10584-008-9473-2.

Dinniman, M. S., Klinck, J. M., and Hofmann, E. E. 2012. Sensitivity of circumpolar deep water transport and ice shelf basal melt along the West Antarctic Peninsula to changes in the winds. Journal of Climate, 25(14): 4799–4816. doi:10.1175/jcli-d-11-00307.1.

Ducklow, H. W., Baker, K., Martinson, D. G., Quetin, L. B., Ross, R. M., Smith, R. C., Stammerjohn, S. E., *et al*. 2007. Marine pelagic ecosystems: the West Antarctic Peninsula. Philosophical Transactions of the Royal Society of London B, 362: 67–94.

Ducklow, H., Clarke, A., Dickhut, R., Doney, S. C., Geisz, H., Huang, K., Martinson, D. G., *et al*. 2012. The marine system of the Western Antarctic Peninsula. *In* Antarctic Ecosystems: An Extreme Environment in a Changing World, pp. 121–159. Ed. by A. Rogers, N. Johnston, E. Murphy, and A. Clarke. Blackwell, London. 564 pp.

Ducklow, H. W., Fraser, W. R., Meredith, M. P., Stammerjohn, S. E., Doney, S. C., Martinson, D. G., Sailley, S. F., *et al*. 2013. West Antarctic Peninsula: an ice-dependent coastal marine ecosystem in transition. Oceanography, 26(3): 190–203.

Foxton P. 1966. The distribution and life history of *Salpa thompsoni* Foxton with observations on a related species *S. gerlachei* Foxton. Discovery Reports, 34: 1–116.

Fyfe, J. C. 2006. Southern Ocean warming due to human influence, Geophysical Research Letters, 33: L19701, doi:10.1029/2006GL027247.

Gagné, M-È., Gillett, N. P., and Fyfe, J. C. 2015. Observed and simulated changes in Antarctic sea ice extent over the past 50 years, Geophysical Research Letters, 42: 90–95, doi:10.1002/2014GL062231.

Gille, S. T. 2008. Decadal-scale temperature trends in the Southern Hemisphere Ocean. Journal of Climate, 21(18): 4749–4765.

Gutt, J., Bertler, N., Bracegirdle, T. J., Buschmann, A., Comiso, J., Hosie, G., Isla, E., *et al*. 2014. The Southern Ocean ecosystem under multiple climate change stresses – an integrated circumpolar assessment. Global Change Biology, 21: 1434-1453, doi:10.1111/gcb.12794.

Hall, A., and Visbeck, M. 2002. Synchronous variability in the Southern Hemisphere atmosphere, sea ice, and ocean resulting from the annular mode. Journal of Climate, 15(21): 3043–3057.

Ho, M., Kiem, A. S., and Verdon-Kidd, D. C. 2012. The Southern Annular Mode: a comparison of indices. Hydrology and Earth System Sciences, 16: 967–982.

Hosie, G. W., Fukuchi, M., and Kawaguchi, S. 2003. Development of the Southern Ocean Continuous Plankton Recorder Survey. Progress in Oceanography, 58(2–4): 263–283.

Hosie, G., Mormede, S., Kitchener, J., Takahashi, K., and Raymond, B. 2014. Near surface zooplankton communities. *In* The CAML/SCAR-MarBIN Biogeographic Atlas of the Southern Ocean, pp. 422–430. Ed. by C. De Broyer, P. Koubbi, H. Griffiths, B. Danis, B. David, S. Grant, J. Gutt, *et al*. Scientific Committee on Antarctic Research, Cambridge, UK. 498 pp.

Johnston, B. M, and Gabric, A. J. 2011. Interannual variability in estimated biological productivity in the Australian sector of the Southern Ocean in 1997–2007. Tellus, 63B: 266–286.

Langlais, C. E., Rintoul, S. R., and Zika, J. D. 2015. Sensitivity of Antarctic Circumpolar Current transport and eddy activity to wind patterns in the Southern Ocean. Journal of Physical Oceanography, 45: 1051–1067, doi:10.1175/JPO-D-14-0053.1.

Lee, C. I., Pakhomov, E., Atkinson, A., and Siegel, V. 2010. Long-term relationships between the marine environment, krill and salps in the Southern Ocean. Journal of Marine Biology, 2010: 1–18, doi:10.1155/2010/410129.

Loeb, V. J., and Santora, J. A. 2012. Population dynamics of *Salpa thompsoni* near the Antarctic Peninsula: growth rates and interannual variations in reproductive activity (1993–2009). Progress in Oceanography, 96: 93–107.

Loeb, V., Siegel, V., Holm-Hansen, O., Hewitt, R., Fraser, W., Trivelpiece, W., and Trivelpiece, S. 1997. Effects of sea-ice extent and krill or salp dominance on the Antarctic food web. Nature, 387: 897–900.

Mackey, A., Atkinson, A., Hill, S., Ward, P., Cunningham, N. J., Johnson, N., and Murphy, E. J. 2012. Antarctic macrozooplankton of the southwest Atlantic sector and Bellingshausen Sea: baseline historical (Discovery Investigations, 1928–1935) distributions related to temperature and food, with projections for subsequent ocean warming. Deep-Sea Research II, 59–60: 130–146.

Martinson, D. G., Stammerjohn, S. E., Iannuzzi, R. A., Smith, R. C., and Vernet, M. 2008. Western Antarctic Peninsula physical oceanography and spatio-temporal variability. Deep-Sea Research II, 55(18–19): 1964–1987.

Matear, R. J., Chamberlain, M. A., Sun, C., and Feng, M. 2013. Climate change projection of the Tasman Sea from an Eddy-resolving Ocean Model. Journal of Geophysical Research: Oceans, 118(6): 2961–2976.

Matear, R. J., and Lenton, A. 2008. Impact of historical climate change on the Southern Ocean carbon cycle. Journal of Climate, 21(22): 5820–5834.

McLeod, D. J, Hosie, G. W., Kitchener, J. A., Takahashi, K. T., and Hunt, B. P. V. 2010. Zooplankton atlas of the Southern Ocean: The Southern Ocean Continuous Plankton Recorder Survey (1991-2008). Polar Science, 4(2): 353–385, doi:10.1016/j.polar.2010.03.004.

Meredith, M. P., and King, J. C. 2005. Rapid climate change in the ocean west of the Antarctic Peninsula during the second half of the 20th century. Geophysical Research Letters, 32(19): L19604, doi:10.1029/2005GL024042.

Meskhidze, N., Nenes, A., Chameides, W. L., Luo, C., and Mahowald, N. 2007. Atlantic Southern Ocean productivity: Fertilization from above or below? Global Biogeochemical Cycles, 21: GB2006, doi:10.1029/2006GB002711.

Moffat, C., Beardsley, R. C., Owens, B., and van Lipzig, N. 2008. A first description of the Antarctic Peninsula Coastal Current. Deep-Sea Research II, 55: 277–293.

Montes-Hugo, M., Doney, S. C., Ducklow, H. W., Fraser, W., Martinson, D., Stammerjohn, S. E., and Schofield, O. 2009. Recent changes in phytoplankton communities associated with rapid regional climate change along the Western Antarctic Peninsula. Science, 323: 470–1473.

Moore, J. K., and Abbott, M. R. 2000. Phytoplankton chlorophyll distributions and primary production in the Southern Ocean, Journal of Geophysical Research: Oceans, 105: 28709–28722.

National Geophysical Data Center. 2006. 2-minute Gridded Global Relief Data (ETOPO2) v2. National Geophysical Data Center, NOAA. doi:10.7289/V5J1012Q.

Oke, P. R., and England, M. H. 2004. Oceanic response to changes in the latitude of the Southern Hemisphere subpolar westerly winds. Journal of Climate, 17(5): 1040–1054.

Orsi, A. H. and Harris, U. 2001(updated 2015). Locations of the various fronts in the Southern Ocean. Australian Antarctic Data Centre-CAASM Metadata (http://data.aad.gov.au/aadc/metadata/metadata_redirect.cfm?md=/AMD/AU/southern_ocean_fronts).

Orsi, A. H., Whitworth III, T., and Nowlin Jr., W. D. 1995. On the meridional extent and fronts of the Antarctic Circumpolar Current. Deep-Sea Research I, 42(5): 641–673.

Pakhomov, E. A., Atkinson, A., Meyer, B., Oettl, B., and Bathmann, U. 2004. Daily rations and growth of larval krill *Euphausia superb* in the Eastern Bellingshausen Sea during austral autumn. Deep-Sea Research II, 51: 2185–2198.

Pakhomov, E. A., Dubischar, C. D., Strass, V., Brichta, M., and Bathmann, U. V. 2006. The tunicate *Salpa thompsonia* ecology in the Southern Ocean. I. Distribution, biomass, demography and feeding ecophysiology. Marine Biology, 149: 609–623.

Prézelin, B. B., Hofmann, E. E., Mengelt, C., and Klinck, J. M. 2000. The linkage between upper circumpolar deep water (UCDW) and phytoplankton assemblages on the west Antarctic Peninsula Continental Shelf. Journal of Marine Research, 58: 165–202.

Saba, G. K., Fraser, W. R., Saba, V. S., Iannuzzi, R. A., Coleman, K. E, Doney, S. C., Ducklow, H. W., *et al*. 2014. Winter and spring controls on the summer food web of the coastal West Antarctic Peninsula. Nature Communications, 5: 4318, doi:10.1038/ncomms5318.

Schneider, D. P., Deser, C., and Okumura, Y. 2012. An assessment and interpretation of the observed warming of West Antarctica in the austral spring. Climate Dynamics, 38(1–2): 323–347.

Sokolov, S. 2008. Chlorophyll blooms in the Antarctic Zone south of Australia and New Zealand in reference to the Antarctic Circumpolar Current fronts and sea ice forcing, Journal of Geophysical Research, 113: C03022, doi:10.1029/2007JC004329.

Sokolov, S., and Rintoul, S. R. 2009a. Circumpolar structure and distribution of the Antarctic Circumpolar Current fronts: 1. Mean circumpolar paths. Journal of Geophysical Research, 114: C11018, doi:10.1029/2008JC005108.

Sokolov, S., and Rintoul, S. R. 2009b. Circumpolar structure and distribution of the Antarctic Circumpolar Current fronts: 2. Variability and relationship to sea surface height. Journal of Geophysical Research, 114: C11019, doi:10.1029/2008JC005248.

Stammerjohn, S. E., Martinson, D. G., Smith, R. C., Yuan, X., and Rind, D. 2008. Trends in Antarctic annual sea ice retreat and advance and their relation to ENSO and Southern Annular Mode variability, Journal of Geophysical Research, 113: C03S90, doi:10.1029/2007JC004269.

Stammerjohn, S., Massom, R., Rind, D., and Martinson, D. 2012. Regions of rapid sea ice change: an interhemispheric seasonal comparison. Geophysical Research Letter, 39(6): L06501, doi:10.1029/2012GL050874.

Steinberg, D. K., Martinson, D. G., and Costa, D. P. 2012. Two decades of pelagic ecology of the Western Antarctic Peninsula. Oceanography, 25(3): 56–67, http://dx.doi.org/10.5670/oceanog.2012.75.

Steinberg, D. K., Ruck, K. E., Gleiber, M. R., Garzio, L. M., Cope, J. S., Bernard, K. S., Stammerjohn, S. E., *et al*. 2015. Long-term (1993–2013) changes in macrozooplankton off the Western Antarctic Peninsula. Deep-Sea Research I, 101: 54–70.

Talley L. D., Pickard G. L., Emery W. J., and Swift J. H., 2011. Descriptive Physical Oceanography: An Introduction (Sixth edn), Elsevier, Boston. 560 pp.

Thompson, D. W., Wallace, J. M., and Hegerl, G. C. 2000. Annular modes in the extratropical circulation. Part II: Trends. Journal of Climate, 13(5): 1018–1036.

Turner, J., Colwell, S. R., Marshall, G. J., Lachlan-Cope, T. A., Carleton, A. M., Jones, P. D., Lagun, V., *et al*. 2005. Antarctic climate change during the last 50 years. International Journal of Climatology, 25(3): 279–294.

Vaughan, D. G., Marshall, G. J., Connolley, W. M., Parkinson, C., Mulvaney, R., Hodgson, D. A., King, J. C., *et al*. 2003. Recent rapid regional climate warming on the Antarctic Peninsula. Climatic Change, 60: 243–274.

van Oijen, T., van Leeuwe, M. A., Granum, E., Weissing, F. J., Bellerby, R. G. J., Gieske, W. W. C., and de Baar, H. J. W. 2004. Light rather than iron controls photosynthate production and allocation in Southern Ocean phytoplankton populations during austral autumn. Journal of Plankton Research, 26: 885–890.

von der Heyden, B. P., Roychoundhury, A. N., Mtshali, T. N., Tyliszczak, T., and Myneni, S. C. B. 2012. Chemically and geographically distinct solid-phase iron pools in the Southern Ocean. Science, 338: 1199.

Ward, P., Tarling, G, A., and Thorpe, S. E. 2014. Mesozooplankton in the Southern Ocean: Spatial and temporal patterns from Discovery Investigations. Progress in Oceanography, 120: 305–319.

Whitehouse, M. J., Meredith, M. P. Rothery, P., Atkinson, A., Ward, P., and Korb, R. E. 2008. Rapid warming of the ocean around South Georgia, Southern Ocean, during the 20th century: forcings, characteristics and implications for lower trophic levels. Deep-Sea Research I, 55: 1218–1228.

7 Indian Ocean

Peter A. Thompson, Todd D. O'Brien, Kirsten Isensee, Laura Lorenzoni, and Lynnath E. Beckley

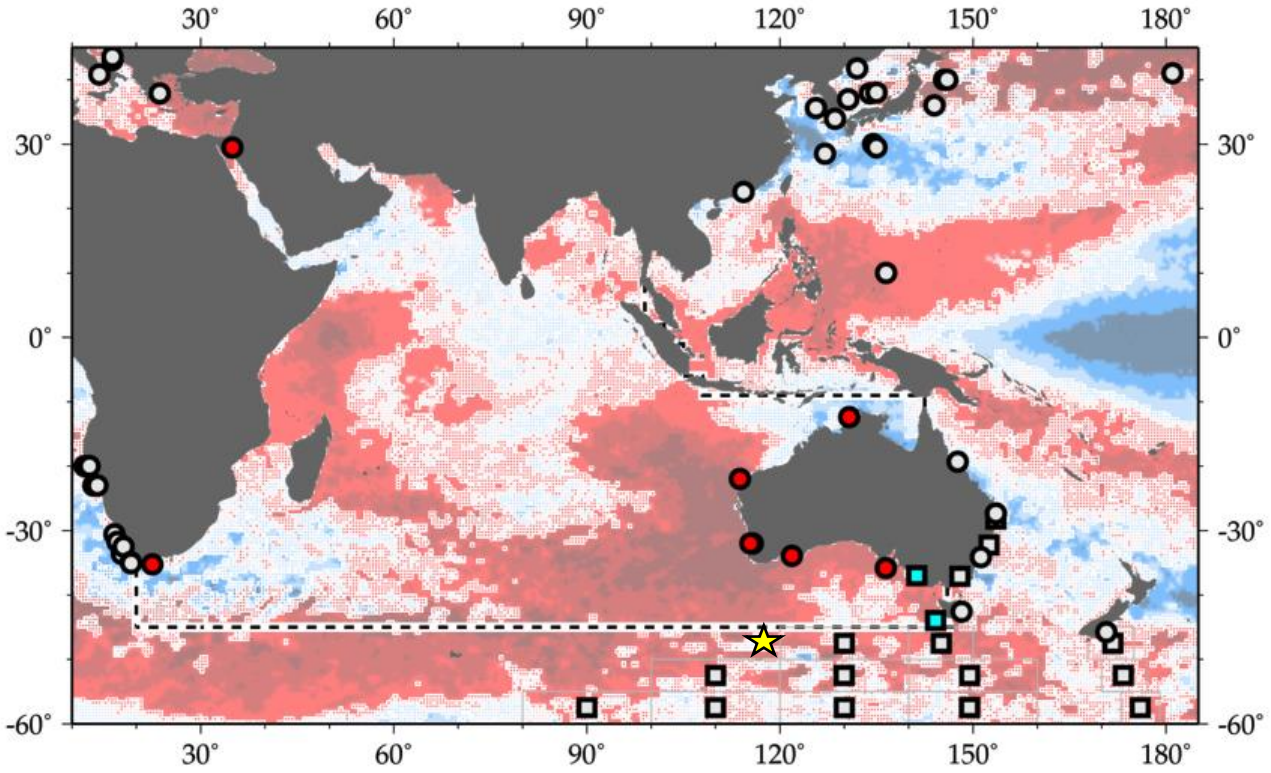

Figure 7.1. Map of IGMETS-participating Indian Ocean time series on a background of a 10-year time-window (2003–2012) sea surface temperature trends (see also Figure 7.3). At the time of this report, the Indian Ocean collection consisted of 10 time series (coloured symbols of any type), of which two were Continuous Plankton Recorder surveys (blue boxes) and one was estuarine (yellow star). Dashed lines indicate boundaries between IGMETS regions. Uncoloured (gray) symbols indicate time series being addressed in a different regional chapter (e.g. Southern Ocean, North/South Pacific, South Atlantic). See Table 7.3 for a listing of this region's participating sites. Additional information on the sites in this study is presented in the Annex.

Participating time-series investigators

Uli Bathmann, Frank Coman, Claire Davies, Ruth Eriksen, Mitsuo Fukuchi, Amatzia Genin, Graham Hosie, Jenny Huggett, Takahashi Kunio, Felicity McEnnulty, Anthony Richardson, Malcolm Robb, Don Robertson, Karen Robinson, Yonathan Shaked, Anita Slotwinkski, Peter A. Thompson, Mark Tonks, and Julian Uribe-Palomino

This chapter should be cited as: Thompson, P. A., O'Brien, T. D., Isensee, K., Lorenzoni, L., and Beckleyiebe, L.E. 2017. Indian Ocean. I*n* What are Marine Ecological Time Series telling us about the ocean? A status report, pp. 113–132. Ed. by T. D. O'Brien, L. Lorenzoni, K. Isensee, and L. Valdés. IOC-UNESCO, IOC Technical Series, No. 129. 297 pp.

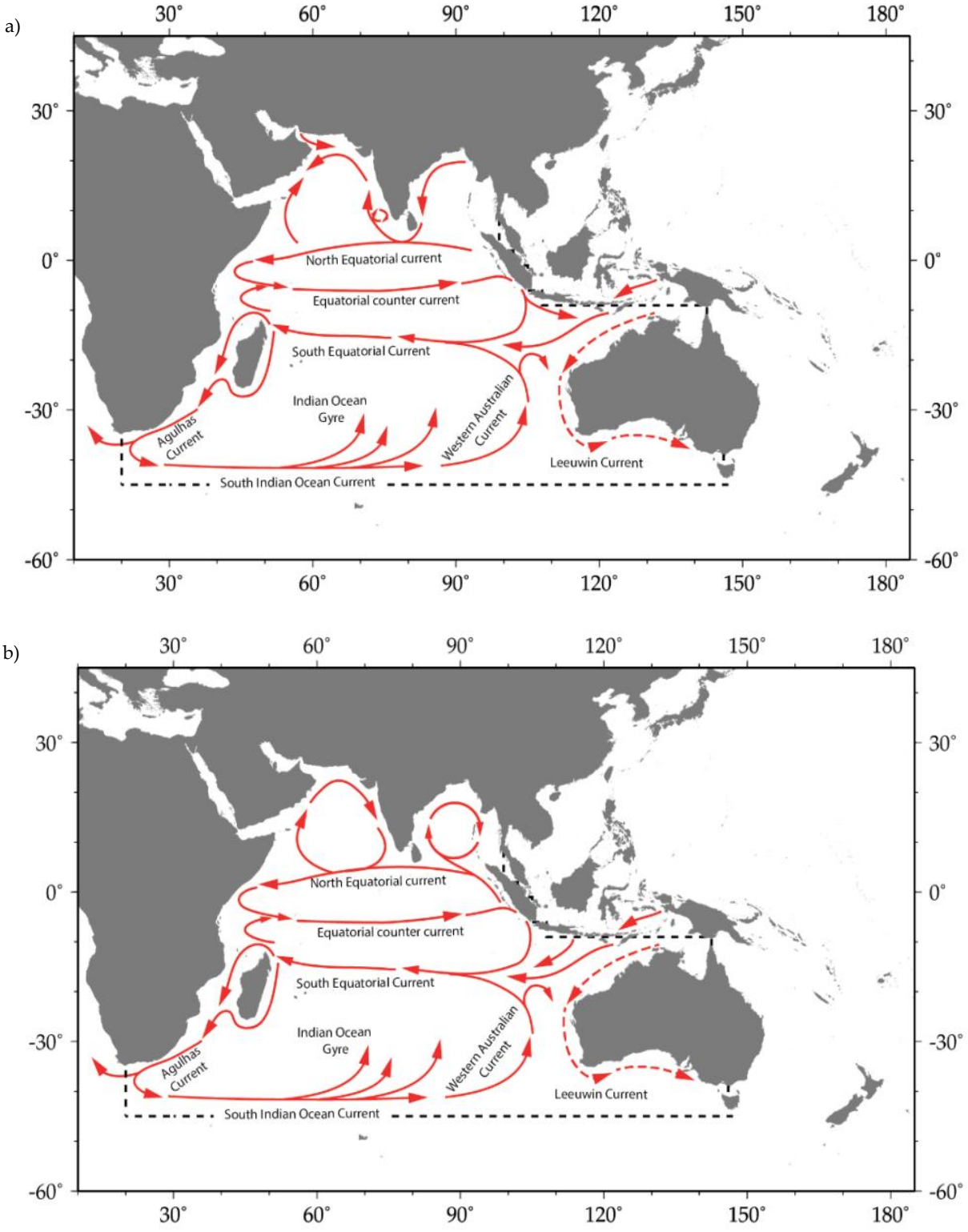

Figure 7.2. Major Indian Ocean Currents (adapted from Schott *et al.*, 2009). a) Late Northeast Monsoon (March–April); b) Late Southwest Monsoon (September–October).

7.1 Introduction

With a southern boundary historically ranging from 60°S to the Antarctic continent, the Indian Ocean is the fourth largest ocean with an area of up to 74 million km^2. As the IGMETS analysis required non-overlapping ocean regions for its spatiotemporal trend calculations, and likewise could only assign each time series to a single region, a boundary of 45°S was used to define and separate the Indian Ocean region from the Southern Ocean region. This modified area, ca. 7800 km wide and stretching from about 25°N to 45°S, had an area of 56.8 million km^2. Unlike the North Atlantic and North Pacific oceans, the Eurasian landmass in the north precludes high-latitude cooling of surface waters in the northern Indian Ocean. There is, however, some low-latitude exchange of water between the Pacific and Indian oceans via the Indonesian Throughflow. The only large shelf areas are the shallow seas north of Australia, which are regions of strong tidal dissipation. There are a number of significant meridional ridges and several deep basins extending below 5000 m. Within the Indian Ocean, there are several marginal seas, gulfs, and bays, with the Indian subcontinent separating the two most prominent, namely the Arabian Sea and the Bay of Bengal. The Arabian Sea, extending between roughly 10–23°N and 51–74°E, reaches depths >3000 m over most of its area and has two important regions: the Gulf of Aden to the southwest, connecting with the Red Sea, and the Gulf of Oman to the northwest, which connects with the Persian Gulf. The Bay of Bengal, which occupies an area of 2 172 000 km^2, receives input from a number of rivers, the most important being the Ganges–Brahmaputra river system.

This river system delivers large quantities of sediment to the Bengal Fan, which causes depth in the Bay of Bengal to decrease gradually from 4000 m south of Sri Lanka to ≤ 2000 m at 18°N (Tomczak and Godfrey, 2003; Galy *et al*., 2007). The circulation of the northern Indian Ocean is dominated by the monsoons and their seasonal switching between strong southwest winds during June–September and weaker northeast winds in October–March (Talley *et al*., 2011). The winds drive a reversal of the surface currents in both the Bay of Bengal and Arabian Sea (Figure 7.2). In particular, the western boundary current in the Arabian Sea, the Somali Current, flows northward in boreal summer and then reverses to flow largely southward in boreal winter. The summer pattern of wind and current stimulates a strong current and upwelling along the coast from Somalia to Oman (Beal and Chereskin, 2003). The northern hemisphere summer monsoons provide intense rainfall between 10–20°N and 70–120°E, which is of considerable importance to agriculture in the region. The tropical southern Indian Ocean typically has a wet monsoon between November and March that produces rainfall around 5–10°S and across the entire basin. In contrast, the austral winter (April–October) monsoon creates some upwelling along the west coasts of Java and Sumatra (Wyrtki, 1962) that tends to be strongest during El Niño events (Susanto *et al*., 2001). The Agulhas Current is a strong western boundary current that transports 70 Sv poleward at 31°S, with flow that varies from 9 to 121 Sv at velocities of up to 2 m s^{-1} at 35°S (Boebel *et al*., 1998; Bryden *et al*., 2005). As the Agulhas Current reaches the southern tip of Africa, most of the water is reflected to the east by the "westerly wind drift" (Lutjeharms and van Ballegooyen, 1988) along the subtropical front (STF). However, a modest volume of warm, saline Indian Ocean water is transported into the South Atlantic through the Agulhas leakage. It has been suggested that the Agulhas leakage is an important component of the climate system (Beal *et al*., 2011). The STF is a long narrow feature stretching from the east coast of South America, through the South Atlantic, Indian, and South Pacific oceans to the west coast of South America. It separates the warm, salty subtropical waters from colder, fresher Antarctic waters. The STF region is high in eddy kinetic energy and develops large coccolithophorid blooms in summer (Balch *et al*., 2011, 2016).

The Leeuwin Current forms the eastern boundary current for the Indian Ocean and is unusual, as it flows poleward albeit with much less volume (ca. 5 Sv) than the Agulhas Current (Godfrey and Ridgway, 1985). The poleward flow of warm, fresher water typically peaks in May or June (Figure 7.2). The buoyant Leeuwin Current also flows eastward through the Great Australian Bight along the south coast of Australia in winter suppressing upwelling along its length (Ridgway and Condie, 2004). The oligotrophic southern Indian Ocean central gyre has previously been estimated to be growing in size in response to climate drivers (Jena *et al*., 2013; Signorini *et al*., 2015).

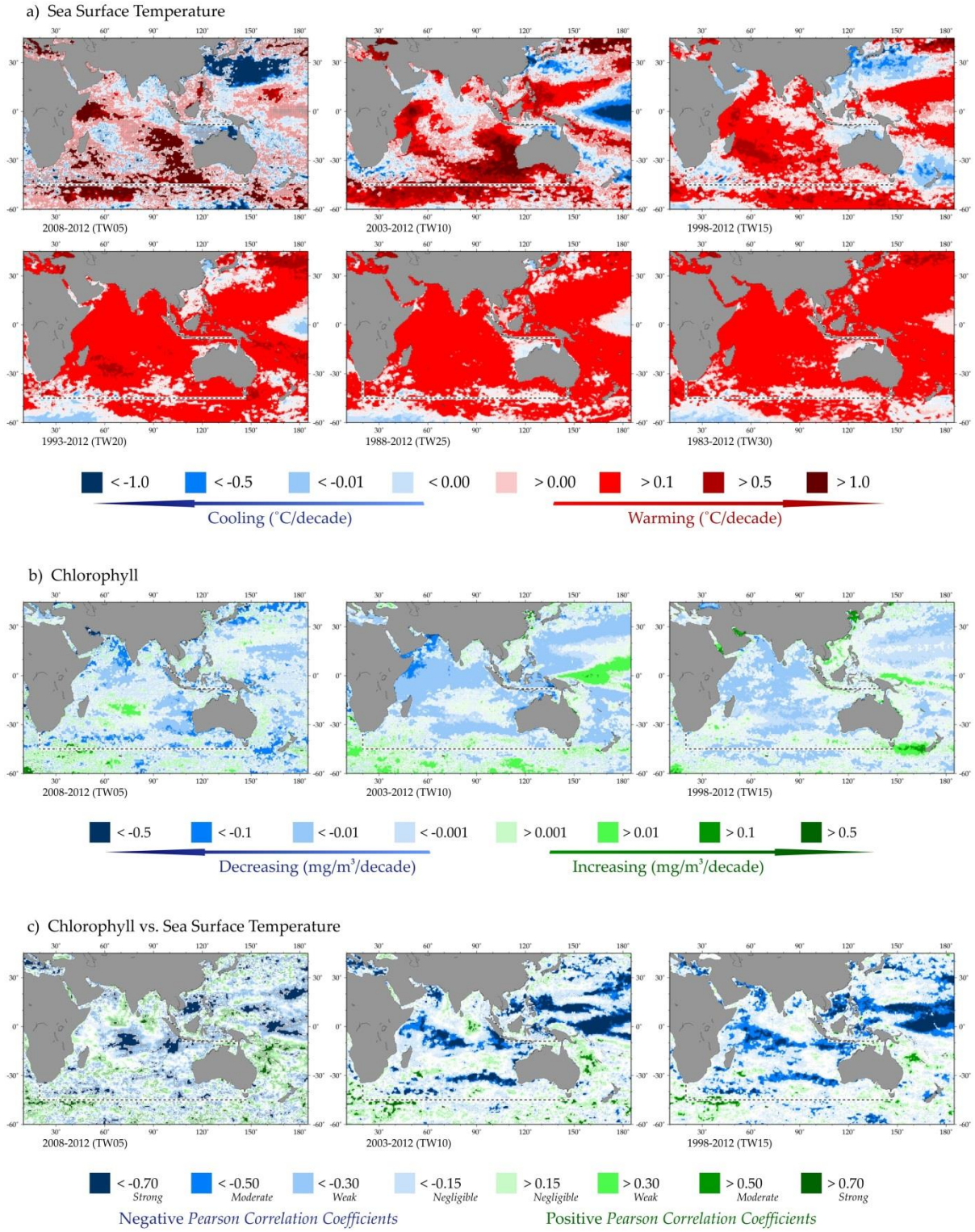

Figure 7.3. Annual trends in Indian Ocean sea surface temperature (SST) (a) and sea surface chlorophyll (CHL) (b), and correlations between chlorophyll and sea surface temperature for each of the standard IGMETS time-windows (c). See "Methods" chapter for a complete description and methodology used.

7.2 General patterns in temperature and phytoplankton biomass

For the entire Indian Ocean, the overwhelming trend in temperature has been upwards (Figure 7.3; Table 7.1). During 1983–2012, ca. 98% of the Indian Ocean was warming, 81.9% showed a significant temperature increase > 0.1 and ≤ 0.5°C decade^{-1} (Table 7.1). This was the greatest proportion of warming for any ocean on the planet (Chapter 10) and is associated with a range of climate cycles including the relatively long positive phase of the Interdecadal Pacific Oscillation (Han *et al*., 2014). Over this same time-period, only 0.5% of the Indian Ocean was found to be significantly cooling (Table 7.1).

The analysis over multiple 5-year time-windows shows that temperature changes were more rapid and more variable over shorter intervals (Table 7.1; Figure 7.3). For example, 19.3% of the Indian Ocean was warming at a high rate of > 1.0°C decade^{-1} over the 5-year window (2008–2012), but this rate was not observed over the 15-year time-window (1998–2012). Between 2008 and 2012, the statistically significant rates of warming ranged from –1.0 to +1.0°C decade^{-1} (Figure 7.4a). Over the longer temporal window from 1983 to 2012, these rates tended to be 5–10-fold less variable ranging from –0.5 to +0.5°C decade^{-1} (Figure 7.4b). Notwithstanding the influence of statistics itself, the declining variability in the rate of temperature changes suggests that the shorter-term climate cycles predominately have periods that are less than 30 years. Consider that the proportion of the Indian Ocean warming rose 0.75% year^{-1} as the time series lengthened from 0 to 20 years, then only 0.23% year^{-1} as the time series was extended another 10 years (Table 7.1). The slowing in the spatial expansion and consolidation of the rate at an intermediate value suggests that the variability associated with shorter-term climatic signals in the Indian Ocean (e.g. Indian Ocean Dipole, El Niño Southern Oscillation) is reduced when using a linear model and more than 20 years of data.

More than 79% of the Indian Ocean experienced a decline in surface chlorophyll *a* over the 15-year time-period from 1998 to 2012, while only 20.3% had an increase (Figure 7.3). The proportion of the Indian Ocean experiencing a decline in chlorophyll *a* was the greatest for any ocean (Table 7.1; Chapter 10) and highly correlated with warming (Figure 7.3). The main areas of cooling and increasing chlorophyll *a* were associated with just four regions: (i) the Arabian Sea and surrounding areas (Red Sea and Persian Gulf), (ii) along the south-west coasts of Sumatra and the Sunda Islands, (iii) south from Madagascar, and (iv) along the subtropical front (STF) at ca. 40–45°S (Figure 7.3). The spatial pattern of increasing chlorophyll *a* tended to vary depending on the temporal window considered, but was arguably most consistent along the STF.

There was significant cooling in the Red Sea, Arabian Sea, Persian Gulf, and along the coasts of Oman and Yemen between 1998 and 2012 (Figure 7.3). Almost none of this regional cooling was evident over the longer 30-year time-window, suggesting that it was strongly influenced by relatively short climatic cycles such as the Indian Ocean Dipole (IOD) and ENSO. It is also possible that this regional cooling was caused by greater seasonal upwelling associated with an increased frequency of stronger IOD and ENSO events that were predicted as a response to climate change (Cai *et al*., 2015).

The Arafura and Timor seas north of Australia also trended colder during 1998–2012. It is probable that this colder trend resulted from the strong positive IOD in 2011 and 2012 and a weakening La Niña (Meyers *et al*., 2007). The IOD primarily affects the pelagic ecology of this region through upwelling favourable winds (Currie *et al*., 2013; Kämpf, 2015).

There was a relatively broad region of cooling off south-east Africa below Madagascar where the Southeast Madagascar and Agulhas currents normally transport considerable amounts of warm water southward (Yamagami and Tozuka, 2015). Although the Southeast Madagascar Current flow is associated with ENSO, this cooling was consistent throughout the different time-windows (Figure 7.3), suggesting a longer-term effect. The source of this surface cooling is unclear. A possibility is the multidecadal rise in subtropical wind stress and increased Southeast Madagascar Current flow (Backeberg *et al*., 2012). The increased South Madagascar Current resulted in a substantial rise in eddy kinetic energy and, in turn, promoted greater vertical mixing for this region (Backeberg *et al*., 2012). Similarly, the region showed mesoscale patches of warming, consistent with increased Agulhas and Southeast Madagascar Current flow.

Table 7.1. Relative spatial areas (% of the total region) and rates of change within within the Indian Ocean region that are showing increasing or decreasing trends in sea surface temperature (SST) for each of the standard IGMETS time-windows. Numbers in brackets indicate the % area with significant ($p < 0.05$) trends. See "Methods" chapter for a complete description and methodology used.

Latitude-adjusted SST data field surface area = 56.8 million km^2	**5-year** (2008–2012)	**10-year** (2003–2012)	**15-year** (1998–2012)	**20-year** (1993–2012)	**25-year** (1988–2012)	**30-year** (1983–2012)
Area (%) w/ increasing SST trends ($p < 0.05$)	**66.7%** (*26.4%*)	**76.0%** (*47.4%*)	**82.6%** (*58.1%*)	**96.7%** (*87.9%*)	**96.2%** (*89.4%*)	**97.8%** (*91.9%*)
Area (%) w/ decreasing SST trends ($p < 0.05$)	33.3% (*4.2%*)	24.0% (*4.5%*)	17.4% (*4.6%*)	3.3% (*0.8%*)	3.8% (*0.7%*)	2.2% (*0.5%*)
> 1.0°C decade^{-1} warming ($p < 0.05$)	24.8% (*19.3%*)	7.8% (*7.8%*)	0.0% (*0.0%*)	0.0% (*0.0%*)	0.0% (*0.0%*)	0.0% (*0.0%*)
0.5 to 1.0°C decade^{-1} warming ($p < 0.05$)	18.8% (*6.1%*)	19.0% (*18.3%*)	6.6% (*6.5%*)	2.9% (*2.9%*)	0.1% (*0.1%*)	0.0% (*0.0%*)
0.1 to 0.5°C decade^{-1} warming ($p < 0.05$)	18.1% (*0.9%*)	38.5% (*20.9%*)	**60.3%** (*49.2%*)	**86.2%** (*83.3%*)	**84.2%** (*83.3%*)	**82.2%** (*81.9%*)
0.0 to 0.1°C decade^{-1} warming ($p < 0.05$)	5.0% (*0.0%*)	10.7% (*0.5%*)	15.7% (*2.3%*)	7.6% (*1.7%*)	11.9% (*6.0%*)	15.6% (*10.0%*)
0.0 to –0.1°C decade^{-1} cooling ($p < 0.05$)	4.1% (*0.0%*)	8.7% (*0.1%*)	7.1% (*0.1%*)	2.0% (*0.1%*)	2.7% (*0.1%*)	1.7% (*0.1%*)
–0.1 to –0.5°C decade^{-1} cooling ($p < 0.05$)	15.0% (*0.5%*)	12.7% (*2.4%*)	9.7% (*3.9%*)	1.2% (*0.6%*)	1.1% (*0.6%*)	0.5% (*0.3%*)
–0.5 to –1.0°C decade^{-1} cooling ($p < 0.05$)	8.7% (*1.5%*)	2.3% (*1.8%*)	0.6% (*0.6%*)	0.1% (*0.1%*)	0.0% (*0.0%*)	0.0% (*0.0%*)
> –1.0°C decade^{-1} cooling ($p < 0.05$)	5.5% (*2.2%*)	0.3% (*0.2%*)	0.1% (*0.1%*)	0.0% (*0.0%*)	0.0% (*0.0%*)	0.0% (*0.0%*)

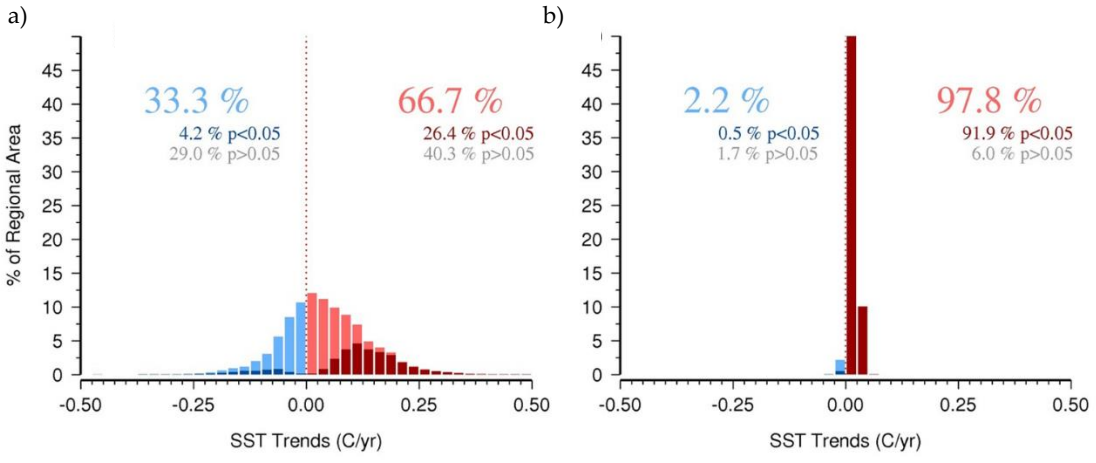

Figure 7.4. The range of SST trends observed over different temporal windows in the Indian Ocean. (a) From 2008 to 2012, 33.3% (66.7%) of the area was cooling (warming); while 4.2% (26.4%) was cooling (warming) significantly ($p < 0.05$). Rates of cooling and warming ranged from –0.50 to +0.50°C year^{-1}. (b) Over the longer-term from 1983 to 2012, the rates of temperature change were much more constrained, ranging from –0.05 to 0.075°C year^{-1}. Over this 30-year period, only 2.2% (97.8) of the area was cooling (warming), while 0.5% (91.9%) was cooling (warming) significantly ($p < 0.05$).

It is suggested that stronger increasing eddy kinetic energy observed across the Agulhas retroflection (Swart *et al*., 2015) added to this spatial mosaic of mesoscale variability in warming and cooling trends. The spatial pattern of patchy cooling extended across the entire Indian Ocean at ca. 40°S, suggesting that this effect can be seen a long way eastward along the edge of the STF. There was also cooling south of Africa between 20–60°E and 50–60°S. This probably relates to the long-term positive trend in the SAM (Swart *et al*., 2015), which increases the westerly flow along 60°S, decreasing SST to lower-than-normal values (Lovenduski and Gruber, 2005; Verdy *et al*., 2006).

Between 1998 and 2012, there were upward trends in chlorophyll *a* within the southern Red Sea, Persian Gulf, and patches through the Gulf of Oman and Arabian Sea off the coasts of Yemen and Oman that largely coincide with regions of declining SST. The latter are regions of upwelling that are known to respond to stronger winds during the summer southwest monsoon season (Yi *et al*., 2015). The trends in chlorophyll *a* are clearly dependent on the temporal window selected with downward trends for most of this region over the shorter 10-year window from 2003 to 2012. Over the shortest temporal window from 2008 to 2012, trends in chlorophyll *a* were mixed across the region, although quite strongly negative in the Persian Gulf (Figure 7.3). A 60-year reconstruction of summer blooms based on SST suggested that regional summer chlorophyll *a* concentrations might have peaked during the very strong upwelling of 1966 (Roxy *et al*., 2016).

The rise in chlorophyll *a* from 1998 to 2012 along the coasts of Java and Sumatra, weakly through the Timor and Arafura seas, and into the Gulf of Carpentaria was in regions that respond to positive ENSO and IOD conditions (Currie *et al*., 2013). These climatic indices were positive on average and trending positive throughout this 15-year period. Indeed, the 15-year period started with predominant El Niño episodes and progressed to include several moderate-to-strong La Niña events in the latter half. The mechanisms potentially driving an increase in chlorophyll *a* across this diverse region include upwelling favorable winds off Java and Sumatra, increased runoff into the Gulf of Carpentaria, and greater interocean exchange from the Pacific to the Indian Ocean for the shallow Arafura and Timor seas.

There were patches of increased chlorophyll *a* southeast of Africa and south of Madagascar observed across all three temporal windows. These patches were also evident across the Indian Ocean sector near the STF. In these regions, the patchy spatial distribution of the increasing chlorophyll *a* has a strong resemblance to the spatial pattern of increased SSH and increasing eddy kinetic energy observed during 1993–2009 (Backeberg *et al*., 2012). Thus, the spatial nature of the increased phytoplankton in this region can be hypothesized to be associated with increased eddy pumping (Falkowski *et al*., 1991). Eastward, along the STF, it is likely that eddies with increased deep mixing at this convergence zone have created this mosaic of increased and decreased chlorophyll *a*. The most pronounced increases in phytoplankton along the Indian Ocean sector of the STF were observed close to Tasmania, where the STF interacts with a strengthening East Australian Current (Figure 7.3).

Mostly at latitudes > 45°S, although occasionally closer to the equator, there were scattered regions where chlorophyll *a* was trending upwards. A positive SAM has been associated with changes in the ocean meridional overturning circulation, including increased upwelling of nutrient-rich waters in the region of 60°S (Hall and Visbeck, 2002), as well as a shallower surface mixed layer depth (Lovenduski and Gruber, 2005). The ENSO also exerts an influence on phytoplankton in this region; for example, when a positive SAM aligns with a positive ENSO event, eddy kinetic energy increases significantly (Langlais *et al*., 2015). Between 35 and 60°S, the spatial patterns of SST and chlorophyll *a* trends were quite consistent across all temporal windows examined. However, during 2003–2012, the warming and greening was broader, but patchier. The trend and average condition of both ENSO and SAM cycles were positive during these 10 years, factors that have been previously linked to increased chlorophyll *a* in these regions (Lovenduski and Gruber, 2005). During this time, the deeply mixed surface layer of the Subantarctic Zone (SAZ) and Polar Front Zone (PFZ) apparently became more conducive for phytoplankton growth. The mechanism for this response is hypothesized to be the upwelling of iron or shallowing of the surface mixed layer (Carranza and Gille, 2015).

During 2008–2012, the south Indian central gyre cooled, and a broad increase in chlorophyll *a* was also observed in that area. The explanation for this strong reversal of the longer-term trend is not evident at this point and may merit further investigation. Indeed, most research has shown the subtropical gyres to be expanding, warming, and declining in phytoplankton (Jena *et al*., 2013; Signorini *et al*., 2015).

Table 7.2. Five-year trends (TW05, 2008–2012) in the time series of observations from *in situ* sites in the South Pacific (not including Continuous Plankton Recorder sites).

Site-ID	Lat (°E) Long (°S)	SST	S	Oxy	NO3	CHL	Cope-pods	Dia.	Dino.	Dia.: Dino.
au-40114 SO CPR Aurora	19.18 147.37	+	-	*n/a*	*n/a*	-	-	*n/a*	*n/a*	*n/a*
au-40205 AusCPR MEAD Line	27.20 153.33	*n/a*	*n/a*	*n/a*	*n/a*	*n/a*	*n/a*	*n/a*	*n/a*	*n/a*
au-50102 IMOS NRS – Darwin	34.05 151.15	*n/a*	*n/a*	*n/a*	*n/a*	*n/a*	*n/a*	*n/a*	*n/a*	*n/a*
au-50103 IMOS NRS – Esperance	42.35 148.14	+	-	-	-	+	+	-	-	-
au-50104 IMOS NRS – Kangaroo Island	36.5 73.0	-	-	-	-	-	-	-	-	-
au-50106 IMOS NRS – Ningaloo	23.1 70.47	*n/a*	*n/a*	*n/a*	*n/a*	*n/a*	*n/a*	*n/a*	*n/a*	*n/a*
au-50108 IMOS NRS – Rottnest Island	4.8 82.00	*n/a*	-	*n/a*	*n/a*	-	*n/a*	-	*n/a*	-
il-10101 Gulf of Eilat NMP Station A	16.00 75.00	-	-	-	-	-	-	-	-	-
za-30202 ABCTS Mossel Bay	11.99 78.97	*n/a*	*n/a*	*n/a*	*n/a*	*n/a*	*n/a*	-	*n/a*	*n/a*

$p > 0.05$ negative positive

7.3 Trends from *in situ* time series

There is a dire paucity of ecological long-term time-series data openly available for the Indian Ocean (Figure 7.5). Most of the small number of time series extend for < 10 years. The lack of these data makes it nearly impossible to even describe the current status of the ecosystem and its pelagic biota or their temporal trends at the basin scale.

The most heavily sampled region is the coastal zone around Australia, extending from Darwin (12°S 131°E) to Tasmania (42°S 148°E), mostly in the Longhurst biogeographical province No. 2 (Longhurst, 2007), the Indonesian and Australian Coastal Province (Figure 7.6). The footprint of these stations indicates that they can represent temperature and chlorophyll *a* temporal trends across a large portion of the adjacent shelf (Oke and Sakov, 2012; Jones *et al*., 2015). Within the Australian portion of this province, the Leeuwin Current (LC) is a strong influence bringing warm, low-salinity, silicate-rich water southward from the tropics (Thompson *et al*., 2011). During 2008–2012, two stations, Esperance and Rottnest Island (Table 7.2), showed the most signs of greater LC effects, such as increasing SST, decreases in salinity, declining dissolved oxygen (DO), and fewer diatoms (Figure 7.5). Copepod biomass rose at both these sites, as did chlorophyll *a* at Esperance (Figure 7.5). The latter result is in strong contrast to the general trend of declining chlorophyll *a* within this region (Figure 7.3), possibly reflecting a more localized effect at this near-shore station or the increased intrusion of productive STF eddies onto the shelf (Schodlok *et al*., 1997; Cresswell and Griffin, 2004). The nearby estuarine site in the Swan River had 10-year trends of increasing temperature, chlorophyll *a*, and DO, but declines in phosphate and dinoflagellates. These are strongly influenced by declining rainfall (Thompson *et al*., 2015). The Kangaroo Island site is also located in Longhurst No. 2 near the extreme eastern end of the Indian Ocean. This site is influenced by wind-driven upwelling with weak links to ENSO and SAM (Nieblas *et al*., 2009). The site showed declines in nitrate, zooplankton, diatoms, and the diatom/dinoflagellate ratio, with a modest increase in salinity from 2008 to 2012 (Table 7.2; Figure 7.5). The declines in the proportion of diatoms and diatom/dinoflagellate were found at three stations along the bottom of Australia. Consistent with satellite data, the time series from the Gulf of Eilat site in the northern Red Sea showed a strong increase in temperature and dissolved oxygen and a weak increase in chlorophyll *a* between 2008 and 2012 (Table 7.2).

Salinity, nitrate, phosphate, and silicate all trended down over the 5-year time-window between 2008 and 2012. The only other time series currently available from the Indian Ocean is at the western extreme at Mossel Bay on the Agulhas Bank. This is one of two regions on the Bank that have been sampled since 1979 (Hutchings *et al*., 1995). There was a strong negative trend in zooplankton biomass over the 15-year time-window from 1998 to 2012 (Table 7.2).

In summary, across the few *in situ* time series available for the Indian Ocean, the trends in temperature were generally upward, while salinity trended down. Trends in nitrate were also generally downward, but other nutrients and biology were variable. These results suggest that local or shorter-term complexities in the oceanography are important in determining ecosystem responses even in the presence of a pervasive warming trend.

7.4 Consistency with previous analysis

Over the 15-year time-period from 1998 to 2012, the average IOD and ENSO indices were positive and trending positive, while the SAM was positive, but trending slightly more negative. These shorter climatic cycles impact most significantly on the Indian Ocean environment and its ecology. The environmental impacts tend to oscillate, with some level of periodicity associated with these climate cycles (Eccles and Tziperman, 2004; Yamagata *et al*., 2003; Fogt *et al*., 2009).

The ENSO climatic driver is the primary source of inter-annual variability in climate throughout most of the Pacific Ocean and portions of the Indian Ocean (Weiqing *et al*., 2014; Cai *et al*., 2015). It is a coupled ocean and atmosphere cycle that can be represented by the Southern Oscillation Index (SOI) based on the difference in surface air pressure between Tahiti and Darwin (Australia).

A persistently positive SOI (lower pressure over Darwin than Tahiti) is a La Niña event. During such an event, strong Pacific trade winds and surface currents push warm water in the tropics westward causing increasing SST, increased steric height, greater rainfall, and reduced SSS. The increased volume of seawater transported from the Pacific Ocean to the Indian Ocean by a La Niña event has been estimated at 5 Sv (Meyers, 1996), and this contributes to a stronger Leeuwin Current.

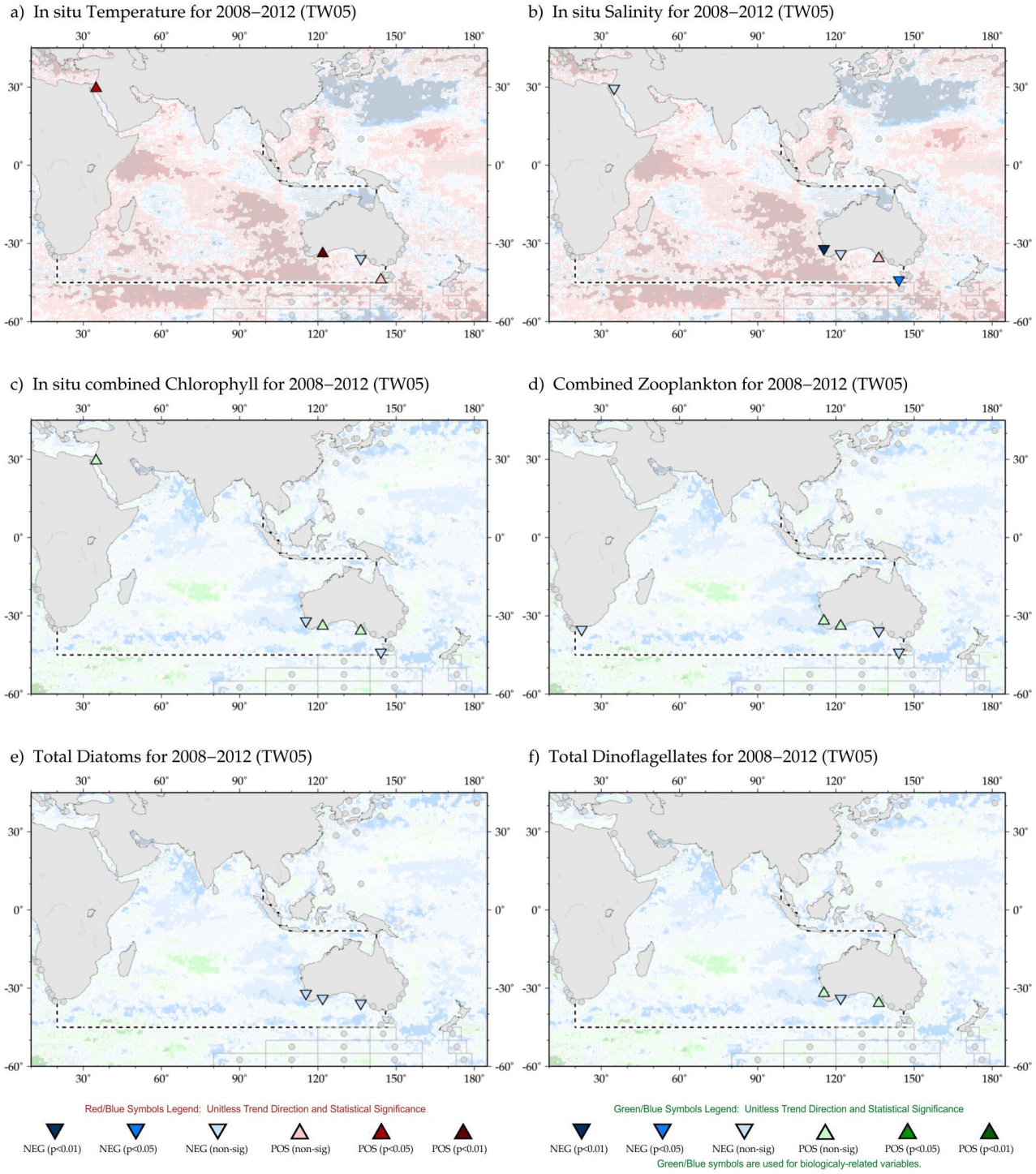

Figure 7.5. Map of Indian Ocean region time-series locations and trends for select variables and IGMETS time-windows. Upward-pointing triangles indicate positive trends; downward triangles indicate negative trends. Gray circles indicate time-series sites that fell outside of the current study region or time-window. Additional variables and time-windows are available through the IGMETS Explorer (http://IGMETS.net/explorer). See "Methods" chapter for a complete description and methodology used.

The intensity of the IOD is represented by an anomalous SST gradient between the western equatorial Indian Ocean (50–70°E and 10°S–10°N) and the southeastern equatorial Indian Ocean (90–110°E and 10°S–0°N; Saji *et al*., 1999). This gradient is also known as the Dipole Mode Index (DMI). Typically, significant anomalies appear around June, intensify in the following months, and peak in October. During a positive IOD, anomalously strong winds push warm water west towards Africa, decreasing upwelling in that region, and increasing upwelling (lower SST) along the west coast of Sumatra (Alory *et al*., 2007). A positive IOD is also associated with reduced rainfall in Indonesia and northern Australia. Lastly, during a positive Southern Annular Mode (SAM) event, the southern hemisphere westerly winds tend to move farther southward and increase in intensity (Gong and Wang, 1999; Thompson *et al*., 2000). This results in stronger cold water upwelling at high latitudes, anomalous downwelling around 45°S, and a strengthening of the Antarctic Circumpolar Current (Hall and Visbeck, 2002; Oke and England, 2003). There is significant temporal variability in the SAM, but over the last 50+ years, the SAM index has been positive and on the rise (Thompson *et al*., 2000; Abram *et al*., 2014); this rise has been linked to anthropogenic factors that include ozone depletion (Fyfe *et al*., 1999).

The analyses presented here are broadly consistent with previous work in the Indian Ocean in terms of warming and the biological responses. However, there are also some discrepancies. For example, some studies of phytoplankton biomass using remote sensing have reported declines in parts or most of the north Indian Ocean (Gregg and Rousseaux, 2014; Roxy *et al*., 2016), in the Equatorial Indian Ocean (Gregg and Rousseaux, 2014), and in the central gyre of the southern Indian Ocean (Jena *et al*., 2013; Signorini *et al*., 2015). The choice of time and space scale used in the analysis clearly influences the result. Shorter time-periods are prone to detecting responses to shorter climatic cycles. For example, the 5-year analysis presented here showed increasing chlorophyll *a* in the south Indian Ocean central gyre (Longhurst 33) during 2008–2012, suggesting a possible link to an intermediate climate cycle (e.g. ENSO or IOD). In addition, the analysis of trends at smaller spatial scales is clearly demonstrating important patterns that can be overlooked if averaging at a larger spatial scale.

Long-term changes to sea surface temperature, surface salinity, and dissolved oxygen in the Indian Ocean have all been previously investigated (e.g. Durack and Wijffels, 2010; Stramma *et al*., 2010; Cai *et al*., 2015). The physical changes in the Indian Ocean are the best studied and are the best resolved through a combination of considerable observational effort and modeling. Chemical and biological studies that are sufficient to detect significant temporal trends are very scarce. The long-term trends of increasing CO_2 and decreasing O_2 at depth tend to change slowly making reasonable predictions of their trends possible from low-frequency sampling. The Bay of Bengal has a shallow low DO layer that extends south of the equator and is expanding (Stramma *et al*., 2010), with the potential to disrupt fisheries (Stramma *et al*., 2012). This low DO layer appears to be high in nitrate and CO_2, and low in pH (Waite *et al*., 2013). The seasonal dynamics of other chemical and the biological components, especially in the euphotic zone, require monthly sampling to resolve trends (Henson, 2014).

The lack of biological monitoring in the Indian Ocean severely limits our ability to understand the effects of climate variability on ecological processes and biodiversity (Dobson, 2005). In addition, the heterogenetic spatial and temporal distributions of biota can make it much more challenging to detect long-term trends or broad spatial patterns. For example, the seasonal variability in phytoplankton biomass can be significant and change annually, requiring sustained and consistent sampling to detect any type of longer-term trend. Thus, detecting a relatively small climate signal requires long-term, carefully designed sampling regimes. Trends in the basic biology of phytoplankton, primary production, zooplankton, and secondary production are known from only a few points in the Indian Ocean. More numerous are reports of significant and rapid range expansions by pelagic biota in response to the changing climate (McLeod *et al*., 2012; Sunday *et al*., 2015). The lack of fisheries-independent stock assessments, the potential for unreported fishing effort, and the instability in catch per unit effort (cpue) means that a robust measure of trends for many populations of fish species is not available at the basin scale.

In the next section, we present some of the most notable changes that have been reported in the literature for the Indian Ocean and compare them to the available data for this report using a geographic framework (Longhurst, 2007).

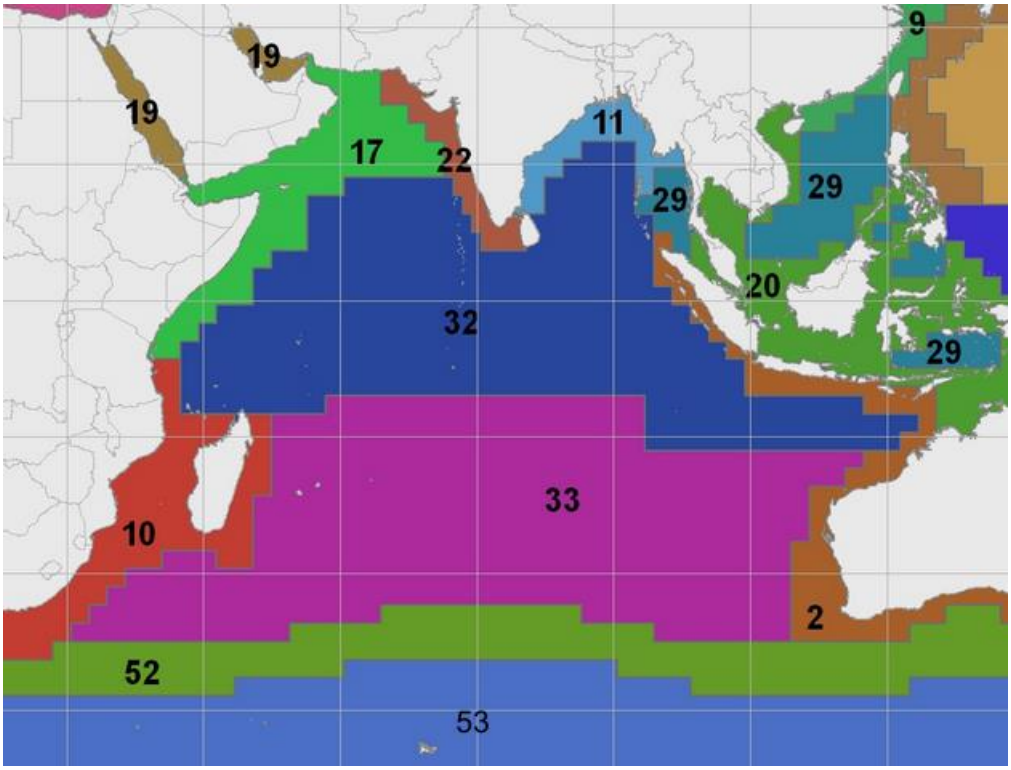

Figure 7.6. The Indian Ocean and surrounding marginal seas separated into biogeographical provinces after Longhurst (1995, 2007). The provinces are based on the types of physical forces that determine the pelagic ecology, particularly the distribution of phytoplankton (*et al*., 2013). Indian Ocean provinces include the: Northwest Arabian Upwelling (17), Red Sea and Persian Gulf (19), East Africa Coastal (10), Australia–Indonesia Coastal (2), Subtropical Convergence (52), Subantarctic (53), East India Coastal (11), West India Coastal (22), Archipelago Deep Basin (29), India Monsoon Gyres (32), and India Subtropical Gyre. (33).

7.4.1 Northwest Arabian upwelling province (Longhurst 17), Red Sea and Persian Gulf province (Longhurst 19)

A series of cruises to this region during the 1990s produced significant insights into the pelagic ecology (Smith, 2005), especially the biological responses to monsoonal forcing (Wiggert *et al*., 2005). Unfortunately, there are limited *in situ* time-series data to assess long-term ecological trends. A regional peak in satellite chlorophyll *a* was observed in 2003 associated with a negative SLA and low SST (Prakash *et al*., 2012). Similarly, a very low SST and strong upwelling was observed in 1966 (Roxy *et al*., 2016). The patchy increases in satellite chlorophyll *a* scattered across the northwest Arabian upwelling province seen over the 5- and 15-year temporal windows may reflect positive IOD and negative ENSO events during the early monsoon season (Currie *et al*., 2013). At this time, the considerable interannual variability and local effects of climate cycles make it difficult to conclude whether the region will experience a longer-term trend towards increased upwelling under prolonged climate change (Bakun, 1990; Goes *et al*., 2005; Prakash and Ramesh, 2007; Narayan *et al*., 2010; Sydeman *et al*., 2014). The significant positive chlorophyll *a* trend in the Gulf of Oman and Persian Gulf, especially observed in the 15-year time-window, is consistent with reports of large blooms of the green form of *Noctiluca scintillans* (Gomes *et al*., 2014). This mixotrophic dinoflagellate, which grows fastest when grazing, has been increasing globally (Harrison *et al*., 2011). Gomes *et al*. (2014) linked the rise in *N. scintillans* with eutrophication and indicated that it was coincident with declining subsurface dissolved oxygen. The 15-year trend of increasing satellite-detected chlorophyll *a* in the Red Sea reported herein has been investigated by Raitsos *et al*. (2015), who suggest that the physical mechanism stimulating primary production is related to ENSO climate

variability in monsoonal winds and nutrient injection from the Indian Ocean, allowing the southern Red Sea to bloom. Unfortunately, the only IGMETS time-series data available from the Red Sea is from the Gulf of Eilat in the far north and well away from this 15-year trend of increasing phytoplankton. In the Gulf of Eilat, the warming and declining nutrients are consistent with the generally expected responses to climate change (Laufkötter *et al*., 2015).

7.4.2 East Africa coastal province (Longhurst 10)

The zooplankton biomass on the Agulhas Bank has declined 57% since 1988 (J. Huggett, pers. comm.). In particular, abundance of the large calanoid zooplankton *Calanus agulhas* has decreased significantly. Available information suggests that increasing SST and predation by anchovy (*Engraulis capensis*) and sardine (*Sardinops sagax*) may be the primary causes (J. Huggett, pers. comm.), a relationship that has been observed nearby on the west coast of Africa (Verheye *et al*., 1998). Increasing SST has been frequently associated with declining populations of large macrozooplankton (Daufresne *et al*., 2009). This province has spatially heterogeneous trends in physical and ecological characteristics that are apparently associated with changing coastal boundary currents (Backeberg *et al*., 2012).

7.4.3 Australia–Indonesia coastal province (Longhurst 2)

Lower SST, greater upwelling, and more chlorophyll *a* off Java and Sumatra have been previously linked to a positive IOD and negative ENSO during September–November (Currie *et al*., 2013). Based on *in situ* data from Rottnest Island (1951–2002), a warming trend of ca. 0.012° $year^{-1}$ has been reported for the west coast of Australia (Thompson *et al*., 2009), which is consistent with the 30-year SST trend reported here. The La Niña event of 2011 was associated with a pronounced increase in water temperature (Feng *et al*., 2013), a decline in zooplankton biomass, and significantly more of the picoplankton *Prochlorococcus* and *Synechococcus*, which are most abundant in the tropics (Thompson *et al*., 2015).

7.4.4 Subtropical convergence province (Longhurst 52)

The subtropical convergence and the subtropical front separates the more saline subtropical waters from the fresher subantarctic waters. The physical drivers are spatially and temporally dynamic (Graham and de Boer, 2013).

The province stretches across the South Atlantic, Indian, and South Pacific oceans and has high eddy kinetic energy and substantial westward flow. In this report, the STF showed evidence of increased chlorophyll *a* across the South Atlantic, South Pacific, and South Indian oceans. In the Indian Ocean, it is possible that this increase is related to large blooms of coccolithophores, which occur in mid-summer (Brown and Yoder, 1994; Balch *et al*., 2011). There is evidence of a diversity of *Emiliania huxleyi* morphotypes (Cubillos *et al*., 2007; Cook *et al*., 2011) and a poleward expansion of these taxa (Winter *et al*., 2014).

7.4.5 Subantarctic province (Longhurst 53)

This province is only rarely within the 45°S limit ascribed to the Indian Ocean for the purpose of this report (Orsi *et al*., 1995). Unfortunately, *in situ* time-series data from this province and within the Indian Ocean sector are very rare. One exceptional dataset was published by Hirawake *et al*. (2005) from regular cruises between Tokyo and the Antarctic continent once a year. The authors reported an increase in chlorophyll *a* over their time series (1965–2002, a trend which is consistent with the remotely-sensed data analyzed herein.

7.5 Conclusions

The Indian Ocean had the greatest extent of warming of all oceans, with 91.8% of its area showing a significant positive trend over 30 years, compared with the Atlantic (88.6%), Pacific (65.9%), Arctic (79.2%), and Southern (31.8%) oceans. In addition to having a high degree of warming, the Indian Ocean also had the greatest proportion of its area (55.1%) showing a significant ($p < 0.05$) decline in chlorophyll *a* between 1998 and 2012. The 51 million km^2 of warming in the Indian Ocean may reflect the fact that the northern Indian Ocean is landlocked at ca. 25°N and, therefore, has no high-latitude, seasonal deep mixing to supply cold surface water.

Across the entire Indian Ocean, a few relatively small and mostly upwelling regions, previously identified as productive (Carr *et al*., 2006), have shown remarkable resilience to warming or declining chlorophyll *a* over the past 30 or 15 years, respectively. These regions off Sumatra and Java, off Somalia and Oman, in the Arabian and Red Seas, and along the STF all showed areas of temperature stability or decline and an increase in chlorophyll *a* during 1998–2012. Upwelling was predicted to intensify under global warming (Bakum, 1990), and there is evidence of this happening in the Indian Ocean. The rise in phytoplankton along the STF is consistent with some coarse-scale modeling of the ocean in 2090 (Marinov *et al*., 2013), although the mechanism and proposed taxonomic shift towards diatoms cannot be confirmed. It should be noted that these regions are the overwhelming minority of the Indian Ocean, with only 0.5% of the area tending significantly downward in temperature over 30 years and 4.8% trending significantly upward for chlorophyll *a* over a 15-year time-period.

Given the spatial scale of warming in the Indian Ocean, it seems likely that climate impacts on marine ecosystems will be most pronounced in this ocean. At the same time, the Indian Ocean has very few *in situ* biogeochemical time series that can be used to assess impacts of climate change on biota or biodiversity. The few time series that exist in the IGMETS database are all on the continental shelves of just two continents, leaving vast areas completely unmonitored. Still, new insights have arisen from examining trends over sequential time-steps and from the effort to couple physical observations with observed biological responses, including *in situ* observations. These *in situ* observations allow unprecedented insights into trends in ecology driven by climate. Previous research on ecological responses of the Indian Ocean to climate change at the basin-scale have been largely model-based (Currie *et al*., 2013), limited to trends detected by remote sensing, or a few local case studies. This IGMETS report is the first effort to bring multiple *in situ* time series together to provide a global synthesis and basin-scale comparisons of long-term trends.

Table 7.3. Time-series sites located in the IGMETS Indian Ocean region. Participating countries: Australia (au), Israel (il), and South Africa (za). Year-spans in red text indicate time series of unknown or discontinued status.

No.	IGMETS-ID	Site or programme name	Year-span	T	S	Oxy	Ntr	Chl	Mic	Phy	Zoo
1	au-10101	Swan River Estuary: S01 Blackwall Reach *(Southwestern Australia)*	1994–present	X	X	X	X	X	-	X	-
2	au-40114	SO-CPR Aurora 140-160-B4245 *(Southern Ocean)* *see Southern Ocean Annex A4)*	2008–present	X	X	-	-	X	-	-	X
3	au-40205	AusCPR MEAD Line *(Australian Coastline)* *see Southern Ocean Annex A4)*	2010–present	-	-	-	-	X	-	X	X
4	au-50102	IMOS National Reference Station Darwin *(Northern Australia)*	2011–present	X	X	-	X	X	X	X	X
5	au-50103	IMOS National Reference Station Esperance *(Southern Australia)*	2009–present	X	X	X	X	X	X	X	X
6	au-50104	IMOS National Reference Station Kangaroo Island *(Southern Australia)*	2008–present	X	X	-	X	X	X	X	X
7	au-50106	IMOS National Reference Station Ningaloo *(Western Australia)*	2010–present	X	X	-	X	X	X	X	X
8	au-50108	IMOS National Reference Station Rottnest Island *(Southwestern Australia)*	2009–present	X	X	-	X	X	X	X	X
9	il-10101	Gulf of Eilat Aqaba NMP Station A *(Gulf of Eilat – Gulf of Aqaba)*	2003–present	X	X	X	X	X	-	-	-
10	za-30202	ABCTS Mossel Bay Monitoring Line *(Agulhas Bank)*	1988–present	-	-	-	-	-	-	-	X

7.6 References

Abram, N. J., Mulvaney, R., Vimeux, F., Phipps, S. J., Turner, J., and England, M. H. 2014. Evolution of the Southern Annular Mode during the past millennium. Nature Climate Change, 4(7): 564–569.

Alory, G., Wijffels, S., and Meyers, G. 2007. Observed temperature trends in the Indian Ocean over 1960–1999 and associated mechanisms. Geophysical Research Letters, 34: L02606.

Backeberg, B. C., Penven, P., and Rouault, M. 2012. Impact of intensified Indian Ocean winds on mesoscale variability in the Agulhas system. Nature Climate Change, 2: 1–5.

Bakun, A. 1990. Global climate change and intensification of coastal ocean upwelling, Science, 247: 198–201.

Balch W. M., Drapeau D. T., Bowler B. C., Lyczkowski, E., Booth, E. S., and Alley, D. 2011. The contribution of coccolithophores to the optical and inorganic carbon budgets during the Southern Ocean Gas Exchange Experiment: new evidence in support of the "Great Calcite Belt" hypothesis. Journal of Geophysical Research, 116: C00F06.

Balch, W. M., Bates, N. R., Lam, P. J., Twining, B. S., Rosengard, S. Z., Bowler, B. C., Drapeau, D. T., *et al*. 2016. Factors regulating the Great Calcite Belt in the Southern Ocean and its biogeochemical significance. Global Biogeochemical Cycles, 30: 1124–1144, doi:10.1002/2016GB005414.

Beal, L. M., and Chereskin, T. K. 2003. The volume transport of the Somali current during the 1995 southwest monsoon. Deep-Sea Research II, 50: 2077–2089.

Beal, L. M., De Ruijter, W. P. M., Biastoch, A., and Zahn, R. 2011. On the role of the Agulhas system in ocean circulation and climate. Nature, 472(7344): 429–436.

Boebel, O., Rae, C. D., Garzoli, S., Lutjeharms, J., Richardson, P., Rossby, T., Schmid, C., *et al.* 1998. Float experiment studies interocean exchanges at the tip of Africa. EOS, 79(1): 7–8.

Brown, C. W., and Yoder, J. A. 1994. Coccolithophorid blooms in the global ocean, Journal of Geophysical Research, 99: 7467–7482.

Bryden, H. L., Beal, L. M., and Duncan, L. M. 2005. Structure and transport of the Agulhas Current and its temporal variability. Journal of Oceanography, 61: 479–492, doi:10.1007/s10872-005-0057-8.

Cai, W., Santoso, A., Wang, G., Yeh, S-W., An, S-I., Cobb, K. M., Collins, M., *et al*. 2015. ENSO and greenhouse warming. Nature Climate Change, 5: 849–859, doi:10.1038/nclimate2743.

Carr, M., Friedrichs, M. A. M., Schmeltz, M., Aita, M. N., Antoine, D., Arrigo, K. R., Asanuma, I., *et al*. 2006. A comparison of global estimates of marine primary production from ocean color. Deep-Sea Research II, 53: 741–770.

Carranza, M. M., and Gille, S. T. 2015. Southern Ocean wind-driven entrainment enhances satellite chlorophyll-a through the summer. Journal of Geophysical Research: Oceans, 120: 304–323, doi:10.1002/2014JC010203.

Cook, S. S., Whittock, L., Wright, S. W., and Hallegraeff, G. M. 2011. Photosynthetic pigment and genetic differences between two Southern Ocean morphotypes of *Emiliania huxleyi* (Haptophyta). Journal of Phycology, 47: 615–626.

Cubillos, J. C., Wright, S. W., Nash, G., de Salas, M. F., Griffiths, B., Tilbrook, B., Poisson, A., *et al*. 2007. Calcification morphotypes of the coccolithophorid *Emiliania huxleyi* in the Southern Ocean: Changes in 2001 to 2006 compared to historical data. Marine Ecological Progress Series, 348: 47–54.

Cresswell, G. R., and Griffin, D. A. 2004. The Leeuwin Current, eddies and sub-Antarctic waters off south-western Australia. Marine Freshwater Research, 55: 267–276.

Currie, J. C., Lengaigne, M., Vialard, J., Kaplan, D. M., Aumont, O., Naqvi, S. W. A., and Maury, O. 2013. Indian Ocean Dipole and El Niño/Southern Oscillation impacts on regional chlorophyll anomalies in the Indian Ocean. Biogeosciences, 10: 6677–6698.

Daufresne, M., Lengfellner, K., and Sommer, U. 2009. Global warming benefits the small in aquatic ecosystems. Proceedings of the National Academy of Sciences of the United States of America, 106: 12788–12793.

Dobson, A. 2005. Monitoring global rates of biodiversity change: challenges that arise in meeting the Convention on Biological Diversity (CBD) 2010 goals. Philosophical Transactions of the Royal Society B, 360: 229–241.

Durack, P. J., and Wijffels, S. E. 2010. Fifty-year trends in global ocean salinities and their relationship to broad-scale warming. Journal of Climate, 23: 4342–4362.

Eccles, F., and Tziperman, E. 2004. Nonlinear effects on ENSO's period. Journal of Atmospheric Science, 61: 474–482.

Falkowski, P. G., Ziemann, D., Kolber, Z., and Bienfang, P. K. 1991. Role of eddy pumping in enhancing primary production in the ocean. Nature, 352(6330): 55–58.

Feng, M., McPhaden, M. J., Xie, S., and Hafner, J. 2013. La Niña forces unprecedented Leeuwin Current warming in 2011. Scientific Reports 3: 1277, doi:10.1038/srep01277.

Fogt, R. L., Perlwitz, J., Monaghan, A. J., Bromwich, D. H., Jones, J. M., and Marshall, G. J. 2009. Historical SAM variability. Part II: twentieth-century variability and trends from reconstructions, observations, and the IPCC AR4 models. Journal of Climate, 22: 5346–5365.

Fyfe, J. C., Boer, G. J., and Flato, G. M. 1999. The Arctic and Antarctic Oscillations and their projected changes under global warming. Geophysical Research Letters, 26: 1601–1604.

Galy, V., France-Lanord, C., Beyssac, O., Faure, P., Kudrass, H., and Palhol, F. 2007. Efficient organic carbon burial in the Bengal fan sustained by the Himalayan erosional system. Nature, 450: 407–410.

Godfrey, J. S., and Ridgway, K. R. 1985. The large-scale environment of the poleward-flowing Leeuwin current, Western Australia: longshore steric height gradients, wind stresses and geostrophic flow. Journal of Physical Oceanography, 15: 481–495.

Goes, J. I., Thoppil, P. G., Gomes, H. D., and Fasullo, J. T. 2005. Warming of the Eurasian landmass is making the Arabian Sea more productive. Science, 308: 545–547.

Gomes, H. D. R., Goes, J., Matondkar, S. G. P., Buskey, E. J., Basu, S., Parab, S., and Thoppil, P. 2014. Massive outbreaks of *Noctiluca scintillans* blooms in the Arabian Sea due to spread of hypoxia. Nature Communications, 5: 4862, doi:10.1038/ncomms5862.

Gong, D., and Wang, S. 1999. Definition of Antarctic oscillation index. Geophysical Research Letters, 26: 459–462.

Graham, R. M., and De Boer, A. M. 2013. The Dynamical Subtropical Front, Journal of Geophysical Research, 118: 5676–5685, doi:10.1002/jgrc.20408.

Gregg, W. W., and Rousseaux, C. S. 2014. Decadal trends in global pelagic ocean chlorophyll: A new assessment integrating multiple satellites, in situ data, and models. Journal of Geophysical Research: Oceans, 119: 5921–5933, http://dx.doi.org/10.1002/2014JC010158.

Hall, A., and Visbeck, M. 2002. Synchronous variability in the Southern Hemisphere atmosphere, sea ice, and ocean resulting from the annular mode. Journal of Climate, 15: 3043–3057.

Han, W., Vialard, J., McPhaden, M. J., Lee, T., Masumoto, Y., Feng, M., and de Ruijter, W. P. M. 2014. Indian Ocean decadal variability: a review. Bulletin of the American Meteorological Society, 95: 1679–1703.

Harrison, P. J., Furuya, K., Glibert, P., Xu, J., Liu, H. B., Yin, K., Lee, J. H. W., *et al*. 2011. Geographical distribution of red and green *Noctiluca scintillans*. Chinese Journal of Oceanology and Limnology, 29: 807–831, doi:10.1007/s00343-011-0510-z.

Henson, S. A. 2014. Slow science: the value of long ocean biogeochemistry records. Philosophical Transactions of the Royal Society A, 372(2025), doi:10.1098/rsta.2013.0334.

Hirawake, T., Odate, T., and Fukuchi, M. 2005. Long-term variation of surface phytoplankton chlorophyll *a* in the Southern Ocean during 1965–2002. Geophysical Research Letters, 32(2005): L05606, http://dx.doi.org/10.1029/2004GL021394.

Hutchings, L., Verheye, H. M., Mitchell-Innes, B. A., Peterson, W. T., Huggett, J. A., and Painting, S. J. 1995. Copepod production in the southern Benguela system. ICES Journal of Marine Science, 52: 439–455.

Jena, B., Sahu, S., Avinash, K., and Swain, D. 2013. Observation of oligotrophic gyre variability in the South Indian Ocean: Environmental forcing and biological response. Deep-Sea Research I, 80: 1–10.

Jones, E. M., Doblin, M. A., Matear, R., and King, E. 2015. Assessing and evaluating the ocean-colour footprint of a regional observing system. Journal of Marine Systems, 143: 49–61.

Kämpf, J. 2015. Undercurrent-driven upwelling in the northwestern Arafura Sea. Geophysical Research Letters, 42: 9362–9368, doi:10.1002/2015GL066163.

Langlais, C., Rintoul, S., and Zika, J. 2015. Sensitivity of Antarctic circumpolar transport and eddy activity to wind patterns in the Southern Ocean. Journal of Physical Oceanography, 45: 1051–1067, doi:10.1175/JPO-D-14-0053.1.

Laufkötter, C., Vogt, M., Gruber, N., Aita-Noguchi, M., Aumont, O., Bopp, L., Buitenhuis, E., *et al*. 2015. Drivers and uncertainties of future global marine primary production in marine ecosystem models. Biogeosciences, 12: 6955–6984, doi:10.5194/bg-12-6955-2015.

Longhurst, A. 1995. Seasonal cycles of pelagic production and consumption. Progress in Oceanography, 36: 77–167.

Longhurst, A. 2007. Ecological Geography of the Sea, 2nd edn. Academic Press, San Diego. 542 pp.

Lovenduski, N. S., and Gruber, N. 2005. The impact of the Southern Annular Mode on Southern Ocean circulation and biology. Geophysical Research Letters, 32: L11603, doi:10.1029/2005GL022727.

Lutjeharms, J. R. E., and van Ballegooyen, R. C. 1988. The retroflection of the Agulhas Current. Journal of Physical Oceanography, 18: 1570–1583.

Marinov, I., Doney, S. C., Lima, I. D., Lindsay, K., Moore, J. K., and Mahowald, N. 2013. North–south asymmetry in the modeled phytoplankton community response to climate change over the 21st century. Global Biogeochemical Cycles, 27: 1274–1290, doi:10.1002/2013GB004599.

McLeod, D. J., Hallegraeff, G. M., Hosie, G. M., and Richardson, A J. 2012. Climate-driven range expansion of the red-tide dinoflagellate *Noctiluca scintillans* into the Southern Ocean. Journal of Plankton Research, 34: 332–337.

Meyers, G. 1996. Variation of the Indonesian throughflow and the El Niño-Southern Oscillation. Journal of Geophysical Research, 101: 12255–12263.

Meyers, G., McIntosh, P., Pigot, L., and Pook, M. 2007. The years of El Niño, La Niña, and interactions with the tropical Indian Ocean. Journal of Climate, 20: 2872–2880, doi:10.1175/JCLI4152.1.

Narayan, N., Paul, A., Mulitza, S., and Schulz, M. 2010. Trends in coastal upwelling intensity during the late 20th century. Ocean Science, 6: 815–823, doi:10.5194/os-6-815-2010.

Nieblas, A. E., Sloyan, B. M., Coleman, R., and Richardson, A. J. 2009. Variability of biological production in low wind-forced regional upwelling systems: a case study off southeastern Australia. Limnology and Oceanography, 54: 1548–1558.

Oke, P. R., and England, M. H. 2003. Oceanic response to changes in the latitude of the Southern Hemisphere subpolar westerly winds. Journal of Climate, 17: 1040–1054.

Oke, P. R., and Sakov, P. 2012. Assessing the footprint of a regional ocean observing system. Journal of Marine Systems, 105–108: 30–51.

Orsi, A. H., Whitworth III, T., and Nowlin Jr., W. D. 1995: On the meridional extent and fronts of the Antarctic Circumpolar Current. Deep-Sea Research I, 42: 641–673.

Prakash, P., Prakash, S., Rahaman, H., Ravichandran, M., and Nayak, S. 2012. Is the trend in chlorophyll-a in the Arabian Sea decreasing? Geophysical Research Letters, 39: L23605, doi:10.1029/2012GL054187.

Prakash, S., and Ramesh, R. 2007. Is the Arabian Sea getting more productive? Current Science, 92: 667–671.

Raitsos, D. E., Yi, X., Platt, T., Racault, M., Brewin, R. J. W., Pradhan, Y., Papadopoulos, V. P., *et al*. 2015. Monsoon oscillations regulate fertility of the Red Sea. Geophysical Research Letters, 42: 855–862, doi:10.1002/2014GL062882.

Reygondeau, G., Longhurst, A., Martinez, E., Beaugrand, G., Antoine, D., and Maury, O. 2013. Dynamic biogeochemical provinces in the global ocean. Global Biogeochemical Cycles, 27: 1–13, doi:10.1002/gbc.20089.

Ridgway, K. R., and Condie, S. A. 2004. The 5500-km-long boundary flow off western and southern Australia. Journal of Geophysical Research: Oceans, 109: C04017, doi:0.1029/2003JC001921.

Roxy, M. K., Modi, A., Murtugudde, R., Valsala, V., Panickal, S., Prasanna Kumar, S., Ravichandran, M., *et al*. 2016. A reduction in marine primary productivity driven by rapid warming over the tropical Indian Ocean. Geophysical Research Letters, 43: 826–833, doi:10.1002/2015GL066979.

Saji, N. H., Goswami, B. N., Vinayachandran, P. N., and Yamagata, T. 1999. A dipole mode in the tropical Indian Ocean. Nature, 401: 360–363.

Schodlok, M. P., Tomczak, M., and White, N. 1997. Deep sections through the South Australian Basin and across the Australian-Antarctic Discordance. Geophysical Research Letters, 24: 2785–2788.

Schott, F. A., Xie, S-P., and McCreary Jr., J. P. 2009. Indian Ocean circulation and climate variability. Reviews of Geophysics, 47: RG1002, doi:10.1029/2007RG000245.

Signorini, S. R., Franz, B. B., and McClain, C. R. 2015. Chlorophyll variability in the oligotrophic gyres: mechanisms, seasonality and trends. Frontiers in Marine Science, http://dx.doi.org/10.3386/fmars.2015.0001

Smith, A. L. 2005. The Arabian Sea of the 1990s: New Biogeochemical Understanding. Progress in Oceanography, 65: 113–115.

Stramma, L., Schmidtko, S., Levin, L. A., and Johnson, G. C. 2010. Ocean oxygen minima expansions and their biological impacts. Deep-Sea Research I, Oceanographic Research Papers, 57(4): 587–595.

Stramma, L., Prince, E. D., Schmidtko, S., Luo, J., Hoolihan, J. P., Visbeck, M., Wallace, D. W. R., *et al*. 2012. Expansion of oxygen minimum zones may reduce available habitat for tropical pelagic fishes. Nature Climate Change, 2: 33–37.

Sunday, J. M., Pecl, G. T., Frusher, S., Hobday, A. J., Hill, N., Holbrook, N. J., Edgar, G. J., *et al*. 2015. Species traits and climate velocity explain geographic range shifts in an ocean-warming hotspot. Ecology Letters, 18: 944–953.

Susanto, R. D., Gordon, A. L., and Zheng, Q. 2001. Upwelling along the coasts of Java and Sumatra and its relation to ENSO. Geophysical Research Letters, 28(8): 1599–1602.

Swart, N. C., Fyfe, J. C., Gillett, N., and Marshall, G. J. 2015. Comparing trends in the Southern Annular Mode and Surface Westerly Jet. Journal of Climate, 28: 8840–8859, doi:http://dx.doi.org/10.1175/JCLI-D-15-0334.1.

Sydeman, W. J., García-Reyes, M., Schoeman, D. S., Rykaczewski, R. R., Thompson, S. A., Black, B. A., and Bograd, S. J. 2014. Climate change and wind intensification in coastal upwelling ecosystems. Science, 345(6192): 77–80.

Talley, L. D., Pickard, G. L., Emery, W. J., and Swift, J. H. 2011. Descriptive Physical Oceanography: An Introduction (Sixth edn). Elsevier, Boston. 560 pp.

Thompson, D. W. J., Wallace, J. M., and Hegerl, G. C. 2000. Annular modes in the Extratropical Circulation. Part II: Trends. Journal of Climate, 13: 1018–1036.

Thompson, P. A., Baird, M. E., Ingleton, T., and Doblin, M. A. 2009. Long-term changes in temperate Australian coastal waters and implications for phytoplankton. Marine Ecology Progress Series, 384: 1–19.

Thompson, P. A., Bonham, P., Rochester, W., Doblin, M. A., Waite, A. M., Richardson, A., and Rousseaux, C. 2015. Climate variability drives plankton community composition changes: an El Niño to La Niña transition around Australia. Journal of Plankton Research, 37(5): 966–984, doi:10.1093/plankt/fbv069.

Thompson, P. A., Wild-Allen, K., Lourey, M., Rousseaux, C., Waite A. M., Feng, M., and Beckley, L. E. 2011. Nutrients in an oligotrophic boundary current: Evidence of a new role for the Leeuwin Current. Progress in Oceanography, 91: 345–359.

Tomczak, M., and Godfrey, J. S. 2003. Regional Oceanography: an Introduction. Daya Publishing House, Delhi, India. 390 pp.

Verdy, A., Marshall, J., and Czaja, A. 2006. Sea surface temperature variability along the path of the Antarctic Circumpolar Current, Journal of Physical Oceanography, 36: 1317–1331.

Verheye, H. M., Richardson, A. J., Hutchings. L., Marska. G., and Gianakouros, D. 1998. Long-term trends in the abundance and community structure of coastal zooplankton in the southern Benguela system, 1951–1996. South African Journal of Marine Science, 19: 317–332.

Waite, A. M., Rossi, V., Roughan, M., Tilbrook, B., Thompson, P. A., Feng, M., Wyatt, A. S. J., *et al*. 2013. Formation and maintenance of high-nitrate, low pH layers in the Eastern Indian Ocean and the role of nitrogen fixation. Biogeosciences, 10: 5691–5702.

Weiqing, H., Vialard, J., McPhaden, M. J., Lee, T., Masumoto, Y., Feng, M., and de Ruijter, W. P. M. 2014. Indian Ocean decadal variability: a review. Bulletin of the American Meteorological Society, 95: 1679–1703.

Wiggert, J. D., Hood, R. R., Banse, K., and Kindle, J. C. 2005. Monsoon-driven biogeochemical processes in the Arabian Sea. Progress in Oceanography, 65: 176–213, doi: 10.1016/j.pocean.2005.03.008.

Winter, A., Henderiks, J., Beaufort, L., Rickaby, R. E. M., and Brown, C. W. 2014. Poleward expansion of the coccolithophore *Emiliania huxleyi*. Journal of Plankton Research, 36: 316–325.

Wyrtki, K. 1962. The upwelling in the region between Java and Australia during the south-east monsoon. Marine Freshwater Research, 13: 217–225.

Yamagata, T., Behera, S. K. Rao, S. A., Guan, Z., Ashok, K., and Saji, H. N. 2003. Comments on dipoles, temperature gradient, and tropical climate anomalies. Bulletin of the American Meteorological Society, 84: 1418–1422.

Yamagami, Y., and Tozuka, T. 2015. Interannual variability of South Equatorial Current bifurcation and western boundary currents along the Madagascar coast, Journal of Geophysical Research: Oceans, 120: 8551–8557.

Yi, B., Yang, P., Dessler, A., and da Silva, A. M. 2015. Response of aerosol direct radiative effect to the East Asian Summer Monsoon. IEEE Geoscience and Remote Sensing Letters, 12(3): 597–600.

8 South Pacific Ocean

Peter A. Thompson, Todd D. O'Brien, L. Lorenzoni, and Anthony J. Richardson

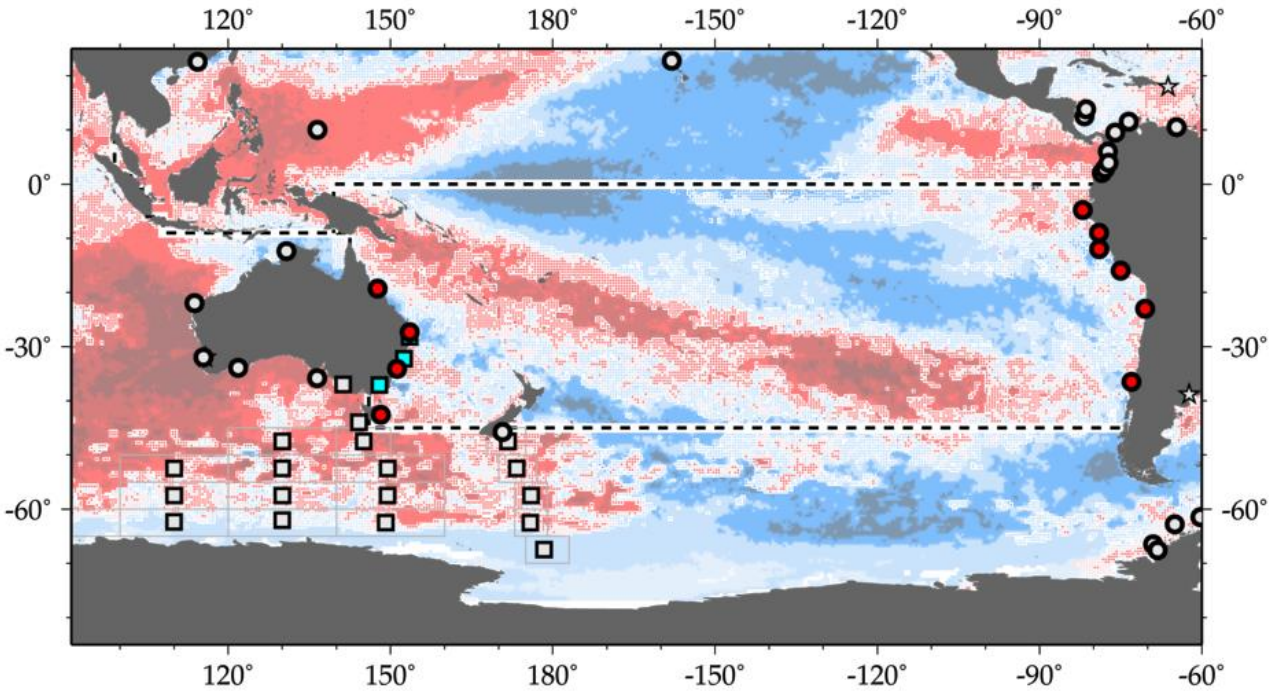

Figure 8.1. Map of IGMETS-participating South Pacific time series on a background of a 10-year time-window (2003–2012) sea surface temperature trends (see also Figure 8.3). At the time of this report, the South Pacific collection consisted of 13 time series (coloured symbols of any type), of which three were from Continuous Plankton Recorder surveys (blue boxes) and none were from estuarine areas (yellow stars). Dashed lines indicate boundaries between IGMETS regions. Uncoloured (gray) symbols indicate time series being addressed in a different regional chapter (e.g. Southern Ocean, North Pacific, Indian Ocean). See Table 8.4 for a listing of this region's participating sites. Additional information on the sites in this study is presented in Annex A.6.

Participating time-series investigators

Patricia Ayon, Frank Coman, Claire Davies, Ruth Eriksen, Ruben Escribano, Jesus Ledesma Rivera, Felicity McEnnulty, Anthony J. Richardson, Anita Slotwinkski, Mark Tonks, and Julian Uribe-Palomino

This chapter should be cited as: Thompson, P. A., O'Brien, T. D., Lorenzoni, L., and Richardson, A. J. 2017. The South Pacific Ocean. I*n* What are Marine Ecological Time Series telling us about the ocean? A status report, pp. 133–151. Ed. by T. D. O'Brien, L. Lorenzoni, K. Isensee, and L. Valdés. IOC-UNESCO, IOC Technical Series, No. 129. 297 pp.

8.1 Introduction

After the North Pacific, the South Pacific Ocean (Figure 8.1) is the second largest body of water considered in this report. The surface currents of the South Pacific are strongly influenced by the predominantly westerly wind near the southern boundary (45°S) and easterly winds near the equator (Figure 8.2). Along the southern boundary of the South Pacific, strong easterly flow is found at the subtropical front (STF) and in the Antarctic Circumpolar Current (ACC). The westward return flow is primarily by the South Equatorial Current (SEC) (Figure 8.2; Roemmich and Cornuelle, 1990). A portion of the easterly flow passes between South America and Antarctica, but part of it curves northward and flows along the west coast of South America as the Humboldt (or Chile–Peru) Current. The quasi stationary South Pacific high atmospheric pressure zone near 100°W, between 20 and 35°S, deflects winds toward the equator and contributes to the ~15 Sv (Sv = sverdrup = 10^6 m^3 s^{-1}; Wijffels *et al*., 2001) strength of the Humboldt Current (Wyrtki, 1963), one of the most productive eastern boundary currents (EBCs) in the global oceans. Strong wind-induced upwelling along the Peru and Chile coastlines results in large phytoplankton blooms, a substantial biomass of zooplankton, and some of the world's largest annual fish catches (Fiedler *et al*., 1991; Daneri *et al*., 2000; Pennington *et al*., 2006; Chavez and Messié, 2009; Correa-Ramirez *et al*., 2012).

The Humboldt Current bifurcates around 25°S (Fuenzalida *et al*., 2008); the offshore branch heads northwest and the more coastal branch continues along the coast of Peru. Both branches eventually turn mainly westward as part of the SEC that flows from South America to the western Pacific. The SEC divides as it approaches Australia producing at least three major branches, one of the most important being the East Australian Current (EAC). The EAC is the Western Boundary Current (WBC) of the southwestern Pacific and is associated with the South Pacific subtropical gyre (Mata *et al*., 2000). The EAC is significantly weaker than other WBCs in terms of volume transport, with ca. 15 Sv mean annual flow (Mata *et al*., 2000). It flows poleward along the eastern Australian coast carrying warm water from tropical to mid latitudes. It separates from the continent at 30–34°S, where about two-thirds of the flow moves eastward and then continues down the east coast of New Zealand before going farther eastward (Godfrey *et al*., 1980; Ridgway and Godfrey, 1997). In the region where the EAC

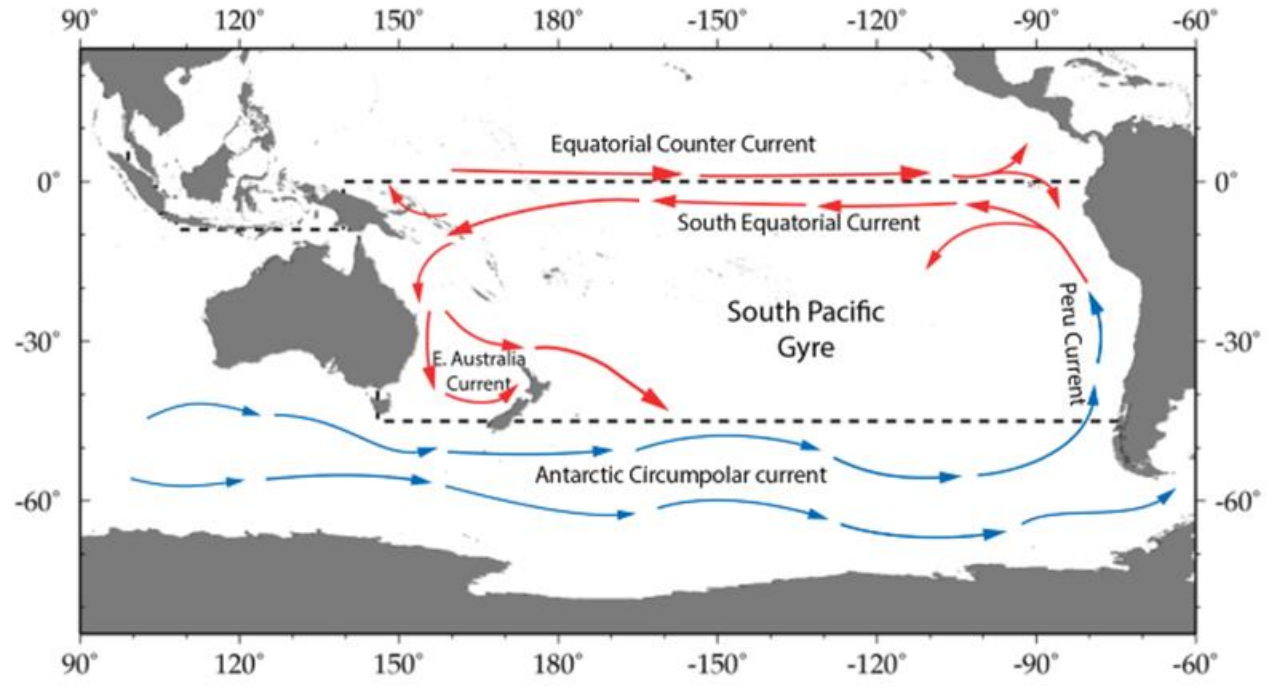

Figure 8.2. Schematic major current systems in the IGMETS-defined South Atlantic region. Red arrows indicate generally warmer water currents; blue arrows indicate generally cooler water currents.

veers eastward, the remaining ca. one-third of the EAC continues south past Tasmania as an eddy field (Mata *et al*., 2006; O'Kane *et al*., 2011; Macdonald *et al*., 2013; Cetina-Heredia *et al*., 2014). The seasonal, interannual and decadal changes of the EAC, together with the high variability induced by the mesoscale eddies, dominate circulation features along the east coast of Australia and influence the biogeochemistry and ecology of the region (Cetina-Heredia *et al*., 2014).

In the western tropical Pacific between 10°Nand 10°S and centred around 170°E, the Pacific Warm Pool (WP) is characterized by high sea surface temperatures (SST, 28–29°C) and low sea surface salinities (SSS, <35), the latter induced by heavy rainfall (Wyrtki, 1989). Along much of the northern edge of the South Pacific and extending into the central gyre is a large region of very high solar radiation (ca. 200 W m^{-2}), warming the ocean, causing considerable evaporation, and producing large net precipitation along the intertropical convergence zone (ITCZ) near the equator (Meehl *et al*., 2008). Farther south at ca. 15–25°S and centred at ca. 124°W, the warming produces a region of very high net evaporation and high surface salinities (SSS >36; Hasson *et al*., 2013). This pool of high-salinity water seasonally migrates eastward during austral summer and westward during austral winter, driven by changes in the intensity of the South Pacific Convergence Zone and easterly winds. However, a net migration westward of the salinity maximum over the past 20 years has been noted (Hasson *et al*., 2013).

A high pressure zone tends to persist over Australia during austral summer (December–February), directing winds that deflect equatorial trade winds poleward and creating the strong South Pacific Convergence Zone (SPCZ) (Vincent, 1994; Vincent *et al*., 2011). While the SPCZ is best developed during austral summer, it is present year-round, extending from New Guinea (0° 150°E) east–southeastward to about 30°S 120°W. In its northwestern sector, the SPCZ merges with the Intertropical Convergence Zone (ITCZ). This low-level atmospheric convergence and precipitation zone is one of the major components of South Pacific climate and is responsible for a large fraction of South Pacific precipitation, especially during austral summer (Vincent, 1994; Brown *et al*., 2011; Vincent *et al*., 2011).

Important drivers of oceanic ecology such as currents, upwelling, tides, irradiance, temperature, and nutrients show significant variation across a range of time- and space scales producing a complex spatial and temporal pattern of trends. This report focuses on time-scales of 5–30 years and spatial scales from hundreds to millions of square kilometers. Most of the multiyear and large spatial-scale variability in the physics, biogeochemistry, and ecology of the South Pacific is modulated by "shorter" natural climatic cycles such as El Niño Southern Oscillation (ENSO), the Interdecadal Pacific Oscillation (IPO), and Southern Annular Mode (SAM). These natural cycles often have a more profound effect on SST differences between years than the long-term rise of ca. 0.03°C $decade^{-1}$ since 1850 (Rayner *et al*., 2006).

El Niño Southern Oscillation (ENSO) is a coupled ocean and atmosphere cycle consisting of a weakening and strengthening of the easterly trade winds over the tropical Pacific and with a consequent impact on sea surface temperatures (Wang *et al*., 2012a). It fluctuates between warm (El Niño) and cold (La Niña) conditions in the tropical Pacific (Rayner *et al*., 2003; McPhaden *et al*., 2006; Annex A6). During El Niño, the easterly trade winds weaken, the reduced westward flow at the equator results in the migration of warm surface water eastward, and the upwelling along the west coast of South America substantially decreases. La Niña is characterized by stronger trade winds, warmer surface waters in the western Pacific, and cold water at the equator in the central and eastern Pacific (Rasmusson and Carpenter, 1982; Philander, 1990; Trenberth, 1997; Pennington *et al*., 2006). ENSO affects many other regions through teleconnections in the atmosphere and ocean and tends to cycle between 2–7 years (McPhaden *et al*., 2006). Depending on the temporal window and region selected, this cycle can make the surface ocean warmer or colder.

The Interdecadal Pacific Oscillation (IPO) is a pattern of Pacific climate variability similar to ENSO in character, but which persists for much longer. It is a robust, recurring pattern centred over the mid-latitude Pacific basin with a 20–30-year period (Biondi *et al*., 2001). During negative IPOs, the SPCZ moves southwest, similar to La Niña events (Folland *et al*., 2002). The recent hiatus in global warming has been associated with a persistent negative IPO that commenced in about 2000 (Dai *et al*., 2015; Trenberth, 2015). In late 2014, there were signs that the IPO might be shifting to a more positive phase.

During a positive Southern Annular Mode (SAM) event, the southern hemisphere westerly winds tend to move farther south and increase in intensity (Thompson and Wallace, 2000). This results in stronger cold water upwelling at high latitudes, anomalous downwelling

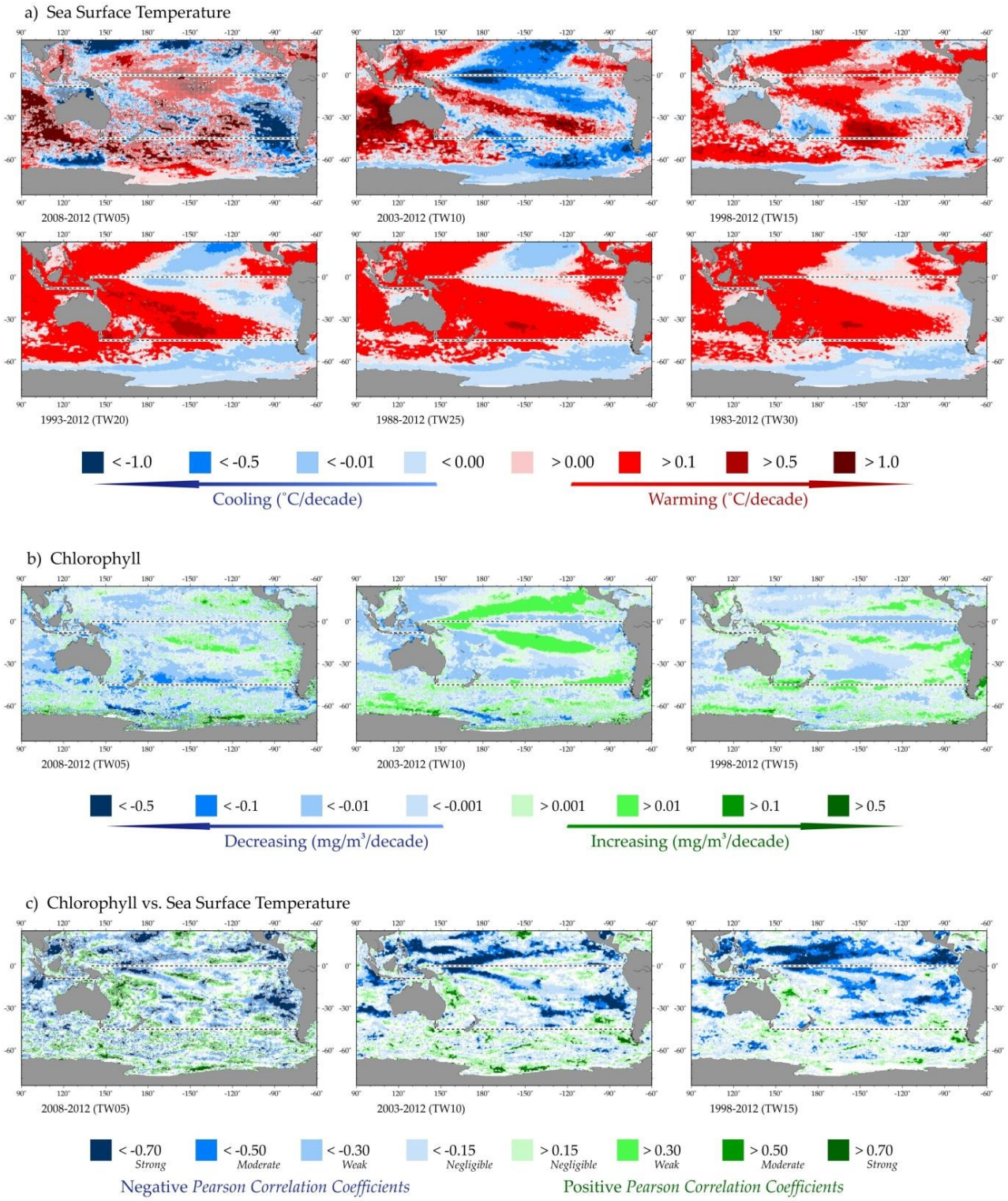

Figure 8.3. Annual trends in South Pacific sea surface temperature (SST) (a) and sea surface chlorophyll (CHL) (b), and correlations between chlorophyll and sea surface temperature for each of the standard IGMETS time-windows (c). See "Methods" chapter for a complete description and methodology used.

around 45°S, and a strengthening of the Antarctic Circumpolar Current (Hall and Visbeck, 2002; Oke and England, 2004). Variations in the SAM have been shown to be correlated with SST anomalies in the central tropical Pacific (Ding *et al*., 2012). There is significant temporal variability in the SAM, but over the last 50+ years, the SAM index has been positive and on the rise (Thompson and Wallace, 2000; Abram *et al*., 2014). This rise has been linked to anthropogenic factors which include ozone depletion (Fyfe *et al*., 1999).

The following sections describe spatial and temporal patterns in temperature and chlorophyll *a* observed during 1983–2012 in the South Pacific as well as patterns in the biogeochemistry and ecology of the region as seen from satellite and ship-based time-series data compiled by IGMETS. How these may relate to ocean circulation and climate drivers is also explored. More detailed tables and maps can be obtained from the IGMETS Explorer tool (http://igmets.net/explorer/).

8.2 General patterns of temperature and phytoplankton biomass

8.2.1 30-year trends in SST

Over the past 30 years (1983–2012), 84.4% of the South Pacific has warmed (Figure 8.3; Table 8.1), of which 67.3% was significant ($p < 0.05$). Although the spatial extent of warming was substantial, it was more limited than in the Indian, Arctic or Atlantic oceans. Long-term, 30-year warming was most pronounced in the western Pacific, spanning from the equator to 50°S along 150°E. This large area of warming extended eastward from Australia toward South America, but also contracted poleward. There was another smaller region of warming at the equator around 95°W. Close to the South American continent, there were two regions of persistent cooling: a larger one off northern Chile and southern Peru (ca. 10–30°S) and a smaller one at ca. 40–50°S. Over the 30-, 25-, and 20-year temporal windows, the larger cooling region extended west and north all the way to the equator (Figure 8.2).

This spatial pattern of warm and cool areas was mostly driven by a combination of long-term global warming and changes in the phase of the Interdecadal Pacific Oscillation (IPO; Dong and Zhou, 2014; Dong and Dai, 2015). The multidecadal cooling trend was associated with a change in phase of IPO from positive to negative around 1998/1999 (Dong and Zhou, 2014) as well as more frequent occurrences of central Pacific-type El Niño events (Chavez *et al*., 2003; Sohn *et al*., 2013). The change in the IPO also enhanced the east–west thermal contrast that produced an intensification of global monsoon precipitation (Wang *et al*., 2012b), trade winds across the Pacific (England *et al*., 2014), and a greater contrast in sea level pressure (SLP) between the eastern and western tropical Pacific (Merrifield, 2011). These changes in surface wind, precipitation, and SLP in the tropical Pacific over the past 30 years may also have led to a general increase in the Walker circulation (Liu and Curry, 2006; Sohn and Park, 2010; Sohn *et al*., 2013; Kosaka and Xie, 2013). The fact that over 80% of the South Pacific warmed since 1983, however, suggests that global warming dominated over the ENSO, IPO, and SAM cycles.

8.2.2 15-, 10-, and 5-year trends in SST

Over the periods 1998–2012 and 2003–2012 (15- and 10-year windows, respectively), a strong band of warming was visible extending roughly along the trajectory of the SPCZ south and east from Papua New Guinea to about 100°W (Figure 8.3). The area of South Pacific warming over the 15-year time-window was 65.1% (Table 8.1; Figure 8.3). Between 2003 and 2012, the spatial extent of warming was reduced to only 36.7%, and the majority of the South Pacific (63.3%) was cooling at a rate of –0.1°C year^{-1}. Over this 10-year period, some of the strongest cooling trends were in the region of the western Pacific warm pool (Figure 8.3; Table 8.1). This decadal cooling trend has been largely attributed to La Niña-like conditions (Kosaka and Xie, 2013), the negative phase of the IPO (Dong and Zhou, 2014; Meehl *et al*., 2014), and a strengthening in Pacific trade winds (England *et al*., 2014). During the shorter 5-year window (2008–2012), the cooling still prevailed, but only over 50.4% of the South Pacific (Figure 8.3; Table 8.1).

Table 8.1. Relative spatial areas (% of the total region) and rates of change within the South Pacific region that are showing increasing or decreasing trends in sea surface temperature (SST) for each of the standard IGMETS time-windows. Numbers in brackets indicate the % area with significant ($p < 0.05$) trends. See "Methods" chapter for a complete description and methodology used.

Latitude-adjusted SST data field surface area = 68.8 million km²	**5-year** (2008–2012)	**10-year** (2003–2012)	**15-year** (1998–2012)	**20-year** (1993–2012)	**25-year** (1988–2012)	**30-year** (1983–2012)
Area (%) w/ increasing SST trends ($p < 0.05$)	**50.4%** (*5.6%*)	36.7% (*15.5%*)	**65.1%** (*31.0%*)	**67.4%** (*52.1%*)	**88.3%** (*68.1%*)	**84.4%** (*67.3%*)
Area (%) w/ decreasing SST trends ($p < 0.05$)	49.6% (*12.2%*)	**63.3%** (*38.4%*)	34.9% (*14.7%*)	32.6% (*11.8%*)	11.7% (*0.7%*)	15.6% (*5.3%*)
> 1.0°C decade^{-1} warming ($p < 0.05$)	11.2% (*4.5%*)	0.9% (*0.9%*)	0.3% (*0.3%*)	0.0% (*0.0%*)	0.0% (*0.0%*)	0.0% (*0.0%*)
0.5 to 1.0°C decade^{-1} warming ($p < 0.05$)	15.5% (*1.1%*)	8.2% (*7.7%*)	5.6% (*5.6%*)	8.1% (*8.1%*)	1.2% (*1.2%*)	0.9% (*0.9%*)
0.1 to 0.5°C decade^{-1} warming ($p < 0.05$)	18.3% (*0.1%*)	20.9% (*6.9%*)	41.5% (*24.6%*)	45.6% (*42.6%*)	**61.9%** (*60.7%*)	**58.7%** (*58.2%*)
0.0 to 0.1°C decade^{-1} warming ($p < 0.05$)	5.4% (*0.0%*)	6.7% (*0.1%*)	17.7% (*0.5%*)	13.6% (*1.4%*)	25.3% (*6.1%*)	24.8% (*8.3%*)
0.0 to –0.1°C decade^{-1} cooling ($p < 0.05$)	5.3% (*0.0%*)	7.7% (*0.2%*)	13.0% (*0.2%*)	18.9% (*1.7%*)	10.9% (*0.2%*)	14.3% (*4.0%*)
–0.1 to –0.5°C decade^{-1} cooling ($p < 0.05$)	16.7% (*0.4%*)	33.6% (*17.5%*)	20.7% (*13.3%*)	13.7% (*9.9%*)	0.7% (*0.5%*)	1.3% (*1.3%*)
–0.5 to –1.0°C decade^{-1} cooling ($p < 0.05$)	13.8% (*2.8%*)	18.8% (*17.6%*)	1.2% (*1.2%*)	0.1% (*0.1%*)	0.0% (*0.0%*)	0.0% (*0.0%*)
> –1.0°C decade^{-1} cooling ($p < 0.05$)	13.8% (*9.1%*)	3.1% (*3.1%*)	0.0% (*0.0%*)	0.0% (*0.0%*)	0.0% (*0.0%*)	0.0% (*0.0%*)

Table 8.2. Relative spatial areas (% of the total region) and rates of change within the South Pacific region that are showing increasing or decreasing trends in phytoplankton biomass (CHL) for each of the standard IGMETS time-windows. Numbers in brackets indicate the % area with significant ($p < 0.05$) trends. See "Methods" chapter for a complete description and methodology used.

Latitude-adjusted CHL data field surface area = 68.8 million km²	**5-year** (2008–2012)	**10-year** (2003–2012)	**15-year** (1998–2012)
Area (%) w/ increasing CHL trends ($p < 0.05$)	27.0% (*6.0%*)	39.4% (*22.1%*)	41.5% (*20.0%*)
Area (%) w/ decreasing CHL trends ($p < 0.05$)	**73.0%** (*36.3%*)	**60.6%** (*39.9%*)	**58.5%** (*40.4%*)
> 0.50 mg m^{-3} decade^{-1} increasing ($p < 0.05$)	0.2% (*0.1%*)	0.0% (*0.0%*)	0.1% (*0.1%*)
0.10 to 0.50 mg m^{-3} decade^{-1} increasing ($p < 0.05$)	1.4% (*0.5%*)	0.5% (*0.4%*)	1.0% (*0.9%*)
0.01 to 0.10 mg m^{-3} decade^{-1} increasing ($p < 0.05$)	15.6% (*5.3%*)	23.4% (*18.8%*)	16.1% (*13.0%*)
0.00 to 0.01 mg m^{-3} decade^{-1} increasing ($p < 0.05$)	9.8% (*0.2%*)	15.4% (*2.9%*)	24.3% (*6.1%*)
0.00 to –0.01 mg m^{-3} decade^{-1} decreasing ($p < 0.05$)	13.7% (*1.8%*)	22.3% (*8.7%*)	33.6% (*18.0%*)
–0.01 to –0.10 mg m^{-3} decade^{-1} decreasing ($p < 0.05$)	**52.4%** (*29.2%*)	36.8% (*30.0%*)	24.5% (*22.0%*)
–0.10 to –0.50 mg m^{-3} decade^{-1} (decreasing) ($p < 0.05$)	6.5% (*5.0%*)	1.2% (*0.9%*)	0.5% (*0.3%*)
> –0.50 mg m^{-3} decade^{-1} (decreasing) ($p < 0.05$)	0.4% (*0.3%*)	0.3% (*0.3%*)	0.0% (*0.0%*)

8.2.3 15-year trends in chlorophyll *a*

The dominant trend for surface chlorophyll *a* has been to decline in the South Pacific (Figure 8.3; Table 8.2). The South Pacific, however, had regions of positive and negative trends in chlorophyll *a*, depending on the region and the temporal window considered. In the tropics, there was often a relationship between warming and declining chlorophyll *a*, while across most of the temporal windows and much of the South Pacific, significant relationships between SST and chlorophyll *a* were relatively rare (Figure 8.3, bottom). Over the 15-year time-window, chlorophyll *a* declined over 58.5% (40.4%, $p < 0.05$) of the South Pacific. Most of this decline occurred in the South Pacific gyre or in the tropical eastern Pacific (Figure 8.3). The South Pacific gyre itself has been estimated to be growing at 245 766 km^2 $year^{-1}$ (or 1.4% $year^{-1}$) between 1998 and 2006 (Polovina *et al*., 2008). The decline in chlorophyll *a* within the tropical eastern Pacific was observed in a similar analysis by Gregg and Rousseaux (2014) and suggested to be linked to ENSO. Significant increases in chlorophyll *a* were observed at about 10°S and between 20 and 40°S off the coast of South America, along the Subtropical Front (STF) stretching from Tasmania to South America, and along the trajectory of the SPCZ. These observations agree with other findings based on satellite observations (Vantrepotte and Melin, 2011; Siegel *et al*., 2013; Gregg and Rousseaux, 2014). Greater chlorophyll *a* concentrations in the Humboldt Current are consistent with suggestions of increasing upwelling intensity as a result of climate change (Bakun, 1990; Gutiérrez *et al*., 2011; Sydeman *et al*., 2014). The eddies along the STF appear to support substantial blooms of coccolithophores (Balch *et al*., 2011, 2016) during austral summer (December–January). ENSO may also exert an influence on phytoplankton along the STF; for example, when a positive SAM aligns with a positive ENSO event, the eddy kinetic energy and number of eddies increases significantly (Langlais *et al*., 2015). Over the 15-year time-window, the highest rate of chlorophyll *a* increase was > 0.01 mg chlorophyll *a* m^{-3} $year^{-1}$ measured in the southern Tasman Sea. This appears to be associated with greater EAC eddy pumping and an increase in winter intrusions of the STF into the Tasman Sea (Matear *et al*., 2013; Kelly *et al*., 2015).

8.2.3 10-year trends in chlorophyll *a*

Between 2003 and 2012, 60.6% (39.9% significant with $p < 0.05$) of the South Pacific showed a decline in chlorophyll *a* (Table 8.2; Figure 8.3). At the same time, a marked increase in chlorophyll *a* was observed in a band across the South Pacific from about 0°E and 160°E to 20°S and 100°W. The chlorophyll *a* increase overlapped part of the SPCZ, running north of, but parallel to, the band of strongly warming SST (Figure 8.3). A similar spatial pattern of increasing chlorophyll *a* was also evident over the 15 years between 1998 and 2012. There was a strikingly similar spatial pattern of temporal trends in temperature and chlorophyll *a* in the North Pacific (see Chapter 9, Figure 9.4) over this 100-year window. The cooler, more productive waters in the central South Pacific have been attributed, in part, to a strengthening of the Pacific trade winds (England *et al*., 2014). At ca. 40–45°S off the coast of southern Chile, there was another region with a strong positive chlorophyll *a* trend over 10 years. This increase in chlorophyll *a* was positively correlated with SST (Figure 8.3).

Despite the cooler equatorial waters during the 10-year time-window, the upwelling zone of the tropical Pacific and off the Peruvian coast showed a decline in chlorophyll *a*. It has been suggested that this may be a result of ENSO (Gregg and Rousseaux, 2014). Finally, chlorophyll *a* patterns near the Chilean coast during this period were heterogeneous, but generally correlated negatively with temperature (Figure 8.3, bottom).

8.2.4 5-year trends in chlorophyll *a*

Over the most recent and shortest temporal window (2008–2012), declining chlorophyll *a* was observed over 73% (36.3% at $p < 0.05$) of the South Pacific (Table 8.2). Over this 5-year period, there were strong declines in chlorophyll *a* north of the STF and in the region of the western Pacific warm pool close to Papua New Guinea. Although considerably weaker, the spatial pattern of an increase in chlorophyll *a* spreading eastward and at an angle away from the equator across the Pacific was also evident over this time-window (Figure 8.3). A patchy, but broad, increase in remotely-sensed chlorophyll *a* was evident east of Australia through the southern Coral Sea and northern Tasman Sea as far east as 160°E (Figure 8.3). Some of these patches showed a strong positive

correlation with SST. Explanations for these positive correlations in the open ocean are largely hypothetical, although predicted by some models and potentially attributable to (i) more diazotrophs (Dutkiewicz *et al.*, 2014), (ii) potential increase in eddy pumping (McGillicuddy *et al.*, 1998) associated with increasing eddy kinetic energy, and (iii) the strengthening of the EAC (Matear *et al.*, 2013). Sporadic increases in chlorophyll *a* were also observed off Chile in the region where the current flow along the STF interacts with the subtropical water mass.

8.3 Trends from *in situ* time series

In the western South Pacific, there are four *in situ* time series (Figure 8.4; Table 8.3), all in Australian waters (Lynch *et al.*, 2014). In addition, there are three *in situ* time series of phytoplankton and zooplankton data constructed from Continuous Plankton Recorder routes along the Australian shelf break. The Australian time series commenced after 2007 and only have data for the 5-year temporal window (2008–2012). The tropical site of Yongala (19°S) off northeast Australia is within the Great Barrier Reef Lagoon and broadly influenced by coastal processes. Yongala showed increasing *in situ* temperatures during 2008–2012. Sites farther south at Port Hacking (34°S) and Maria Island (43°S) all cooled between 2008 and 2012 (Figure 8.4), reversing the longer-term trends for warming that had been measured in that region at a rate of ca. 0.75°C century^{-1} and 2.2°C century^{-1}, respectively (Thompson *et al.*, 2009). Generally, the waters along the east Australian continental shelf have been warming in association with the strengthening of the South Pacific gyre (Ridgway, 2007; Hill *et al.*, 2011). Where the shelf is narrow (Port Hacking) or the STF periodically intrudes (Maria Island), however, the short-term or local trends can vary.

Table 8.3. Five-year trends (TW05, 2008–2012) in the time series of observations from the *in situ* sites in the South Pacific (not including Continuous Plankton Recorder sites).

Site-ID	Lat (°E) Long (°S)	SST	S	Oxy	NO3	CHL	Cope-pods	Dia.	Dino.	Dia.: Dino.
au-50109 Yongala	19.18 147.37	+	+	*n/a*	*n/a*	+	-	+	-	+
au-50107 North Stradbroke Island	27.20 153.33	*n/a*	-	*n/a*	+	-	+	-	-	-
au-50101 Port Hacking	34.05 151.15	-	+	*n/a*	+	+	*n/a*	-	-	-
au-50105 Maria Island	42.35 148.14	-	+	-	+	+	+	-	-	-
cl-30101 Concep-tion 18	36.50 73.00	*n/a*	*n/a*	*n/a*	*n/a*	*n/a*	*n/a*	*n/a*	*n/a*	*n/a*
cl-30102 Bay of Mejillones	23.10 70.47	*n/a*	*n/a*	*n/a*	*n/a*	*n/a*	*n/a*	*n/a*	*n/a*	*n/a*
pe-30101 IMARPE A	4.80 82.00	*n/a*	*n/a*	*n/a*	*n/a*	*n/a*	*n/a*	*n/a*	*n/a*	*n/a*
pe-30102 IMARPE B	9.00 79.00	*n/a*	*n/a*	*n/a*	*n/a*	*n/a*	*n/a*	*n/a*	*n/a*	*n/a*
pe-30103 IMARPE C	16.00 75.00	*n/a*	*n/a*	*n/a*	*n/a*	*n/a*	*n/a*	*n/a*	*n/a*	*n/a*
pe-30104 IMARPE Callao	11.99 78.97	*n/a*	*n/a*	+	-	-	*n/a*	*n/a*	*n/a*	*n/a*

$p > 0.05$ negative positive $p < 0.05$ negative positive

From 2008 to 2012, *in situ* salinity trends were weak, tending to increase at three sites and decline at one site along the east coast of Australia (Figure 8.4). Over the same time-period, nitrate concentrations increased weakly at three mid-latitude stations (North Stradbroke Island, Port Hacking, and Maria Island). Nitrate concentrations at Pork Hacking have been rising since the 1950s (Thompson *et al*., 2009; Kelly *et al*., 2015). The strengthening EAC, a positive IPO, and the La Niña of 2010–2011 are likely to have reduced downwelling and shallowed the pynocline along the east coast of Australia (Gibbs *et al*., 1998), potentially providing more nutrients to the euphotic zone. Between 2008 and 2012, silicate concentrations increased at North Stradbroke Island, Port Hacking, and Maria Island, reversing strong 30-year declines at the latter two sites (Thompson *et al*., 2009). The La Niña event of 2011 broke the "Millennium Drought" for eastern Australia (Dijk *et al*., 2013), with the second highest rainfalls ever recorded and many rivers flooding over their banks. The increased silicate potentially reflects the input of substantial silicate-rich runoff.

Between 2008 and 2012, the *in situ* chlorophyll *a* concentrations rose significantly at three sites along the mid to northeast coast of Australia, while trends were weaker and mixed at sites farther south (Figure 8.4). The spatial footprint of Australian sites at North Stradbroke Island and Maria Island are known to reflect changes in chlorophyll *a* and temperature over broad regions of the South Coral Sea and Tasman Sea, respectively (Oke and Sakov, 2012; Jones *et al*., 2015). In some cases, the positive *in situ* chlorophyll *a* trends observed along the Australian coast contrasted with the weak trends measured using satellite remote sensing, highlighting the difference that may exist between these measurements in coastal areas and the need to use caution when interpreting data from just one source (Pennington *et al*., 2006).

Zooplankton and phytoplankton data from the east coast of Australia in 2008–2012 were available from seven sites where trends in total copepod biomass were mixed: four positive and three negative (Figure 8.3). The two significant positive trends in zooplankton from the CPR route on the mid-east coast coincided with *in situ* measurements of increasing chlorophyll *a* by CPR colour index. On the eastern coast of Australia (North Stradbroke Island site), a strong trend in increasing copepod biomass was also found, but with weakly decreasing *in situ* chlorophyll *a*. In addition, all three sites with increasing copepod biomass were in regions of increasing SST (Figure 8.3).

Off the Australian east coast, diatoms increased at three of seven sites (Figure 8.4g); the most significant increase was observed in offshore sites near the separation zone at about 30°S where most of the EAC turns eastward to flow across the Tasman Sea. Dinoflagellates also increased at these mid-coast sites. Trends at the more coastal and the most southerly stations tended to be weak and negative. The surface nutrient concentrations along the east coast of Australia are extremely low (Condie and Dunn, 2006), with low silicate previously reported to limit diatom blooms (Grant, 1971). Between the La Niña of 1999, during the millennium drought and prevailing El Niño conditions, diatoms declined significantly along Australia's east coast (Ajani *et al*., 2016). However, the 2008–2012 data suggest that diatoms recovered at Yongala, while dinoflagellates declined and the diatom/dinoflagellate ratio increased (Figures 8.4g, f; Table 8.3).

In the eastern South Pacific, *in situ* time series were scarce. Based on satellite data, the region has been broadly cooling throughout all temporal windows. At the Peruvian site of Callao (11°S), nutrients (nitrate, phosphate, and silicate) have generally declined, with nitrate and silicate decreasing from 1998 to 2012 (Figure 8.4). Callao also showed declines in chlorophyll *a* for the same time-period. The negative trend is consistent with satellite data. The recent decline in phytoplankton has been attributed to warmer conditions induced by the ENSO. Over the longer period of 15 years, the Callao time series of chlorophyll *a* was still negative, while the Bay of Mejillones showed a positive trend. Satellite data indicated that, during 1998–2012, the region was experiencing spatially heterogeneous increases (Vargas *et al*., 2007; Chavez and Messié, 2009; Chavez *et al*., 2011; Gutierrez *et al*., 2011) and decreases (Thomas *et al*., 2009) in chlorophyll *a* (Figure 8.3).

Two zooplankton time series were available along the west coast of South America from 23°S (Bay of Mejillones) and ca. 36°S (Concepción Station). The temporal trends in zooplankton biomass were generally weak, sometimes positive and sometimes negative. For example, a weak positive trend in zooplankton biomass was found over 15 years (1998–2012) in the Bay of Mejillones. The notable exception was a statistically significant, negative trend in zooplankton biomass off southern Chile at the Concepción site between 2003 and 2012.

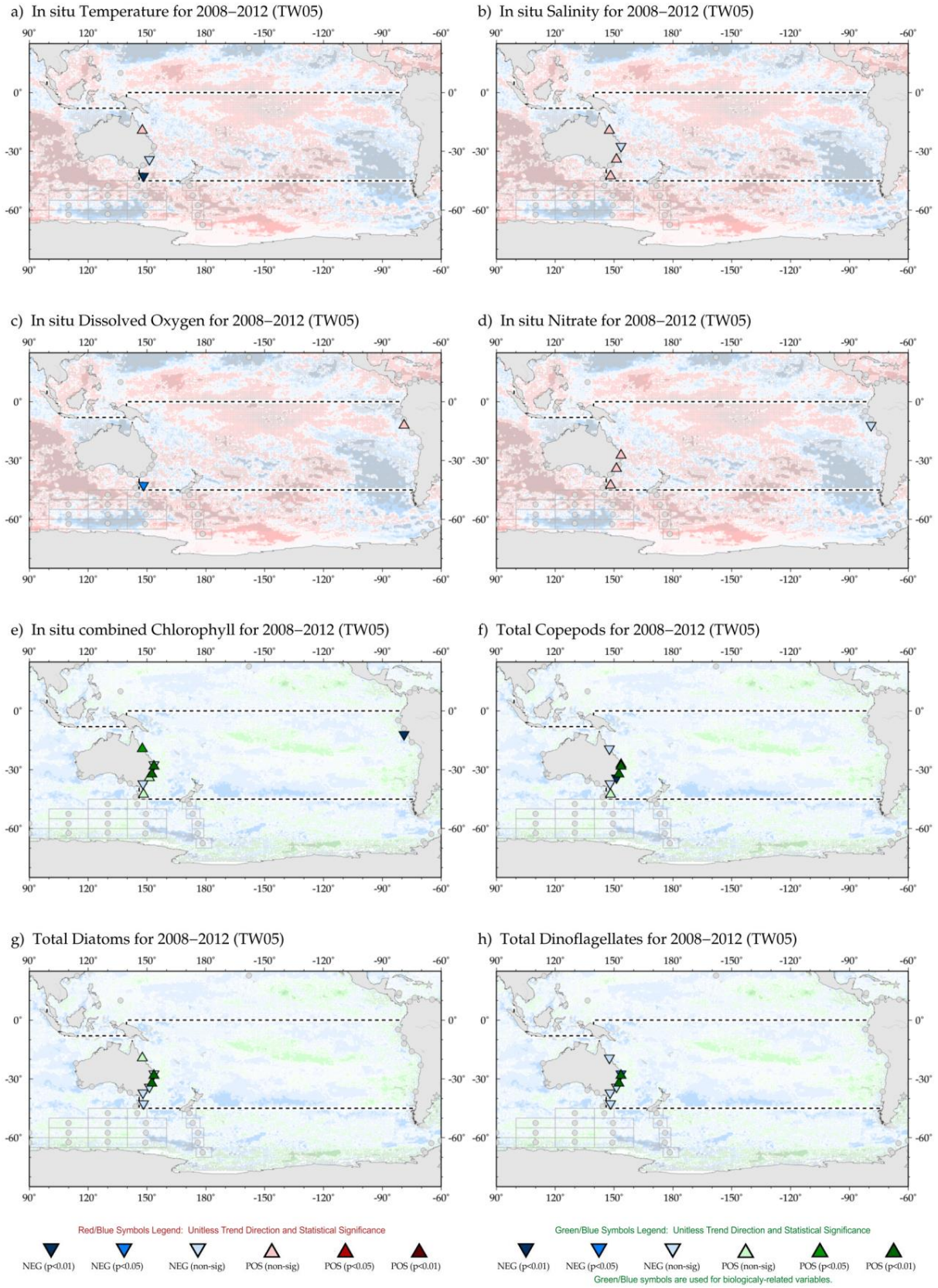

Figure 8.4. Map of South Pacific region time-series locations and trends for select variables and IGMETS time-windows. Upward-pointing triangles indicate positive trends; downward triangles indicate negative trends. Gray circles indicate time-series sites that fell outside of the current study region or time-window. Additional variables and time-windows are available through the IGMETS Explorer (http://IGMETS.net/explorer). See "Methods" chapter for a complete description and methodology used.

This trend occurred in spite of declining SST and increasing upwelling (Escribano *et al*., 2012). As noted by Escribano *et al*. (2012), zooplankton biomass is sensitive to the timing and scale of upwelling. Ayon *et al*. (2008) suggested that zooplankton biomass is positively correlated with seasonal temperature, and thus persistent upwelling may be a negative factor for zooplankton abundance. Zooplankton abundance rose 50% from 1981 to 2002 off Peru, but in 2002, it was still only one-fourth of the peak biomass observed in 1967 (Ayón *et al*., 2008). Ayón *et al*. (2008) also reported a positive correlation between zooplankton and anchovy biomass.

Dissolved oxygen (DO) trends were only available from two sites in the entire South Pacific: off Tasmania and in the Peruvian upwelling (Callao). Off Tasmania, the 2008–2012 trends were weakly negative. At ca. 11°S off Peru, DO trends were positive and statistically significant over the 15 years between 1998 and 2012. Combined with the declining SST (satellite data only), the 15 years of increasing DO observed at Callao support the hypothesis of a more vigorous upwelling in this boundary current in response to climate change (Bakun, 1990) and/or a response to the intensification of the trade winds in the Pacific (England *et al*., 2014).

8.4 Comparisons with other studies

The long-term rate of warming for southern hemisphere oceans has been 0.03°C decade^{-1} (Rayner *et al*., 2006), although across the entire South Pacific basin, this trend was found to be statistically insignificant over the last 60 years (Hoegh-Guldberg *et al*., 2014). Yet, the IGMETS analysis for 2008–2012 in the South Pacific showed 11.2% (4.5% at $p < 0.05$) of the surface ocean was warming at > 1.0°C decade^{-1} and a similar rate of cooling was found over 13.8% (9.1% at $p < 0.05$). Clearly, there is a need to consider subbasin-scale variability and the role of natural climatic cycles. These regional patterns in SST have been attributed to both human-induced global warming (Stott *et al*., 2010) and natural climatic cycles (e.g. IPO, ENSO; Dong and Zhou, 2014; England *et al*., 2014; Dong and Dai, 2015; Karl *et al*., 2015). The combination of progressive global warming, the IPO, and ENSO seem to account for most of the temporal and spatial patterns in SST trends observed over the last 30 years in the tropical Pacific (Dong and Dai, 2015).

The proportion of the South Pacific that is warming is rising much faster than the proportional increase in SST (Polovina and Woodworth, 2012). The long-term cooling SST trend in much of the eastern South Pacific is consistent with suggestions of increasing upwelling intensity as a result of climate change (Bakun, 1990; Sydeman *et al*., 2014), changes in the subtropical gyre circulation (Cai *et al*., 2005; Schneider *et al*., 2007), and changes in the Pacific wind regime (England *et al*., 2014). The dramatic cooling observed in this analysis over large parts of the South Pacific during the 2003–2012 time-window has also been noted by several studies and attributed to natural climate variability, tied specifically to La Niña-like decadal cooling (Kosaka and Xie, 2013) and wind-induced cooling (England *et al*., 2014). Natural climatic cycles have also affected surface salinity in the region. The negative IPO and strong La Niña of 2010–2011 saw a southwest shift in the SPCZ, bringing more precipitation to the South Pacific (Salinger *et al*., 2001; Folland *et al*., 2002; Cai and Rensch, 2012). At the same time, equatorial rainfall moved eastward along the ITCZ. Similarly, there has been a significant freshening in the western tropical Pacific, extending eastward under the low-salinity ITCZ and SPCZ regions (Durack and Wijffels, 2010).

The trends reported herein for satellite-derived chlorophyll *a* are similar to those previously published (Gregg and Conkright, 2002; Thomas *et al*., 2012; Siegel *et al*., 2013; Gregg and Rousseaux, 2014). For large portions of the South Pacific, there is a tendency for chlorophyll *a* to covary negatively with SST (Martinez *et al*., 2006; Vantrepotte and Mélin, 2011), a pattern consistent with warming SST being associated with a deeper surface mixed layer and reduced nutrient availability (Thomas *et al*., 2009; Hofmann *et al*., 2011, Doney *et al*., 2012). There were also regions of positive covariation between SST and chlorophyll *a* previously reported in the tropics north and west of Australia (Martinez *et al*., 2006) along the STF (Vantrepotte and Mélin, 2011) and in parts of the central gyre (Signorini *et al*., 2015). For regions where the mixed-layer depth is too deep for net positive phytoplankton growth during most of the year, e.g. along the STF, a positive relationship of chlorophyll *a* with SST is predictable. A similar covariation has been found in Humboldt Current off Peru and northern Chile (Thomas *et al*., 2009), where wind and chlorophyll phenology are out of phase and mixed-layer depth and light play a significant role in surface chlorophyll concentrations (Echevin *et al*., 2008). The major impacts of these changes are increasingly evident and amenable to modelling that accounts for both the physical supply and biological losses of carbon, oxygen, and nutrients (e.g. Deutsch *et*

al., 2006, 2011). For example, changes in chlorophyll *a* within the Tasman Sea are well described in models and estimated into the future by climatic forcings (Matear *et al*., 2013). Climate-related changes to phytoplankton taxa have also been modelled (Bopp *et al*., 2005), statistically estimated (Barnes *et al*., 2011), extrapolated using remote sensing (Polovina and Woodworth, 2012; Uitz *et al*., 2015), and modelled using a combination of both (Gregg and Rouseaux, 2014). One general outcome that seems highly likely is a shift to smaller taxa as the oceans continue to warm (Barnes *et al*., 2011).

The tropical Pacific has seen a dramatic decline in oxygen concentration; some of the steepest declines were measured under the western Pacific warm pool, while the lowest concentrations were in the eastern tropical Pacific (Stramma *et al*., 2010). In 2012, the trend was observed as -1 μmol kg^{-1} $year^{-1}$ between 2°N and 8°S at about 86°W (Czeschel *et al*., 2015). This oxygen consumption was associated with significantly increased phosphate and nitrate concentrations in the oxygen-minimum zone. The biological effects of the declining oxygen concentrations include vertical compression of habitat for species with high oxygen requirements such as tuna (Prince and Goodyear, 2006). The increasing nutrient concentrations at depth also imply the sequestering of more nutrients below a strengthening pycnocline, potentially reducing primary production. However, the extent of low oxygen regions in the Pacific has been linked to equatorial Pacific wind regime (Deutsch *et al*., 2014).

Previous analysis (Thompson *et al*., 2009) showed mostly increasing nutrient concentrations in the shelf waters of eastern Australia, results which are largely consistent with IGMETS. A notable exception was the detection of a change from declining to increasing silicate during 2008–2012 in the more recent IGMETS analysis. The mixed positive and negative trends observed for *in situ* nutrients may be associated with changes in circulation, thermocline depth, and/or changes in ecosystems induced by the different climate modes operating in the Pacific (Pennington *et al*., 2006; Chavez *et al*., 2011).

8.5 Conclusions

Long-term trends in fundamental characteristics of the environment, such as temperature and salinity, are increasingly evident. For example, over the past 30 years, significant surface warming has been recorded over nearly tenfold more area of the South Pacific than surface cooling (67.3% vs. 5.3%, respectively). A strong physical coupling with planktonic ecology and biology is evident in the South Pacific, with a dominant warming pattern and significantly declining phytoplankton populations. The southeastern Pacific upwelling system continues to show intensification (Vargas *et al*., 2007), while the tropical Pacific and subtropical gyre mostly exhibited declining trends in surface chlorophyll *a*. Prediction of the future ecological state of this important system requires understanding the physical drivers and their ecological consequences throughout the foodwebs, particularly the impact changes may have on ecosystem services at a regional scale. Modelling has been used to predict trends in phytoplankton community composition within the South Pacific (Polovina and Woodworth, 2012; Rousseaux and Gregg, 2015), but these have very limited taxonomic resolution. The time series included in IGMETS provide the means to test, validate, and improve ecological models of trophic links and trophic efficiency across an ample spectrum of phytoplankton and zooplankton taxonomic groups and predict potential changes that may occur within Pacific Ocean foodwebs in response to climate variability.

While "short" climate cycles such as ENSO have been associated with changes in copepod abundance in the Pacific (White *et al*., 1995, Thompson *et al*., 2015), reports of long-term trends in macrozooplankton biomass or taxa in the South Pacific are extremely rare (Ajani *et al*., 2016). In other ocean basins, there have been stronger links established between zooplankton community composition and climate-related increases in temperature (Richardson and Schoeman, 2004; Chiba *et al*., 2006). Some researchers have also suggested links between the abundance of some jellyfish (Cnidaria) and climate (Richardson, 2008), but the hypothesis is supported by only a few case studies from other oceans (reviewed by Purcell, 2005). For this section, zooplankton data were available only in a handful of locations, and the same is true for most of the other biogeochemical and ecological variables. Indeed, our understanding of the climatic effects on marine ecology, such as phytoplankton community composition, zooplankton productivity, and fish populations in the South Pacific remains rudimentary mostly due to a lack of data. Our knowledge of the spatial scale of ecological changes is limited to a few regions with time-series data. For example, during the 2010 La Niña event, there was a poleward extension of some dominant tropical taxa, such as *Prochlorococcus* and *Synechococcus*, and a decline in macrozooplankton (Thomp-

son *et al*., 2015). These apparent La Niña effects could have extended throughout the southwestern Pacific. Similarly, there have been large range expansions for some easily observed taxa such as *Noctiluca* (Thompson *et al*., 2009; Harrison *et al*., 2011; McLeod *et al*., 2012), raising concerns about rapid, but unobserved, changes in the basic ecology of our oceans (Doney *et al*., 2012). These very substantial expansions in regions of rapid warming suggest that physical transport of suitable habitat may be the controlling mechanism. The location of existing time series in the South Pacific also limits our knowledge of ecological changes to the continental shelf. While coastal sites can be used to warn of changes, such as low oxygen and high carbon dioxide water coming near shore (Chan *et al*., 2008), given the rapid rate of expanding low oxygen zones, it may be beneficial to have more offshore monitoring (Deutsch *et al*., 2015).

Table 8.4. Time-series sites located in the IGMETS South Pacific region. Participating countries: Argentina (ar), Brazil (br), Namibia (na), United Kingdom (uk), South Africa (za), Australia (au), Chile (il), and Peru (pe). Year-spans indicated in red belong to time series which were terminated. Year-spans in red text indicate time series of unknown or discontinued status. IGMETS-IDs in red text indicate time series without a description entry in Annex 6.

No.	IGMETS-ID	Site or programme name	Year-span	T	S	Oxy	Ntr	Chl	Mic	Phy	Zoo
1	au-40201	AusCPR BRSY Line – North (*Australian Coastline*)	2009–present	-	-	-	-	X	-	X	X
2	au-40202	AusCPR BRSY Line – South (*Australian Coastline*)	2009–present	-	-	-	-	X	-	X	X
3	au-40204	AusCPR SYME Line – South (*Australian Coastline*)	2009–present	-	-	-	-	X	-	X	X
4	au-50101	IMOS National Reference Station – Port Hacking (*Southeastern Australia*)	2002–present	X	X	-	X	X	X	X	X
5	au-50105	IMOS National Reference Station – Maria Island (*Tasmania*)	2009–present	X	X	X	X	X	X	X	X
6	au-50107	IMOS National Reference Station – North Stradbroke Island (*Eastern Australia*)	2008–present	-	X	-	X	X	X	X	X
7	au-50109	IMOS National Reference Station – Yongala (*Northeastern Australia*)	2009–present	X	X	-	X	X	X	X	X
8	cl-30101	Concepcion Station 18 (*Chilean Coast*)	2002–present	-	-	-	-	-	-	-	X
9	cl-30102	Bay of Mejillones (*Chilean Coast*)	1988–present	-	-	-	-	-	-	-	X
10	pe-30101	IMARPE Region A *(Eastern South Pacific)*	1962–2005 (?)	-	-	-	-	-	-	-	X
11	pe-30102	IMARPE Region B *(Eastern South Pacific)*	1962–2005 (?)	-	-	-	-	-	-	-	X
12	pe-30103	IMARPE Region C *(Eastern South Pacific)*	1964–2005 (?)	-	-	-	-	-	-	-	X
13	pe-30104	IMARPE Callao *(Eastern South Pacific)*	2001–present	-	-	X	X	X	-	-	-

8.6 References

Abram, N. J., Mulvaney, R., Vimeux, F., Phipps, S. J., Turner, J., and England, M. H. 2014. Evolution of the Southern Annular Mode during the past millennium. Nature Climate Change, 4: 564–569.

Ajani, P., Hallegraeff, G. M., Allen, D., Coughlan, A., Richardson, A. J., Armand, L. K., Ingelton, T., *et al*. 2016. Establishing baselines: a review of eighty years of phytoplankton diversity and biomass in south-eastern Australia. Oceanography and Marine Biology: An Annual Review, 54: 387–412.

Ayón, P., Criales-Hernandez, M. I., Schwamborn, R., and Hirche, H-J. 2008. Zooplankton research off Peru: A review. Progress in Oceanography, 79(2): 238–255.

Bakun, A. 1990. Global climate change and intensification of coastal ocean upwelling. Science, 247: 198–201.

Balch, W. M., Bates, N. R., Lam, P. J., Twining, B. S., Rosengard, S. Z., Bowler, B. C., Drapeau, D. T., *et al*. 2016. Factors regulating the Great Calcite Belt in the Southern Ocean and its biogeochemical significance. Global Biogeochemical Cycles, 30: doi:10.1002/2016GB005414.

Balch, W. M., Drapeau, D. T., Bowler, B. C., Lyczkowski, E., Booth, E. S., and Alley, D. 2011. The contribution of coccolithophores to the optical and inorganic carbon budgets during the Southern Ocean Gas Exchange Experiment: new evidence in support of the "Great Calcite Belt" hypothesis. Journal of Geophysical Research, 116: C00F06, doi:10.1029/2011JC006941.

Barnes, C., Irigoien, X., De Oliveira, J. A. A., Maxwell, D., and Jennings, S. 2011. Predicting marine phytoplankton community size structure from empirical relationships with remotely sensed variables. Journal of Plankton Research, 33: 13–24.

Biondi, F., Gershunov, A., and Cayan, D. R. 2001. North Pacific decadal climate variability since 1661. Journal of Climate, 14(1): 5–10, doi:10.1175/1520-442(2001)014.

Bopp, L., Aumont, O., Cadule, P., Alvain, S., and Gehlen, M. 2005. Response of diatoms distribution to global warming and potential implications: A global model study. Geophysical Research Letters, 32(19): doi:10.1029/2005GL023653.

Brown, J. R., Power, S. B., Delage, F. P., Colman, R. A., Moise, A. F., and Murphy, B. F. 2011. Evaluation of the South Pacific Convergence Zone in IPCC AR4 climate model simulations of the twentieth century. Journal of Climate, 24(6): 1565–1582, doi:10.1175/2010JCLI3942.1.

Cai, W., and Rensch, P. 2012. The 2011 southeast Queensland extreme summer rainfall: a confirmation of a negative Pacific Decadal Oscillation phase? Geophysical Research Letters, 39(8): doi:10.1029/2011GL050820.

Cai, W. J., Shi, G., Cowan, T., Bi, D. and Ribbe, J. 2005. The response of southern annular mode, the East Australian Current, and the southern midlatitude ocean circulation to global warming. Journal of Geophysical Research Letters, 32: doi:10.1029/2005GL024701.

Cetina-Heredia, P., Roughan, M., van Sebille, E., and Coleman, M. A. 2014. Long-term trends in the East Australian Current separation latitude and eddy driven transport. Journal of Geophysical Research: Oceans, 119: doi:10.1002/2014JC010071.

Chan, F., Barth, J. A., Lubchenco, J., Kirincich, A., Weeks, H., Peterson, W. T., and Menge, B. A. 2008. Emergence of anoxia in the California Current large marine ecosystem. Science, 319(5865): 920–920.

Chavez F. P., and Messié, M. 2009. A comparison of eastern boundary upwelling ecosystems. Progress in Oceanography, 83: 80–96.

Chavez, F. P., Messié, M., and Pennington, J. T. 2011. Marine primary production in relation to climate variability and change. Annual Review of Marine Science, 3: 227–260.

Chavez, F. P., Ryan, J., Lluch-Cota, S. E., and Ñiquen, M. 2003. From anchovies to sardines and back: multidecadal change in the Pacific Ocean. Science, 299(5604): 217–221.

Chiba, S., Tadokoro, K., Sugisaki, H., and Saino, T. 2006. Effects of decadal climate change on zooplankton over the last 50 years in the western subarctic North Pacific. Global Change Biology, 12(5): 907–920.

Condie, S. A., and Dunn, J. R. 2006. Seasonal characteristics of the surface mixed layer in the Australasian region: implications for primary production regimes and biogeography. Marine and Freshwater Research, 57(6): 569–590.

Correa-Ramirez, M. A., Hormazabal, S. E., and Morales, C. E. 2012. Spatial patterns of annual and interannual surface chlorophyll-a variability in the Peru–Chile Current System. Progress in Oceanography, 92: 8–17.

Czeschel, R., Stramma, L., Weller, R. A., and Fischer, T. 2015. Circulation, eddies, oxygen, and nutrient changes in the eastern tropical South Pacific Ocean. Ocean Science, 11: 455–470, doi:10.5194/os-11-455-2015.

Dai, A., Fyfe, J. C., Xie, S. P., and Dai, X. 2015. Decadal modulation of global surface temperature by internal climate variability. Nature Climate Change, 5(6): 555–559, doi:10.1038/nclimate2605.

Daneri, G., Dellarossa, V., Quiñones, R., Jacob, B., Montero, P., and Ulloa, O. 2000. Primary production and community respiration in the Humboldt Current System off Chile and associated oceanic areas. Marine Ecology Progress Series, 197: 41–49.

Deutsch, C., Berelson, W., Thunell, R., Weber, T., Tems, C., McManus, J., Crusius, J., *et al*. 2014. Centennial changes in North Pacific anoxia linked to tropical trade winds. Science, 345(6197): 665–668.

Deutsch, C., Brix, H., Ito, T., Frenzel, H., and Thompson, L. 2011. Climate-forced variability of ocean hypoxia. Science, 333(6040): 336–339.

Deutsch, C., Emerson, S., and Thompson, L. 2006. Physical-biological interactions in North Pacific oxygen variability. Journal of Geophysical Research: Oceans, 111: C09S90, doi:10.1029/2005JC003179.

Deutsch, C., Ferrel, A., Seibel, B., Pörtner, H. O., and Huey, R. B. 2015. Climate change tightens a metabolic constraint on marine habitats. Science, 348(6239): 1132–1135.

Dijk, A. I., Beck, H. E., Crosbie, R. S., Jeu, R. A., Liu, Y. Y., Podger, G. M., Timbal, B., *et al*. 2013. The Millennium Drought in southeast Australia (2001–2009): Natural and human causes and implications for water resources, ecosystems, economy, and society. Water Resources Research, 49(2): 1040–1057.

Ding, Q., Steig, E. J., Battisti, D. S., and Wallace, J. M. 2012. Influence of the tropics on the Southern Annular Mode. Journal of Climate, 25(18): 6330–6348, doi:http://dx.doi.org/10.1175/JCLI-D-11-00523.1.

Doney, S. C., Ruckelshaus, M., Duffy, J., Barry, J. P., Chan, F., English, C. A., Galindo, H. M., *et al*. 2012. Climate change impacts on marine ecosystems. Annual Review of Marine Science, 4: 11–37, doi:10.1146/annurev-marine-041911-111611.

Dong, B., and Dai, A. 2015. The influence of the Interdecadal Pacific Oscillation on temperature and precipitation over the globe. Climate Dynamics, 45(9-10): 2667–2681, doi:10.1007/s00382-015-2500-x.

Dong, L., and Zhou, T. 2014. The formation of the recent cooling in the eastern tropical Pacific Ocean and the associated climate impacts: A competition of global warming, IPO, and AMO. Journal of Geophysical Research: Atmosphere, 119: 11272–11287, doi:10.1002/2013JD021395.

Durack, P. J., and Wijffels, S. E. 2010. Fifty-year trends in global ocean salinities and their relationship to broad-scale warming. Journal of Climate, 23(16): 4342–4362, http://dx.doi.org/10.1175/2010JCLI3377.1.

Dutkiewicz, S., Ward, B. A., Scott, J. R., and Follows, M. J. 2014. Understanding predicted shifts in diazotroph biogeography using resource competition theory. Biogeosciences, 11: 5445–5461, doi:10.5194/bg-11-5445-2014.

Echevin, V., Aumont, O., Ledesma, J., and Flores, G. 2008. The seasonal cycle of surface chlorophyll in the Peruvian upwelling system: a modelling study. Progress in Oceanography, 79: 167–176.

England, M. H., McGregor, S., Spence, P., Meehl, G. A., Timmermann, A., Cai, W., Gupta, A. S., *et al*. 2014. Recent intensification of wind-driven circulation in the Pacific and the ongoing warming hiatus. Nature Climate Change, 4(3): 222–227.

Escribano, R., Hidalgo, P., Fuentes, M., and Donoso, K. 2012. Zooplankton time series in the coastal zone off Chile: Variation in upwelling and responses of the copepod community. Progress in Oceanography, 97–100: 174–186.

Fiedler, P. C., Philbrick, V., and Chavez, F. P. 1991. Oceanic upwelling and productivity in the eastern tropical Pacific. Limnology and Oceanography, 36: 1834–1850.

Folland, C. K., Renwick, J. A., Salinger, M. J., and Mullan, A. B. 2002. Relative influences of the Interdecadal Pacific Oscillation and ENSO in the South Pacific Convergence Zone. Geophysical Research Letters, 29: 21-1–21-4.

Fuenzalida, R., Schneider, W., Garcés-Vargas, J., and Bravo, L. 2008. Satellite altimetry data reveal jet-like dynamics of the Humboldt Current. Journal of Geophysical Research, 113: C07043, doi:10.1029/2007JC004684.

Fyfe, J. C., Boer, G. J., and Flato, G. M. 1999. Arctic and Antarctic oscillations and their projected changes under global warming. Geophysical Research Letters, 26(11): 1601–1604.

Gibbs, M. T., Middleton, J. H., and Marchesiello, P. 1998. Baroclinic response of Sydney shelf waters to local wind and deep ocean forcing, Journal of Physical Oceanography, 28: 178–190.

Grant, B. R. 1971. Variation in silicate concentration at Port Hacking station, Sydney, in relation to phytoplankton growth. Marine and Freshwater Research, 22(1): 49–54.

Godfrey, J. S., Cresswell, G. R., Golding, T. J., Pearce, A. F., and Boyd, R. 1980. The separation of the east Australian current. Journal of Physical Oceanography, 10(3): 430–440.

Gregg, W. W., and Conkright, M. E. 2002. Decadal changes in global ocean chlorophyll. Geophysical Research Letters, 29(11): 20–21, doi:10.1029/2002GL014689.

Gregg, W. W., and Rousseaux, C. S. 2014. Decadal trends in global pelagic ocean chlorophyll: A new assessment integrating multiple satellites, in situ data, and models. Journal of Geophysical Research: Oceans, 119: 5921–5933, doi:10.1002/2014JC010158.

Gutiérrez, D., Bouloubassi, I., Sifeddine, A., Purca, S., Goubanova, K., Graco, M., Field, D., *et al*. 2011. Coastal cooling and increased productivity in the main upwelling zone off Peru since the mid-twentieth century. Geophysical Research Letters, 38: L07603, doi:10.1029/2010GL046324.

Hall, A., and Visbeck, M. 2002. Synchronous variability in the Southern Hemisphere atmosphere, sea ice, and ocean resulting from the Annular Mode. Journal of Climate, 15(21): 3043–3057.

Harrison, P. J., Furuya, K., Glibert, P., Xu, J., Liu, H. B., Yin, K., Lee, J. H. W., *et al*. 2011. Geographical distribution of red and green Noctiluca scintillans. Chinese Journal of Oceanology and Limnology, 29: 807–831, doi:10.1007/s00343-011-0510-z.

Hasson, A., Delcroix, T., and Boutin, J. 2013. Formation and variability of the South Pacific Sea Surface Salinity maximum in recent decades. Journal of Geophysical Research: Oceans, 118: 5109–5116, doi:10.1002/jgrc.20367.

Hill, K. L., Rintoul, S. R., Ridgway, K., and Oke, P. R. 2011. Decadal changes in the South Pacific western boundary current system revealed in observations and reanalysis state estimates. Geophysical Research Letters, 116: doi: 10.1029/2009JC005926.

Hoegh-Guldberg, O., Cai, R., Poloczanska, E. S., Brewer, P. G., Sundby, S., Hilmi, K., Fabry, V. J., *et al*. 2014. The Ocean. *In* Climate Change 2014: Impacts, Adaptation, and Vulnerability. Part B: Regional Aspects, pp. 1655–1731. Ed. by V. R. Barros, C. B. Field, D. J. Dokken, M. D. Mastrandrea, K. J. Mach, T. E. Bilir, M. Chatterjee, *et al.* Contribution of Working Group II to the Fifth Assessment Report of the Intergovernmental Panel on Climate Change, Cambridge University Press, Cambridge and New York. 688 pp.

Hofmann, M., Worm, B., Rahmstorf, S., and Schellnhuber, H. J. 2011. Declining ocean chlorophyll under unabated anthropogenic CO_2 emissions. Environmental Research Letters, 6(3): 034035, doi:10.1088/1748-9326/3/034035.

Jones, E. M., Doblin, M. A., Matear, R., and King, E. 2015. Assessing and evaluating the ocean-colour footprint of a regional observing system. Journal of Marine Systems, 143: 49–61.

Karl, T. R., Arguez, A., Huang, B., Lawrimore, J. H., McMahon, J. R., Menne, M. J., Peterson, T. C., *et al*. 2015. Possible artifacts of data biases in the recent global surface warming hiatus. Science, 348(6242): 1469–1472.

Kelly, P., Clementson, L., and Lyne, V. 2015. Decadal and seasonal changes in temperature, salinity, nitrate, and chlorophyll in inshore and offshore waters along southeast Australia. Journal of Geophysical Research: Oceans, 120: 4226–4244.

Kosaka, Y., and Xie, S. P. 2013. Recent global-warming hiatus tied to equatorial Pacific surface cooling. Nature, 501(7467): 403–407.

Langlais, C., Rintoul, S., and Zika, J. 2015. Sensitivity of Antarctic circumpolar transport and eddy activity to wind patterns in the Southern Ocean. Journal Physical Oceanography, 45: 1051–1067, doi:10.1175/JPO-D-14-0053.1.

Liu, J., and Curry, J. A. 2006. Variability of the tropical and subtropical ocean surface latent heat flux during 1989–2000. Geophysical Research Letters, 33(5): doi: 10.1029/2005GL024809.

Lynch, T. P., Morello, E. B., Evans, K., Richardson, A. J., Rochester, W., Steinberg, C. R., Roughan, M., *et al*. 2014. IMOS national reference stations: a continental-wide physical, chemical and biological coastal observing system. PLoS ONE, 9(12): e113652, doi:10.1371/journal.pone.0113652.

Macdonald, H. S., Roughan, M., Baird, M. E., and Wilkin, J. 2013. A numerical modeling study of the East Australian Current encircling and overwashing a warm-core eddy. Journal of Geophysical Research: Oceans, 118: 301–315, doi:10.1029/2012JC008386.

Martinez, P., Lamy, F., Robinson, R. S., Pichevin, L., and Billy, I. 2006. Atypical δ15N variations at the southern boundary of the East Pacific oxygen minimum zone over the last 50 ka. Quaternary Science Reviews, 25: 3017–3028.

Mata, M. M., Tomczak, M., Wijffels, S., and Church, J. A. 2000. East Australian Current volume transports at 30 S: Estimates from the World Ocean Circulation Experiment hydrographic sections PR11/P6 and the PCM3 current meter array. Journal of Geophysical Research: Oceans, 105(C12): 28509–28526.

Mata, M. M., Wijffels, S. E., Church, J. A., and Tomczak, M. 2006. Eddy shedding and energy conversions in the East Australian Current. Journal of Geophysical Research, 111: C09034, doi:10.1029/2006JC003592.

Matear, R. J., Chamberlain, M. A., Sun, C., and Feng, M. 2013. Climate change projection of the Tasman Sea from an eddy-resolving ocean model. Journal of Geophysical Research, 118: 2961–2976, doi:10.1002/jgrc.20202.

McGillicuddy, D. J., Robinson, A. R., Siegel, D. A., Jannasch, H. W., Johnson, R., Dickeys, T., McNeil, J., *et al*. 1998. Influence of mesoscale eddies on new production in the Sargasso Sea. Nature, 394(6690): 263–266.

McLeod, D. J., Hallegraeff, G. M., Hosie, G. M., and Richardson, A. J. 2012. Climate-driven range expansion of the red-tide dinoflagellate *Noctiluca scintillans* into the Southern Ocean. Journal of Plankton Research, 34: 332–337.

McPhaden, M. J., Zebiak, S. E., and Glantz, M. H. 2006. ENSO as an integrating concept in earth science. Science, 314(5806): 1740–1745.

Meehl, G. A., Arblaster, J. M., Branstator, G., and van Loon, H. 2008. A coupled air–sea response mechanism to solar forcing in the Pacific region. Journal of Climate, 21: 2883–2897, doi:http://dx.doi.org/10.1175/2007JCLI1776.1.

Meehl, G. A., Teng, H., and Arblaster, J. M. 2014. Climate model simulations of the observed early-2000s hiatus of global warming. Nature Climate Change, 4(10): 898–902, doi:10.1038/nclimate2357.

Merrifield, M. A. 2011. A shift in western tropical Pacific sea level trends during the 1990s. Journal of Climate, 24(15): 4126–4138.

O'Kane, T. J., Oke, P. R., and Sandery, P. A. 2011. Predicting the east Australian current. Ocean Modelling, 38(3): 251–266, doi:10.1016/j.ocemod.2011.04.003.

Oke, P. R., and England, M. H. 2004. Oceanic response to changes in the latitude of the Southern Hemisphere subpolar westerly winds. Journal of Climate, 17(5): 1040–1054.

Oke, P. R., and Sakov, P. 2012. Assessing the footprint of a regional ocean observing system. Journal of Marine Systems, 105–108: 30–51.

Pennington, J. T., Mahoney, K. L., Kuwahara, V. S., Kolber, D. D., Calienes, R., and Chavez, F. P. 2006. Primary production in the eastern tropical Pacific: a review. Progress in Oceanography, 69: 285–317.

Philander, S. G. 1990. El Nino, La Niña, and the Southern Oscillation. Academic Press, San Diego. 293 pp.

Polovina, J. J., Howell, E. A., and Abecassis, M. 2008. The ocean's least productive waters are expanding. Geophysical Research Letters, 35: L03618, http://dx.doi.org/10.1029/2007GL031745.

Polovina, J. J., and Woodworth, P. A. 2012. Declines in phytoplankton cell size in the subtropical oceans estimated from satellite remotely-sensed temperature and chlorophyll, 1998–2007, Deep-Sea Research II, 77–80: 82–88, http://dx.doi.org/10.1016/j.dsr2.2012.04.006.

Prince, E. D., and Goodyear, C. P. 2006. Hypoxia-based habitat compression of tropical pelagic fishes. Fisheries Oceanography, 15(6): 451–464.

Purcell, J. E. 2005. Climate effects on formation of jellyfish and ctenophore blooms: a review. Journal of the Marine Biological Association of the United Kingdom, 85: 461–476.

Rasmusson, E. M., and Carpenter, T. H. 1982. Variations in tropical sea surface temperature and surface wind fields associated with the Southern Oscillation/El Nino. Monthly Weather Review, 110: 354–384.

Rayner, N. A., Parker, D. E., Horton, E. B., Folland, C. K., Alexander, L. V., Rowell, D. P., Kent, E. C., *et al.* 2003. Global analyses of sea surface temperature, sea ice, and night marine air temperature since the late nineteenth century. Journal of Geophysical Research, 108(D14): 4407, doi:10.1029/2002JD002670.

Rayner, N. A., Brohan, P., Parker, D. E., Folland, C. K., Kennedy, J. J., Vanicek, M., Ansell, T. J., *et al*. 2006. Improved analyses of changes and uncertainties in sea surface temperature measured *in situ* since the mid-nineteenth century: the HadSST2 dataset. Journal of Climate, 19: 446–469.

Richardson, A. 2008. In hot water: zooplankton and climate change. ICES Journal of Marine Science, 65(3): 279–295, doi:10.1093/icesjms/fsn028.

Richardson, A. J., and Schoeman, D. S. 2004. Climate impact on plankton ecosystems in the Northeast Atlantic. Science, 305(5690): 1609–1612, doi:10.1126/science.1100958.

Ridgway, K. R. 2007. Long-term trend and decadal variability of the southward penetration of the East Australian Current. Geophysical Research Letters, 34: L13613, doi:10.1029/2007GL030393.

Ridgway, K. R., and Godfrey, J. S. 1997. Seasonal cycle of the East Australian Current. Journal of Geophysical Research, 102(C10): 22921–22936, doi:10.1029/97JC00227.

Roemmich, D., and Cornuelle, B. 1990. Observing the fluctuations of gyre-scale ocean circulation: a study of the subtropical South Pacific. Journal of Physical Oceanography, 20: 1919–1934, doi:http://dx.doi.org/10.1175/1520-0485(1990)020<1919:OTFOGS>2.0.CO;2.

Rousseaux, C. S., and Gregg, W. W. 2015. Recent decadal trends in global phytoplankton composition. Global Biogeochemical Cycles, 29: 1674–1688, doi: 10.1002/2015GB005139.

Salinger, M. J., Renwick, J. A., and Mullan, A. B. 2001. Interdecadal Pacific oscillation and south Pacific climate. International Journal of Climatology, 21(14): 1705–1721, doi:10.1002/joc.691.

Schneider, W., Fukasawa, M., Garcés-Vargas, J., Bravo, L., Uchida, H., Kawano, T., and Fuenzalida, R. 2007. Spin-up of South Pacific subtropical gyre freshens and cools the upper layer of the eastern South Pacific Ocean. Geophysical Research Letters, 34(24): L24606, doi:10.1029/2007GL031933,2007.

Siegel, D. A., Behrenfeld, M. J., Maritorena, S., McClain, C. R., Antoine, D., Bailey, S. W., Bontempi, P. S., *et al*. 2013. Regional to global assessments of phytoplankton dynamics from the SeaWiFS mission. Remote Sensing of Environment, 135: 77–91.

Signorini, S. R., Franz, B. A., and McClain, C. R. 2015. Chlorophyll variability in the oligotrophic gyres: mechanisms, seasonality and trends. Frontiers in Marine Science, 2(1): doi:10.3389/fmars.2015.000001.

Sohn, B. J., and Park, S. C. 2010. Strengthened tropical circulations in past three decades inferred from water vapor transport. Journal of Geophysical Research: Atmospheres, 115: D15112, doi:10.1029/2009JD013713.

Sohn, B. J., Yeh, S. W., Schmetz, J., and Song, H. J. 2013. Observational evidences of Walker circulation change over the last 30 years contrasting with GCM results. Climate Dynamics, 40(7–8): 1721–1732.

Stott, P. A., Gillett, N. P., Hegerl, G. C., Karoly, D. J., Stone, D. A., Zhang, X., and Zwiers, F. 2010. Detection and attribution of climate change: a regional perspective. Wiley Interdisciplinary Reviews: Climate Change, 1(2): 192–211.

Stramma, L., Schmidtko, S., Levin, L. A., and Johnson, G. C. 2010. Ocean oxygen minima expansions and their biological impacts. Deep-Sea Research I: Oceanographic Research Papers, 57(4): 587–595.

Sydeman, W. J., García-Reyes, M., Schoeman, D. S., Rykaczewski, R. R., Thompson, S. A., Black, B. A., and Bograd, S. J. 2014. Climate change and wind intensification in coastal upwelling ecosystems. Science, 345(6192): 77–80.

Thomas, A. C., Brickley, P., and Weatherbee, R. 2009. Interannual variability in chlorophyll concentrations in the Humboldt and California Current systems. Progress in Oceanography, 83(1–4): 386–392, doi: 10.1016/j.pocean.2009.07.020.

Thomas, A. C., Strub, P. T., Weatherbee, R. A., and James, C. 2012. Satellite views of Pacific chlorophyll variability: Comparisons to physical variability, local versus nonlocal influences and links to climate indices. Deep-Sea Research II, 77–80: 99–116, http://dx.doi.org/10.1016/j.dsr2.2012.04.008.

Thompson, D. W., and Wallace, J. M. 2000. Annular modes in the extratropical circulation. Part I: Month-to-month variability. Journal of Climate, 13(5): 1000–1016.

Thompson P. A., Baird, M. E., Ingleton, T., and Doblin, M. A. 2009. Long-term changes in temperate Australian coastal waters: implications for phytoplankton, Marine Ecological Progress Series, 394: 1–19, doi: 10.3354/meps08297.

Thompson, P. A., Bonham, P., Rochester, W., Doblin, M. A., Waite, A. M., Richardson, A., and Rousseaux, C. 2015. Climate variability drives plankton community composition changes: an El Niño to La Niña transition around Australia. Journal of Plankton Research, 37(5): 966–984, doi: 10.1093/plankt/fbv069.

Trenberth, K. E. 1997. The definition of El Niño. Bulletin of the American Meteorological Society, 78: 2771–2777.

Trenberth, K. E. 2015. Has there been a hiatus? Science, 349: 691–692.

Uitz, J., Stramski, D., Reynolds, R. A., and Dubranna, J. 2015. Assessing phytoplankton community composition from hyperspectral measurements of phytoplankton absorption coefficient and remote-sensing reflectance in open-ocean environments. Remote Sensing of Environment, 171: 58–74, doi:10.1016/j.rse.2015.09.027.

Vantrepotte, V., and Mélin, F. 2011. Inter-annual variations in the SeaWiFS global chlorophyll a concentration (1997–2007). Deep-Sea Research I, 58: 429–441.

Vargas, G., Pantoja, S., Rutllant, J. A., Lange, C. B., and Ortlieb, L. 2007. Enhancement of coastal upwelling and interdecadal ENSO-like variability in the Peru-Chile Current since late 19th century. Geophysical Research Letters, 34: L13607, doi:10.1029/2006GL028812.

Vincent, D. G. 1994. The South Pacific convergence zone (SPCZ): A review. Monthly Weather Review, 122(9): 1949–1970.

Vincent, E. M., Lengaigne, M., Menkes, C. E., Jourdain, N. C., Marchesiello, P., and Madec, G. 2011. Interannual variability of the South Pacific Convergence Zone and implications for tropical cyclone genesis. Climate Dynamics, 36(9–10): 1881–1896.

Wang, B., Liu, J., Kim, H. J., Webster, P. J., and Yim, S. Y. 2012b. Recent change of the global monsoon precipitation (1979–2008). Climate Dynamics, 39(5): 1123–1135.

Wang, C., Deser, C., Yu, J-Y., DiNezio, P., and Clement, A. 2012a. El Niño and Southern Oscillation (ENSO): A Review. *In* Coral Reefs of the Eastern Pacific: Persistence and Loss in a Dynamic Environment, pp. 85–106. Ed. by P. W. Glynn, D. P. Manzello, and I. C. Enochs. Springer Netherlands. 657 pp.

White, J. R., Zhang, X., Welling, L. A., Roman, M. R., and Dam, H. G. 1995. Latitudinal gradients in zooplankton biomass in the tropical Pacific at 140 W during the JGOFS EqPac study: Effects of El Niño. Deep-Sea Research II: Topical Studies in Oceanography, 42(2): 715–733.

Wijffels, S. E., Toole, J. M., and Davis, R. 2001. Revisiting the South Pacific subtropical circulation: A synthesis of World Ocean Circulation Experiment observations along 32°S. Journal of Geophysical Research, 106: 19481–19513.

Wyrtki, K. 1963. The horizontal and vertical field of motion in the Peru Current. Bulletin of the Scripps Institution of Oceanography, 8: 313–344.

Wyrtki, K. 1989. Some thoughts about the west Pacific warm pool. *In* Proceedings of the Western Pacific International Meeting and Workshop on Toga Coare, Nouméa, New Caledonia, 24-30 May 1989, pp. 99-109. Ed. by J. Picaut Joël, R. Lukas, and T. Delcroix. ORSTOM, Centre de Nouméa.

9 North Pacific Ocean

Andrew R. S. Ross, R. Ian Perry, James R. Christian, Todd D. O'Brien, Laura Lorenzoni, Frank E. Muller-Karger, William R. Crawford, Angelica Peña, and Kirsten Isensee

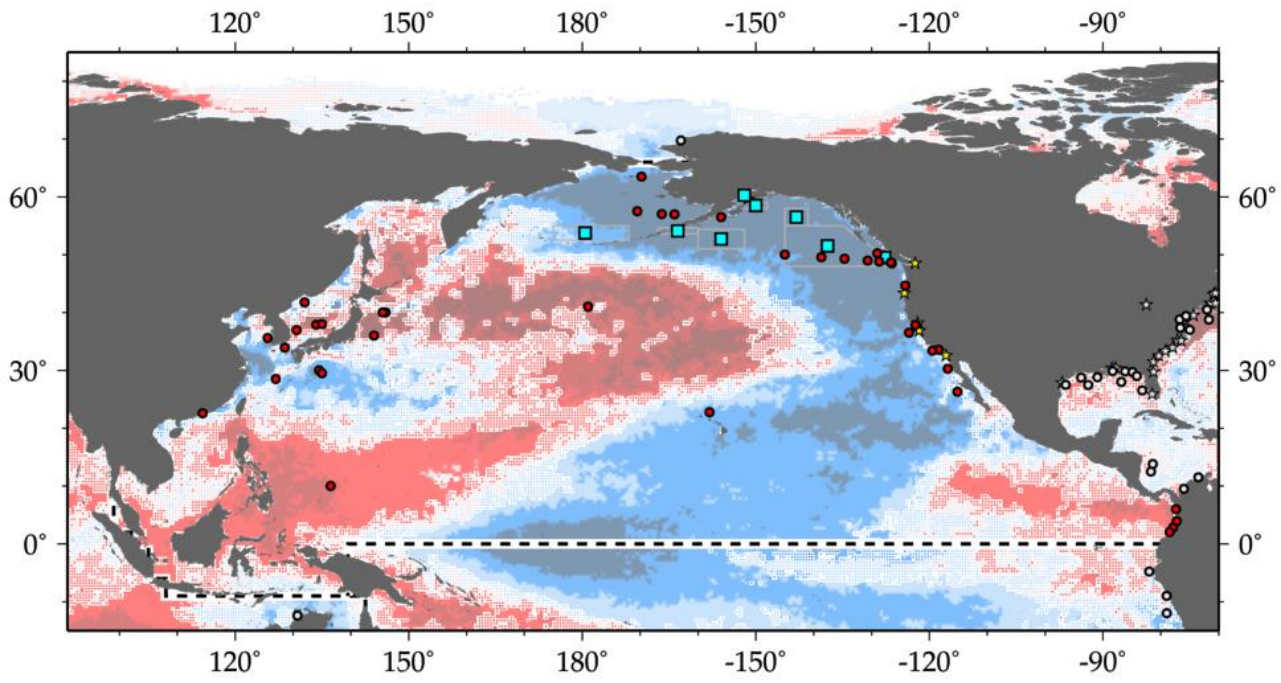

Figure 9.1. Map of IGMETS-participating North Pacific time series on a background of a 10-year time-window (2003–2012) sea surface temperature trends (Figure 9.4). At the time of this report, the North Pacific collection consisted of 54 time series (coloured symbols of any type), of which eight were from Continuous Plankton Recorder subareas (blue boxes), and six were from estuarine areas (yellow stars). Dashed lines indicate boundaries between IGMETS regions. Uncoloured (gray) symbols indicate time series being addressed in a different regional chapter (e.g. Arctic Ocean, South Pacific). See Table 9.3 for a listing of this region's participating sites. Additional information on the sites in this study is presented in the Annex.

Participating time-series investigators

Sonia Batten, Robert Bidigare, David Caron, Sanae Chiba, Matthew J. Church, James E. Cloern, John E. Dore, Janet Duffy-Anderson, Lisa Eisner, Luisa Espinosa, Ed Farley, Jennifer L. Fisher, Jed Fuhrman, Moira Galbraith, Troy Gunderson, Masao Ishii, Young-Shil Kang, David M. Karl, Diane Kim, Michael Landry, Bertha E. Lavaniegos, Ricardo M. Letelier, Roger Lukas, Dave Mackas, Roberta Marinelli, Sam McClatchie, Cheryl A. Morgan, Jeffrey Napp, Todd O'Brien, Mark Ohman, Ian Perry, William T. Peterson, Al Pleudemann, Dwayne Porter, Marie Robert, Andrew R.S. Ross, Sei-ichi Saitoh, Robert Weller, and Kedong Yin

This chapter should be cited as: Ross, A. R. S., Perry, R. I., Christian, J. R., O'Brien, T. D., Lorenzoni, L., Muller-Karger, F. E., Crawford, W. R., *et al.* 2017. North Pacific. I*n* What are Marine Ecological Time Series telling us about the ocean? A status report, pp. 153–169. Ed. by T. D. O'Brien, L. Lorenzoni, K. Isensee, and L. Valdés. IOC-UNESCO, IOC Technical Series, No. 129. 297 pp.

9.1 Introduction

The North Pacific (Figure 9.1) covers an area equivalent to just over one-fifth of the surface of the world's oceans (85 million km^2) and accounts for almost one-fourth of their total volume (331 million km^3). It includes the deepest point in the ocean (10.9 km in the Marianas Trench) and has the greatest average depth (4.3 km) of any ocean basin (Eakins and Sharman, 2010). The North Pacific consists of a large central oceanic region surrounded by a number of boundary currents and marginal seas (McKinnell and Dagg, 2010). These include the Alaska Stream and currents in the Bering Sea that link the Pacific with the Arctic Ocean. They also include the North Equatorial Current, the California Current and Alaska Current to the east, and the Oyashio Current, Kuroshio Current, Sea of Okhotsk, Sea of Japan/East Sea, and Yellow and East China seas to the west. The oceanic region contains a large subtropical gyre to the south and a smaller subarctic gyre to the north, divided by the North Pacific Current.

Pacific Ocean currents (Figure 9.2) follow the general pattern of those in the Atlantic (Bowditch, 2002), although the greater size and semi-enclosed boundaries of the Pacific result in circulation patterns that respond more ideally to the Coriolis effect and symmetrical wind patterns in the two hemispheres (Longhurst, 2007). The North Equatorial Current is driven westward by trade winds before turning north near the Philippines to become the warm Kuroshio Current, which joins the cool southward Oyashio Current to form the eastward Kuroshio–Oyashio Extension (KOE) and North Pacific Current. Western boundary currents like the Kuroshio and the North Atlantic Gulf Stream play an important role in climate change, acting as "hot spots" where the thermodynamic effects of the ocean on the atmosphere are intensified (Minobe *et al.*, 2008; Wu *et al.*, 2012). Changes in the position of the Kuroshio Current and the large meanders that form in this current also affect marine ecology and navigation in the western boundary region (McKinnell and Dagg, 2010). The KOE and North Pacific Current mark the northern boundary of the North Pacific Subtropical Gyre, the largest ecosystem in the surface ocean (Karl, 1999). The Alaska Current, which becomes the Alaska Stream after turning southwest along the Alaskan Peninsular, forms part of the anticlockwise Alaska Gyre and produces large clockwise mesoscale eddies west of Sitka and Haida Gwaii (formerly the Queen Charlotte Islands) that propagate westward into the gyre. Haida eddies play an important role in the offshore transport of zooplankton (Batten and Crawford, 2005) and iron (Johnson *et al.*, 2005) to the high-

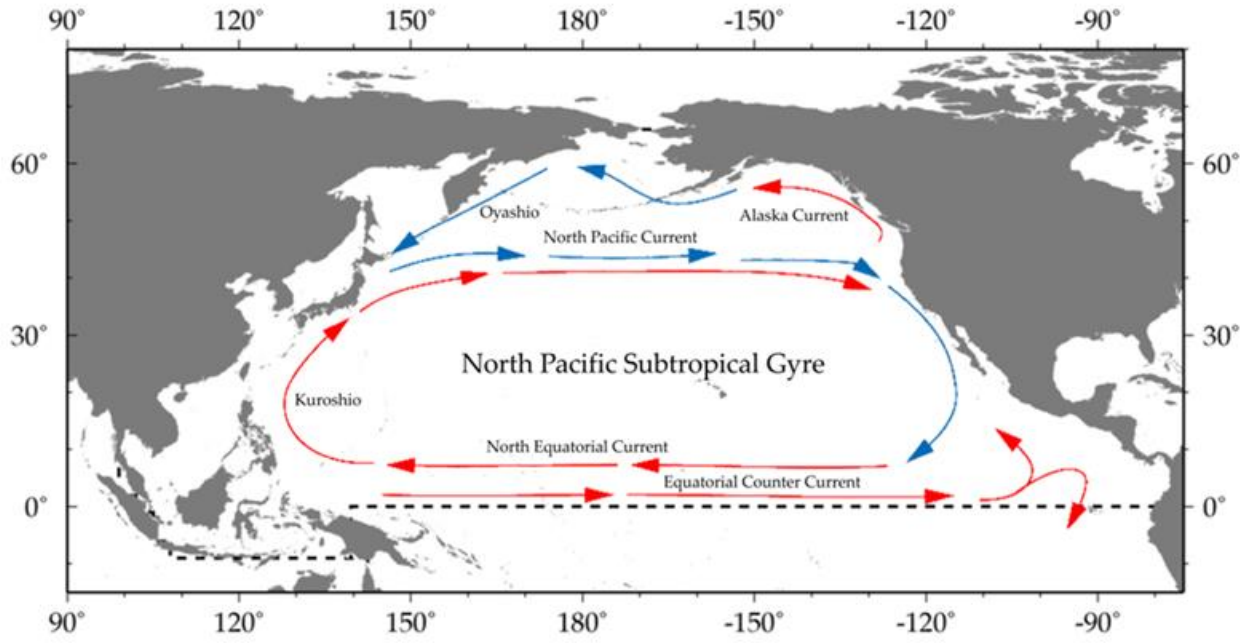

Figure 9.2. Schematic major current systems in the IGMETS-defined North Pacific region. Red arrows indicate generally warmer water currents; blue arrows indicate generally cooler water currents.

nutrient/low-chlorophyll waters of the subarctic Northeast Pacific. Water from the Alaska Current also enters the Bering Sea, forming part of the anticlockwise Bering Sea Gyre. Some of this water flows south into the Oyashio Current, which together with the Alaska Stream forms part of the anticlockwise Western Subarctic Gyre as it turns east to join the North Pacific Current, completing the North Pacific Subarctic Gyre. Water from the Alaska Current also drifts north through the Bering Strait into the Chukchi Sea, contributing to the circulation of the Arctic Ocean (Chapter 3).

The North Pacific lies at the end of the "ocean conveyor belt" (Zenk, 2001) where cold, nutrient-rich, deep water originating from the North Atlantic and Southern Ocean flows northward across the equator (Bowditch, 2002). Upwelling along the eastern boundary of the North Pacific supports high levels of productivity in the coastal waters of western Canada and the United States (McKinnell and Dagg, 2010), but also contributes to the local impacts of ocean acidification, due to the high amounts of dissolved inorganic carbon that accumulate in subsurface waters (Feely *et al.*, 2008; Haigh *et al.*, 2015).

The climate of the North Pacific is characterized by strong interdecadal variability, which arises from modulation of the El Niño–Southern Oscillation (ENSO) signal by the Aleutian Low (AL) and North Pacific Oscillation (NPO). These major atmospheric systems drive two predominant ocean modes: the Pacific Decadal Oscillation (PDO) and the North Pacific Gyre Oscillation (NPGO), respectively (Figure 9.3). The resulting variability gives rise to distinct physical and biological responses in the North Pacific (McKinnell and Dagg, 2010; Di Lorenzo *et al.*, 2013). The Oceanic Niño Index (ONI) is a measure of the anomaly of ocean surface temperature in the east-central equatorial Pacific (Figure 9.3) and defines the occurrence of El Niño and La Niña episodes (http://www.cpc.ncep.noaa.gov/products/analysis_monitoring/ensostuff/ensoyears.shtml). The North Pacific Index (NPI) is the area-weighted sea level pressure over part of the North Pacific and is a useful indicator of the intensity and areal extent of the Aleutian Low (Wallace and Gutzler, 1981; Trenberth and Hurrell, 1994). The PDO is the first mode of ocean surface temperature variability in the North Pacific (Mantua *et al.*, 1997; Zhang *et al.*, 1997) and is often positive during El Niño years (Figure 9.3). PDO variability is slower than that of the ONI and it is usually a good indicator of temperature

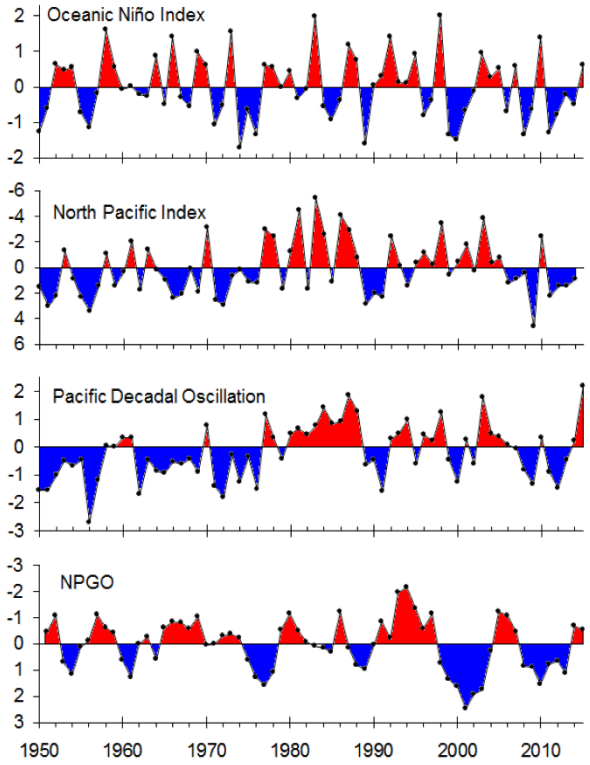

Figure 9.3. North Pacific climate indices, November–March averages (Chandler *et al.*, 2015).

patterns that persist for a decade or more. The NPGO is the second dominant mode of sea surface height variability in the Northeast Pacific and closely tracks the second mode of North Pacific SST (Di Lorenzo *et al.*, 2008). NPGO dynamics are driven by atmospheric variability in the North Pacific and capture the extratropical influence of central Pacific El Niños. When the NPGO is positive, the westerly winds over the eastern North Pacific are often stronger than normal, and the west coast of North America and eastern Gulf of Alaska are cool. These conditions have dominated in most winters from 1999 to 2013, except between 2004 and 2007 (Figure 9.3). The AL/PDO system describes many of the ecosystem fluctuations in the North Pacific (Di Lorenzo *et al.*, 2009). However, long-term time series like CalCOFI (us-50301/2) and Line-P (ca-50901) show decadal-scale fluctuations that are apparently unconnected with the PDO. The NPGO, which is associated with changes in the strength of the subtropical and subarctic gyres, explains the dominant interdecadal fluctuations in salinity, nutrient upwelling, and chlorophyll in many regions of the Northeast Pacific (Di Lorenzo *et al.*, 2009) as well as important state transitions in marine ecosystems (Cloern *et al.*, 2010; Perry and Masson, 2013).

Table 9.1. Relative spatial areas (% of the total region) and rates of change within the North Pacific region that are showing increasing or decreasing trends in sea surface temperature (SST) for each of the standard IGMETS time-windows. Numbers in brackets indicate the % area with significant ($p < 0.05$) trends. See "Methods" chapter for a complete description and methodology used.

Latitude-adjusted SST data field surface area = 85.4 million km²	**5-year** (2008–2012)	**10-year** (2003–2012)	**15-year** (1998–2012)	**20-year** (1993–2012)	**25-year** (1988–2012)	**30-year** (1983–2012)
Area (%) w/ increasing SST trends ($p < 0.05$)	42.8% (*7.9%*)	44.6% (*26.4%*)	**65.3%** (*41.8%*)	**65.0%** (*49.1%*)	**67.9%** (*56.5%*)	**75.7%** (*64.7%*)
Area (%) w/ decreasing SST trends ($p < 0.05$)	**57.2%** (*19.9%*)	**55.4%** (*41.4%*)	34.7% (*18.9%*)	35.0% (*24.1%*)	32.1% (*21.3%*)	24.3% (*16.8%*)
> 1.0°C decade^{-1} warming ($p < 0.05$)	9.2% (*4.9%*)	3.8% (*3.8%*)	0.8% (*0.8%*)	0.1% (*0.1%*)	0.0% (*0.0%*)	0.0% (*0.0%*)
0.5 to 1.0°C decade^{-1} warming ($p < 0.05$)	10.7% (*2.4%*)	10.0% (*9.1%*)	6.0% (*5.9%*)	6.5% (*6.5%*)	0.7% (*0.7%*)	1.8% (*1.8%*)
0.1 to 0.5°C decade^{-1} warming ($p < 0.05$)	17.1% (*0.7%*)	24.7% (*13.3%*)	46.6% (*34.4%*)	44.9% (*40.7%*)	**50.6%** (*49.0%*)	**55.4%** (*54.9%*)
0.0 to 0.1°C decade^{-1} warming ($p < 0.05$)	5.8% (*0.0%*)	6.1% (*0.2%*)	11.9% (*0.7%*)	13.6% (*1.9%*)	16.6% (*6.8%*)	18.6% (*8.0%*)
0.0 to –0.1°C decade^{-1} cooling ($p < 0.05$)	5.6% (*0.0%*)	5.0% (*0.1%*)	9.1% (*0.3%*)	8.1% (*0.5%*)	11.6% (*1.9%*)	9.9% (*2.8%*)
–0.1 to –0.5°C decade^{-1} cooling ($p < 0.05$)	18.3% (*0.5%*)	16.6% (*7.9%*)	20.8% (*13.8%*)	22.6% (*19.3%*)	20.4% (*19.2%*)	14.3% (*14.1%*)
–0.5 to –1.0°C decade^{-1} cooling ($p < 0.05$)	13.5% (*3.9%*)	22.2% (*21.8%*)	4.4% (*4.4%*)	4.3% (*4.3%*)	0.1% (*0.1%*)	0.0% (*0.0%*)
> –1.0°C decade^{-1} cooling ($p < 0.05$)	19.8% (*15.4%*)	11.5% (*11.5%*)	0.4% (*0.4%*)	0.0% (*0.0%*)	0.0% (*0.0%*)	0.0% (*0.0%*)

Table 9.2. Relative spatial areas (% of the total region) and rates of change within the North Pacific region that are showing increasing or decreasing trends in phytoplankton biomass (CHL) for each of the standard IGMETS time-windows. Numbers in brackets indicate the % area with significant ($p < 0.05$) trends. See "Methods" chapter for a complete description and methodology used.

Latitude-adjusted CHL data field surface area = 85.4 million km²	**5-year** (2008–2012)	**10-year** (2003–2012)	**15-year** (1998–2012)
Area (%) w/ increasing CHL trends ($p < 0.05$)	23.6% (*2.9%*)	40.8% (*21.2%*)	34.2% (*13.0%*)
Area (%) w/ decreasing CHL trends ($p < 0.05$)	**76.4%** (*35.8%*)	**59.2%** (*37.3%*)	**65.8%** (*42.7%*)
> 0.50 mg m^{-3} decade^{-1} increasing ($p < 0.05$)	0.9% (*0.3%*)	0.3% (*0.3%*)	0.6% (*0.5%*)
0.10 to 0.50 mg m^{-3} decade^{-1} increasing ($p < 0.05$)	2.9% (*0.5%*)	3.2% (*1.9%*)	4.0% (*3.3%*)
0.01 to 0.10 mg m^{-3} decade^{-1} increasing ($p < 0.05$)	11.8% (*1.9%*)	25.2% (*16.3%*)	15.4% (*8.0%*)
0.00 to 0.01 mg m^{-3} decade^{-1} increasing ($p < 0.05$)	8.0% (*0.2%*)	12.0% (*2.9%*)	14.2% (*1.2%*)
0.00 to –0.01 mg m^{-3} decade^{-1} decreasing ($p < 0.05$)	11.6% (*1.1%*)	16.7% (*6.7%*)	37.5% (*21.9%*)
–0.01 to –0.10 mg m^{-3} decade^{-1} decreasing ($p < 0.05$)	47.7% (*23.7%*)	39.2% (*28.6%*)	27.5% (*20.4%*)
–0.10 to –0.50 mg m^{-3} decade^{-1} (decreasing) ($p < 0.05$)	14.8% (*9.7%*)	2.9% (*1.7%*)	0.7% (*0.4%*)
> –0.50 mg m^{-3} decade^{-1} (decreasing) ($p < 0.05$)	2.3% (*1.3%*)	0.3% (*0.2%*)	0.1% (*0.1%*)

The following describes the main patterns observed from 1983 to 2012 in North Pacific time-series data compiled by IGMETS and how these relate to known ocean circulation patterns, climate drivers, and previous reports regarding the spatial and temporal variability of marine ecosystems in this region. More detailed tables and maps for the North Pacific and other regions can be obtained from the IGMETS Explorer tool:

http://igmets.net/explorer/

9.2 General patterns of temperature and phytoplankton biomass

Time series of gridded, large-scale, satellite-derived sea surface temperature (SST) and surface chlorophyll (CHL) indicate a general warming accompanied by an overall decrease in phytoplankton biomass in the North Pacific (Tables 9.1 and 9.2). During the 30 years from 1983 to 2012, >75% of the North Pacific (64.7% at $p < 0.05$) underwent warming, whereas 24.3% (16.8% at $p < 0.05$) underwent cooling. The pattern of warming resembles the characteristic "wedge and horseshoe" configuration of the PDO, which is the dominant mode of variability at this time-scale, along with the underlying anthropogenic (secular) trend (Figure 9.4a). During the 15 years from 1998 to 2012, about 35% (18.9% at $p < 0.05$) of North Pacific surface water underwent cooling and 65.3% (41.8% at $p < 0.05$) underwent warming (Table 9.1). Cooling occurred primarily in the eastern North Pacific from the Bering Sea and Alaska Gyre to the California Current and across the southeast North Pacific (Figure 9.4a). Cooling of the Kuroshio Current was also apparent during this period, although the observed pattern may also reflect changes in the position of the Kuroshio axis, which is linked to the PDO (Di Lorenzo *et al*., 2013). The onset of these changes appears to coincide with the abrupt shift from El Niño to La Niña conditions in summer 1998.

Satellite-derived surface chlorophyll data are available for the 15 years from 1998 to 2012. During this period, a decrease in chlorophyll was observed in 65.8% (42.7% at $p < 0.05$) of the surface area of the North Pacific (Table 9.2), mainly in the central oceanic region (Figure 9.4b). At the same time, chlorophyll was seen to increase in 34.2% (13% at $p < 0.05$) of the North Pacific, including parts of the North American west coast, eastern subarctic and equatorial Pacific, and coasts of the Okhotsk and Bering seas. During the 10 years from 2003 to 2012, chlorophyll decreased in 59.2% (37.3% at $p < 0.05$) and increased in 40.8% (21.2% at $p < 0.05$) of the North Pacific. This period coincided with significant cooling over 55.4% (41.8% *at* $p < 0.05$) of the ocean's surface (Table 9.1) and with the appearance of a large patch of chlorophyll to the south, aligned roughly with the North Equatorial Current (Figure 9.4b).

A similar patch was observed in the northern South Pacific during the same period (Chapter 8), the divergence of these features in the eastern equatorial Pacific reflecting the symmetry of the prevailing wind patterns and the influence of Ekman transport (Longhurst, 2007). Direct correlation of chlorophyll with SST (Figure 9.4c) shows that warming tends to be associated with lower phytoplankton biomass over much of the North Pacific, except for parts of the western boundary, central subtropical, and subarctic regions. In the western subarctic Pacific, winter mixed layers are deep and, in some seasons, thermal stratification may promote phytoplankton growth by increasing access to light (Dutkiewicz *et al*., 2001).

9.3 Trends from *in situ* time series

The *in situ* time-series datasets available for the North Pacific are fewer in number than for the North Atlantic (Chapter 4), but are relatively well distributed, providing data from the eastern, western, subarctic, and/or subtropical North Pacific, depending on which parameter is selected (Figure 9.5). They include ship-based measurements of SST and chlorophyll which, when superimposed on the corresponding gridded data, show good overall agreement between *in situ* and satellite-based observations (Figure 9.5a). A selection of other *in situ* variables, combined with gridded SST for the 10-year time-window (Figures 9.5b–h), illustrate how local and regional trends in physical, chemical, and biological parameters can be compared and related and how powerful this approach is for understanding trends in the biogeochemistry of the North Pacific. For example, *in situ* measurements of surface nitrate (Figure 9.5b), salinity (Figure 9.5g), and dissolved oxygen (Figure 9.5h) show a general increase in the eastern and subarctic North Pacific during the 10-year time-window (2003–2012), whereas SST shows the opposite trend. Conversely, in the western North Pacific, warmer SST was largely associated with a decrease in surface salinity, nutrients, and oxygen concentrations. The inverse relationship between temperature and nutrients (nitrate, phosphate,

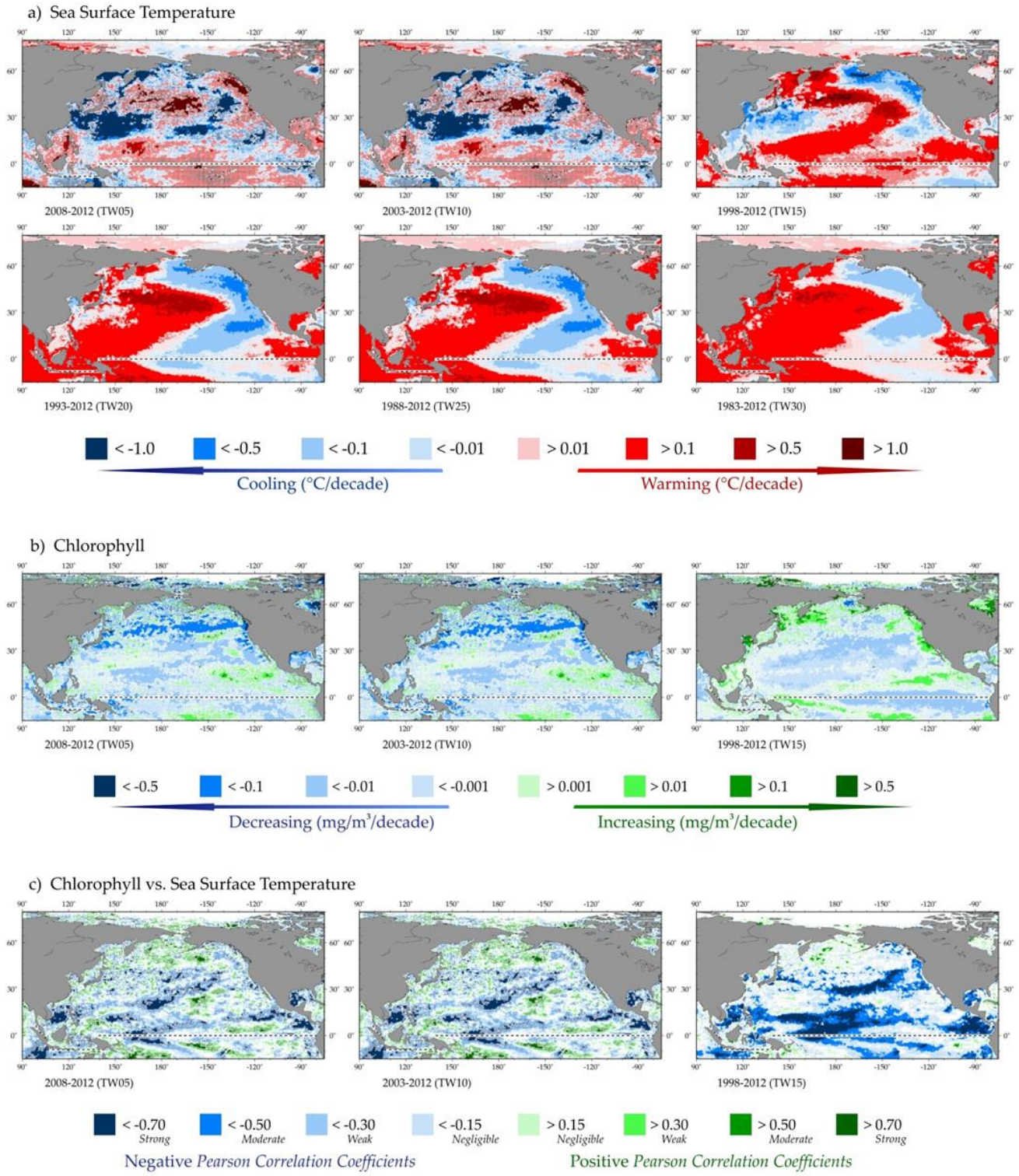

Figure 9.4. Annual trends in North Pacific sea surface temperature (SST) (a) and sea surface chlorophyll (CHL) (b), and correlations between chlorophyll and sea surface temperature for each of the standard IGMETS time-windows (c). See "Methods" chapter for a complete description and methodology used.

and silicate) predominates across the North Pacific over the 30-year time-window (1983–2012) and is consistent with a reduction in the mixing of nutrients into surface waters due to stratification.

Another way of looking at overall trends across the North Pacific is to consider the proportion of available time series that show an increasing or decreasing trend for each *in situ* parameter within a particular time-window. These data can be normalized by expressing them as a percentage of the total number of available sites, making it easier to compare different variables (Figure 9.6). Many of the *in situ* variables in the North Pacific show temporal trends that change in magnitude or direction halfway through the 30-year period from 1983 to 2012, coinciding with the major shift from El Niño to La Niña conditions in 1998 (Figure 9.6c).

For example, the long-term, 30-year trend for *in situ* phytoplankton data is one of increasing chlorophyll (Figure 9.6d), but this trend appears to have slowed since 1998 (Figures 9.6a–c). Considering that most of the *in situ* time series are located in northern and/or coastal waters, with few in tropical or subtropical oceanic waters, these trends are consistent with the assessment of surface chlorophyll based on satellite data (Figure 9.4), which suggests an overall increase in phytoplankton biomass near coastal areas. However, the inclusion of the four equatorial Colombian coastline REDCAM time series (see Table 9.3) contributes to the predominant number of *in situ* measurements showing an increase in temperature between 2008 and 2012 (Figure 9.6a), which contrasts with the overall cooling trend observed in satellite SST across the North Pacific during the same 5-year period (Table 9.1). Neverthless, nitrate time-series measurements show the same inverse relationship with *in situ* temperature (Figure 9.6) as with satellite SST (Figure 9.5b). The available *in situ* data also suggest that zooplankton and diatoms have decreased in most time series during the past 15 years (Figures 7.6a–c). Time series that show increasing chlorophyll are sometimes associated with decreases in zooplankton, especially in the subarctic North Pacific.

Pairwise correlation of *in situ* parameters with Reynolds SST or satellite chlorophyll data allows for an investigation of potential cause-and-effect relationships between these variables. Such a comparison shows synchrony between *in situ* and local gridded SST data (Figure 9.7), but suggests that there is no clear relationship between *in situ* SST and satellite chlorophyll measurements (Figure 9.8), based on the available data. Indeed, there is little correlation between *in situ* parameters and the local gridded chlorophyll data other than an overall positive correlation with nitrate and phytoplankton biomass (Figure 9.8c). In contrast, nitrate, chlorophyll, salinity, and dissolved oxygen time series generally show negative correlations with gridded SST (Figure 9.7). Most phytoplankton time series also showed a negative correlation between the diatom/dinoflagellate ratio and SST (Figure 9.7), as opposed to the positive correlation between this ratio and satellite chlorophyll (Figure 9.8), although the latter is more variable. The majority of zooplankton, diatom, and dinoflagellate time series were positively correlated with SST over the last 10 years (Figure 9.7b). However, it should be born in mind that these basin-scale relationships may not apply at the local or regional level. Furthermore, as mentioned above, the available *in situ* time series cover only a small and mainly peripheral area of the North Pacific, whereas the gridded SST and chlorophyll data cover the entire basin. This, together with the possibility of seasonal effects, may account for apparent discrepancies between *in situ* and satellite-based trends. Increasing time series coverage of the North Pacific would help to address this issue.

9.4 Comparison with other studies

Changing conditions of the North Pacific have been the focus of multiple studies. Fisheries and Oceans Canada (DFO) has been preparing annual State of the Pacific Ocean (SOPO) reports on conditions in the subarctic Northeast Pacific since 1999 (http://www.dfo-mpo.gc.ca/oceans/publications/index-eng.html) using data from oceanic and coastal time series such as the Line-P (ca-50901-6) and offshore Vancouver Island (ca-50301-2) monitoring programmes. Similarly, the North Pacific Marine Science Organization (PICES) has prepared two Special Publications on Marine Ecosystems of the North Pacific Ocean covering the periods 1998–2003 and 2003–2008 (PICES, 2004; McKinnell and Dagg, 2010) using time-series data provided by PICES member nations and participating international organizations such as SAHFOS/Pacific CPR (uk-40201-8). These documents provide a wealth of information on changes in the climate and oceanography of the North Pacific, with which the last 15 years of this IGMETS assessment (1998–2012) can be compared. The first North Pacific Ecosystems

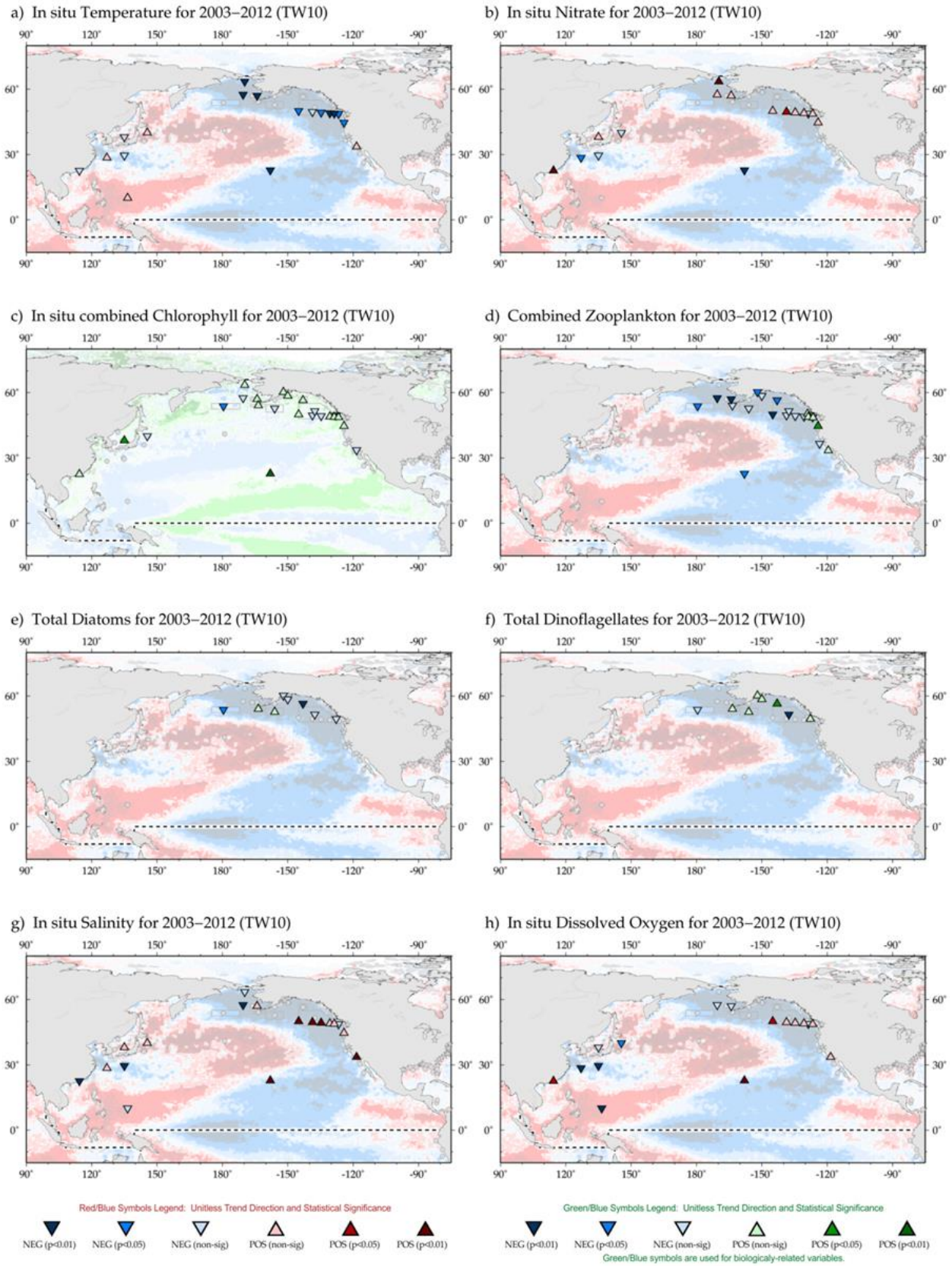

Figure 9.5. Map of North Pacific region time-series locations and trends for select variables and IGMETS time-windows. Upward-pointing triangles indicate positive trends; downward triangles indicate negative trends. Gray circles indicate time-series site that fell outside of the current study region or time-window. Additional variables and time-windows are available through the IGMETS Explorer (http://IGMETS.net/explorer). See "Methods" chapter for a complete description and methodology used.

Status Report (PICES, 2004) describes the emergence of a new climate pattern between 1998 and 2002 associated with a cooling along the eastern boundary and warming of the central North Pacific. SOPO reports for this period (DFO, 2000–2002) describe a return to relatively normal conditions of temperature and plankton ecology following the El Niño/La Niña transition in 1998, although the 2002 SOPO report (DFO, 2003) describes anomalously warm waters in the subarctic Northeast Pacific and the shallowest mixed layer on record at that time.

This period coincides with the onset of significant changes in temporal and spatial trends of SST and chlorophyll (Figure 9.4) and in many of the *in situ* parameters included in this assessment (Figure 9.6).

The warmer conditions of the western North Pacific noted in this report have also been studied by other authors. For example, Park *et al*. (2012) reported that the western boundary of the subtropical North Pacific showed the greatest rate of warming of all oceans between 1981 and 2005. They attributed the temperature increase to rapid changes in both the Siberian High and Aleutian Low which, in turn, affected the subtropical gyre circulation of the North Pacific. Progressive warming in the Okhotsk Sea since the 1950s has also been observed (Nakanowatari *et al*., 2007). Cravatte *et al*. (2009) report on the consistent warming and freshening of the Western Pacific Warm Pool, an area that was observed to consistently increase in SST over the different time-windows examined here.

Variability in chlorophyll concentration across the North Pacific is largely connected to climate modes. For example, suppressed equatorial upwelling during El Niño events leads to a reduced nutrient supply, which affects primary production in the tropical Pacific and reduces chlorophyll concentrations. This also induces an asymmetric response of ocean chlorophyll to El Niño and La Niña in the central Pacific (Vantrepotte and Mélin, 2009; Park *et al*., 2011), a feature that can be seen in the data presented here. The SOPO report for 2006 (DFO, 2007) describes the onset of La Niña conditions and, at that time, the largest phytoplankton (coccolithophore) bloom ever recorded off Vancouver Island on the Canadian west coast. This period is encompassed by the 10-year IGMETS time-window (2003–2012), during which the percentage surface area of the North Pacific in which chlorophyll increased was greater than for other time-windows (Table 9.2), which suggests a slowing of the long-term downward trend in the open ocean. This was also the period during which the greatest number of *in situ* time series showed an increase in phytoplankton biomass (Figure 9.6b). The normally dominant PDO climate pattern shifted abruptly to its negative phase in 2007, coinciding with La Niña conditions and ushering in an unusually cool 5-year period (2008–2012).

The general decrease in surface chlorophyll noted here in the open North Pacific, as determined by satellite observations, is consistent with observations made by Polovina *et al*. (2008) and Signorini *et al*. (2015), who report on the expansion of low surface chlorophyll areas in the subtropical North Pacific from 1998 to 2006 and from 1998 to 2013, respectively, accompanied by significant increases in average sea surface temperature. This is also consistent with the reported increase in stratification in both subtropical oceanic and subarctic coastal waters. In the coastal eastern and western North Pacific, as well as near the western tropical Pacific, the higher chlorophyll concentrations that have been observed over the past 15 years have been linked to changes in nitrate concentrations and variation in the PDO (Rykaczewski and Dunne, 2010; Chiba *et al*., 2012). While some models project an increase in size of the Western Pacific Warm Pool (Matear *et al*., 2015), there may not be a significant change in primary productivity in the area despite the continued temperature increase.

Climate modes also impact the ecological variability of the North Pacific (Doney *et al*., 2012; Litzow and Mueter, 2014). For example, in the eastern North Pacific, zooplankton communities north and south of the southern California Bight have opposite trends following the shift from El Niño to La Niña in 1998 (McKinnell and Dagg, 2010), signifying a major geographical shift in patterns of lower trophic level productivity in response to climate change. This inverse relationship appears to be captured in the *in situ* zooplankton data for the 10-year time-window presented in this report (Figure 9.5d), further illustrating the coherence between this assessment and previously published reports on changing conditions in the North Pacific. The second North Pacific Ecosystem Status Report (McKinnell and Dagg, 2010) also describes 2003–2008 as a period of enhanced climatic and ecological variability, particularly in the eastern North Pacific where extreme values in some time series were observed. Similarly, Canadian SOPO reports (DFO, 2005–2007) document unusually warm conditions from 2004 to 2006, accompanied by an overall decrease in zooplankton and a shift to warm-water species along the Canadian west coast. These observations are consistent

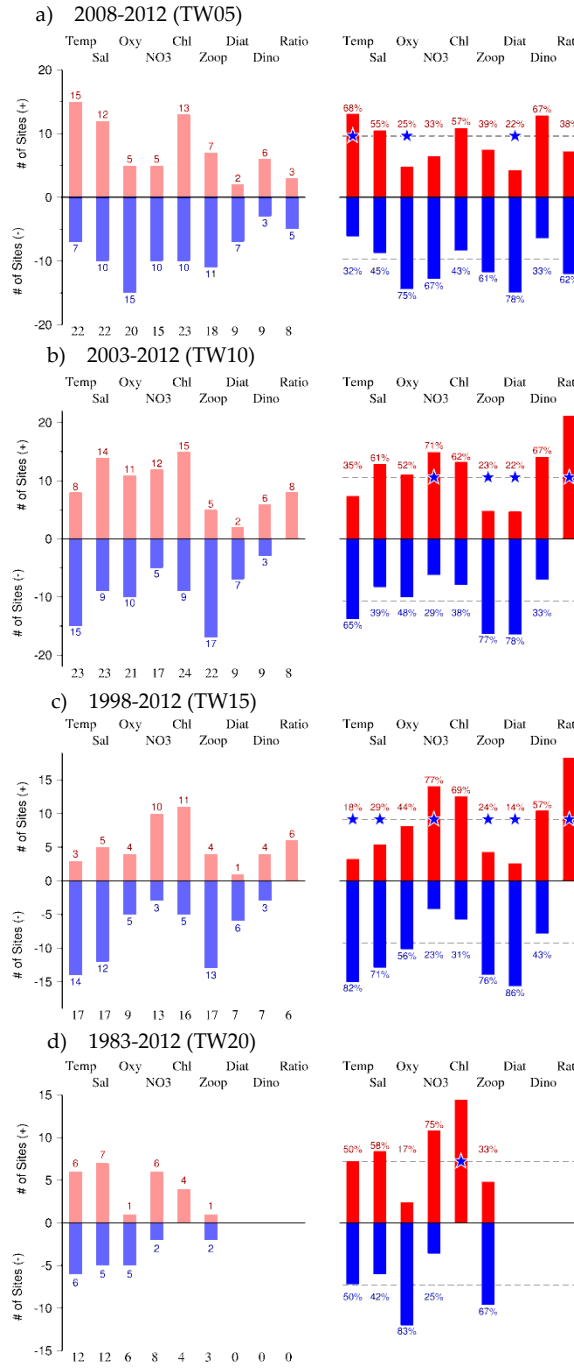

Figure 9.7. Absolute (left) and relative (%, right) frequency of positive and negative trends in selected variables from *in situ* time series in the North Pacific region computed for the 5-, 10-, 15-, and 30-year IGMETS time-windows. The 50% relative frequency is indicated by dashed lines in the left panels. A star symbol on the dashed line indicates a statistically significant difference ($p < 0.05$) from 50% positive/negative correlations. See "Methods" chapter for a complete description and methodology used.

Figure 9.6. Absolute (left) and relative (%, right) frequency of positive and negative correlations between selected *in situ* North Pacific time-series variables and corresponding gridded sea surface temperature (SST) for the 5-, 10-, 15-, and 30-year IGMETS time-windows. The 50% relative frequency is indicated by dashed lines in the left panels. A star symbol on the dashed line indicates a statistically significant difference ($p < 0.05$) from 50% positive/negative correlations. See "Methods" chapter for a complete description and methodology used.

with what was found for the time-window 2003–2010 in this assessment. From 2007 onwards, however, northern species of zooplankton once again predominated in western Canadian coastal waters (DFO, 2008–2011), illustrating the dynamic relationship between SST and the distribution of cold- and warm-water species.

The decrease in surface salinity of the northern and western North Pacific, as observed in this assessment (Figure 9.5g), has been attributed to changes in precipitation, evaporation, and sea ice. For example, Ohshima *et al*. (2014) attribute most of the freshening of the Okhotsk Sea to reduced sea ice production, with minor influences from variations in precipitation and evaporation over the region. Similarly, Hosoda *et al*. (2009) suggest that variations in precipitation and evaporation are the drivers behind the freshening of the northern North Pacific. The second North Pacific Ecosystem Status Report also describes long-term downward trends in surface oxygen and phosphate in the Oyashio Current that slowed after 1998 and show decadal variability linked to the PDO.

9.5 Conclusions

The North Pacific has undergone significant changes in ocean climate during the past three decades. Based on satellite SST measurements, > 75% (64% at $p < 0.05$) of its surface area has undergone significant warming since 1983. The patterns of change suggest that the PDO has been the dominant mode of climate variability in the North Pacific between 1983 and 2012. It is interesting to note that the subarctic Northeast Pacific has experienced little or no overall warming during this period, due to the dominance of a positive PDO prior to 1997 and negative PDO after 1998. However, marked variability in SST has been observed, with episodes of warming in 2002, 2004, and 2010 interspersed with periods of cooling, particularly since 2008 due to the combined effects of La Niña and a negative, cooling PDO phase. These changes and the resulting variability in key ocean parameters are captured in the IGMETS dataset and confirmed by other assessments of ocean conditions in the North Pacific.

Long-term time series in the central, subarctic northeast, and western North Pacific show an increase in phytoplankton biomass during the past 30 years. However, satellite observations suggest that over 65% of the surface of the North Pacific has experienced a decline in chlorophyll concentration since 1998. Available time-

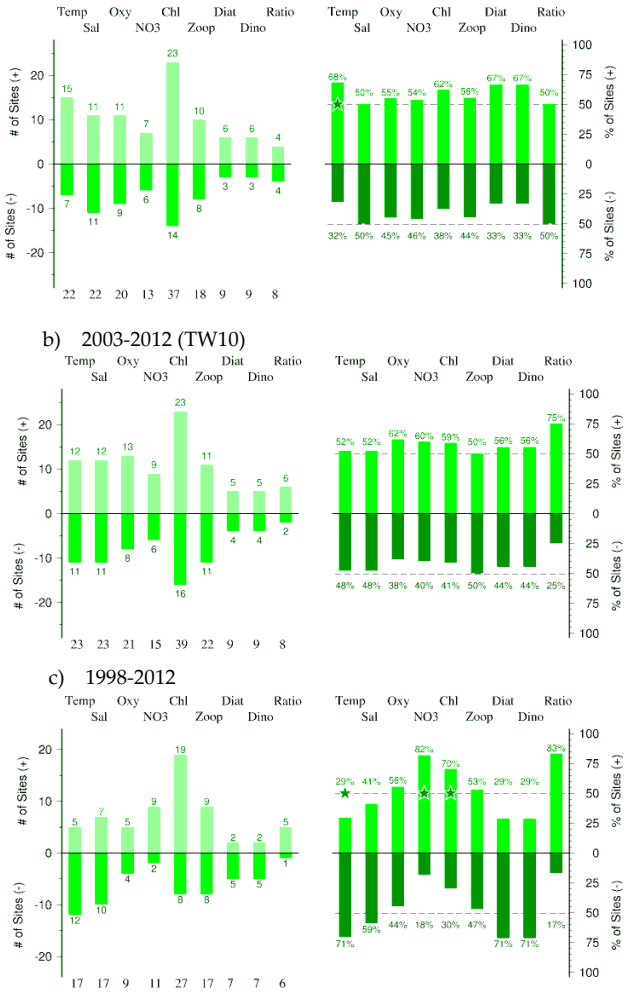

Figure 9.8. Absolute (left) and relative (%, right) frequency of positive and negative correlations between selected *in situ* North Pacific time series variables and corresponding gridded satellite chlorophyll for the 5-, 10-, and 15-year IGMETS time-windows. The 50% relative frequency is indicated by dashed lines in the left panels. A star symbol on the dashed line indicates a statistically significant difference ($p < 0.05$) from 50% positive/negative correlations. See "Methods" chapter for a complete description and methodology used.

series show an increase in zooplankton biomass in the waters off Hawaii, southern Vancouver Island, and the western United States during the last 15 years, but an overall decrease at most other locations, with no significant correlation between zooplankton biomass and chlorophyll. Nutrients, salinity, and dissolved oxygen at the ocean surface appear to be negatively correlated with SST across the North Pacific. Maintaining and, where possible, increasing the number of time series in this region would enhance our ability to identify and assess the impacts of long- and short-term climate change on North Pacific marine ecosystems.

Table 9.3. Regional listing of participating time series for the IGMETS North Pacific. Participating countries: Canada (ca), Colombia (co), China/Hong Kong (hk), Japan (jp), Republic of Korea (kr), Mexico (mx), United Kingdom (uk), and United States (us). Year-spans in red text indicate time series of unknown or discontinued status. IGMETS-IDs in red text indicate time series without a description entry in the Annex A7.

No.	IGMETS-ID	Site or programme name	Year-span	T	S	Oxy	Ntr	Chl	Mic	Phy	Zoo
1	ca-50301	Northern Vancouver Island – Offshore *(Canadian Pacific Coast)*	1983–present	-	-	-	-	-	-	-	X
2	ca-50302	Southern Vancouver Island – Offshore *(Canadian Pacific Coast)*	1979–present	-	-	-	-	-	-	-	X
3	ca-50901	Line P – P26 – OWS Papa *(Northeast North Pacific)*	1956–present	X	X	X	X	X	-	-	X
4	ca-50902	Line P – P20 *(Northeast North Pacific)*	1968–present	X	X	X	X	X	-	-	X
5	ca-50903	Line P – P16 *(Northeast North Pacific)*	1968–present	X	X	X	X	X	-	-	X
6	ca-50904	Line P – P12 *(Northeast North Pacific)*	1968–present	X	X	X	X	X	-	-	X
7	ca-50905	Line P – P08 *(Northeast North Pacific)*	1968–present	X	X	X	X	X	-	-	X
8	ca-50906	Line P – P04 *(Northeast North Pacific)*	1968–present	X	X	X	X	X	-	-	X
9	co-30110	REDCAM Department of Cauca *(Colombia Coastline)*	2002–present	X	X	X	-	-	-	-	-
10	co-30111	REDCAM Department of Choco *(Colombia Coastline)*	2002–present	X	X	X	-	-	-	-	-
11	co-30112	REDCAM Department of Narino *(Colombia Coastline)*	2002–present	X	X	X	-	-	-	-	-
12	co-30113	REDCAM Department of Valle del Cauca *(Colombia Coastline)*	2002–present	X	X	X	-	-	-	-	-
13	hk-30101	Hong Kong EPD Marine Water Quality Monitoring *(Hong Kong)*	1991–present	X	X	X	X	X	-	X	-
14	jp-30104	PM Line *(Japan Sea)*	1972–2002 (?)	-	-	-	-	-	-	-	X
15	jp-30101	Kuroshio Current *(Western North Pacific)*	1951–2002 (?)	X	-	-	-	-	-	-	X
16	jp-30102	Oyashio Current *(Western North Pacific)*	1951–2004 (?)	X	-	-	-	-	-	-	X
17	jp-30103	Oyashio–Kuroshio Transition *(Western North Pacific)*	1951–2004 (?)	X	-	-	-	-	-	-	X
18	jp-30201	Bering Sea – HUFO *(Bering Sea)*	1955–2006 (?)	-	-	-	-	-	-	-	X
19	jp-30202	Central North Pacific – HUFO *(North Pacific)*	1979–2000 (?)	-	-	-	-	-	-	-	X

No.	IGMETS-ID	Site or programme name	Year-span	T	S	Oxy	Ntr	Chl	Mic	Phy	Zoo
20	jp-30401	JMA East China Sea *(East China Sea)*	1965–present	X	X	X	X	-	-	-	-
21	jp-30402	JMA Japan Sea *(Japan Sea)*	1964–present	X	X	X	X	X	-	-	-
22	jp-30403	JMA Philippine Sea *(Philippine Sea)*	1965–present	X	X	X	X	X	-	-	-
23	jp-30404	JMA Southeast Hokkaido *(Northwest North Pacific)*	1965–present	X	X	X	X	X	-	-	-
24	jp-30405	JMA 137E Transect *(Lower Philippine Sea)*	1970–present	X	X	X	X	-	-	-	-
25	kr-30103	Korea East *(Japan Sea)*	1965–2006 (?)	-	-	-	-	-	-	-	X
26	kr-30104	Northeast Korea – Russian Sampling *(Japan Sea)*	1988–2007 (?)	-	-	-	-	-	-	-	X
27	kr-30102	Korea South *(East China Sea)*	1965–2006 (?)	-	-	-	-	-	-	-	X
28	kr-30101	Korea West *(Yellow Sea)*	1965–2006 (?)	-	-	-	-	-	-	-	X
29	mx-30101	IMECOCAL Northern Baja – NB *(Southeastern North Pacific)*	1998–present	-	-	-	-	-	-	-	X
30	mx-30102	IMECOCAL Southern Baja – SB *(Southeastern North Pacific)*	1998–present	-	-	-	-	-	-	-	X
31	uk-40201	Pacific CPR – Southern Bering Sea *(Northeastern North Pacific)*	2000–present	-	-	-	-	X	-	X	X
32	uk-40202	Pacific CPR – Aleutian Shelf *(Northeastern North Pacific)*	2000–present	-	-	-	-	X	-	X	X
33	uk-40203	Pacific CPR – Western Gulf of Alaska *(Northeastern North Pacific)*	2000–present	-	-	-	-	X	-	X	X
34	uk-40204	Pacific CPR – Alaskan Shelf *(Northeastern North Pacific)*	2004–present	-	-	-	-	X	-	X	X
35	uk-40205	Pacific CPR – Cook Inlet *(Northeastern North Pacific)*	2004–present	-	-	-	-	X	-	X	X
36	uk-40206	Pacific CPR – Northern Gulf of Alaska *(Northeastern North Pacific)*	1997–present	-	-	-	-	X	-	X	X
37	uk-40207	Pacific CPR – Offshore BC *(Northeastern North Pacific)*	1997–present	-	-	-	-	X	-	X	X
38	uk-40208	Pacific CPR – BC Shelf *(Northeastern North Pacific)*	2000–present	-	-	-	-	X	-	X	X
39	us-10201	Hawaii Ocean Time series – HOT *(Central North Pacific)*	1988–present	X	X	X	X	X	X	-	X

No.	IGMETS-ID	Site or programme name	Year-span	T	S	Oxy	Ntr	Chl	Mic	Phy	Zoo
40	us-10301	USC WIES San Pedro Ocean Time series – SPOT *(Eastern North Pacific)*	2000–present	X	X	X	X	X	-	-	-
41	us-30401	Central Bay *(San Francisco Bay)*	1978–present	X	X	X	X	X	X	X	-
42	us-50301	CalCOFI California Current region – CC *(California Current)*	1951–present	-	-	-	-	-	-	-	X
43	us-50302	CalCOFI Southern California region – SC *(Southern California Current)*	1951–present	-	-	-	-	-	-	-	X
44	us-50401	Western Kodiak Island – EcoFOCI *(Gulf of Alaska)*	1981–present	-	-	-	-	-	-	-	X
45	us-50501	Newport Line NH-5 *(Newport-Oregon)*	1969–present	X	X	-	X	X	-	-	X
46	us-50601	EMA-1: Eastern Bering Sea – East *(Southeastern Bering Shelf)*	1999–present	X	X	X	X	X	-	-	X
47	us-50602	EMA-2: Eastern Bering Sea – West *(Southwestern Bering Shelf)*	2002–present	X	X	X	X	X	-	-	X
48	us-50603	EMA-3: Northern Bering Sea *(Northern Bering Sea)*	2002–present	X	X	X	X	X	-	-	X
49	us-60106	NERRS Elkhorn Slough *(Northeastern North Pacific)*	2001–present	X	X	X	X	X	-	-	-
50	us-60113	NERRS Kachemak Bay *(Northeastern North Pacific)*	2003–present	X	X	X	X	X	-	-	-
51	us-60120	NERRS Padilla Bay *(Northeastern North Pacific)*	2009–present	X	X	X	X	X	-	-	-
52	us-60123	NERRS San Francisco Bay *(Northeastern North Pacific)*	2008–present	X	X	X	X	X	-	-	-
53	us-60124	NERRS South Slough *(Northeastern North Pacific)*	2002–present	X	X	X	X	X	-	-	-
54	us-60125	NERRS Tijuana River *(Northeastern North Pacific)*	2004–present	X	X	X	X	X	-	-	-

9.6 References

Batten, S. D., and Crawford, W. R. 2005. The influence of coastal origin eddies on oceanic plankton distribution in the eastern Gulf of Alaska. Deep-Sea Research II, 52: 991–1009.

Bowditch, N. 2002. American Practical Navigator: An Epitome of Navigation and Nautical Astronomy. Publication No. 9. National Imagery and Mapping Agency, Bethesda, MD. 879 pp.

Chandler, P. C., King, S. A., and Perry, R. I. (Eds). 2015. State of the physical, biological and selected fishery resources of Pacific Canadian marine ecosystems in 2014. Canadian Technical Report of Fisheries and Aquatic Science, 3131. 211 pp.

Chiba, S., Batten, S., Sasaoka, K., Sasai, Y., and Sugisaki, K. 2012. Influence of the Pacific Decadal Oscillation on phytoplankton phenology and community structure in the western North Pacific. Geophysical Research Letters, 39: L15603, doi:10.1029/2012GL052912.

Cloern, J. E., Hieb, K. A., Jacobsen, T., Sanso, B., Di Lorenzo, E., Stacey, M. T., Largier, J. L., *et al*. 2010. Biological communities in San Francisco Bay track large-scale climate forcing over the North Pacific. Geophysical Research Letters, 37: L21602, http://dx.doi.org/10.1029/2010GL044774.

Cravatte, S., Delcroix, T., Zhang, D., McPhaden, M. J., and Leloup, J. 2009. Observed freshening and warming of the western Pacific warm pool. Climate Dynamics, 33: 565–589, doi:10.1007/s00382-009-0526-7.

DFO. 2000. http://waves-vagues.dfo-mpo.gc.ca/Library/324619.pdf.

DFO. 2001. http://waves-vagues.dfo-mpo.gc.ca/Library/324620.pdf.

DFO. 2002. http://waves-vagues.dfo-mpo.gc.ca/Library/265807.pdf.

DFO. 2003. http://waves-vagues.dfo-mpo.gc.ca/Library/324622.pdf.

DFO. 2005. http://waves-vagues.dfo-mpo.gc.ca/Library/324624.pdf.

DFO. 2006. http://www.dfo-mpo.gc.ca/Library/324625.pdf.

DFO. 2007. http://www.dfo-mpo.gc.ca/Library/328475.pdf.

DFO. 2008. http://www.dfo-mpo.gc.ca/csas-sccs/publications/SAR-AS/2008/SAR-AS2008_028_e.pdf.

DFO. 2009. http://www.dfo-mpo.gc.ca/csas-sccs/publications/SAR-AS/2009/2009_030_e.pdf.

DFO. 2010. http://www.dfo-mpo.gc.ca/csas-sccs/publications/sar-as/2010/2010_034_e.pdf.

DFO. 2011. http://www.dfo-mpo.gc.ca/csas-sccs/Publications/SAR-AS/2011/2011_032-eng.pdf.

Di Lorenzo, E., Combes, V., Keister, J. E., Strub, P. T., Thomas, A. C., Franks, P. J. S., Ohman, M. D., *et al*. 2013. Synthesis of Pacific Ocean climate and ecosystem dynamics. Oceanography, 26(4): 69–81.

Di Lorenzo, E., Fiechter, J., Schneider, N., Bracco, A., Miller, A. J., Franks, P. J. S., Bograd, S. ., *et al*. 2009. Nutrient and salinity decadal variations in the central and eastern North Pacific. Geophysical Research Letters, 36: L14601, doi:10.1029/2009GL038261.

Di Lorenzo, E., Schneider, N., Cobb, K. M., Franks, P. J. S., Chhak, K., Miller, A. J., McWilliams, J. C., *et al*. 2008. North Pacific Gyre Oscillation links ocean climate and ecosystem change. Geophysical Research Letters, 35: L08607, doi:10.1029/2007GL032838.

Doney, S. C., Ruckelshaus, M., Duffy, J. E., Barry, J. P., Chan, F., English, C. A., Galindo, H. M., *et al*. 2012. Climate change impacts on marine ecosystems. Annual Review of Marine Science, 4: 11–37, doi:10.1146/annurev-marine-041911-111611.

Dutkiewicz, S., Follows, M., Marshall, J., and Gregg, W. W. 2001. Interannual variability of phytoplankton abundances in the North Atlantic. Deep-Sea Research II, 48: 2323–2344.

Eakins, B. W., and Sharman, F. 2010. Volumes of the World's Oceans from ETOPO1. NOAA National Geophysical Data Center, Boulder, CO.

Feely, R. A., Sabine, C. L., Hernandez-Ayon, J. M., Ianson, D., and Hales, B. 2008. Evidence for upwelling of corrosive "acidified" water onto the Continental Shelf. Science, 320: 1490–1492.

Haigh, R., Ianson, D., Holt, C. A., Neate, H. E., and Edwards, A. M. 2015. Effects of ocean acidification on temperate coastal marine ecosystems and fisheries in the Northeast Pacific. PLoS One, 10(2): e0117533, https://doi:10.1371/journal.pone.0117533.

Hosoda, S., Suga, T., Shikama, N., and Mizuno, K. 2009. Global surface layer salinity change detected by Argo and its implication for hydrological cycle intensification. Journal of Oceanography, 65: 579–586.

Johnson, K. W., Miller, L. A., Sutherland, N. E., and Wong, C. S. 2005. Iron transport by mesoscale Haida eddies in the Gulf of Alaska. Deep-Sea Research II, 52: 933–953.

Karl, D. M. 1999. A sea of change: biogeochemical variability in the North Pacific Subtropical Gyre. Ecosystems, 2(3): 181–214.

Litzow, M. A., and Mueter, F. J. 2014. Assessing the ecological importance of climate regime shifts: An approach from the North Pacific Ocean. Progress in Oceanography, 120: 110–119, http://dx.doi.org/10.1016/j.pocean.2013.08.003.

Longhurst, A. 2007. Ecological Geography of the Sea, 2nd edn. Elsevier, San Diego. 398 pp.

Mantua, J. N., Hare, S. R., Zhang, Y., Wallace, J. M., and Francis, R. C. 1997. A Pacific interdecadal climate oscillation with impacts on salmon production. Bulletin of the American Meteorological Society, 78: 1069–1080.

Matear, R. J., Chamberlain, M. A, Sun, C., and Feng, M. 2015. Climate change projection for the western tropical Pacific Ocean using a high-resolution ocean model: Implications for tuna fisheries. Deep-Sea Research II: Topical Studies in Oceanography, 113: 22–46, http://dx.doi.org/10.1016/j.dsr2.2014.07.003.

McKinnell, S. M., and Dagg, M. J. (Eds). 2010. Marine Ecosystems of the North Pacific Ocean, 2003-2008. PICES Special Publication, 4. 393 pp.

Minobe, S., Kuwano-Yoshida, A., Komori, N., Xie, S-P., and Small, R. J. 2008. Influence of the Gulf Stream on the troposphere. Nature, 452: 206–209.

Nakanowatari, T., Ohshima, K. I., and Wakatsuchi, M. 2007. Warming and oxygen decrease of intermediate water in the northwestern North Pacific, originating from the Sea of Okhotsk, 1955–2004. Geophysical Research Letters, 34: L04602, doi:10.1029/2006GL028243.

Ohshima, K. I., Nakanowatari, T., Riser, S., Volkov, Y., and Wakatsuchi, M. 2014. Freshening and dense shelf water reduction in the Okhotsk Sea linked with sea ice decline. Progress in Oceanography, 126: 71–79, http://dx.doi.org/10.1016/j.pocean.2014.04.020.

Park, J-Y., Kug, J-S. F., Park, J., Yeh, S-W., and Jang, C. J. 2011. Variability of chlorophyll associated with El Niño–Southern Oscillation and its possible biological feedback in the equatorial Pacific. Journal of Geophysical Research, 116: C10001, doi:10.1029/2011JC007056.

Park, J-Y., Yoon, J-H , Youn, Y-H., and Vivier, F. 2012. Recent warming in the Western North Pacific in relation to rapid changes in the atmospheric circulation of the Siberian High and Aleutian Low systems. Journal of Climate, 25: 3476–3493, doi:http://dx.doi.org/10.1175/2011JCLI4142.1.

Perry, R. I., and Masson, D. 2013. An integrated analysis of the marine social-ecological system of the Strait of Georgia, Canada over the past four decades, and development of a regime shift index. Progress in Oceanography, 115: 14–27.

PICES. 2004. Marine Ecosystems of the North Pacific. PICES Special Publication, 1. 280 pp.

Polovina, J. J., Howell, E. A., and Abecassis, M. 2008. Ocean's least productive waters are expanding. Geophysical Research Letters 35: L03618, doi:10.1029/2007GL031745.

Rykaczewski, R. R., and Dunne, J. P. 2010. Enhanced nutrient supply to the California Current Ecosystem with global warming and increased stratification in an earth system model. Geophysical Research Letters, 37: L21606, doi: 10.1029/2010GL045019.

Signorini, S. R., Franz, B. A., and McClain, C. R. 2015. Chlorophyll variability in the oligotrophic gyres: mechanisms, seasonality and trends. Frontiers in Marine Science, 2(1): doi: 10.3389/fmars.2015.00001.

Trenberth, K. E., and Hurrell, J. W. 1994. Decadal atmosphere-ocean variations in the Pacific. Climate Dynamics, 9: 303–319.

Vantrepotte, V., and Mélin, F. 2009. Temporal variability of 10-year global SeaWiFS time series of phytoplankton chlorophyll *a* concentration. ICES Journal of Marine Science, 66(7): 1547-1556, doi:https://doi.org/10.1093/icesjms/fsp107.

Wallace, J. M., and Gutzler, D. S. 1981. Teleconnections in the Geopotential Height Field during the Northern Hemisphere Winter. Monthly Weather Review, 109: 784–812.

Wu, L., Cai, W., Zhang, L., Nakamura, H., Timmermann, A., Joyce, T., McPhaden, M. J., *et al*. 2012. Enhanced warming over the global subtropical western boundary currents. Nature Climate Change, 2: 161–166.

Zenk, W. 2001. Abyssal currents. *In* Encyclopedia of Ocean Sciences, pp. 12–28. Ed. by J. H. Steele, K. K. Turekian, and S. A. Thorpe. Elsevier. 3399 pp.

Zhang, Y., Wallace, J. M., and Battisti, D. S. 1997. ENSO-like interdecadal variability: 1900-93. Journal of Climate, 10: 1004–1020.

10 Global Overview

Laura Lorenzoni, Todd D. O'Brien, Kirsten Isensee, Heather Benway, Frank E. Muller-Karger, Peter A. Thompson, Michael Lomas, and Luis Valdés

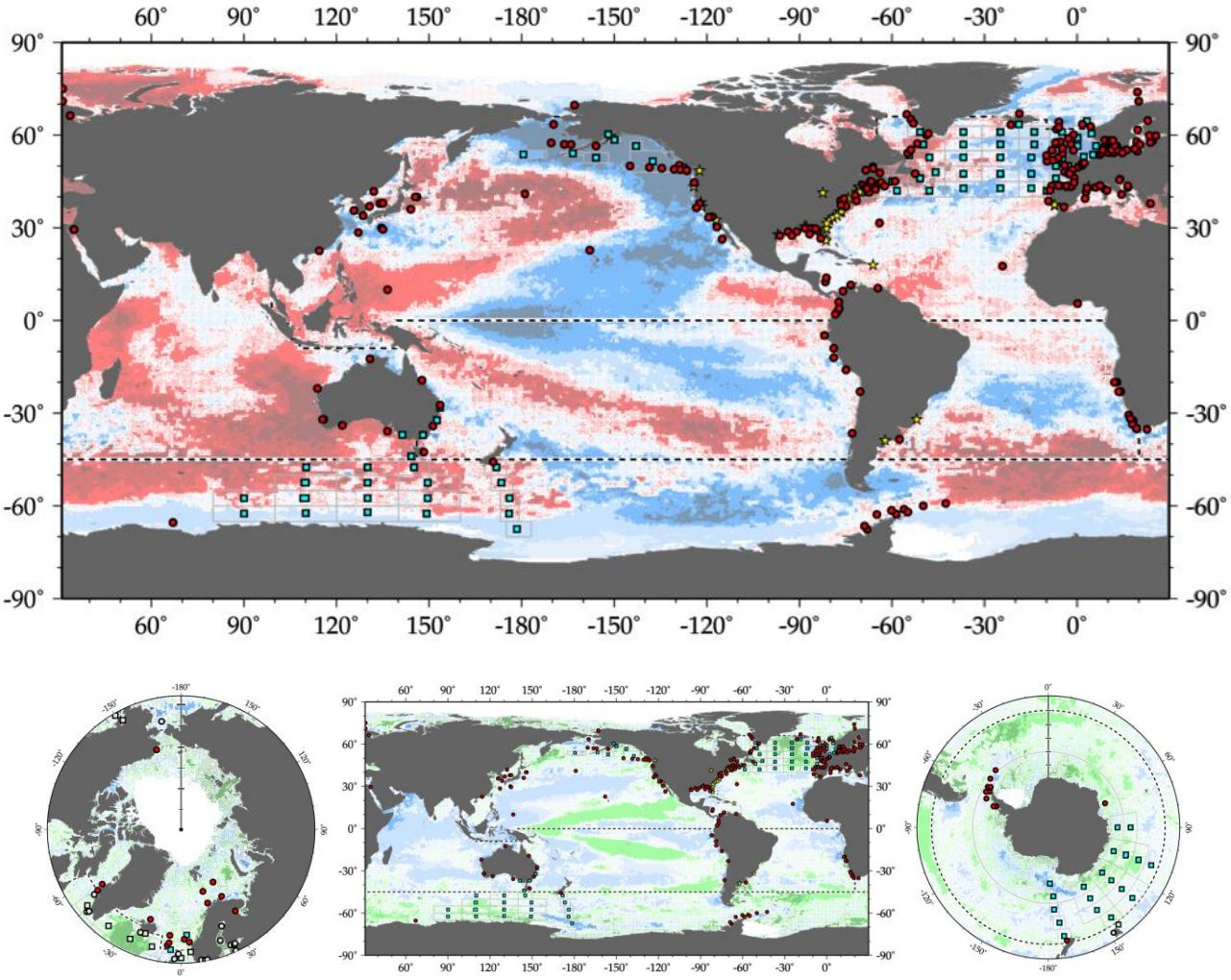

Figure 10.1. Maps of IGMETS-participating time series on a background of 10-year (2003–2012) sea surface temperature trends (top panel, see also Figure 10.4a) or on a background of 10-year sea surface chlorophyll trends (bottom panel, see also Figure 10.4b). These maps show 344 time series (coloured symbols of any type), of which 71 were from Continuous Plankton Recorder subareas (blue boxes) and 46 were from estuarine areas (yellow stars). Dashed lines indicate boundaries between IGMETS regions. Additional information on the sites in this study is presented in the Annex.

Participating time-series investigators

Eric Abadie, Jose L. Acuna, M. Teresa Alvarez-Ossorio, Anetta Ameryk, Jeff Anning, Elvire Antajan, Georgia Asimakopoulou, Yrene Astor, Angus Atkinson, Patricia Ayon, Alexey Babkov, Hermann Bange, Ana Barbosa, Nick Bates, Uli Bathmann, Sonia Batten, Beatrice Bec, Radhouan Ben-Hamadou, Claudia Benitez-Nelson, Carla F. Berghoff, Robert Bidigare, Antonio Bode, Maarten Boersma, Angel Borja, Alexander Brearley, Eileen Bresnan, Cecilie Broms, Juan Bueno, Mario O. Carignan, Craig Carlson, David Caron, Jacob Carstensen, Gerardo Casas, Benoit Casault, Claudia Castellani, Fabienne Cazassus, Georgina Cepeda, Paulo Cesar Abreu, Jacky Chauvin, Sanae Chiba, Luis Chicharo, Epaminondas Christou, Matthew J. Church, Andrew Clarke, James E. Cloern, Rudi Cloete, Nathalie Cochennec-Laureau, Andrew Cogswell, Amandine Collignon, Yves Collos, Frank Coman, Maria Constanza Hozbor, Kathryn Cook, Dolores Cortes, Joana Cruz, Daniel Cucchi Colleoni, Kim Currie, Padmini Dalpadado, Claire Davies, Alejandro de la Sota, Alessandra de Olazabal, Laure Devine, Emmanuel Devred, Iole Di Capua, Rita Domingues, Anne Doner, John E. Dore, Antonina dos Santos, Hugh Ducklow, Janet Duffy-Anderson, Joerg Dutz, Martin Edwards, Lisa Eisner, Joao Pedro Encarnacao, Ruth Eriksen, Ruben Escribano, Luisa Espinosa, Tone Falkenhaug, Ana Faria, Ed Farley, Maria Luz Fernandez de Puelles, Susana Ferreira, Bjorn Fiedler, Jennifer L. Fisher, James Fishwick, Serena Fonda-Umani, Almudena Fontan, Janja France, Javier Franco, Jed Fuhrman, Mitsuo Fukuchi, Eilif Gaard, Moira Galbraith, Peter Galbraith, Helena Galvao, Pep Gasol, Amatzia Genin, Astthor Gislason, Anne Goffart, Renata Goncalves, Rafael Gonzalez-Quiros, Gabriel Gorsky, Annika Grage, Hafsteinn Gudfinnsson, Kristinn Gudmundsson, Valeria Guinder, Troy Gunderson, David Hanisko, Jon Hare, Roger Harris, Erica Head, Jean-Henri Hecq, Simeon Hill, Richard Horaeb, Graham Hosie, Jenny Huggett, Keith Hunter, Anda Ikauniece, Arantza Iriarte, Masao Ishii, Solva Jacobsen, Marie Johansen, Catherine Johnson, Jacqueline Johnson, Young-Shil Kang, David M. Karl, So Kawaguchi, Kevin Kennington, Diane Kim, Georgs Kornilovs, Arne Kortzinger, Alexandra Kraberg, Anja Kreiner, Nada Krstulovic, Takahashi Kunio, Inna Kutcheva, Michael Landry, Bertha E. Lavaniegos, Aitor Laza-Martinez, Jesus Ledesma Rivera, Alain Lefebvre, Sirpa Lehtinen, Maiju Lehtiniemi, Ezequiel Leonarduzzi, Ricardo M. Letelier, William Li, Priscilla Licandro, Michael Lomas, Christophe Loots, Angel Lopez-Urrutia, Laura Lorenzoni, Roger Lukas, Vivian Lutz, Dave Mackas, Jorge Marcovecchio, Francesca Margiotta, Piotr Margonski, Roberta Marinelli, Jennifer Martin, Douglas Martinson, Daria Martynova, Daniele Maurer, Maria Grazia Mazzocchi, Sam McClatchie, Felicity McEnnulty, Webjorn Melle, Jesus M. Mercado, Michael Meredith, Claire Meteigner, Ana Miranda, Graciela N. Molinari, Nora Montoya, Pedro Morais, Cheryl A. Morgan, Patricija Mozetic, Teja Muha, Frank Muller-Karger, Jeffrey Napp, Florence Nedelec, Ruben Negri, Vanessa Neves, Todd D. O'Brien, Clarisse Odebrecht, Mark Ohman, Lena Omli, Emma Orive, Luciano Padovani, Hans Paerl, Marcelo Pajaro, Evgeny Pakhomov, Kevin Pauley, S.A. Pedersen, Ben Peierls, Pierre Pepin, Myriam Perriere Rumebe, Ian Perry, Tim Perry, William T. Peterson, Roger Pettipas, David Pilo, Sophie Pitois, Al Pleudemann, Stephane Plourde, Arno Pollumae, Dwayne Porter, Lutz Postel, Nicole Poulton, Igor Primakov, Regina Prygunkova, A. Miguel P. Santos, Andy Rees, Michael Reetz, Beatriz Reguera, Malcolm Reid, Christian Reiss, Jasmin Renz, Mickael Retho, Marta Revilla, Maurizio Ribera, Anthony Richardson, Malcolm Robb, Marie Robert, Don Robertson, Karen Robinson, M. Carmen Rodriguez, Andrew Ross, Gunta Rubene, M. Guillermina Ruiz, Tatiana Rynearson, Sei-ichi Saitoh, Rafael Salas, Danijela Santic, Diana Sarno, Michael Scarratt, Renate Scharek, Oscar Schofield, Mary Scranton, Valeria Segura, Sergio Seoane, Stefanija Sestanovic, Yonathan Shaked, Volker Siegel, Mike Sieracki, Joe Silke, Ricardo I. Silva, Ioanna Siokou-Frangou, Milijan Sisko, Anita Slotwinkski, Tim Smyth, Mladen Solic, Dominique Soudant, Carla Spetter, Jeff Spry, Michel Starr, Debbie Steinberg, Deborah Steinberg, Lars Stemmann, Rowena Stern, Solvita Strake, Patrik Stromberg, Glen Tarran, Gordon Taylor, Maria Alexandra Teodosio, Peter Thompson, Robert Thunell, Valentina Tirelli, Others to be added soon, Mark Tonks, Sakhile Tsotsobe, Ibon Uriarte, Julian Uribe-Palomino, Nikolay Usov, Luis Valdés, Victoriano Valencia, Marta M. Varela, Hugh Venables, Marina Vera Diaz, Hans Verheye, Olja Vidjak, Fernando Villate, Maria Delia Viñas, Norbert Wasmund, Robert Weller, George Wiafe, Claire Widdicombe, Karen H. Wiltshire, Malcolm Woodward, Lidia Yebra, Kedong Yin, Cordula Zenk, Soultana Zervoudaki, and Adriana Zingone

This chapter should be cited as: Lorenzoni, L., O'Brien, T. D., Isensee, K., Benway, H., Muller-Karger, F. E., Thompson, P. A., Lomas, M., *et al.* 2017. Global Overview. I*n* What are Marine Ecological Time Series telling us about the ocean? A status report, pp. 171–190. Ed. by T. D. O'Brien, L. Lorenzoni, K. Isensee, and L. Valdés. IOC-UNESCO, IOC Technical Series, No. 129. 297 pp.

10.1 Introduction

The ocean's biological, physical, and chemical characteristics vary across a range of temporal and spatial scales in response to different driving forces. These include short-term and seasonal localized phenomena, such as coastal upwelling and river discharge, as well as meso- and large-scale features like eddies, ocean currents, and the global thermohaline circulation – the conveyor belt (Figure 10.2). The ocean also responds to large-scale climate cycles (e.g. Pacific Decadal Oscillation, El Niño–Southern Oscillation, North Atlantic Oscillation). Changes induced by humans add yet another layer of complexity. Monitoring changes in global marine biological and biogeochemical variables and exploring their relationships with natural variability and anthropogenic forcing is fundamental to improving our capacity to predict how the ocean may respond to future changes as well as associated impacts on marine ecosystem services (Worm *et al*., 2006; Hoegh-Guldberg and Bruno, 2010; Overland *et al*., 2010; Doney *et al*., 2014).

Global ocean phytoplankton biomass and sea surface temperature (SST) have been investigated with a variety of techniques, including satellites and *in situ* sampling. These two variables have significant effects on ecosystem structure and functioning and have been observed to change in response to varying ocean conditions (IPCC, 2013). Several authors have suggested that global phytoplankton biomass has declined over the past several decades in nearly all ocean regions due to increasing SST and stratification (Behrenfeld *et al*., 2006; Henson *et al*., 2010; Vantrepotte and Mélin, 2009, 2011; Beaulieu *et al*., 2013; IPCC, 2013; Siegel *et al*., 2013), while others point to an increase in the North Atlantic where long time series exist (McQuatters-Gollop *et al*., 2011). The relationship among SST, chlorophyll and stratification, however, is not simple; therefore, it is difficult to correlate changes in one with changes in the other on a global scale (Dave and Lozier, 2013; Behrenfeld *et al*., 2015).

Maps of trends help identify regions that experience significant changes over different time-scales and can also provide information on rates of change. Maps of multiple variables help elucidate possible causes for the alterations. Changes are constantly occurring on a global scale; some are related to anthropogenic forcing, and some variables will show changes faster than others, resulting in a widespread debate on the length of time required to observe trends related to climate signals (Henson *et al*., 2010, 2016; Henson, 2014).

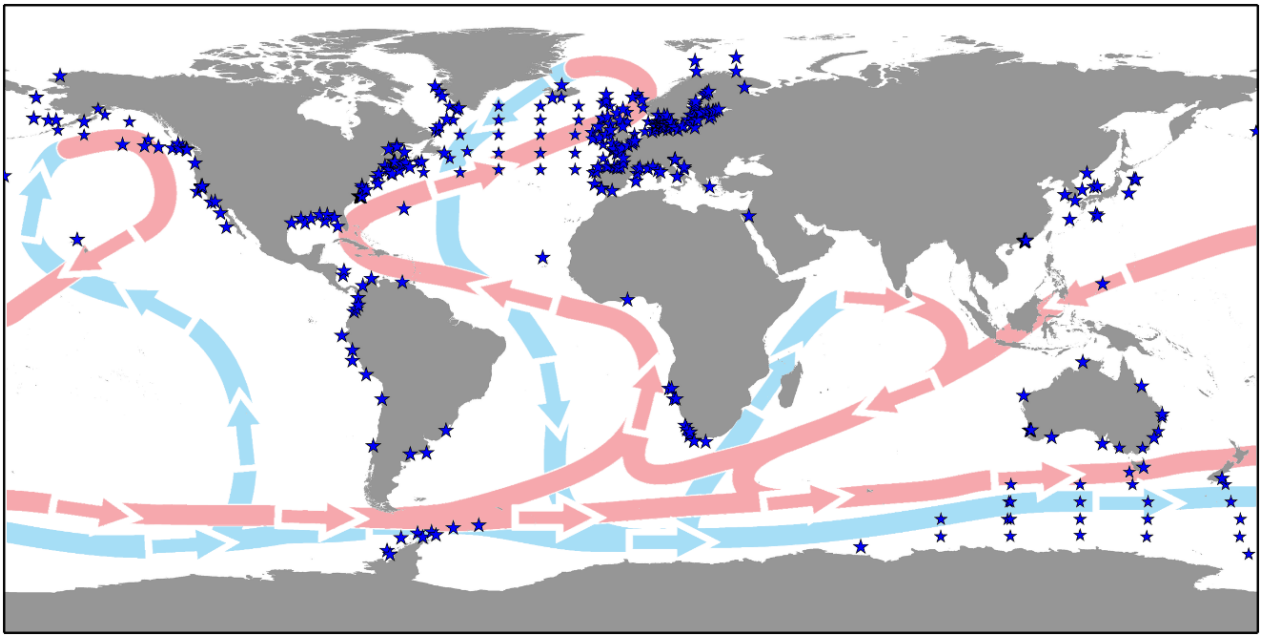

Figure 10.2. Map showing stylized, major global currents that interconnect the world oceans, also known as "the conveyor belt". Blue arrows indicate generally cooler water currents and red arrows indicate generally warmer currents. The dark blue stars indicate the locations of the 344 time series that participated in this study. Additional information on these time series is presented in the Annex.

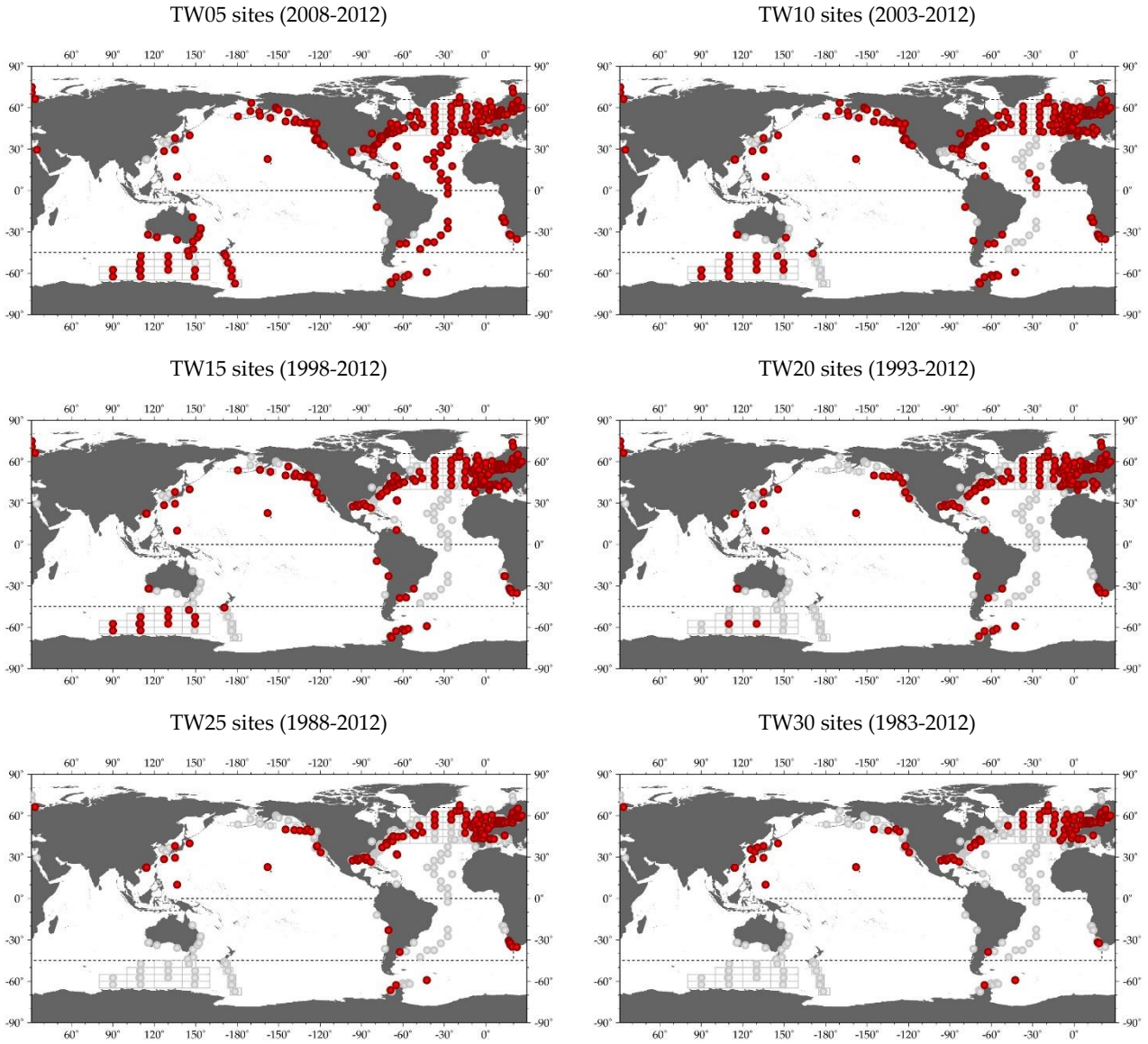

Figure 10.3. Panel of maps showing locations of IGMETS-participating time series based on time-window qualification. Red symbols indicate time-series sites with at least one biological or biogeochemical variable (i.e. excluding temperature- and salinity-only time series) that qualified for that time-window (e.g. TW05, TW20). Light gray symbols indicate sites that did not have enough data from the given time-window to be included in that analysis.

Globally, there are at least 344 ship-based biogeochemical time series that span different lengths and windows of time (Figure 10.1). These time series represent one of the most valuable tools scientists have to characterize and quantify ocean carbon fluxes, biogeochemical processes, and their links to changing climate (Karl, 2010; Chavez *et al*., 2011; Church *et al*., 2013). Coupling these *in situ* biogeochemical measurements and plankton data with satellite observations improves the understanding of changes in the biological, physical, and biogeochemical properties of the global oceans. Satellite data provide an additional layer of information about changing ocean conditions and ecosystems and can help scale-up the relatively sparse shipboard datasets to achieve a broader regional and/or global perspective.

In this chapter, we aim to examine changes in the global oceans, explore possible connections between ocean basins, and identify areas that show significant changes over temporal periods of 10, 15, 20, and 30 years ("time-windows"; the IGMETS "time-windows" analysis is described in Chapter 2). A shorter 5-year time-window analysis is also available to observe short-term fluctua-

tions, though these may not be statistically significant for climate change-related trends. Thirty years of observations provide information on the overall direction of change (if any) of the different ocean variables and present a good basis to start distinguishing between natural variability and long-term, human-induced trends (Henson *et al*., 2010; Henson, 2014). In terms of available biogeochemical and plankton time series, there are tenfold more 5-year time series than 30-year time series. However, going back in time (20 years), most of the time-series sites are located in the North Atlantic (Figure 10.3).

Short time-windows, such as five years, provide information on the speed of some of the changes that are being observed in the ocean and offer insight on short-term fluctuations. The magnitude of natural variability in many biogeochemical variables can mask anthropogenic trends, as is shown in the regional chapters. The ecological and economic consequences of such changes are important, particularly with regard to marine ecosystem goods and services. Analyzing changes in specific time-windows facilitates comparison of trends in different areas and detection of decadal and multidecadal climatic drivers. Clearly, the start and end dates chosen for trend analyses may influence the assessment of the rates of change (IPCC, 2013; Karl *et al*., 2015).

It is not possible yet to fully quantify how much of the ocean's variability is due to anthropogenic drivers; hence, the importance of sustained ocean time-series observations. Only a fraction of the biogeochemical time series around the world reaches or exceeds observations of more than two decades (Figure 10.3). Indeed, many ship-based biogeochemical time-series measurements (e.g. ocean CO_2 system parameters, nutrient concentrations), particularly in the southern hemisphere, were initiated only in the past decade. These various time series provide a "baseline" against which to detect areas that have undergone rapid change.

10.2 General patterns of temperature and phytoplankton biomass

Significant trends in SST were visible at the global scale (over 79% of the ocean) during the past three decades (Figure 10.4a; Table 10.1). In the 30-year time-window (1983–2012), 79.9% (69.8% at $p < 0.05$) of the world's oceans increased in temperature, while 20.1% (13.2% at $p < 0.05$) registered a decrease (Table 10.1). The most significant warming was observed in the Atlantic and Indian oceans (Figure 10.4a; see also the respective regional chapters). Comparing the changes, the positive trend was +0.1 to +0.5°C decade^{-1}. Areas that cooled down had rates of less than –0.1°C decade^{-1}. These observations generally agree with published results that highlight increases in ocean temperatures of ca. 0.1°C decade^{-1} (IPCC, 2013; Karl *et al*., 2015). Non-significant changes were visible only in the western and tropical Pacific Ocean, a portion of the South Atlantic, and in small areas of the Arctic and Antarctic oceans. The warming trend is also visible over a large portion of the global ocean during the past 10–15 years (49.3% in the past 10 years, with 26.3% at $p < 0.05$; 69.3% over the past 15 years, with 44.8% at $p < 0.05$; Figure 10.4a; Table 10.1).

Satellite data coverage of the Arctic region is poor. Changes in SST show that this area is subject to strong interannual and spatial variability linked to changes in albedo (sea ice cover, soot on snow), atmospheric cloud cover, water vapor and black carbon content, and oceanic heat flux (see Serreze and Barry, 2011; and references therein). Compared to the Antarctic (with the exception of the Western Antarctic Peninsula; Meredith and King, 2005; Steig *et al*., 2009), warming over the Arctic during 1983–2012 has been pronounced (85.3%, with 79.2% at $p < 0.05$). While the Arctic Ocean showed a slowdown in its warming during 2003–2012, positive SST trends have prevailed.

In the Southern Ocean, 55.9% (with 44% at $p < 0.05$) of the region cooled during 1983–2012 (Figures 10.4a and 10.5). Areas of cooling are close to the Antarctic coastline, while the warming is observed farther north. One exception is the area adjacent to the Western Antarctic Peninsula; this warming arises largely from increased air temperatures recorded in the region and reduced sea ice cover (Meredith and King, 2005; Steig *et al*., 2009; Ducklow *et al*., 2013). Variations in the Antarctic SST are associated with changes in the polarity of the Southern Oscillation (SO) and the Southern Annular Mode (SAM), as well as the Antarctic Oscillation Index (AAO) (Yu *et al*., 2012). Some of the colder SSTs observed could be attributed to lower air temperatures reported for a large portion of the Antarctic Peninsula (Kwok and Comiso, 2002; Marshall *et al*., 2014). The driver of these negative SST trends is still being debated (Randel and Wu, 1999; Thompson and Solomon, 2002). Over the 15-year time-window, significant warming was observed in most of the measurable surface of the

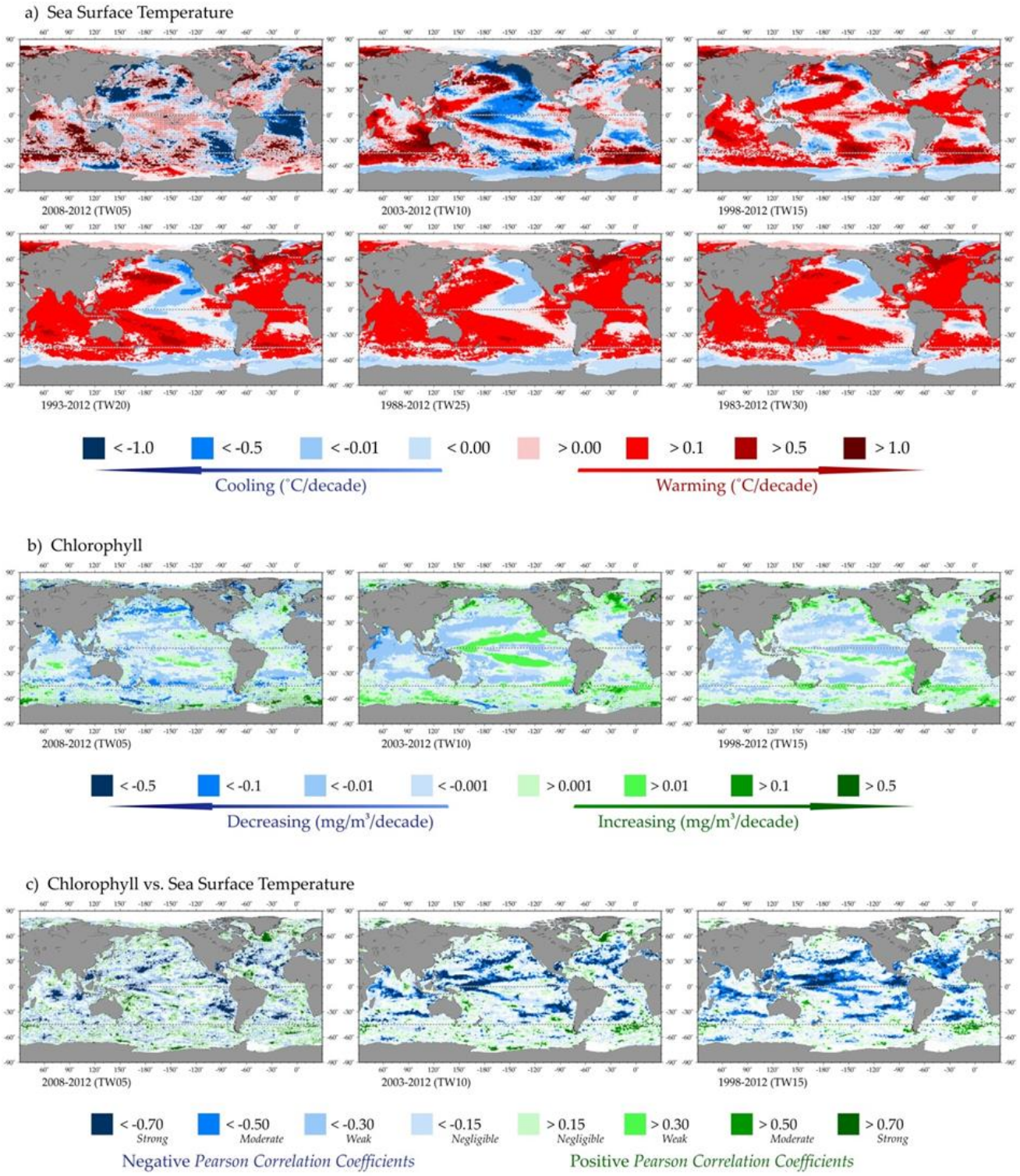

Figure 10.4. Annual trends in global sea surface temperature (SST) (a) and sea surface chlorophyll (CHL) (b) and correlations between chlorophyll and sea surface temperature for each of the standard IGMETS time-windows (c). See "Methods" chapter for a complete description and methodology used.

Southern Ocean (57.5%, of which 40.0% was significant at $p < 0.05$; Table 6.1; Figure 6.2). This pattern reversed over the past 10 years, where ca. 54% of the Southern Ocean exhibited cooling (Table 6.1; Figure 6.2). The Western Antarctic Peninsula was still the exception, where sustained warming was observed in both time-windows (Meredith and King, 2005; Ducklow *et al*., 2013; see Chapter 6). The cooling in the past decade has been, in part, attributed to the ozone hole (Marshall *et al*., 2014).

In the Atlantic Ocean, the subtropical South Atlantic cooling observed over the 30-year time-period is possibly linked to variations in the subtropical anticyclone that arises from decadal-scale, wind-driven ocean temperature fluctuations that occur in a north–south dipole structure (Venegas *et al*., 1997). It could also be a manifestation of an ENSO teleconnection (Nobre and Shukla, 1996; Enfield and Mestas-Nuñez, 2000; Deser *et al*., 2010). The warming of the entire North Atlantic region (99.1%, with 97.3% at $p < 0.05$) over the past three decades has been attributed to both natural and anthropogenic forcings (Knudsen *et al*., 2011; Hoegh-Guldberg *et al*., 2014). Over shorter time-scales, the warming and cooling across the Atlantic were more heterogeneous; during 2003–2012, 50.3% of the Atlantic – the southern north and south parts – warmed, while 49.7% – the northern North and South Atlantic – cooled. In the North Atlantic, air temperatures are largely driven by the NAO, with colder conditions over the Mediterranean and subpolar regions and warmer mid-latitudes (Europe, the north-eastern United States, and parts of Scandinavia) during positive NAO phases (Visbeck *et al*., 2001; Deser *et al*., 2010; Hurrell and Deser, 2010). For this phase, SST reflects a "tripole pattern" with a cold anomaly in the subpolar region, a warm anomaly in the mid-latitudes, and a cold subtropical anomaly between 0 and 30°N (Visbeck *et al*., 2001). The mixed warm/cold trends observed in the North Atlantic over the past decade could be reflecting fluctuations of NAO phases (e.g. strong negative phases in 2009 and 2010, positive in 2012), and possible SST feedback (Hurrell and Deser, 2010; Figure 10.4). The colder SST could also be the result of changes in the Atlantic meridional overturning circulation (AMOC), as suggested by Rahmstorf *et al*. (2015).

Cooling observed in the western and tropical Pacific Ocean over the past 30 years is likely related to interannual–multidecadal oscillations like the El Niño Southern Oscillation (ENSO), the Interdecadal Pacific Oscillation (IPO), and the Pacific Decadal Oscillation (PDO) (Chavez *et al*., 2003, 2011). Pacific SST is strongly correlated with these climate indices (Enfield *et al*., 2001; Alexander *et al*., 2002). The warming and cooling of the Pacific under the changing regimes is not uniform; the central North and South Pacific are out of phase with the eastern Pacific. Chavez *et al*. (2003) identified one "warm" period (from about 1975 to the late 1990s) and two cooler periods (from the early 1950s to about 1975 and from the late 1990s to around 2012). In the 15-year time-window, a particular pattern emerged in the Pacific Ocean with warming across the equatorial Pacific. In 1998–2012, 65.2% of the Pacific warmed (37% at $p < 0.05$), and these areas were located mostly near the equator and in the central North and South Pacific; 34.8% cooled (17.0% at $p < 0.05$; see Figure 7.2). That pattern can be tied to ENSO (Deser *et al*., 2010). However, when analyzing the 10-year time-window, the Pacific exhibited a general cooling over 59% of its area (40% at $p < 0.05$). This is largely linked to La Niña-like conditions (Kosaka and Xie, 2013) and a change in phase of IPO from positive to negative around 1998/1999 (Dong and Zhou, 2014).

The Indian Ocean exhibited strong, consistent warming across all time-windows. From 1983 to 2012, 97.8% of the Indian Ocean warmed (91.9% at $p < 0.05$; Figure 10.4). The warming is associated with a range of climate cycles, including the IPO (Han *et al*., 2014). Over shorter time-scales (10–15 years), while the sustained warming prevailed, the spatial extent decreased (Table 10.1), likely due to variability induced by shorter-term climatic signals (e.g. Indian Ocean Dipole, ENSO).

The chlorophyll (Chl *a*) trends, as derived from satellite data, show that, overall, ca. 60% of the ocean has exhibited decreasing concentrations over the past 15 years (Figures 10.4 and 10.5), which is consistent with previous studies (Polovina *et al*., 2008; Henson *et al*., 2010; Siegel *et al*., 2013; Gregg and Rousseaux, 2014; Signorini *et al*., 2015). In general, changes in chlorophyll are inversely related to SST (Table 10.1; Figure 10.4). The increase in global Chl *a* concentrations observed in the 10-year time-window, relative to the 15-year window, might be attributable to somewhat cooler SSTs. In the Pacific Ocean, in particular, higher Chl *a* concentrations were observed in the subtropics, between roughly 10 and 30°, both north and south of the equator. This region corresponds to areas experiencing cooling and possibly becoming more productive (increased mixed-layer depth), due to La Niña-like conditions (Siegel *et al*., 2013; Signorini *et al*., 2015). The influences of circulation pat

Table 10.1. Relative spatial areas (% of the total region) and rates of change that are showing increasing or decreasing trends in sea surface temperature (SST) for each of the standard IGMETS time-windows. Numbers in brackets indicate the % area with significant ($p < 0.05$) trends. See "Methods" chapter for a complete description and methodology used.

Latitude-adjusted SST data field surface area = 361.9 million km²	**5-year** (2008–2012)	**10-year** (2003–2012)	**15-year** (1998–2012)	**20-year** (1993–2012)	**25-year** (1988–2012)	**30-year** (1983–2012)
Area (%) w/ increasing SST trends ($p < 0.05$)	**52.9%** (*14.8%*)	49.3% (*26.3%*)	**69.3%** (*44.8%*)	**74.1%** (*60.8%*)	**79.4%** (*67.5%*)	**79.9%** (*69.8%*)
Area (%) w/ decreasing SST trends ($p < 0.05$)	47.1% (*16.4%*)	**50.7%** (*29.7%*)	30.7% (*15.0%*)	25.9% (*15.6%*)	20.6% (*13.0%*)	20.1% (*13.2%*)
> 1.0°C decade^{-1} warming ($p < 0.05$)	14.3% (*9.4%*)	4.2% (*4.2%*)	0.6% (*0.6%*)	0.1% (*0.1%*)	0.0% (*0.0%*)	0.0% (*0.0%*)
0.5 to 1.0°C decade^{-1} warming ($p < 0.05$)	14.5% (*3.8%*)	11.3% (*10.6%*)	7.3% (*7.2%*)	6.0% (*6.0%*)	1.9% (*1.9%*)	1.6% (*1.6%*)
0.1 to 0.5°C decade^{-1} warming ($p < 0.05$)	17.4% (*1.3%*)	25.0% (*11.2%*)	46.4% (*35.2%*)	**54.9%** (*51.7%*)	**59.6%** (*58.5%*)	**58.4%** (*58.1%*)
0.0 to 0.1°C decade^{-1} warming ($p < 0.05$)	6.8% (*0.3%*)	8.8% (*0.3%*)	15.1% (*1.8%*)	13.1% (*3.0%*)	17.8% (*7.0%*)	19.9% (*10.1%*)
0.0 to –0.1°C decade^{-1} cooling ($p < 0.05$)	5.3% (*0.1%*)	9.5% (*1.4%*)	12.6% (*2.8%*)	12.5% (*4.1%*)	12.6% (*5.4%*)	14.0% (*7.2%*)
–0.1 to –0.5°C decade^{-1} cooling ($p < 0.05$)	14.9% (*0.9%*)	24.2% (*11.9%*)	16.3% (*10.4%*)	12.3% (*10.4%*)	8.1% (*7.6%*)	6.1% (*5.9%*)
–0.5 to –1.0°C decade^{-1} cooling ($p < 0.05$)	12.2% (*4.1%*)	13.2% (*12.6%*)	1.6% (*1.6%*)	1.1% (*1.1%*)	0.0% (*0.0%*)	0.0 %
> –1.0°C decade^{-1} cooling ($p < 0.05$)	14.6% (*11.2%*)	3.9% (*3.8%*)	0.1% (*0.1%*)	0.0 %	0.0 %	0.0 %

Table 10.2 Relative spatial areas (% of the total region) and rates of change that are showing increasing or decreasing trends in phyto-plankton biomass (CHL) for each of the standard IGMETS time-windows. Numbers in brackets indicate the % area with significant ($p < 0.05$) trends. See "Methods" chapter for a complete description and methodology used.

Latitude-adjusted CHL data field surface area = 361.9 million km²	**5-year** (2008–2012)	**10-year** (2003–2012)	**15-year** (1998–2012)
Area (%) w/ increasing CHL trends ($p < 0.05$)	28.9% (*4.9%*)	40.9% (*16.4%*)	37.8% (*14.6%*)
Area (%) w/ decreasing CHL trends ($p < 0.05$)	**71.1%** (*32.1%*)	**59.1%** (*33.7%*)	**62.2%** (*38.4%*)
> 0.50 mg m^{-3} decade^{-1} increasing ($p < 0.05$)	1.6% (*0.6%*)	0.7% (*0.5%*)	0.9% (*0.8%*)
0.10 to 0.50 mg m^{-3} decade^{-1} increasing ($p < 0.05$)	5.1% (*1.4%*)	4.0% (*2.3%*)	3.7% (*2.8%*)
0.01 to 0.10 mg m^{-3} decade^{-1} increasing ($p < 0.05$)	14.5% (*2.7%*)	22.6% (*11.8%*)	17.2% (*8.9%*)
0.00 to 0.01 mg m^{-3} decade^{-1} increasing ($p < 0.05$)	7.7% (*0.2%*)	13.5% (*1.8%*)	16.0% (*2.1%*)
0.00 to –0.0 mg m^{-3} decade^{-1} decreasing ($p < 0.05$)	9.6% (*0.8%*)	17.3% (*5.2%*)	30.1% (*14.9%*)
–0.01 to –0.10 mg m^{-3} decade^{-1} decreasing ($p < 0.05$)	45.3% (*21.4%*)	37.4% (*25.7%*)	30.8% (*22.8%*)
–0.10 to –0.50 mg m^{-3} decade^{-1} (decreasing) ($p < 0.05$)	12.7% (*7.7%*)	3.9% (*2.4%*)	1.2% (*0.6%*)
> –0.50 mg m^{-3} decade^{-1} (decreasing) ($p < 0.05$)	3.4% (*2.1%*)	0.6% (*0.4%*)	0.1% (*0.1%*)

terns caused by the ENSO are clearly distinguishable. Increases over the 10-year time-window are also observed in the Southern Ocean, in the eastern North Atlantic near the Greenland Sea, and in the Arctic Ocean. Similar changes were also noted by other authors (Henson *et al*., 2010; McQuatters-Gollop *et al*., 2011; Siegel *et al*., 2013). Chl *a* changes around Antarctica may be driven by the Antarctic Oscillation, which affects wind intensity and, in turn, mixed-layer depth (Boyce *et al*., 2010). The Chl *a* increases noted in the North Atlantic and Arctic oceans are likely related to the decrease in ice cover and duration (more open water), which have led to associated increases in primary production in the region (Zhang *et al*., 2010; Arrigo and van Dijken, 2011). In general, for the 10-and 15-year time-windows, positive correlations of SST and Chl *a* were more commonly observed at high latitudes, suggesting drivers other than temperature for the enhanced productivity (Doney, 2006). The only ocean basin that showed a consistent decline in Chl *a* concentrations over time was the Indian Ocean, though some regions, such as the South China Sea and the subtropical front, showed no trend.

It is important to stress that the aforementioned trends derived from satellite observations are only for a portion of the surface ocean. Satellite-derived SST and Chl *a* are limited to the first optical depth, which can vary from a few to several tens of metres, depending on the optical properties of the water (Morel *et al*., 2007). It is also important to bear in mind that changes observed in Chl *a* can be associated with physiological changes and changes in phytoplankton biomass or biased by high concentrations of coloured dissolved organic matter (CDOM) (Siegel *et al*., 2005; Behrenfeld *et al*., 2015).

10.3 Trends from *in situ* time series

Only a few *in situ* time series have sufficient data to show reliable trends in biogeochemical variables over the past 30 years. Indeed, the North Atlantic, Baltic Sea, and Mediterranean Sea are some of the only locations where such time-series information exists, which enable us to track how the biology and biogeochemistry may have been changing over the past 30 years. Continuous satellite chlorophyll concentration data are only available since the late 1990s.

Over time-scales of less than a decade, it is difficult to distinguish between natural and anthropogenic forcing

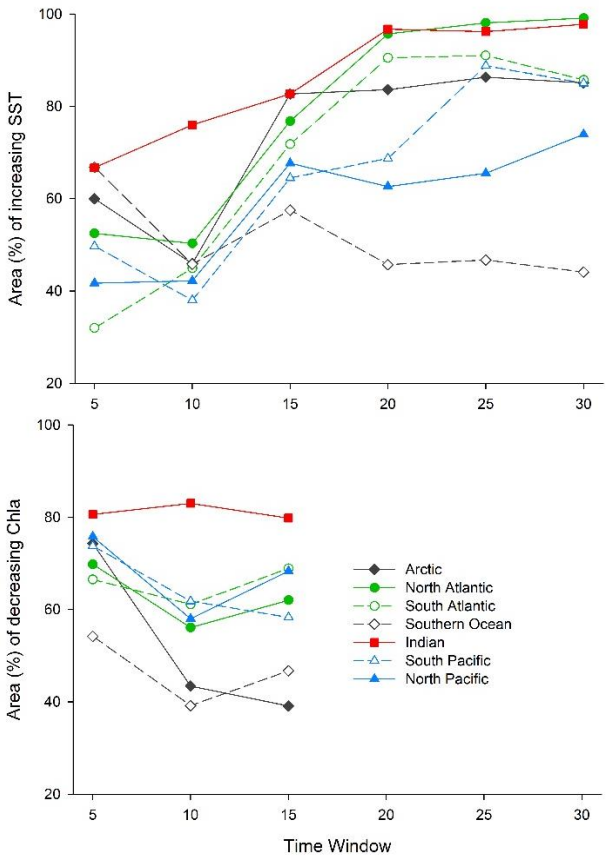

Figure 10.5. Percent spatial area of increasing sea surface temperature (SST; top) and decreasing chlorophyll *a* (Chl *a*; bottom) measurements per ocean over different time-windows, as derived by satellite measurements.

(Overland *et al*., 2006; Karl, 2010; Henson, 2014). Statistical significance of results can also be questionable. For this reason, this chapter's analysis of satellite data was done for time-windows of 10 or more years. However, for *in situ* time series, even short time-scale data provide valuable information. Most of the time series collecting measurements today span ≤ 10 years. Thus, we will provide a short summary of biogeochemical trends from *in situ* time series, especially focusing over the past fifteen, ten, and five years, but, where possible, including those few that have measurements with longer time-spans.

Over the 30-, 15-, 10-, and 5-year periods, most of the *in situ* time-series data report an increase in Chl *a* concentrations throughout the world's oceans, contrasting with some of the satellite data (Table 10.2; Figure 10.9). It is particularly interesting to note that the majority of the time series are located in coastal areas, where local drivers affect primary production and chlorophyll concentrations. Indeed, the *in situ* time series and satellite Chl *a* trends highlight the differences between coastal and

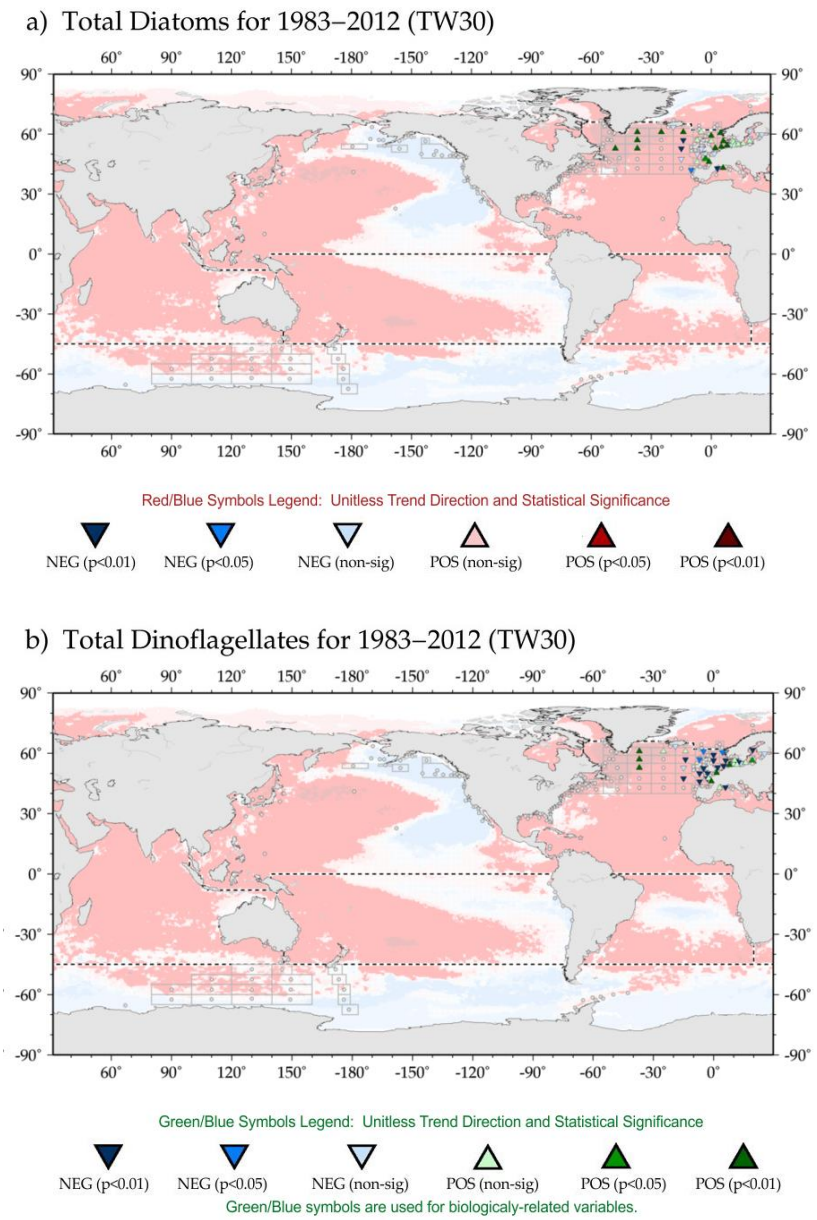

Figure 10.6. Global 30-year trends (1983–2012; TW30) of diatom (a) and dinoflagellate (b) concentrations; background colours indicate rates of change in gridded SST obtained from Reynolds OIv2SST.

open-ocean ecosystems. Special caution must be used when averaging oceanic regions (Yuras *et al*., 2005), and the inclusion of continental margins in primary production or carbon-flux estimates for the world's oceans has to be considered (Laws *et al*., 2000; Müller-Karger *et al*., 2005).

While it is generally accepted that phytoplankton become less abundant with rising ocean temperatures due to increased stratification and less nutrient availability (Richardson and Schoeman, 2004; Gruber, 2011), it has been suggested that global warming can also boost phytoplankton abundance and that phytoplankton physiology responds favorably to such changes (Richardson and Schoeman, 2004; Kempt and Villareal, 2013; Behrenfeld *et al*., 2015). A shift towards more upwelling-favorable winds and subsequently enhanced coastal upwelling in response to greenhouse warming can lead to higher primary production (Bakun, 1990; Sydeman *et al*., 2014). Similarly, a rise in phytoplankton concentrations due to higher metabolic rates and extended permanence within the euphotic zone in regions of warming has been proposed (Richardson and Schoeman, 2004). Ocean warming can also have other effects on plankton abundance, such as an uneven shift in bloom timing and location of various plankton groups (phenology – match/mismatch) (Richardson, 2008; Henson *et al*., 2013; Barton *et al*., 2016). Higher stratification and more

nutrient-depleted conditions in the surface ocean may lead to changes in ecosystem structure, where smaller phytoplankton will dominate (Bopp *et al*., 2005). Higher ocean CO_2 concentrations (ocean acidification) could lead to higher phytoplankton biomass, depicted as higher Chl *a* concentrations, as a result of excess carbon consumption and/or higher photosynthetic rates (Riebesell *et al*., 2007; Riebesell and Tortell, 2011). Nevertheless, primary producers such as coccolithophores are reported to have a species-specific reaction towards ocean acidification, and general patterns are not easy to identify (Meyer and Riebesell, 2015; Riebesell and Gattuso, 2015). In addition, it has been suggested that the combination of higher CO_2 concentrations coupled with increased light exposure can negatively impact marine primary producers (Gao *et al*., 2012). The regional chapters provide more details on the complex responses of marine organisms to concurrent changes in CO_2 concentrations, ocean temperature, and nutrient availability.

Over the 30-year time-window, increases in diatoms and dinoflagellates were observed in the western and northern North Atlantic (Figure 10.6). McQuatters-Gollop *et al*. (2011) reported increases in phytoplankton in most regions of the North Atlantic after 1980. While this trend seems to be robust, this region exhibits highly variable phytoplankton blooms. These are linked to the North Atlantic Oscillation (NAO), and the magnitude of blooms is related to the mixed-layer depth (Henson *et al*., 2009). It has also been suggested that variations in phytoplankton abundance can be related to expanding or contracting niches as ocean conditions change (Irwin *et al*., 2012; Barton *et al*., 2016). Over shorter time-windows, the changes observed in North Atlantic and Mediterranean phytoplankton abundance are spatially heterogeneous. For example, some parts of the Mediterranean showed a decline in diatom concentrations over the past decade, consistent with reports of a shift from diatom-dominated phytoplankton populations toward non-siliceous types in response to decreasing silica and nitrate concentrations (Goffart *et al*., 2002). A relative lack of phytoplankton data precludes comparable analyses in other ocean basins.

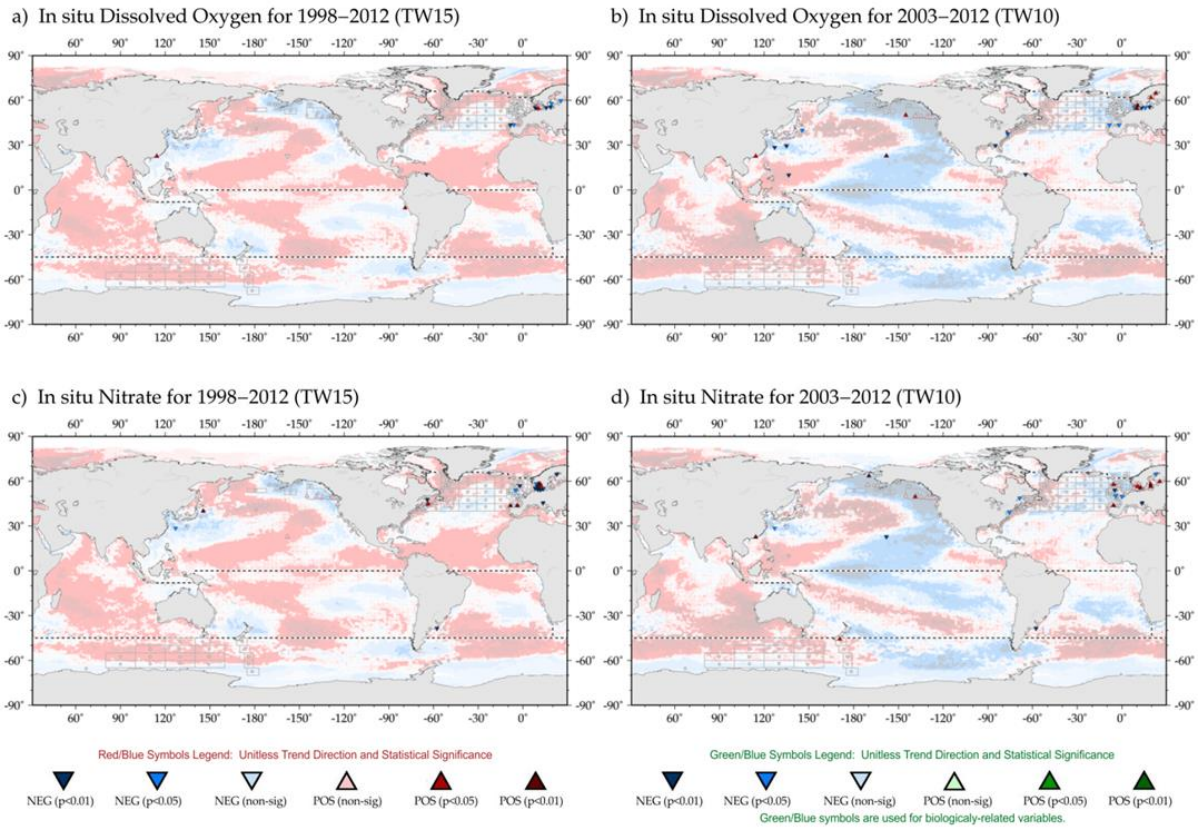

Figure 10.7. Global 15-and-10-year trends (1998–2012 (TW15) and 2003–2012 (TW10), respectively) (a), dissolved oxygen (b); and nitrate concentration (NO_3) (c and d). Background colours indicate rates of change in gridded SST obtained from Reynolds OIv2SST. Variable names according to the IGMETS Explorer (http://igmets.net/explorer/).

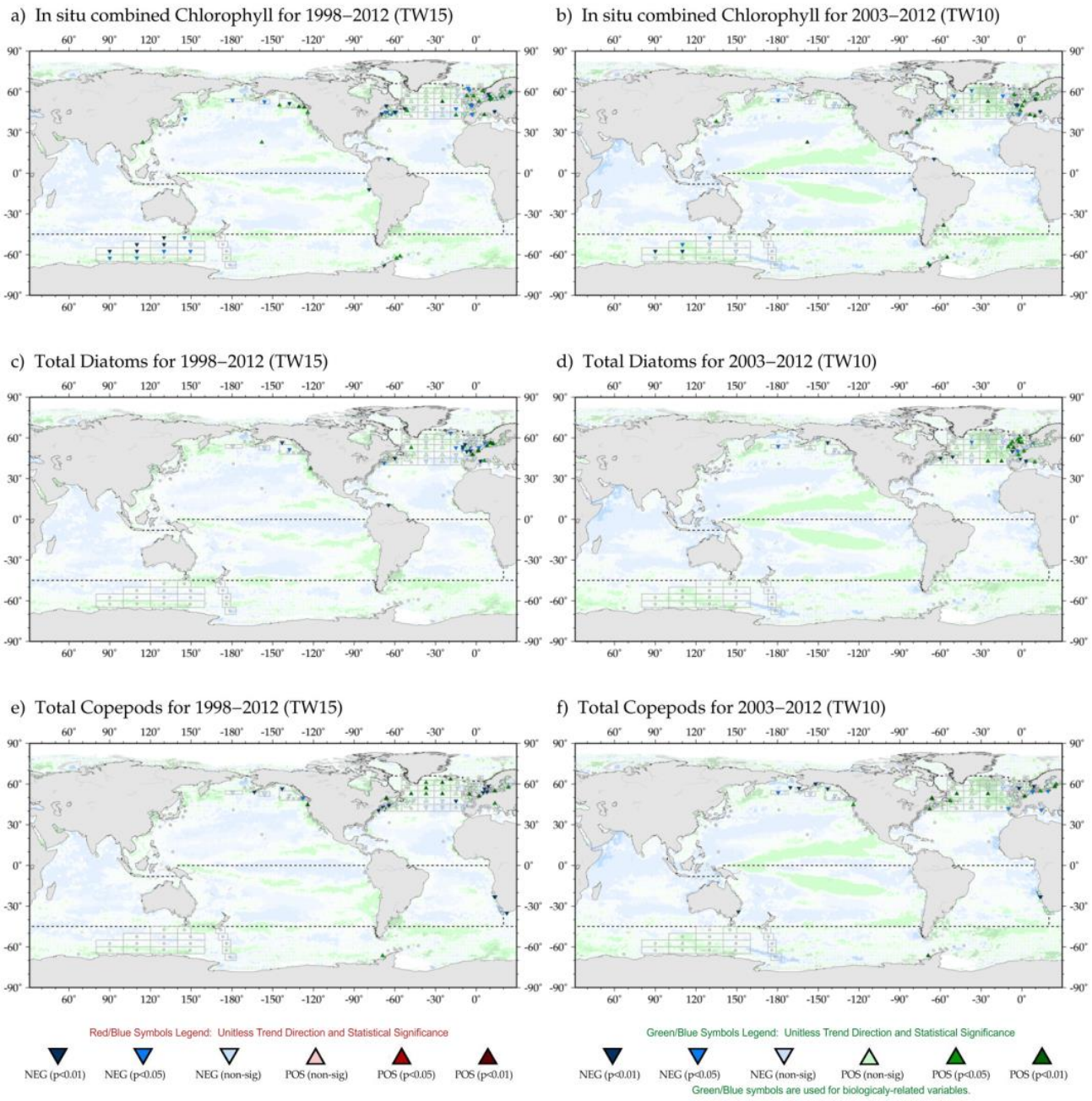

Figure 10.8. Global 15-and-10-year trends (1998–2012 (TW15) and 2003–2012 (TW10), respectively) of *in situ* Chl *a* (a and b); diatom concentration (c and d); and zooplankton (e and f). Background colours indicate rates of change in Chl *a* from SeaWiFS/MODIS-A. Variable names according to the IGMETS Explorer (http://igmets.net/explorer/).

The NAO has been invoked to explain changes in zooplankton populations in the Mediterranean and North Atlantic (Mazzocchi *et al*., 2007; Siokou-Frangou *et al*., 2010; García-Comas *et al*., 2011). Over the past three decades, copepods have largely decreased in the western North Atlantic, but have increased in the eastern North Atlantic and Mediterranean Sea. However, copepod abundance has been highly variable in space and time (Figure 10.8); for example, increases in copepods were observed in the western North Atlantic over the 10-and 5-year windows. Locations of increased Chl *a* were often associated with areas of higher zooplankton biomass, illustrating the foodweb connectivity.

However, most of the changes in zooplankton were non-significant (more information available at http://igmets.net/explorer); this suggests that changes in zooplankton population within the past 15 years may be mostly responding to local drivers (e.g. nutrient inputs and local bloom dynamics), as opposed to large-scale climate drivers (Beaugrand and Reid, 2003; Lejeusne *et al*., 2010). It is important to note that changes within global zooplankton communities (e.g. species composition, seasonal changes), which are key ecosystem characteristics, were not assessed in this global analysis due to limited zooplankton species data, especially outside of the North Atlantic region.

Trends in nutrient concentrations spanning the 5–15-year periods were highly variable across time-series sites (Figures 10.7, 10.9, and 10.10; more information available at http://igmets.net/explorer). At the global level, nitrate is negatively correlated with temperature, which is typical of upwelling systems (Kamykowski and Zentara, 1986, 2005). However, at the local scale, and particularly in coastal regions, other processes may complicate this signal. For example, biologically-driven variability (e.g. taxonomic composition, size structure and abundance of phytoplankton communities) strongly influences nutrient uptake and availability (Richardson, 2008; Mills and Arrigo, 2010; Martiny *et al*., 2013), as do changes in agricultural practices (e.g. fertilizer use and runoff to coastal waters) (Caraco and Cole, 1999; Brodie and Mitchell, 2005). Many of the time series that report increases in nutrient concentrations are located in areas where there has been an increase in Chl *a* (Figure 10.4).

Over time-scales of 10 and 15 years, oxygen data were available for some areas. Surface oxygen concentrations appear to increase in some stations (e.g. North Pacific), while decreasing in others (e.g. off the coast of Spain; Figure 10.7). Looking closely at temperature and oxygen, those locations that exhibited increased oxygen concentrations are located in areas where cooling was observed, as well as high Chl *a* concentrations. Conversely, those stations that showed a decrease in oxygen were in areas that registered warming (Figure 10.7). Thus, these observations are consistent with the predicted temperature-dependent behavior of oxygen (Figure 10.10; Gruber, 2011). Examining even shorter (e.g. 5-year) time-windows, higher variability in oxygen trends was visible (Figure 10.9; i.e. some of the stations that exhibited positive trends change to negative, e.g. the northeastern Pacific), highlighting that local processes exert important controls. However, the pattern stayed consistent with the SST data; areas with increasing temperature were characterized by decreasing oxygen concentrations (Keeling *et al*., 2010; Gruber, 2011). It is important to remember that surface oxygen concentrations depend largely on ocean-atmosphere exchange.

The responses of phytoplankton, zooplankton, and other biogeochemical variables to changes in ocean conditions, as well as the interplay among all of the drivers, vary across regions and are addressed in more detail in each of the regional chapters.

10.4 Conclusions – major findings

Ship-based biogeochemical time series provide the high-quality biological, physical, and chemical measurements that are needed to detect climate change-driven trends in the ocean, assess associated impacts on marine food-webs, and ultimately improve our understanding of changes in marine biodiversity and ecosystems. While the spatial "footprint" of a single time series may be limited (see also Henson *et al*., 2016), coupling observations from multiple time series with synoptic satellite data can improve our understanding of critical processes such as ocean productivity, ecosystem variability, and carbon fluxes on a larger spatial-scale.

By examining the behavior and sensitivity of a variety of physical, chemical, and biological ocean variables over a range of time-scales, some general trends have been highlighted in this chapter. The analyses presented here show a generalized warming trend over the past 30 years. These results are consistent with the IPCC (2013) report as well as other research which have shown significant ocean warming and shifts in the biology over the past several decades. There are, however, regional differences in temperature trends, depending on the time-window considered. These differences are driven by regional and temporal expressions of large-scale climatic forcing and atmospheric teleconnections that can intensify warming and cooling trends in different regions of the ocean. This regional and temporal variability affects biogeochemical cycling (i.e. oxygen, nutrient, carbon), marine foodwebs, and ecosystem services.

The capacity to identify and differentiate anthropogenic and natural climate variations and trends depends largely on the length and location of the time series. Most of the ship-based ecological time series are concentrated in the coastal ocean. Coastal zones are some of the most

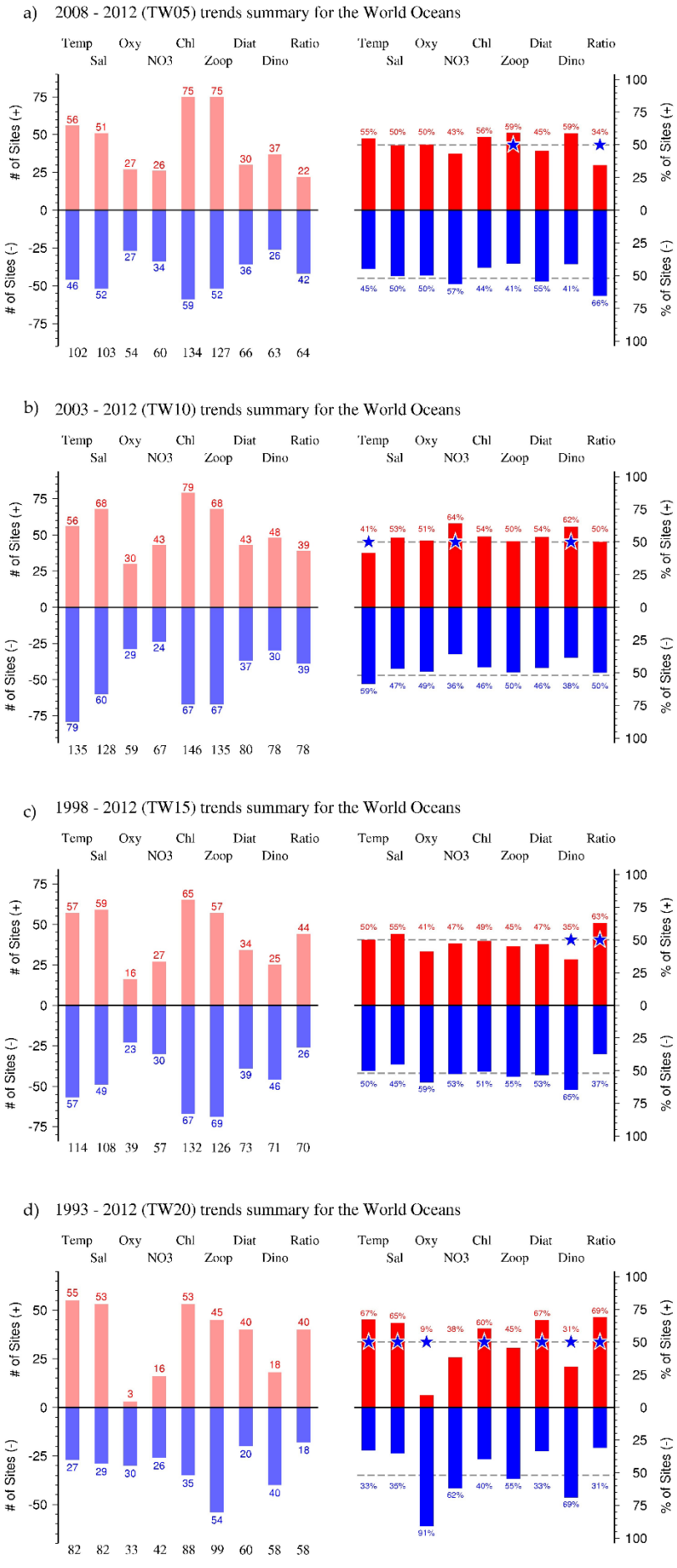

Figure 10.9. BODE (Brief Overviews of Dynamic Ecosystems) plots showing positive and negative trends in selected variables from *in situ* time series in the world's oceans. Time-windows (5, 10, 20, and 30) are indicated in each figure. Significant trends are indicated by the star symbol. Left side illustrates the trend for the absolute number of sites (in no.); panels on the right indicate the percentage of sites showing increasing or decreasing trends. The total number of sites included in this calculation is shown below the figures. Temp: *in situ* temperature; Sal: *in situ* salinity; Oxy: *in situ* oxygen; NO3: *in situ* nitrate; Phyto: *in situ* chlorophyll; Zoop: *in situ* total zooplankton; Diat: *in situ* total diatoms; Dino: *in situ* total dinoflagellates; Ratio: *in situ* ratio of diatoms to dinoflagellates. Data for the 20-year trends for phytoplankton and zooplankton are largely located in the North Atlantic.

productive areas of the ocean and play a critical role in the global carbon cycle (Müller-Karger *et al*., 2005; Chen and Borges, 2009). These areas are important providers of ecosystem goods and services (e.g. food, recreation). Coastal ecosystems are highly dynamic, with strong influences from both ocean and land processes, and are thus more vulnerable to natural and anthropogenic climate forcing. The results shown here highlight differences in biogeochemical trends between coastal and open-ocean regions and among different time-windows. This lends insight into the dominant drivers of coastal and open-ocean ecosystem change and the impacts of decadal (or longer) climate patterns.

While coastal zones in North America and Europe are being monitored, there is a conspicuous lack of biogeochemical time series in other coastal regions around the world, not to mention an almost complete absence of such observational platforms in the open ocean, which limits the capacity of analyses such as presented in this report. A more globally-distributed network of time-series observations over multiple decades will be needed to differentiate between natural and anthropogenic variability. Currently, ocean colour satellite data provide the only synoptic, quasi-biological assessment of the world's oceans, while satellite sea surface temperature, as well as Argo floats, provide information on some of the oceans' physical properties. If biogeochemical time series are essential to documenting and understanding the effects of climate change on ocean resources, how will we maintain and augment the current network of ship-based biogeochemical time series under increased funding pressure? Shrinkage in the already inadequate biogeochemical observing network may result in reductions in sampling and/or long gaps in time-series activities, which will significantly hinder our ability to detect a climate-driven signal. With the development of new technologies, a limited suite of new automated biogeochemical measurements will be possible, but may not be readily accessible to many regions of the world. The majority of biological analysis needed to detect species shift and biodiversity changes will require *in situ* ship-based sampling. This calls for the necessity of securing long-term funding for the maintenance of ship-based time series, together with commitment and support from the global (and not just scientific) community. Without consistent, uninterrupted measurements, it will be impossible to understand the changes and consequences of climate change on the oceans' biogeochemical cycles, biological pump, and marine ecosystems.

A reduction in monitoring capabilities also has important implications for our capacity to predict how the provision of ocean ecosystem services will change in the future and may hamper the establishment of sustainable management strategies. *In situ* measurements are not only critical to monitor ocean health, but also to develop and validate ocean and climate models. As stated previously, *in situ* measurement can serve as a constant biodiversity and ecosystem health "thermometer" used to monitor and predict how goods and services provided by marine ecosystems will be affected in the future (e.g. food resources, flood control, filtering, detoxification; Worm *et al*., 2006; Barange *et al*., 2014). Management of these important marine ecosystem services rely on the high-quality biological and biogeochemical data that time series provide on a regular basis, particularly in coastal areas.

a) 2003–2012 (TW10) correlations between SST and ecological parameters

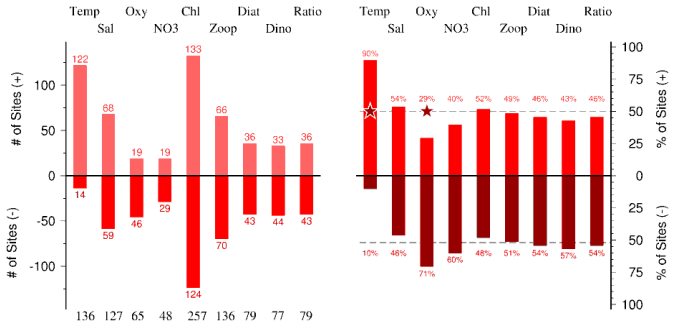

b) 2003–2012 (TW10) correlations between Chl *a* and ecological parmeters

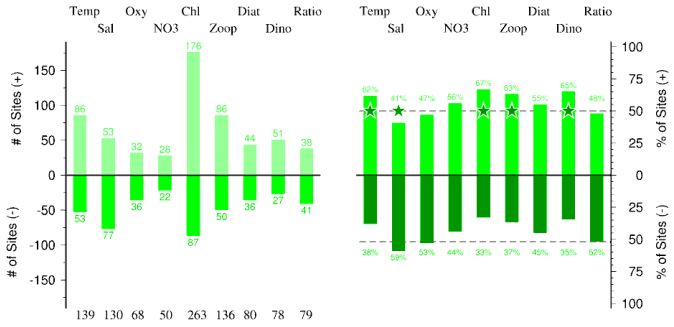

Figure 10.10. Frequency of positive and negative correlations between variables from *in situ* time series and gridded SST (Reynolds OIv2SST) and Chl *a* (satellite derived) computed for a 10-year time-window (2003–2012). Significant trends are indicated by the star symbol. Left side of the figures illustrates the correlation for the absolute number of sites; panels on the right side indicate the percentage of sites showing positive or negative correlation.

10.5 References

Alexander, M. A., Bladé, I., Newman, M., Lanzante, J. R., Lau, N-C., and Scott, J. D. 2002. The atmospheric bridge: the influence of ENSO teleconnections on air–sea interaction over the global oceans. Journal of Climate, 15: 2205–2231, doi:http://dx.doi.org/10.1175/1520-0442(2002)015<2205:TABTIO>2.0.CO;2.

Arrigo, K. R., and van Dijken, G. L. 2011. Secular trends in Arctic Ocean net primary production. Journal of Geophysical Research, 116: C09011, doi:10.1029/2011JC007151.

Bakun, A. 1990. Global climate change and intensification of coastal ocean upwelling. Science, 247(4939): 198–201.

Barange, M., Merino, G., Blanchard, J. L., Scholtens, J., Harle, J., Allison, E. H., Allen, J. I., *et al*. 2014. Impacts of climate change on marine ecosystem production in societies dependent on fisheries. Nature Climate Change, 4(3): 211–216, doi:10.1038/NCLIMATE2119.

Barton, A. D., Irwin, A. J., Finkel, Z. V., and Stock, C. A. 2016. Anthropogenic climate change drives shift and shuffle in North Atlantic phytoplankton communities. Proceedings of the National Academy of Sciences, 113(11): 2964–2969.

Beaugrand, G., and Reid, P. C. 2003. Long-term changes in phytoplankton, zooplankton and salmon linked to climate. Global Change Biology, 9: 801–817, doi:10.1046/j.1365-2486.2003.00632.x.

Beaulieu, C., Henson, S. A., Sarmiento, J. L., Dunne, J. P., Doney, S. C., Rykaczewski, R. R., and Bopp, L. 2013. Factors challenging our ability to detect long-term trends in ocean chlorophyll. Biogeosciences, 10: 2711–2724, doi:10.5194/bg-10-2711-2013.

Behrenfeld, M. J., O'Malley, R. T., Boss, E. S., Westberry, T. K., Graff, J. R., Halsey, K. H., Milligan, A. J., *et al*. 2015. Revaluating ocean warming impacts on global phytoplankton. Nature Climate Change, 6(3): 323–330, doi:10.1038/NCLIMATE2838.

Behrenfeld, M. J., O'Malley, R. T., Siegel, D. A., McClain, C. R., Sarmiento, J. L., Feldman, G. C., Milligan, A. J., *et al*. 2006. Climate-driven trends in contemporary ocean productivity. Nature, 444(7120): 752–755.

Bopp, L., Aumont, O., Cadule, P., Alvain, S., and Gehlen, M. 2005. Response of diatoms distribution to global warming and potential implications: A global model study. Geophysical Research Letters, 32(19): L19606, doi:10.1029/2005GL023653.

Boyce, D. G. Lewis, M. R., and Worm, B. 2010. Global phytoplankton decline over the past century. Nature, 466(7306): 591–596, doi:10.1038/nature09268.

Brodie, J. E., and Mitchell, A. W. 2005. Nutrients in Australian tropical rivers: changes with agricultural development and implications for receiving environments. Marine and Freshwater Research, 56: 279–302.

Caraco, N. F., and Cole, J. J. 1999. Human impact on nitrate export: an analysis using major world rivers. Ambio, 28: 167–170.

Chavez, F. P., Messié, M., and Pennington, J. T. 2011. Marine primary production in relation to climate variability and change. Annual Review of Marine Science, 3: 227–260.

Chavez, F. P., Ryan, J., Lluch-Cota, S. E., and Ñiquen, M. 2003. From anchovies to sardines and back: multidecadal change in the Pacific Ocean. Science, 299(5604): 217–221.

Chen, C. T. A., and Borges, A. V. 2009. Reconciling opposing views on carbon cycling in the coastal ocean: continental shelves as sinks and near-shore ecosystems as sources of atmospheric CO_2. Deep-Sea Research II: Topical Studies in Oceanography, 56(8): 578–590, doi:10.1016/j.dsr2.2009.01.001.

Church, M. J., Lomas, M. W., and Müller-Karger, F. 2013. Sea change: Charting the course for biogeochemical ocean time-series research in a new millennium. Deep-Sea Research II: Topical Studies in Oceanography, 93: 2–15.

Dave, A. C., and Lozier, M. S. 2013. Examining the global record of interannual variability in stratification and marine productivity in the low-latitude and mid-latitude ocean. Journal of Geophysical Research: Oceans, 118: 3114–3127, doi:10.1002/jgrc.20224.

Deser, C., Phillips, A. S., and Alexander, M. A. 2010. Twentieth century tropical sea surface temperature trends revisited. Geophysical Research Letters, 37(10): L1070, doi: 10.1029/2010GL043321.

Doney, S. C. 2006. Oceanography—Plankton in a warmer world, Nature, 444(7120): 695–696, doi:10.1038/444695a.

Doney, S. C., Bopp, L., and Long, M. C. 2014. Historical and future trends in ocean climate and biogeochemistry. Oceanography, 27(1): 108–119, http://dx.doi.org/10.5670/oceanog.2014.14.

Dong, L., and Zhou, T. 2014. The formation of the recent cooling in the eastern tropical Pacific Ocean and the associated climate impacts: A competition of global warming, IPO, and AMO. Journal of Geophysical Research: Atmospheres, 119(19): 11272–11287, doi:10.1002/2013JD021395.

Ducklow, H. W., Fraser, W. R., Meredith, M. P., Stammerjohn, S. E., Doney, S. C., Martinson, D. G., Sailley, S. F., *et al*. 2013. West Antarctic Peninsula: An ice-dependent coastal marine ecosystem in transition. Oceanography, 26(3): 190–203, http://dx.doi.org/10.5670/oceanog.2013.62.

Enfield, D. B., and Mestas-Nuñez, A. M. 2000. Global modes of ENSO and non-ENSO sea surface temperature variability and their associations with climate. *In* El Niño and the Southern Oscillation: Multiscale Variability and Global and Regional Impacts, pp. 89–112). Ed. by H. F. Diaz, and V. Markgraf. Cambridge University Press. 512 pp.

Enfield, D. B., Mestas-Nuñez, A. M., and Trimble, P. J. 2001. The Atlantic multidecadal oscillation and its relation to rainfall and river flows in the continental US. Geophysical Research Letters, 28(10): 2077–2080.

Gao, K., Xu, J., Gao, G., Li, Y., Hutchins, D. A., Huang, B., Wang, L., *et al*. 2012. Rising CO_2 and increased light exposure synergistically reduce marine primary productivity. Nature Climate Change, *2*(7): 519–523.

García-Comasa, C., Stemmanna, L., Ibaneza, F., Berlinea, L., Mazzocchi, M., Gasparinia, G. S., Picherala, M., *et al*. 2011. Zooplankton long-term changes in the NW Mediterranean Sea: Decadal periodicity forced by winter hydrographic conditions related to large-scale atmospheric changes? Journal of Marine Systems, 87(3–4): 216–226.

Goffart, A., Hecq, J. H., and Legendre, L. 2002. Changes in the development of the winter-spring phytoplankton bloom in the Bay of Calvi (NW Mediterranean) over the last two decades: a response to changing climate? Marine Ecology Progress Series, 236: 45–60, doi:10.3354/meps236045.

Gregg, W. W., and Rousseaux, C. S. 2014. Decadal trends in global pelagic ocean chlorophyll: A new assessment integrating multiple satellites, *in situ* data, and models. Journal of Geophysical Research: Oceans, 119(9): 5921–5933.

Gruber, N. 2011. Warming up, turning sour, losing breath: ocean biogeochemistry under global change. Philosophical Transactions of the Royal Society A, 369: 1980–1996, doi:10.1098/rsta.2011.0003.

Han, W., Vialard, J., McPhaden, M. J., Lee, T., Masumoto, Y., Feng, M., and De Ruijter, W. P. 2014. Indian Ocean decadal variability: A review. Bulletin of the American Meteorological Society, 95(11): 1679–1703.

Henson, S. A. 2014. Slow science: the value of long ocean biogeochemistry records. Philosophical Transactions of the Royal Society A, 372(2025): doi:10.1098/rsta.2013.0334.

Henson, S. A., Beaulieu, C., and Lampitt, R. 2016. Observing climate change trends in ocean biogeochemistry: when and where. Global Change Biology, *22*(4): 1561–1571.

Henson, S., Cole, H., Beaulieu, C., and Yool, A. 2013. The impact of global warming on seasonality of ocean primary production. Biogeosciences, 10(6): 4357–4369, doi:10.5194/bg-10-4357-2013.

Henson, S. A., Dunne, J., and Sarmiento, J. L. 2009. Decadal variability in North Atlantic phytoplankton blooms. Journal of Geophysical Research, 114: C04013, doi:10.1029/2008JC005139.

Henson, S. E., Sarmiento, J., Dunne, J., Bopp, L., Lima, I., Doney, S., John, J., *et al*. 2010. Detection of anthropogenic climate change in the satellite records of ocean chlorophyll and productivity. Biogeosciences, 7: 621–640.

Hoegh-Guldberg, O., and Bruno, J. F. 2010. The impact of climate change on the world's marine ecosystems. Science, 328: 1523–1528.

Hoegh-Guldberg, O., Cai, R., Poloczanska, E. S., Brewer, P. G., Sundby, S., Hilmi, H., Fabry, V. J., *et al*. 2014. The Ocean. *In* Climate Change 2014: Impacts, Adaptation, and Vulnerability. Part B: Regional Aspects, pp. 1655–1731. Ed. by V. R. Barros, C. B. Field, D. J. Dokken, M. D. Mastrandrea, K. J. Mach, T. E. Bilir, M. Chatterjee, *et al.* Contribution of Working Group II to the Fifth Assessment Report of the Intergovernmental Panel on Climate Change, Cambridge University Press, Cambridge and New York. 688 pp.

Hurrell, J. W., and Deser, C. 2010. North Atlantic climate variability: The role of the North Atlantic Oscillation. Journal of Marine Systems, 79 (3–4): 231–244.

IPCC. 2013. Climate Change 2013: The Physical Science Basis. Contribution of Working Group I to the Fifth Assessment Report of the Intergovernmental Panel on Climate Change. Ed. by T. F. Stocker, D. Qin, G-K. Plattner, M. Tignor, S. K. Allen, J. Boschung, A. Nauels, *et al*. Cambridge University Press, Cambridge and New York. 1535 pp.

Irwin, A. J., Nelles, A., M., and Finkel, Z. V. 2012. Phytoplankton niches estimated from field data. Limnology and Oceanography, 57(3): 787–797, doi:10.4319/lo.2012.57.3.0787.

Kamykowski, D., and Zentara, J. 1986. Predicting plant nutrient concentrations from temperature and sigma-t in the world ocean. Deep-Sea Research, 33: 89–105.

Kamykowski, D., and Zentara, J. 2005. Changes in world ocean nitrate availability through the 20th century. Deep-Sea Research I, 52: 1719–1744.

Karl, D. M. 2010. Oceanic ecosystem time-series programs. Oceanography, 23(3): 104–125.

Karl, T. R., Arguez, A., Huang, B., Lawrimore, J. H., McMahon, J. R., Menne, M. J., Peterson, T. C., *et al*. 2015. Possible artifacts of data biases in the recent global surface warming hiatus. Science, 348(6242): 1469–1472, doi: 10.1126/science.aaa5632.

Keeling, R. F., Körtzinger, A., and Gruber, N. 2010. Ocean deoxygenation in a warming world. Annual Review of Marine Science, 2: 199–229.

Kempt, A. E., and Villareal, T. A. 2013. High diatom production and export in stratified waters – A potential negative feedback to global warming. Progress in Oceanography, 119: 4–23.

Knudsen, M. F., Seidenkrantz, M. S., Jacobsen, B. H., and Kuijpers, A. 2011. Tracking the Atlantic Multidecadal Oscillation through the last 8,000 years. Nature Communications, 2: 178.

Kosaka, Y., and Xie, S. P. 2013. Recent global-warming hiatus tied to equatorial Pacific surface cooling. Nature, 501(7467): 403–407.

Kwok, R., and Comiso, J. C. 2002. Spatial patterns of variability in Antarctic surface temperature: Connections to the Southern Hemisphere Annular Mode and the Southern Oscillation. Geophysical Research Letters, 29(14): 50-1–50-4, doi:10.1029/2002GL015415.

Laws, E. A., Falkowski, P. G., Smith, W. O., Ducklow, H., and McCarthy, J. J. 2000. Temperature effects on export production in the open ocean. Global Biogeochemical Cycles, 14(4): 1231–1246.

Lejeusne, C., Chevaldonné, P., Pergent-Martini, C., Boudouresque, C. F., and Pérez, T. 2010. Climate change effects on a miniature ocean: the highly diverse, highly impacted Mediterranean Sea. Trends in Ecology & Evolution, 25(4): 250–260, doi:http://dx.doi.org/10.1016/j.tree.2009.10.009.

Marshall, J., Armour, K. C., Scott, J. R., Kostov, Y., Hausmann, U., Ferreira, D., Shepherd, T. G., *et al*. 2014. The ocean's role in polar climate change: asymmetric Arctic and Antarctic responses to greenhouse gas and ozone forcing. Philosophical Transactions of the Royal Society A, 372: 20130040, doi:10.1098/rsta.2013.0040.

Martiny, A. C., Pham, C. T. A., Primeau, F. W., Vrugt, J. A., Moore, J. K., Levin, S. A., and Lomas, M. W. 2013. Strong latitudinal patterns in the elemental ratios of marine plankton and organic matter. Nature Geoscience, 6(4): 279–283, doi:http://dx.doi.org/10.1038/ngeo1757.

Mazzocchi, M. G., Christoub, E. D., Di Capuaa, I., Fernández de Puellesc, M., Fonda-Umanid, S., Molineroe, J. C., Nivalf, P., *et al*. 2007. Temporal variability of *Centropages typicus* in the Mediterranean Sea over seasonal-to-decadal scales. Progress in Oceanography, 72(2–3): 214–232, doi:http://dx.doi.org/10.1016/j.pocean.2007.01.004.

Meredith, M. P., and King, J. C. 2005. Rapid climate change in the ocean west of the Antarctic Peninsula during the second half of the 20th century. Geophysical Research Letters, 32: L19604, doi:10.1029/2005GL024042.

Meyer, J., and Riebesell, U. 2015. Reviews and syntheses: Responses of coccolithophores to ocean acidification: a meta-analysis. Biogeosciences, 12(6): 1671–1682, doi:10.5194/bg-12-1671-2015.

Mills, M. M., and Arrigo, K. R. 2010. Magnitude of oceanic nitrogen fixation influenced by the nutrient uptake ratio of phytoplankton. Nature Geoscience, *3*(6): 412–416.

Morel, A., Gentili, B., Claustre, H., Babin, M., Bricaud, A., Ras, J., and Tieche, F. 2007. Optical properties of the "clearest" natural waters. Limnology and Oceanography, 52(1): 217–229.

McQuatters-Gollop, A., Reid, P. C., Edwards, M., Burkill, P. H., Castellani, C., Batten, S., Gieskes, W., *et al*. 2011. Is there a decline in marine phytoplankton? Nature, 472(7342): E6–E7.

Müller-Karger, F. E., Varela, R., Thunell, R., Luerssen, R., Hu, C., and Walsh, J. J. 2005. The importance of continental margins in the global carbon cycle. Geophysical Research Letters, 32: L01602, doi:10.1029/2004GL021346.

Nobre, P., and Shukla, J. 1996. Variations of sea surface temperature, wind stress, and rainfall over the tropical Atlantic and South America. Journal of Climate, 9: 2464–2479, doi:http://dx.doi.org/10.1175/1520-0442(1996)009<2464:VOSSTW>2.0.CO;2.

Overland, J. E., Alheit, J., Bakun, A., Hurrell, J. W., Mackas, D. L., and Miller, A. J. 2010. Climate controls on marine ecosystems and fish populations. Journal of Marine Systems, 79(3): 305–315.

Overland, J. E., Percival, D. B., and Mofjeld, H. O. 2006. Regime shifts and red noise in the North Pacific. Deep-Sea Research I: Oceanographic Research Papers, 53(4): 582–588.

Polovina, J. J., Howell, E. A., and Abecassis, M. 2008. Ocean's least productive waters are expanding. Geophysical Research Letters, 35: L03618, doi:10.1029/2007GL031745.

Rahmstorf, S., Feulner, G., Mann, M. E., Robinson, A., Rutherford, S., and Schaffernicht, E. J. 2015. Exceptional twentieth-century slowdown in Atlantic Ocean overturning circulation. Nature Climate Change, 5(5): 475–480, doi:10.1038/NCLIMATE2554.

Randel, W. J., and Wu, F. 1999. Cooling of the Arctic and Antarctic polar stratosphere due to ozone depletion. Journal of Climate, 12: 1467–1479, doi:10.1175/1520-0442(1999)012<1467:COTAAA>2.0.CO;2.

Richardson, A. J., and Schoeman, D. S. 2004. Climate impact on plankton ecosystems in the Northeast Atlantic. Science, 305(5690): 1609–1612, doi:10.1126/science.1100958.

Richardson, A. 2008. In hot water: zooplankton and climate change. ICES Journal of Marine Science, 65(3): 279–295, doi:10.1093/icesjms/fsn028.

Riebesell, U., and Gattuso, J-P. 2015. Lessons learned from ocean acidification research. Nature Climate Change, 5(1): 12–14.

Riebesell, U., Schulz, K. G., Bellerby, R. G. J., Botros, M., Fritsche, P., Meyerhöfer, M., Neill, C., *et al*. 2007. Enhanced biological carbon consumption in a high CO^2 ocean. Nature, 450(7169): 545–548.

Riebesell, U., and Tortell, P. D. 2011. Effects of ocean acidification on pelagic organisms and ecosystems. *In* Ocean Acidification, pp. 99–121. Ed. by J-P. Gattuso, and L. Hansson. Oxford University Press. 326 pp.

Serreze, M. C., and Barry, R. G. 2011. Processes and impacts of Arctic amplification: A research synthesis. Global and Planetary Change, 77(1–2): 85–96, doi:http://dx.doi.org/10.1016/j.gloplacha.2011.03.004.

Siegel, D. A., Maritorena, S., Nelson, N. B., Behrenfeld, M. J., and McClain, C. R. 2005. Colored dissolved organic matter and its influence on the satellite-based characterization of the ocean biosphere. Geophysical Research Letters, 32: L20605, doi:10.1029/2005GL024310.

Siegel, D. A., Behrenfeld, M. J., Maritorena, S., McClain, C. R., Antoine, D., Bailey, S. W., Bontempi, P. S., *et al*. 2013. Regional to global assessments of phytoplankton dynamics from the SeaWiFS mission. Remote Sensing of Environment, 135: 77–91.

Signorini, S. R., Franz, B. A., and McClain, C. R. 2015. Chlorophyll variability in the oligotrophic gyres: mechanisms, seasonality and trends. Frontiers in Marine Science, 2: 1, doi:10.3389/fmars.2015.00001.

Siokou-Frangou, I., Christaki, U., Mazzocchi, M. G., Montresor, M., Ribera d'Alcalá, M., Vaqué, D., and Zingone, A. 2010. Plankton in the open Mediterranean Sea: a review. Biogeosciences, 7, 1543-1586.

Steig, E. J., Schneider, D. P., Rutherford, S. D., Mann, M. E., Comiso, J. E., and Shindell, D. T. 2009. Warming of the Antarctic ice-sheet surface since the 1957 International Geophysical Year. Nature, 457: 459–462.

Sydeman, W. J., García-Reyes, M., Schoeman, D. S., Rykaczewski, R. R., Thompson, S. A., Black, B. A., and Bograd, S. J. 2014. Climate change and wind intensification in coastal upwelling ecosystems. Science, 345(6192): 77–80.

Thompson, D. W. J., and Solomon, S. 2002. Interpretation of recent southern hemisphere climate change. Science, 296(5569): 895–899, doi:10.1126/science.1069270.

Vantrepotte, V., and Mélin, F. 2009. Temporal variability of 10-year global SeaWiFS time series of phytoplankton chlorophyll a concentration. ICES Journal of Marine Science, 66(7): 1547–1556, doi:10.1093/icesjms/fsp107.

Vantrepotte, V., and Mélin, F. 2011. Inter-annual variations in the SeaWiFS global chlorophyll a concentration (1997–2007). Deep-Sea Research I: Oceanographic Research Papers, 58(4): 429–441.

Venegas, S. A., Mysak, L. A., and Straub, D. N. 1997. Atmosphere–ocean coupled variability in the South Atlantic. Journal of Climate, 10: 2904–2920, doi:http://dx.doi.org/10.1175/1520-0442(1997)010<2904:AOCVIT>2.0.CO;2.

Visbeck, M. H., Hurrell, J. W., Polvani, L., and Cullen, H. M. 2001. The North Atlantic Oscillation: Past, present, and future. Proceedings of the National Academy of Sciences of the United States of America, 98(23): 12876–12877, doi:10.1073/pnas.231391598.

Worm, B., Barbier, E. B., Beaumont, N., Duffy, J. E., Folke, C., Halpern, B. S., Jackson, J. B. C., *et al*. 2006. Impacts of biodiversity loss on ocean ecosystem services. Science, 314(5800): 787–790, doi:10.1126/science.1132294.

Yu, L., Zhang, Z., Zhou, M., Zhong, S., Lenschow, D., Hsu, H., Wu, H., *et al*. 2012. Influence of the Antarctic Oscillation, the Pacific–South American modes and the El Niño–Southern Oscillation on the Antarctic surface temperature and pressure variations. Antarctic Science, 24(01): 59–76.

Yuras, G., Ulloa, O., and Hormazábal, S. 2005. On the annual cycle of coastal and open ocean satellite chlorophyll off Chile (18°–40°S). Geophysical Research Letters, 32(23), doi:http://dx.doi.org/10.1029/2005GL023946.

Zhang, J., Spitz, Y. H., Steele, M., Ashjian, C., Campbell, R., Berline, L., and Matrai, P. 2010. Modeling the impact of declining sea ice on the Arctic marine planktonic ecosystem. Journal of Gephysical Research, 115: C10015, doi:10.1029/2009JC005387.

Annex

Description of time-series programmes

The time-series sites and programmes participating in the IGMETS analysis are individually described in the following pages. The sections of this Annex are sorted by major ocean basins, following the ocean conveyor belt starting in the Arctic Ocean (A1), North Atlantic (A2), South Atlantic (A3), Southern Ocean (A4), Indian Ocean (A5), South Pacific (A6), and finishing in the North Pacific Ocean (A7). In addition to the brief information provided within each text summary here, a unique identifier/web link is provided to access detailed information about each time-series site.

This Annex does not include every marine time series in the world. IGMETS focuses on ship-based, *in situ* time series with at least one biogeochemical and/or ecological variable (e.g. nutrients, pigments, or plankton). Some time series did not participate in this initial study because their data were proprietary or it was not possible to contact them due to changes in staffing or outdated contact information.The Annex lists only time-series sites where data were shared, highlighting the important collaborative and scientific contributions made. As IGMETS is an ongoing activity, new time series will be included and their new datasets will be added beyond this first report. Updated information is available in the online IGMETS metabase (http://igmets.net/metabase).

Two example IGMETS time-series site summary figures are shown below. These figures indicate the geographic location and available variable classes submitted to IGMETS. In some cases, additional variable types may exist, but were not provided to IGMETS for this report. The left figure is an example of a multiple-site Southern Ocean project (KRILLBASE) for which only zooplankton data were available. The right figure is a single-site programme from the North Atlantic (CARIACO) for which data from all of the IGMETS variable classes were available.

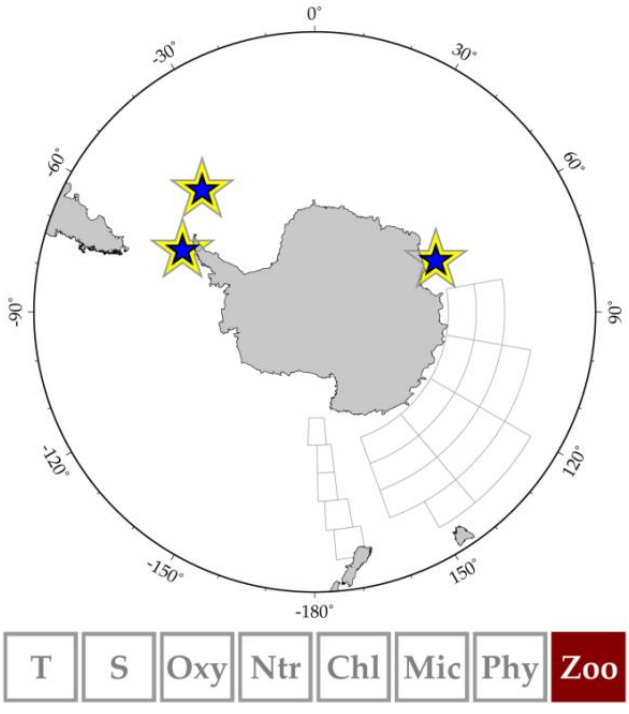

KRILLBASE (uk-30402)
http://igmets.net/sites/?id=**uk-30402**

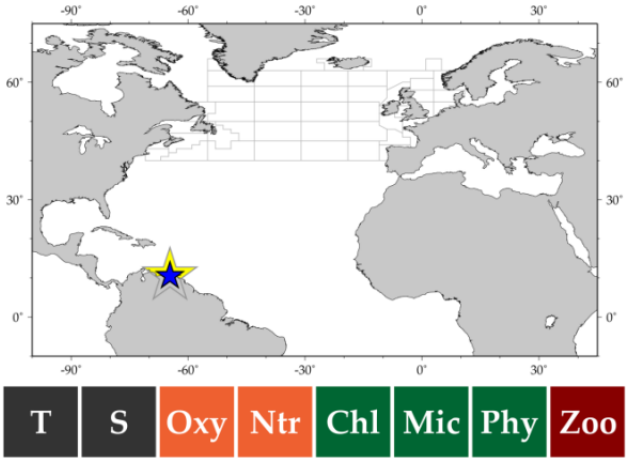

CARIACO Ocean Time Series (ve-10101)
http://igmets.net/sites/?id=**ve-10101**

In situ variable icons: **T** = temperature, **S** = salinity, **Oxy** = dissolved oxygen, **Ntr** = nutrients, **Chl** = chlorophyll/pigments, **Mic** = microbial plankton, **Phy** = phytoplankton, **Zoo** = zooplankton

A1 Arctic Ocean

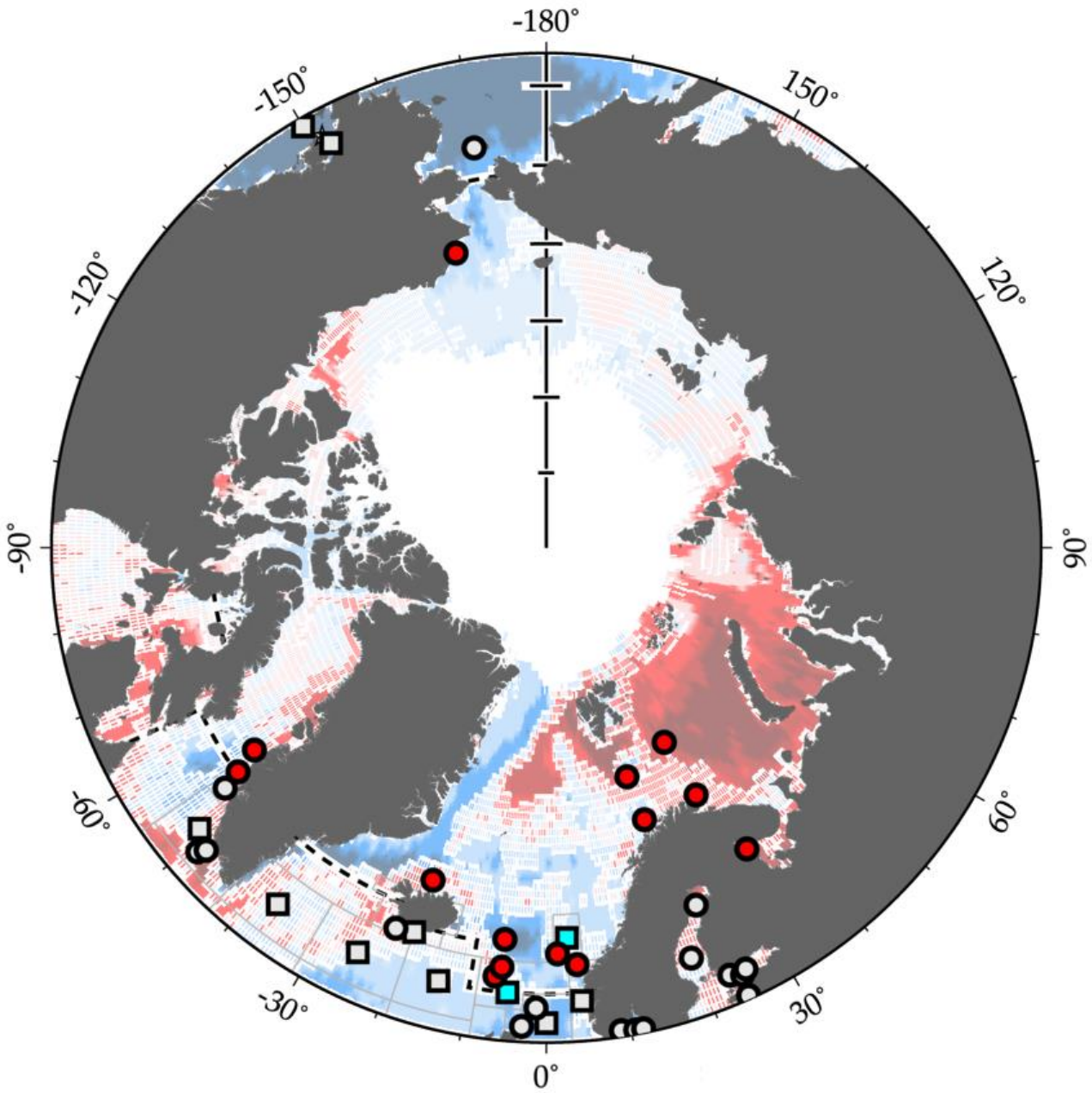

Figure A1. Map of IGMETS-participating Arctic Ocean time series on a background of a 10-year time-window (2003–2012) sea surface temperature trends (see also Chapter 3). At the time of this report, the Arctic Ocean collection consisted of 16 time series (coloured symbols of any type), of which two were from Continuous Plankton Recorder subareas (blue boxes). Dashed lines indicate boundaries between IGMETS regions. Uncoloured (gray) symbols indicate time series being addressed in a different regional chapter (e.g. North Atlantic, North Pacific).

Table A1. Time-series sites located in the IGMETS Arctic Ocean region. Participating countries: Denmark (dk), Faroe Islands (fo), Iceland (is), Norway (no), Russia (ru), United Kingdom (uk), and United States (us). Year-spans in red text indicate time series of unknown or discontinued status. IGMETS-IDs in red text indicate time series without a description entry in this Annex.

No.	IGMETS-ID	Site or programme name	Year-span	T	S	Oxy	Ntr	Chl	Mic	Phy	Zoo
1	dk-10101	Hellefiske Bank – S1 *(West Greenland)*	1950–1984 (?)	X	-	-	-	-	-	-	X
2	dk-10102	Sukkertop Bank – S2 *(West Greenland)*	1950–1984 (?)	X	-	-	-	-	-	-	X
3	fo-30101	Faroe Islands Shelf *(Faroe Islands)* *see North Atlantic Annex (A2)*	1991–present	X	-	-	X	X	-	-	X
4	fo-30102	Norwegian Sea Transect – North *(North Faroe Islands)*	1990–present	X	-	-	-	X	-	-	X
5	fo-30103	Norwegian Sea Transect – South *(North Faroe Islands)*	1990–present	X	-	-	-	X	-	-	X
6	is-30101	Siglunes Transect *(North Iceland)*	1952–present	X	X	-	-	X	-	-	X
7	no-50101	Svinøy Transect – East *(Norwegian Sea)*	1994–present	-	-	-	-	X	-	-	X
8	no-50102	Svinøy Transect – West *(Norwegian Sea)*	1994–present	-	-	-	-	X	-	-	X
9	no-50201	Fugløya-Bjørnøya Transect – North *(Western Barents Sea)*	1990–present	X	X	-	-	X	-	-	X
10	no-50202	Fugløya-Bjørnøya Transect – South *(Western Barents Sea)*	1990–present	X	X	-	-	X	-	-	X
11	no-50301	Vardø-Nord Transect – North *(Central Barents Sea)*	1990–present	X	X	-	-	X	-	-	X
12	no-50302	Vardø-Nord Transect – South *(Central Barents Sea)*	1990–present	X	X	-	-	X	-	-	X
13	ru-10101	Kartesh D1 *(White Sea)*	1961–present	X	X	-	-	-	-	-	X
14	uk-40101	SAHFOS-CPR A01 *(Norwegian Sea)*	1958–present	-	-	-	-	X	-	X	X
15	uk-40114	SAHFOS-CPR B04 *(Southern Norwegian Sea)*	1958–present	-	-	-	-	X	-	X	X
16	us-50604	EMA-4: Chukchi Sea *(Chukchi Sea)*	2003–present	X	X	-	X	X	-	-	-

Norwegian Sea Transect

Country: Faroe Islands

IGMETS-ID: fo-30102 / fo-30103
see also Faroe Island Shelf (North Atlantic, fo-30101)

Eilif Gaard, Solva Jacobsen, and Karin Margretha H. Larsen

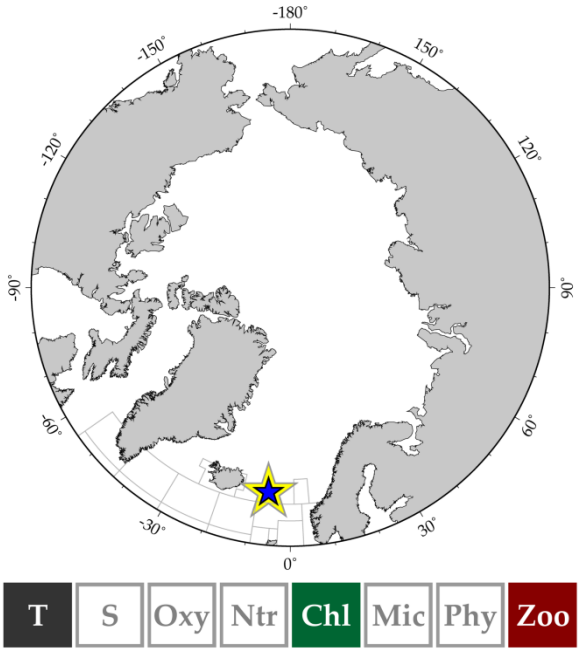

The Faroe Marine Research Institute conducts monitoring of hydrography, chlorophyll *a*, and zooplankton at a transect at 6°W extending from 62°N on the Faroe Shelf and northward to 64°30′N in the Norwegian Sea. The southern part of the transect is characterised by warm Atlantic water flowing from the southwest, while the northern part contains cold East Atlantic water, flowing from the northwest. These two water masses meet and form the Iceland–Faroe Front approximately halfway on the transect. The transect covers warm Atlantic water that is transported into the Nordic seas. Furthermore, the region is an important feeding area for pelagic planktivorous fish during spring and summer. The monitoring aims to understand temporal variability in ocean climate and linkages between environmental variables, plankton, and pelagic fish. The time series, which were established in 1990, are conducted 3–4 times annually. Profiles of temperature, salinity, chlorophyll, and PAR are measured down to ca. 1300 m. Zooplankton is collected from 50 m depth to the surface with WP-2 nets.

Siglunes Transect (Northern Iceland)

Country: Iceland

IGMETS-ID: is-30101
see also Selvogsbanki Transect (North Atlantic, is-30102)

Astthor Gislason, Hafsteinn Gudfinnsson, and Kristinn Gudmundsson

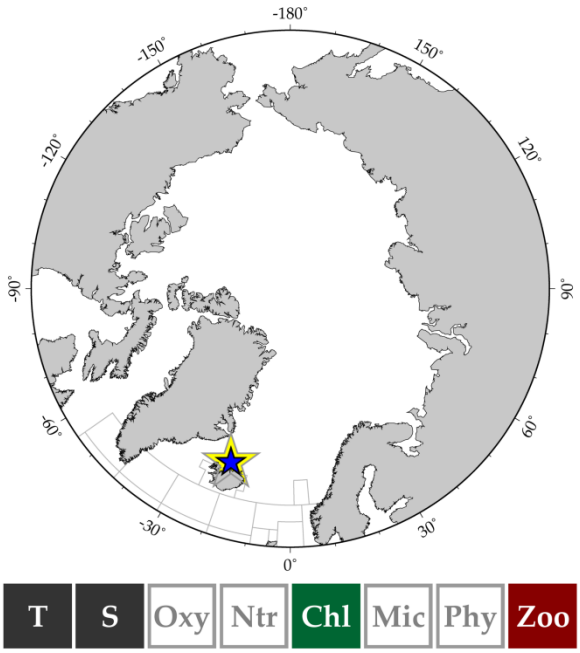

The Icelandic monitoring programme for hydrography, nutrients, phytoplankton, and zooplankton consists of a series of standard transects around Iceland perpendicular to the coastline. In the 1960s, sampling was started at stations along transects north and east of Iceland. Additional transect lines south and west were added in the 1970s. Currently, there are approximately 90 stations, with sampling carried out at these stations every year in May and June. In this IGMETS study, we have included data from the Siglunes Transect, off northern Iceland, and the Selvogsbanki Transect, in western south Iceland. These two transects represent conditions from two very different water bodies. The Siglunes Transect contains plankton communities and hydrography primarily from subarctic, polar waters, while the Selvogsbanki Transect community and conditions predominantly represent North Atlantic water. As such, the Iceland contribution to IGMETS is found in both the Arctic Ocean (Chapter 3) and the North Atlantic (Chapter 4) sections.

Related information: http://www.hafro.is/index_eng.php

Svinøy Transect (Norwegian Sea)

County: Norway

IGMETS-ID: no-50101 / no-50102

Webjørn Melle and Cecilie Broms

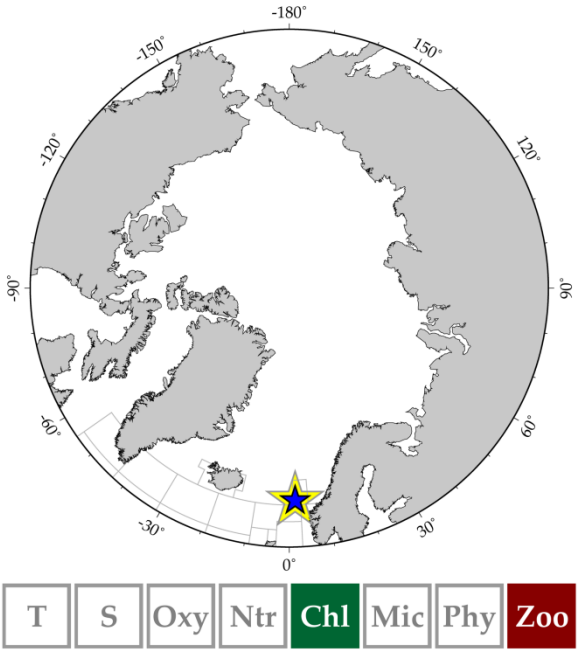

The Svinøy Transect is located in the southern part of the Norwegian Sea. The Institute of Marine Research (IMR) Monitoring Programme established this transect in the mid-1990s. For mesozooplankton, the transect is, by default, sampled 4–6 times each year with a WP-2 net (56-cm diameter, 180-µm mesh) from 200 m depth to the surface. The Svinøy transect is split into two sections called Svinøy Transect East and Svinøy Transect West. Svinøy Transect East is generally located on the shallow shelf and frontal area and is influenced by Norwegian coastal water. Svinøy Transect West is generally located in and influenced by Atlantic water. A chlorophyll bloom occurs in late April and early May, with a protracted post-bloom. The dominant contributor to mesozooplankton biomass is *Calanus finmarchicus*, with a tendency for earlier production in coastal water compared to Atlantic water (Broms and Melle, 2007; Bagøien *et al*., 2012).

Fugløya–Bjørnøya Transect (western Barents Sea)
Vardø–Nord Transect (central Barents Sea)

Country: Norway

IGMETS-ID: no-50201 / no-50301

Padmini Dalpadado

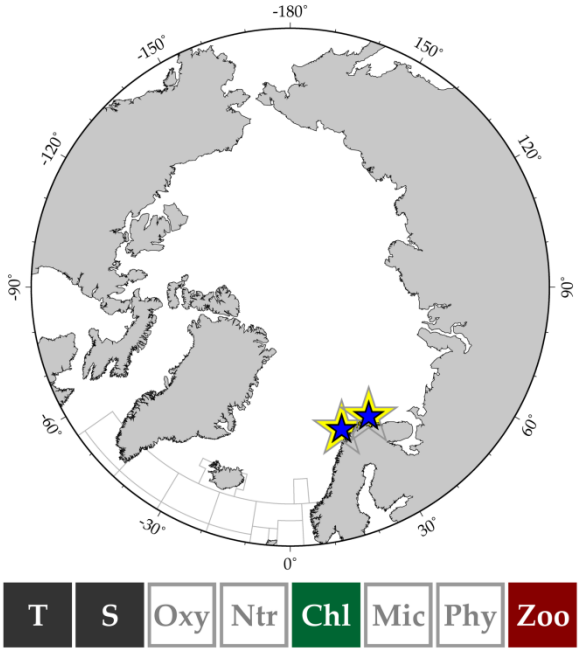

Zooplankton was collected vertically between the bottom and the surface with WP-2 plankton nets (180-mm mesh, diameter of 56 cm) along two standard sections, Fugløya–Bjørnøya (FB) and Vardø–Nord (VN). The FB and VN sections are located, respectively, in the western (Barents Sea opening) and central Barents Sea. Standard sections were sampled up to six times per year, covering most seasons. The biomass (g m^{-2}) data are available for three different size fractions; 2000, 2000–1000, and 1000–180 µm. The biomass for different seasons is available for both sections, allowing the exploration season dynamics of mesozooplankton. Hydrographical parameters such as temperature and salinity as well as chlorphyll, nitrate, and silicate data are also accessible for the two sections. In addition, mesozooplankton species composition (*Calanus finmarchicus*, *C. glacialis*, *C. hyperboreus*, and other species) and their abundance have been monitored since 1995 at four selected stations from the FB section.

White Sea Hydrology and Zooplankton Time Series (Kartesh D1)

Country: Russia

IGMETS-ID: ru-10101

Nikolay Usov, Daria Martynova, Inna Kutcheva, Igor Primakov, Regina Prygunkova, Vyacheslav Smirnov, and Alexey Babkov

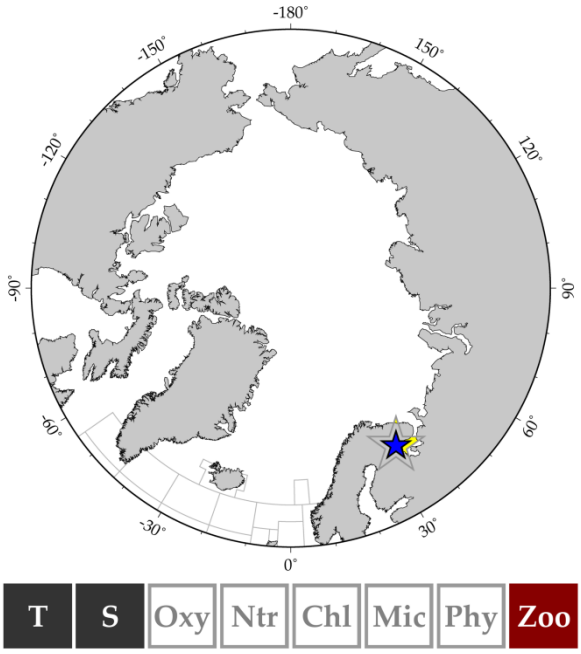

The zooplankton and hydrology monitoring at the D1 station was established in 1957 to understand life cycles of planktonic animals, long-term trends of zooplankton abundance, and abiotic factors influencing those biological variables. D1 is situated in Chupa Inlet (66°19.861'N 33°39.818'E), which opens to the sea, so this point is representative of the coastal zone of Kandalaksha Bay of the White Sea and similar inlets along the coast of the bay (Berger and Dahle, 2001). Zooplankton sampling and temperature, salinity, chlorophyll *a*, turbidity, and dissolved organic matter measurements are conducted every 10 days during the ice-free period of the year and monthly from the ice (Usov *et al*., 2013). Zooplankton is sampled by vertical tows at depths of 0–10, 10–25, and 25–60 m. Other parameters are measured along vertical profiles with 1 Hz frequency. Until 2005, only temperature and salinity were measured at 0, 5, 10, 15, 25, 50 m, and the bottom.

Related information: http://www.zin.ru/kartesh

North Atlantic Continuous Plankton Recorder (CPR) survey

Country: United Kingdom

IGMETS-ID: uk-40101 / uk-40114
see also entry in the North Atlantic chapter

Martin Edwards, Priscilla Licandro, Claudia Castellani, and Rowena Stern

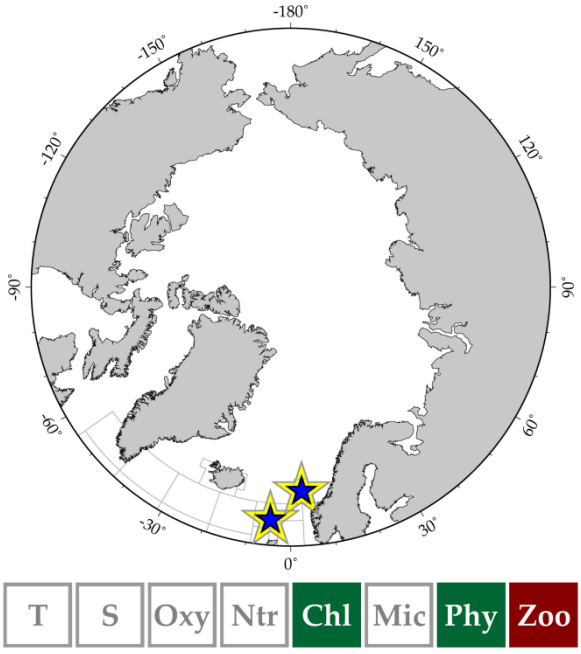

The Continuous Plankton Recorder (CPR) survey is a long-term, subsurface, marine plankton monitoring programme consisting of a network of CPR transects towed monthly across the major geographical regions of the North Atlantic. It has been operating in the North Sea since 1931, with some standard routes existing with virtually unbroken monthly coverage back to 1946. After each tow, the CPR samples are returned to the laboratory for routine analysis, including the estimation of phytoplankton biomass (Phytoplankton Colour Index, PCI) and the identification of up to 500 different phytoplankton and zooplankton taxa (Warner and Hays, 1994). Direct comparisons between the Phytoplankton Colour Index and other chlorophyll *a* estimates, including SeaWiFS satellite estimates, indicate strong positive correlations (Batten *et al*., 2003; Raitsos *et al*., 2005).

Ecosystem Monitoring and Assessment Program (EMA) – Chukchi Sea

Country: United States

IGMETS-ID: us-50604
see also EMA Eastern and Northern Bering Sea (North Pacific, us-50601/us-50602/us-50603)

Lisa Eisnor, Ed Farley, and Jeffrey Napp

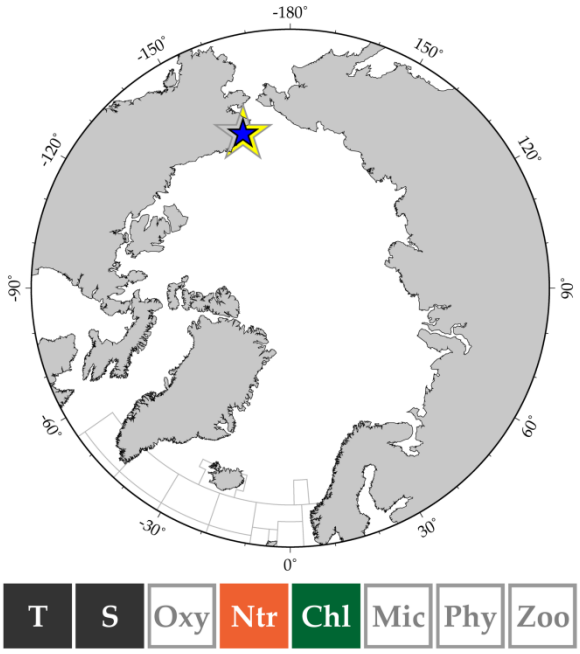

The NOAA Alaska Fisheries Science Center (AFSC) Ecosystem Monitoring and Assessment (EMA) Program's overall goal is to improve and reduce uncertainty in stock assessment models of commercially important fish species through concurrent collection of fish and oceanography data. Surface trawl and midwater acoustics are used to measure fish abundance, size, distribution, diet, and energetic status. CTDs with auxiliary sensors for chlorophyll *a* fluorescence, light attenuation, photosynthetic available radiation (PAR), and dissolved oxygen, and attached Niskin water bottles are used to collect vertical profiles of hydrography, nutrients, and chlorophyll a (total and size-fractionated). Oblique and vertical tows over the water column (150- and 505-µm nets) are used to collect zooplankton taxa. These fisheries oceanographic observations are used to connect climate change and spatial variability in large marine ecosystems to early marine survival of commercially important fish species in the Gulf of Alaska, Eastern Bering Sea, and Chukchi Sea.

A2 North Atlantic Ocean
North Atlantic Proper

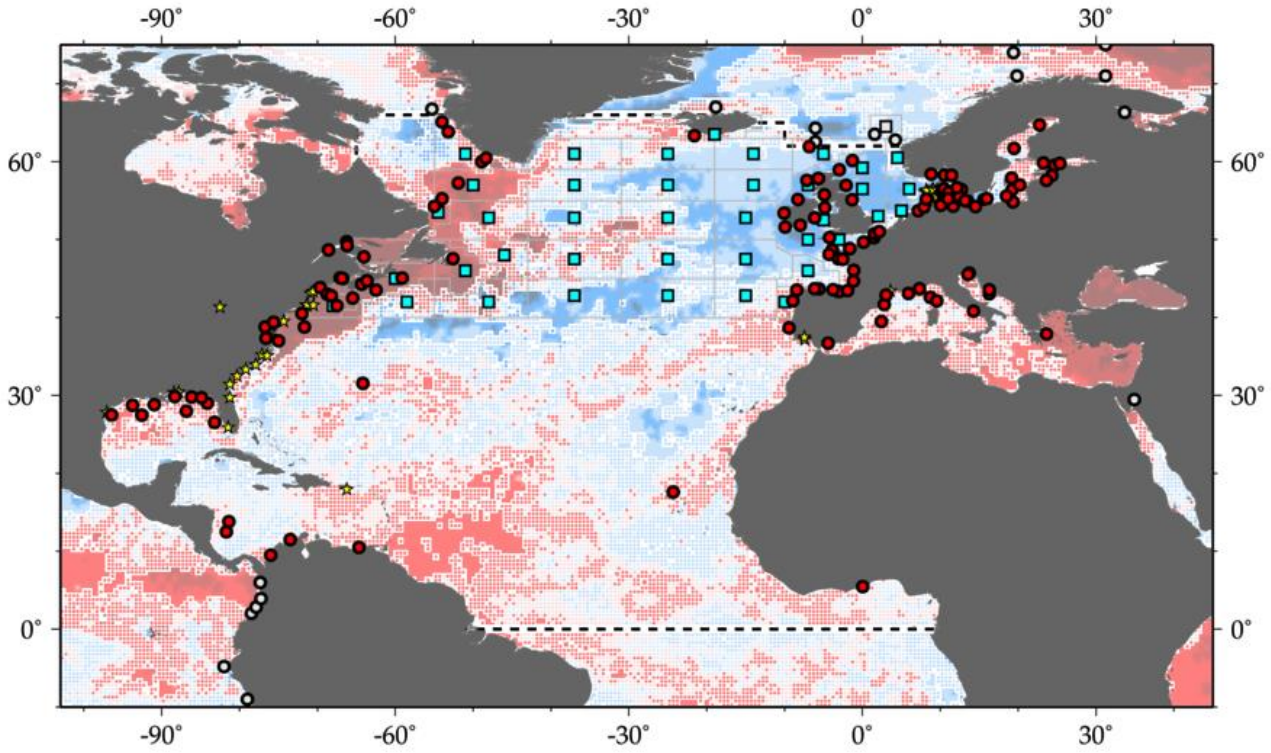

Figure A2.1. Map of IGMETS-participating North Atlantic time series on a background of a 10-year time-window (2003–2012) sea surface temperature trends (see also Chapter 4). At the time of this report, the North Atlantic collection consisted of 211 time series (coloured symbols of any type), of which 39 were from Continuous Plankton Recorder subareas (blue boxes) and 37 were from estuarine areas (yellow stars). Dashed lines indicate boundaries between IGMETS regions. Uncoloured (gray) symbols indicate time series being addressed in a different regional chapter (e.g. Arctic Ocean, South Pacific). Due to the number of sites in the North Atlantic proper (154), the Baltic Sea and Mediterranean Sea have their own Annex subsections.

Table A2.1. Time-series sites located in the IGMETS North Atlantic (not including the Baltic Sea and Mediterranean Sea) region. Participating countries: Canada (ca), Colombia (co), Germany (de), Denmark (dk), Spain (es), Faroe Islands (fo), France (fr), Ghana (gh), Ireland (ie), Isle of Man (im), Iceland (is), Portugal (pt), United Kingdom (uk), United States (us), and Venezuela (ve). Year-spans in red text indicate time series of unknown or discontinued status. IGMETS-IDs in red text indicate time series without a description entry in this Annex.

No.	IGMETS-ID	Site or programme name	Year-span	T	S	Oxy	Ntr	Chl	Mic	Phy	Zoo
1	ca-50101	AZMP Halifax Line 2 *(Scotian Shelf)*	1997–present	X	-	-	-	X	-	-	X
2	ca-50102	AZMP Prince 5 *(Bay of Fundy)*	1999–present	X	-	-	-	X	-	-	X
3	ca-50201	AR7W Zone 1 *(Labrador Shelf)*	1996–present	X	X	-	-	X	-	-	X
4	ca-50202	AR7W Zone 2 *(Labrador Slope)*	1996–present	X	X	-	-	X	-	-	X
5	ca-50203	AR7W Zone 3 *(Central Labrador Sea)*	1996–present	X	X	-	-	X	-	-	X
6	ca-50204	AR7W Zone 4 *(Eastern Labrador Sea)*	1996–present	X	X	-	-	X	-	-	X
7	ca-50205	AR7W Zone 5 *(Greenland Shelf)*	1996–present	X	X	-	-	X	-	-	X
8	ca-50401	Bedford Basin *(Northwestern North Atlantic)*	1967–present	X	X	-	X	X	X	-	-
9	ca-50501	Bay of Fundy *(Northwestern Atlantic shelf)*	1988–2012 discontinued	X	X	-	-	X	-	X	-
10	ca-50601	AZMP Station 27 *(Newfoundland Shelf)*	1960–present	X	-	-	-	X	-	-	X
11	ca-50701	AZMP Anticosti Gyre *(Gulf of St Lawrence)*	1999–present	X	-	-	-	X	-	-	X
12	ca-50702	AZMP Gaspe Current *(Gulf of St Lawrence)*	1999–present	X	-	-	-	X	-	-	X
13	ca-50703	AZMP Rimouski *(Gulf of St Lawrence)*	2005–present	X	X	-	X	X	-	-	X
14	ca-50704	AZMP Shediac *(Gulf of St Lawrence)*	1999–present	X	X	-	X	X	-	-	X
15	ca-50801	Central Scotian Shelf *(Northwestern Atlantic shelf)*	1996–present	X	X	-	X	X	X	-	-
16	ca-50802	Eastern Scotian Shelf *(Northwestern Atlantic)*	1997–present	X	X	-	X	X	X	-	-
17	ca-50803	Western Scotian Shelf *(Northwestern Atlantic)*	1997–present	X	X	-	X	X	X	-	-
18	co-30101	REDCAM Isla de San Andres *(Southwestern Caribbean)*	2002–present	X	X	X	-	-	-	-	-
19	co-30102	REDCAM Isla de Provencia *(Southwestern Caribbean)*	2002–present	X	X	X	-	-	-	-	-

No.	IGMETS-ID	Site or programme name	Year-span	T	S	Oxy	Ntr	Chl	Mic	Phy	Zoo
20	co-30103	REDCAM Western Colombia–Caribbean Shelf *(Southwestern Caribbean)*	2002–present	X	X	X	-	-	-	-	-
21	co-30104	REDCAM Eastern Colombia–Caribbean Shelf *(Southwestern Caribbean)*	2002–present	X	X	X	-	-	-	-	-
22	de-10101	Nordeney WQ-W2 *(Southern North Sea)*	1999–2008 (?)	X	X	-	X	-	-	X	-
23	de-30201	Helgoland Roads *(Southeastern North Sea)*	1962–present	X	X	-	X	-	X	X	X
24	de-30301	Cape Verde Ocean Observatory *(Tropical Eastern North Atlantic)*	2006–present	X	X	X	X	-	-	-	-
27	dk-30101	North Sea: DNAMAP-1510007 *(Baltic Sea)* *see Baltic Sea Annex (A2)*	1989–present	X	X	X	X	X	-	X	-
28	dk-30105	Ringkobing Fjord: DNAMAP-1 *(Baltic Sea)* *see Baltic Sea Annex (A2)*	1980–present	X	X	X	X	X	-	X	-
29	dk-30106	Nissum Fjord: DNAMAP-22 *(Baltic Sea)* *see Baltic Sea Annex (A2)*	1983–present	X	X	X	X	X	-	X	-
30	dk-30107	Nissum Bredning: DNAMAP-3702-1 *(Baltic Sea)* *see Baltic Sea Annex (A2)*	1982–present	X	X	X	X	X	-	X	-
31	dk-30110	Lister Dyb: DNAMAP-3 *(Baltic Sea)* *see Baltic Sea Annex (A2)*	1993–present	X	X	X	X	X	-	X	-
32	es-30101	BILBAO 35 Time Series *(Inner Bay of Biscay)*	1998–present	X	X	X	-	X	-	-	X
33	es-30102	URDAIBAI 35 Time Series *(Inner Bay of Biscay)*	1997–present	X	Xs	X	-	X	-	-	X
34	es-30201	AZTI Station D2 *(Southeastern Bay of Biscay)*	1986–present	X	X	X	X	X	-	X	-
35	es-30401	Nervion River Estuary E1 *(Southern Bay of Biscay)*	2000–present	X	X	-	-	-	-	X	-
36	es-50101	RADIALES Santander Station 4 *(Southern Bay of Biscay)*	1991–present	X	X	*	X	*	*	-	X
37	es-50102	RADIALES A Coruna Station 2 *(Northwestern Iberian coast)*	1988–present	X	X	X	X	X	X	X	X
38	es-50103	RADIALES Gijon/Xixon Station 2 *(Southern Bay of Biscay)*	2001–present	X	X	*	X	X	X	X	X
39	es-50104	RADIALES Vigo Station 3 *(Northwest Iberian coast)*	1994–present	X	X	-	X	X	-	-	X
40	es-50105	RADIALES Cudillero Station 2 *(Southern Bay of Biscay)*	1992–present	X	X	X	X	X	*	-	X

No.	IGMETS-ID	Site or programme name	Year-span	T	S	Oxy	Ntr	Chl	Mic	Phy	Zoo
41	fo-30101	Faroe Islands Shelf *(Faroe Islands)*	1991–present	X	-	-	X	X	-	-	X
42	fr-50101	REPHY Antifer Ponton Petrolier *(English Channel)*	1989–present	X	X	X	X	X	-	X	-
43	fr-50102	REPHY At So *(English Channel)*	1987–present	X	X	-	X	X	-	X	-
44	fr-50103	REPHY Donville *(English Channel)*	2002–present	X	X	X	X	X	-	X	-
45	fr-50104	REPHY Pen al Lann *(English Channel)*	1987–present	X	X	X	-	X	-	X	-
46	fr-50105	REPHY Point 1 SRN Boulogne *(English Channel)*	1992–present	X	X	-	X	X	-	X	-
47	fr-50106	REPHY Kervel *(Bay of Biscay)*	1987–present	X	X	-	-	X	-	X	-
48	fr-50107	REPHY Le Cornard *(Bay of Biscay)*	1987–present	X	X	X	-	X	-	X	-
49	fr-50108	REPHY Men er Roue *(Bay of Biscay)*	1987–present	X	X	-	X	X	-	X	-
50	fr-50109	REPHY Ouest Loscolo *(Bay of Biscay)*	1987–present	X	X	-	X	X	-	X	-
51	fr-50110	REPHY Teychan Bis *(Bay of Biscay)*	1999–present	X	X	-	X	X	-	X	-
52	fr-50201	Gravelines Station *(English Channel)*	1993–present	-	-	-	-	-	-	-	X
53	ie-30101	East Coast Ireland *(Ireland)*	1990–present	-	-	-	-	-	-	X	-
54	ie-30102	Northwest Coast Ireland *(Ireland)*	1990–present	-	-	-	-	-	-	X	-
55	ie-30103	South Coast Ireland *(Ireland)*	1990–present	-	-	-	-	-	-	X	-
56	ie-30104	Southwest Coast Ireland *(Ireland)*	1990–present	-	-	-	-	-	-	X	-
57	ie-30105	West Coast Ireland *(Ireland)*	1990–present	-	-	-	-	-	-	X	-
58	im-10101	Cypris Station – Isle of Man *(Irish Sea)*	1954–2009 (?)	X	X	X	X	X	-	X	-
59	is-30102	Selvogsbanki Transect *(South Iceland)*	1971–present	X	X	-	-	X	-	-	X
60	no-50401	Arendal Station 2 *(North Sea)*	1994 – present	X	X	X	X	X	-	-	X
61	pt-30101	Cascais Bay *(Portuguese Coast)*	2005–present	X	X	-	-	-	-	-	X

No.	IGMETS-ID	Site or programme name	Year-span	T	S	Oxy	Ntr	Chl	Mic	Phy	Zoo
62	pt-30201	Guadiana Lower Estuary *(Southwest Iberian Peninsula)*	1996–present	X	X	-	-	X	-	-	X
63	pt-30301	Guadiana Upper Estuary *(Southwest Iberian Peninsula)*	1996–present	X	X	-	X	X	X	X	-
64	uk-30101	Stonehaven *(Northwest North Sea)*	1997–present	X	X	-	X	X	-	X	X
65	uk-30102	Loch Ewe *(Northwest North Sea)*	2002–present	X	X	-	X	X	-	X	X
66	uk-30103	Loch Maddy *(Northwest North Sea)*	2003– 2011 (?)	X	X	-	X	-	-	X	-
67	uk-30104	Mill Port *(Northwest North Sea)*	2005– 2013 (?)	X	-	-	-	-	-	X	-
68	uk-30105	Scalloway – Shetland Isles *(Northwest North Sea)*	2001–present	X	X	-	X	-	-	X	-
69	uk-30106	Scapa Bay – Orkney *(Northwest North Sea)*	2001–present	X	X	-	X	-	-	X	-
70	uk-30201	Plymouth L4 *(Western English Channel)*	1988–present	X	X	X	X	X	X	X	X
71	uk-30301	Dove *(North Sea)*	1971–2002 discontinued	-	-	-	-	-	-	-	X
72	uk-30601	Atlantic Meridional Transect (AMT)	1995-present	X	X	X	X	X		X	X
73	uk-40106	SAHFOS–CPR A06 *(South Iceland)*	1958–present	-	-	-	-	X	-	X	X
74	uk-40111	SAHFOS–CPR B01 *(Northeastern North Sea)*	1958–present	-	-	-	-	X	-	X	X
75	uk-40112	SAHFOS–CPR B02 *(Northwestern North Sea)*	1958–present	-	-	-	-	X	-	X	X
76	uk-40114	SAHFOS–CPR B04 *(Southern Norwegian Sea)*	1958–present	-	-	-	-	X	-	X	X
77	uk-40115	SAHFOS–CPR B05 *(Southeast Iceland)*	1958–present	-	-	-	-	X	-	X	X
78	uk-40116	SAHFOS–CPR B06 *(Southwest Iceland)*	1958–present	-	-	-	-	X	-	X	X
79	uk-40117	SAHFOS–CPR B07 *(Southeast Greenland)*	1958–present	-	-	-	-	X	-	X	X
80	uk-40118	SAHFOS–CPR B08 *(Southwest Greenland)*	1962–present	-	-	-	-	X	-	X	X
81	uk-40121	SAHFOS–CPR C01 *(Eastern Central North Sea)*	1958–present	-	-	-	-	X	-	X	X
82	uk-40122	SAHFOS–CPR C02 *(Western Central North Sea)*	1958–present	-	-	-	-	X	-	X	X

No.	IGMETS-ID	Site or programme name	Year-span	T	S	Oxy	Ntr	Chl	Mic	Phy	Zoo
83	uk-40123	SAHFOS–CPR C03 *(Irish Sea)*	1958–present	-	-	-	-	X	-	X	X
84	uk-40124	SAHFOS–CPR C04 *(Northwest Scotland and Ireland)*	1958–present	-	-	-	-	X	-	X	X
85	uk-40125	SAHFOS–CPR C05 *(Northeast Central North Atlantic)*	1958–present	-	-	-	-	X	-	X	X
86	uk-40126	SAHFOS–CPR C06 *(Central North Atlantic)*	1958–present	-	-	-	-	X	-	X	X
87	uk-40127	SAHFOS–CPR C07 *(Northwest Central North Atlantic)*	1959–present	-	-	-	-	X	-	X	X
88	uk-40128	SAHFOS–CPR C08 *(Labrador)*	1959–present	-	-	-	-	X	-	X	X
89	uk-40131	SAHFOS–CPR D01 *(Southeast North Sea)*	1958–present	-	-	-	-	X	-	X	X
90	uk-40132	SAHFOS–CPR D02 *(Southwest North Sea)*	1958–present	-	-	-	-	X	-	X	X
91	uk-40133	SAHFOS–CPR D03 *(English Channel)*	1958–present	-	-	-	-	X	-	X	X
92	uk-40134	SAHFOS–CPR D04 *(South Ireland)*	1958–present	-	-	-	-	X	-	X	X
93	uk-40135	SAHFOS–CPR D05 *(Eastern Central North Atlantic)*	1958–present	-	-	-	-	X	-	X	X
94	uk-40136	SAHFOS–CPR D06 *(Central North Atlantic)*	1958–present	-	-	-	-	X	-	X	X
95	uk-40137	SAHFOS–CPR D07 *(Western Central North Atlantic)*	1959–present	-	-	-	-	X	-	X	X
96	uk-40138	SAHFOS–CPR D08 *(Western Central North Atlantic)*	1959–present	-	-	-	-	X	-	X	X
97	uk-40139	SAHFOS–CPR D09 *(Labrador Shelf)*	1959–present	-	-	-	-	X	-	X	X
98	uk-40144	SAHFOS–CPR E04 *(Bay of Biscay)*	1958–present	-	-	-	-	X	-	X	X
99	uk-40145	SAHFOS–CPR E05 (*Eastern Southern North Atlantic*)	1958–present	-	-	-	-	X	-	X	X
100	uk-40146	SAHFOS–CPR E06 (*Southern North Atlantic*)	1961–present	-	-	-	-	X	-	X	X
101	uk-40147	SAHFOS–CPR E07 (*Southern North Atlantic*)	1961–present	-	-	-	-	X	-	X	X
102	uk-40148	SAHFOS–CPR E08 (*Western Southern North Atlantic*)	1960–present	-	-	-	-	X	-	X	X
103	uk-40149	SAHFOS–CPR E09 (*Off Newfoundland Shelf*)	1960–present	-	-	-	-	X	-	X	X

No.	IGMETS-ID	Site or programme name	Year-span	T	S	Oxy	Ntr	Chl	Mic	Phy	Zoo
104	uk-40150	SAHFOS–CPR E10 (*Off Scotian Shelf*)	1961–present	-	-	-	-	X	-	X	X
105	uk-40154	SAHFOS–CPR F04 (*Off Iberian Shelf*)	1958–present	-	-	-	-	X	-	X	X
106	uk-40155	SAHFOS–CPR F05 (*Eastern Southern North Atlantic*)	1963–present	-	-	-	-	X	-	X	X
107	uk-40156	SAHFOS–CPR F06 (*Central Southern North Atlantic*)	1967–present	-	-	-	-	X	-	X	X
108	uk-40157	SAHFOS–CPR F07 (*Central Southern North Atlantic*)	1963–present	-	-	-	-	X	-	X	X
109	uk-40158	SAHFOS–CPR F08 (*Central Southern North Atlantic*)	1963–present	-	-	-	-	X	-	X	X
110	uk-40159	SAHFOS–CPR F09 (*Western Southern North Atlantic*)	1962–present	-	-	-	-	X	-	X	X
111	uk-40160	SAHFOS–CPR F10 (*Off Gulf of Maine*)	1961–present	-	-	-	-	X	-	X	X
112	us-10101	Bermuda Atlantic Time Series (*BATS*)	1982–present	X	X	X	X	X	X	-	X
113	us-10401	Boothbay (*Northwestern Atlantic shelf*)	2000–present	X	X	-	-	X	X	-	-
114	us-30101	Upper Chesapeake – Maryland (*Chesapeake Bay*)	1984–2002 (?)	-	-	-	-	-	-	-	X
115	us-30102	Lower Chesapeake – Virginia (*Chesapeake Bay*)	1985–2002 (?)	-	-	-	-	-	-	-	X
116	us-30201	Narragansett Bay (*Northwestern Atlantic*)	1959–present	X	X	-	X	X	-	-	-
117	us-30301	Neuse River Estuary NR000 (*Outer Banks – North Carolina*)	1994–present	X	X	X	X	X	-	-	-
118	us-30302	Pamlico Sound PS1 (*Outer Banks – North Carolina*)	2000–present	X	X	X	X	X	-	-	-
119	us-50101	EcoMon Gulf of Maine – GOM (*Gulf of Maine*)	1977–present	-	-	-	-	-	-	-	X
120	us-50102	EcoMon Georges Bank – GBK (*Georges Bank*)	1977–present	-	-	-	-	-	-	-	X
121	us-50103	EcoMon Southern New England – SNE (*Southern New England*)	1977–present	-	-	-	-	-	-	-	X
122	us-50104	EcoMon Mid-Atlantic Bight – MAB (*Mid-Atlantic Bight*)	1977–present	-	-	-	-	-	-	-	X
123	us-50105	EcoMon Gulf of Maine CPR line (*Gulf of Maine*)	1961–2012 discontinued	-	-	-	-	-	-	-	-
124	us-50106	EcoMon Mid-Atlantic Bight CPR line (*Mid-Atlantic Bight*)	1975–2012 discontinued	-	-	-	-	-	-	-	-

No.	IGMETS-ID	Site or programme name	Year-span	T	S	Oxy	Ntr	Chl	Mic	Phy	Zoo
125	us-50201	SEAMAP: Texas/Lousiana Shelf WEST (*Gulf of Mexico*)	1982–present	-	-	-	-	-	-	-	X
126	us-50202	SEAMAP: Texas/Louisiana Shelf CENTRAL (*Gulf of Mexico*)	1982–present	-	-	-	-	-	-	-	X
127	us-50203	SEAMAP: Texas/Lousiana Shelf EAST (*Gulf of Mexico*)	1982–present	-	-	-	-	-	-	-	X
128	us-50204	SEAMAP: Mississippi/Alabama Shelf (*Gulf of Mexico*)	1982–present	-	-	-	-	-	-	-	X
129	us-50205	SEAMAP: Florida Shelf NORTH-WEST (*Gulf of Mexico*)	1986–present	-	-	-	-	-	-	-	X
130	us-50206	SEAMAP: Florida Shelf NORTH-EAST (*Gulf of Mexico*)	1986–present	-	-	-	-	-	-	-	X
131	us-50207	SEAMAP: Florida Shelf SOUTH (*Gulf of Mexico*)	1982–present	-	-	-	-	-	-	-	X
132	us-50208	Northeast Off-shelf Region – SEAMAP (*Gulf of Mexico*)	1982–present	-	-	-	-	-	-	-	X
133	us-50209	Northwest Off-Shelf Region – SEAMAP (*Gulf of Mexico*)	1982–present	-	-	-	-	-	-	-	X
134	us-60101	NERRS ACE Basin	2001–present	X	X	X	X	X	-	-	-
135	us-60102	NERRS Apalachicola	2002–present	X	X	X	X	X	-	-	-
136	us-60103	NERRS Chesapeake Bay MD	2003–present	X	X	X	X	X	-	-	-
137	us-60104	NERRS Chesapeake Bay VA	2002–present	X	X	X	X	X	-	-	-
138	us-60105	NERRS Delaware	2001–present	X	X	X	X	X	-	-	-
139	us-60107	NERRS Grand Bay	2004–present	X	X	X	X	X	-	-	-
140	us-60108	NERRS Great Bay	2001–present	X	X	X	X	X	-	-	-
141	us-60109	NERRS Guana Tolomato Matanzas	2002–present	X	X	X	X	X	-	-	-
142	us-60111	NERRS Jacques Cousteau	2002–present	X	X	X	X	X	-	-	-
143	us-60112	NERRS Jobos Bay – Puerto Rico	2001–present	X	X	X	X	X	-	-	-
144	us-60115	NERRS Mission-Aransas	2007–present	X	X	X	X	X	-	-	-

No.	IGMETS-ID	Site or programme name	Year-span	T	S	Oxy	Ntr	Chl	Mic	Phy	Zoo
145	us-60116	NERRS Narragansett Bay	2002–present	X	X	X	X	X	-	-	-
146	us-60117	NERRS North Inlet – Winyah Bay	2001–present	X	X	X	X	X	-	-	-
147	us-60118	NERRS North Carolina	2001–present	X	X	X	X	X	-	-	-
148	us-60119	NERRS Old Woman Creek	2002–present	X	X	X	X	X	-	-	-
149	us-60121	NERRS Rookery Bay	2002–present	X	X	X	X	X	-	-	-
150	us-60122	NERRS Sapelo Island	2004–present	X	X	X	X	X	-	-	-
151	us-60126	NERRS Wells	2004–present	X	X	X	X	X	-	-	-
152	us-60127	NERRS Weeks Bay	2001–present	X	X	X	X	X	-	-	-
153	us-60128	NERRS Waquoit Bay	2002–present	X	X	X	X	X	-	-	-
154	ve-10101	CARIACO Ocean Time Series (*Cariaco Basin off Venezuela*)	1995–present	X	X	X	X	X	X	X	X

Atlantic Zone Monitoring Program (AZMP) Halifax Line 2, Prince 5

Country: Canada

IGMETS-ID: ca-50101, ca-50102

Catherine Johnson, Erica Head, Emmanuel Devred, Marc Ringuette, and Dave Hebert

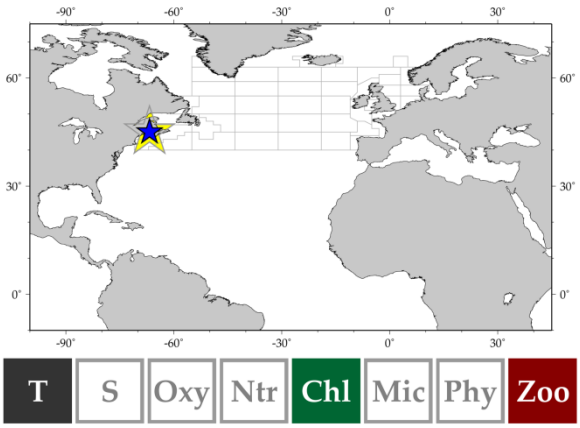

The Halifax Line 2 (HL2) station has been sampled semi-monthly since 1999 by the Atlantic Zone Monitoring Program (AZMP). AZMP was implemented by Fisheries and Oceans Canada in 1998 to (i) characterize and understand the causes of ocean variability at seasonal, interannual, and decadal scales, (ii) establish relationships among biological, chemical, and physical variability, and (iii) provide adequate data to support sound development of ocean activities. HL2 is located on the central Scotian Shelf, 11 km from the Nova Scotia coast, and has a bottom depth of 149 m. It exhibits strong annual-scale temperature variation, and its water properties are influenced both by cold, low salinity waters of the equatorward flowing Nova Scotia Current and by onshelf transport of warmer, saltier waters.

The Prince-5 time-series station has been sampled semi-monthly since 1999 by the Atlantic Zone Monitoring Program (AZMP), and a temperature and salinity time series extends back to the 1920s at the station. The Prince-5 station is located in the coastal outer Bay of Fundy and has a bottom depth of 95 m. It is strongly influenced by tidal mixing, and its water properties and plankton community reflect mixing of nearshore waters and waters of the outer Bay of Fundy, which are similar to the central Gulf of Maine.

AZMP performs a core set of observations including hydrography, oxygen, nutrients, chlorophyll, and zooplankton at the stations.

Related information: http://www.meds-sdmm.dfo-mpo.gc.ca/isdm-gdsi/azmp-pmza/index-eng.html

AR7W Greenland Shelf, Canada

Country: Canada

Site name (IGMETS-ID):

AR7W Zone 1 – Labrador Shelf (ca-50201)
AR7W Zone 2 – Labrador Slope (ca-50202),
AR7W Zone 3 – Central Labrador Sea (ca-50203)
AR7W Zone 4 – Eastern Labrador Sea (ca-50204)
AR7W Zone 5 – Greenland Shelf (ca-50205)

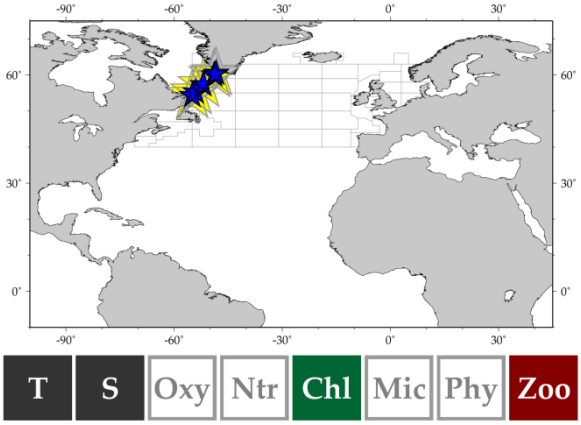

Erica Head, Marc Ringuette Igor Yashayaev, and Kumiko Azetsu-Scott

The Labrador Sea Monitoring Program collects physical, chemical, and biological oceanographic observations at fixed stations on the Atlantic Repeat Hydrography Line 7 West (AR7W) between southern Labrador and southwest Greenland. AR7W has been occupied annually (typically in May) since 1990, with biological measurements since 1994. The Labrador Sea is an area where intermediate-depth water masses are formed through winter convective sinking of dense surface water, transporting carbon dioxide and other important ocean properties to the lower limb of the ocean's Meridional Overturning Circulation. The Labrador Sea is also a key region for modification of the Labrador Current system, which influences oceanographic and ecosystem conditions downstream on the Atlantic Canadian shelf. As an important reservoir for the ecologically significant zooplankter *Calanus finmarchicus*, the Labrador Sea deep convection area meets the criteria for Ecologically or Biologically Significant Area adopted by the Conference of the Parties to the UNEP Convention on Biological Diversity.

Bedford Basin Monitoring Program (BBMP)

Country: Canada

IGMETS-ID: ca-50401

Andrew Cogswell and William Li

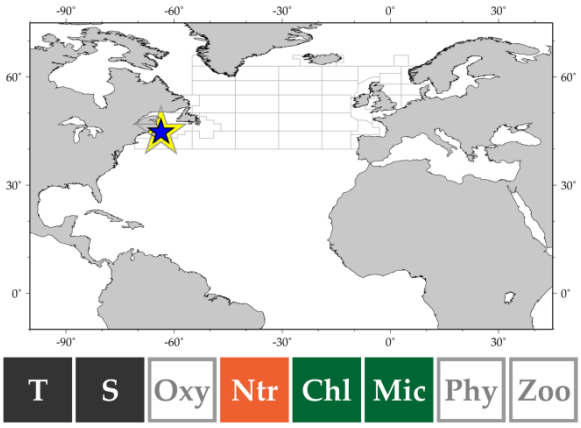

Bedford Basin is a small embayment that forms the inner portion of Halifax Harbour, Nova Scotia, Canada. It is encircled by the largest urban population centre in eastern Canada. For 30 years after the establishment of the Bedford Institute of Oceanography in 1962, the Basin served as an easily accessible body of water for marine research, as opportunity permitted. In 1992, regular oceanographic observation was initiated to record the state of the plankton ecosystem on a sustained basis. Weekly measurements are made of selected properties that characterize the physical, chemical, biological, and optical environments of the water column. This programme of research and monitoring delineates normal conditions in the Basin and discerns ecological change over long periods of time. The Compass Buoy station in Bedford Basin may be considered the inshore terminus of the Scotian Shelf Halifax Line of the Atlantic Zone Monitoring Program conducted by Fisheries and Oceans Canada.

Related information: http://www.bio.gc.ca/science/monitoring-monitorage/bbmp-pobb/bbmp-pobb-eng.php

St. Andrews Biological Station Phytoplankton Time Series – Bay of Fundy

Country: Canada

IGMETS-ID: ca-50501

Jennifer Martin

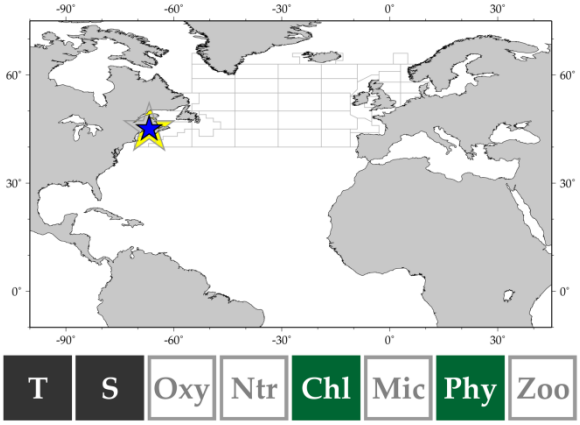

The St. Andrews Biological Station Phytoplankton Time Series was established in the Quoddy Region of the Bay of Fundy, eastern Canada in 1987. Purposes of the phytoplankton study were to (i) establish baseline data on phytoplankton populations since little detailed work had been published since earlier studies by Gran and Braarud (1935); (ii) identify harmful algal species that could potentially cause harm to the salmon aquaculture industry; (iii) provide an early warning to shellfish and finfish industries; (iv) observe new species to the region; and (v) determine patterns and trends in phytoplankton populations. The Bay of Fundy, has the largest tides in the world (exceeding 16 m), with a tidal range of 8.3 m in the Quoddy Region. Oscillation time is 13 h, and currents can be up to 2 m s^{-1}, resulting in vigorous mixing in some areas. Samples are collected weekly for phytoplankton, temperature, nutrients, salinity, and fluorescence from late April to late May and monthly during all other months.

AZMP Station 27

Country: Canada

IGMETS-ID: ca-50601

Pierre Pepin and Eugene Colbourne

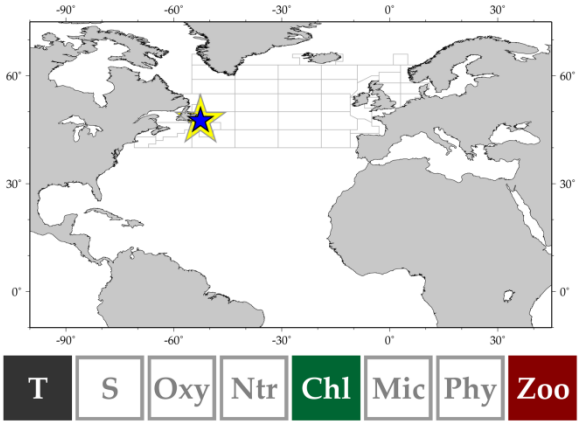

Station 27 has been sampled semi-monthly since 1999 under the Atlantic Zone Monitoring Program (AZMP), building on systematic oceanographic observations at the station extending back to 1947. AZMP was implemented by Fisheries and Oceans Canada in 1998 to (i) characterize and understand the causes of ocean variability at seasonal, interannual, and decadal scales, (ii) establish relationships among biological, chemical, and physical variability, and (iii) provide adequate data to support sound development of ocean activities. Station 27 is about 7 km off St. John's Harbour, Newfoundland in a water depth of 176 m. It is located in the Avalon Channel in the inshore branch of equatorward-flowing Labrador Current and exhibits strong annual-scale variations in temperature and salinity. AZMP performs a core set of observations including hydrography, oxygen, nutrients, chlorophyll, and zooplankton at the station.

Related information: http://www.meds-sdmm.dfo-mpo.gc.ca/isdm-gdsi/azmp-pmza/index-eng.html

Atlantic Zone Monitoring Program (AZMP): Rimouski and Shediac Valley stations

Country: Canada

Station name (IGMETS-ID):

AZMP Anticosti Gyre (ca-50701)
AZMP Gaspé Current (ca-50702)
AZMP Rimouski (ca-50703)
AR7W Shediac Valley (ca-50704)

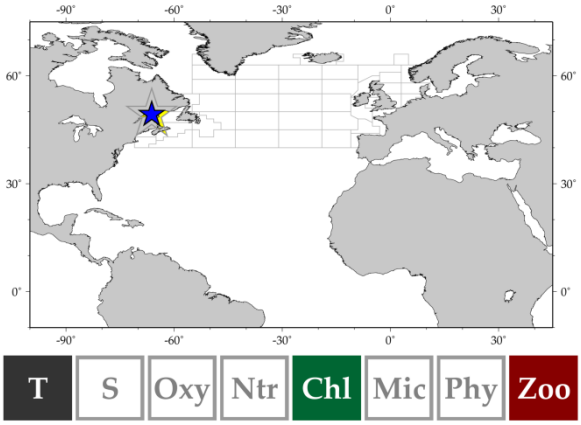

Stéphane Plourde, Michael Scarratt, Michel Starr, Peter Galbraith, and Laure Devine

The Atlantic Zone Monitoring Program (AZMP) was implemented by Fisheries and Oceans Canada to detect, track, and predict changes in the state and productivity of the Northwest Atlantic. AZMP is essential in order to tackle major issues such as the impact of climate change or to support the ecosystem approach to ensure conserving resources and protecting the marine environment. The Rimouski (depth: 335 m) and Shediac Valley (depth: 84 m) stations are two high-frequency sampling sites located in the western Gulf of St. Lawrence that are sampled on a weekly (Rimouski) or monthly (Shediac) basis from early spring to late autumn. On each visit to these stations, a CTD profile is performed and samples for phytoplankton, nutrients, and extracted chlorophyll are collected using Niskin bottles at fixed depths. Finally, zooplankton is vertically sampled from the bottom to the surface with a ring net (75-cm diameter, 200-µm mesh).

Related information: http://www.bio.gc.ca/science/monitoring-monitorage/azmp-pmza-eng.php
http://ogsl.ca/en/azmp/context.html

Atlantic Zone Monitoring Program (AZMP): Scotian Shelf

Country: Canada

Site name (IGMETS-ID):

AZMP Central Scotian Shelf (ca-50801)
AZMP Eastern Scotian Shelf (ca-50802)
AZMP Western Scotian Shelf (ca-50803)

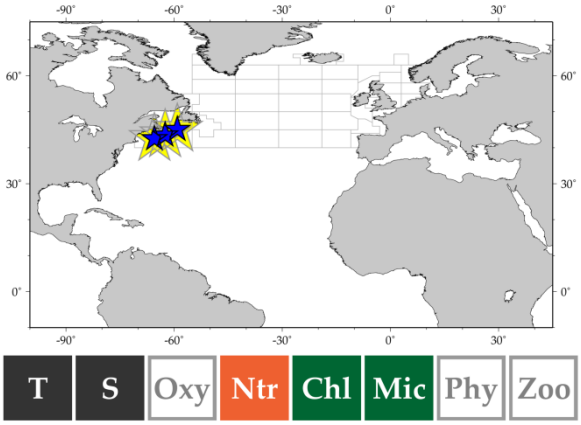

Andrew Cogswell, Catherine Johnson, David Hebert, and William Li

AZMP was implemented by Fisheries and Oceans Canada in 1997 for monitoring the Northwest Atlantic to understand, describe, and forecast the state of the ocean environment and marine ecosystem and to relate those changes to the predator–prey relationships of marine resources. AZMP works to protect the marine environment by providing data to support the sound development of ocean activities. The sampling regime consists of (i) seasonal and/or opportunistic sampling along 11 sections for information on the variability of the physical environment in the whole Northwest Atlantic region; (ii) higher-frequency temporal sampling (biological, chemical, and physical variables) at six accessible fixed sites for smaller time-scale dynamics in representative areas; (iii) satellite remote sensing of sea surface temperature and chlorophyll for broad synoptic spatial coverage of ocean data fields; and complemented by (iv) data from other sources (e.g. Continuous Plankton Recorder) and of other types (e.g. meteorological data, groundfish surveys).

Related information: http://www.meds-sdmm.dfo-mpo.gc.ca/isdm-gdsi/azmp-pmza/index-eng.html

REDCAM

Country: Colombia

Site names (IGMETS-ID):

REDCAM Isla de San Andres (co-30101)
REDCAM Isla de Provencia (co-30102)
REDCAM Western Colombia-Caribbean Shelf (co-30103)
REDCAM Eastern Colombia-Caribbean Shelf (co-30104)

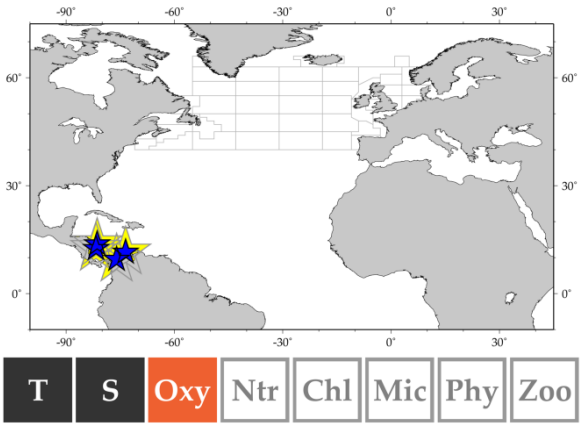

The Colombian Marine Environment Monitoring Network (REDCAM) was initiated in 2001 for the purpose of grouping multiple institutions and their efforts necessary to evaluate the chemical and sanitary quality of the marine and estuarine waters of Colombia. It is composed of 16 nodes and a main server located at INVEMAR (Santa Marta). Each node includes hardware and software for input and retrieval tables and cartographic information about the quality of marine and coastal waters of Colombia. It was established as a network of field stations that cover most of the Colombian coast. Since 2001 and twice a year at each node, it has been registering the values of the main physicochemical and bacteriological variables that characterize the quality of the marine and estuarine waters. Based on this information, the following zones have been identified as critical for its marine and coastal pollution: Santa Marta, Cartagena, Barranquilla, Morrosquillo, Uraba, and San Andres at the Caribbean coast and Buenaventura, Guapi, and La Tola at the Pacific coast.

Helgoland Roads

Country: Germany

IGMETS-ID: de-30201

Karen H. Wilshire, Alexandra Kraberg, Maarten Boersma, and Jasmin Renz

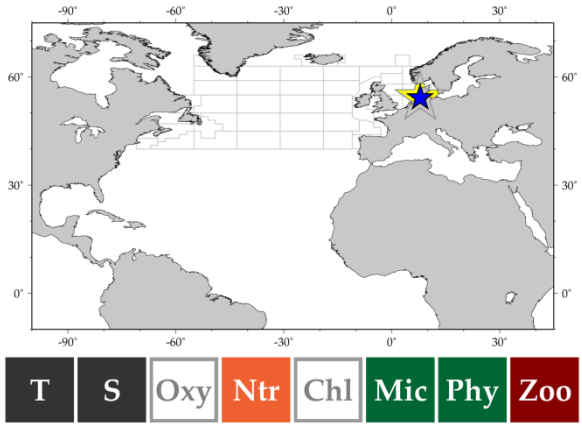

The Helgoland Roads time series, located at the island of Helgoland in the German Bight, ca. 60 km off the German mainland (54°11'N 7°54'E), is one of the richest temporal marine datasets available. The dataset comprises a phytoplankton time series (started in 1962 and sampled daily) and a zooplankton time series (started in 1975 and sampled three times a week) along with time series for inorganic nutrients, salinity, and temperature and several shorter time series (e.g. chlorophyll and other data from ferrybox systems).

The high sampling frequency of the Helgoland Roads time series has provided a unique opportunity to study long-term trends in abiotic and biotic parameters, but also ecological phenomena, such as seasonal interactions between different foodweb components, niche properties, and the dynamics and timing of the spring bloom. It has also facilitated close examination of the dynamics of new species appearing in the local ecosystem.

Related information: http://www.awi.de/en/research/research_divisions/biosciences/shelf_sea_ecology/long_term_studies/helgoland_roads_long_term_data_series/

Cape Verde Ocean Observatory – CVOO

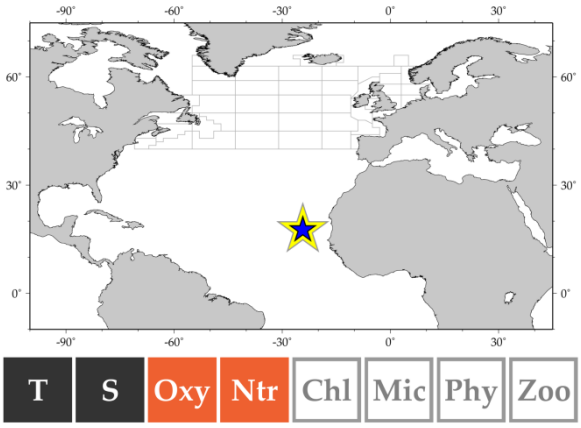

Country: Germany

IGMETS-ID: de-30301

Björn Fiedler, Arne Körtzinger, Pericles Silva, and Johannes Karstensen

CVOO (17°35′N 24°17′W), established in 2006, is located in the open eastern tropical North Atlantic (ETNA), 100 km northeast of the Cape Verde archipelago and downwind of the Mauritanian upwelling region (Fiedler, 2013). The Cape Verde Atmospheric Observatory (CVAO) is colocated 100 km downwind of CVOO and measures the marine boundary layer without terrestrial contaminations. CVOO represents open-ocean oligotrophic conditions; it is at the rim of an oxygen minimum zone (OMZ) in the ETNA. Observations are based on ship-based monthly sampling (0–500 m) with the local research vessel "Islândia" and an interdisciplinary full-depth mooring (3600 m) equipped with a variety of physical and biogeochemical sensors. Ship-based sampling frequency varies due to weather conditions and logistical constraints. RV "Islândia" is equipped with state-of-the-art instruments to collect temperature, salinity, biological parameters, nutrients, dissolved carbon, and oxygen. Novel observational platforms (gliders and profiling floats) are used within the framework of CVOO.

Related information: http://cvoo.geomar.de

BILBAO 35 Time Series

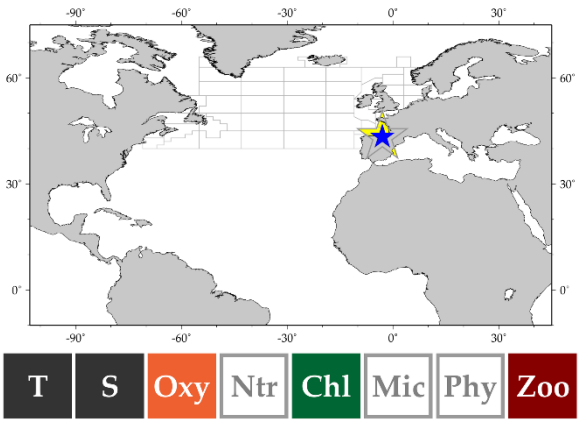

Country: Spain

IGMETS-ID: es-30101

Fernando Villate, Ibon Uriarte, and Arantza Iriarte

The BILBAO 35 Time-Series, established in the outer part of the Estuary of Bilbao in Abra Harbour (Basque coast, inner Bay of Biscay), constitutes the outermost sampling site of an environmental and plankton-monitoring programme carried out in five salinity sites (35, 34, 33, 30, and <30) along the estuary. The series was initiated in 1997 to report mesozooplankton changes in relation to water conditions and hydroclimatologic forces in the most perturbed estuary of the Basque coast. It also aims to contribute to understanding the combined effect of climate change and local human perturbations on plankton ecosystems of temperate coastal areas. The Bilbao 35 site (43°20′N 3°01′W) shows an annual chlorophyll maximum in summer (Iriarte *et al*., 2010), and it is sampled nearly every month to obtain profiles of temperature, salinity, and dissolved oxygen, collect zooplankton samples, and gather water samples for chlorophyll determination at mid-depth below the halocline.

URDAIBAI 35 Time Series

Country: Spain

IGMETS-ID: es-30102

Fernando Villate, Ibon Uriarte, and Arantza Iriarte

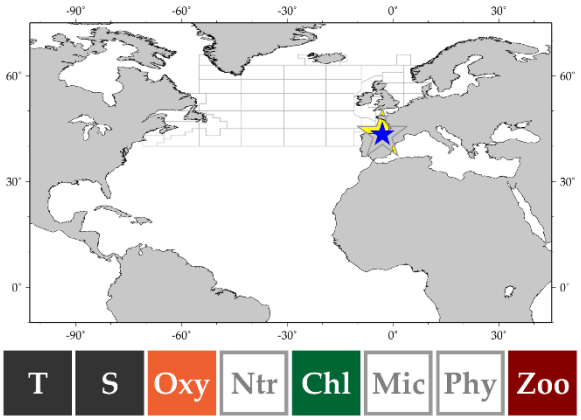

The URDAIBAI 35 Time-Series is established in the mouth of the Estuary of Urdaibai (Basque coast, inner Bay of Biscay) and constitutes the outermost sampling site of an environmental- and plankton-monitoring programme carried out in four salinity sites (35, 33, 30, and 26) along the estuary. The series was initiated in 1997 to report mesozooplankton changes in relation to water conditions and hydroclimatologic forces in this well-conserved estuary located within a biosphere reserve. The aim was also to contribute to understanding the combined effect of climate change and local human perturbations on plankton ecosystems of temperate coastal areas. The Urdaibai 35 site (43°24´N 2°41´W) shows a bimodal chlorophyll cycle with a maximum in early spring (Iriarte *et al*., 2010), and it is sampled nearly every month to obtain profiles of temperature, salinity, and dissolved oxygen, collect zooplankton samples, and gather water samples for chlorophyll determination at mid-depth below the halocline.

AZTI Station D2

Country: Spain

IGMETS-ID: es-30201

Marta Revilla, Almudena Fonán, Ángel Borja, and Victoriano Valencia

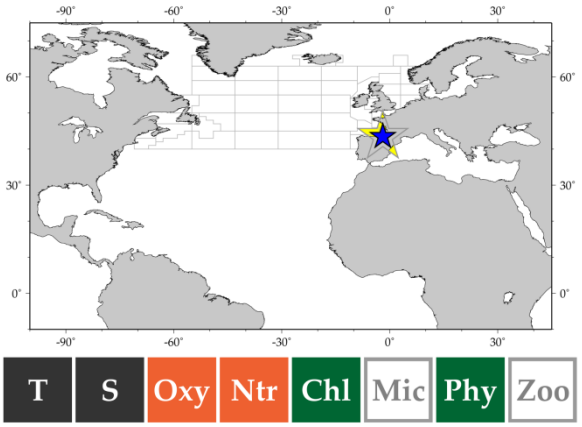

D2 station (43°27'N 01°55'W) was established in 1986 in the southeastern part of the Bay of Biscay (North Atlantic region). This station is located 13.1 km offshore at a depth of 110 m. Due to its distance from the main pollution sources on land, it is considered to be unaffected by anthropogenic influences. Freshwater content is low (2.3‰ at the surface). The longest time series involves temperature, salinity, and phytoplankton biomass (chlorophyll *a*) data collected by means of CTD continuous vertical profiles. Although irregularly sampled, eight surveys per year have been conducted on average (Revilla *et al*., 2010). In addition, phytoplankton abundance and composition together with environmental variables (e.g. nutrients) have been monitored since 2002. The time series aims to understand oceanometeorological processes and how they can affect fisheries. Since 2002, this station has also been used as a reference site for the assessment of environmental/ecological quality in the context of the European Directives.

Related information: http://www.azti.es/marine-research/

Nervión River Estuary

Country: Spain

IGMETS-ID: es-30401

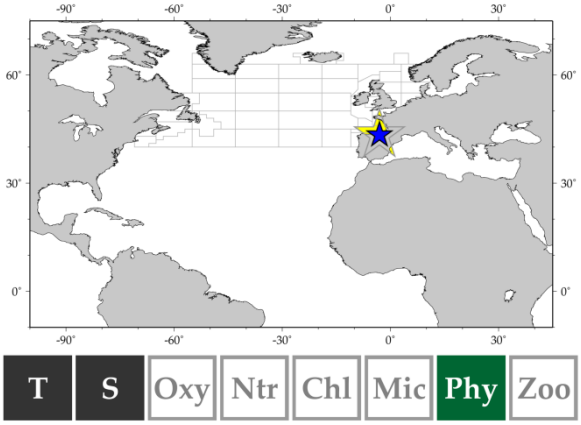

Emma Orive, Javier Franco, Aitor Laza-Martinez, Sergio Seoane, Alejando de la Sota, and Marta Revilla

The River Nervión Estuary, also known as Bilbao Estuary and Nervión–Ibaizabal Estuary, is a small mesotidal estuary located in the northeast part of the Bay of Biscay (Atlantic Ocean, northern Spain). It is channeled for most its length (about 25 km) and consist of two well-differentiated parts: the inner and middle segments, which are narrow (about 100 m in width) and shallow (about 10 m in depth), whereas the outer segment is a semi-enclosed bay of about 2 km in width and about 25 m maximum depth. In recent years, and particularly after the implementation of the European Water Framework Directive of 2000, it has been the subject of several monitoring programmes dealing with the study of the abundance and composition of plankton populations, among other bioindicators. The outer estuary contains a very active harbour and two beaches that have been recovered for bathing following the construction of a wastewater treatment plant serving most populated areas and industries.

RADIALES

Country: Spain

Site name (IGMETS-ID):

RADIALES Santander (es-50101)
RADIALES A Coruña (es-50102)
RADIALES Gijón/Xixón (es-50103)
RADIALES Vigo (es-50104)
RADIALES Cudillero (es-50105)

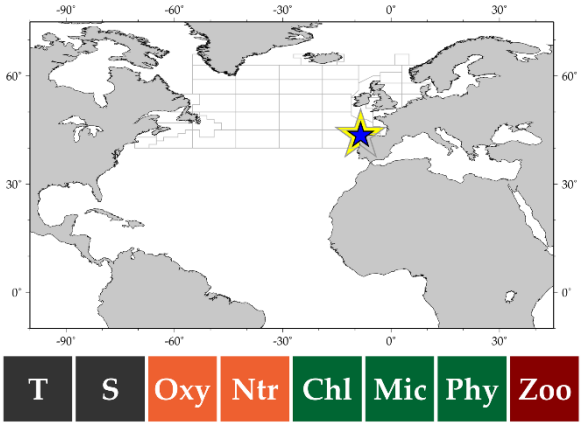

Antonio Bode, Jorge Luis Valdés, Jose Luis Acuña, Marta Álvarez, Maria Teresa Álvarez-Ossorio, Ricardo Anadón, José Manuel Cabanas, Gerardo Casas, Xose-Anxelu Guitiérrez-Morán, Nicolás González, César González-Pola, Rafael González-Quirós, Mikel Latasa, Alicia Lavín, Ángel López-Urrutia, Ana Miranda, Enrique Nogueira, Beatriz Reguera, José-María Rodríguez, M. Carmen Rodriguez, Francisco Rodriguez-Hernández, Manuel Ruiz-Villarreal, Renate Scharek, Eva Teira, Manuel Varela, Marta Varela

The RADIALES time-series programme has been monitoring shelf waters in northern Spain since 1990. Core observations include ship-based hydrographic, biogeochemical, and plankton measurements at monthly intervals in five oceanographic sections along the Iberian shelf. RADIALES aims at understanding and modelling the response of the marine ecosystem to the sources of temporal variability in oceanographic and planktonic components, particularly focusing on those factors and processes affecting biological production and potentially altering ecosystem services. Located in a key transitional biogeographic region, RADIALES allows for the analysis of variability in the coastal ecosystem in a gradient from the seasonal upwelling off Galicia to the temperate waters of the southern Bay of Biscay. This gradient encompasses changes in biological productivity, biodiversity, and biogeochemical fluxes. RADIALES is supported by base funds of the Instituto Español de Oceanografía (IEO) complemented by funds from competitive research projects. In addition, several universities collaborate with the programme.

Related information: http://www.seriestemporales-ieo.com/

Faroe Islands Shelf

Country: Faroe Islands

IGMETS-ID: fo-30101

Eilif Gaard, Solva Jacobsen, and Karin Margretha H. Larsen

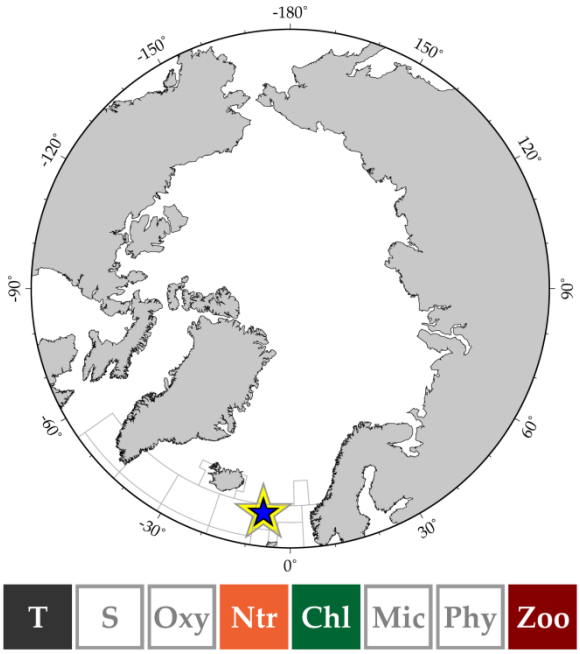

The Faroe Shelf water is relatively well separated from the surrounding ocean by a persistent front that surrounds the shelf at the 100–150 m bottom depth contour. The shelf water contains a neritic ecosystem. In order to study the influences of environmental variables on plankton and fish larvae in the ecosystem, the Faroe Marine Research Institute operates two time series: one in spring (last week of April) and one in midsummer (second half of June). The spring time series was established in 1994 and contains ca. 30 stations on the shelf and the surrounding ocean for monitoring hydrography and Chl *a* (CTD and fluorescence profiles) combined with spectrophotometric analysis of chlorophyll *a*. Zooplankton is collected with bongo net tows, using 100- and 200-µm mesh nets, respectively. *Calanus finmarchicus* egg production is monitored at selected stations. The summer time series was established in 1994 and includes profiles of temperature, salinity, Chl *a*, and nutrients at 50 stations on the shelf and the surrounding ocean. In order to study short-term variability and dynamics of the Faroe Shelf oceanography and plankton, the Faroe Marine Research Institute conducts frequent monitoring of temperature, salinity, Chl *a*, and nutrients at a coastal station on the Faroe Shelf. Seawater from 18-m depth at a tidally well-mixed location is pumped into the station. This seawater is representative of the central shelf areas. The time series was established in 1995. Temperature is measured continuously, and samples for salinity and nutrient analysis are collected twice a week throughout the year. Chlorophyll *a* is analysed on a weekly basis between April and September.

French Phytoplankton and Phycotoxin Monitoring Network (REPHY)

Country: France

Site name (IGMETS-ID):

REPHY Antifer Ponton Petrolier (English Channel) (fr-50101),
REPHY At So (English Channel) (fr-50102)
REPHY Donville (English Channel) (fr-50103)
REPHY Pen al Lann (English Channel) (fr-50104)
REPHY Point 1 SRN Boulogne (English Channel) (fr-50105)
REPHY Kervel (Bay of Biscay) (fr-50106)
REPHY Le Cornard (Bay of Biscay) (fr-50107)
REPHY Men er Roue (Bay of Biscay) (fr-50108)
REPHY Quest Loscolo (Bay of Biscay) (fr-50109)
REPHY Teychan Bis (Bay of Biscay) (fr-50110)

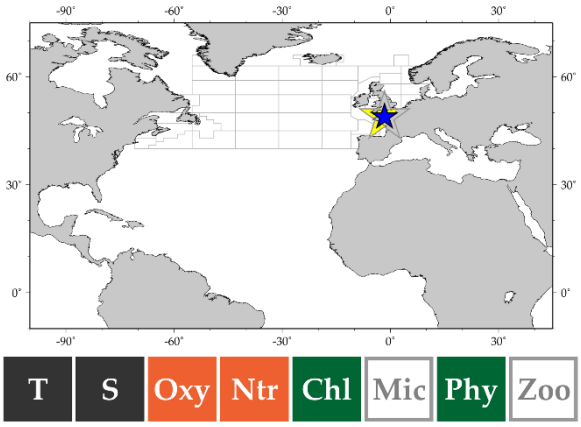

Dominique Soudant, Jacky Chauvin, Mickael Retho, Nathalie Cochennec-Laureau, and Claire Méteigner

The French Phytoplankton and Phycotoxin Monitoring Network (REPHY) was set up in 1984 to (i) enhance knowledge of phytoplankton communities, (ii) safeguard public health, and (iii) protect the marine environment (Belin, 1998). Phytoplankton along the French coast has been sampled up to twice a month since 1987 at 12 coastal laboratories. For that purpose, the French coast is divided into a hierarchy of sites and subsites common to three regional networks: the English Channel, the Bay of Biscay, and the Mediterranean Sea.

Within the English Channel, the REPHY Point 1 SRN Boulogne and At So sites are both shallow and characterized by a macrotidal regime, especially the latter, which is also more sheltered. Sampling started in 1987 at At So and five years later at Point 1 SRN Boulogne. Ancillary measurements of temperature, salinity, chlorophyll *a*, phaeopigments, inorganic nutrient concentrations, and turbidity are also routinely measured (usually 15 samples per year). Oxygen was incorporated in 2007 at both sites.

Men er Roue, Ouest Loscolo, Le Cornard, and Teychan Bis are four REPHY sites in the Bay of Biscay. These sites are all shallow, meso- to macrotidal, with differing wave exposure, from sheltered in Teychan Bis to moderately exposed at Ouest Loscolo and Le Cornard. From 1987 onwards, the basic environmental variables (salinity, temperature, and turbidity) are measured together with phytoplankton composition and abundance. Variables such as inorganic nutrient concentrations, chlorophyll *a*, phaeopigments, and oxygen were included in the time series of most of the sites later in different years.

Gravelines Station

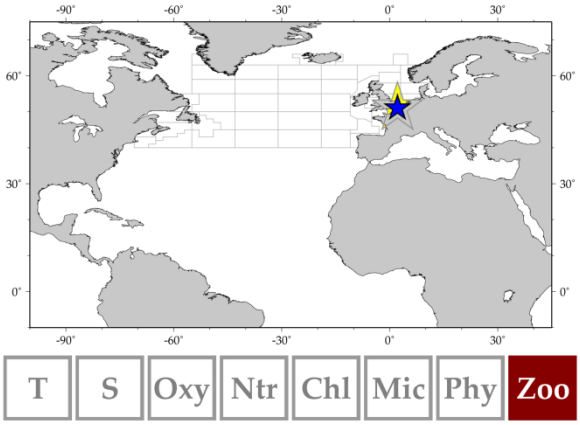

Country: France

IGMETS-ID: fr-50201

Elvire Antaja, Christophe Loots, and Alain Lefebvre

The French Research Institute for Exploitation of the Sea (Ifremer) has established a monthly time series of zooplankton species since 1978 at Gravelines, a station located in the western port of Dunkirk at the lower end of the southern bight of the North Sea. This ecological survey is done in the framework of a research programme designed to observe environmental evolution on the site of a nuclear power plant. The Gravelines Station is located in the entrance of the channel inflow to the power plant and is not impacted by the power plant water discharge. The monitoring at Gravelines Station also includes the following parameters measured on a weekly basis: temperature, ammonium, nitrate, chlorophyll *a*, phaeopigment concentrations, and phytoplankton abundance.

Related information: http://wwz.Ifremer.fr/manchemerdunord

Time Series Stations Ireland

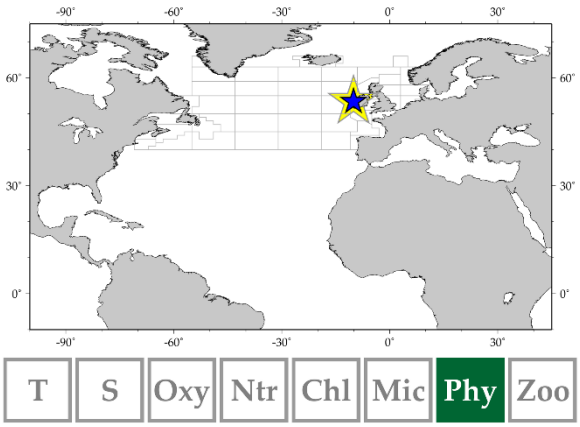

Country: Ireland

Site name (IGMETS-ID):

East Coast Ireland (ie-30101)
Northwest Coast Ireland (ie-30102)
South Coast Ireland(ie-30103)
Southwest Coast Ireland (ie-30104)
West Coast Ireland (ie-30105)

Joe Silke and Rafael Salas

The Marine Institute in Ireland carries out a national phytoplankton monitoring programme which extends back to the late 1980s. This includes a harmful algal blooms (HABs) monitoring service that warns producers and consumers of concentrations of toxic plankton in Irish coastal waters that could contaminate shellfish or cause fish deaths and also a series of sentinel stations that are monitored for the European Water Framework. Since 1990, data have been captured in a systematic manner and logged into an electronic database. Principal component analysis of the dataset resulted in five groups of sites. Based on the data extracted and amalgamated from these regions, it is deemed to be a good representation of the phytoplankton flora for these regions. Sites were sampled by a variety of methods, either surface samples, discrete Ruttner sampling bottles, or tube samplers. Following fixing by Lugol's iodine, they were analysed using the Utermöhl method. Species were identified and enumerated, and cell counts were expressed in cells l^{-1}. Average sea surface temperatures for western and southern waters of Ireland range from 8–10°C in winter to 14–17°C in summer and tend to be several degrees higher than the eastern waters. As the water column stratifies in summer, a surface-to-bottom temperature difference of up to 6°C is typical of waters along the Atlantic shelf and Celtic Sea. Along the coast, turbulent tidal currents are sufficient to prevent establishment of stratification, and the water remains mixed throughout the year. The boundary between mixed and stratified waters in summer is marked by tidal fronts that influence the composition and density of phytoplankton community in these areas.

Related information: http://www.marine.ie/habs

Selvogsbanki Transect (southern Iceland)

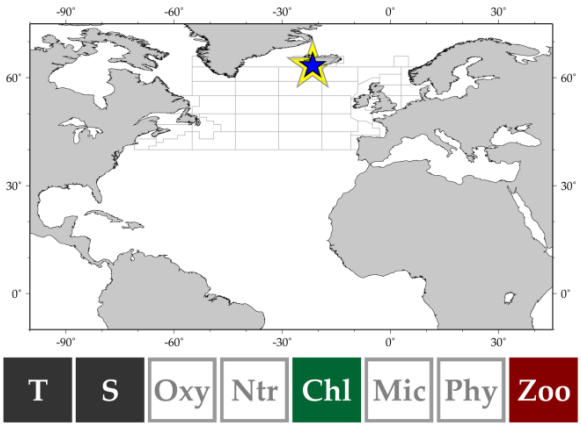

Country: Iceland

IGMETS-ID: is-30102

see also Siglunes Transect (Arctic Ocean, is-30101)

Astthor Gislason, Hafsteinn Gudfinnsson, and Kristinn Gudmundsson

The Icelandic monitoring programme for hydrography, nutrients, phytoplankton, and zooplankton consists of a series of standard transects around Iceland perpendicular to the coastline. In the 1960s, sampling was started at stations along transects north and east of Iceland. Additional transect lines south and west were added in the 1970s. Currently, there are ca. 90 stations, with sampling carried out at these stations every year in May and June. In this IGMETS study, we have included data from the Siglunes Transect off northern Iceland and the Selvogsbanki Transect off southwestern Iceland. These two transects represent conditions from two very different water bodies. The Siglunes Transect contains plankton communities and hydrography primarily from subarctic, polar waters, while the Selvogsbanki Transect community and conditions predominantly represent North Atlantic water. As such, the Iceland contribution to IGMETS is found in both the Arctic Ocean (Chapter 3) and the North Atlantic (Chapter 4) sections.

Related information: http://www.hafro.is/index_eng.php

Arendal Station 2

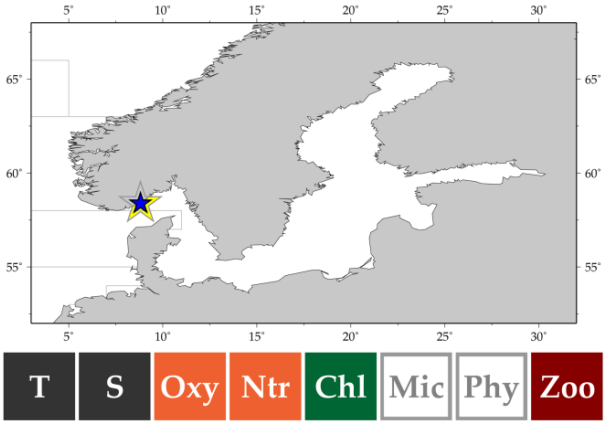

Country: Norway

IGMETS-ID: no-50401

Tone Falkenhaug and Lena Omli

The zooplankton time series at Arendal Station 2 in northern Skagerrak was established in 1994 by the Institute of Marine Research (IMR, Norway) with the objective of monitoring the environmental status in coastal waters and documenting long-term changes in the plankton communities. The site is located at 58°23'N 08°49'E, 1 nautical mile offshore from the IMR Flødevigen Research Station in a water depth of 105 m. The Skagerrak is located downstream of the North Sea, the Baltic Sea, and the Kattegat. Water bodies of different origin enter and influence the site, which is characterized by strong seasonal variations in temperature, light, and nutrients. Sampling at Arendal Station 2 is carried out twice a month. Zooplankton is sampled from 50 m to the surface using vertical ring net tows (180-µm mesh). Data on hydrography and samples for nutrients and chlorophyll are collected using a CTD profiler fitted with a water bottle rosette.

Cascais Watch (Cascais Bay)

Country: Portugal

IGMETS-ID: pt-30101

Antonina dos Santos, Miguel P. Santos, João Pastor, and Alexandra Silva

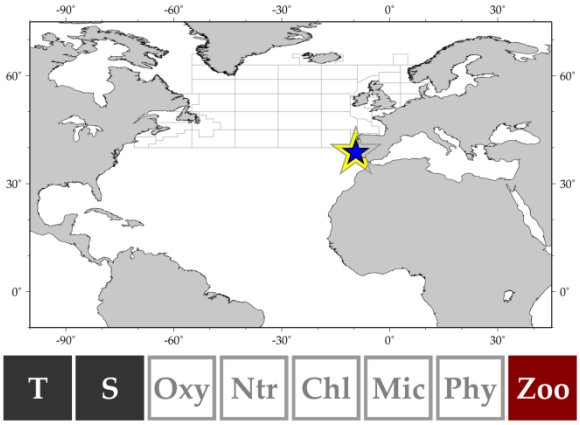

The Cascais site (since 2005) is a station of the Oceanography and Plankton Group of IPMA for providing long-term oceanographic information capable of detecting seasonal and interannual changes in plankton related to environmental conditions. The station is located off Cascais, outside the Tejo River estuary at 38°40'N 09°26'W at the west coast of Portugal. The site is considered to be under the influence of the Eastern North Atlantic Upwelling System in spring and summer. This seasonal upwelling is responsible for the high phytoplankton production which promotes stable zooplankton abundance throughout the year (Santos *et al*., 2007). Environmental parameters such as temperature, salinity, and fluorescence are collected *in situ* (CTD) and measured along with zoo- and phytoplankton sampling to obtain diversity and abundance of plankton taxa. Monthly precipitation and upwelling index values are also obtained. Plankton assemblages are very diverse and include temperate, subtropical, and tropical species.

Guadiana Lower Estuary

Country: Portugal

IGMETS-ID: pt-30201

Maria Alexandra Teodósio, Joana Cruz, Pedro Morais, Marco Mattos, Joao Pedro Encarnacao, Renata Goncalves, Susana Ferreira, Teja Muha, Vanessa Neves, Vania Baptista, and Luis Chicharo

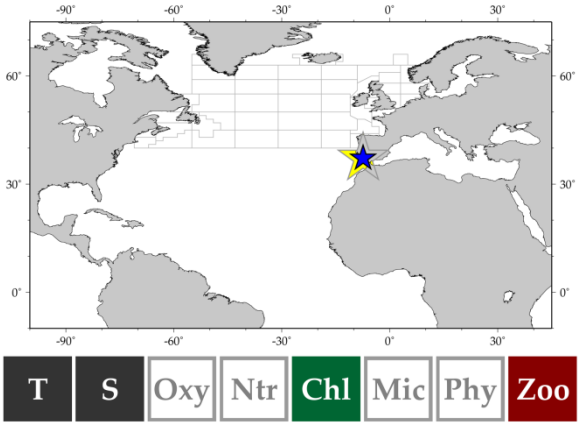

The Lower Guadiana Estuary time series, established in the south Iberia Peninsula in 1997, aims at understanding linkages between hydrological and zooplanktonic processes and how these change over time. It also aims at monitoring early phases of invasive species. The sampling conducted nearly every month includes a programme at two stations located at 37°13'N 07°24'W and 37°07'N 07°24'W, with depth ranging from 5 to 30 m and using a WP-2 net.The construction of the large Alqueva Dam, whose construction began in the upper estuary in 1999 and was completed in 2002, increased freshwater flow regulation in the area. As a consequence, the Guadiana estuary shifts between being freshwater-dominated during winter and flood periods and registering a marine influence during most of the year. In recent years, a reduction in productivity and an increase of invasive species was reported: *Blackfordia virginica* (Chícharo *et al*., 2009), *Maeotias marginata* (Muha *et al*., 2017), *Fundulus heteroclitus* (Gonçalves *et al*., 2015), *Mnemiopsis leidyi* (Cruz *et al*., subm.). The flow stability seems to facilitate introductions for different species while the natural flow regime, with low and high freshwater discharge, discourage invasions, as native biota has evolved in response to overall flow regime. An integrated management approach – i.e. freshets released from dams to control the populations– was proposed to minimize or mitigate the putative impacts of these species in the Guadiana estuary.

Guadiana Upper Estuary

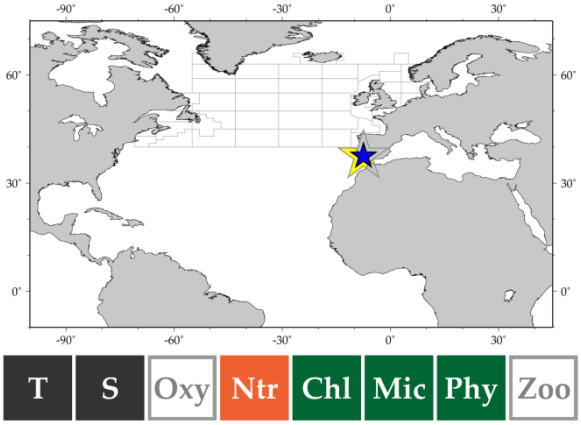

Country: Portugal

IGMETS-ID: pt-30301

Ana B. Barbosa, Rita B. Domingues, and Helena M. Galvão

Monitoring the Guadiana Upper Estuary by the Aquatic Microbiology Laboratory at Universidade do Algarve (autumn 1996 to autumn 2010) was aimed at studying cyanobacteria bloom dynamics in the freshwater zone in the period before, during, and after construction of the Alqueva Dam. This huge dam, completed in 2003, is located 150 km upstream and has a total catchment of 55 000 km², further restricting river flow from 75 to 81%. The Guadiana River situated in an arid Mediterranean region has a torrential flow regime varying markedly both seasonally and interannually, thus exerting a strong regulating influence on chlorophyll maxima, which typically occur in the upper estuary. Potentially toxic cyanobacteria predominated in the freshwater zone from mid-summer to late autumn due to seasonal shifts in nutrients (Rocha *et al*., 2002). The Alqueva Dam construction was hypothesized to increase intensity of cyanobacteria blooms, but contributed instead to oligotrophication and the disappearance of cyanobacteria blooms in the upper estuary (Galvão *et al*., 2012).

Stonehaven, East Scotland

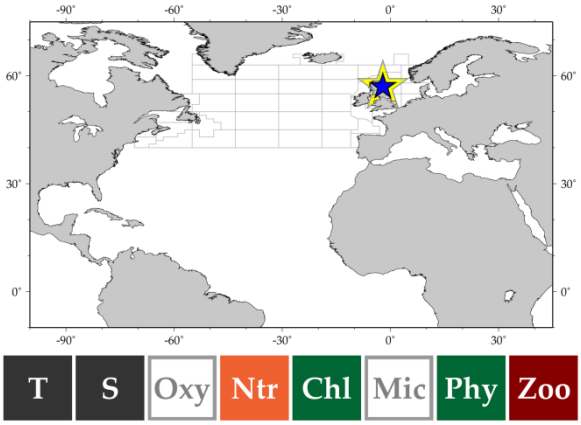

Country: United Kingdom

IGMETS-ID: uk-30101

Eileen Bresnan and Kathryn Cook

The Marine Scotland Science (MSS) Stonehaven sampling site is located in the northern North Sea at 56°57'N 02°06'W, ca. 5 km offshore. It is part of a network of coastal ecosystem monitoring sites operated by MSS around the Scottish coast to provide information on baseline environmental conditions that act as reference sites to fulfil the requirements of the EU Water Framework Directive and to test the development of tools to identify "Good Environmental Status" for the Marine Strategy Framework Directive. The origins of water passing down the Scottish east coast lie mainly north and west of Scotland and are a variable mix of coastal and oceanic Atlantic waters. The site has a water depth of 50 m and has been sampled weekly since 1997. A wide range of parameters are measured, including surface and near-seabed temperature, salinity, nutrient concentrations, carbon chemistry, integrated (0–10 m) chlorophyll concentrations, and phytoplankton and zooplankton community composition.

Related information: http://www.gov.scot/Resource/Doc/295194/0099701.pdf

Loch Ewe, West Scotland

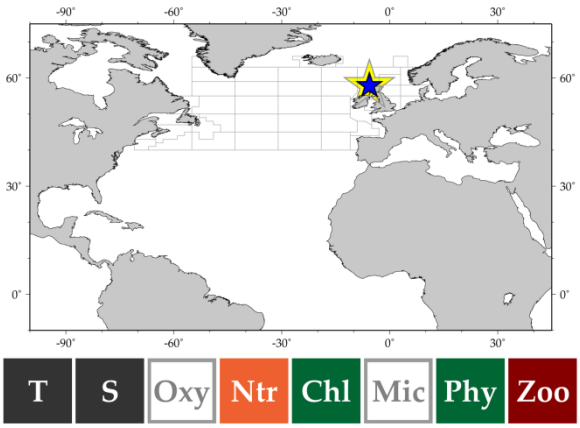

Country: United Kingdom

IGMETS-ID: uk-30102

Eileen Bresnan and Kathryn Cook

The Marine Scotland Science (MSS) Loch Ewe sampling site is located at 57°51'N 05°39'W ca. 0.5 km offshore in a sea loch. It is part of a network of coastal ecosystem monitoring sites operated by MSS around the Scottish coast to provide information on baseline environmental conditions that act as reference sites to fulfil the requirements of the EU Water Framework Directive and to test the development of tools to identify "Good Environmental Status" for the Marine Strategy Framework Directive. To the north, the loch opens into the North Minch and then the eastern Atlantic. Water movements in this loch are complex and strongly influenced by wind and tide. The site has a water depth of 40 m and has been sampled weekly since 2002. A wide range of parameters are measured including surface and near-seabed temperature, salinity, nutrient concentrations, integrated (0–10 m) chlorophyll concentrations, and phytoplankton and zooplankton community composition.

Related information: http://www.gov.scot/Resource/Doc/295194/0099701.pdf

Loch Maddy

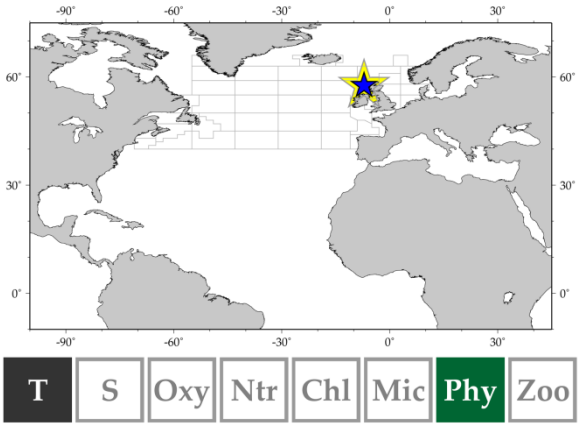

Country: United Kingdom

IGMETS-ID: uk-30103

Eileen Bresnan

Loch Maddy (Site 38, 57°36'N 07°08'W) is located on the Island of North Uist, part of the Western Isles. It is a unique site with a diverse saline lagoon system opening into the sea loch, which contains a mix of rocky reefs and soft-sediment habitats. This system supports a rich diversity of marine life and, as a result, has been designated a marine special area of conservation (SAC). Loch Maddy has been participating in the Marine Scotland Science Coastal Ecosystem Monitoring Programme since 2003.

Related information: http://www.gov.scot/Resource/Doc/295194/0099701.pdf

Millport, The Clyde

Country: United Kingdom

IGMETS-ID: uk-30104

Eileen Bresnan

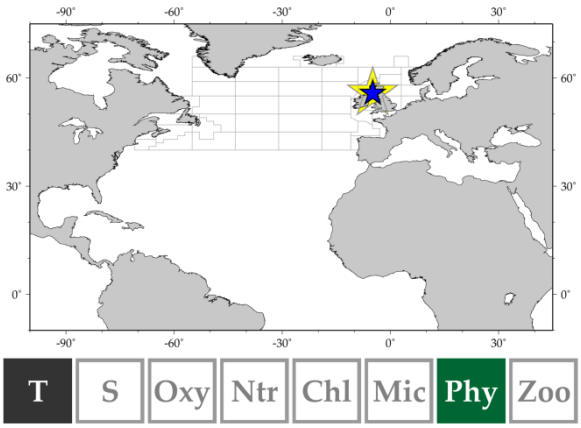

The Marine Scotland Science (MSS) Millport sampling site is located at 55°44'N 04°54'W. It is part of a network of coastal ecosystem monitoring sites operated by MSS around the Scottish coast to provide information on baseline environmental conditions. Millport is situated on the Isle of Cumbrae in the Clyde Sea. The monitoring site is at Keppel Pier where there is one of the longest time series of temperature data in the UK. Monitoring for phytoplankton began in this site in 2005. Samples are collected by the Field Studies Centre on the Island.

Related information: http://www.gov.scot/Resource/Doc/295194/0099701.pdf

Scalloway, Shetland Island

Country: United Kingdom

IGMETS-ID: uk-30105

Eileen Bresnan

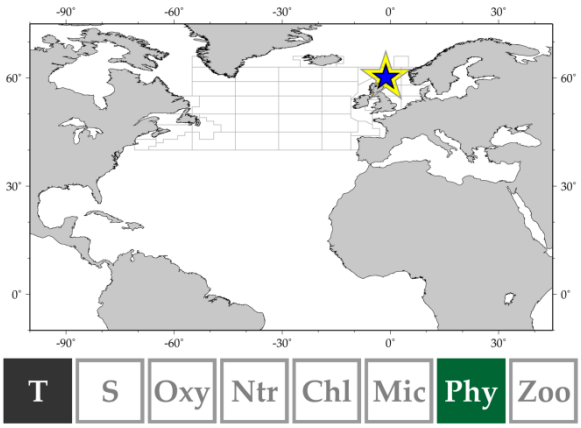

The Marine Scotland Science (MSS) Scapa Bay sampling site is located at 60°08'N 01°16'W. It is part of a network of coastal ecosystem monitoring sites operated by MSS around the Scottish coast to provide information on baseline environmental conditions that act as reference sites to fulfil the requirements of the EU Water Framework Directive and to test the development of tools to identify "Good Environmental Status" for the Marine Strategy Framework Directive. The Shetland Islands lie over 100 miles north of the UK mainland. Atlantic water from west of the UK enters the North Sea between Orkney and Shetland and also around northeast Shetland. Scalloway is located on the southwest coast of Shetland. Sampling is performed by the North Atlantic Fisheries College. The site has been sampled weekly since 2001. A range of parameters are measured including temperature, salinity, nutrient concentrations, and phytoplankton community composition.

Related information: http://www.gov.scot/Resource/Doc/295194/0099701.pdf

Scapa Bay, Orkney Islands

Country: United Kingdom

IGMETS-ID: uk-30106

Eileen Bresnan

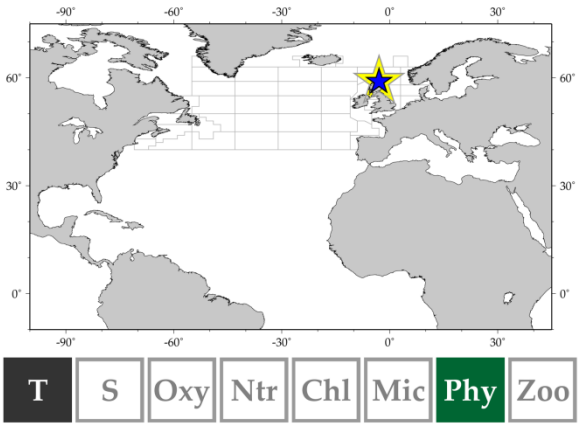

The Marine Scotland Science (MSS) Scapa Bay sampling site is located at 58°57'N 02°58'W. It is part of a network of coastal ecosystem monitoring sites operated by MSS around the Scottish coast to provide information on baseline environmental conditions that act as reference sites to fulfil the requirements of the EU Water Framework Directive and to test the development of tools to identify "Good Environmental Status" for the Marine Strategy Framework Directive. The Orkney Islands are an archipelago of over 70 islands which lie 50 miles north of the UK mainland. The Scapa Bay monitoring site is located at Scapa Pier, and samples are collected by Orkney Islands Harbour Council on a voluntary basis. The site has been sampled weekly since 2001. A range of parameters are measured including temperature, salinity, nutrient concentrations, and phytoplankton community composition.

Related information: http://www.gov.scot/Resource/Doc/295194/0099701.pdf

Plymouth L4

Country: United Kingdom

IGMETS-ID: uk-30201

Tim Smyth, James Fishwick, Malcolm Woodward, Glen Tarran, Ruth Airs, Claire Widdicombe, and Angus Atkinson

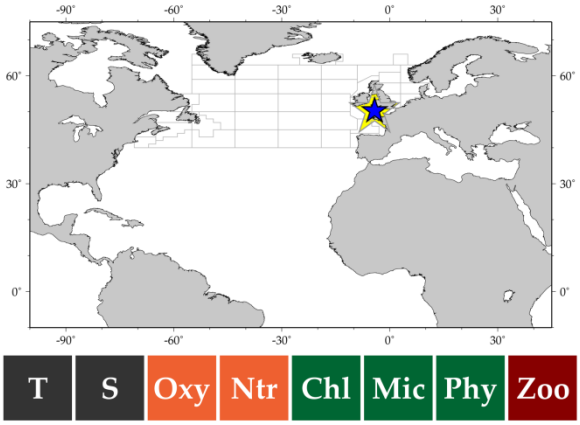

L4 is one of a series of stations, now known as the Western Channel Observatory, that have been sampled periodically for over a century. Sampling of L4 (13 km from Plymouth, ca. 50 m water depth) has been on weekly basis since 1988. Another site, E1 lying further offshore, is sampled fortnightly. Buoys at both sites provide finer resolution. L4 provides both a time series and a biodiversity reference site, since a wide range of process measurements, including the benthos, augment the monitoring. Trophic levels up to fish are covered, including Plymouth Marine Laboratory's measurements on physics, optics, nutrients, flow cytometry, HPLC-pigments, and the identification of over 300 phytoplankton and zooplankton taxa. Although the L4 site is dynamic, it stratifies seasonally, and the high-resolution profiling allow insights into processes at a great range of scale from extreme weather events, through seasonality, up to decadal and longer-term changes.

Related information: http://www.westernchannelobservatory.org.uk/

Atlantic Meridional Transect (AMT)

Country: United Kingdom

IGMETS-ID: uk-30601 – uk-30624

Andy Rees

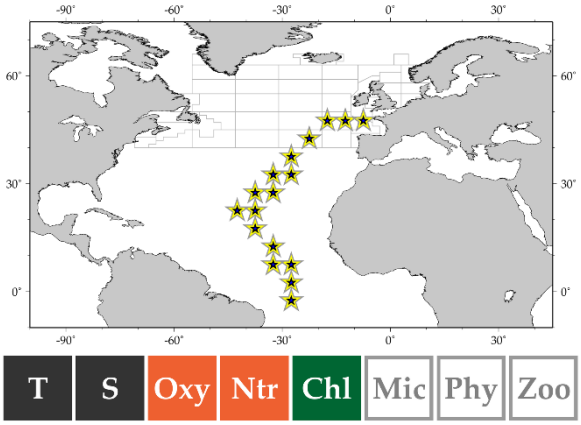

The Atlantic Meridional Transect (AMT) is a multidisciplinary programme which undertakes biological, chemical, and physical oceanographic research during an annual voyage between the UK and destinations in the South Atlantic. AMT began in 1995, with scientific aims to assess mesoscale to basin-scale phytoplankton processes, functional interpretation of bio-optical signatures and seasonal, regional, and latitudinal variations in mesozooplankton dynamics. The programme provided a platform for international scientific collaboration, including the calibration and validation of SeaWiFS measurements and products. The measurements of hydrographic and bio-optical properties, plankton community structure, and primary production completed during the first 12 transects (1995–2000) represent the most coherent set of repeated biogeochemical observations over ocean-basin scales. This unique dataset has led to several important discoveries concerning the identification of oceanic provinces, validation of ocean-colour algorithms, distributions of picoplankton, the identification of new regional sinks of carbon dioxide, and variability in rates of primary production and respiration. In 2002, the programme restarted (2002–2006) and broadened to address a suite of cross-disciplinary questions concerning ocean plankton ecology, biogeochemistry, and their links to atmospheric processes. The programme is coordinated and led by Plymouth Marine Laboratory in collaboration with the National Oceanography Centre.

Related information: http://www.amt-uk.org/

The spatial subsetting and analysis of the AMT time series was still being processed at the time of the preparation of this report, and data were, therefore, not included in the analysis presented in Chapter 4. Upon incorporation in the IGMETS assessment, the AMT contribution will be available online (http://igmets.net/explorer).

North Atlantic Continuous Plankton Recorder (CPR) survey

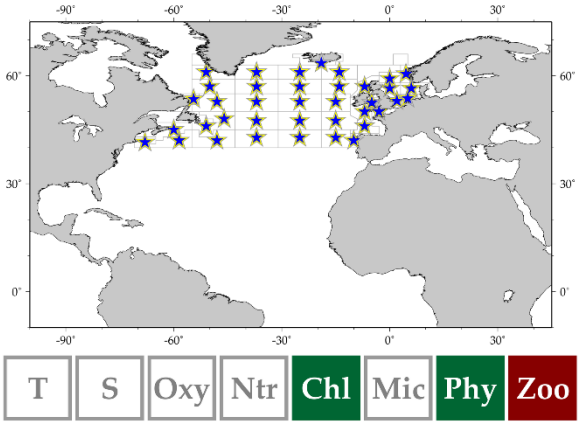

Country: United Kingdom

IGMETS-ID: uk-40106, uk-40111, uk-40112; uk-40114 through uk-40118, uk-40121 through uk-40128, uk-40131 through uk-40139, uk-40144 through uk-40150, uk-40154 through uk-40160 *see also entry in the Arctic Ocean Annex*

Martin Edwards, Priscilla Licandro, Claudia Castellani, and Rowena Stern

The Continuous Plankton Recorder (CPR) survey is a long-term, subsurface, marine plankton monitoring programme consisting of a network of CPR transects towed monthly across the major geographical regions of the North Atlantic. It has been operating in the North Sea since 1931, with some standard routes existing with virtually unbroken monthly coverage back to 1946. After each tow, the CPR samples are returned to the laboratory for routine analysis, including the estimation of phytoplankton biomass (Phytoplankton Colour Index, PCI) and the identification of up to 500 different phytoplankton and zooplankton taxa (Warner and Hays, 1994). Direct comparisons between the Phytoplankton Colour Index and other chlorophyll *a* estimates, including SeaWiFS satellite estimates, indicate strong positive correlations (Batten *et al*., 2003; Raitsos *et al*., 2005).

Related information: http://sahfos.org/

Bermuda Atlantic Time–series Study

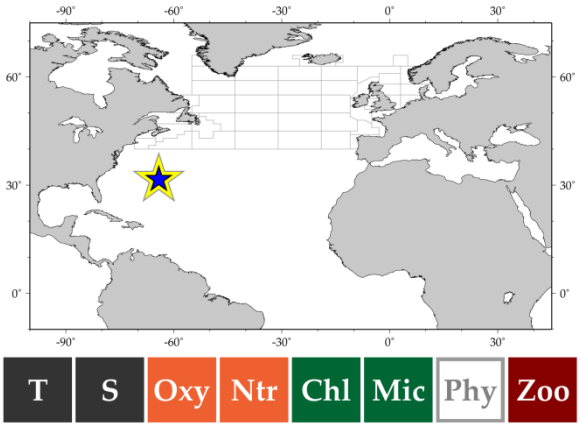

Country: United States

IGMETS-ID: us-10101

Nicholas R. Bates, Rodney J. Johnson, Deborah K. Steinberg, and Michael W. Lomas

The Bermuda Atlantic Time-series Study (BATS) programme has sampled the northwestern Sargasso Sea on a biweekly (January–April) to monthly basis (biweekly during January–April) since October 1988. The primary objective of the core BATS programme continues to be an improved understanding of the time-variable processes and mechanisms that control the biogeochemical cycling of carbon and related elements in the surface ocean. This study region is largely representative of other oligotrophic ocean regions, but does have a strong seasonal signal, with increased deep mixing and a seasonal peak in primary production in spring, followed by strong depletion of inorganic carbon in the surface ocean in summer (Lomas *et al*., 2013). With 25+ years of measurements for many chemical, physical, and biological variables, we are able to move beyond descriptions of seasonal and interannual variability to examination of multiyear trends (Bates *et al*., 2014) and potential climatic controls on organic matter production, export, and remineralization.

Related information: http://bats.bios.edu

Boothbay – Maine

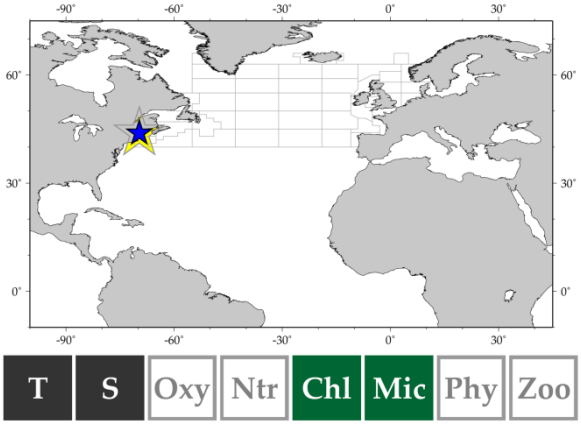

Country: United States

IGMETS-ID: us-10401

Nicole Poulton and Mike Sieracki

Boothbay is a small mesotidal embayment located along mid-coast Maine, USA, with no major river input. Circulation is dominated by strong semi-diurnal tidal mixing with offshore Gulf of Maine coastal waters. The monitoring site was initiated from a floating dock in 2000 located near the State of Maine's Department of Marine Resources. The purpose of the study is to monitor long-term physical and chemical changes and phytoplankton population dynamics. Weekly observations at high tide of phytoplankton, bacteria, and eukaryotic heterotrophs are made using flow cytometry. Temperature, salinity (refractometer measurements), and size-fractionated chlorophyll *a* are also determined. Flow cytometric ataxonomic groups are defined and enumerated (*Synechococcus*, cryptophytes, and total phytoplankton < 20 µm). Microplankton taxonomic distribution (15–300 µm) and abundance are collected using an imaging cytometer, FlowCAM (Sieracki *et al*., 1998). As of 2012, nutrients and zooplankton abundance and composition (vertical net tows) have also been determined.

Related information: http://fac.bigelow.org/

Narragansett Bay

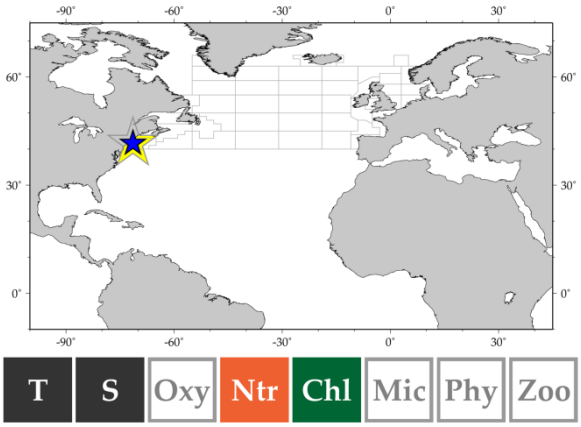

Country: United States

IGMETS-ID: us-30201

Tatiana Rynearson and Ted Smayda

Narragansett Bay, Rhode Island is a highly productive estuary located on the east coast of North America. Regarded as one of the world's longest-running plankton time series, samples have been collected weekly from Narragansett Bay since the 1950s. Samples are collected once a week for temperature, salinity, turbidity, size-fractionated chlorophyll *a*, and nutrients. Microplankton community composition (species identification and abundance) is determined using a light microscope to quantify live samples. The species list for the >10-µm size fraction includes 246 different species or species complexes of protists. Samples are also collected for the determination of copepod and ctenophore concentrations. The full dataset has been available to the public since 1999.

Related information: http://www.gso.uri.edu/phytoplankton/

Neuse River Estuary

Country: United States

IGMETS-ID: us-30301

Pamlico Sound

Country: United States

IGMETS-ID: us-30301

Hans Paerl and Ben Peierls

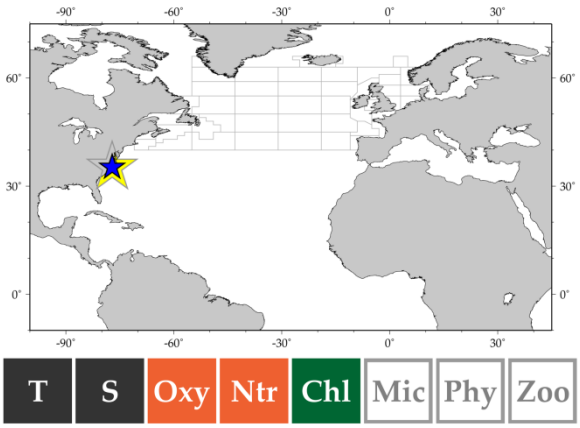

The Neuse River Estuary (NRE) Modeling and Monitoring Program (ModMon) is a partnership between the University of North Carolina (NC) Institute of Marine Sciences, the NC Department of Environmental and Natural Resources–Division of Water Resources, and the Neuse River Compliance Association that has been collecting and analyzing water quality data on the NRE since 1994. ModMon was created following declines in NRE water quality and in support of nutrient management actions. The NRE is a shallow (3.8 m mean depth), river- and wind-driven, intermittently mixed estuary in eastern NC that is a tributary of Pamlico Sound (4.9 m mean depth), the USA's largest lagoonal estuary. The programme consists of eleven sites in the NRE and nine sites in southwestern Pamlico Sound spanning a gradient of freshwater to seawater salinity. Profiles of *in situ* temperature, salinity, dissolved oxygen, pH, turbidity, and chlorophyll fluorescence are collected at each site, along with surface and near-bottom water samples for nutrient, organic matter, primary productivity, and phytoplankton diagnostic pigment analyses.

EcoMon Time Series

Country: United States

Site name (IGMETS-ID):

EcoMon – Gulf of Maine (us-50101)
EcoMon – Georges Bank (us-50102)
EcoMon – Southern New England (us-50103)
EcoMon – Mid-Atlantic Bight (us-50104)
EcoMon – Gulf of Maine CPR Transects (us-50105)
EcoMon – Mid-Atlantic Bight CPR Transects (us-50106)

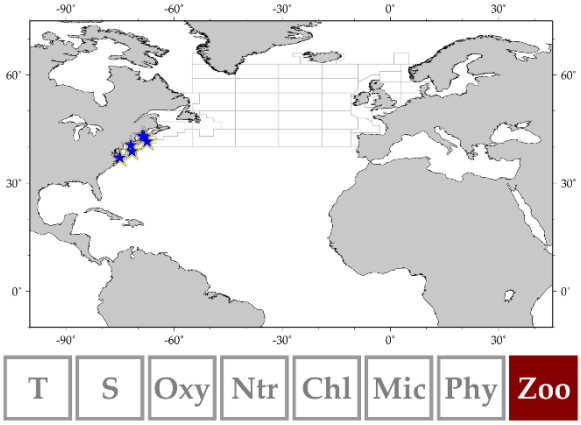

Jon Hare

The Northeast Fisheries Science Center has maintained long-term plankton observing on the Northeast US Shelf using bongo nets towed obliquely to a maximum depth of 200 m. Zooplankton are identified to the lowest taxonomic level possible, and developmental stage is determined for a subset of species. Taxonomic analyses are conducted at the Plankton Sorting and Identification Center in Szczecin, Poland. The survey area extends from Cape Hatteras, North Carolina to the western portions of the Scotian Shelf and encompasses four regions: Gulf of Maine, Georges Bank, Southern New England, and Mid-Atlantic Bight. The observations started in 1977 and surveys have occurred 6–8 times a year to resolve the large seasonality in the ecosystem. Since 2013, the seasonal coverage has been cut to four surveys per year. The effort is described more fully in McClatchie *et al*. (2014) and Kane (2007).

The Northeast Fisheries Science Center supported monthly Continuous Plankton Recorder (CPR) transects across the Gulf of Maine and the Mid-Atlantic Bight. Sampling began in the early 1960s in the Gulf of Maine and the mid-1970s in the Mid-Atlantic. The CPR was towed behind merchant vessels, and zooplankton and phytoplankton were identified to the lowest taxonomic level by experts at the NEFSC and the Plankton Sorting and Identification Center in Gydnia, Poland. The monthly sampling well resolved the strong seasonal cycle in the Northeast US Shelf ecosystem. The NEFSC canceled the programmes in 2013, and operations were shifted to the Sir Alister Hardy Foundation for Ocean Science. Samples are not being processed, but are being stored until funds for processing can be found. The effort is described more fully in Jossi and Kane (2013).

SEAMAP Plankton Time Series

Country: United States

Site name (IGMETS-ID):

SEAMAP: Texas/Louisiana Shelf West (us-50201)
SEAMAP: Texas/Lousiana Shelf Central (us-50202)
SEAMAP: Texas/Louisiana Shelf East (us-50203)
SEAMAP: Mississippi/Alabama Shelf (us-50204)
SEAMAP: Florida Shelf (us-50205, us-50206, us50207)
SEAMAP: Northeast Gulf of Mexico (us-50208)
SEAMAP: Northwest Gulf of Mexico (us-50209)

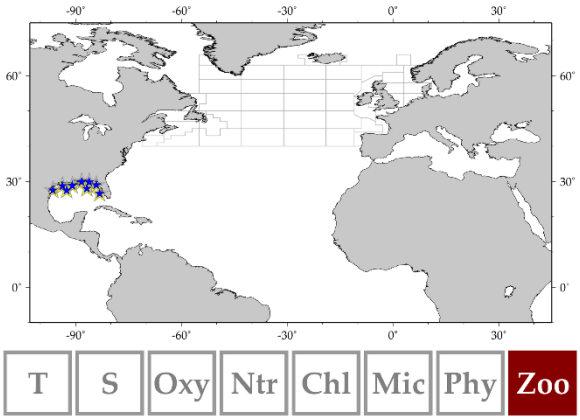

David S. Hanisko and Glenn Zapfe

The SouthEast Area Monitoring and Assessment Program (SEAMAP) is a state/federal/university cooperative programme for collection, management, and dissemination of fishery-independent data and information in the southeastern United States. SEAMAP has been conducting plankton surveys throughout the Gulf of Mexico since 1982. The goal of these surveys has been to assemble a time series of data on the occurrence, abundance, and geographical distribution of fish eggs and larvae, as well as to collect data on selected physical properties of their pelagic habitat (McClatchie *et al*., 2014). The SEAMAP plankton sampling domain covers the entire northern GOM from the 10-m isobath out to the US EEZ and comprises ca. 300 designated sampling sites arranged in a fixed, systematic grid. Intermittent sampling outside the SEAMAP domain has also occurred. Sampling is carried out principally during three dedicated plankton surveys, but is also piggybacked onto other fishery-independent resource surveys. Samples are primarily taken utilizing 60-cm bongo and/or 1 × 2 m neuston nets.

Related information: http://www.gsmfc.org/#:content@3:links@4
http://www.sefsc.noaa.gov/labs/mississippi/surveys/plankton.htm

National Estuarine Research Reserve System (NERRS)
System–wide Monitoring Program (SWMP)

Country: United States

Site name (IGMETS-ID): us-60101 - us-60126

Dwayne Porter (liaison)

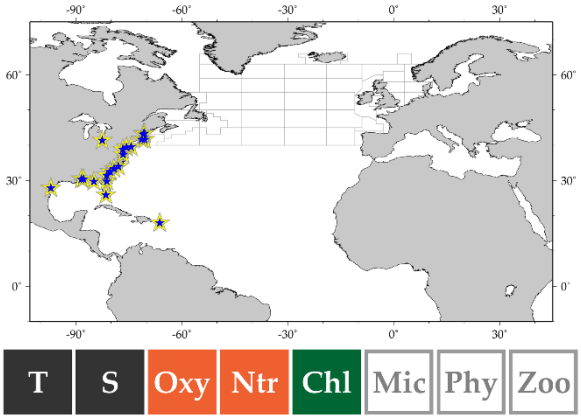

The National Estuarine Research Reserve System (NERRS) is a network of 28 coastal sites designated to protect and study estuarine systems. Established through the Coastal Zone Management Act, the reserves represent a partnership programme between the National Oceanic and Atmosphere Administration (NOAA) and the coastal states. NOAA provides funding and national guidance, and each site is managed on a daily basis by a lead state agency or university with input from local partners.

NERRS acknowledges the importance of both long-term environmental monitoring programmes and data and information dissemination through its support of the NERRS System-wide Monitoring Program (SWMP). The goal of the SWMP is to identify and track short-term variability and long-term changes in the integrity and biodiversity of representative estuarine ecosystems and coastal watersheds for the purpose of contributing to effective national, regional, and site-specific coastal zone management. This comprehensive programme consists of three phased components: estuarine water quality monitoring, biodiversity monitoring, and land-use and habitat change analysis.

The NERRS research reserves encompass 1.3 million acres of estuaries along the US coastlines.

Related information: https://coast.noaa.gov/nerrs/

CARIACO Ocean Time Series, Venezuela

Country: Venezuela

IGMETS-ID: ve-10101

Laura Lorenzoni and Frank Muller-Karger

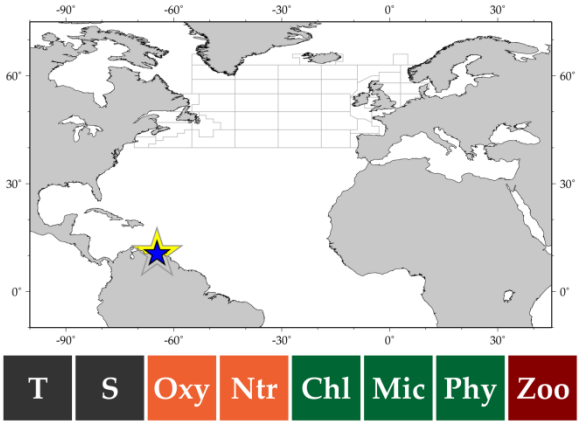

The CARIACO Ocean Time Series Project was established in the Cariaco Basin in November 1995 with support from the Venezuelan Fondo Nacional de Ciencia, Tecnología e Investigación (FONACIT) and the US National Science Foundation (NSF). The Cariaco Basin is a semi-enclosed tectonic depression located on the continental shelf off northern Venezuela in the southern Caribbean Sea. It is composed of two ca. 1400 m deep subbasins that are connected to the Caribbean Sea by two ca. 140 m deep channels. These channels allow for open exchange of near-surface water. The restricted circulation below the 140-m sill, coupled with highly productive surface waters due to seasonal wind-driven coastal upwelling (ca. 450 g C m^{-2} $year^{-1}$; Muller-Karger *et a*l., 2010), has led to sustained anoxia below about 250 m. The goal of the project is to understand linkages between oceanographic processes and the production, remineralization, and sinking flux of particulate matter in the Cariaco Basin and how these change over time. It also aims at understanding climatic changes in the region, as well as in the Atlantic Ocean, and how variation in the processes are preserved in sediments accumulating in this anoxic basin. CARIACO conducts near-monthly cruises to the station (10°30′N 64°40′W) to collect a core suite of biogeochemical and ecological samples. It also has a microbiology component, which carries out specific biannual cruises, and a sediment trap mooring which collects particle fluxes biweekly at five depths from ca. 150 m to ca. 1200 m.

Related information: http://imars.marine.usf.edu/cariaco

A2 North Atlantic Ocean
Baltic Sea

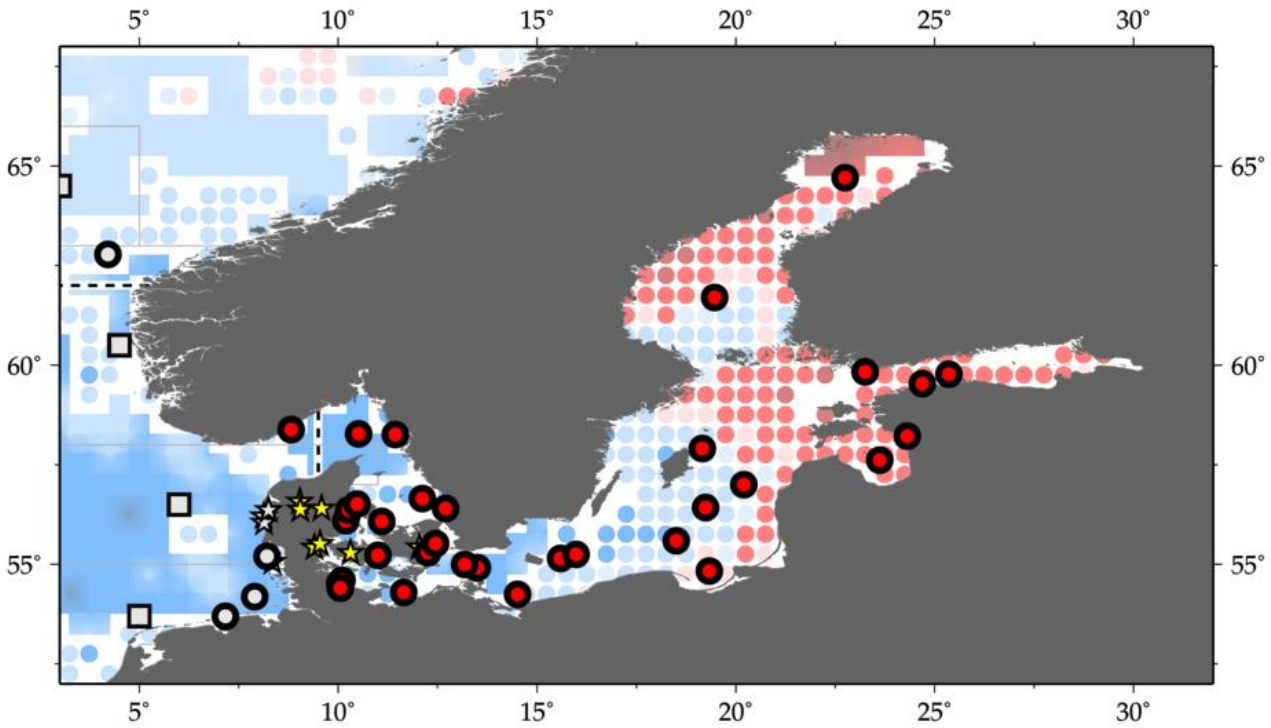

Figure A2.2. Map of IGMETS-participating North Atlantic – Baltic Sea time series on a background of a 10-year time-window (2003–2012) sea surface temperature trends (see also Chapter 4). At the time of this report, the North Atlantic – Baltic Sea collection consisted of 41 time series (coloured symbols of any type), of which seven were from estuarine areas (yellow stars). Uncoloured (gray) symbols indicate time series being addressed in a different regional chapter or subregion (e.g. Arctic Ocean, North Atlantic Proper).

Table A2.2. Time-series sites located in the IGMETS North Atlantic – Baltic Sea region. Participating countries: Germany (de), Denmark (dk), Estonia (ee), Finland (fi), Latvia (lv), Poland (pl), and Sweden (se).

No.	IGMETS-ID	Site or programme name	Year-span	T	S	Oxy	Ntr	Chl	Mic	Phy	Zoo
1	de-10201	Boknis Eck Time Series Station *(Eckernfoerde Bay – SW Baltic Sea)*	1957–present	X	X	X	X	X	X	-	-
2	de-30101	Arkona Basin (*Southern Baltic Sea*)	1979–present	X	X	X	X	X	X	X	X
3	de-30102	Bornholm Basin (*Southern Baltic Sea*)	1979–present	X	X	X	X	X	X	X	-
4	de-30103	Mecklenburg Bight (*Southern Baltic Sea*)	1980–present	X	X	X	X	X	X	X	-
5	de-30104	Eastern Gotland Basin (*Southern Baltic Sea*)	1979–present	X	X	X	X	X	X	X	-
6	dk-30102	Arhus Bugt: DNAMAP-170006 (*Baltic Sea*)	1979–present	X	X	X	X	X	-	X	-
7	dk-30103	Koge Bugt: DNAMAP-1727 (*Baltic Sea*)	1985–present	X	X	X	X	X	-	X	-
8	dk-30104	Hevring Bugt: DNAMAP-190004 (*Baltic Sea*)	1985–present	X	X	X	X	X	-	X	-
9	dk-30108	Logstor Bredning: DNAMAP-3708-1 (*Baltic Sea*)	1980–present	X	X	X	X	X	-	X	-
10	dk-30109	Skive Fjord: DNAMAP-3727-1 (*Baltic Sea*)	1980–present	X	X	X	X	X	-	X	-
11	dk-30111	Alborg Bugt: DNAMAP-409 (*Baltic Sea*)	1981–present	X	X	X	X	X	-	X	-
12	dk-30112	Anholt East: DNAMAP-413 (*Baltic Sea*)	1981–present	X	X	X	X	X	-	X	-
13	dk-30113	Vejle Fjord: DNAMAP-4273 (*Baltic Sea*)	1982–present	X	X	X	X	X	-	X	-
14	dk-30114	Ven: DNAMAP-431 (*Baltic Sea*)	1979–present	X	X	X	X	X	-	X	-
15	dk-30115	Arkona: DNAMAP-444 (*Baltic Sea*)	1979–present	X	X	X	X	X	-	X	-
16	dk-30116	Mariager Fjord: DNAMAP-5503 (*Baltic Sea*)	1979–present	X	X	X	X	X	-	X	-
17	dk-30117	Horsens Fjord: DNAMAP-5790 (*Baltic Sea*)	1981–present	X	X	X	X	X	-	X	-
18	dk-30118	Roskilde Fjord: DNAMAP-60 (*Baltic Sea*)	1979–present	X	X	X	X	X	-	X	-
19	dk-30119	Lillebaelt-South: DNAMAP-6300043 (*Baltic Sea*)	1979–present	X	X	X	X	X	-	X	-
20	dk-30120	Lillebaelt-North: DNAMAP-6870 (*Baltic Sea*)	1979–present	X	X	X	X	X	-	X	-

No.	IGMETS-ID	Site or programme name	Year-span	T	S	Oxy	Ntr	Chl	Mic	Phy	Zoo
21	dk-30121	Odense Fjord: DNAMAP-6900017 (*Baltic Sea*)	1979–present	X	X	X	X	X	-	X	-
22	dk-30122	Gniben: DNAMAP-925 (*Baltic Sea*)	1979–present	X	X	X	X	X	-	X	-
23	dk-30123	Storebaelt: DNAMAP-939 (*Baltic Sea*)	1982–present	X	X	X	X	X	-	X	-
24	dk-30124	Bornholm Deep: DNAMAP-bmpk2 (*Baltic Sea*)	1980–present	X	X	X	X	X	-	X	-
27	ee-10101	Pärnu Bay (*Gulf of Riga*)	1957–present	X	X	-	-	X	-	-	X
28	ee-10201	Tallinn Bay (*Gulf of Finland*)	1959–present	X	X	-	-	X	-	-	X
29	fi-30101	Bothnian Bay Region: Bo3+F2 (*Northern Baltic Sea*)	1959–present	X	X	X	X	X	X	X	X
30	fi-30102	Bothnian Sea Region: SR5+US5b+F64 (*Northern Baltic Sea*)	1959–present	X	X	X	X	X	X	X	X
31	fi-30103	Gulf of Finland Region: LL3A+LL7+LL12 (*Northern Baltic Sea*)	1959–present	X	X	X	X	X	X	X	X
32	fi-30104	Northern Baltic Proper Region: BY15+BY38+LL17+LL23 (*Northern Baltic Sea*)	1959–present	X	X	X	X	X	X	X	X
33	lv-10101	Station 121 (*Gulf of Riga*)	1959–present	X	X	-	-	X	-	-	X
34	lv-10201	Eastern Gotland Basin (*Central Baltic Sea*)	1959–present	X	X	X	X	X	-	-	X
35	pl-30101	Gdansk Basin (*Baltic Sea*)	1959–present	X	X	-	X	X	X	X	X
36	pl-30102	Bornholm Basin (*Baltic Sea*)	1959–present	X	X	-	X	X	X	X	X
37	pl-30103	Pomeranian Bay (*Baltic Sea*)	1979–present	X	X	-	X	X	X	X	-
38	pl-30104	Southern Gotland Basin (*Baltic Sea*)	1959–present	X	X	X	-	X	-	-	X
39	se-50101	SMHI A17 (*Sweden*)	1982–present	X	X	X	X	X	X	X	X
40	se-50102	SMHI Anholt East (*Kattegat*)	1959–present	X	X	X	X	X	X	X	X
41	se-50103	SMHI Slaggo (*Sweden*)	1959–present	X	X	X	X	X	X	X	X

Boknis Eck Time series Station

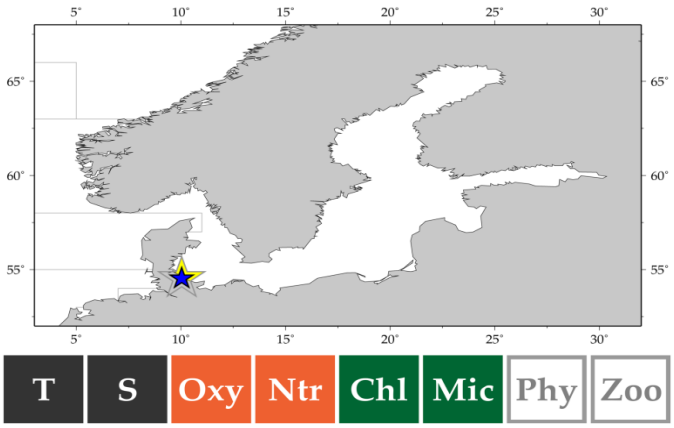

Country: Germany

IGMETS-ID: de-10201

The Boknis Eck Time series Station (BE) is located at the entrance to Eckernförde Bay (54°31'N 10°02'E; water depth 28 m, muddy sediments) in the south-western Baltic Sea. Samples are taken from six depths on a monthly basis. Salinity, temperature, phosphate, and O_2 data have been recorded since 1957. Chlorophyll *a* measurements started in 1960. Additional nutrients (nitrate, nitrite, ammonium, and silicate) and Secchi depths are available since 1979 and 1986, respectively. Since riverine and groundwater inputs are negligible, the overall hydrographic setting at BE is dominated by the regular inflow of North Sea water through the Kattegat and the Great Belt. Seasonal stratification usually occurs from mid-March until mid-September and causes pronounced hypoxia, which sporadically become anoxic. The location of BE is ideal to study (i) a coastal ecosystem under the influence of pronounced changes of salinity and (ii) biogeochemical processes sensitive to changes in dissolved oxygen.

Related information: http://www.bokniseck.de

IOW Baltic Sea Time Series

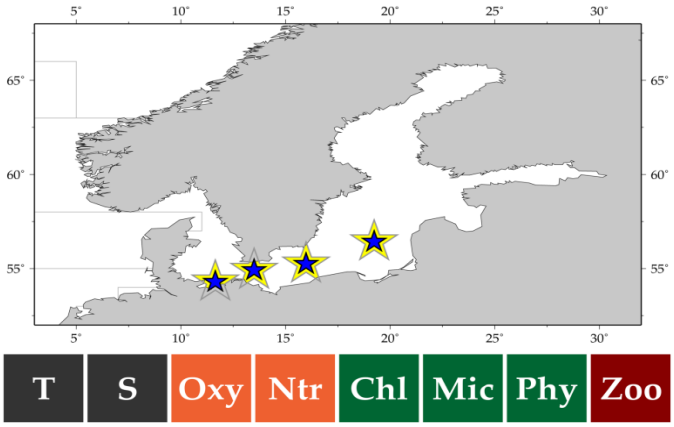

Country: Germany

Site name (IGMETS-ID):

Arkona Basin (de-30101)
Bornholm Basin (de-30102)
Mecklenburg Bight (de-30103)
Eastern Gotland Basin (de-30104)

Norbert Wasmund and Jörg Dutz

The IOW Baltic Sea Time Series, established in 1979 within the framework of the Helsinki Commission (HELCOM), records long-term changes in plankton abundance, frequency, and biodiversity in relation to climatic and anthropogenic forcing. Monitored sites extend from the western Belt Sea and the Arkona Sea to the Bornholm and eastern Gotland Basin along a pronounced salinity and depth gradient that exerts a strong influence on local plankton. A periodical inflow of seawater and an outflow of Baltic brackishwater cause particularly strong variability in the plankton composition of the western areas. IOW conducts five cruises a year collecting physical, chemical, and biological core data in February, March, May, August, and November. Integrated surface samples for phytoplankton biomass and chlorophyll *a* concentration from the upper 10 m are taken at 10 stations. Zooplankton abundance/biomass is monitored at nine stations, with the sampling depth adjusted to seasonal stratification.

Danish National Aquatic Monitoring and Assessment Program (DNAMAP)

Country: Denmark

IGMETS-ID: dk-30101 – dk-30124 (24 sites)

Jacob Carstensen

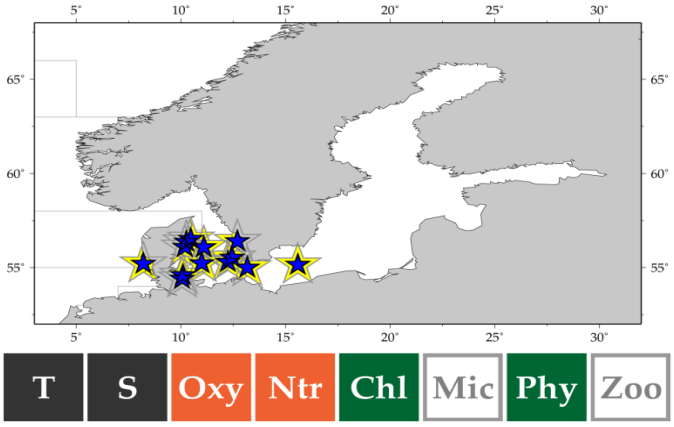

The Danish National Aquatic Monitoring and Assessment Program (DNAMAP) was established in 1989 with the aim of reporting coastal ecosystems responses to nutrient reductions (ca. 50% for N and >80% for P). DNAMAP was based on previous regional and national monitoring activities. The marine monitoring component includes hydrochemistry, phytoplankton, zooplankton, benthic vegetation, benthic macrofauna, harmful substances, and their effects on biota. Sampling and analyses were carried out according to common protocols, and data have been reported to the national database for marine data. Almost 100 stations scattered over estuaries, coastal, and open waters have been monitored for up to four decades. Estuaries and coastal waters are shallow (typically < 10 m), intermittently stratified and impacted by land-based inputs, whereas the open-water stations are permanently stratified due to the exchange of brackish Baltic Sea water with water from the North Sea. The monitoring data provide an excellent example of coastal ecosystem recovery from eutrophication.

Pärnu Bay Time Series

Country: Estonia

IGMETS-ID: ee-10101

Arno Põllumäe, Mart Simm and Maria Põllupüü

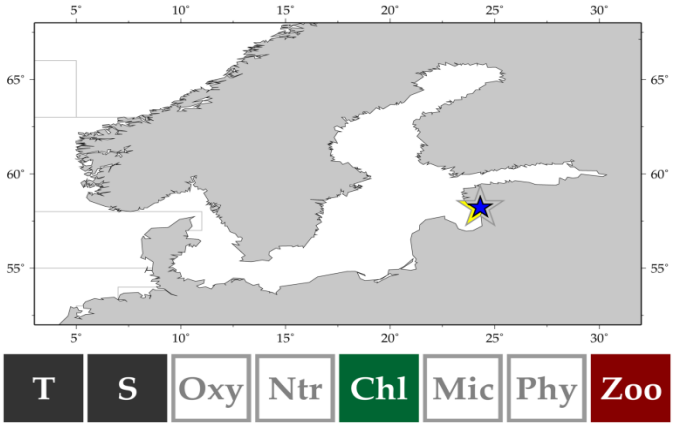

Pärnu Bay in northeastern part of the Gulf of Riga (Baltic Sea) is the site of the longest consistent marine biological sampling in Estonia. Zooplankton sample collection started in 1957 to assess feeding conditions for herring (*Clupea harengus membras*). Since 1993, three stations inside the shallow (10 m) Bay have been a part of the Estonian national marine monitoring programme, which started simultaneous sampling of zooplankton, phytoplankton, macrozoobenthos, and nutrients several times a year. In 2000, frequency of sampling was raised to 12 cruises per year. The salinity of Pärnu Bay is slightly lower than that in the Gulf of Riga, with an average salinity of 5 psu. Pärnu Bay also suffers from heavy anthropogenic eutrophication, with nitrate and phosphate coming into the Bay from the town of Pärnu and the Pärnu River. Because of the port and low biodiversity of local species, the Bay has also been an important foothold for some new invasions.

Tallinn Bay Time Series

Country: Estonia

IGMETS-ID: ee-10201

Arno Põllumäe

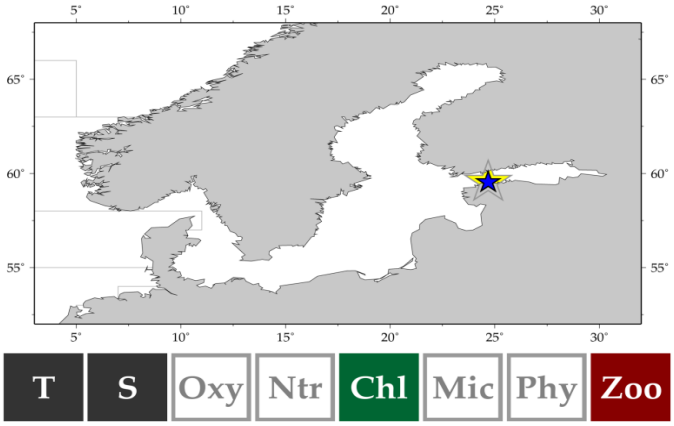

The Tallinn Bay Time Series started in 1993 as one of many monitoring stations around Estonia within the Estonian National Monitoring Program. The main objective of this monitoring programme has been to assess the Baltic Sea ecosystem response to eutrophication. During the 1990s, the frequency of sampling was 1–4 times a year, and the parameters monitored were oceanography, phytoplankton, zooplankton, and macrozoobenthos. In 2001, the frequency of sampling of the Tallinn Bay Time Series was increased to 12 cruises a year. The depth of the monitoring station is 45 m. Tallinn Bay is an exposed water body in the central part of the Gulf of Finland (Baltic Sea) and the time series characterizes typical coastal environments of the entire Gulf that are subjected to high anthropogenic pressure.

Northern Baltic Sea Time Series

Country: Finland

Site name (IGMETS-ID):

SYKE Bothnian Bay (fi-30101)
SYKE Bothnian Sea (fi-30102)
SYKE Gulf of Finland (fi-30103)
SYKE Baltic Proper (fi-30104)

Maiju Lehtiniemi and Sirpa Lehtinen

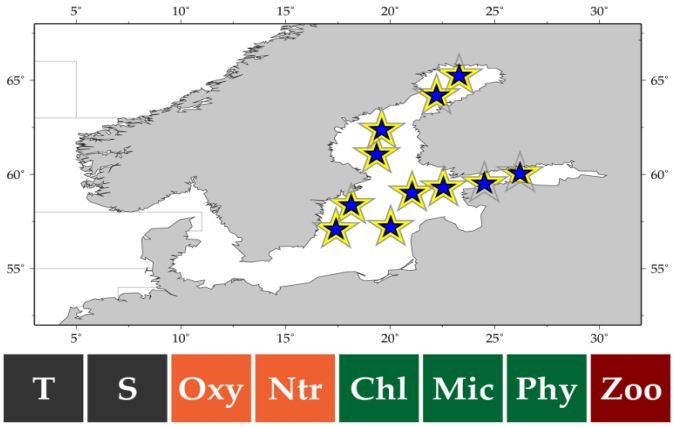

The Northern Baltic Sea Time Series, established in 1979 in the gulfs of Finland and Bothnia, northern Baltic Proper, and the Åland Sea aims at understanding the ecosystem changes in the pelagic zone and the linkages between regional climatic changes and plankton production. The semi-enclosed brackishwater Baltic Sea is connected to the North Sea via narrow straits in the west, and its salinity is regulated by irregular salt water intrusions through the straits and by river inflow of freshwater. It experiences high seasonal temperature variation and partial ice cover every winter and is characterized by strong vertical stratification of both salinity and temperature. Northern Baltic Sea sampling is conducted by the Finnish Environment Institute (SYKE) once a year in August for phyto- and zooplankton and three times a year for hydrographical parameters on board RV "Aranda".

Central Gulf of Riga Time Series (Station 121)

Country: Latvia

IGMETS-ID: lv-10101

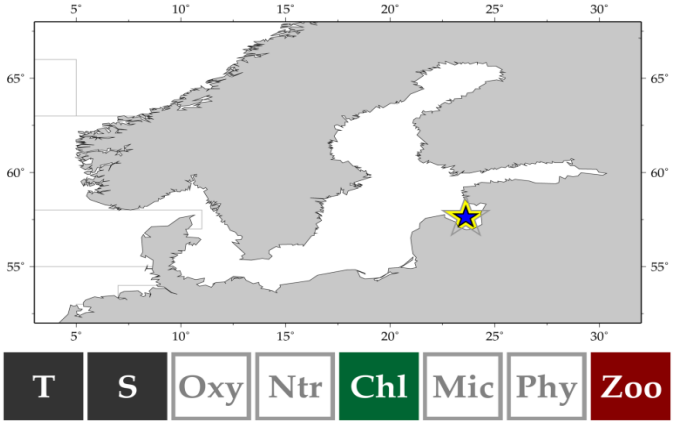

The Central Gulf of Riga Time Series were started in 1974 for physical-chemical parameters and in 1993 for biological parameters as part of a marine monitoring programme to assess the status of the marine environment and to follow trends in ecosystem components. The Gulf of Riga is the third largest gulf in the Baltic Sea, receiving substantial freshwater and nutrient loads, while at the same time being seasonally stratified and having a salinity of 2–6 psu. Time series are represented by one measurement and sampling point at 57°37′N 23°37′E visited three times a year and located out of the impact zone of inflowing freshwater to characterize the deeper and more stable part of the Gulf. Therefore, effects of long-term atmospheric processes and related oceanographic and biological changes can be detected (Jurgensone *et al*., 2011).

Eastern Gotland Basin (Station 37)

Country: Latvia

IGMETS-ID: lv-10201

Gunta Rubene and Solvita Strāķe

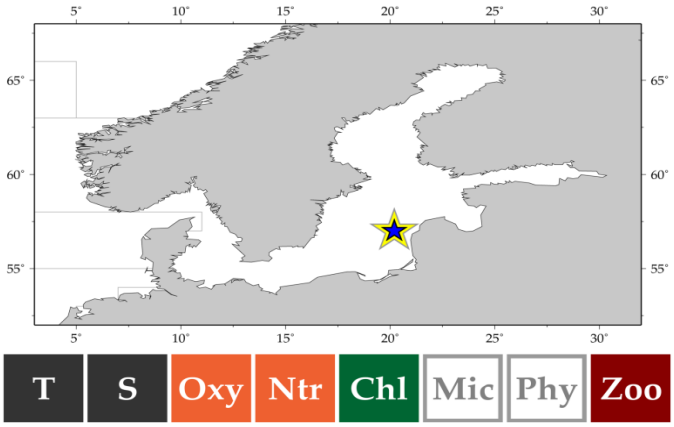

The Eastern Gotland Basin Station 37 (57°02′N 19°06′E) is located in the central Baltic Sea, ICES Subdivision 28. The deeper part of this site could be characterized by an anoxic zone formed at a depth of 249 m. Two different time-series periods have been visible here for sea surface water temperature and salinity, with a regime of lower temperature and higher salinity until the 1990s and the opposite trends afterwards. The time series of the eastern Gotland Basin (zooplankton, temperature, and salinity) has been collected since 1959 to investigate fish resources, regulation of utilization, and reproduction. Zooplankton has been sampled using a Juday net (upper ring diameter – 36 cm, mesh size 160 μm) covering the water column to a maximum depth of 100 m. Hydrological variables were collected using a bathometer until 2005, but subsequently with a CTD probe in the upper water layer (0–10m). All the variables have been sampled once a season (May, August, and October).

Related information: http://www.bior.lv

Southern Baltic Proper (NMFRI Monitoring)

Country: Poland

Site name (IGMETS-ID):

Gdansk Basin (pl-30101)
Bornholm Basin (pl-30102)
Pomeranian Bay (pl-30103)
Southern Gotland Basin (pl-30104)

Anetta Ameryk, Sławomira Gromisz, Janina Kownacka, Marianna Pastuszak, Mariusz Zalewski, and Piotr Margonski

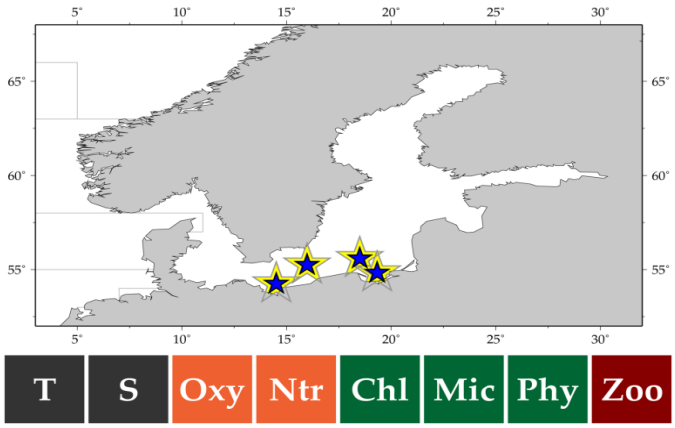

A phytoplankton database was created by the National Marine Fisheries Research Institute (NMFRI), and samples have been collected and analyzed by experts from NMFRI. Nutrients and chlorophyll *a* have been monitored since 1977, while phytoplankton taxa since 1987. Each study area is a rectangle containing several sampling stations. Monitoring of the Gdańsk Basin and Pomeranian Bay is important as both areas are significantly influenced by the Vistula and Oder rivers, respectively. Samples are collected using 2- to 5-l Nansen or Niskin bottles at five fixed depth strata between 0 and 10 m. Frequent cruises, 6–10 times a year, were organized in the 1980s and only twice a year, in spring and summer, over the last ten years. The database has many gaps, especially in the region of Pomeranian Bay.

Zooplankton samples are collected within the Baltic Sea HELCOM COMBINE Monitoring Programme. The Maritime Branch of the Institute of Meteorology and Water Management is responsible for collecting the samples along the southern coast of the Baltic Sea (in the Polish EEZ). Over the 30 years of monitoring, zooplankton have been analyzed by several experts working in various institutions. The dataset starts in 1979, with two stations located in the Bornholm and southern Gotland basins. Since 1986, a third sampling location in the Gdansk Basin was added. Vertical hauls of the WP-2 net with 100-µm mesh size were used. Stratified samples are presented here as an average of the whole water column) were collected in the layers from the bottom to the halocline (included), from the top of the halocline to the thermocline (included), and from the top of the thermocline to the surface. The frequency of sampling varied in time (3–6 times a year), but spring and summer conditions can be described for each year.

Swedish Meteorological and Hydrological Institute Time Series

Country: Sweden

Site name (IGMETS-ID):

SMHI Å17 (se-50101)
SMHI Anholt East (se-50102)
SMHI Släggö (se-50103)

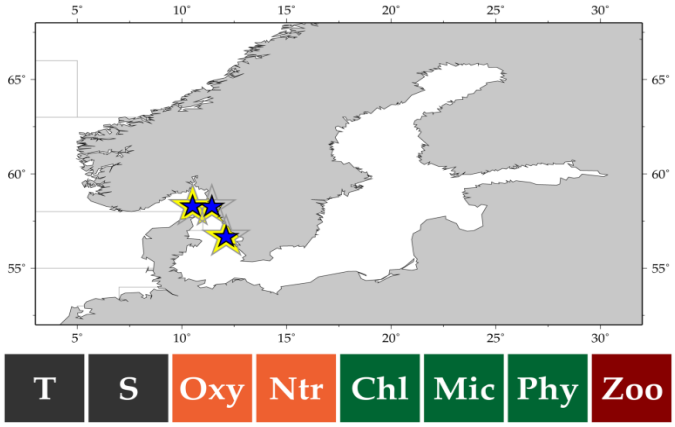

Patrik Strömberg and Marie Johansen

The Swedish National Oceanographic Data Centre is financed by the Swedish Agency for Marine and Water Management (SWAM) and part of SMHI (Swedish Meteorological and Hydrological Institute) and hosts Swedish marine environmental monitoring data comprising biogeochemistry, physics, and zooplankton. Data are publicly available and downloadable from sharkweb.smhi.se, and there is a machine–machine interface at this website making it possible to harvest data. The earliest record dates to June 1979 (two records in total); more data are added every year. Time series are more complete after 2007; for 2013, there are 174 records. As of 19 March 2015, there were 1519 zooplankton records. Since 2007, SMHI samples monthly in the Baltic Sea and along the Swedish west coast in accordance with the HELCOM manual. For zooplankton, a WP-2 net (90-µm mesh) is used. SMHI released an updated version of the website in 2015 that enabled many improvements, including the possibility to download physical and chemical data. Time-series data availability increased from 1971–2014 (44 years) to 1893–2014 (122 years).

A2 North Atlantic Ocean
Mediterranean Sea

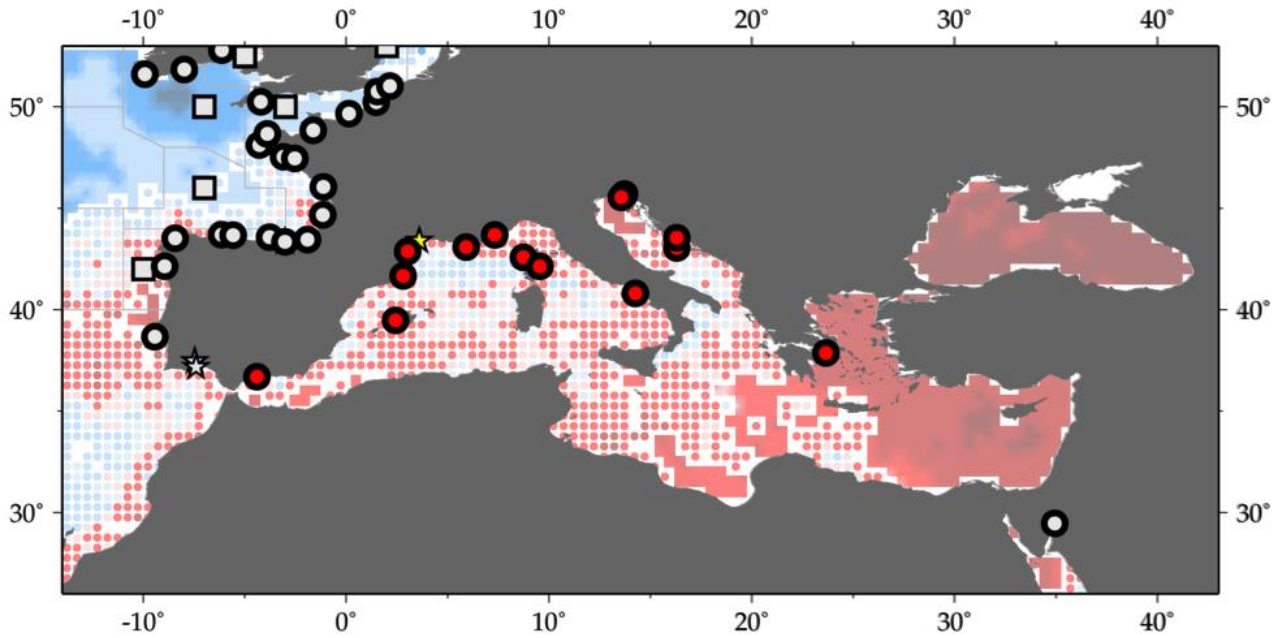

Figure A2.3. Map of IGMETS-participating North Atlantic – Mediterranean Sea time series on a background of a 10-year time-window (2003–2012) sea surface temperature trends (see also Chapter 4). At the time of this report, the North Atlantic – Mediterranean Sea collection consisted of 16 time series (coloured symbols of any type), of which one was from estuarine areas (yellow star). Uncoloured (gray) symbols indicate time series being addressed in a different subregion (e.g. North Atlantic Proper).

Table A2.3. Time-series sites located in the IGMETS North Atlantic – Mediterranean Sea region. Participating countries: Belgium (be), Spain (es), France (fr), Greece (gr), Croatia (hr), Italy (it), and Slovenia (si).

No.	IGMETS-ID	Site or programme name	Year-span	T	S	Oxy	Ntr	Chl	Mic	Phy	Zoo
1	be-10101	PHYTOCLY Time Series *(Bay of Calvi)*	1988–present	-	-	-	X	X	-	-	-
2	es-30301	Blanes Bay *(Northwest Mediterranean)*	1992–present	X	X	-	X	X	X	-	-
3	es-50201	IEO Mallorca Baleares Station *(Mallorca Channel)*	1994–present	X	X	-	-	X	-	-	X
4	es-50301	IEO ECOMÁLAGA *(Alboran Sea)*	1992–present	X	X	-	X	X	-	-	X
5	fr-10101	Villefranche Point B *(Cote d'Azur)*	1995–present	-	-	-	-	-	-	-	X
6	fr-10201	Thau Lagoon *(Mediterranean Sea)*	1965–present	X	X	-	X	X	X	X	-
7	fr-50111	REPHY Diana Centre *(Mediterranean Sea)*	1987–present	X	X	X	X	X	-	X	-
8	fr-50112	REPHY Lazaret A *(Western Mediterranean)*	1987–present	X	X	X	-	X	-	X	-
9	fr-50113	REPHY Parc Leucate 2 *(Mediterranean Sea)*	1987–present	X	X	-	-	X	-	X	-
10	fr-50114	REPHY Villefranche *(Mediterranean Sea)*	1995–present	X	X	-	-	-	-	X	-
11	gr-10101	Saronikos Gulf S11 *(Aegean Sea)*	1987–present	-	-	-	-	X	-	-	X
12	hr-10101	Stoncica *(Central Adriatic Sea)*	1959–present	-	-	-	-	-	X	-	X
13	hr-10102	Kastela Bay *(Central Adriatic Sea)*	1994–present	-	-	-	-	-	X	-	-
14	it-30101	Gulf of Naples LTER-MC *(Tyrrhenian Sea)*	1984–present	X	X	-	X	X	-	X	X
15	it-30201	C1-LTER Gulf of Trieste *(Northern Adriatic Sea)*	1970–present	-	-	-	-	-	-	-	X
16	si-10101	Gulf of Trieste – MBS Buoy *(Northern Adriatic Sea)*	1990–present	X	X	X	X	X	-	X	-

PHYTOCLY Time Series

Country: Belgium

IGMETS-ID: be-10101

Anne Goffart, Amandine Collignon, and Jean-Henri Hecq

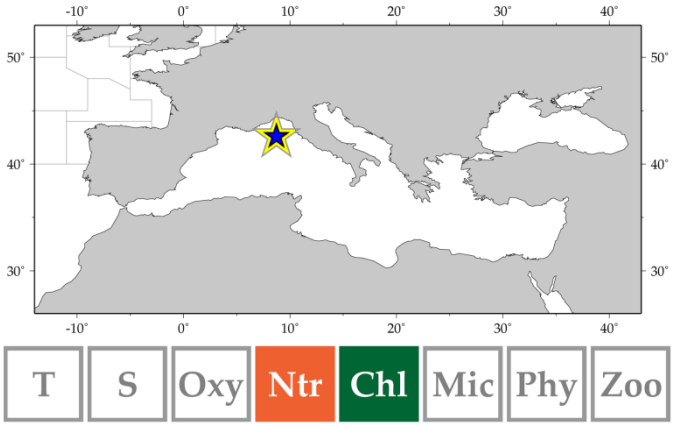

The PHYTOCLY Time Series, established in 1979 in the Bay of Calvi (Corsica, northwestern Mediterranean), aims to investigate the effects of climate forcing on surface nutrient replenishment as well on phyto- and zooplankton dynamics. The Bay of Calvi is a well-preserved and low-runoff system, with high water quality. It opens to the north to the Ligurian Sea and is characterized by a narrow continental shelf (mean width ca. 3 km) and the presence of a deep canyon (mean depth ca. 600 m), which enhances shelf–slope exchanges. The trophic character of the Bay of Calvi changes yearly and ranges from very oligotrophic (low seasonal variability) to mesotrophic (well-marked increases in nutrient concentrations, chlorophyll *a*, and zooplankton during the winter–spring period). A third regime occurs during severe winters and is characterized by specific wind conditions when Mediterranean "high nutrient – low chlorophyll" conditions occurred. Sampling and analysis were supported by the University of Liège (Belgium), Stareso SA (Calvi, France), Ifremer (France), the French Water Agency (PACA-Corsica) and the Territorial Collectivity of Corsica.

Blanes Bay

Country: Spain

IGMETS-ID: es-30301

Josep M Gasol, Ramon Massana, Rafel Simó, Celia Marrasé, Silvia G. Acinas, Carlos Pedrós-Alió, Carles Pelejero, M. Montserrat Sala, Eva Calvo, Dolors Vaqué, and Francesc Peters

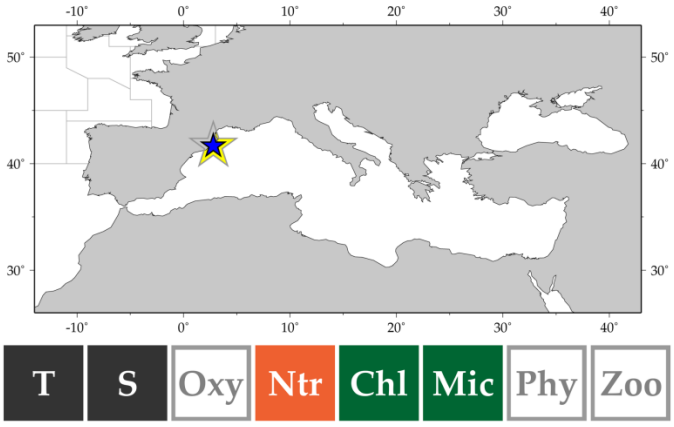

The Blanes Bay Microbial Observatory is placed in an open east-facing bay in the northwestern Mediterranean Catalan coast about 70 km north of Barcelona. It is a good example of an oligotrophic (relatively nutrient-poor) coastal ecosystem relatively unaffected by human influences. It is also one of the sites for which more information exists on the ecology of the Mediterranean planktonic environment dating back to the 1940s. Current monitoring, which started in 2000, is focused on biogeochemistry and microbial diversity.

The site is at about 0.5 miles offshore over 20 m depth. An oceanographic fully-operated buoy is operative nearby. The station is at the limit between the rocky coast of the "Costa Brava" and the sandy coast southward, with very limited riverine influence. Dominant southwestern water circulation drives away the Tordera River outflow south of the site. A nearby submarine canyon sporadically introduces offshore seawater to the site.

Related information: http://www.icm.csic.es/bio/projects/icmicrobis/bbmo

IEO Mallorca Baleares Station

Country: Spain

IGMETS-ID: es-50201

Maria Luz Fernandez de Puelles

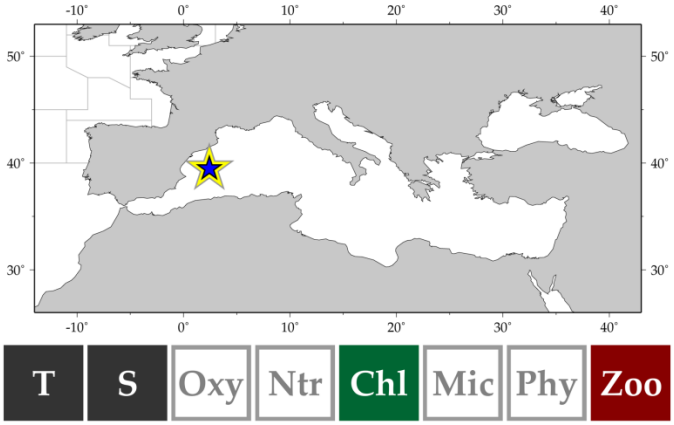

Mallorca Station (75 m depth) is located southwest of Mallorca Island (39°29′N 02°26′E) and has been sampled every 10 days between January 1994 and December 2005. Sampling since 2007 has only been seasonally. CTD data were also recorded. Zooplankton was sampled by bottom–surface oblique hauls with bongo net with 250- and 100-µm mesh. A General Oceanic flowmeter was fitted to estimate the volume of filtered water. Samples are split into subsamples for biomass and taxonomic analysis, with the latter preserved with 4% neutralized formaldehyde. All groups are identified, with the main focus on copepods and cladocerans to the species level. Subsamples for biomass are frozen (–20°C) for subsequent estimation as dry weight.

This area experiences regular influxes of northern Mediterranean and Atlantic waters and their broad range of temperatures and salinities. A seasonal cycle of temperature includes a mixing period during winter followed by a stratified period of more than six months (May–October), which coincides with the lowest zooplankton biomass. Phytoplankton blooms generally occur in January, but sometimes in late spring. Zooplankton biomass peaks in winter (March), spring (May), and at the end of summer (September), during which copepods are the dominant zooplankton group.

IEO ECOMÁLAGA

Country: Spain

IGMETS-ID: es-50301

Lidia Yebra, Jesús M. Mercado, and Dolores Cortés

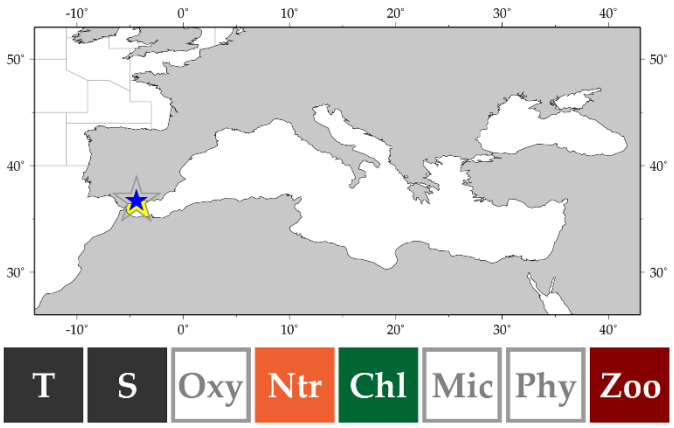

The ECOMÁLAGA time series operated by the Instituto Español de Oceanografía (IEO) sampled Málaga Bay during 1992–2007. In 2010, quarterly sampling of hydrochemical and biological variables restarted with the aim of assessing the environmental status of marine pelagic communities as well as the impact of human-induced activities on the plankton community structure. Station MA2 is located in northwestern Alboran Sea (36°42′N 04°24′E), with a bottom depth of 28 m. The region presents high variability in hydrochemical conditions. This is due to the presence of an anticyclonic gyre originated by the jet of Atlantic water than enters the Mediterranean through the Strait of Gibraltar. Also, within the shelf, frontal areas appear associated with westerly wind-induced upwelling events. Plankton production along the coast is significantly higher than in offshore waters (Mercado *et al*., 2014) and is among the highest in the entire Mediterranean Sea.

Northwestern Mediterranean Sea Zooplankton Time Series (Point B)

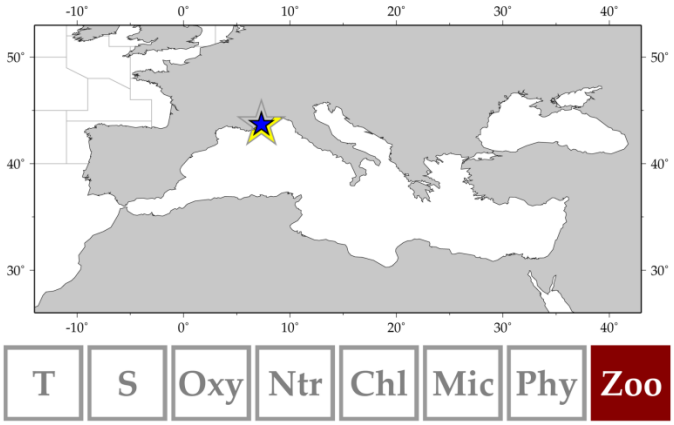

Country: France

IGMETS ID: fr-10101

Fabien Lombard, Lars Stemmann, Gabriel Gorsky, Amanda Elineau, and Corinne Desnos

The Villefranche Point B dataset consists of more than 30 years of samples collected off Villefranche at 43°41'N 07°19'E. Samples were collected by a vertical tow from bottom to surface (75–0 m) using a Juday-Bogorov net (1996–2003, 330-µm mesh) and WP-2 net (1995–2012, 200-µm mesh). The sampling site is located at the mouth of the bay over a bathymetry of 80 m and is thus open to the Ligurian Sea. Zooplankton abundance was counted from ongoing and historical samples using the wet-bed image scanning technique of ZooScan (Gorsky *et al.*, 2010).

Zooplankton abundance was highest during years with well-mixed winter periods (in the 1980s), followed by a general decline, with rising water temperatures and increasing stratification in the 1990s (Garcia-Comas *et al.*, 2011). After 2000, the mesozooplankton abundance again reached the levels seen in the 1980s (Vandrome *et al.*, 2012).

Thau Lagoon Time-Series

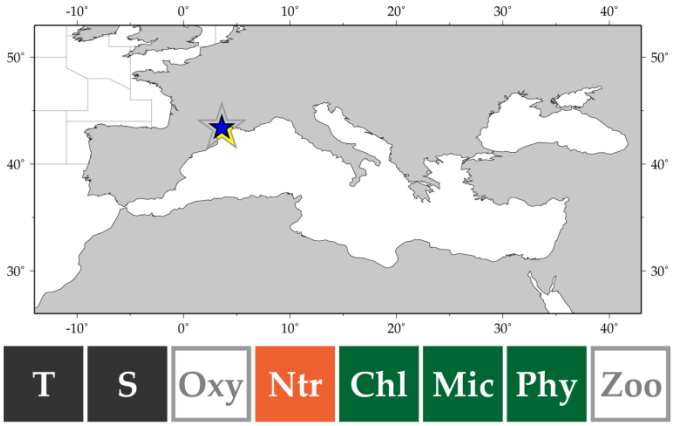

Country: France

IGMETS-ID: fr-10201

Yves Collos, Béatrice Bec and Eric Abadie

The Thau Lagoon Time-Series, established in Thau Lagoon in 1971, aims at understanding linkages between physical and chemical variables, phytoplankton species, and oyster production and how these change over time. It also aims at understanding regional climatic changes and how variations in these processes affect oyster production. The Thau Lagoon is a semi-enclosed lagoon located in southern France that is connected to the Mediterranean Sea by three narrow channels. Systematic observations of physical (temperature, salinity) and chemical (nutrient concentrations) properties have been made since 1971, and biological (phytoplankton > 5 µm) properties have been monitored since 1987. Picophytoplankton (picoeukaryotes and picocyanobacteria) has been counted by flow cytometry since 1991. The lagoon harbors *Ostreococcus tauri*, the smallest eukaryote in the world (Courties *et al.*, 1994). Sampling frequency is twice monthly, but can increase to weekly or more during periods favorable to harmful algae.

French Phytoplankton and Phycotoxin Monitoring Network (REPHY)

Country: France

Site name (IGMETS-ID):

REPHY Diana Centre (fr-50111)
REPHY Lazaret A (fr-50112)
REPHY Parc Leucate 2 (fr-50113)
REPHY Villefranche (fr-50114)

see also REPHY in the North Atlantic Annex

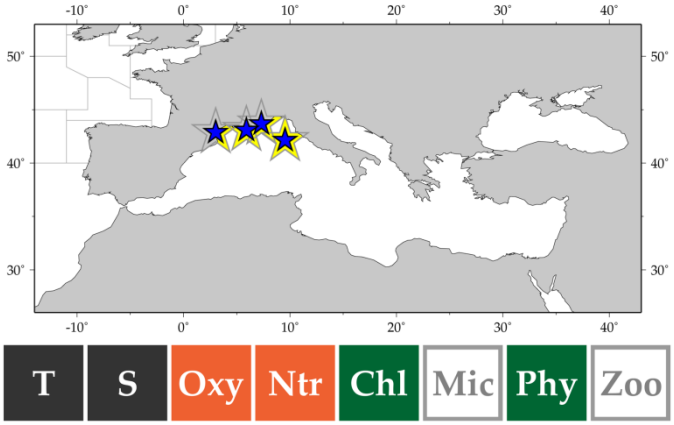

Dominique Soudant and Eric Abadie

The French Phytoplankton and Phycotoxin Monitoring Network (REPHY) was set up in 1984 with three objectives: (i) enhance knowledge of phytoplankton communities, (ii) safeguard public health, and (iii) protect the marine environment (Belin, 1998). Phytoplankton along the French coast has been sampled up to twice a month since 1987 at 12 coastal laboratories. For that purpose, the French coast is divided into a hierarchy of sites and subsites common to three regional networks: the English Channel, the Bay of Biscay, and the Mediterranean Sea.

Lazaret A and Diana Centre are two Mediterranean REPHY sites. Lazaret A is located in well-mixed waters, with a medium-depth, sandy bottom within Toulon Bay. Diana Center is located in shallow, less-mixed waters of a coastal lagoon in Corse and features a muddy bottom. As with the Bay of Biscay and English Channel REPHY sites, sampling started in 1987, with salinity, temperature, turbidity, and oxygen measured concomitantly from the beginning or one year thereafter. Chlorophyll *a* and pheopigments started at Diana Centre in 1988 and at Lazaret A in 1999. This latter site is sampled twice a month on average, whereas fewer samples (17 on average from 10 months) are taken annually at Diana Centre.

Saronikos S11, Aegean Sea

Country: Greece

IGMETS-ID: gr-10101

Soultana Zervoudaki, Epaminondas Christou, and Assimakopoulou Georgia

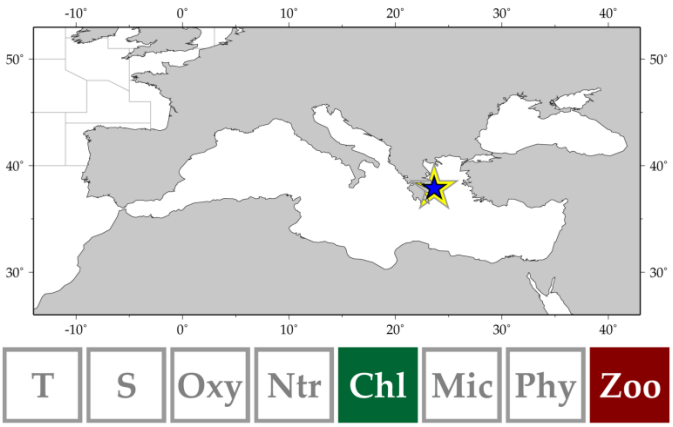

Saronikos S11 (37°52′N 23°38′E) time series is located in the Saronikos Gulf in the Aegean Sea (eastern Mediterranean) with a bottom depth of 78 m. This area receives treated sewage effluents from the Athens metropolitan area through a deep underwater outlet situated near Psitallia Islet on the northeast side of the Gulf. Since 1987, the marine environment has been seasonally and interannually monitored in order to assess *inter alia* any short- and long-term effects on plankton. Average temperature in this station has seasonal cycles, with minima in March (14°C) and maxima in September (23°C). Salinity ranges between 38 and 39, depending on the variability of the inflow of Aegean water (Kontoyiannis *et al*., 2005; Kontoyiannis, 2010). Chlorophyll *a* shows clear annual cycles, with sharp peaks around 2 mg m^{-3} in spring. The area has been classified as mesotrophic, having good water quality (Simboura *et al*., 2014).

Station Stončica

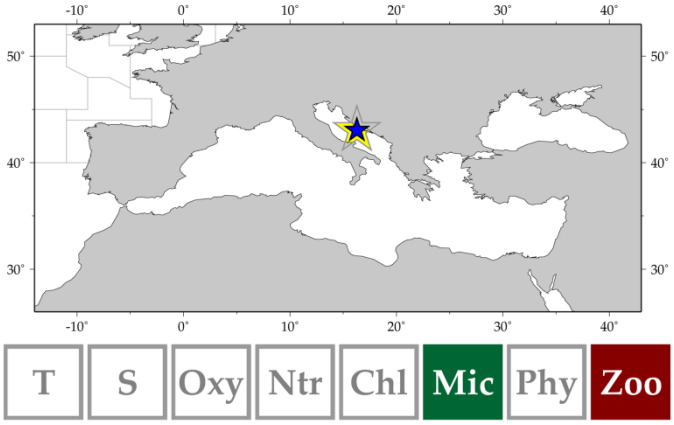

Country: Croatia

IGMETS-ID: hr-10101

Mladen Solic, Olja Vidjak, Nada Krstulovic, Danijela Santic, and Stefanija Sestanovic

Station Stončica is located in the central part of the Adriatic Sea (43°02′N 16°17′E), with a maximum depth of 107 m. The area is strongly influenced by the incoming Mediterranean water (Levantine Intermediate Water). The Stončica site is considered as a reference for the oligotrophic open waters of the central Adriatic and has been under regular monitoring from as early as the 1950s, resulting in several multidecadal datasets of bacterial, phyto-, and mesozooplankton abundance and/or their respective production and biomass measured on a near-monthly basis. Plankton data are accompanied by concurrent temperature, salinity, nutrient, and oxygen concentration measurements in the water column. Stončica dataseries were analyzed in several publications, aiming at understanding natural plankton cycles and fluctuation patterns and identifying climate–population connections in the water column (Baranović *et al.*, 1993; Šolić *et al.*, 1997; Berline *et al.*, 2012; Grbec *et al.*, 2009).

Station Kaštela Bay

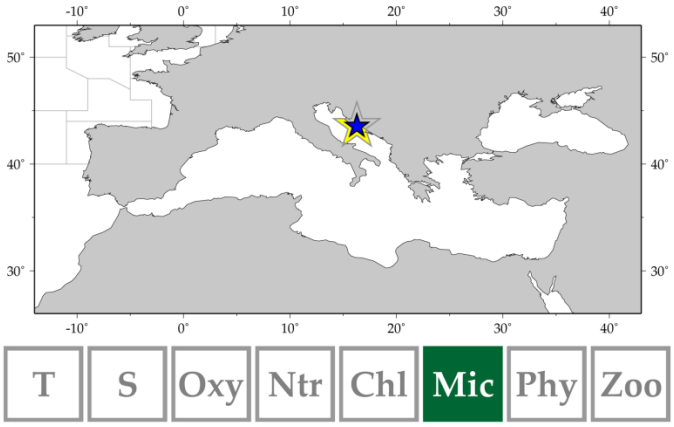

Country: Croatia

IGMETS-ID: hr-10102

Mladen Solic, Nada Krstulovic, Danijela Santic, and Stefanija Sestanovic

Station Kaštela Bay (38-m depth) is located in one of the largest bays on the eastern Adriatic coast (43°32′N 16°23′E). The River Jadro discharges into the eastern part, with an average annual inflow of 10 m^{-3} s^{-1}. The Bay encompasses a total area of 61 km^2 and a volume of 1.4 km^3, with a densely populated narrow coastal strip and some industrial activities along the coast. For decades, the Bay was severely eutrophicated; however, recent investigations point to considerable improvement in water quality (Kušpilić *et al.*, 2009). Long-term monitoring of the ecological status of the Bay conducted at this site produced long sets of bacterial, phyto-, and zooplankton data (abundance, production, and biomass) measured near-monthly, accompanied by temperature, salinity, nutrient, and oxygen measurements. Available data were tested in the context of anthropogenic impacts, water quality, biodiversity, and climate change (Šolić *et al.*, 2010; Ninčević-Gladan *et al.*, 2015).

Gulf of Naples LTER–MC

Country: Italy

IGMETS-ID: it-30101

Adriana Zingone, Maria Grazia Mazzocchi, Diana Sarno, Iole Di Capua, Francesca Margiotta, and Maurizio Ribera d'Alcalà

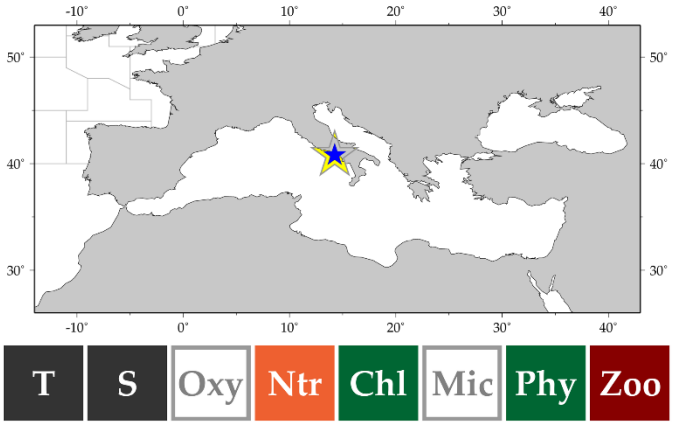

The MareChiara Time-Series was established in 1984 in the Gulf of Naples (Tyrrhenian Sea, western Mediterranean) with the aim of understanding plankton variability and its relationships with external forcing, including anthropogenic disturbance and climate change. The sampling site LTER-MC (40°49′N 14°15′E) is located over the 75-m isobath, 2 nautical miles off the coast of the densely populated city of Naples at the boundary between the eutrophic coastal zone and the offshore oligotrophic waters. The site has been part of the European and international LTER networks since 2006. Sampling was fortnightly until July 1991 and has been weekly since February 1995, with an interruption between the two periods. Numerous physical, chemical, and biological variables are regularly recorded, and metagenomic analyses have been conducted in recent years. Presently, first results are available on the website weekly in real-time. Laboratory experiments are conducted to test hypotheses stemming from field studies.

Related information: http://szn.macisteweb.com/

C1–LTER (Gulf of Trieste)

Country: Italy

IGMETS-ID: it-30201

Valentina Tirelli, Serena Fonda Umani, and Alessandra de Olazabal

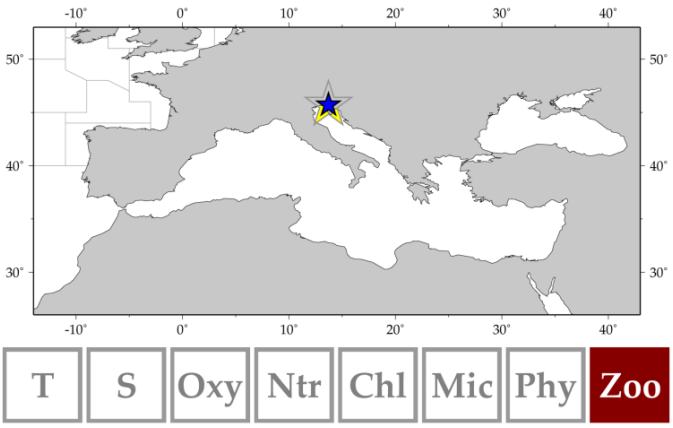

The station C1 is located in the Gulf of Trieste in the northernmost part of the Adriatic Sea. In 2006, it was formally included in the Italian network of long-term ecological research sites (LTER-Italy). Zooplankton are collected by vertical hauls from 15 m to the surface using a WP-2 net (200-µm mesh). Sampling has been ongoing since April 1970, with a major interruption from January 1981 to February 1986, inclusive. The sampling frequency is monthly and was fortnightly during a few months in the 1980s and in 2002–2004. The time-series station C1, established by the University of Trieste, was later taken over by the Laboratory of Marine Biology of Trieste after its formal institution in December 1979 and, since October 2005, has been handled by the Division of Oceanography (OCE) of the OGS (Istituto Nazionale di Oceanografia e Geofisica Sperimentale) of Trieste.

Related information: http://nettuno.ogs.trieste.it/ilter/BIO

Gulf of Trieste – MBS Buoy

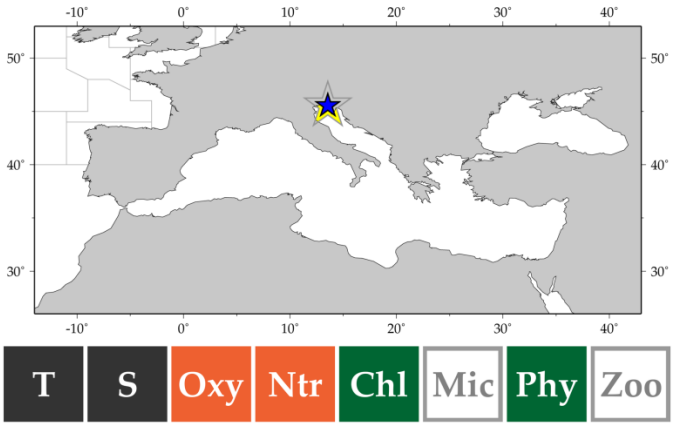

Country: Slovenia

IGMETS-ID: si-10101

Patricija Mozetič, Janja Francé, Neli Glavaš, Vlado Malačič, and Milijan Šiško

This time series in the southeastern part of the Gulf of Trieste (northern Adriatic Sea) was established in 1990 when the national monitoring programme became operational. The time series aims at understanding the variability in phytoplankton community structure in relation to physical and chemical properties of coastal waters (Mozetič *et al*., 2012) and distinguishing between natural fluctuations and those induced by anthropogenic activities. The Gulf of Trieste (surface area 600 km^2, volume 9.5 km^3, maximum depth 25 m) is affected by water-mass exchange with the northern Adriatic, local meteorological conditions, and freshwater inputs (Malačič *et al*., 2006). Events of hypoxia/anoxia and accumulation of mucous aggregates have characterized the area in the recent past. Sampling of physical, chemical, and biological parameters of the water column is carried out monthly at a relatively non-impacted station located in the vicinity of the oceanographic MBS buoy (45°54′N 13°55′E).

Related information: http://www.nib.si/mbp/

A3 South Atlantic Ocean

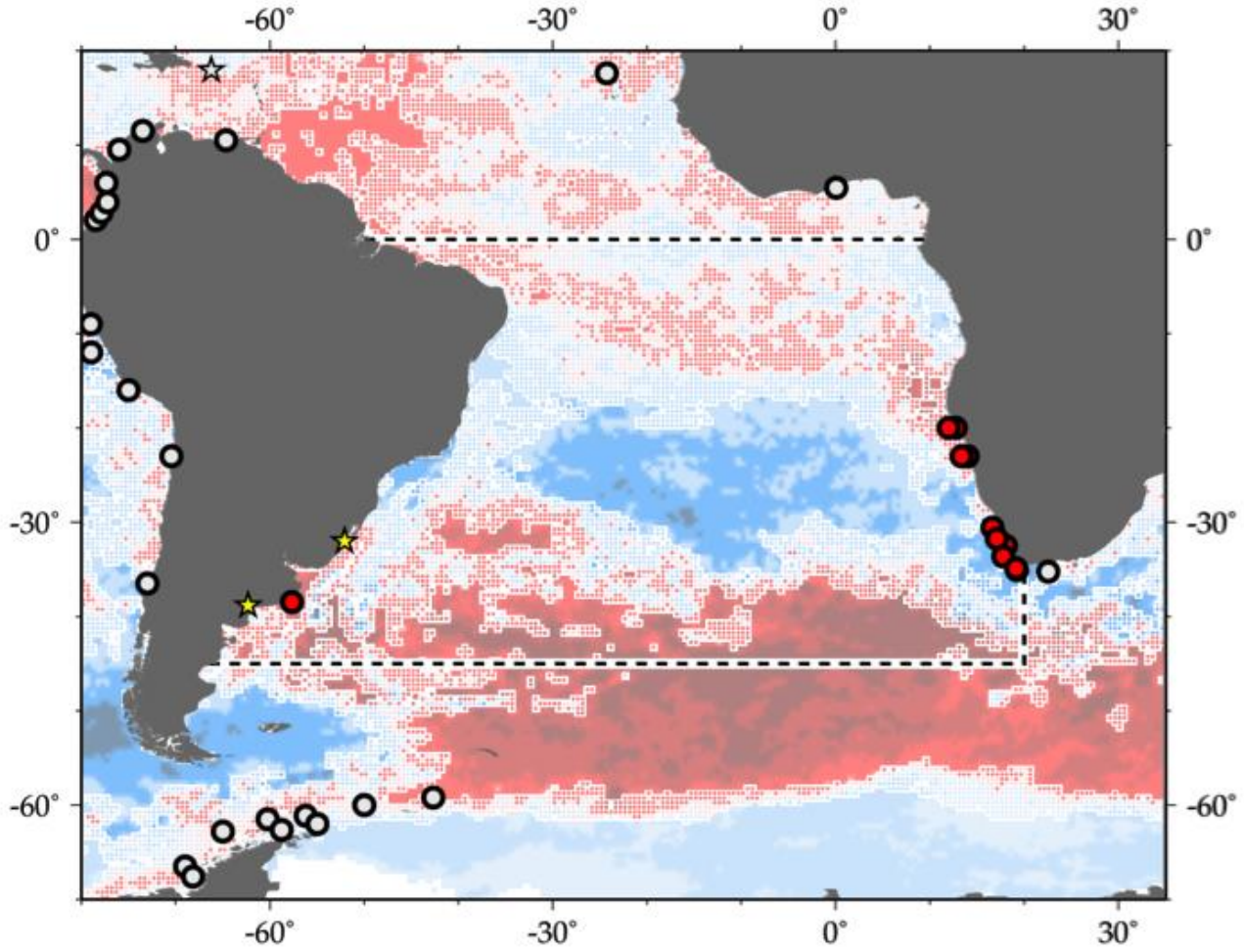

Figure A3. Map of IGMETS-participating South Atlantic time series on a background of a 10-year time-window (2003–2012) sea surface temperature trends (see also Chapter 5). At the time of this report, the South Atlantic collection consisted of 13 time series (coloured symbols of any type), of which two were from estuarine areas (yellow stars). Dashed lines indicate boundaries between IGMETS regions. Uncoloured (gray) symbols indicate time series being addressed in a different regional chapter (e.g. Southern Ocean, North Atlantic, and South Pacific).

Table A3. Time-series sites located in the IGMETS South Atlantic region. Participating countries: Argentina (ar), Brazil (br), Namibia (na), United Kingdom, (uk), and South Africa (za). Year-spans in red text indicate time series of unknown or discontinued status. IGMETS-IDs in red text indicate time series without a description entry in this Annex.

No.	IGMETS-ID	Site or programme name	Year-span	T	S	Oxy	Ntr	Chl	Mic	Phy	Zoo
1	ar-10101	Puerto Cuatreros *(Bahia Blanca Estuary)*	1975–present	X	X	X	X	X	-	-	-
2	ar-10201	EPEA – Estacion Permanente de Estudios Ambientales *(Argentine Coastal Waters)*	2000–present	X	X	-	X	X	X	-	-
3	br-10101	Patos Lagoon Estuary – Phyto-plankton Time Series *(Southeastern Brazil)*	1993–present	X	X	-	X	X	X	X	-
4	na-10101	Walvis Bay 23S shelf *(Northern Benguela Current)*	1978–present	X	X	X	-	-	-	-	X
5	na-10102	Namibia 20S shelf *(Northern Benguela Current)*	2002–present	-	-	-	-	-	-	-	X
6	na-10103	Walvis Bay 23S offshore *(Northern Benguela Current)*	1978–present	X	X	X	-	-	-	-	X
7	na-10104	Namibia 20S offshore *(Northern Benguela Current)*	2002–present	-	-	-	-	-	-	-	X
8	uk-30601	Atlantic Meridional Transect (AMT)	1995–present	X	X	X	X	X		X	X
9	za-10101	St Helena Bay *(Southern Benguela Current)*	1951–present	X	X	-	-	-	-	-	X
10	za-30101	SBCTS-A: North West Coast *(Southern Benguela Current)*	1988–present	-	-	-	-	-	-	-	X
11	za-30102	SBCTS-B: Central West Coast *(Southern Benguela Current)*	1988–present	-	-	-	-	-	-	-	X
11	za-30103	SBCTS-C: South West Coast *(Southern Benguela Current)*	1988–present	-	-	-	-	-	-	-	X
12	za-30104	SBCTS-D: Western Agulhas Bank *(Southern Benguela Current)*	1988–present	-	-	-	-	-	-	-	X
13	za-30201	ABCTS Danger Point Monitoring Line *(Agulhas Bank)*	1988–present	-	-	-	-	-	-	-	X

Puerto Cuatreros, Bahia Blanca Estuary

Country: Argentina

IGMETS-ID: ar-10101

Jorge Marcovecchio, Valeria Guinder, and Carla Spetter

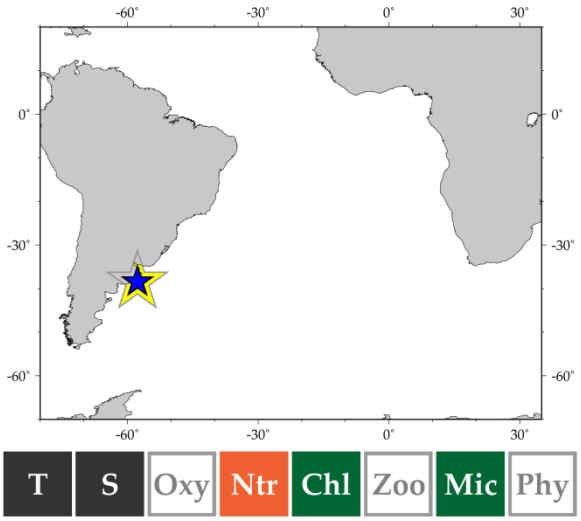

The Bahia Blanca Estuary, located in the southwest part of the Buenos Aires Province, Argentina, is a mesotidal estuary (Perillo *et al*., 2001). The mean tidal amplitude ranges from 2.2 to 3.5 m, the spring tidal amplitude ranges from 3 to 4 m, and the highest tidal amplitudes occur near the head of the estuary (Perillo *et al*., 2001). The estuary is formed by a series of northwest- to southeast-oriented tidal channels separated by extensive tidal flats, salt marsh patches, and islands (Perillo, 1995).

The sampling site is located at the inner zone of this estuary in Cuatreros Port, which is considered a chemically representative site of this zone (Freije and Marcovecchio, 2004).

EPEA (Estación Permanente de Estudios Ambientales)

Country: Argentina

IGMETS-ID: ar-10201

Ruben Negri, Vivian A. Lutz, Carla F. Berghoff, Mario O. Carignan, Georgina Cepeda, Daniel Cucchi Colleoni, Marina Vera Diaz, María Constanza Hozbor, Ezequiel Leonarduzzi, Graciela N. Molinari, Nora Montoya, Luciano Padovani, Marcelo Pájaro, M. Guillermina Ruiz, Valeria Segura, Ricardo I. Silva, and María Delia Viñas

The main objective of the EPEA time series (38°28′S 57°41′E) is to understand the annual and interannual dynamics of environmental variables and all components of plankton and follow possible long-term changes. It has been sampled monthly (with unfortunate gaps) since 2000. Variables measured include temperature, salinity, oxygen, nutrients, light penetration, absorption by particulate matter (phytoplankton and non-algal particles) and coloured dissolved organic material, chlorophyll *a*, pigment composition, bacterio-, phyto- (pico, nano, and micro), zoo-, and ichtyoplankton. The station is characterized by a temperate regime; annual range of SST: 10–21°C and salinity: 33.5–34.1. The hydrographic system is a transition between high-salinity coastal waters and mid-shelf waters. Under exceptional conditions, salinity can drop due to the influence of the Río de la Plata. Several unusual phytoplankton events, linked to large spatial and temporal scales, were detected during these years. EPEA forms part of the Latin American network Antares.

Patos Lagoon Estuary (PLE) Phytoplankton Time Series

Country: Brazil

IGMETS-ID: br-10101

Clarisse Odebrecht and Paulo Cesar Abreu

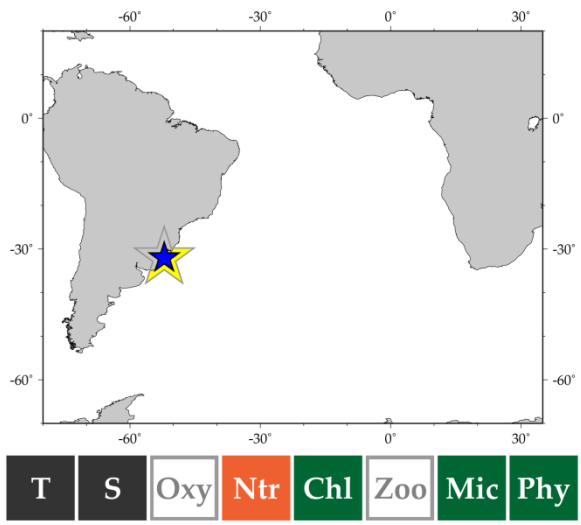

Large interannual phytoplankton variations observed in the 1980s instigated the establishment of the Patos Lagoon Estuary (PLE) Phytoplankton Time Series carried out in the framework of the Brazilian Long-Term Ecological Research (BR-LTER). The

main objective is to identify the natural and anthropic impacts on the PLE and adjacent coast. PLE (ca. 1000 km²) is a warm-temperate shallow and choked (only one long and narrow entrance) estuary where water exchanges with the Atlantic Ocean occur through a stabilized inlet, mainly controlled by winds and freshwater discharge, whereas tides are not significant. Peaks of river discharge are associated with El Niño episodes and turn the system riverine. Environmental (water temperature, salinity, Secchi disk depth, and concentrations of dissolved inorganic nutrients) and biotic properties (chlorophyll *a*, phytoplankton) have been measured monthly since 1993, providing the longest phytoplankton time series in Brazil.

Related information: http://www.peld.furg.br

Walvis Bay (23°S) Time Series

Country: Namibia

IGMETS-ID: na-10101 / na-10103

Anja Kreiner, Richard Horaeb, Hans Verheye, Fabienne Cazassus, Rudi Cloete, and Sakhile Tsotsobe

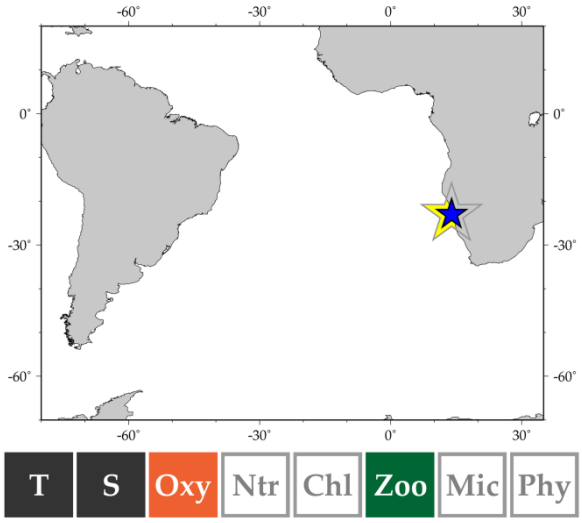

The National Marine Information and Research Centre (NatMIRC) in Swakopmund, Namibia started zooplankton monitoring in 2000 within an intense routine monitoring (Monthly Oceanographic Monitoring - MOM) programme on the 23°S line just outside Walvis Bay in an important fisheries nursing area. Sampling was done ca. monthly for the first five years, but since 2005, sampling has been done about eight times a year. Stations are positioned 2, 5, 10, 20, 30, 40, 50, 60, and 70 nautical miles from the coast. Sampling is done using a UNESCO WP-2 net equipped with a 200-µm mesh and in the upper 200 m of the water column (or 10 m from the bottom, if shallower). Apart from zooplankton, environmental parameters (temperature, salinity, and dissolved oxygen) are measured at every station. Zooplankton time series can reveal changes in environmental regimes, including turning points or regime shifts, which are important to understand for successful fisheries management.

Namibia (20°S) Time Series

Country: Namibia

IGMETS-ID: na-10102 / na-10104

Richard Horaeb and Rudi Cloete

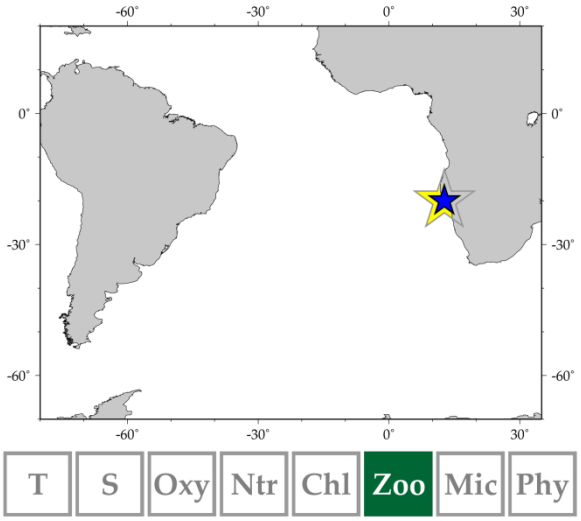

Within the Monthly Oceanographic Monitoring (MOM) Programme of the National Marine Information and Research Centre (NatMIRC) in Swakopmund, Namibia, zooplankton samples along with oceanographic data, such as SST, salinity, oxygen, and chlorophyll *a*, have been collected regularly since March 2005 along the transect at 20°S. Sampling stations are located at 2, 5, 10, 20, 30, 40, 50, 60, and 70 nautical miles from the coast. Sampling is done using a UNESCO WP-2 net equipped with a 200-µm mesh and in the upper 200 m of the water column (or 10 m from the bottom, if shallower). Changes in zooplankton species composition can be indicators of changes in environmental regimes and thus give important information for sustainable fisheries management.

Atlantic Meridional Transect (AMT) – South

Country: United Kingdom

IGMETS-ID: uk- 30601 to uk-30624

Andy Rees

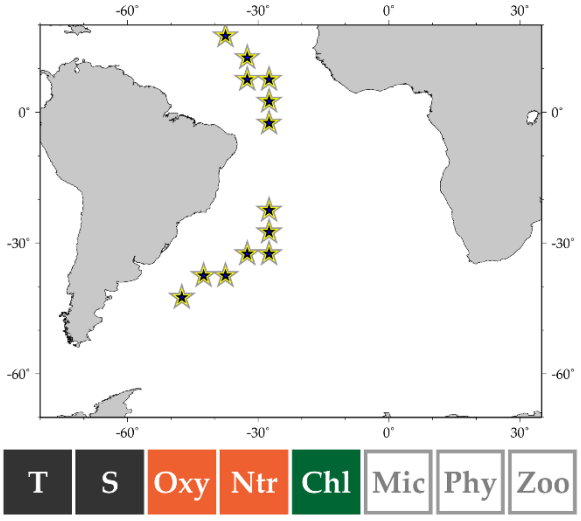

The Atlantic Meridional Transect (AMT) is a multidisciplinary programme which undertakes biological, chemical, and physical oceanographic research during an annual voyage between the UK and destinations in the South Atlantic. AMT began in 1995, with scientific aims to assess mesoscale to basin-scale phytoplankton processes, the functional interpretation of bio-optical signatures, and the seasonal, regional, and latitudinal variations in mesozooplankton dynamics. The programme provided a platform for international scientific collaboration, including the calibration and validation of SeaWiFS measurements and products. The measurements of hydrographic and bio-optical properties, plankton community structure, and primary production completed during the first 12 transects (1995–2000) represent the most coherent set of repeated biogeochemical observations over ocean basin-scales. This unique dataset has led to several important discoveries concerning the identification of oceanic provinces, validation of ocean colour algorithms, distributions of picoplankton, the identification of new regional sinks of carbon dioxide, and variability in rates of primary production and respiration. In 2002, the programme restarted (2002–2006) and broadened to address a suite of cross-disciplinary questions concerning ocean plankton ecology, biogeochemistry, and their links to atmospheric processes. The programme is coordinated and led by the Plymouth Marine Laboratory in collaboration with the National Oceanography Centre.

Related information: http://www.amt-uk.org/

The spatial subsetting and analysis of the AMT time series was still being processed at the time of the preparation of this report, and data were, therefore, not included in the analysis presented in Chapter 5. Upon incorporation in the IGMETS assessment, the AMT contribution will be available online (http://igmets.net/explorer).

St Helena Bay Copepod Time Series

Country: South Africa

IGMETS-ID: za-10101

Hans Verheye and Jenny Huggett

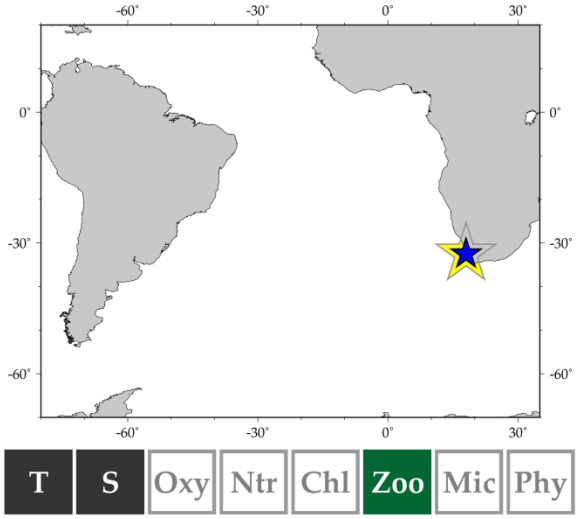

St Helena Bay (32°50′S), on the west coast of South Africa, is one of the most productive regions of the Benguela Current Large Marine Ecosystem (BCLME), one of the world's four productive upwelling regions of the eastern boundary current systems. It is the centre of pelagic fish recruitment and has been the focus of environmental, plankton, and fisheries research and monitoring since the early 1950s when the pelagic fishery developed in South Africa. The copepod time series (1951–2010) was constructed based on retrospective analysis of abundance and species composition of copepods in samples collected within 60 nautical miles from the coast in the bay during several fisheries-oriented, plankton dynamics and environmental sampling programmes since 1951. The analysis focused on austral autumn (April–June), the time when recruitment of anchovy (*Engraulis encrasicolus*) and sardine (*Sardinops sagax*) is at its peak. Details on sampling time, strategy, gear, and sample analysis are described in Verheye *et al*. (1998).

Southern Benguela Copepod Time Series

Country: South Africa

Site Name (IGMETS-ID):

North West Coast (IGMETS-ID: za-30101)
Central West Coast (IGMETS-ID: za-30102)
South West Coast (IGMETS-ID: za-30103)
Western Agulhas Bank (IGMETS-ID: za-30104)

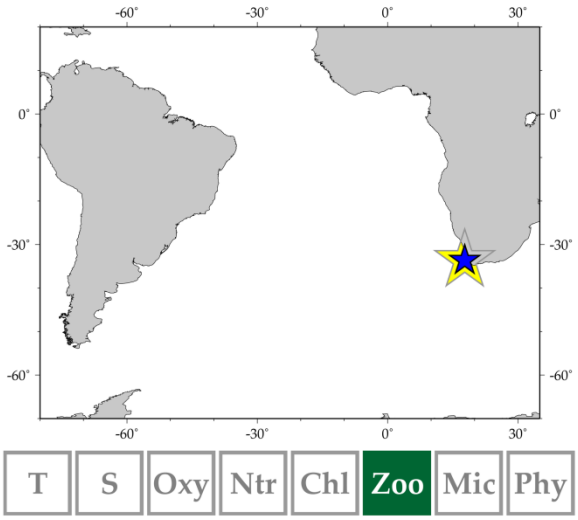

Jenny Huggett and Hans Verheye

The Benguela system is one of the four major eastern boundary upwelling systems of the world, characterized by high productivity and large pelagic fish populations. The Southern Benguela extends from the Orange River in the north (the boundary between South Africa and Namibia) to Cape Agulhas on the south coast of South Africa, the approximate longitude of the (warm) Agulhas Current retroflection. Upwelling-favourable, southeasterly winds reach a maximum during austral spring and summer, with the upwelling season extending from September to March. The system has been subdivided into four areas for spatial analysis (Huggett *et al*., 2009). Three regions on the west coast correspond to upwelling cells, as defined by Shannon and Nelson (1996): (i) the Namaqua (Hondeklipbaai) cell in the extreme north, designated the North West Coast (NWC), extending from the mouth of the Orange River to 31°S; (ii) the Columbine cell, designated the Central West Coast (CWC), extending from 31°S to Cape Columbine; and (iii) the Cape Peninsula cell in the south, called the South West Coast (SWC), extending from Cape Columbine to Cape Point. The fourth area, the Western Agulhas Bank (WAB), extends eastward from Cape Point to Cape Agulhas on the south coast. The west coast is an important nursery area for pelagic fish in winter, whereas the adult fish spawn mainly in summer on the south coast. Biannual monitoring of zooplankton, with a focus on copepods as important prey items for pelagic fish, was initiated in 1988. Vertical bongo net (200-µm mesh) hauls to a depth of 200 m were used to collect zooplankton along stratified random transects crossing the continental shelf, perpendicular to the coast, during hydroacoustic pelagic surveys in late spring/early summer (November/December) and late autumn/early winter (May/June). All copepods were counted and identified to stage, species, or category, as described in Huggett *et al*. (2009).

Agulhas Bank Copepod Time Series – Danger Point

Country: South Africa

IGMETS-ID: za-30201

see also Mossel Bay (za-30202) in the Indian Ocean section

Jenny Huggett

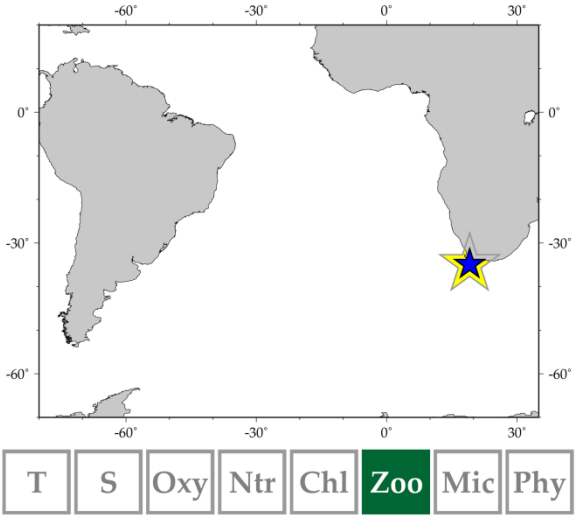

The Agulhas Bank is a wide continental shelf that forms the southern tip of the African continent. The eastern shelf is bounded by the warm, fast-flowing Agulhas Current, which retroflects at ca. 20°S, south of Cape Agulhas. The Agulhas Bank serves as a spawning ground for many commercially important fish, including sardine, round herring (*Etrumeus whiteheadi*), and anchovy. Copepods, which comprise 90% of the zooplankton carbon on the Agulhas Bank, provide an important food source for these pelagic fish as well as for juvenile squid. A single large (ca. 3 mm) species of copepod (*Calanus agulhensis*) dominates the copepod community in terms of biomass and has a centre of distribution associated with a semi-permanent ridge of cool, upwelled water south of Mossel Bay (Huggett and Richardson, 2000). Annual monitoring of copepod abundance and species composition on the Agulhas Bank was initiated in 1988 during austral spring (November/December). This time of year coincides with peak spawning by anchovy. Sampling was conducted along transects crossing the continental shelf, perpendicular to the coast, at two locations: one on the western Agulhas Bank near Danger Point (19°30′E) and one on the eastern Agulhas Bank near Mossel Bay (22°E). Zooplankton were collected using vertical bongo net (200-µm mesh) hauls to a maximum depth of 200 m during routine hydroacoustic surveys of pelagic fish. All copepods were counted and identified to stage, species, or category, as described in Huggett *et al*. (2009).

A4 Southern Ocean

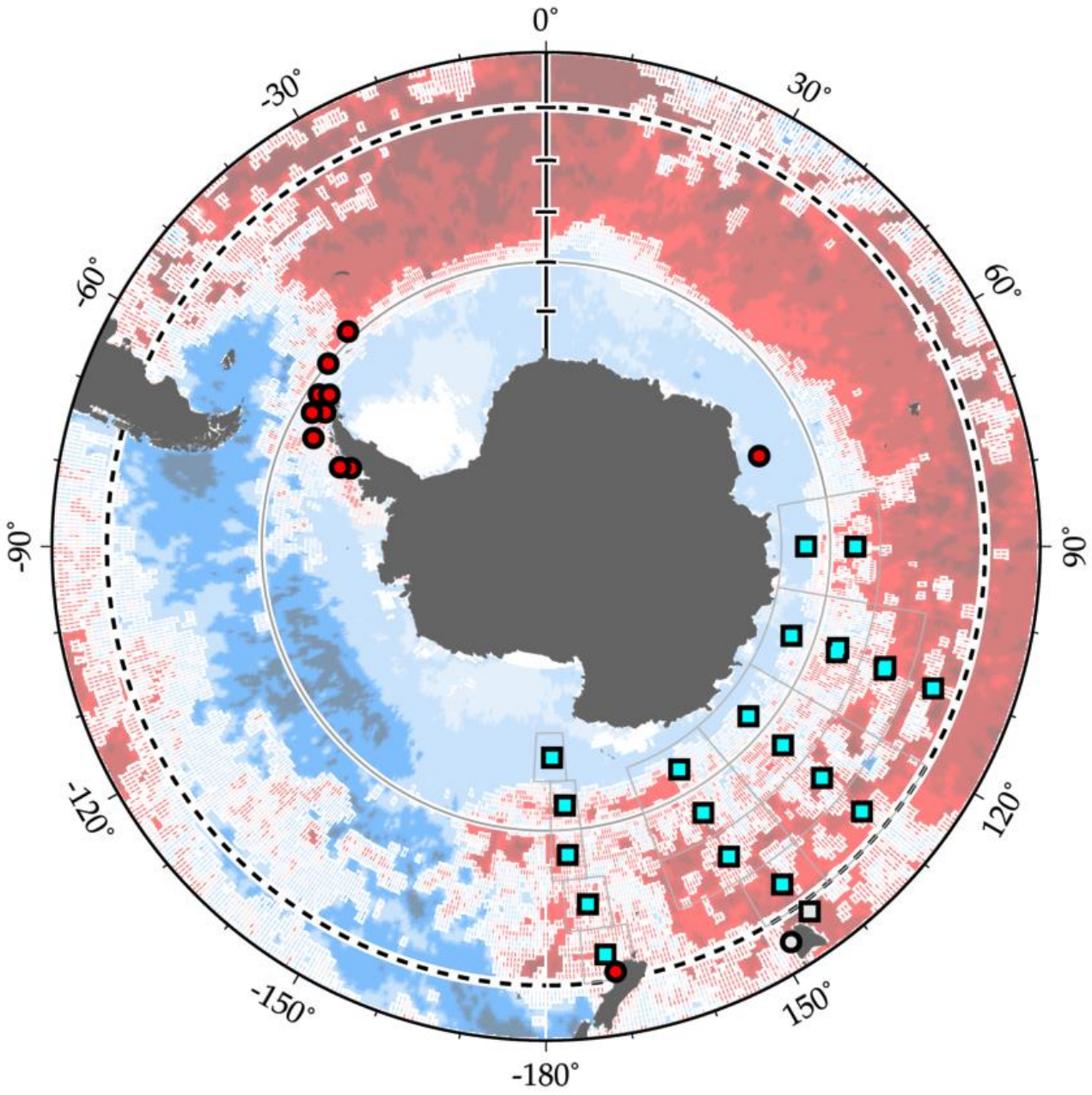

Figure A4. Map of IGMETS-participating Southern Ocean time series on a background of a 10-year time-window (2003–2012) sea surface temperature trends (see also Chapter 6). At the time of this report, the Southern Ocean collection consisted of 32 time series (coloured symbols of any type), of which 21 were from Continuous Plankton Recorder subareas (blue boxes). The dashed line at 45°S indicates the boundary between the IGMETS Southern Ocean region and other IGMETS regions in this report (e.g. South Pacific, South Atlantic, Indian Ocean), while the gray line at 60°S indicates the Antarctic Treaty boundary. Uncoloured (gray) symbols indicate time series being addressed in a different regional chapter.

Table A4. Time-series sites located in the IGMETS Southern Ocean region. Participating countries: New Zealand (nz), United Kingdom (uk), United States (us), and multiple countries (zz). Year-spans in red text indicate time series of unknown or discontinued status. IGMETS-IDs in red text indicate time series without a description entry in this Annex.

No.	IGMETS-ID	Site or programme name	Year-span	T	S	Oxy	Ntr	Chl	Mic	Phy	Zoo
1	nz-10101	Munida Time Series (*Western South Pacific*)	1998–present	X	X	-	X	X	-	-	-
2	uk-30401	KRILLBASE: Atkinson Krill Study (*Southern Ocean*)	1976–2003 (?)	-	-	-	-	-	-	-	X
3	uk-30402	KRILLBASE: Antarctic Peninsula and western Scotia Sea (*Southern Ocean*)	1975–present	-	-	-	-	-	-	-	X
4	uk-30403	KRILLBASE: Eastern Scotia Sea and South Georgia (*Southern Ocean*)	1975–present	-	-	-	-	-	-	-	X
5	uk-30404	KRILLBASE: Indian Ocean Sector (*Southern Ocean*)	1981–2006 (?)	-	-	-	-	-	-	-	X
6	uk-30501	Rothera Time Series (RaTS) (*Southern Ocean*)	1998–present	X	X	-	-	X	-	-	-
7	us-30501	Palmer Station Antarctica LTER (*Antarctic*)	1989–present	X	X	X	X	X	-	-	X
8	us-50701	AMLR Elephant Island – EI (*Southern Ocean*)	1995–present	X	X	-	-	X	-	-	-
9	us-50702	AMLR South – SA (*Southern Ocean*)	1995–present	X	X	-	-	X	-	-	-
10	us-50703	AMLR West – WA (*Southern Ocean*)	1995–present	X	X	-	-	X	-	-	-
11	us-50704	AMLR Joinville Island – JI (*Southern Ocean*)	1997–present	X	X	-	-	X	-	-	-
12	zz-40101	SCAR SO-CPR Aurora 080-100-B5560 (*Southern Ocean*)	1991–present	X	X	-	-	X	-	-	X
13	zz-40102	SCAR SO-CPR Aurora 080-100-B6065 (*Southern Ocean*)	1991–present	X	X	-	-	X	-	-	X
14	zz-40103	SCAR SO-CPR Aurora 100-120-B5055 (*Southern Ocean*)	1998–present	X	X	-	-	X	-	-	X
15	zz-40104	SCAR SO-CPR Aurora 100-120-B5560 (*Southern Ocean*)	1991–present	X	X	-	-	X	-	-	X
16	zz-40105	SCAR SO-CPR Aurora 100-120-B6065 (*Southern Ocean*)	1997–present	X	X	-	-	X	-	-	X
17	zz-40106	SCAR SO-CPR Aurora 120-140-B4550 (*Southern Ocean*)	1998–present	X	X	-	-	X	-	-	X
18	zz-40107	SCAR SO-CPR Aurora 120-140-B5055 (*Southern Ocean*)	1997–present	X	X	-	-	X	-	-	X
19	zz-40108	SCAR SO-CPR Aurora 120-140-B5560 (*Southern Ocean*)	1995–present	X	X	-	-	X	-	-	X

No.	IGMETS-ID	Site or programme name	Year-span	T	S	Oxy	Ntr	Chl	Mic	Phy	Zoo
20	zz-40109	SCAR SO-CPR Aurora 120-140-B6065 (*Southern Ocean*)	1995–present	X	X	-	-	X	-	-	X
21	zz-40110	SCAR SO-CPR Aurora 140-160-B4550 (*Southern Ocean*)	1999–present	X	X	-	-	X	-	-	X
22	zz-40111	SCAR SO-CPR Aurora 140-160-B5055 (*Southern Ocean*)	1995–present	X	X	-	-	X	-	-	X
23	zz-40112	SCAR SO-CPR Aurora 140-160-B5560 (*Southern Ocean*)	1995–present	X	X	-	-	X	-	-	X
24	zz-40113	SCAR SO-CPR Aurora 140-160-B6065 (*Southern Ocean*)	1997–present	X	X	-	-	X	-	-	X
25	zz-40131	SCAR SO-CPR Shirase E108111-S4550 (*Southern Ocean*)	2000–present	X	X	-	-	X	-	-	X
26	zz-40132	SCAR SO-CPR Shirase E108111-S5055 (*Southern Ocean*)	1999–present	X	X	-	-	X	-	-	X
27	zz-40133	SCAR SO-CPR Shirase E108111-S5560 (*Southern Ocean*)	1999–present	X	X	-	-	X	-	-	X
28	zz-40151	SCAR SO-CPR Aotea B4550 (*Southern Ocean*)	2008–present	-	-	-	-	-	-	-	X
29	zz-40152	SCAR SO-CPR Aotea B5055 (*Southern Ocean*)	2008–present	-	-	-	-	-	-	-	X
30	zz-40153	SCAR SO-CPR Aotea B5560 (*Southern Ocean*)	2008–present	-	-	-	-	-	-	-	X
31	zz-40154	SCAR SO-CPR Aotea B6065 (*Southern Ocean*)	2008–present	-	-	-	-	-	-	-	X
32	zz-40155	SCAR SO-CPR Aotea B6570 (*Southern Ocean*)	2008–present	-	-	-	-	-	-	-	X

Munida Time Series

Country: New Zealand

IGMETS-ID: nz-10101

Kim Currie, Keith Hunter and Malcolm Reid

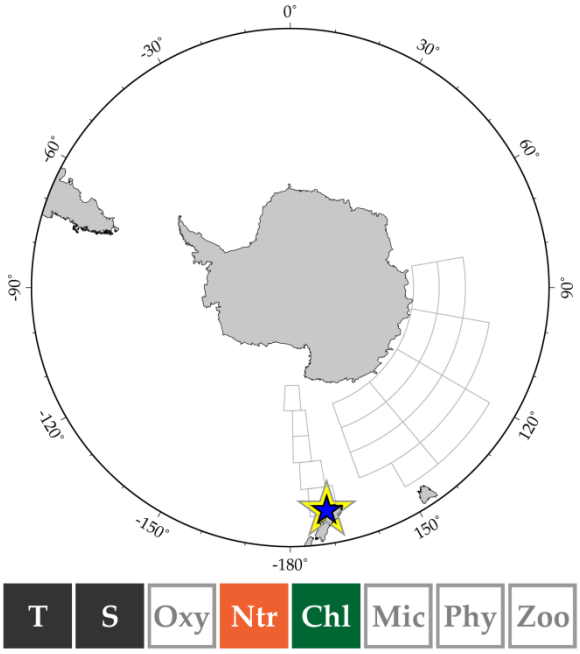

The Munida Time Series is a surface transect extending 65 km off the southeast coast of New Zealand and including neritic, modified subtropical, and subantarctic surface waters (SASW). The time series was established in 1998 to study the role of these waters in the uptake of atmospheric carbon dioxide and the seasonal, interannual, and long-term changes of the carbonate chemistry. Cruises are bimonthly and consist of surface measurements plus a depth station in SASW. All water masses are a sink for atmospheric carbon dioxide (Currie *et al.*, 2011), and the seasonal cycles of dissolved inorganic carbon are primarily driven by net community production (Brix *et al.*, 2013; Jones *et al.*, 2013), with modification by the annual cycle of sea surface temperature. Aspects of trace metal chemistry, nitrogen cycling, and bacterial production have been studied on a shorter-term basis, embedded within the main programme.

KRILLBASE: a circumpolar database of Antarctic krill and salps

Countries: United Kingdom, Germany, Canada, United States, and Australia

Site Name (IGMETS-ID):

Atkinson Krill Study (uk-30401)
Antarctic Peninsula and Western Scotia Sea (uk-30402)
Eastern Scotia Sea and South Georgia (uk-30403)
Indian Ocean Sector (uk-30404)

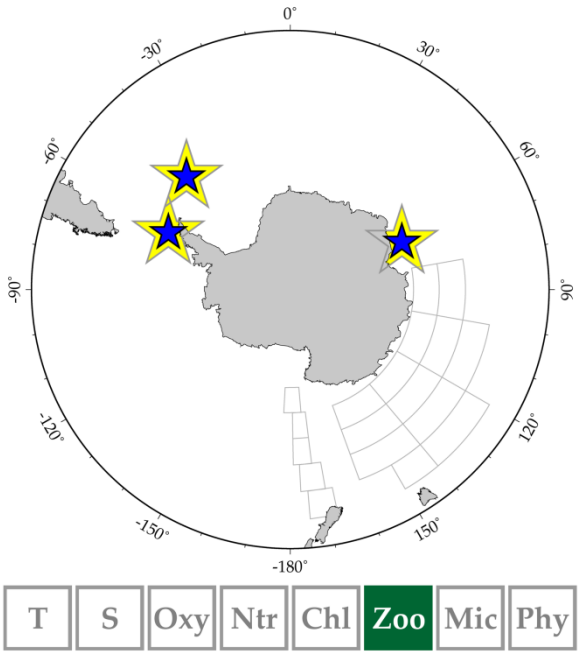

Angus Atkinson, Volker Siegel, Evgeny Pakhomov, Simeon Hill, Christian Reiss, Debbie Steinberg, and So Kawaguchi

Standardized monitoring of *Euphausia superba* and salps only dates from the 1990s and in a few sites. However, a wealth of historical data exists from various countries all focusing on a narrow "slice" of Antarctica. KRILLBASE has mined and compiled all available scientific net-haul data into a single searchable database. This active project so far contains about 15 000 net hauls for abundance of salps and postlarval krill, with many individual krill length measurements. The best coverage is December–March in the Atlantic and Indian sectors (1926–1939, post-1976). This composite dataset needs careful analysis because the methods were not standardized. However, it is more than the sum of its parts and allows a diversity of analyses, e.g. meso- and circumpolar-scale dynamics, changes with time and krill demographics. KRILLBASE includes state-funded programmes (see above) which require direct prior communication for access to their parts of the dataset.

Related information: http://www.iced.ac.uk/science/krillbase.htm

Rothera Time Series (RaTS)

Country: United Kingdom

IGMETS-ID: uk-30501

Hugh Venables, Alexander Brearley, Andrew Clarke, and Michael Meredith

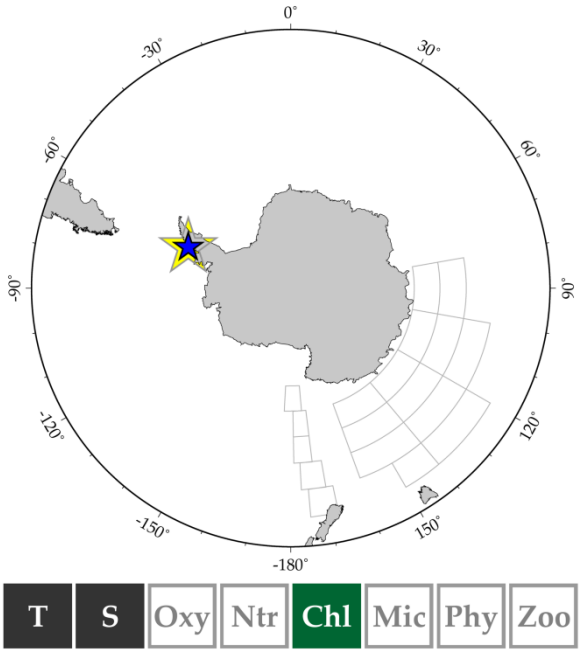

The western Antarctic Peninsula (WAP) warmed more rapidly than any other region in the southern hemisphere during the second half of the 20th century. To understand the impacts of this change on the interdisciplinary marine environment, the Rothera Time Series (RaTS) was instigated in 1997 to make the high-quality, sustained ocean measurements required. RaTS involves quasi-weekly profiling of the physical properties (temperature, salinity, density) of the water column at the WAP from rigid inflatable boats plus sampling for a range of biogeochemical and biological parameters. The suite of measurements includes chlorophyll concentration, nutrients, isotopic tracers of ice melt, carbonate system parameters, and so on. Uniquely, RaTS includes full ocean measurements in winter, including sampling though holes cut in sea ice when the ocean surface is completely frozen. These winter measurements have resulted in the attainment of some of the most important new insights into the functioning of the oceanographic and biological systems.

Related information: https://www.bas.ac.uk/project/rats/

Palmer Station Antarctica–LTER

Country: United States

IGMETS-ID: us-30501

Hugh Ducklow, Debbie Steinberg, Oscar Schofield, Michael Meredith, and Douglas Martinson

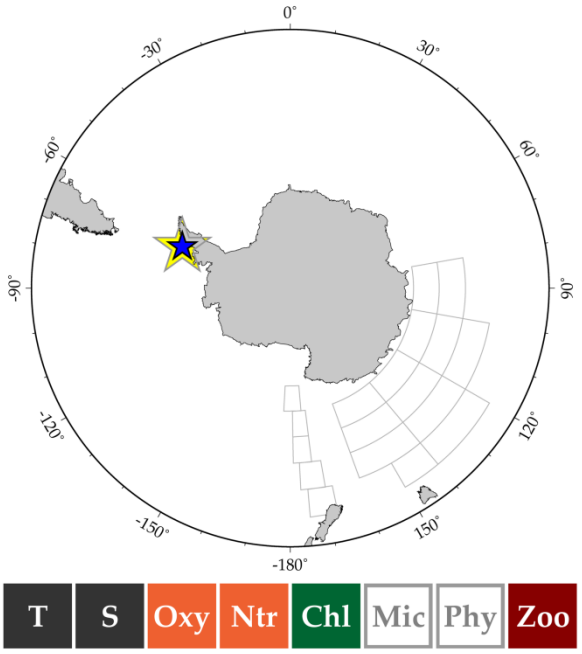

Palmer Station Antarctica (LTER) is an interdisciplinary polar marine research programme established in 1990 as part of a national network of long-term ecological research sites created by the US National Science Foundation (NSF). The western Antarctic Peninsula (WAP) is distinctive among the Antarctic regions with its north–south orientation, direct exposure to prevailing westerly atmospheric winds and complex ocean circulation patterns. The extent, duration, and seasonality of sea ice and inputs from glacial meltwater are strong influences on the ecological and biogeochemical processes in the coastal marine ecosystem. Sea ice is the principal physical determination of variability in the coastal marine ecosystem. In fact, the life cycles of most organisms are influenced by the seasonal changes.

To study these changes on a global-scale, Palmer LTER examines the region, which is a series of dynamic, interconnected systems encompassing an immediate coastal region (0 300 m deep), a continental shelf region (300–1000 m deep), and a continental slope region (>1000 m deep). Yearly between the months of October and April, semi-weekly observations of nearshore process studies are made from Palmer Station. These are complemented in January (austral summer in the Antarctic) by a regional-scaled LTER cruise.

Related information: http://pal.lternet.edu

AMLR

Country: United States

Site name (IGMETS-ID):

AMLR Elephant Island – EI (us-50701)
AMLR South – SA (us-50702)
AMLR West – WA (us-50703)
AMLR Joinville Island – JI (us-50704)

Christian Reiss

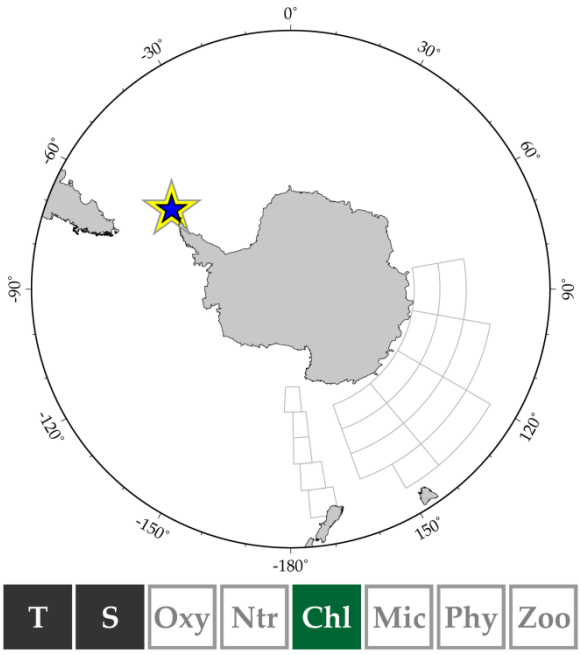

The Antarctic Ecosystem Research Division (AERD) conducts research to fulfill NOAA's mandate of providing scientific advice that supports US interests related to resource management by the Commission for the Conservation of Antarctic Marine Living Resources (CCAMLR), of which the US is a member country. NOAA Fisheries' Antarctic research is mandated by the US Antarctic Marine Living Resources (AMLR) Convention Act of 1984; thus, the programme of work undertaken and managed by the AERD is widely known as the US AMLR Program. The US AMLR Program is internationally recognized for its ongoing contributions to ecosystem-based management of fisheries that impact krill, finfishes, krill-dependent predators, and other components of the Antarctic ecosystem. Since 1986, the AERD has managed the US AMLR Program's field studies in Antarctic waters to investigate the effects of commercial fisheries on the marine ecosystem, including effects on local seal and seabird populations. Studies conducted by US AMLR/AERD researchers include (i) an annual research vessel survey to map prey distribution and abundance and to measure environmental variables in a study area off the Antarctic Peninsula; (ii) research at land stations to determine effects of fishing on pinniped and seabird populations during their reproductive cycles; and (iii) accounting for the status and role of mesopelagic species such as myctophids, *Pleurogramma*, and so on.

Related information: http://swfsc.noaa.gov/aerd/

SCAR SO–CPR – Southern Ocean Continuous Plankton Recorder

IGMETS ID: zz-40101 – zz-40131 – zz-40151

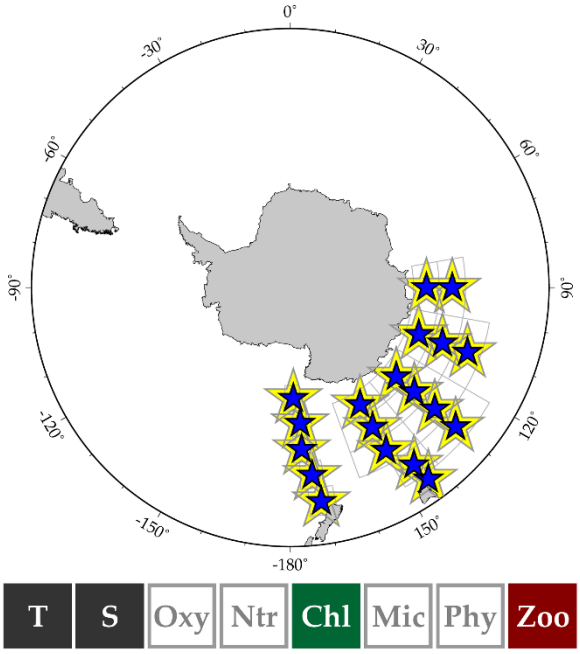

The SCAR SO-CPR Survey was established in 1991 to map the spatial-temporal patterns of zooplankton biodiversity and then to use the sensitivity of plankton to environmental change as early warning indicators of the health of the Southern Ocean. CPRs are towed from research, supply, and fishing vessels which usually also collect environmental data such as SST, salinity, fluorometry, light, and other meteorological parameters while underway. Sixteen ships from ten countries have participated to date providing a near circum-Antarctic survey. Most tows are conducted in the region south of Africa eastward to the Ross Sea. All zooplankton in 5-nautical-mile-equivalent sections are identified to the lowest possible taxa, usually species, and counted. Antarctic krill (*Euphausia superba*) and other euphausiids are identified to the developmental stage. Counts are combined with averaged environmental data for each 5 nautical miles. Approximately 250 000 nautical miles have been sampled representing ca. 50 000 samples for about 250 zooplankton taxa. The dataset is a SCAR business product.

For the purposes of the IGMETS analysis, the SCAR SO-CPR data set was divided into twenty sub-areas (indicated by the gray box outlines in the map above), similar to the sub-areas and methods used for the North Atlantic and North Pacific CPR programs.

A5 Indian Ocean

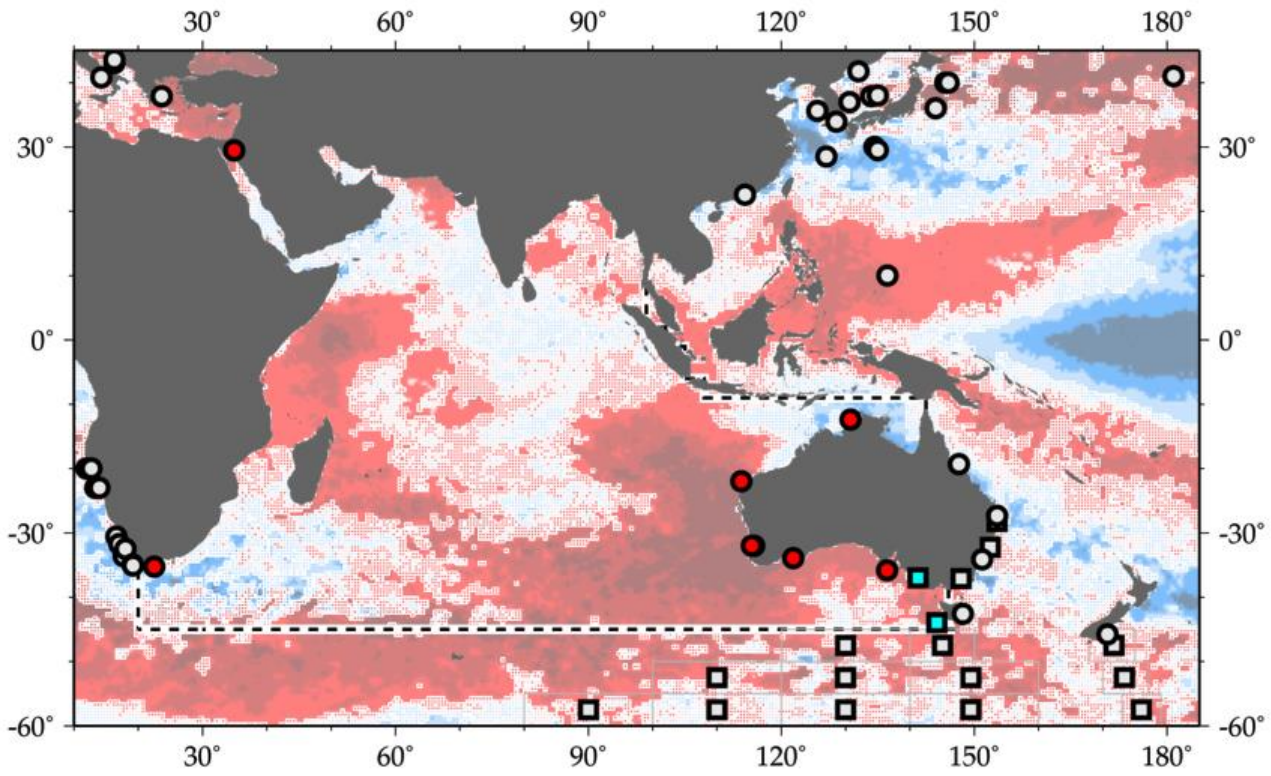

Figure A5. Map of IGMETS-participating Indian Ocean time series on a background of a 10-year time-window (2003–2012) sea surface temperature trends (see also Chapter 7). At the time of this report, the Indian Ocean collection consisted of 10 time series (coloured symbols of any type), of which two were Continuous Plankton Recorder subareas (blue boxes) and one was estuarine (yellow star). Dashed lines indicate boundaries between IGMETS regions. Uncoloured (gray) symbols indicate time series being addressed in a different regional chapter (e.g. Southern Ocean, North/South Pacific, South Atlantic).

Table A5. Time-series sites located in the IGMETS Indian Ocean subarea. Participating countries: Australia (au), Israel (il), and South Africa (za).

No.	IGMETS-ID	Site or programme name	Year-span	T	S	Oxy	Ntr	Chl	Mic	Phy	Zoo
1	au-10101	Swan River Estuary: S01 Blackwall Reach *(Southwestern Australia)*	1994–present	X	X	X	X	X	-	X	-
2	au-40114	SO-CPR Aurora 140-160-B4245 *(Southern Ocean)* *see Southern Ocean Annex A4)*	2008–present	X	X	-	-	X	-	-	X
3	au-40205	AusCPR MEAD Line *(Australian Coastline)* *see Southern Ocean Annex A4)*	2010–present	-	-	-	-	X	-	X	X
4	au-50102	IMOS National Reference Station Darwin *(Northern Australia)*	2011–present	X	X	-	X	X	X	X	X
5	au-50103	IMOS National Reference Station Esperance *(Southern Australia)*	2009–present	X	X	X	X	X	X	X	X
6	au-50104	IMOS National Reference Station Kangaroo Island *(Southern Australia)*	2008–present	X	X	-	X	X	X	X	X
7	au-50106	IMOS National Reference Station Ningaloo *(Western Australia)*	2010–present	X	X	-	X	X	X	X	X
8	au-50108	IMOS National Reference Station Rottnest Island *(Southwestern Australia)*	2009–present	X	X	-	X	X	X	X	X
9	il-10101	Gulf of Eilat Aqaba NMP Station A *(Gulf of Eilat – Gulf of Aqaba)*	2003–present	X	X	X	X	X	-	-	-
10	za-30202	ABCTS Mossel Bay Monitoring Line *(Agulhas Bank)*	1988–present	-	-	-	-	-	-	-	X

Swan River Estuary

Country: Australia

IGMETS-ID: au-10101

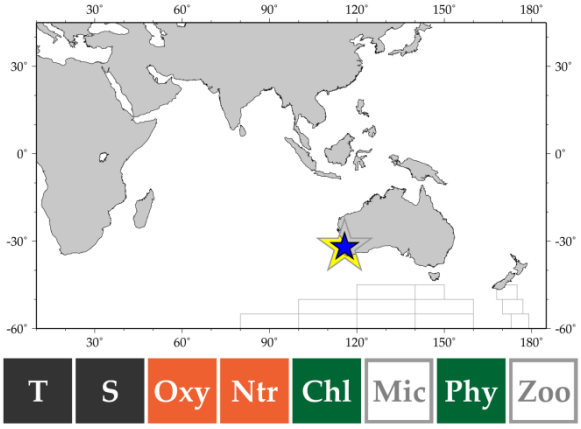

The Swan and Canning rivers flow through the heart of metropolitan Perth, a city of more than 1.5 million people and the capital of Western Australia. The Swan (Derbal Yerrigan) and Canning (Djarlgarra or Dyarlgarro) rivers are 72 and 110 km long, respectively. Together, these two rivers and their tributaries drain a catchment area of 2090 km^2. The Swan–Canning river system is typified by a large urban and agricultural catchment and relatively shallow and slow-moving river conditions. These factors as well as sandy soils and a climate of diminishing rainfall and long hot summers make the system vulnerable to a suite of environmental issues. The Swan River Trust has a series of initiatives and monitoring programmes in place aimed at improving water quality in the Swan and Canning rivers and their tributaries.

Integrated Marine Observing System's (IMOS) – IMOS National Reference Station – Darwin

Country: Australia

IGMETS-ID: au-50102

Anthony J. Richardson, Frank Coman, Claire Davies, Ruth Eriksen, Felicity McEnnulty, Anita Slotwinski, Mark Tonks, and Julian Uribe-Palomino

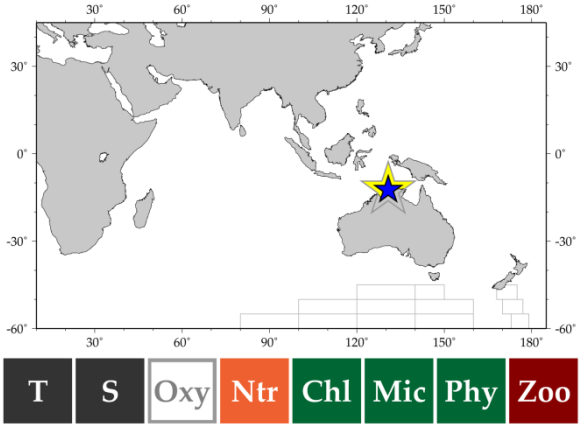

Darwin (12°40′S 130°77′E) is one of seven National Reference Stations that comprise IMOS. The NRSs are designed to provide regular baseline information to understand how large-scale, long-term change and variability in the global ocean are affecting Australia's coastal ecosystems. The goal is to develop multidecadal time series of the physical and biogeochemical properties of Australia's coastal seas, informing research into ocean change, climate variability, ocean circulation, and ecosystem responses. The Darwin NRS is situated close to the largest town in Northern Australia, and its population has a considerable impact on the ecosystem. This dataset contains seasonal data on zooplankton biomass and species composition collected since June 2011 using a 100-µm mesh dropnet deployed to 18 m. The corresponding biogeochemical datasets including temperature, salinity, nutrients, chlorophyll, and phytoplankton abundance are available through the AODN portal https://portal.aodn.org.au/.

Related information: http://imos.org.au/anmnnrs.html

Integrated Marine Observing System's (IMOS) – IMOS National Reference Station – Esperance

Country: Australia

IGMETS-ID: au-50103

Anthony J. Richardson, Frank Coman, Claire Davies, Ruth Eriksen, Felicity McEnnulty, Anita Slotwinski, Mark Tonks, and Julian Uribe-Palomino

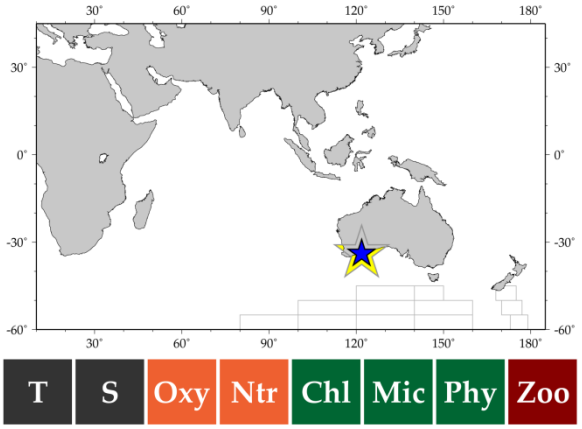

Esperance (33°93'S 121°85'E) is one of two National Reference Stations that was dropped from the original set of nine moorings that comprise IMOS. The NRSs are designed to provide regular baseline information to understand how large-scale, long-term change and variability in the global ocean are affecting Australia's coastal ecosystems. The goal is to develop multidecadal time series of the physical and biogeochemical properties of Australia's coastal seas, informing research into ocean change, climate variability, ocean circulation, and ecosystem responses. The Esperance NRS was isolated and logistically challenging to sample monthly; it operated between May 2009 and July 2013. This dataset contains seasonal data on zooplankton biomass and species composition collected using a 100-µm mesh dropnet deployed to 45 m. The corresponding biogeochemical datasets including temperature, salinity, nutrients, chlorophyll, and phytoplankton abundance are available through the AODN portal https://portal.aodn.org.au/.

Related information: http://imos.org.au/anmnnrs.html

Integrated Marine Observing System's (IMOS) – IMOS National Reference Station – Kangaroo Island

Country: Australia

IGMETS-ID: au-50104

Anthony J. Richardson, Frank Coman, Claire Davies, Ruth Eriksen, Felicity McEnnulty, Anita Slotwinski, Mark Tonks, and Julian Uribe-Palomino

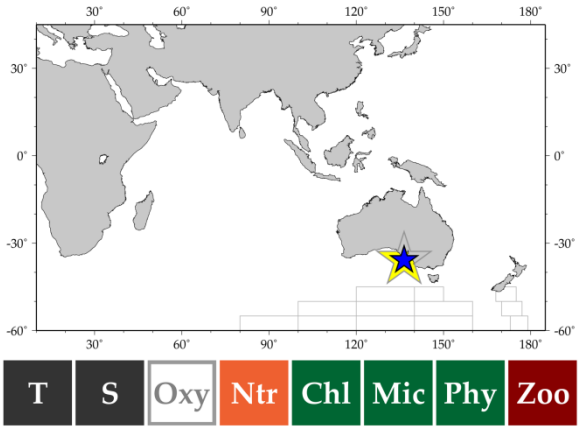

Kangaroo Island (35°83'S 136°44'E) is one of seven National Reference Stations that comprise IMOS. The NRSs are designed to provide regular baseline information to understand how large-scale, long-term change and variability in the global ocean are affecting Australia's coastal ecosystems. The goal is to develop multidecadal time series of the physical and biogeochemical properties of Australia's coastal seas, informing research into ocean change, climate variability, ocean circulation, and ecosystem responses. The Kangaroo Island NRS is part of a mooring array that monitors the large seasonal coastal upwelling of water that occurs along the region's continental shelf during summer. This dataset contains seasonal data on zooplankton biomass and species composition collected since November 2009 using a 100-µm mesh dropnet deployed to 100 m. The corresponding biogeochemical datasets including temperature, salinity, nutrients, chlorophyll, and phytoplankton abundance are available through the AODN portal https://portal.aodn.org.au/.

Related information: http://imos.org.au/anmnnrs.html

Integrated Marine Observing System's (IMOS) – IMOS National Reference Station – Ningaloo

Country: Australia

IGMETS-ID: au-50106

Anthony J. Richardson, Frank Coman, Claire Davies, Ruth Eriksen, Felicity McEnnulty, Anita Slotwinski, Mark Tonks, and Julian Uribe-Palomino

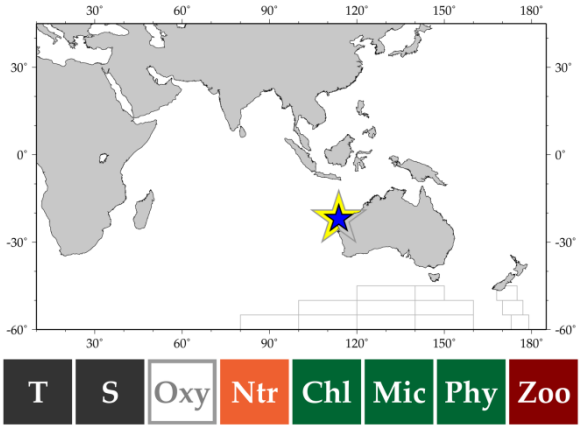

Ningaloo (21°99'S 113°78'E) is one of two National Reference Stations that was dropped from the original set of nine moorings that comprise IMOS. The NRSs are designed to provide regular baseline information to understand how large-scale, long-term change and variability in the global ocean are affecting Australia's coastal ecosystems. The goal is to develop multidecadal time series of the physical and biogeochemical properties of Australia's coastal seas, informing research into ocean change, climate variability, ocean circulation, and ecosystem responses. The Ningaloo NRS was isolated and logistically challenging to sample monthly; it operated between November 2010 and August 2013. This dataset contains seasonal data on zooplankton biomass and species composition collected using a 100-µm mesh dropnet deployed to 25 m. The corresponding biogeochemical datasets including temperature, salinity, nutrients, chlorophyll, and phytoplankton abundance are available through the AODN portal https://portal.aodn.org.au/.

Related information: http://imos.org.au/anmnnrs.html

Integrated Marine Observing System's (IMOS) – IMOS National Reference Station – Rottnest Island

Country: Australia

IGMETS-ID: au-50108

Anthony J. Richardson, Frank Coman, Claire Davies, Ruth Eriksen, Felicity McEnnulty, Anita Slotwinski, Mark Tonks, and Julian Uribe-Palomino

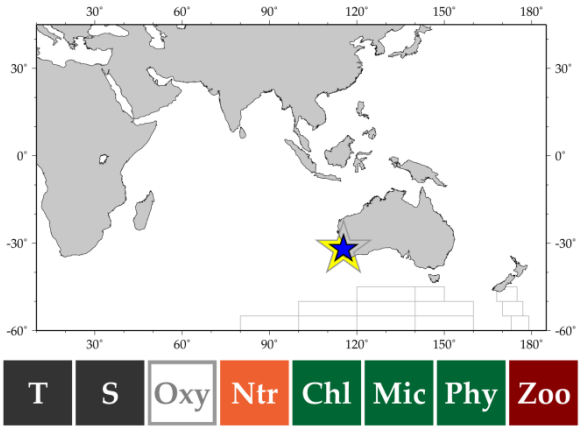

Rottnest Island (32°S 115°42'E) is one of seven National Reference Stations that comprise IMOS. The NRSs are designed to provide regular baseline information to understand how large-scale, long-term change and variability in the global ocean are affecting Australia's coastal ecosystems. The goal is to develop multidecadal time series of the physical and biogeochemical properties of Australia's coastal seas, informing research into ocean change, climate variability, ocean circulation, and ecosystem responses. The Rottnest Island NRS is sited at an historical mooring, operating since 1951 to monitor variability in the Leeuwin Current. This dataset contains seasonal data on zooplankton biomass and species composition collected since December 2009 using a 100-µm mesh dropnet deployed to 45 m. The corresponding biogeochemical datasets include temperature, salinity, nutrients, chlorophyll, and phytoplankton abundance are available through the AODN portal https://portal.aodn.org.au/.

Related information: http://imos.org.au/anmnnrs.html

Gulf of Eilat/Aqaba NMP Station A

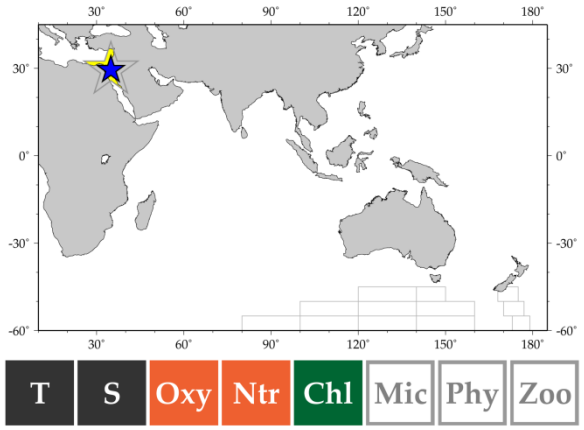

Country: Israel

IGMETS-ID: il-10101

Yonathan Shaked and Amatzia Genin

Israel's national monitoring programme (NMP) monitors habitats at the northern end of the Gulf of Eilat/Aqaba (Red Sea) within Israel's borders. The programme was initiated in 2003 by Israel's Ministry of Environmental Protection to provide administrators with scientific data.

The Gulf is a deep narrow basin surrounded by an arid landmass. SST reaches ca. 28°C in summer, but, the deep waters are uniquely always about 21°C, forcing a low SST limit that accommodates some of the world's northernmost coral reefs. Winter cooling promotes water column mixing, sometimes deeper than 800 m, that supply scarce nutrients to the upper waters.

The NMP's scope includes both deep and shallow habitats. Monthly cruises sample the water column (to > 700 m depth) and shallow waters along the Israeli coast. Reefs and other shallow habitats are surveyed annually, and various supplementary measurements aid data analyses.

An annual report (Hebrew, English abstract and figure legends) and all data are available online.

Related information: http://www.iui-eilat.ac.il/Research/NMPmeteodata.aspx

Agulhas Bank Copepod Time Series – Mossel Bay

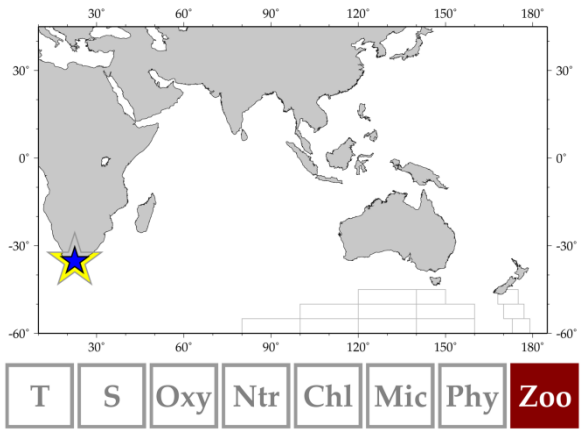

Country: South Africa

IGMETS-ID: za-30202

Jenny Huggett

The Agulhas Bank is a wide continental shelf that forms the southern tip of the African continent. The eastern shelf is bounded by the warm, fast-flowing Agulhas Current which retroflects at ca. 20°S, south of Cape Agulhas. The Agulhas Bank serves as a spawning ground for many commercially important fish including sardine, round herring, and anchovy. Copepods, which comprise 90% of the zooplankton carbon on the Bank, provide an important food source for these pelagic fish as well as for juvenile squid. A single large (ca. 3 mm) species of copepod (*Calanus agulhensis*) dominates the copepod community in terms of biomass and has a centre of distribution associated with a semi-permanent ridge of cool, upwelled water south of Mossel Bay (Huggett and Richardson, 2000). Annual monitoring of copepod abundance and species composition on the Agulhas Bank was initiated in 1988 during austral spring (November/December). This time of year coincides with peak spawning by anchovy. Sampling was conducted along transects crossing the continental shelf, perpendicular to the coast, at two locations: one on the western Agulhas Bank near Danger Point (19°30'E) and one on the eastern Agulhas Bank near Mossel Bay (22°E). Zooplankton were collected using vertical bongo net (200-µm mesh) hauls to a maximum depth of 200 m during routine hydroacoustic surveys of pelagic fish. All copepods were counted and identified to stage, species, or category, as described in Huggett *et al*. (2009).

A6 South Pacific Ocean

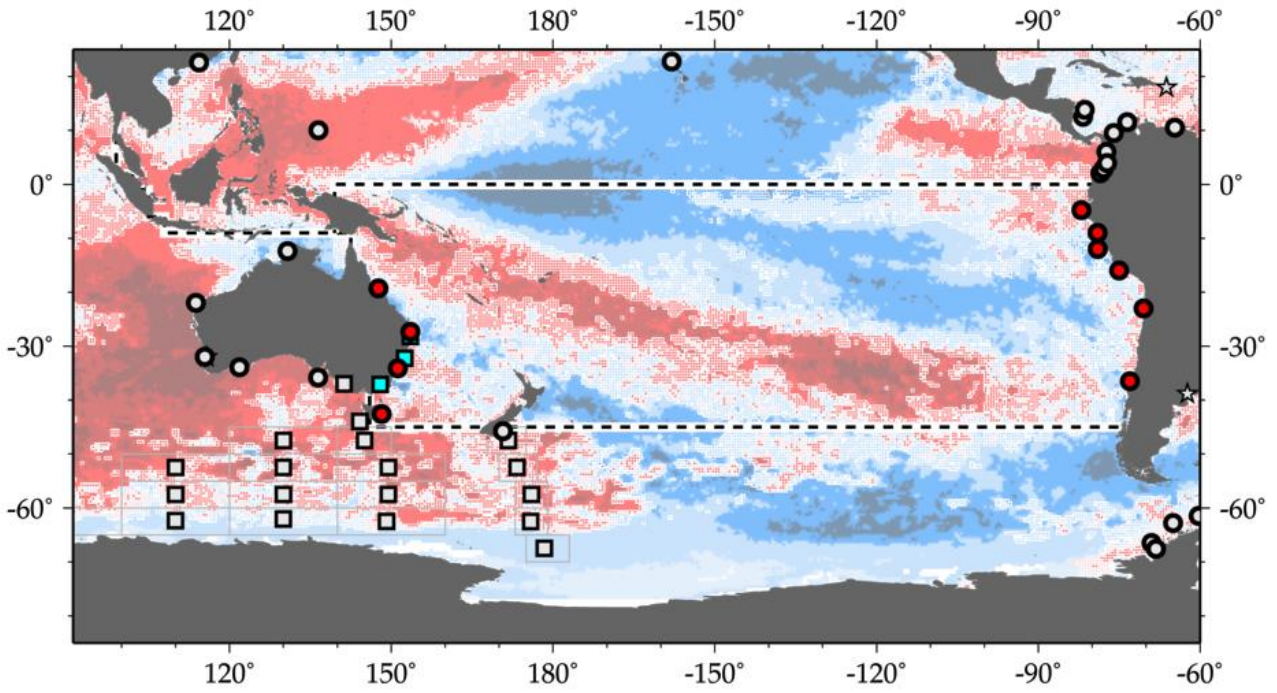

Figure A6. Map of IGMETS-participating South Pacific time series on a background of a 10-year time-window (2003–2012) sea surface temperature trends (see also Chapter 7). At the time of this report, the South Pacific collection consisted of 13 time series (coloured symbols of any type), of which three were from Continuous Plankton Recorder subareas (blue boxes) and none were from estuarine areas (yellow stars). Dashed lines indicate boundaries between IGMETS regions. Uncoloured (gray) symbols indicate time series being addressed in a different regional chapter (e.g. Southern Ocean, North Pacific, Indian Ocean).

Table A6. Time-series sites located in the IGMETS South Pacific region. Participating countries: Australia (au), Chile (il), and Peru (pe). Year-spans indicated in red belong to time series which were terminated. Year-spans in red text indicate time series of unknown or discontinued status. IGMETS-IDs in red text indicate time series without a description entry in this Annex.

No.	IGMETS-ID	Site or programme name	Year-span	T	S	Oxy	Ntr	Chl	Mic	Phy	Zoo
1	au-40201	AusCPR BRSY Line – North (*Australian Coastline*)	2009–present	-	-	-	-	X	-	X	X
2	au-40202	AusCPR BRSY Line – South (*Australian Coastline*)	2009–present	-	-	-	-	X	-	X	X
3	au-40204	AusCPR SYME Line – South (*Australian Coastline*)	2009–present	-	-	-	-	X	-	X	X
4	au-50101	IMOS National Reference Station – Port Hacking (*Southeastern Australia*)	2002–present	X	X	-	X	X	X	X	X
5	au-50105	IMOS National Reference Station – Maria Island (*Tasmania*)	2009–present	X	X	X	X	X	X	X	X
6	au-50107	IMOS National Reference Station – North Stradbroke Island (*Eastern Australia*)	2008–present	-	X	-	X	X	X	X	X
7	au-50109	IMOS National Reference Station – Yongala (*Northeastern Australia*)	2009–present	X	X	-	X	X	X	X	X
8	cl-30101	Concepcion Station 18 (*Chilean Coast*)	2002–present	-	-	-	-	-	-	-	X
9	cl-30102	Bay of Mejillones (*Chilean Coast*)	1988–present	-	-	-	-	-	-	-	X
10	pe-30101	IMARPE Region A *(Eastern South Pacific)*	1962–2005 (?)	-	-	-	-	-	-	-	X
11	pe-30102	IMARPE Region B *(Eastern South Pacific)*	1962–2005 (?)	-	-	-	-	-	-	-	X
12	pe-30103	IMARPE Region C *(Eastern South Pacific)*	1964–2005 (?)	-	-	-	-	-	-	-	X
13	pe-30104	IMARPE Callao *(Eastern South Pacific)*	2001–present	-	-	X	X	X	-	-	-

Australian Continuous Plankton Recorder Sites

Country: Australia

Site name (IGMETS-ID):

AusCPR BRSY Line - North (au-40201)
AusCPR BRSY Line – South (au-40202)
AusCPR SYME Line – South (au-40204)
AusCPR MEAD Line (au-40205)

Anthony Richardson, Claire Davies, Frank Coman, Ruth Eriksen, Felicity McEnnulty, Anita Slotwinski, Mark Tonks, and Julian Uribe-Palomino

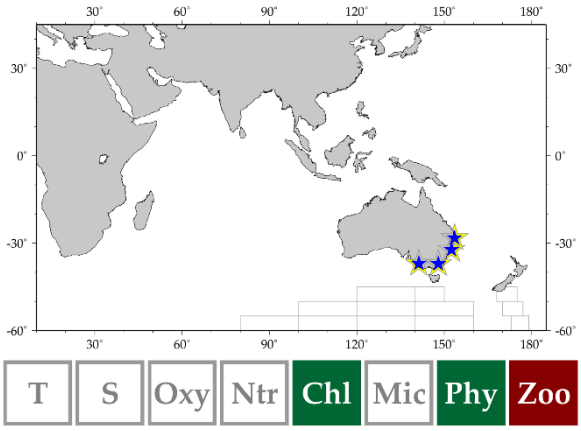

The AusCPR Survey is a joint project of CSIRO Oceans and Atmosphere and the Australian Antarctic Division (AAD) to measure plankton communities as a guide to the health of Australia's oceans. The survey is part of the Integrated Marine Observing System (IMOS), a national collaborative programme to observe Australia's marine environments. The aims of the survey are to:

- map plankton biodiversity and distribution
- develop the first long-term plankton baseline for Australian waters
- document plankton changes in response to climate change
- provide indices for fisheries management
- detect harmful algal blooms
- validate satellite remote sensing
- initialize and test ecosystem models

The survey has sampled throughout Australia, but concentrates on the East Australian Current, the Great Australian Bite, and the Great Barrier Reef. The dataset is freely available through the AODN (https://portal.aodn.org.au/) and provides researchers and policy makers with environmental and climatic indicators on harmful algal blooms, eutrophication, pollution, climate change, and fisheries.

Related information: http://imos.org.au/auscontinuousplanktonrecorder.html
https://portal.aodn.org.au

Integrated Marine Observing System's (IMOS): IMOS National Reference Station – Port Hacking

Country: Australia

IGMETS-ID: au-50101

Anthony J. Richardson, Frank Coman, Claire Davies, Ruth Eriksen, Felicity McEnnulty, Anita Slotwinski, Mark Tonks, and Julian Uribe-Palomino

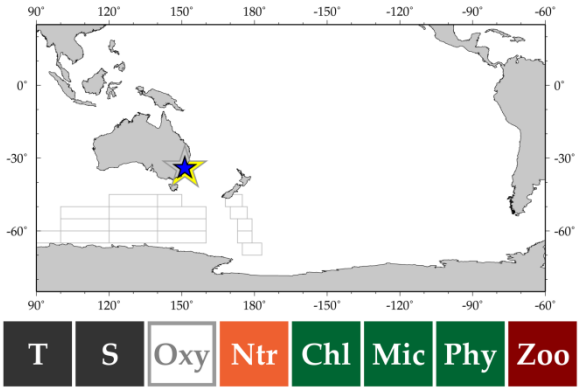

Port Hacking (34°12'S 151°23'E) is one of seven National Reference Stations that comprise IMOS. The NRSs are designed to provide regular baseline information to understand how large-scale, long-term change and variability in the global ocean are affecting Australia's coastal ecosystems. The goal is to develop multidecadal time series of the physical and biogeochemical properties of Australia's coastal seas, informing research into ocean change, climate variability, ocean circulation, and ecosystem responses. The Port Hacking NRS is sited on an historical mooring operating since 1953 looking at the East Australian Current and its movement away from the coast. This dataset contains seasonal data on zooplankton biomass and species composition collected since 2002 using a 100-µm mesh dropnet deployed to 100 m. The corresponding biogeochemical datasets from February 2009 including temperature, salinity, nutrients, chlorophyll, and phytoplankton abundance are available through the AODN portal https://portal.aodn.org.au/.

Related information: http://imos.org.au/anmnnrs.html

Integrated Marine Observing System's (IMOS): IMOS National Reference Station – Maria Island

Country: Australia

IGMETS-ID: au-50105

Anthony J. Richardson, Frank Coman, Claire Davies, Ruth Eriksen, Felicity McEnnulty, Anita Slotwinski, Mark Tonks, and Julian Uribe-Palomino

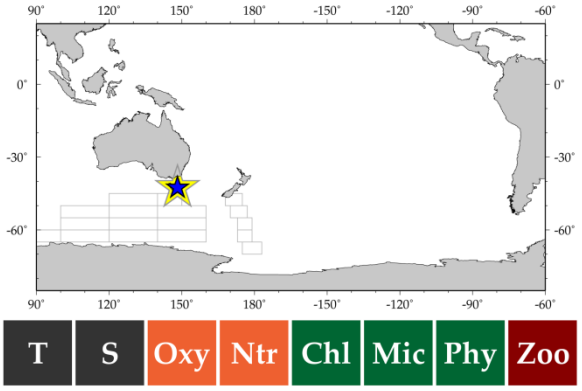

Maria Island (42°60'S 148°23'E) is one of seven National Reference Stations that comprise IMOS. The NRSs are designed to provide regular baseline information to understand how large-scale, long-term change and variability in the global ocean are affecting Australia's coastal ecosystems. The goal is to develop multidecadal time series of the physical and biogeochemical properties of Australia's coastal seas, informing research into ocean change, climate variability, ocean circulation, and ecosystem responses. The Maria Island NRS is sited at an historical mooring operating since 1944 where ocean temperatures are rising faster than anywhere else in Australia due to the increasing incursion of the East Australian Current. This dataset contains seasonal data on zooplankton biomass and species composition collected since April 2009 using a 100-µm mesh dropnet deployed to 80 m. The corresponding biogeochemical datasets including temperature, salinity, nutrients, chlorophyll, and phytoplankton abundance are available through the AODN portal https://portal.aodn.org.au/.

Related information: http://imos.org.au/anmnnrs.html

Integrated Marine Observing System's (IMOS): IMOS National Reference Station – North Stradbroke Island

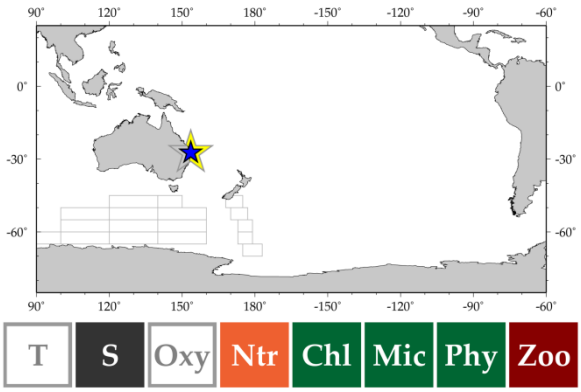

Country: Australia

IGMETS-ID: au-50107

Anthony J. Richardson, Frank Coman, Claire Davies, Ruth Eriksen, Felicity McEnnulty, Anita Slotwinski, Mark Tonks, and Julian Uribe-Palomino

North Stradbroke Island (27°35'S 153°56'E) is one of seven National Reference Stations that comprise IMOS. The NRSs are designed to provide regular baseline information to understand how large-scale, long-term change and variability in the global ocean are affecting Australia's coastal ecosystems. The goal is to develop multidecadal time series of the physical and biogeochemical properties of Australia's coastal seas, informing research into ocean change, climate variability, ocean circulation, and ecosystem responses. The North Stradbroke Island NRS is well placed for measuring the effects of the East Australian Current as it is located where the Current is strongest and most coherent. This dataset contains seasonal data on zooplankton biomass and species composition collected since September 2008 using a 100-µm mesh dropnet deployed to 60 m. The corresponding biogeochemical datasets including temperature, salinity, nutrients, chlorophyll, and phytoplankton abundance are available through the AODN portal https://portal.aodn.org.au/.

Related information: http://imos.org.au/anmnnrs.html

Integrated Marine Observing System's (IMOS): IMOS National Reference Station – Yongala

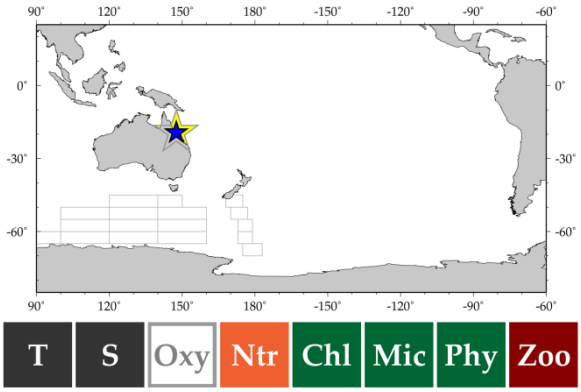

Country: Australia

IGMETS-ID: au-50109

Anthony J. Richardson, Frank Coman, Claire Davies, Ruth Eriksen, Felicity McEnnulty, Anita Slotwinski, Mark Tonks, and Julian Uribe-Palomino

Yongala (19°31'S 147°62'E) is one of seven National Reference Stations that comprise the Australian Integrated Marine Observing System's (IMOS). The NRSs are designed to provide regular baseline information to understand how large-scale, long-term change and variability in the global ocean are affecting Australia's coastal ecosystems. The goal is to develop multidecadal time series of the physical and biogeochemical properties of Australia's coastal seas, informing research into ocean change, climate variability, ocean circulation, and ecosystem responses. The Yongala NRS is situated in the lagoon of the central Great Barrier Reef, where there are concerns about the impacts of eutrophication. This dataset contains seasonal data on zooplankton biomass and species composition collected since September 2009 using a 100-µm mesh dropnet deployed to 26 m. The corresponding biogeochemical datasets including temperature, salinity, nutrients, chlorophyll, and phytoplankton abundance are available through the AODN portal https://portal.aodn.org.au/.

Related information: http://imos.org.au/anmnnrs.html

Concepción Station 18

Bay of Mejillones

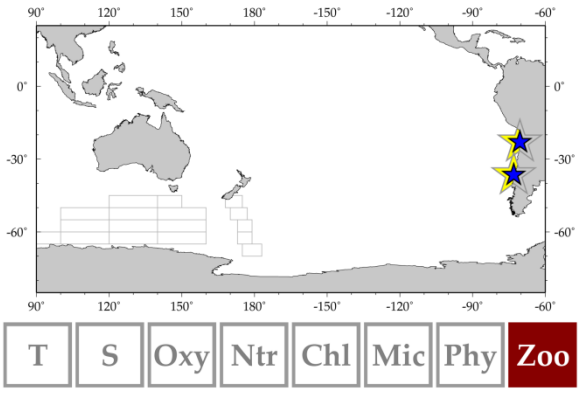

Country: Chile

IGMETS-ID: cl-30101, cl-30102

Ruben Escribano

In August 2002 in the central/southern region of Chile, the COPAS oceanographic centre initiated a time-series study at Station 18 on the continental shelf (ca. 90 m depth) of Concepción. Zooplankton are sampled on a nearly monthly basis using a 1-m² Tucker trawl equipped with 200-µm mesh nets. The net has a calibrated flowmeter to estimate the volume sampled. Oblique tows are made from 80 m to the surface between 12 pm and 4 pm (daylight hours). The net collects integrated samples from 0 to 80 m and also stratified samples from 80 to 50 m and 50 to 0 m. In 1988, a time series of zooplankton was initiated at Antofagasta in the Bay of Mejillones. Prior to 2010, this site was only sampled twice a year (summer and winter). Since 2010, nearly monthly sampling has been done at the site. Samples were obtained with a 200-µm WP-2 net towed from between 50 m and 20 m to the surface. Water volume filtered was estimated from the depth of deployment. All sampling was performed during daylight hours.

Related information: http://copas.udec.cl/eng/research/serie/
http://copas.udec.cl/eng/

Instituto del Mar del Perú (IMARPE) Time Series

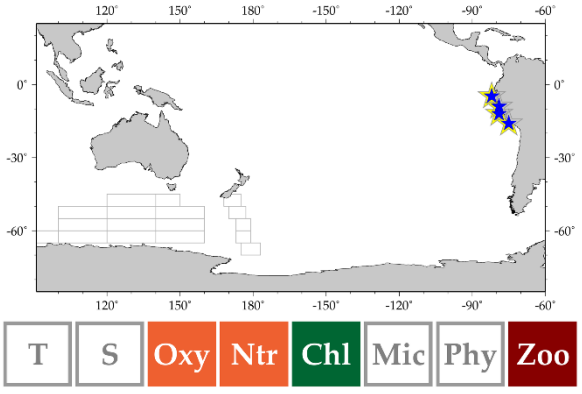

Country: Peru

Site name (IGMETS-ID):

IMARPE Region A (pe-30101),
IMARPE Region B (pe-30102)
IMARPE Region C (pe-30103)

Patricia Ayon

IMARPE has always focused on fisheries. Zooplankton samples were a byproduct of ichthyoplankton sampling, which was conducted on all pelagic, demersal, or hydrographic surveys. Between 1961 and 2006, 150 surveys were carried out, with > 10 000 samples collected. Surveys covered up to 500 km from the coast between 3°30′ and 18°20′S, although over 95% of the samples were collected within 100 km of the coastline. Two types of standard surveys for zooplankton sampling have evolved with time. The first type is the Hensen Net Program in which zooplankton data have been collected since 1964 on pelagic fish, demersal fish, and oceanographic surveys, where a Hensen net (330-µm mesh, 60 cm diameter) has been towed vertically from 50 m to the surface. The stations are located on a predefined meander-shaped cruise track covering the whole coastal area of Peru, although the cruise track was sometimes modified. Zooplankton samples were only taken at stations where echograms indicated fish were present and fish trawling should also be conducted. Since 1996, additional zooplankton sampling has been conducted where distance between trawl positions was >20 nautical miles. The second type is the Fixed Coastal Stations Program on transects perpendicular to the coast near Paita, San José, and Callao, with horizontal surface tows taken since 1994 with a WP2 net. Additionally, since 2004, oblique bongo net tows (60-cm diameter, 300-µm mesh size) have been included.

A7 North Pacific Ocean

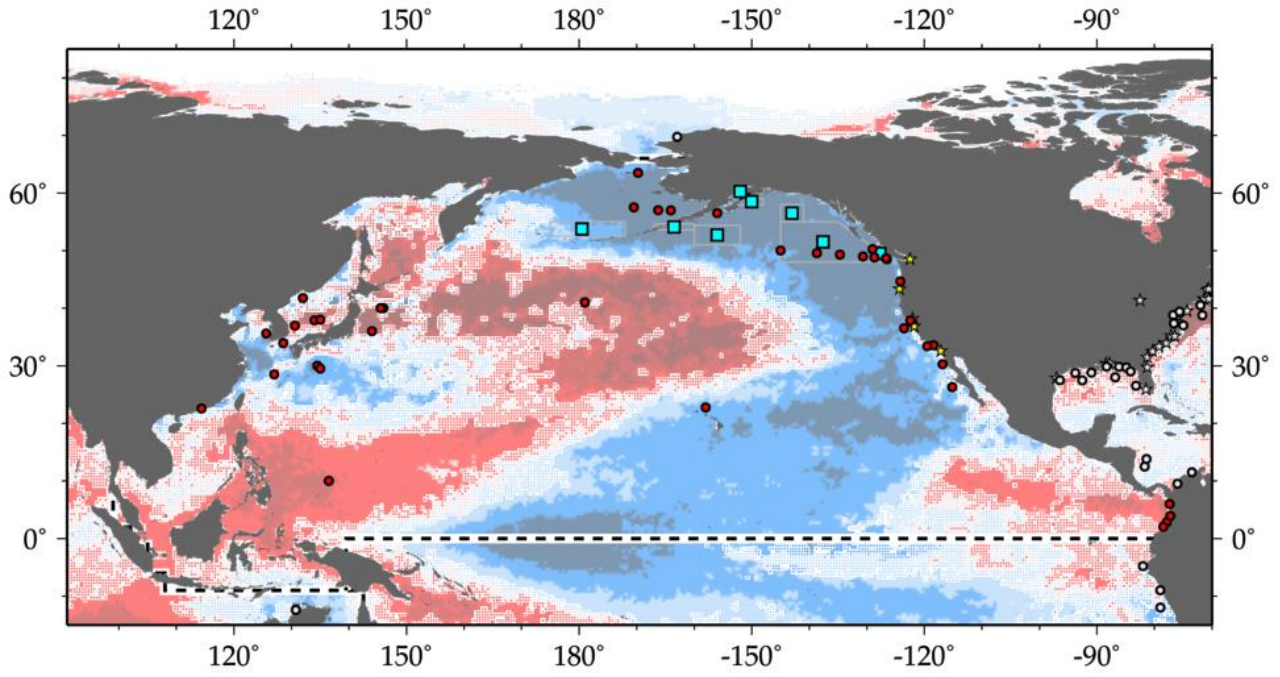

Figure A7. Map of IGMETS-participating North Pacific time series on a background of a 10-year time-window (2003–2012) sea surface temperature trends (see also Chapter 8). At the time of this report, the North Pacific collection consisted of 54 time series (coloured symbols of any type), of which eight were from Continuous Plankton Recorder subareas (blue boxes), and six were from estuarine areas (yellow stars). Dashed lines indicate boundaries between IGMETS regions. Uncoloured (gray) symbols indicate time series being addressed in a different regional chapter (e.g. Arctic Ocean, South Pacific).

Table A7. Time-series sites located in the IGMETS North Pacific region. Participating countries: Canada (ca), Colombia (co), China – Hong Kong (hk), Japan, (jp), Republic of Korea (kr), Mexico (mx), United Kingdom (uk), and United States (us). Year-spans in red text indicate time series of unknown or discontinued status. IGMETS-IDs in red text indicate time series without a description entry in this Annex.

No.	IGMETS-ID	Site or programme name	Year-span	T	S	Oxy	Ntr	Chl	Mic	Phy	Zoo
1	ca-50301	Northern Vancouver Island – Offshore *(Canadian Pacific Coast)*	1983–present	-	-	-	-	-	-	-	X
2	ca-50302	Southern Vancouver Island – Offshore *(Canadian Pacific Coast)*	1979–present	-	-	-	-	-	-	-	X
3	ca-50901	Line P – P26 – OWS Papa *(Northeast North Pacific)*	1956–present	X	X	X	X	X	-	-	X
4	ca-50902	Line P – P20 *(Northeast North Pacific)*	1968–present	X	X	X	X	X	-	-	X
5	ca-50903	Line P – P16 *(Northeast North Pacific)*	1968–present	X	X	X	X	X	-	-	X
6	ca-50904	Line P – P12 *(Northeast North Pacific)*	1968–present	X	X	X	X	X	-	-	X
7	ca-50905	Line P – P08 *(Northeast North Pacific)*	1968–present	X	X	X	X	X	-	-	X
8	ca-50906	Line P – P04 *(Northeast North Pacific)*	1968–present	X	X	X	X	X	-	-	X
9	co-30110	REDCAM Department of Cauca *(Colombia Coastline)*	2002–present	X	X	X	-	-	-	-	-
10	co-30111	REDCAM Department of Choco *(Colombia Coastline)*	2002–present	X	X	X	-	-	-	-	-
11	co-30112	REDCAM Department of Narino *(Colombia Coastline)*	2002–present	X	X	X	-	-	-	-	-
12	co-30113	REDCAM Department of Valle del Cauca *(Colombia Coastline)*	2002–present	X	X	X	-	-	-	-	-
13	hk-30101	Hong Kong EPD Marine Water Quality Monitoring *(Hong Kong)*	1991–present	X	X	X	X	X	-	X	-
14	jp-30104	PM Line *(Japan Sea)*	1972–2002 (?)	-	-	-	-	-	-	-	X
15	jp-30101	Kuroshio Current *(Western North Pacific)*	1951–2002 (?)	X	-	-	-	-	-	-	X
16	jp-30102	Oyashio Current *(Western North Pacific)*	1951–2004 (?)	X	-	-	-	-	-	-	X
17	jp-30103	Oyashio–Kuroshio Transition *(Western North Pacific)*	1951–2004 (?)	X	-	-	-	-	-	-	X
18	jp-30201	Bering Sea – HUFO *(Bering Sea)*	1955–2006 (?)	-	-	-	-	-	-	-	X
19	jp-30202	Central North Pacific – HUFO *(North Pacific)*	1979–2000 (?)	-	-	-	-	-	-	-	X

No.	IGMETS-ID	Site or programme name	Year-span	T	S	Oxy	Ntr	Chl	Mic	Phy	Zoo
20	jp-30401	JMA East China Sea *(East China Sea)*	1965–present	X	X	X	X	-	-	-	-
21	jp-30402	JMA Japan Sea *(Japan Sea)*	1964–present	X	X	X	X	X	-	-	-
22	jp-30403	JMA Philippine Sea *(Philippine Sea)*	1965–present	X	X	X	X	X	-	-	-
23	jp-30404	JMA Southeast Hokkaido *(Northwest North Pacific)*	1965–present	X	X	X	X	X	-	-	-
24	jp-30405	JMA 137E Transect *(Lower Philippine Sea)*	1970–present	X	X	X	X	-	-	-	-
25	kr-30103	Korea East *(Japan Sea)*	1965–2006 (?)	-	-	-	-	-	-	-	X
26	kr-30104	Northeast Korea – Russian Sampling *(Japan Sea)*	1988–2007 (?)	-	-	-	-	-	-	-	X
27	kr-30102	Korea South *(East China Sea)*	1965–2006 (?)	-	-	-	-	-	-	-	X
28	kr-30101	Korea West *(Yellow Sea)*	1965–2006 (?)	-	-	-	-	-	-	-	X
29	mx-30101	IMECOCAL Northern Baja – NB *(Southeastern North Pacific)*	1998–present	-	-	-	-	-	-	-	X
30	mx-30102	IMECOCAL Southern Baja – SB *(Southeastern North Pacific)*	1998–present	-	-	-	-	-	-	-	X
31	uk-40201	Pacific CPR – Southern Bering Sea *(Northeastern North Pacific)*	2000–present	-	-	-	-	X	-	X	X
32	uk-40202	Pacific CPR – Aleutian Shelf *(Northeastern North Pacific)*	2000–present	-	-	-	-	X	-	X	X
33	uk-40203	Pacific CPR – Western Gulf of Alaska *(Northeastern North Pacific)*	2000–present	-	-	-	-	X	-	X	X
34	uk-40204	Pacific CPR – Alaskan Shelf *(Northeastern North Pacific)*	2004–present	-	-	-	-	X	-	X	X
35	uk-40205	Pacific CPR – Cook Inlet *(Northeastern North Pacific)*	2004–present	-	-	-	-	X	-	X	X
36	uk-40206	Pacific CPR – Northern Gulf of Alaska *(Northeastern North Pacific)*	1997–present	-	-	-	-	X	-	X	X
37	uk-40207	Pacific CPR – Offshore BC *(Northeastern North Pacific)*	1997–present	-	-	-	-	X	-	X	X
38	uk-40208	Pacific CPR – BC Shelf *(Northeastern North Pacific)*	2000–present	-	-	-	-	X	-	X	X
39	us-10201	Hawaii Ocean Time series – HOT *(Central North Pacific)*	1988–present	X	X	X	X	X	X	-	X

No.	IGMETS-ID	Site or programme name	Year-span	T	S	Oxy	Ntr	Chl	Mic	Phy	Zoo
40	us-10301	USC WIES San Pedro Ocean Time series – SPOT *(Eastern North Pacific)*	2000–present	X	X	X	X	X	-	-	-
41	us-30401	Central Bay *(San Francisco Bay)*	1978–present	X	X	X	X	X	X	X	-
42	us-50301	CalCOFI California Current region – CC *(California Current)*	1951–present	-	-	-	-	-	-	-	X
43	us-50302	CalCOFI Southern California region – SC *(Southern California Current)*	1951–present	-	-	-	-	-	-	-	X
44	us-50401	Western Kodiak Island – EcoFOCI *(Gulf of Alaska)*	1981–present	-	-	-	-	-	-	-	X
45	us-50501	Newport Line NH-5 *(Newport-Oregon)*	1969–present	X	X	-	X	X	-	-	X
46	us-50601	EMA-1: Eastern Bering Sea – East *(Southeastern Bering Shelf)*	1999–present	X	X	X	X	X	-	-	X
47	us-50602	EMA-2: Eastern Bering Sea – West *(Southwestern Bering Shelf)*	2002–present	X	X	X	X	X	-	-	X
48	us-50603	EMA-3: Northern Bering Sea *(Northern Bering Sea)*	2002–present	X	X	X	X	X	-	-	X
49	us-60106	NERRS Elkhorn Slough *(Northeastern North Pacific)*	2001–present	X	X	X	X	X	-	-	-
50	us-60113	NERRS Kachemak Bay *(Northeastern North Pacific)*	2003–present	X	X	X	X	X	-	-	-
51	us-60120	NERRS Padilla Bay *(Northeastern North Pacific)*	2009–present	X	X	X	X	X	-	-	-
52	us-60123	NERRS San Francisco Bay *(Northeastern North Pacific)*	2008–present	X	X	X	X	X	-	-	-
53	us-60124	NERRS South Slough *(Northeastern North Pacific)*	2002–present	X	X	X	X	X	-	-	-
54	us-60125	NERRS Tijuana River *(Northeastern North Pacific)*	2004–present	X	X	X	X	X	-	-	-

Vancouver Island Time Series

Country: Canada

Site name (IGMETS-ID):

Northern Vancouver Island (ca-50301)
Southern Vancouver Island (ca-50302)

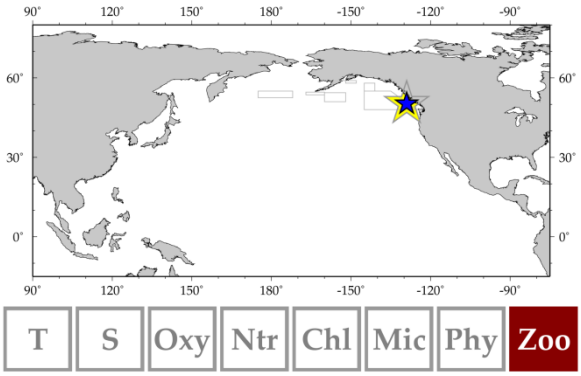

Ian Perry, Moira Galbraith, Dave Mackas, and Doug Yelland

The La Perouse Zooplankton Monitoring Program started in 1979 by sampling the southern continental shelf and shelf break west of Vancouver Island, British Columbia, Canada (Mackas *et al*., 2001, 2006, 2007). In 1990, this survey was expanded to include off northern Vancouver Island, but with low sampling intensity and taxonomic resolution in 1991–1995 (Mackas *et al*., 2004, 2006). This programme began with four surveys a year (spring, summer, autumn, winter) to understand regional seasonality, but recently has decreased to two surveys a year (May and September). Sampling gear and methods have remained consistent: a dual-net (bongo) sampler with black 236-μm mesh and TSK flowmeter hauled vertically 10 m off the bottom on the shelf or a maximum of 250 m on the slope and offshore areas. One side is used for size fractionated biomass and the other for taxonomic identifications, including life stage. A CTD and/or Rosette profile is also done at each station where a zooplankton tow is taken. The areas being covered under the La Perouse Program have expanded to include survey lines along the entire west coast of Vancouver Island and into the Strait of Georgia. Additional sampling is undertaken by other DFO surveys to this region to survey other seasons. Zooplankton and ichthyoplankton data are archived in the IOS Zooplankton Database.

Data from each sampling period are spatially averaged within each region (geometric mean), and sample-number-weighted averages of the survey means are used to calculate average seasonal cycles = climatologies (to 2005) for each region. Within-region and within-time-period anomalies are calculated as log(observation/climatology), and these are then averaged within year (and sometimes across groups of taxa and across adjoining spatial regions) to give the time series of annual anomalies. For information or access to these data, contact Ian Perry (general enquiries), Moira Galbraith (plankton data), or Doug Yelland (hydrographic data).

Ocean Station Papa and Line P

Country: Canada

IGMETS-ID: ca-50901 – ca-50906

Marie Robert, Moira Galbraith, Andrew Ross, Ian Perry, and Dave Mackas

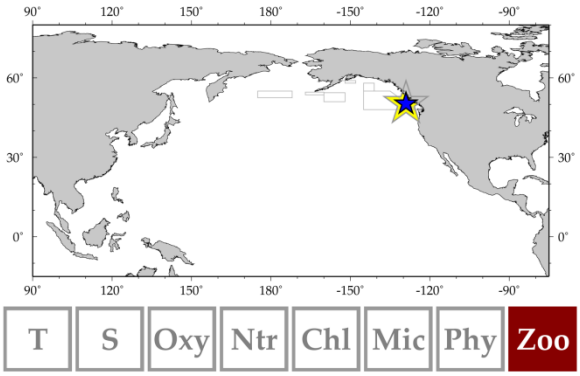

Line P is a long standing programme which surveys a 1400-km long section west of Vancouver Island, Canada, three times a year. It is composed of 27 stations spread from the mouth of Juan de Fuca Strait (P1 at 48°35'N 125°30'W) to Ocean Station Papa (50°N 145°W). Of these 27 stations, seven are major stations (P2, P4, P8, P12, P16, P20, and P26) where a whole suite of properties are measured, including biogeochemical and ecological samples. At the other stations, CTD profiles collect physical and some chemical data via sensors. Ocean Station Papa is the site of a large array of moorings. Past years have seen moored sediment traps and the Canadian SOLAS moorings. Present moorings are serviced by various US agencies and universities. Data have been collected along this line since 1956 and show evidence of the impact of climate variability on ocean productivity. Although the main focus of the Line P Program is ocean monitoring, is it a fantastic basis for various research projects. Line P data can be accessed at www.waterproperties.ca/linep.

Zooplankton records collected on these surveys are archived in the IOS Zooplankton Database. Data start in 1956 and go to 1980 on a monthly basis for Station Papa: P26. Samples were taken using a NorPac or SCOR vertical net haul using 350-µm mesh from a depth of 150 m. Early samples (1956–1964) consisted of total biomass measurements. In 1965–1967, major taxonomic groups were enumerated: copepods, amphipods, euphausiids, chaetognaths, and medusae. During 1968–1980, more detailed identification of zooplankton began, but only for selected species. In 1987, bongo nets were introduced using black Nitex 236-µm mesh. This apparatus has paired 2.5-m socks with 0.5-m^2 mouth opening. One side was used for taxonomic identification of zooplankton and the other for size-fractionated biomass. Zooplankton sampling on the Line P Monitoring Program started in 1995; samples were taken from 150 m to the surface using the same methods described for 1987. In 2003, the maximum sampling depth was changed to 250 m so as to sample below the diel migrators of the open ocean.

Related information: http://www.waterproperties.ca/linep

REDCAM – Pacific Sites

Country: Colombia

Site name (IGMETS-ID):

REDCAM Department of Cauca (co-30110)
REDCAM Department of Choco (co-30111)
REDCAM Department of Narino (co-30112)
REDCAM Department of Valle del Cauca (co-30113)

see also REDCAM in North Atlantic (co-30101 to co-30104)

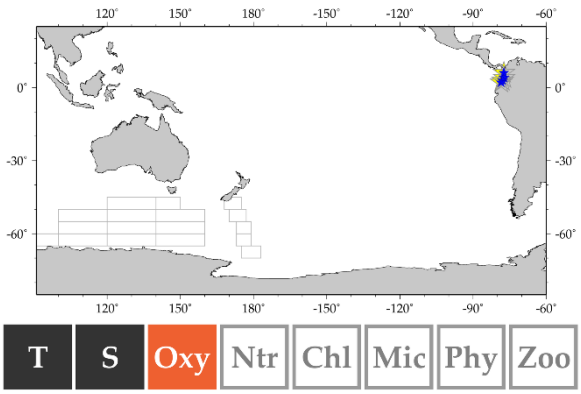

The Colombian Marine Environment Monitoring Network (REDCAM) was initiated in 2001 to group the institutions and the efforts necessary to evaluate the chemical and sanitary quality of the marine and estuarine waters of Colombia. It is composed of 16 nodes and a main server located at INVEMAR (Santa Marta). Each node includes hardware and software for input and retrieval tables and cartographic information about the quality of marine and coastal waters of Colombia. It was established as a network of field stations that covers most of the Colombian coasts. Since 2001 and twice a year at each node, it has been registering the values of the main physicochemical and bacteriological variables that characterize the quality of the marine and estuarine waters. Based on this information, the following zones have been identified as critical for its marine and coastal pollution: Santa Marta, Cartagena, Barranquilla, Morrosquillo, Uraba, and San Andres at the Caribbean coast and Buenaventura, Guapi, and La Tola at the Pacific coast.

Hong Kong EPD Marine Water Quality Monitoring – Pearl River (Hong Kong)

Country: China (Hong Kong)

IGMETS-ID: hk-30101

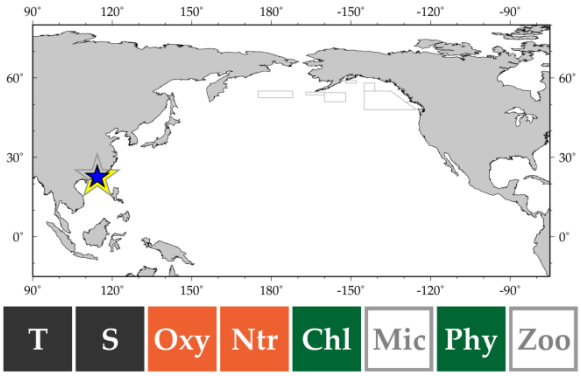

The Environmental Protection Department (EPD) of the Hong Kong SAR Government monitors the water quality of some 1700 km² of the territory's marine waters. The purpose of this programme is to (i) indicate the state of health of marine waters; (ii) assess compliance with the statutory Water Quality Objectives (WQOs); (iii) reveal long-term changes in water quality; and (iv) provide a basis for the planning of pollution control strategies.

The Hong Kong waters are divided into ten Water Control Zones (WCZs). A range of physical and chemical parameters, including temperature, pH, salinity, turbidity, and dissolved oxygen, are measured *in situ* by a CTD. In addition, water and sediment samples are collected and sent to the laboratories for the analysis of some 40 parameters, such as nutrients, metals, organics, and coliform bacteria. Water-quality monitoring is generally conducted once a month, whereas sediment quality monitoring is done twice a year.

Related information: http://wqrc.epd.gov.hk/en/overview/index.aspx

Japanese Meteorological Agency oceanographic monitoring

Country: Japan

Site name (IGMETS-ID):

JMA East China Sea (jp-30401)
JMA Japan Sea (jp-30402)
JMA Philippine Sea (jp-30403)
JMA Southeast Hokkaido (jp-30404)
JMA 137E Transect (jp-30405)

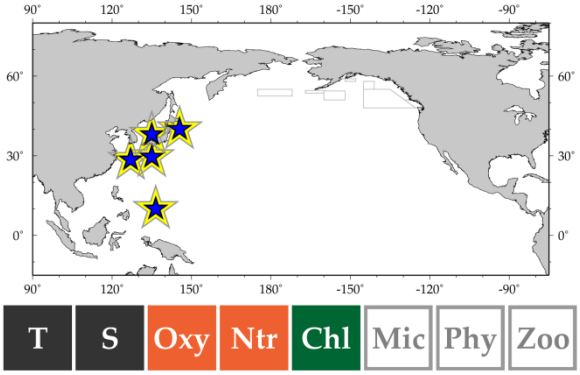

Toshiya Nakano and Masao Ishii

Section 137 E in the western North Pacific was established in 1967 by J. Masuzawa and his colleagues at the Japan Meteorological Agency. This section encompasses the coastal zone of Japan, Kuroshio Recirculation Gyre and North Equatorial Current zone in the subtropics, North Equatorial Countercurrent, and the tropical warm pool near Indonesia. The longest time series involves temperature, salinity, oxygen, nutrients, and DIC (1994–) in the water column and underway, and pCO_2 in surface seawater (1983–) and in the atmosphere. Recently, they have been sampled seasonally or biannually at station intervals of 1° latitude for CTDO2 and 1–5° for biogeochemical variables. This high-frequency section aims to understand the trend of ocean warming, salinity change (freshening), ocean circulation change, deoxygenation, anthropogenic CO_2 storage and acidification, air–sea CO_2 flux, and so on that are associated with climate variability/change and anthropogenic CO_2 emission.

Related information: http://www.data.jma.go.jp/gmd/kaiyou/db/vessel_obs/data-report/html/ship/ship_e.php

Baja California Zooplankton Time Series

Country: Mexico

Site name (IGMETS-ID):

Northern Baja California Zooplankton Time Series (mx-30101)
Southern Baja California Zooplankton Time Series (mx-30102)

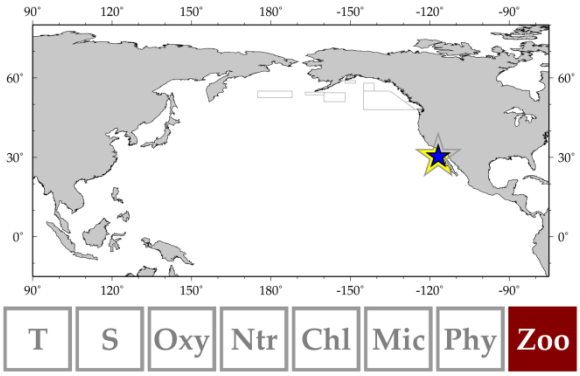

Bertha E. Lavaniegos

The Baja California Zooplankton Time Series are derived from biological material collected by IMECOCAL cruises since September 1997 in the subtropical sector of the California Current. The aim is to provide data of biomass and abundance by functional groups and species in order to understand the composition of and changes in the zooplankton component at different temporal scales. The California Current is an eastern boundary upwelling ecosystem. Subarctic water upstream presents low temperature and salinity, with both increasing downstream. From late summer to early winter, a major influence of subtropical oceanic water is observed associated with branching of the California Current off northern Baja California, with a return flow (poleward) along the coast, weakening the rest of the current that continues equatorward. During the spring transition, the California Current is renewed, and strong winds enhance coastal upwelling. The coastal shelf is narrow, except for Vizcaino Bay and the Gulf of Ulloa. The topography, winds, and circulation determine strong onshore–offshore differences in zooplankton communities and, to a lesser extent, from north to south.

A summary of the zooplankton time series for the period 1997-2013 is offered by Lavaniegos et al. (2015).

Related information: http://imecocal.cicese.mx/

Pacific Continuous Plankton Recorder survey

Country: Multiple countries

Site name (IGMETS-ID):

Southern Bering Sea (uk-40201)
Aleutian Shelf (uk-40202)
Western Gulf of Alaska (uk-40203)
Alaskan Shelf (uk-40204)
Cook Inlet (uk-40205)
Northern Gulf of Alaska (uk-40206)
Offshore BC (Oceanic Northeast Pacific between 48 and 55°N) (uk-40207)
BC Shelf (uk-40208)

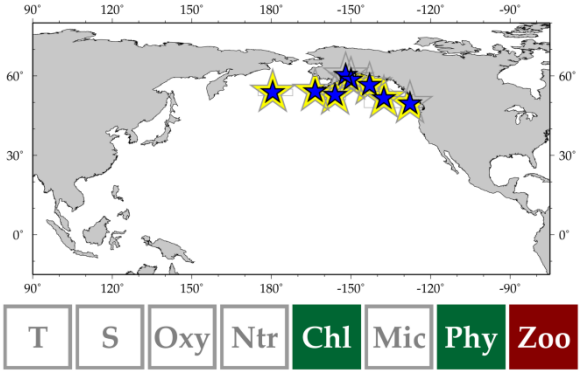

Sonia Batten

Continuous Plankton Recorders (CPR) were first deployed in the North Pacific in 2000. The purpose of the programme is to provide taxonomically resolved data on lower-trophic-level abundance and distribution. Seasonal resolution is also possible since transects are sampled multiple times a year between spring and autumn. This enables interannual variability to be determined and the influence of ocean climate on marine productivity to be assessed. The CPR is towed behind merchant ships at about 7 m depth on their regular routes. It samples continuously, although the transect is divided into discrete 10-nautical-mile samples during processing. Samples are examined microscopically to identify and enumerate plankton. While all data are available on request, data here have been binned into distinct oceanographically meaningful regions (such as shelf distinct from offshore), which incorporate the extent and variability of the ships' transect positions between tows.

Related information: http://www.pices.int/projects/tcprsotnp/main.aspx

Hawaii Ocean Time Series (HOT)

Country: United States

IGMETS-ID: us-10201

Matthew J. Church, David M. Karl, Roger Lukas, Robert Bidigare, John E. Dore, Ricardo M. Letelier, Michael Landry, Robert Weller, and Al Pleudemann

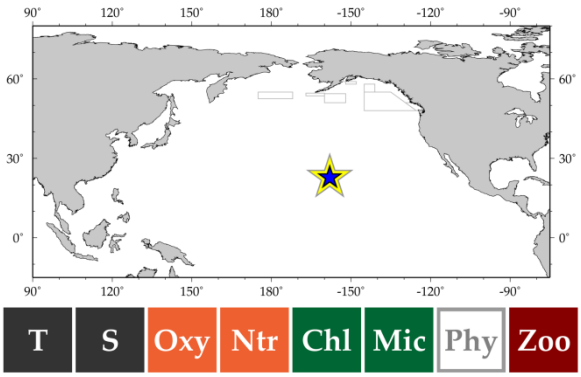

Since 1988, the Hawaii Ocean Time Series (HOT) programme has conducted near-monthly research cruises to the open-ocean field site Station ALOHA (22°75'N 158°W) to examine time variability in biogeochemical and physical processes in the North Pacific Subtropical Gyre (NPSG). The resulting measurements provide information on interactions between ocean climate and ecosystem variability in the NPSG and quantify time-variability in reservoirs and fluxes of carbon (C) and associated bioelements (nitrogen, oxygen, phosphorus, and silicon). HOT programme measurements are enabling quantification of long-term trends in upper-ocean carbonate system properties (including pH and dissolved inorganic carbon) and highlighting key biological and physical processes mediating air–sea carbon exchange in this ecosystem (Karl and Church, 2014). Despite a persistently oligotrophic upper ocean, HOT programme measurements indicate net community productivity ranges between ca. 1.5 and 4 mol C m^{-2} $year^{-1}$. Moreover, the carbon cycle appears sensitive to variability in ocean climate, including regional-scale changes in evaporation and precipitation.

Related information: http://hahana.soest.hawaii.edu/hot/

USC WIES San Pedro Ocean Time Series (SPOT)

Country: United States

IGMETS-ID: us-10301

Roberta Marinelli, David Caron, Jed Fuhrman, Troy Gunderson, and Diane Kim

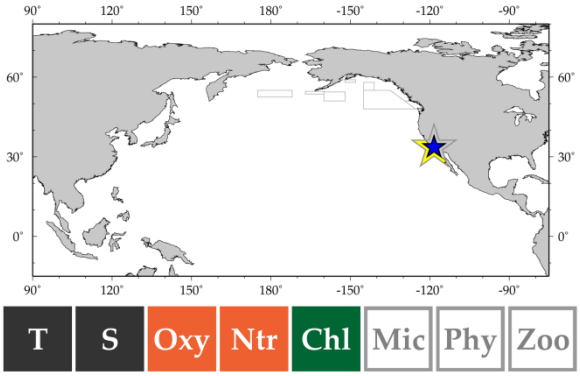

The San Pedro Ocean Time Series (SPOT) was established in 1998 by the USC Wrigley Institute for Environmental Studies to study basic oceanographic processes at a near-coastal site in the Southern California Bight. Near Los Angeles, CA, the SPOT station (33°33′N 118°24′W) provides a unique vantage point to study human impacts on the ocean environment. Biogeochemical and physical water-column properties measured monthly by ship demonstrate low surface chlorophyll *a* concentrations (< 2 μg L^{-1}) year-round. Relatively shallow mixing in winter (mixed layer depth maximum of ca. 50 m) stimulates slight increases in chlorophyll *a* concentrations in spring. Depth of the deep chlorophyll *a* maximum varies seasonally (< 20–60 m), and the site is persistently hypoxic (< 1 ml L^{-1}) below ca. 300 m to the bottom of the San Pedro Basin (ca. 890 m). In September 2000, the NSF USC Microbial Observatory (now Dimensions of Biodiversity) began complementing SPOT collections with microbiological (archaea, bacteria, microbial eukaryotes) and virus data.

Related information: http://dornsife.usc.edu/spot/

California Cooperative Oceanic Fisheries Investigations (CalCOFI)

Country: United States

Site name (IGMETS-ID):

CalCOFI California Current region (us-50301)
CalCOFI Southern California region (us-50302)

Sam McClatchi, Edward Weber, Ralf Goericke, and Mark Ohman

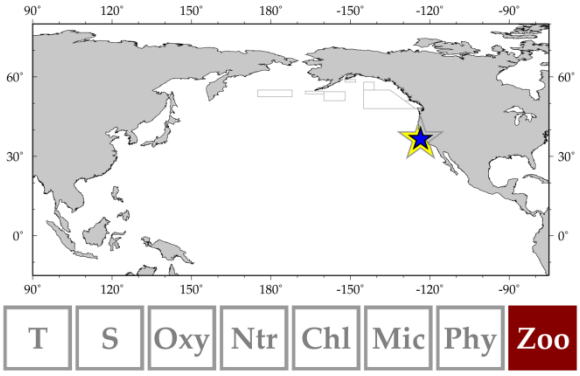

The California Cooperative Oceanic Fisheries Investigations (CalCOFI) programme is a joint research effort by the US National Oceanic and Atmospheric Administration Southwest Fisheries Science Center, University of California Scripps Institution of Oceanography, and California Department of Fish and Wildlife. Joint fisheries and oceanography surveys have been conducted regularly by the CalCOFI programme since 1951 and are currently conducted quarterly.

Vertical, oblique, and surface tows are collected routinely on CalCOFI cruises. Several important changes have occurred in sampling methods for collecting icthyoplankton. In 1969, tow depths were extended from 140 to 210 m, and nets were changed from 0.55-mm mesh silk to 0.505-mm mesh nylon. In 1977, oblique tows were changed from using 1-m bridled ringnets (denoted C1 in the data) to 0.71-m bridleless bongo nets (denoted CB). See Hewitt (1980), Brinton and Townsend (1981), and Ohman and Smith (1995) for details.

Related information: http://www.calcofi.org/
http://coastwatch.pfeg.noaa.gov/erddap/search/index.html?page=1&itemsPerPage=1000&searchFor=calcofi

Western Kodiak Island (Western Gulf of Alaska) – EcoFOCI

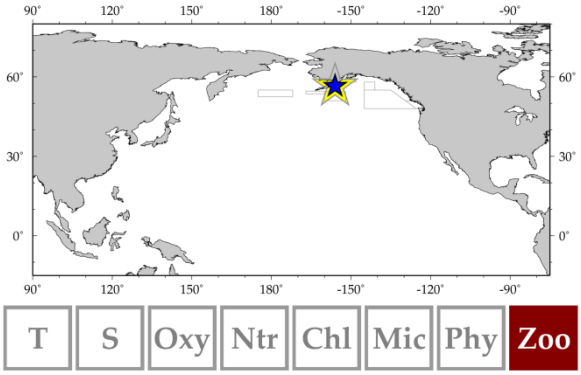

Country: United States

IGMETS-ID: us-50401

Janet Duffy-Anderson

Ecosystems and Fisheries Oceanography Coordinated Investigations (EcoFOCI) is a joint research programme between the Alaska Fisheries Science Center (NOAA/NMFS/AFSC) and the Pacific Marine Environmental Laboratory (NOAA/OAR/PMEL). FOCI was established by NOAA in 1984 to study the variability in recruitment success of commercially valuable finfish and shellfish in Alaskan waters. The project initially studied walleye pollock (*Gadus chalcogrammus*) in the western Gulf of Alaska. From FOCI to EcoFOCI, the programme has broadened to ecosystems research in the North Pacific and Alaskan waters, drawing on multiple scientific disciplines, and matching NOAA scientists with academia as part of NOAA's Cooperative Institute partnership.

The goal of our ecosystems research is to determine the influence of physical and biological environments on marine populations and their subsequent impact on fisheries. We work towards understanding ecosystem dynamics, applying that understanding to fisheries resource management, and analyzing observations in the context of climate and ocean changes. EcoFOCI scientists integrate field, laboratory, and modeling studies and work on many time-scales (seasonal, annual, decadal, and longer). Our research regions include the Gulf of Alaska, the Aleutian Passes, the Bering Sea, and the Chukchi Sea.

Related information: http://www.ecofoci.noaa.gov/

Newport Hydrographic (NH) and Zooplankton Time Series

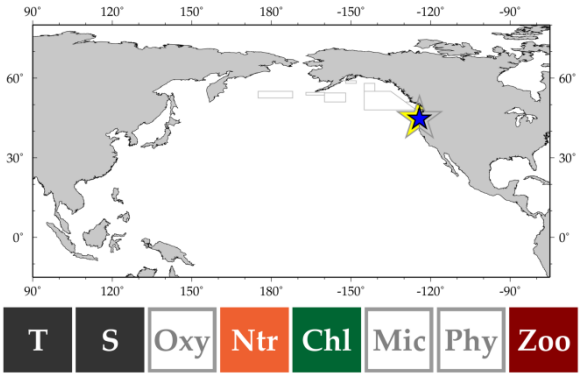

Country: United States

IGMETS-ID: us-50501

William T. Peterson, Jennifer L. Fisher, Cheryl A. Morgan, and Jay O. Peterson

The Newport Hydrographic (NH) and Zooplankton Time Series characterizes ocean conditions in the Northern California Current, which is a region of high productivity driven by seasonal coastal upwelling and large-scale ocean gyre circulation (Peterson *et al.*, 2014). Hydrographic and zooplankton data are collected at seven stations across the shelf 2–46 km from shore off Newport, Oregon (44°65'N). Biophysical data have been (and continue to be) collected biweekly–monthly since 1996. Zooplankton are sampled vertically from just above the bottom to the surface with a 0.5-m plankton net using a 202-µm mesh. Organisms are enumerated and expressed as carbon biomass (mg C m^{-3}) after appropriate conversions. Full water-column profiles of temperature, salinity, chlorophyll fluorescence, and oxygen are collected with a Seabird CTD. Surface water is analyzed for chlorophyll *a* concentration and nutrients.

Related information: www.nwfsc.noaa.gov/oceanconditions

National Estuarine Research Reserve System (NERRS)
System–wide Monitoring Program (SWMP)

Country: United States

Site name (IGMETS-ID): us-60101 - us-60126

Dwayne Porter (liason)

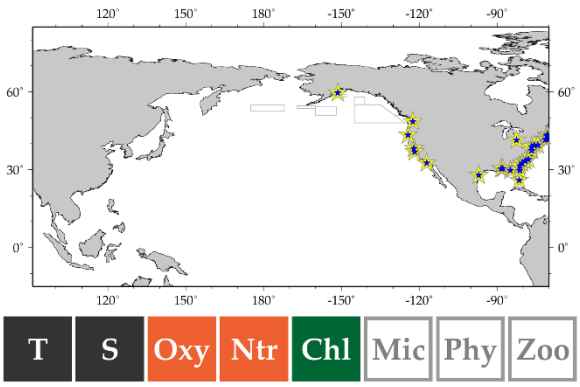

The National Estuarine Research Reserve System (NERRS) is a network of 28 coastal sites designated to protect and study estuarine systems. Established through the Coastal Zone Management Act, the reserves represent a partnership programme between the National Oceanic and Atmosphere Administration (NOAA) and the coastal states. NOAA provides funding and national guidance, and each site is managed on a daily basis by a lead state agency or university with input from local partners.

NERRS acknowledges the importance of both long-term environmental monitoring programmes and data and information dissemination through its support of the NERRS System-wide Monitoring Program (SWMP). The goal of SWMP is to identify and track short-term variability and long-term changes in the integrity and biodiversity of representative estuarine ecosystems and coastal watersheds for the purpose of contributing to effective national, regional, and site-specific coastal zone management. This comprehensive programme consists of three phased components: estuarine water quality monitoring, biodiversity monitoring, and land-use and habitat-change analysis.

The NERRS research reserves encompass 1.3 million acres of estuaries along the US coastlines.

Related information: https://coast.noaa.gov/nerrs/

A8 Annex References

Bagøien, E., Melle, W., and Kaartvedt, S. 2012. Seasonal development of mixed layer depths, nutrients, chlorophyll and *Calanus finmarchicus* in the Norwegian Sea – A basin-scale habitat comparison. Progress in Oceanography, 103: 58–79.

Bates, N. R., Astor, Y. M., Church, M. J., Currie, K., Dore, J. E., Gonzalez-Davila, M., Lorenzoni, L., *et al*. 2014. Changing ocean chemistry: A time-series view of ocean uptake of anthropogenic CO^2 and ocean acidification. Oceanography, 27(1): 121–141, http://dx.doi.org/10.5670/oceanog.2014.03.

Baranović, A., Šolić, M., and Krstulović, N. 1993. Temporal fluctuations of zooplankton and bacteria in the middle Adriatic Sea. Marine Ecology Progress Series, 92: 65–75.

Batten, S. D., Walne, A. W., Edwards, M., and Groom, S. B. 2003. Phytoplankton biomass from continuous plankton recorder data: an assessment of the phytoplankton colour index. Journal of Plankton Research, 25(7): 697–702.

Belin, C. 1998. French phytoplankton monitoring: an exploration of optimum data presentation. ICES Journal of Marine Science, 55: 705–710.

Berger, V., and Dahle, S. (Eds) 2001. White Sea. Ecology and Environment. Derzhavets Publisher, St. Petersburg – Tromsø. 158 pp.

Berger, V., Naumov, A., Zubaha, M., Usov, N., Smolyar, I., Tatusko, R., and Levitus, S. 2003. 36-Year Time Series (1963-1998) of Zooplankton, Temperature and Salinity in the White Sea. S-Petersburg – Washington, 2003, 362 pp.

Berline L., Siokou-Frangou, I., Marasović, I., Vidjak, O., Fernández de Puelles, Ma L., Mazzocchi, M. G., Assimakopoulou, G., *et al*. 2012. Intercomparison of six Mediterranean zooplankton time series. Progress in Oceanography, 97/100: 76–91.

Brinton, E., and Townsend, A. W. 1981. A comparison of euphausiid abundances from bongo and 1-m CalCOFI nets. California Cooperative Oceanic Fisheries Investigations Report, 22: 111–125.

Brix, H., Currie, K. I., and Mikaloff Fletcher, S. 2013. Seasonal variability of the carbon cycle in subantarctic surface water in the South West Pacific. Global Biogeochemical Cycles, 27: 1–12.

Broms, C., and Melle, W. 2007. Seasonal development of *Calanus finmarchicus* in relation to phytoplankton bloom dynamics in the Norwegian Sea. Deep Sea Research Part II: Topical Studies in Oceanography, 54(23): 2760–2775.

Chícharo M.A., Leitão, T., Range, P., Gutierrez, C., Morales, J., Morais, P., and Chícharo, L. 2009. Alien species in the Guadiana Estuary (SE-Portugal/SW-Spain): *Blackfordia virginica* (Cnidaria, Hydrozoa) and Palaemon macrodactylus (Crustacea, Decapoda): potential impacts and mitigation measures. Aquatic Invasions, 4 (3): 501-506. DOI: 10.3391/ai.2009.4.3.11

Courties, C., Vaquer, A., Troussellier, M., Lautier, J., Chrétiennot-Dinet, M. J., Neveux, J., Machado, C., *et al*. 1994. Smallest eukaryotic organism. Nature, 370(6487): 255–255.

Currie, K. I., Reid, M. R., and Hunter, K. A. 2011. Interannual variability of carbon dioxide drawdown by subantarctic surface water near New Zealand. Biogeochemistry, 104: 23–34.

Fiedler, B. 2013. CO^2 and O^2 dynamics and ocean-atmosphere fluxes in the Eastern Tropical North Atlantic. Doctoral thesis. Christian Albrechts Universität Kiel, Germany. 162 pp.

Freije, R. H., and Marcovecchio, J. E. 2004. Oceanografía química. *In* Ecosistema del Estuario de Bahía Blanca, pp. 69–78. Ed. by M. C. Piccolo, and M. S. Hoffmeyer. Instituto Argentino de Oceanografía, Bahía Blanca, Buenos Aires, Argentina.

Galvão, H. M., Reis, M. P., Domingues, R. B., Caetano, S. M., Mesquita, S., Barbosa, A. B., Costa, C., *et al*. 2012. Ecological tools for the management of cyanobacteria blooms in the Guadiana River Watershed, Southwest Iberia. *In* Studies on Water Management Issues, pp. 159–192. Ed. by M. Kumarasamy. InTech. 286 pp.

Garcia-Comas, C., Stemmann, L., Ibanez, F., Berline, L., Mazzocchi, M. G., Gasparini, S., Picheral, M., *et al.* 2011. Zooplankton long-term changes in the NW Mediterranean Sea: Decadal periodicity forced by winter hydrographic conditions related to large-scale atmospheric changes? Journal of Marine Systems, 87(3–4): 216–226.

Gonçalves, R., Correia, A.D., Atanasova, N., Teodósio, M.A., Ben-Hamadou, R., and Chícharo, M.A. 2015. Environmental factors affecting larval fish community in the salt marsh area of Guadiana estuary (Algarve, Portugal). Sci. Mar., 79(1), doi: http://dx.doi.org/10.3989/scimar.04081.08A

Gorsky, G., Ohman, M. D., Picheral, M., Gasparini, S., Stemmann, L., Romagnan, J. B., Cawood, A., *et al*. 2010. Digital zooplankton image analysis using the ZooScan integrated system. Journal of Plankton Research, 32(3): 285–303.

Gran, H. H., and Braarud, T. 1935. A quantitative study of the phytoplankton in the Bay of Fundy and the Gulf of Maine (including observations on hydrography, chemistry, and turbidity). Journal of the Biological Board of Canada, 1: 279–467.

Grbec, B., Morović, M., Kušpilić, G., Matijević, S., Matić, F., Beg Paklar, G., and Ninčević, Ž. 2009. The relationship between the atmospheric variability and productivity in the Adriatic Sea area. Journal of the Marine Biological Association of the United Kingdom, 89(8): 1549–1558.

Hewitt, R. 1980. Distributional atlas of fish larvae in the California Current region: northern anchovy, *Engraulis mordax* Girard, 1966 through 1979. California Cooperative Oceanic Fisheries Investigations Atlas 28. 101 pp.

Huggett, J. A., and Richardson, A. J. 2000. A review of the biology and ecology of *Calanus agulhensis* off South Africa. ICES Journal of Marine Science, 57(6): 1834–1849.

Huggett, J. A., Verheye, H. M., Escribano, R., and Fairweather, T. 2009. Copepod biomass, size composition and production in the Southern Benguela: spatio-temporal patterns of variation, and comparison with other eastern boundary upwelling systems. Progress in Oceanography, 83: 197–207.

Iriarte, A., Aravena, G., Villate, F., Uriarte, I., Ibáñez, B., Llope, M., and Stenseth, N. 2010. Dissolved oxygen in contrasting estuaries of the Bay of Biscay: effects of temperature, river discharge and chlorophyll. *Marine Ecology Progress Series*, 418: 57–71.

Jones, K., Currie, K. I., McGraw, C. M., and Hunter, K. A. 2013. The effect of coastal processes on phytoplankton biomass and primary production within the near-shore Subtropical Frontal Zone. Estuarine, Coastal and Shelf Science, 124: 44–55.

Jossi, J. W., and Kane, J. 2013. An atlas of the dominant zooplankton collected along a Continuous Plankton Recorder transect between Massachusetts USA and Cape Sable NS, 1961-2008. US Department of Commerce, Northeast Fisheries Science Center Reference Document, 13-12. 104 pp.

Jurgensone, I., Carstensen, J., Ikauniece, A., and Kalveka, B., 2011. Long-term changes and controlling factors of phytoplankton community in the Gulf of Riga (Baltic Sea). Estuaries and Coasts, 34(6): 1205–1219.

Kane, J. 2007. Zooplankton abundance trends on Georges Bank, 1977–2004. ICES Journal of Marine Science, 64(5): 909–919.

Karl, D. M., and Church, M. J. 2014. Microbial oceanography and the Hawaii Ocean Time-series programme. Nature Reviews Microbiology, 12(10): 699–713.

Kontoyiannis, H. 2010. Observations on the circulation of Saronikos Gulf: A Mediterranean embayment sea-border of Athens/Greece. Journal of Geophysical Research, 115 (C6): doi:10.1029/2008JC005026.

Kontoyiannis, H., Balopoulos, E., Gotsis-Skretas, O., Pavlidou, A., Assimakopoulou, G., and Papageorgiou, E. 2005. The hydrology and biochemistry of the Cretan Straits (Antikithira and Kassos Straits) revisited in the period June 1997–May 1998. Journal of Marine Systems, 53(1): 37–57.

Kušpilić, G., Marasović, I., Krstulović, N., Šolić, M., Ninčević-Gladan, Ž.,; Bojanić, N., Vidjak, O., *et al*., 2009. Restoration potential of eutrophic waters adjacent to large cities: lessons from the coastal zone of Croatia. *In* Proceedings of the International Workshop: Impact of Large Coastal Mediterranean Cities on Marine Ecosystems, Alexandria, Egypt, 10–12 February 2009, pp. 117–120. Ed. by M. Angelidis, F. Brian, J-F. Cadiou, S. Kholeif, J. Oh, A. Rodriguez y Baena, and M. Scoullos. Commission Internationale pour l'Exploration Scientifique de la Mer Méditerranée, Monaco, Technical Report. 240 pp.

Lavaniegos B.E., Molina-González O. and Murcia-Riaño M. 2015. Zooplankton functional groups from the California Current and climate variability during 1997-2013. CICIMAR Oceánides 30(1):45-62.

Lomas, M. W., Bates, N. R., Johnson, R. J., Knap, A. H, Steinberg, D. K., and Carlson, C. A. 2013. Two decades and counting: 23-years of sustained open ocean biogeochemical measurements in the Sargasso Sea. Deep-Sea Research II, 93:16–32, doi: 10.1016/j.dsr2.2013.01.008.

Mackas, D. L., Batten, S., and Trudel, M. 2007. Effects on zooplankton of a warmer ocean: recent evidence from the Northeast Pacific. Progress in Oceanography, 75: 223–252.

Mackas, D. L., Peterson, W. T., Ohman, M. D., and Lavaniegos, B. E. 2006. Zooplankton anomalies in the California Current system before and during the warm ocean conditions of 2005. Geophysical Research Letters, 3: L22S07, doi:10.1029/2006GL027930.

Mackas, D. L., Peterson, W. T., and Zamon, J. E. 2004. Comparisons of interannual biomass anomalies of zooplankton communities along the continental margins of British Columbia and Oregon. Deep-Sea Research II, 51: 875–896.

Mackas, D. L., Thomson, R. E., and Galbraith, M. 2001. Changes in the zooplankton community of the British Columbia continental margin, and covariation with oceanographic conditions, 1985-1999. Canadian Journal of Fisheries and Aquatic Sciences, 58: 685–702.

Malačič, V., Celio, M., Čermelj, B., Bussani, A., and Comici, C. 2006. Interannual evolution of seasonal ther-mocline properties in the Gulf of Trieste (northern Adriatic) 1991-2003. Journal of Geophysical Research, 111: 1–16.

Martynova D., Usov N., Falk-Petersen S., Bathmann U. Monitoring keystone components of sub-Arctic food webs – ecosystem dynamics of the White Sea. - Fact Sheet by: EUR-OCEANS Knowledge Transfer Unit, hosted by the GLOBEC IPO at Plymouth Marine Laboratory, KTU N11, October 2008.

McClatchie, S., Duffy-Anderson, J., Field, J. C., Goericke, R., Griffith, D., Hanisko, D. S., Hare, J. A., *et al*. 2014. Long time series in US fisheries oceanography. Oceanography, 27(4): 48–67, http://dx.doi.org/10.5670/oceanog.2014.86.

Mercado, J. M., Sala, I., Salles, S., Cortés, D., Ramírez, T., Liger, E., Yebra, L., *et al*. 2014. Effects of community composition and size structure on light absorption and nutrient uptake of phytoplankton in contrasting areas of the Alboran Sea. Marine Ecology Progress Series, 499: 47–64.

Morais, P., Chícharo, M. A., and Chícharo, L. 2009. Changes in a temperate estuary during the filling of the biggest European dam. Science of the Total Environment, 407: 2245–2259.

Mozetič, P., Francé, J., Kogovšek, T., Talaber, I., and Malej, A. 2012. Plankton trends and community changes in a coastal sea (northern Adriatic): bottom-up vs. top-down control in relation to environmental drivers. Estuarine, Coastal and Shelf Science, 115: 138–148.

Muha T.P., Teodosio, M.A., and Ben-Hamadou, R. 2017. Impact assessment of non-indigenous jellyfish species on the estuarine community dynamic: A model of medusa phase. Estuarine, Coastal and Shelf Science, Volume 187, 5 March 2017, Pages 249–259DOI: 10.1016/j.ecss.2016.10.040

Müller-Karger, F. E., Varela, R., Thunell, R. C., Scranton, M. I., Taylor, G. T., Astor, Y., Benitez-Nelson, C. R., *et al*. 2010. The CARIACO Oceanographic Time Series. *In* Carbon and Nutrient Fluxes in Continental Margins: A Global Synthesis, pp. 454–464. Ed. by K-K. Liu, L. Atkinson, R. Quinones, and L. Talaue-McManus. Springer-Verlag, Berlin. 741 pp.

Ninčević-Gladan, Ž., Bužančić, M., Kušpilić, G., Grbec, B., Matijević, S., Skejić, S., Marasović, I., *et al*. 2015. The response of phytoplankton community to anthropogenic pressure gradient in the coastal waters of the eastern Adriatic Sea. Ecological Indicators, 56: 106–115.

Ohman, M. D., and Smith, P. E. 1995. A comparison of zooplankton sampling methods in the CalCOFI time series. California Cooperative Oceanic Fisheries Investigations Report, 36: 153–158.

Perillo, G. M. E. 1995. Definitions and geomorphologic classifications of estuaries. *In* Geomorphology and Sedimentology of Estuaries, pp. 17–47. Ed. by G. M. E. Perillo. Elsevier, Amsterdam. 488 pp.

Perillo, G. M. E., Piccolo, M. C., Parodi, E., and Freije, R. H. 2001. The Bahía Blanca Estuary, Argentina. *In* Coastal Marine Ecosystems of Latin America, pp. 205–217. Ed. by U. Seeliger, and B. Kjerfve. Springer-Verlag, Berlin. 366 pp.

Peterson, W. T., Fisher, J. L., Peterson, J. O., Morgan, C. A., Burke, B. J., and Fresh, K. L. 2014. Applied fisheries oceanography: Ecosystem indicators of ocean conditions inform fisheries management in the California Current. Oceanography, 27: 80–89.

Raitsos, D. E., Reid, P. C., Lavender, S. J., Edwards, M., and Richardson, A. J. 2005. Extending the SeaWiFS chlorophyll data set back 50 years in the northeast Atlantic. Geophysical Research Letters, 32(6): L06603, doi:10.1029/2005GL022484.

Revilla, M., Borja, Á., Fontán, A., Franco, J., González, M., and Valencia, V. 2010. A two-decade record of surface chlorophyll a and temperature in offshore waters of the Basque country (southeastern Bay of Biscay). Revista de Investigación Marina, 17(2): 13–20.

Rocha, C., Galvão, H., and Barbosa, A. 2002. Role of transient silicon limitation in the development of cyanobacteria blooms in the Guadiana estuary, south-western Iberia. Marine Ecology Progress Series, 228: 35–45.

Santos, A. M. P., Chícharo, A., dos Santos, A., Moita, T., Oliveira, P. B., Peliz, A., and Ré, P. 2007. Physical biological interactions in the life history of small pelagic fish in the Western Iberia Upwelling Ecosystem. Progress in Oceanography, 74: 192–209.

Shannon, L. V., and Nelson, G. 1996. The Benguela: large scale features and processes and system variability. *In* The South Atlantic: Present and Past Circulation, pp. 163–210. Ed. by G. Wefer, W. H. Berger, G. Siedler, and D. Webb. Springer-Verlag, Berlin. 644 pp.

Sieracki, C. K., Sieracki, M. E., and Yentsch, C. S. 1998. An imaging-in-flow system for automated analysis of marine microplankton. Marine Ecology Progress Series, 168: 285–296.

Simboura, N., Zenetos, A., and Pancucci-Papadopoulou, M. A. 2014. Benthic community indicators over a long period of monitoring (2000-2012) of the Saronikos Gulf, Greece, Eastern Mediterranean. Environmental Monitoring and Assessment, 186: 3809–3821.

Šolić, M., Krstulović, N., Kušpilić, G., Ninčević Gladan, Ž., Bojanić, N., Šestanović, S., Šantić, D., *et al*. 2010. Changes in microbial food web structure in response to changed environmental trophic status: A case study of the Vranjic Basin (Adriatic Sea). Marine Environmental Research, 70(2): 239–249.

Šolić, M., Krstulović, N., Marasović, I., Baranović, A., Pucher-Petković, T., and Vučetić, T. 1997. Analysis of time series of planktonic communities in the Adriatic Sea: distinguishing between natural and man-induced changes. Oceanologica Acta, 20(1): 131–143.

Usov, N., Kutcheva, I., Primakov, I., and Martynova, D. 2013. Every species is good in its season: Do the shifts in the annual temperature dynamics affect the phenology of the zooplankton species in the White Sea? Hydrobiologia, 706(1): 11–33.

Vandromme, P., Stemmann, L., Berline, L., Gasparini, S., Mousseau, L., Passafiume, O., Guarini, J-M., *et al*. 2012. Zooplankton communities fluctuations from 1995 to 2005 in the Bay of Villefranche-sur-Mer (Northern Ligurian Sea, France). Biogeosciences, 8: 3143–3158, http://www.obs-vlfr.fr/Rade/RadeZoo/RadZoo /Accueil.html.

Verheye, H. M., Richardson, A. J., Hutchings, L., Marska, G., and Gianakouras, D. 1998. Long-term trends in the abundance and community structure of coastal zooplankton in the southern Benguela system, 1951–1996. South African Journal of Marine Science, 19(1): 317–332.

Warner, A. J., and Hays, G. C. 1994. Sampling by the continuous plankton recorder survey. Progress in Oceanography, 34(2–3): 237–256.

List of Acronyms

A

AAO	Antarctic Oscillation
ACC	Antarctic Circumpolar Current
AMO	Atlantic Multidecadal Oscillation
AMOC	Alantic Meridional Overturning Circulation
AO	Arctic Oscillation

C

CDOM	Coloured Dissolved Organic Matter
CHL/Chla	Chlorophyll
CO2	Carbon dioxide
COPEPOD	Coastal and Oceanic Plankton Ecology,Production, and Observation Database
CPR	Continuous Plankton Recorder

D

DFO	Department of Fisheries and Oceans / Fisheries and Oceans Canada
Diat	Diatom biomass
Dino	Dinoflagellate biomass
DMI	Dipole Mode Index
DO	Dissolved Oxygen

E

EAC	East Australian Current
EBC	Eastern Boundary Current
ENSO	El Niño Southern Oscillation

G

GIN Seas	Greenland Iceland Norwegian Seas
GLOBEC	Global Ocean Ecosystem Dynamics

I

ICES	International Council for the Exploration of the Seas
IEO	Instituto Español de Oceanografía
IGMETS	International Group for Marine Ecological Time Series
IOCCP	International Ocean Carbon Coordination Project
IPCC	Intergovernmental Panel on Climate Change
IOD	Indian Ocean Dipole
IPO	Interdecadal Pacific Oscillation
ITCZ	Intertropical Convergence Zone

J

JGOFS	Joint Global Ocean Flux Study

K

KOE	Kuroshio-Ozashio Extension
KIOST	Korean Institute for Ocean Science and Technology

L

LC	Leeuwin Current

M

MODIS	Moderate Resolution Imaging Spectroradiometer aboard the Terra and Aqua satellites
MSLP	Mean Sea Level Pressure

N

NADW	North Atlantic Deep Water
NAO	North Atlantic Oscillation
NO3	Nitrate
NOAA	National Oceanic and Atmospheric Administration
NPGO	North Pacific Gyre Oscillation
NPI	North Pacific Index
NPO	North Pacific Oscillation

O

OA	Ocean Acidification
OCB	Ocean Carbon & Biogeochemistry
OCCCI	Ocean Colour Climate Change Initiative
OISST	Optimum Interpolation Sea Surface Temperature
ONI	Oceanic Niño index
Oxy/O2	Oxygen

P

PCI	Phytoplankton Colour Index
PDO	Pacific decadal oscillation
PF	Polar Front
Phyto	Phytoplankton
PICES	North Pacific Marine Science Organization
POOZ	Permanently Open Ocean Zone

R

Ratio	Ratio between Diatom and Dinoflagellate biomass

S

SAF	Subantarctic Front
SAHFOS	Sir Alister Hardy Foundation for Ocean Science
Sal	Salinity
SAM	Southern Annular Mode SASW Subantarctic Surface Waters SAZ Subantarctic Zone
SCOR	Scientific Committee on Oceanic Research
SeaWiFS	Sea-Viewing Wide Field of View Sensor
SEC	South Equatorial Current
SMK	Seasonal Mann Kendall Test
SO	Southern Oscillation
SOCPR	Southern Ocean Continuous Plankton Recorder Survey
SOI	Southern Oscillation Index
SOPO	State of the Pacific Ocean Report
SPCZ	South Pacific Convergence Zone
SSS	Sea Surface Salinity
SST	Sea-Surface-Temperature
STF	Subtropical Front
Sv	Sverdrup

T

Temp	Temperature
TW	Time Window

U

UCDW	Upper Circumpolar Deep Water

W

WAP	Western Antarctic peninsula
WBC	Western Boundary Current
WGPME	ICES Working Group on Phytoplankton and Microbial Ecology
WGZE	ICES Working Group on Zooplankton Ecology
WP	Pacific Warm Pool

Z

Zoop	Zooplankton biomass

Acknowledgements

The elaboration of this publication "What are Marine Ecological Time Series telling us about the ocean? A status report" would not have been possible without the dedicated work of hundreds of time-series investigators, who provided not only the data used for the analysis, but also encouraged us, the editors and the authors, during the drafting process and review. We will not be able to mention everyone, but each chapter starts with a list of principle investigators, representing often a team of scientists, who contributed data and comments to the respective section of the report. This comprehensive characterization of the global ocean is based on the information obtained from more than 300 time-series sites in the northern and southern hemisphere, in the open-ocean and coastal areas.

Thanks to the generous financial support by the Korean Institute for Ocean Science and Technology (KIOST) we were able to engage a core group of scientists to form the International Group for Marine Ecological Time Series (IGMETS) and to write the report. KIOST interest in the IOC objectives and its support have been really encouraging.

We would like to warmly thank all the lead authors and co-authors for their commitment and very professional work in the elaboration of this publication, foremost: Nicholas Bates, Antonio Bode, Frank Muller-Karger, Laura Lorenzoni, Michael Lomas, Todd O'Brien, Andrew Ross, Peter Thompson, Luis Valdés, and Peter Wiebe.

We also recognize the generous involvement and support by our partners and the organizations/institutions that employ the IGMETS steering members.

Partners:

- ICES - International Council for the Exploration of the Sea
- IOCCP - International Ocean Carbon Coordination Project
- KIOST - Korean Institute for Ocean Science and Technology, Republic of Korea
- NOAA - National Oceanic and Atmospheric Administration, USA
- OCB - Ocean Carbon and Biogeochemistry, USA
- PICES - North Pacific Marine Science Organization

Steering-member organizations/institutes:

- Bigelow Laboratory, USA
- BIOS - Bermuda Institute of Ocean Sciences, USA
- CSIRO – Commonwealth Scientific and Industrial Research Organisation, Australia
- DFO – Department for Fisheries and Oceans Canada, Canada
- IEO - Instituto Español de Oceanografía, Spain
- NOAA - National Oceanic and Atmospheric Administration, USA
- USF – University of South Florida, USA
- WHOI - Woods Hole Oceanographic Institution, USA

Illustrations are a key part of the publication. We acknowledge Todd O'Brien and COPEPOD (NOAA) for the elaboration of new material specifically designed to be published in this book. We would like to thank in particular Franck Drouet for the elaboration of the ocean currents figures and Martin Wickenden for his patience in assisting during the whole process. Finally, we would also like to thank Emory Anderson for his editorial review of the final document.

Three dedicated workshops of the IGMETS working group were organized within the framework of the 'Ocean Carbon Sources and Sinks' project, and it was a pleasure to work with such a highly motivated team, modifying methodology, discussing the outcomes, and finally drafting the report.

Participating time-series investigators

Eric Abadie, Jose L. Acuna, M. Teresa Alvarez-Ossorio, Anetta Ameryk, Jeff Anning, Elvire Antajan, Georgia Asimakopoulou, Yrene Astor, Angus Atkinson, Patricia Ayon, Alexey Babkov, Espen Bagoien, Hermann Bange, Ana Barbosa, Nick Bates, Uli Bathmann, Sonia Batten, Beatrice Bec, Radhouan Ben-Hamadou, Claudia Benitez-Nelson, Carla F. Berghoff, Robert Bidigare, Antonio Bode, Maarten Boersma, Angel Borja, Alexander Brearley, Eileen Bresnan, Cecilie Broms, Juan Bueno, Mario O. Carignan, Craig Carlson, David Caron, Jacob Carstensen, Gerardo Casas, Benoit Casault, Claudia Castellani, Fabienne Cazassus, Georgina Cepeda, Paulo Cesar Abreu, Jacky Chauvin, Sanae Chiba, Luis Chicharo, Epaminondas Christou, Matthew J. Church, Andrew Clarke, James E. Cloern, Rudi Cloete, Nathalie Cochennec-Laureau, Andrew Cogswell, Amandine Collignon, Yves Collos, Frank Coman, Maria Constanza Hozbor, Kathryn Cook, Dolores Cortes, Joana Cruz, Daniel Cucchi Colleoni, Kim Currie, Padmini Dalpadado, Claire Davies, Alejandro de la Sota, Alessandra de Olazabal, Laure Devine, Emmanuel Devred, Iole Di Capua, Rita Domingues, Anne Doner, John E. Dore, Antonina dos Santos, Hugh Ducklow, Janet Duffy-Anderson, Joerg Dutz, Martin Edwards, Lisa Eisner, Joao Pedro Encarnacao, Ruth Eriksen, Ruben Escribano, Luisa Espinosa, Tone Falkenhaug, Ana Faria, Ed Farley, Maria Luz Fernandez de Puelles, Susana Ferreira, Bjorn Fiedler, Jennifer L. Fisher, James Fishwick, Serena Fonda-Umani, Almudena Fontan, Janja France, Javier Franco, Jed Fuhrman, Mitsuo Fukuchi, Eilif Gaard, Moira Galbraith, Peter Galbraith, Helena Galvao, Pep Gasol, Amatzia Genin, Astthor Gislason, Anne Goffart, Renata Goncalves, Rafael Gonzalez-Quiros, Gabriel Gorsky, Annika Grage, Hafsteinn Gudfinnsson, Kristinn Gudmundsson, Valeria Guinder, Troy Gunderson, David Hanisko, Jon Hare, Roger Harris, Erica Head, Jean-Henri Hecq, Simeon Hill, Richard Horaeb, Graham Hosie, Jenny Huggett, Keith Hunter, Anda Ikauniece, Arantza Iriarte, Masao Ishii, Solva Jacobsen, Marie Johansen, David Johns, Catherine Johnson, Jacqueline Johnson, Young-Shil Kang, David M. Karl, So Kawaguchi, Kevin Kennington, Diane Kim, Georgs Kornilovs, Arne Kortzinger, Alexandra Kraberg, Anja Kreiner, Nada Krstulovic, Takahashi Kunio, Inna Kutcheva, Michael Landry, Stuart Larsen, Bertha E. Lavaniegos, Aitor Laza-Martinez, Jesus Ledesma Rivera, Alain Lefebvre, Sirpa Lehtinen, Maiju Lehtiniemi, Ezequiel Leonarduzzi, Ricardo M. Letelier, William Li, Priscilla Licandro, Michael Lomas, Christophe Loots, Angel Lopez-Urrutia, Laura Lorenzoni, Roger Lukas, Vivian Lutz, Dave Mackas, Jorge Marcovecchio, Francesca Margiotta, Piotr Margonski, Karin Margretha H. Larsen, Roberta Marinelli, Jennifer Martin, Douglas Martinson, Daria Martynova, Daniele Maurer, Maria Grazia Mazzocchi, Sam McClatchie, Felicity McEnnulty, Webjorn Melle, Jesus M. Mercado, Michael Meredith, Claire Meteigner, Ana Miranda, Graciela N. Molinari, Nora Montoya, Pedro Morais, Cheryl A. Morgan, Patricija Mozetic, Teja Muha, Frank Muller-Karger, Jeffrey Napp, Florence Nedelec, Ruben Negri, Vanessa Neves, Todd O'Brien, Clarisse Odebrecht, Mark Ohman, Lena Omli, Emma Orive, Luciano Padovani, Hans Paerl, Marcelo Pajaro, Evgeny Pakhomov, Kevin Pauley, S.A. Pedersen, Ben Peierls, Pierre Pepin, Myriam Perriere Rumebe, Ian Perry, Tim Perry, William T. Peterson, Roger Pettipas, David Pilo, Sophie Pitois, Al Pleudemann, Stephane Plourde, Arno Pollumae, Dwayne Porter, Lutz Postel, Nicole Poulton, Igor Primakov, Regina Prygunkova, A. Miguel P. Santos, Andy Rees, Michael Reetz, Beatriz Reguera, Malcolm Reid, Christian Reiss, Jasmin Renz, Mickael Retho, Marta Revilla, Maurizio Ribera, Anthony Richardson, Marc Ringuette, Malcolm Robb, Marie Robert, Don Robertson, Karen Robinson, M. Carmen Rodriguez, Solveig R Olafsdottir, Andrew Ross, Gunta Rubene, M. Guillermina Ruiz, Tatiana Rynearson, Sei-ichi Saitoh, Rafael Salas, Danijela Santic, Diana Sarno, Michael Scarratt, Renate Scharek, Oscar Schofield, Mary Scranton, Valeria Segura, Sergio Seoane, Stefanija Sestanovic, Yonathan Shaked, Volker Siegel, Mike Sieracki, Joe Silke, Ricardo I. Silva, Ioanna Siokou-Frangou, Milijan Sisko, Anita Slotwinkski, Tim Smyth, Mladen Solic, Dominique Soudant, Carla Spetter, Jeff Spry, Michel Starr, Debbie Steinberg, Deborah Steinberg, Lars Stemmann, Rowena Stern, Solvita Strake, Patrik Stromberg, Glen Tarran, Gordon Taylor, Maria Alexandra Teodosio, Peter Thompson, Robert Thunell, Valentina Tirelli, Others to be added soon, Mark Tonks, Sakhile Tsotsobe, Ibon Uriarte, Julian Uribe-Palomino, Nikolay Usov, Luis Valdés, Victoriano Valencia, Marta M. Varela, Hugh Venables, Marina Vera Diaz, Hans Verheye, Olja Vidjak, Fernando Villate, Maria Delia Viñas, Norbert Wasmund, Robert Weller, George Wiafe, Claire Widdicombe, Karen H. Wiltshire, Malcolm Woodward, Lidia Yebra, Kedong Yin, Cordula Zenk, Soultana Zervoudaki, and Adriana Zingone

DISCOVER OCEAN TIME SERIES

United Nations Educational, Scientific and Cultural Organization

Intergovernmental Oceanographic Commission

IGMETS

Key:

- Marine ecological time series site for which data were provided and included in the International Group for Marine Ecological Time Series analysis.
- Marine ecological time series site for which participation in the initial International Group for Marine Ecological Time Series analysis was not confirmed at the time of this map's creation.

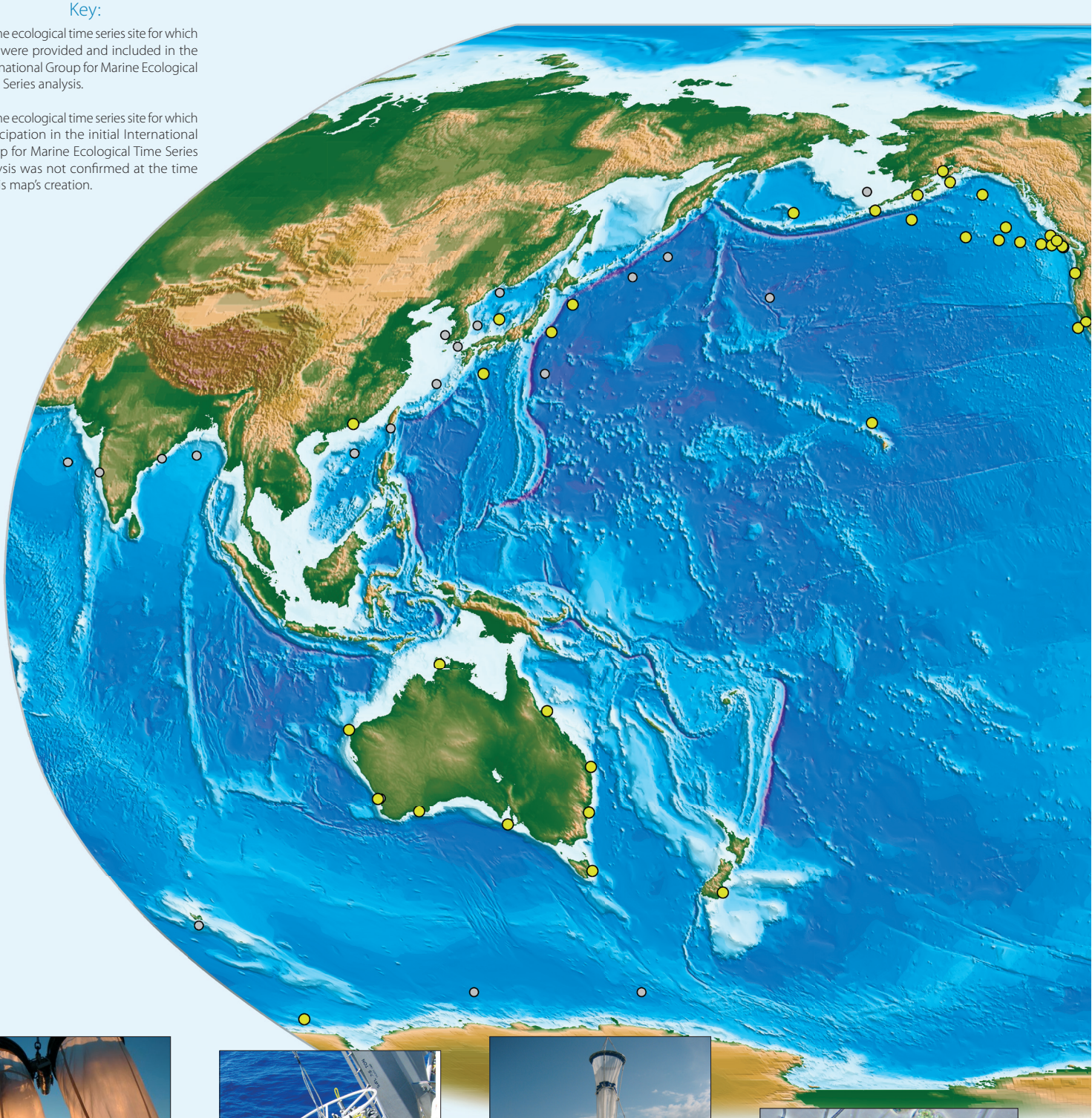

© James R Wilkinson/SIO-CalCOFI

Crew of the NOAA ship Belle M. Shimada recovers the Bongo Net during a CaLCOFI cruise.

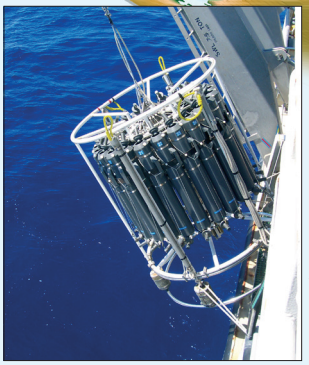

© Digna Rueda

CTD sensor equipped with water sampling rosette deployed at the BATS station.

© Kirsten Isensee

WP2 plankton net deployed in the Baltic Sea.

© Bill Li

Chaetoceros decipiens.

Scientific research vessel Veliger II returning from regular sampling at the Ubatuba station.

Limacina retroversa.

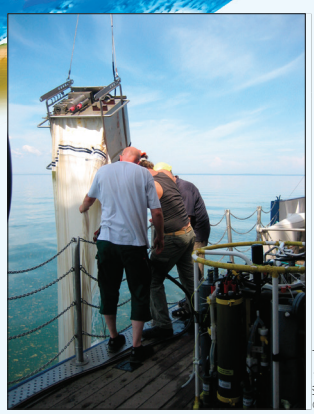

Recovery of a multi-net for plankton analysis in the Baltic Sea during a cyanobacteria bloom.

Sediment trap deployment at the CARIACO station.

Ship-based biogeochemical and ecological time series are one of the most valuable tools to characterize and quantify ocean ecosystems. These programmes continuously provide major breakthroughs in understanding ecosystem variability, allow quantification of the ocean carbon cycle, and help understand the processes that link biodiversity, food webs, and changes in services that benefit human wellbeing. A quantum jump in regional and global ocean ecosystem science can be gained by aggregating observations from the individual time series that are distributed across different oceans and which are managed by different countries. The collective value of these data is greater than that provided by each time series individually. However, maintaining time series requires a commitment by the scientific community and sponsor agencies.

What are Marine Ecological Time Series telling us about the ocean? A status report highlights the importance of continued sampling by existing marine time series authored by the International Group for Marine Ecological Time Series (IGMETS). The report seeks to aggregate time series dispersed around the world in an effort to augment the observing power to look at changes within different ocean regions, to explore plausible reasons and connections at a global level, and to highlight any locations of especially large changes that may be of special importance; in summary, to produce new science.

This publication was possible thanks to the generous financial support by the
Korean Institute for Ocean Science and Technology (KIOST).

What are Marine Ecological Time Series telling us about the ocean? A status report

http://igmets.net

United Nations Educational, Scientific and Cultural Organization | Intergovernmental Oceanographic Commission

KIOST KOREA INSTITUTE OF OCEAN SCIENCE & TECHNOLOGY

IGMETS

Intergovernmental Oceanographic Commission (IOC)
United Nations Educational, Scientific and Cultural Organization (UNESCO)
7 Place Fontenoy, 75352 Paris Cedex 07 SP, France
Tel: +33 1 45 68 39 83/84
Fax: +33 1 45 68 58 12
http://ioc.unesco.org